













*Wiley Eastern University Edition*

By the Late William P. Creager and the Late Joel D. Justin

**HYDROELECTRIC HANDBOOK**

By the Late William P. Creager, the Late Joel D. Justin, and Julian Hinds

**ENGINEERING FOR DAMS, in three volumes**

**I. GENERAL DESIGN**

By the Late William P. Creager, the Late Joel D. Justin, and Julian Hinds

**II. CONCRETE DAMS**

By Julian Hinds, the Late William P. Creager, and the Late Joel D. Justin

**III. EARTH, ROCK-FILL, STEEL AND TIMBER DAMS**

By the Late Joel D. Justin, Julian Hinds, and the Late William P. Creager.

By the Late Joel D. Justin

**EARTH DAM PROJECTS**

By the Late Joel D. Justin and William G. Mervine

**POWER SUPPLY ECONOMICS**

# *Engineering for Dams*

---

*By*

**WILLIAM P. CREAGER**

**JOEL D. JUSTIN**

*and*

**JULIAN HINDS**

*In Three Volumes*

**VOLUME II • CONCRETE DAMS**

*By* **JULIAN HINDS, WILLIAM P. CREAGER**

*and* **JOEL D. JUSTIN**



**WILEY EASTERN PRIVATE LIMITED**  
**NEW DELHI**

**First Edition, 1945**

**Published by Anand R. Kundaji for Wiley Eastern Private Limited,  
J 41 South Extension 1, New Delhi 3 and printed by Sudhir Balsaver  
at Usha Printers, 6 Tulloch Road, Bombay 1. Printed in India**

## PREFACE

During the past decade there has been a marked increase in expenditures for projects involving dams. This increase has led to an intensification of experimental research and a reexamination not only of details and methods of construction but also of many of the theories of design, all of which has resulted in a substantial improvement in the art and science of dam building. It is for this reason that the authors are presenting to the engineering profession a new work on dams which is intended to be a compendium of modern practice in sufficient detail to serve the practicing engineer as well as the student.

It is unfortunate that space does not permit a listing of the many engineers who have assisted the authors with suggestions, data, constructive criticisms, and much actual work. To these the authors are very grateful because, without such great help, this work would not have been possible.

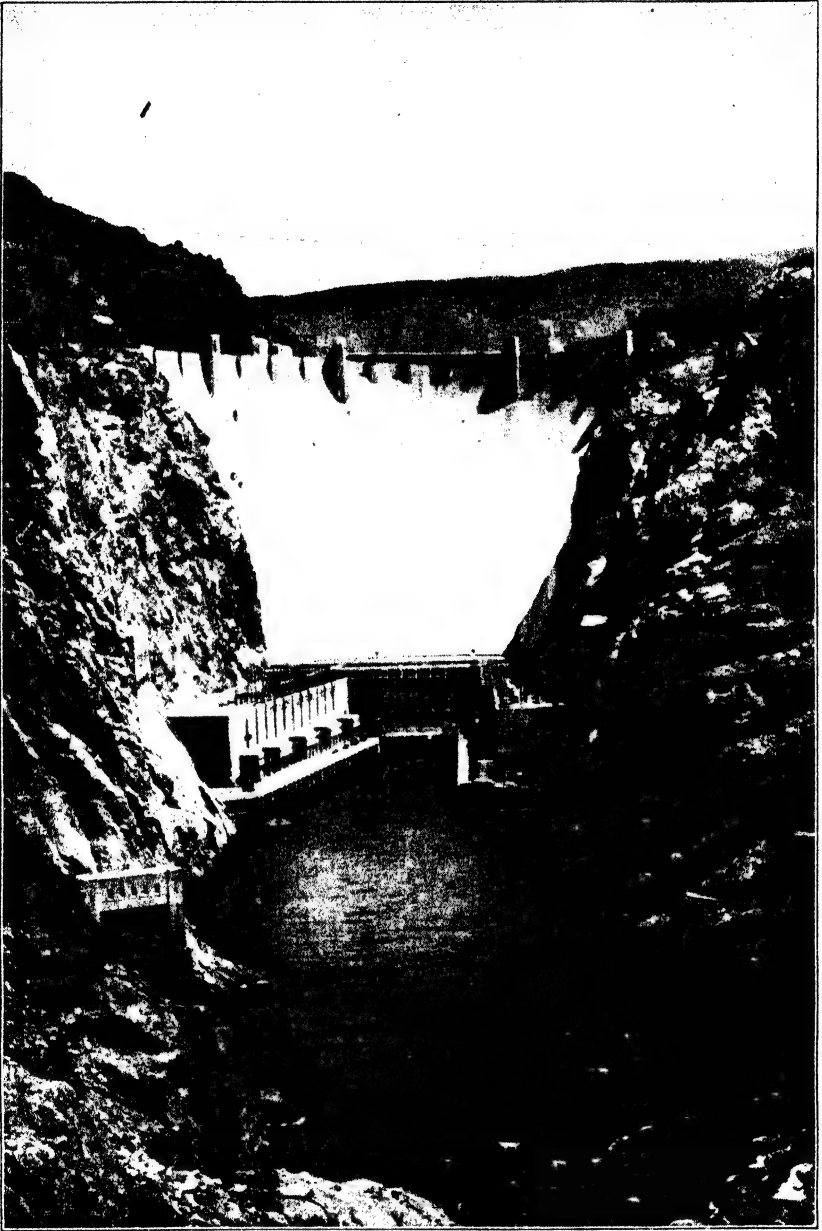
Many of these persons have been mentioned in the text. Special mention should be made of Byron O. McCoy for a large amount of research work and the editing of the entire manuscript.

The authors are also indebted to the many publishers who, without exception, have given ready consent to the reproduction of illustrations from their periodicals; also to a number of government and private bodies which have been unstinting in their aid.

WILLIAM P. CREAGER.  
JOEL D. JUSTIN.  
JULIAN HINDS.

*March, 1944.*





Boulder Dam, the highest in the world (726 feet).

# CONTENTS

In this book article headings are listed in the table of contents only in the volume in which they occur, but all chapter titles for the three volumes are listed in each volume. A complete index covering all three volumes appears in each volume.

## VOLUME I

CHAPTER	PAGE
1 INVESTIGATION OF DAM SITES . . . . .	1
2 THE CHOICE OF TYPE OF DAM . . . . .	40
3 PREPARATION AND PROTECTION OF THE FOUNDATION . . . . .	44
4 HYDRAULIC MODEL STUDIES . . . . .	91
5 FLOOD FLOWS . . . . .	99
6 SPILLWAYS . . . . .	208

## VOLUME II

### CHAPTER 7. FORCES ACT- ING ON DAMS

ARTICLE	PAGE
1 Nomenclature . . . . .	247
2 General Considerations . . . . .	252
3 External Water Pressure . . . . .	252
4 Dynamic and Subatmospheric Effects . . . . .	255
5 Internal Water Pressure—Uplift . . . . .	260
6 Ice Pressure . . . . .	270
7 Earth and Silt Pressures . . . . .	272
8 Wind Pressure . . . . .	274
9 Wave Pressures and Heights . . . . .	274
10 Tides, Setup, and Seiches . . . . .	276
11 The Weight of the Dam . . . . .	277
12 The Weight of the Foundation . . . . .	278
13 Earthquake Forces . . . . .	279
14 Vertical Reaction of the Foundation . . . . .	286
15 Horizontal Foundation Reactions . . . . .	292

### CHAPTER 8. REQUIRE- MENTS FOR STABILITY OF GRAVITY DAMS

1 Causes of Failure . . . . .	293
2 Location of the Resultant . . . . .	294

ARTICLE	PAGE
3 Resistance to Sliding . . . . .	294
4 Compressive Stresses . . . . .	299
5 Tension on Inclined or Vertical Planes . . . . .	302
6 Margin of Safety . . . . .	303
7 Details of Design and Methods of Construction . . . . .	304
8 Comparison of Stresses and Assumptions, Existing Dams . . . . .	304

### CHAPTER 9. GENERAL PRO- CEDURE FOR THE DESIGN OF GRAVITY DAMS

1 General Considerations . . . . .	306
2 Theoretical Cross-Sections . . . . .	306
3 Division into Zones . . . . .	308
4 Description of Zones, Non-overflow Dams, Rectangular Bases . . . . .	309
5 Description of Zones, Spillway Dams, Rectangular Bases . . . . .	311
6 Zones for Irregular Bases and Hollow Dams . . . . .	312
7 Expansion of Fundamental Equations . . . . .	312

## CHAPTER 10. THE DESIGN OF SOLID NONOVERFLOW GRAVITY DAMS

ARTICLE	PAGE
1 Introduction . . . . .	313

### EXAMPLE 1. 200-FOOT NONOVERFLOW DAM

2 Data, Example 1 . . . . .	313
3 Computation of Constants . . . . .	313
4 Top Details . . . . .	314
5 Zone I, Example 1 . . . . .	314
6 Zone II, Example 1 . . . . .	315
7 Zone III, Example 1 . . . . .	316
8 Block 1, Zone III, Analytical Solution . . . . .	316
9 Block 2, Zone III, Trial Solution . . . . .	318
10 Remainder of Zone III . . . . .	320
11 Sliding Factor and Stresses, Base of Zone III . . . . .	321
12 Zone IV, Example 1 . . . . .	322
13 Block 1, Zone IV . . . . .	322
14 Block 2, Zone IV . . . . .	325
15 Remainder of Zone IV . . . . .	325
16 The Completed Section . . . . .	328
17 Required Precision . . . . .	328
18 Permissible Block Depths . . . . .	329
19 Practical Profile . . . . .	329

### EXAMPLE 2. 200-FOOT NONOVERFLOW DAM WITH EARTHQUAKE ALLOWANCE

20 Data, Example 2 . . . . .	330
21 Earthquake Forces . . . . .	330
22 Constants and Top Details . . . . .	331
23 Zone I, Example 2 . . . . .	331
24 Zone II, Example 2 . . . . .	331
25 Block 1, Zone III . . . . .	332
26 Remainder of Zone III . . . . .	334
27 Zone IV . . . . .	334
28 Comparison with Example 1 . . . . .	337

### EXAMPLE 3. 350-FOOT NONOVERFLOW DAM

29 Effect in Lower Zones Shown . . . . .	337
30 Data, Example 3 . . . . .	338
31 Discussion of Constants . . . . .	338
32 Zones I to IV . . . . .	338
33 Bottom of Zone IV . . . . .	340

ARTICLE	PAGE
34 Zone V . . . . .	340
35 Redesign . . . . .	343
36 Comparison of Sections . . . . .	345

### COMPARISON OF NONOVERFLOW DAMS

37 Comparison of Nonoverflow Dams . . . . .	347
---	-----

## CHAPTER 11. THE DESIGN OF SOLID SPILLWAY GRAVITY DAMS

1 Methods of Design . . . . .	357
2 The Shape of the Crest . . . . .	357
3 Discharge Capacity . . . . .	364
4 The Bucket . . . . .	374
5 Backwater Curves . . . . .	374

### EXAMPLE 1. SOLID OVERFLOW DAM

6 Data for Example 1 . . . . .	377
7 Shape and Dimensions of Crest . . . . .	377
8 Water and Silt Pressures . . . . .	377
9 Zones I and Ia, Example 1 . . . . .	378
10 Zone II . . . . .	378
11 Lower Zones . . . . .	382
12 Practical Profile . . . . .	384
13 Stress Conditions near Crest . . . . .	384

### EXAMPLE 2. SOLID OVERFLOW DAM WITH ICE PRESSURE

14 Data for Example 2 . . . . .	385
15 Alternative Loadings . . . . .	385
16 Alternative Designs . . . . .	385

### EXAMPLE 3. THIRTY-FOOT OVERFLOW DAM WITH HYDRAULIC JUMP

17 Data, Example 3 . . . . .	391
18 Depth of Overflow . . . . .	392
19 Shape of Crest . . . . .	393
20 Stability Computations . . . . .	393
21 Possible Undercut Section . . . . .	397

### DETAILS

22 Controlled Crests . . . . .	397
23 Ice on Controlled Crests . . . . .	399
24 Comparison of Solid Spillway Dams . . . . .	399

# CHAPTER 12. INTERNAL STRESSES AND STRESS CONCENTRATIONS IN GRAVITY DAMS

ARTICLE	PAGE
1 Discussion of Secondary Stresses . . . . .	401
2 Need for Knowledge of Internal Stresses . . . . .	402
3 Principal Stresses . . . . .	402
4 Stresses on Oblique Planes . . . . .	402
5 Determination of Principal Stresses . . . . .	403
6 Stress Conditions at the Faces . . . . .	404
7 Analysis at Interior Points . . . . .	404
8 Geometric Analysis of Shears . . . . .	405
9 Geometric Analysis of Horizontal Stresses . . . . .	406
10 Numerical Example of Geometric Method . . . . .	407
11 Algebraic Determination of Shears . . . . .	411
12 Algebraic Determination of Horizontal Stress . . . . .	412
13 Numerical Computation of Principal Stress . . . . .	413
14 Heel and Toe Stresses at the Base . . . . .	413
15 Fillets in Corners . . . . .	414
16 Illustration of Foundation Stress Concentrations . . . . .	415
17 Stress Concentration at Holes . . . . .	417
18 Numerical Examples of Circular Outlet . . . . .	421
19 Rectangular Gallery . . . . .	422
20 Multiple Openings . . . . .	423

# CHAPTER 13. ARCH DAMS

1 Classification of Arch Dams . . . . .	425
---	-----

## CYLINDER THEORY OF DESIGN

2 Theory of Cylinder Action . . . . .	425
3 Example 1, Constant Radius . . . . .	427
4 Example 2, Constant Angle . . . . .	429
5 Example 3, Variable Radius . . . . .	431

## ELASTIC THEORY OF DESIGN

6 Need for Elastic Analysis . . . . .	434
7 Fundamentals of Elastic Theory . . . . .	434

ARTICLE	PAGE
8 Statically Indeterminate Reactions . . . . .	434
9 Equations for Crown Deflections . . . . .	436
10 Foundation Deformations . . . . .	440
11 Summary of Arch Equations . . . . .	449
12 Cancellation of Factor $1/E$ . . . . .	449
13 Physical Constants . . . . .	450

## EXAMPLES OF ELASTIC ANALYSES

14 Example 4, Analytical Analysis . . . . .	454
15 Example 5, Graphic Analysis . . . . .	468
16 Possible Simplifications . . . . .	479
17 The Importance of Temperature Stresses . . . . .	482

## SPECIAL ARCH FORMS

18 Symmetrical Arch . . . . .	486
19 Circular Arch of Uniform Thickness . . . . .	487
20 Fillet Arches . . . . .	492
21 Three-Centered Arches . . . . .	495

## DETERMINING THE DIMENSIONS OF AN ELASTIC ARCH

22 Best Shape for Elastic Arch . . . . .	496
23 Selection of Arch Form . . . . .	496

## THE TRIAL LOAD ANALYSIS OF ARCHED DAMS

24 Outline of Trial Load Theory . . . . .	500
25 Preparation of Preliminary Plan . . . . .	500
26 Horizontal Elements of Dam . . . . .	500
27 Vertical Elements . . . . .	500
28 Interaction of Elements . . . . .	502
29 Factors Influencing Division of Loads . . . . .	504
30 Typical Load Division . . . . .	505

## NUMERICAL EXAMPLE OF TRIAL-LOAD ARCH DAM

31 Example 10, Data . . . . .	505
32 Preliminary Dimensions . . . . .	507
33 Selection of Units for Analysis . . . . .	509
34 First Trial Division of Radial Loads . . . . .	509
35 Cantilever Analysis for Radial and Vertical Loads . . . . .	509

ARTICLE	PAGE	ARTICLE	PAGE
36 First Complete Set of Trial Loads . . . . .	524	17 Stability of Buttresses, Example 1 . . . . .	579
37 Methods of Arch Analysis . . . . .	524	18 Vertical Pressures, Buttresses of Example 1 . . . . .	580
38 Sample Arch Analysis . . . . .	525	19 Inclined Pressures, Buttresses of Example 1 . . . . .	581
39 Tangential Loads . . . . .	533	20 Horizontal Shear, Buttresses of Example 1 . . . . .	582
40 Twisting of the Cantilevers . . . . .	538	21 Recapitulation of Stresses, Buttresses of Example 1 . . . . .	583
41 Twisting of the Arches . . . . .	542	22 Reinforcement of Buttresses, Example 1 . . . . .	583
42 Adjustment for Poisson's Ratio . . . . .	545	23 Example 2, Overflow Slab Dam . . . . .	583
43 Principal Stresses . . . . .	547		
44 Unit Load Patterns for Arches . . . . .	548		
45 Unit Loads for Cantilevers . . . . .	550		
46 Recapitulation of Trial Load Method . . . . .	550		
MODEL TESTS AND EXAMPLES OF ARCH DAMS		MULTIPLE-ARCH DAMS	
47 Model Analysis of Arch Dams . . . . .	551	24 Principles of Design . . . . .	584
48 Examples of Arch Dams . . . . .	553	25 Form of Arches . . . . .	584
		26 Loading and Arch Analysis . . . . .	585
CHAPTER 14. BUTTRESSED CONCRETE DAMS		EXAMPLE OF A MULTIPLE-ARCH DAM	
1 Advantages of Buttressed Dams . . . . .	558	27 Example 3, Nonoverflow Multiple-Arch Dam . . . . .	585
2 Types of Buttressed Dams . . . . .	558	28 Description of Arches, Example 3 . . . . .	586
3 Forces on Buttressed Dams . . . . .	564	29 Arch Stresses, Example 3 . . . . .	586
4 Earthquake Loading for Buttressed Dams . . . . .	564	30 Stability Computations, Example 3 . . . . .	587
5 Spacing of Buttresses . . . . .	565	31 Stresses in Buttresses of Example 3 . . . . .	591
6 Design of the Buttresses . . . . .	565	32 Recapitulation, Example 3 . . . . .	593
7 Beam Stresses in Buttresses . . . . .	567	33 Overflow Multiple-Arch Dam . . . . .	593
8 Inclination of Buttress Faces . . . . .	569	34 Lake Hodges Multiple-Arch Dam . . . . .	593
9 Shrinkage Cracks and Buttress Reinforcement . . . . .	569	35 Florence Lake Multiple-Arch Dam . . . . .	595
10 Buttresses of Uniform Strength . . . . .	570	36 Bartlett Multiple-Arch Dam . . . . .	596
11 Connection of Facing with the Foundation . . . . .	570		
12 Buttressed Dams on Soft Foundations . . . . .	572		
EXAMPLES OF SLAB AND BUTTRESS DAMS		ROUND-HEAD BUTTRESS DAMS	
13 Example 1, Simple Slab Dam . . . . .	572	37 Characteristics of Round-Head Type . . . . .	597
14 Form and Spacing of Buttresses . . . . .	574	38 Rio Salado Round-Head Buttress Dam . . . . .	599
15 Slab Analysis, Example 1 . . . . .	575		
16 Corbel Details, Example 1 . . . . .	575		
		OTHER TYPES OF STRUCTURAL CONCRETE DAMS	
		39 Multiple-Dome Dams . . . . .	601
		40 Triple-Arch Dams . . . . .	603
		41 Slab and Column Dams . . . . .	603

# CONTENTS

xi

## CHAPTER 15. CONCRETE FOR CONCRETE DAMS

ARTICLE	PAGE
1 General . . . . .	604
2 Cement . . . . .	605
3 Fine Aggregate . . . . .	606
4 Coarse Aggregate . . . . .	606
5 Water . . . . .	608
6 Admixtures . . . . .	608
7 Concrete Mixes . . . . .	608
8 Batching and Mixing . . . . .	611

ARTICLE	PAGE
9 Transportation and Placing . . . . .	611
10 Forms and Formed Surfaces . . . . .	612
11 Height of Lifts . . . . .	613
12 Curing and Protection . . . . .	613
13 Joints—Horizontal and Vertical . . . . .	614
14 Temperature Control, Cracking and Checking . . . . .	615
15 Waterproofing . . . . .	616
16 Tests of Concrete and Concrete Materials . . . . .	617

## VOLUME III

CHAPTER	PAGE
16 SOIL TESTS AND THEIR UTILIZATION . . . . .	619
17 EARTH DAMS—GENERAL PRINCIPLES OF DESIGN . . . . .	655
18 STABILITY OF EARTH DAMS . . . . .	715
19 DETAILS OF EARTH DAMS . . . . .	749
20 ROCK-FILL DAMS . . . . .	806
21 STEEL DAMS . . . . .	834
22 TIMBER DAMS . . . . .	843
23 DETAILS AND ACCESSORIES . . . . .	848
24 HEADWATER CONTROL . . . . .	870



## CHAPTER 7

### FORCES ACTING ON DAMS

**1. Nomenclature.** The following nomenclature will apply, in general, to Chapters 7 to 14. Unless definitely mentioned, all forces are stated in pounds and all dimensions in feet.

$A$	Area of a section, area of a watershed in sq miles, angle between wind direction and fetch
$A_a$ $A_x$ $A_y$	Constants in condensed arch dam equations
$a$	Earthquake acceleration = $\alpha g$ , width of block in foundation deformation equations
$\Delta a_a$ $B_a$ $B_x$ $B_y$	Horizontal projection of an arch dam cantilever block (Fig. 37, Chapter 13)
$b$	Constants in condensed arch dam equations
$b$	Length of block in foundation deformation equations, $b_r$ for right side, $b_l$ for left side
$b_g$	A water-load lever arm (Fig. 33, Chapter 13)
$b_r$	Distance from resultant to unbroken face of a cracked arch dam cantilever
$C$	Coefficient of weir discharge (general), a constant
$C'$	Discharge coefficient for a standard overflow dam for "design head" measured to crest
$C_e$	An earthquake factor
$C_F$	Coefficient of thermal expansion
$C_s$	Coefficient for submerged weirs
$C_w$	Discharge coefficient for a sharp-crested weir
$C_a$ $C_x$ $C_y$	Constants in condensed arch dam equations
$c$	Percentage of joint or base of a dam block subjected to hydrostatic uplift pressure; in certain equations = distance from an arch axis
$D$	Average depth of water in set-up equations
$D_a$ $D_x$ $D_y$	Constants in condensed arch dam equations
$d$	Depth of flow over broad-crested weir or in spillway entrance; in general a depth with locally described subscripts
$E$	Modulus of elasticity in compression or tension; $E_F$ for foundation and $E_M$ for masonry
$\{E\}$ $\{E\}$	Composite foundation factors (Eqs. 54 and 54a, Chapter 13)



$E$	A subscript used to designate functions corresponding to reservoir empty; or in arches, functions derived from external loads
$e$	Excentricity, distance from the center of gravity of a section to its mid-point or to a resultant or force; $e_r$ , $e_1$ , and $e'$ are special values of $e$
$c_e$	Distance from center of gravity of a trapezoidal arch dam cantilever section to upstream and downstream kern limits
$e_i$	
$F$	Fetch or length in miles of exposure of a water surface to wind action; temperature change usually above or below annual mean, $F'$ being total from high to low
$\left\{ \begin{matrix} (F) \\ F \end{matrix} \right\}$	Composite foundation factors (Eqs. 54 and 54a, Chapter 13)
$F$	A subscript used to designate functions corresponding to reservoir full; or in arches to indicate foundation functions
$f$	Coefficient of static friction for well-dressed test specimens; unit fiber stress or unit thrust
$f'$	Actual coefficient of static friction at a given joint or base; unit fiber stress at downstream face of a dam
$f''$	Unit fiber stress at upstream face of a dam
$\left\{ \begin{matrix} f_s \\ f_c \end{matrix} \right\}$	Fiber stresses in steel and concrete
$f'_c$	Unit compressive strength of concrete as determined by test at age of 28 days
$\left\{ \begin{matrix} f_s \\ f_i \end{matrix} \right\}$	Fiber stresses at upstream and downstream faces of an arch
$G$	Shear modulus of elasticity
$\left\{ \begin{matrix} (G) \\ G \end{matrix} \right\}$	Composite foundation factors (Eqs. 55 and 55a, Chapter 13)
$g$	Acceleration of gravity = approximately 32.2 ft per sec per sec
$H$	Total height of dam section or total depth of water to be retained; a force or thrust, $H_c$ thrust at arch crown, $H_a$ at arch abutment, $H_1$ = an arbitrarily assumed crown force treated as an external load
$H_0$	Computed thrust at elastic center of an arch
$(H)$	A composite foundation factor (Eq. 56, Chapter 13)
$h$	Vertical distance; height of masonry; head of water, etc.; special subscripts explained where introduced
$\Delta h$	Height of block in gravity section or arch cantilever
$h_c$	Measured head on a spillway crest
$h'_c$	"Design head," depth above crest used in computing the shape of a standard overflow crest
$h_d$	Depth of dam joint below overflow crest
$h_f$	Head lost from contraction or friction
$h_s$	Depth of silt or earth fill
$h_t$	Depth of tailwater
$h_w$	Height of waves
$I$	Moment of inertia of a figure about its center of gravity unless another center is named; $I_c$ for an arch cantilever; $I_n = I$ about the neutral axis of a curved beam
$J$	Ratio of modulus of elasticity of masonry to same for dam foundation
$K$	A velocity factor (Art. 4, Chapter 7); coefficient of weir discharge (Fig. 6, Chapter 11); a constant
$k$	Void ratio of earth, silt, or concrete materials; ratio of maximum to average unit shear across a section
$\left\{ \begin{matrix} k_e \\ k_i \end{matrix} \right\}$	Distances from upstream and downstream faces of an arch dam cantilever to the kern limits
$\left\{ \begin{matrix} k_1 \\ k_2 \end{matrix} \right\}$	Earthquake and masonry weight constants (Eqs. 10 and 11, Chapter 12)

$k_1$	
$k_2$	
$k_3$	
$k_4$	
$k_5$	
$L$	
$l$	Foundation deformation factors
$l_n$	Top width of a dam
$\Delta l$	Unknown length of a horizontal joint; length of a weir or spillway crest; an arch span; $l_i$ = an intradosal arch span
$l_0$	Net length of a weir or spillway crest after deducting for end contractions
$l_i$	Difference in length of joints at top and bottom of dam block, divisible into upstream and downstream portions $\Delta l_u$ and $\Delta l_d$
$M$	Known length of previously determined dam joint
$\Delta M$	Total length of a spillway crest
$M_a$	Moment, momentum, mass
$M_c$	Rate of change of momentum
$M_E$	Moment at the abutment of an arch
$M_n$	Moment about the center or center of gravity of a figure (sometimes use $M_0$ ); moment at the crown of an arch
$M_u$	Moment caused by external loads
$m$	Net moment, including uplift moment, which usually is negative
$n$	Moment caused by uplift
$\Delta n$	Distance from the center of gravity of a figure or base of a dam block; $m'$ is to downstream face, $m''$ is to upstream face
$P$	Number of complete end contractions on a spillway crest; shear ratio (Art. 12, Chapter 13); ratio of $E$ for steel to $E$ for concrete
$\Delta P$	Horizontal deflection increments in an arch dam cantilever caused by moment ( $\Delta n_1$ ) and shear ( $\Delta n_2$ )
$\Sigma(P)$	Horizontal load on a gravity dam; an external load on an arch dam, frequently divided into $P_1$ , $P_2$ , etc.; also divided into components as $P_x$ and $P_y$
$\Sigma(P_x)$	An increment in the value of $P$ , frequently divided into parts as $P_1$ , $P_2$ , etc.; may carry same subscripts as $P$
$P_a$	Algebraic summation of all forces acting on a gravity dam above a given joint, excluding the reaction at the joint; in general any summation of loads $P$ ; may carry same subscripts as $P$
$P_{\phi 0}$	Algebraic summation of moments of forces contained in $\Sigma(P)$ about a given point (do not confuse with $\Sigma P_x$ )
$P_i$	An earthquake force
$P_s$	Accumulated earthquake force at the base of a dam
$P_t$	Ice pressure per linear foot of dam
$P_w$	Horizontal earth or silt pressure
$p$	Total horizontal pressure of tailwater on a dam slice
$p_a$	Total wave pressure against a dam slice
$p_\beta$	A unit pressure or stress in a gravity dam; $p'$ at downstream face, $p''$ at upstream face; <sup>1</sup> a unit water pressure or horizontal pressure per vertical foot of an arch dam cantilever; a pole distance
$s_\beta$	Allowable unit pressure or stress in masonry
$\Delta p$	Unit values of $p$ and $s$ on a plane making an angle of $\beta$ with direction of first principal stress
$p_1$	Difference in adjacent values of $p$
$p_2$	First and second principal stresses, also particular values of $p$

<sup>1</sup> In many functions throughout the book the superscript ' is used to represent values at the downstream face and '' is used to represent values at the upstream face.

$p_e$	Increase in unit water pressure caused by earthquake
$p_h$	Horizontal, inclined, vertical, and normal unit pressures or stresses <sup>1</sup> respectively
$p_i$	
$p_v$	
$p_n$	
$p_0$	Value of $p_e$ at base of dam
$p_r$	Unit vertical reaction at a point in the foundation of a dam exclusive of uplift pressure <sup>1</sup>
$p_u$	Unit effective uplift on a joint or base of a dam. i.e., the unit internal hydrostatic pressure times the area factor $c$ <sup>1</sup>
$p_v$	$p_r + p_u$ <sup>1</sup>
$p_w$	Unit wave pressure
$Q$	A total flow of water passing over a dam or through a channel
$Q_m$	Maximum flood from a given drainage area likely to be exceeded only once in $T$ years
$q$	Flow of water per foot of effective spillway crest
$R$	A reaction or a resultant of forces; may be divided into parts as $R_1$ , $R_2$ , or $R_L$ (left) and $R_R$ (right), etc.
$r$	Radius of a circle; rise of standard overflow crest above upstream corner; a ratio
$r_{c-w}$	Water-cement ratio
$r_e$	Radii to extrados, intrados, center line, and neutral axis of an arch
$r_i$	
$r_c$	
$r_n$	
$S$	Setup caused by wind; total shear on a dam section; curved length of an arch center line
$S_E$	Shear from external loads
$S_f$	Safety factor against sliding
$S_{s-f}$	Shear-friction safety factor
$S_t$	Total tangential shear between arch slices
$s$	Unit shear; $s_h$ and $s_v$ are horizontal and vertical components <sup>1</sup>
$\Delta s$	Length of an arch voussoir; the thickness of an arch dam cantilever slice <sup>1</sup>
$s_a$	Ultimate unit shearing strength of dam or foundation materials
$\Delta s_c$	Distance between centers of adjacent arch voussoirs
$\Delta s_t$	Unit tangential shear between adjacent arch slices
$\Delta s'$	Thickness of cracked arch dam cantilever at midpoint of unbroken portion
$T$	A thrust, compression if positive; a period of time in years
$T_c$	Thrust at crown of an arch
$T_E$	Arch thrust from external loads
$t$	Period of time; thickness of an arch or width of an arch dam cantilever
$t'$	Unbroken thickness of a cracked arch or arch dam cantilever
$t_c$	Crown thickness of an arch ring
$t_e$	Period of vibration for an earthquake (seconds)
$t_s$	Period of vibration of a structure (seconds)
$V$	Velocity, in miles per hour for wind, otherwise in feet per second; subscripts as $V_1$ , $V_2$ , etc., designate special velocities or velocities at special places; volume; shear
$V_a$	Effective velocity of approach to a dam or spillway
$V_a$	Shears at abutment, crown, and elastic center of an arch
$V_c$	
$V_e$	
$V_E$	

<sup>1</sup> Subscripts  $e$  and  $i$  designate values at extrados and intrados in this and other arch dam functions.

$V_h$	Horizontal component of $V$
$W$	Vertical force or weight, subscripts $W_1$ , $W_2$ designate special values
$\Sigma W$	Algebraic summation of the vertical components of all forces acting on a dam above a given joint, including uplift but exclusive of the reaction of the joint
$\Sigma(Wx)$	Algebraic summation of moments of forces contained in $\Sigma(W)$ about a specified point
$W_n$	A net weight or vertical force
$W_s$	Vertical weight of earth or silt (submerged weight if under water)
$W_t$	Vertical weight of tailwater
$W_u$	Total uplift force in a dam slice, at a joint or the foundation
$W_{uv}$	Virtual uplift (see Eq. 90, Chapter 13)
$W_0$	Previously determined accumulated weight above a given joint in dam
$w$	A unit weight
$\Delta w$	An increment of $w$ ; carries same subscript as $w$
$w_1$	Unit weights of masonry and water
$w_2$	
$w_s$	Unit weight of earth or silt fill in air, or submerged weight in water
$w'_s$	Unit dry weight of earth or silt
$x$	In general a distance; one of the coordinates of an arch; a vertical or horizontal lever arm
$\Delta x$	The difference between adjacent values of $x$
$x_a$	The abutment value of $x$ for an arch
$x_0$	The moment arm of a force or a collection of forces about the center of gravity of the base of a dam
$x_r$	The horizontal distance from the upstream extremity of a joint in a dam to the intersection of the resultant with that joint
$y$	Depth below water surface or crest of a dam; one of the coordinates of an arch; a distance
$\Delta y$	Difference between adjacent values of $y$
$y'$	Horizontal distance from center of moments to downstream and upstream extremities of the top joint of a dam block (see Fig. 4, Chapter 10)
$y''$	
$y_a$	Values of $y$ at abutment and elastic center of an arch
$y_0$	
$z$	Horizontal distance from the center of moments to the point of intersection of the resultant with a joint or base
$z'$	Same as $y'$ and $y''$ but for bottom of block (see Fig. 4, Chapter 10)
$z''$	
$\alpha$	Angle of internal friction for earth or silt fill; ratio of earthquake acceleration to $g$ ; half central angle of an arch; in general an angle
$\alpha'$	Angle between a normal to the face of an arch dam and the direction of an earthquake movement
$\beta$	Generally an angle; a part of the central angle in multi-centered or fillet arches; angle between a given plane and plane of first principal stress
$\Delta$	A prefix denoting a difference or a small but finite part
$\partial$	A prefix designating a small or differential quantity
$\partial'\alpha$	(And a number of similar expressions) foundation functions (see Art. 10, Chapter 13)
$\partial's$	
$\partial'n$	
$\partial s$	
$\partial x$	Changes in $s$ , $x$ , $y$ , and $\alpha$ , in arch equations
$\partial y$	
$\partial \alpha$	
$\partial \epsilon$	
$\epsilon$	Distance of the neutral axis of an arch or curved beam from the center
$\zeta$	Hydrostatic pressure intensity factor

$\theta$	Angle of inclination with the vertical <sup>2</sup> of the resultant $R$ of the forces $\Sigma(W)$ and $\Sigma(P)$ ; angle of earthquake motion
$\lambda$	Specific gravity of foundation, masonry, or aggregate particles
$\mu$	Ratio of transverse deformation to direct strain; Poisson's ratio
$\Sigma$	Symbol of summation; subscripts denoting special use explained in text
$\phi$	Angle of inclination with the vertical of the face of a dam <sup>2</sup>
$\partial\phi_1$	Angular deflection per unit height of arch dam cantilever, $\partial\phi_2$ = same for a cracked cantilever
$\psi$	Angle between plane of an arch and the abutment surface

**2. General Considerations.** The first consideration in designing a dam is the determination of the nature of the forces acting on the structure. These forces may be considered as consisting of the following:

- a. Water pressure,
- b. Earth pressure,
- c. Atmospheric pressure,
- d. Ice pressure,
- e. Earthquake forces,
- f. Wind pressure, \*
- g. Wave pressure,
- h. Weight of the dam,
- i. Weight of the foundation,
- j. Reaction of the foundation.

The nature of most of these forces, unfortunately, is such that they do not admit of exact determination. Their amounts, direction, and location must be adopted by the designer after a thorough consideration of all obtainable facts bearing on the case, and with the exercise of his best judgment, based on his experience and that of others who have had to deal with similar problems.

It must always be borne in mind that conditions in no two dams are alike, and that a general theory must never be applied to a particular case without thought as to the possible need of modification to suit the conditions peculiar thereto.

**3. External Water Pressure.** The weight of a cubic foot of fresh water has been determined to be

62.42 lb per cu ft at 32° F

62.26 lb per cu ft at 75° F

62.00 lb per cu ft at 100° F

The weight usually adopted in the design of dams is 62.5 lb per cu ft.

The total pressure,  $P$ , of quiet water on any submerged plane of area  $A$  is

$$P = w_2 A h_3 \quad [1]$$

<sup>2</sup> This is the common definition, as in general the joints and bases are horizontal. For inclined joints or bases the angles  $\theta$  and  $\phi$  should be measured from a normal to the joint or base.

where  $w_2$  is the weight of 1 cu ft of water and  $h_3$  is the distance from the center of gravity of the plane to the surface of the water. The force,  $P$ , is normal to the surface. In the design of dams, this force is usually resolved into its horizontal and vertical components, or these components may be derived directly by applying the head,  $h_3$ , to horizontal and vertical projections of the area,  $A$ .

In Fig. 1, let 1-2 represent a submerged vertical rectangular plane of unit width, measured perpendicular to the paper, having its top edge parallel to and coincident with the surface of the water. As the width of the plane is unity, the length,  $h_2$ , is a measure of its area,  $A$ .<sup>4</sup> The plane 1-2 being rectangular, its center of gravity is at point 4, midway between 1 and 2.

The total pressure,  $P$ , on the plane 1-2 may be obtained from Eq. 1 by substitution, the results being as follows:

$$P = \frac{1}{2}w_2h_2^2 \quad [2]$$

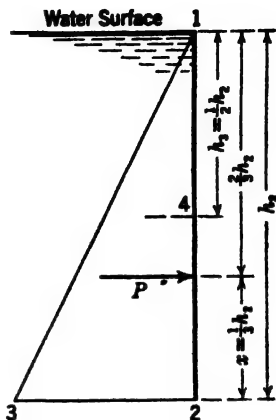


FIG. 1. Triangular water pressure on a vertical plane.

The force,  $P$ , is a distributed force, applied, although unequally, over the entire face. It may be represented by the right triangle 1-2-3, the length of the leg 2-3 of which is proportional to  $w_2h_2$ . Its center of application passes through the center of gravity of the triangle, which is up from the bottom of the face a distance

$$x = \frac{1}{3}h_2 \quad [3]$$

The moment of  $P$  about the lower edge of the surface is

$$Px = \frac{1}{6}w_2h_2^3 \quad [4]$$

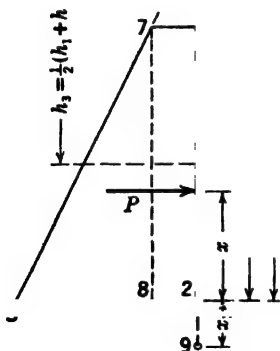


FIG. 2. Trapezoidal water pressure on a vertical plane.

If a portion 1-5 of the face 1-2 is removed, as indicated in Fig. 2, there will be left a vertical submerged face 5-2 of length  $h$ , with its upper edge below the water surface a depth  $h_1$ . The depth to the center of gravity of the surface is  $\frac{1}{2}(h_1 + h_2)$ . Substituting this value for  $h_3$ , and  $h_2 - h_1$  for  $A$  in Eq. 1, and simplifying, the total pressure on the surface is found to be

$$P = \frac{1}{2}w_2(h_2^2 - h_1^2) \quad [5]$$

<sup>4</sup> In the design of dams and where the form of the structure permits, it is customary to consider a slice bounded by two planes perpendicular to the axis of the dam and 1 ft apart, thereby simplifying the calculations by allowing the neglect of the third dimension. Unless specifically stated, it should be assumed, in all that follows, that such a slice is being considered.

The result is the same as if the area of the small triangle 1-5-7 had been subtracted from that of the triangle 1-2-3.

The center of application passes through the center of gravity of the trapezoid 5-2-3-7, which may be found graphically or by the equation

$$x = \frac{1}{3}h \frac{h_2 + 2h_1}{h_2 + h_1} \quad [6]$$

The moment of the force,  $P$ , about the lower edge of the surface may be found by the multiplication of Eqs. 5 and 6, the simplified results being as follows:

$$Px = \frac{1}{3}w_2h^2(h_1 + \frac{1}{3}h) \quad [7]$$

If desired,  $P$  and  $Px$  may be found by dividing the water pressure on the surface, 5-2, into the two parts represented by the rectangle 5-2-8-7 and the triangle 7-8-3 and computing the areas and moments separately. The force represented by the rectangle is

$$P_1 = w_2h_1h \quad [8]$$

For the triangle, the length of the leg 8-3 is  $w_2h$ , and the force, which is equal to the area of the triangle, is

$$P_2 = \frac{1}{2}w_2h^2 \quad [9]$$

The centers of application are  $\frac{1}{2}h$  for  $P_1$ , and  $\frac{1}{3}h$  for  $P_2$ , up from the base so that the moments become

$$P_1x = \frac{1}{2}w_2h^2h_1 \quad [10]$$

$$P_2x = \frac{1}{6}w_2h^3 \quad [11]$$

Eqs. 10 and 11 added together give Eq. 7.

The lever arm about an exterior point, as point 9, Fig. 2, is obtained by adding  $x_1$  to  $x$ .

The submerged faces of dams are frequently inclined, causing the normal water pressures against them to depart from the horizontal. In most dam-design problems, it is convenient to deal separately with the horizontal and vertical components of such forces.

If the plane 1-2 is inclined, as in Fig. 3, the total pressure,  $R$ , on the plane may be resolved into horizontal and vertical components,  $P$  and  $W$ . The horizontal component,  $P$ , will be equal to the pressure on the projection, 2-5, of the plane, 1-2, and its amount, center of application, and moment about the point 2, can be calculated from Eqs. 5, 6, and 7, or from the triangle 3-8-9 and the rectangle 8-9-2-5. The vertical component,  $W$ , will be equal to the weight of water within the boundaries 7-1-2-6, and its center of application will pass through the center of gravity of the figure. The weights of the rectangle 7-1-5-6 and the triangle 1-2-5 may be considered separately if desired.

The horizontal component,  $P$ , of the total water pressure on the upstream face of the dam of Fig. 4 is equal to the total pressure on the plane 8-3 and is determined by Eq. 2. The distance,  $x$ , from point 3 to the center of applica-

tion of the force,  $P$ , is found from Eq. 3. The vertical component,  $W$ , is equal to the weight of water within the area 7-2-3-8 and acts through the center of gravity of that area. For convenience,  $W$  may be divided into the

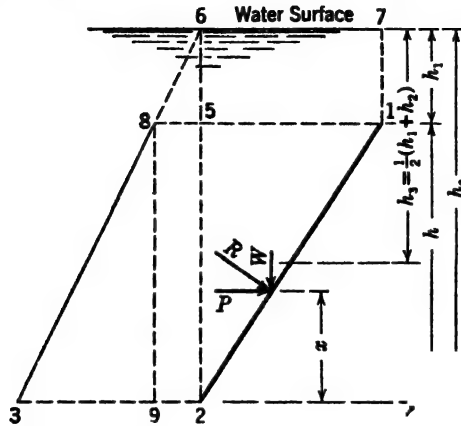


FIG. 3. Water pressure on an inclined plane.

parts 7-2-9-8 and 2-3-9. The tailwater of depth  $h_4$  exerts a pressure in an upstream direction, the value and center of application being determined respectively by Eqs. 2 and 3. The vertical tailwater effect is equal to the weight within the triangle 11-10-4.

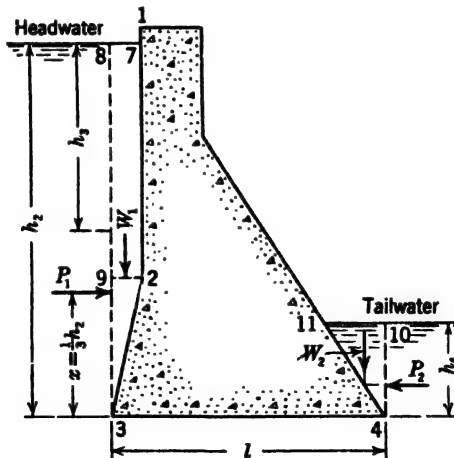


FIG. 4. Water loads on a gravity dam.

**4. Dynamic and Subatmospheric Effects.** (a) *Sharp-crested weir.* The forces acting on an overflow dam are complicated by the motion of the water. Their exact determination is rarely necessary, but the underlying principles should be understood.



Consider the sharp-crested, vertical-faced, aerated weir of Fig. 5. Assume that the velocity of approach is negligible, or zero, and let the diagram 3-5-2 represent the total pressure that would exist were the space 1-3 closed. It is usual to assume that with this space open, permitting overflow, the pressure against the face 1-2 is represented by 1-4-5-2.

If the head corresponding to the approach velocity is appreciable, an increased pressure will exist on portions of the wall. In Fig. 5 let  $h_v = 3-6$  represent the magnitude of the velocity head of approach, and let 6-8 be paral-

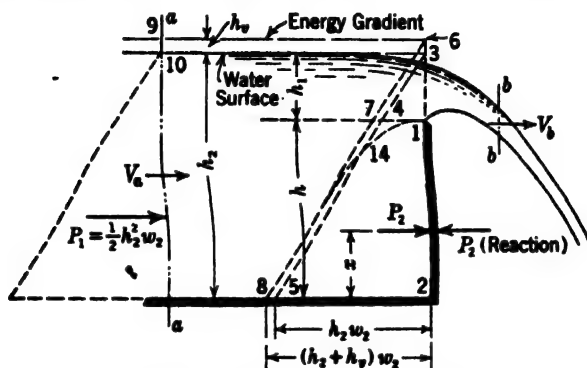


FIG. 5. Aerated sharp-crested weir.

lel to 3-5. The total force against the face 1-2 is usually assumed to be represented by 1-7-8-2.

Actually, the unit pressure at point 1 is zero, and some curve 1-14-8 more accurately represents the true pressures. The shape of this curve depends on the velocity distribution in the approach channel and on other weir flow factors, which usually are not available to the designer. The use of the simple diagram 1-7-8 is on the side of safety for an aerated weir. However, the approximate computation of magnitude of the actual force 1-14-8-2 will be discussed, to obtain a basis for subsequent discussions.

The true horizontal reaction between the wall and the water may be determined by considering the change in horizontal momentum between two sections, such as *a-a* and *b-b*. The *rate of change* of momentum between these sections is

$$\Delta M = w_2 \frac{qV_b}{g} - w_2 \frac{qV_a}{g} \quad [12]$$

where  $\Delta M$  is the change in momentum per second,  $V_a$  and  $V_b$  are the horizontal velocities at *a-a* and *b-b*, respectively; and  $q$  is the discharge per second. The analysis applies to a unit crest length.

A balance is necessary between  $\Delta M$  and the forces acting on the water. Neglecting friction, the only such forces acting parallel to the line of flow are  $P_1$ , the known hydrostatic pressure on the section *a-a* acting downstream;  $P_2$ , the unknown reaction of the weir wall acting upstream on the water; and

$P_0$ , the hydrostatic pressure (if any) across section  $b-b$ , acting upstream. If  $a-a$  is above the drawdown effect of the weir and  $b-b$  is beyond the influence of crest contraction, i.e., where the horizontal velocity component is constant and  $P_0$  is zero, Eq. 12 becomes

$$P_1 - P_2 = \frac{q}{g} w_2 (V_b - V_a) \quad [13]$$

where  $P_1 = \frac{1}{2} w_2 h_2^2$ ;  $q$  is the discharge per foot of weir,  $V_a = q/h_2$ , and  $V_b = K\sqrt{2gh_1}$ ,  $K$  being an experimental constant. Substituting and transposing, Eq. 13 becomes

$$P_2 = \frac{1}{2} h_2^2 w_2 - \frac{q}{g} w_2 \left( K\sqrt{2gh_1} - \frac{q}{h_2} \right) \quad [14]$$

The value of  $q$  is given by Eq. 1, Chapter 11. Values of  $K$  may be determined experimentally, or estimated from the results of experiments previously made. For a sharp-crested, vertical-faced, aerated weir with negligible velocity of approach,  $K$  is about 0.83. For the same conditions, but with the upstream face on a 1 : 1 slope, it is about 0.81. These values are based on horizontal velocity components  $V_A$  as given in Table XVIII, p. 111, of *Masonry Dams*, second edition, by William P. Creager. The description of the construction of this table will aid in the determination of  $V_A$  for other conditions, should such values be required.

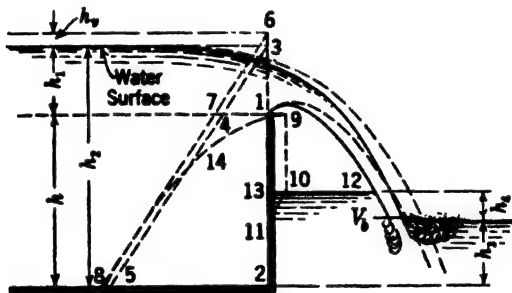


FIG. 6. Nonaerated sharp-crested weir.

(b) *Sharp-crested weir, not aerated.* In the discussion of Fig. 5, the area under the nappe, downstream from the crest, is assumed to be freely aerated. If the atmosphere is excluded from this area, the overfalling water will carry away a portion of the air entrapped in the space 1-12-13, Fig. 6, producing a partial vacuum. The unbalanced pressure of the external air will deflect the nappe from its normal position, shown dotted, to some position such as that shown in solid lines. Water will rise in the space under the nappe to some level, 13-12, having a height,  $h_4$ , above the tailwater level.<sup>5</sup> The pressure at

<sup>5</sup> The rise,  $h_4$ , may be due in part to rebound of water striking the bottom and may exist even without vacuum. This article deals only with that portion of the rise caused by reduced pressure.

the crest then becomes "negative" <sup>6</sup> by an amount equal to  $w_2 h_4$ . The total increase in horizontal reaction over that for the aerated weir of Fig. 5 is represented by the polygon 1-11-10-9 of Fig. 6. By choosing a value of  $K$  corresponding to  $V_1$  just above the tailwater level, the total reaction represented by 1-14-8-2-11-10-9, Fig. 6, may be found from Eq. 14. The determination of  $K$  for the conditions of Fig. 6 is difficult and is avoided by the provision of aeration.

(c) *Overflow-dam crest.* If a structure such as an overflow dam, having exactly the form of the underside of the falling water sheet of Fig. 5, is sub-

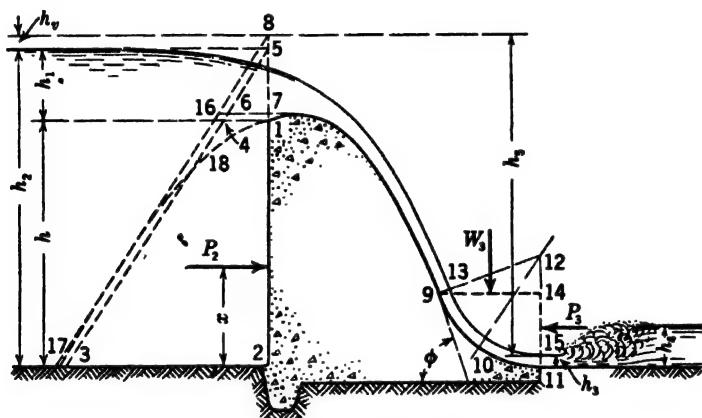


FIG. 7. Overflow dam.

stituted for the sharp-crested weir as illustrated in Fig. 7, the falling sheet will exert no force upon it for such distance as it follows the shape of the nappe. An exact fit between the nappe and the dam profile is possible for only one depth of overflow. For smaller flows, the free fall of the jet is interfered with and a portion of the weight of the water rests on the masonry. This weight is usually neglected. Also,  $P_3$  (Art. 4d) assumes a small positive value, which may be ignored so far as the stability of the dam is concerned.

If the head is increased beyond the value for which the crest is designed, the nappe will tend to follow a wider path, leaving the dam. If this is prevented by lack of aeration, or otherwise, an area of subatmospheric pressure is produced along the face of the dam. Such pressure adds to the overturning effect on the dam. Obviously, it cannot exceed full vacuum, i.e., atmospheric pressure less vapor pressure. If the dam section is of irregular form, there may be local areas where full vacuum actually is approached, but under usual conditions this cannot occur over a large area, as the resulting force would be more than sufficient to deflect the jet against the masonry.

For any ratio of  $h_1$  to the design head, the total reaction may be computed from Eq. 14. If  $h_1$  is equal to the design head, proceed as for Fig. 6, Art. 4b.

<sup>6</sup> The term "negative" will be applied to pressures less than atmospheric.

If  $h_1$  is smaller or larger than the design head, estimate the horizontal component of the velocity at some point such as section 9-13, Fig. 7, and from this compute the value of  $K$ . Even if  $K$  is assumed zero (corresponding to a vertical back face), the computed pressure for any likely case will be much less than full atmospheric on the entire face.

The decreased pressure resulting from any condition causing partial vacuum also has a vertical component, which is usually ignored.

The authors are not prepared to give a simple rule for the height of  $P_2$  above the base of the weir or dam. The primary purpose of Eq. 14 is to permit the designer to determine for cases involving possible vacuum whether the total force appreciably exceeds the area 7-16-17-2 of Fig. 7. If it does, it may be advisable to find the location of  $P_2$  experimentally or by means outside the scope of this book. Conditions requiring such a determination are usually avoided for reasons given below.

For poorly designed crests, the reduction of atmospheric pressure may become intermittent; i.e., a partial vacuum accumulates up to a certain amount, then a break occurs, admitting air, with a sudden return to normal pressure. This is repeated periodically. Such periods sometimes become of very short duration, causing a strong vibration, which may damage the dam.

If the crest is properly formed, it is difficult or impossible to cause the nappe to jump clear, for any reasonable increase in  $h_1$ .<sup>7</sup>

(d) *Dynamic force of tailwater stream.* The downstream face of an overflow dam is usually curved at the base, as illustrated in Fig. 7, to reduce the erosive effect of the falling water. In going around such a curve, the water exerts a reaction on the dam. By determining the value of  $K$ , Eq. 14, at the end of the bucket, as at section 11-15, Fig. 7, this reaction may be included in  $P_2$ . However, unless ignored, it should be computed separately.

Approximate equations for its computation, derived from the momentum theory, are as follows:<sup>8</sup>

$$P_3 = w_2 \frac{q}{g} V(1 - \sin \phi) \quad [15]$$

and

$$W_3 = w_2 \frac{q}{g} V \cos \phi \quad [16]$$

where  $P_3$  is the horizontal force,  $W_3$  the vertical force,  $V$  is the average velocity along the curved face,  $\phi$  the inclination of the face to the vertical at the point of analysis, and other symbols are as previously established. If the depth of tailwater,  $h_3$ , is appreciable, the horizontal force should be increased by the hydrostatic pressure on section 11-15, Fig. 7, thus:

$$P_3 = w_2 \frac{q}{g} V(1 - \sin \phi) + \frac{1}{2} w_2 h_3^2 \quad [17]$$

<sup>7</sup> ROUSE and REID, "Model Research on Spillway Crests," *Civil Eng.*, January 1935.

<sup>8</sup> See DODGE and THOMPSON, *Fluid Mechanics*, McGraw-Hill, 1937, p. 112.

As an approximation,  $V$  may be taken as equal to  $\sqrt{2gh_5}$ . The centers of application of  $P_3$  and  $W_3$  may be taken as passing approximately through the midpoints of 11-14 and 14-9, respectively. The influence of the bucket reaction on the stability of the dam is usually ignored except where the depth of discharge over the crest is very large.

In Fig. 7, the tailwater is shown held away from the dam by the hydraulic jump, and the back pressure due to the depth,  $h_4$ , does not act against the dam. Conditions under which this may be expected, and means of prevention, are discussed in Part IV of Chapter 3.

**5. Internal Water Pressure—Uplift.** (a) *Elements of uplift.* Dams are subjected to water pressure, not only on exposed faces but also on their bases and within the masonry itself. These internal pressures produce uplift. Uplift is the upward pressure of water as it seeps or flows through the dam or its foundations. It causes a reduction in the effective weight of the structure above it. Water causing uplift pressures may enter through pores or imperfections in the foundation, through imperfectly bonded foundation or construction joints, or through pores in the structure itself.

The existence of these forces has been recognized for about half a century and has been the subject of much debate. There is perhaps no other factor in the design of masonry dams about which so little is known and about which there are so many differences of opinion.

Uplift on a unit area at any point in a horizontal section may be considered to have two elements: (1) the *hydrostatic pressure* of the seeping water at that point; and, (2) the percentage,  $c$ , of the unit area on which the hydrostatic pressure acts. These two elements will be considered separately.

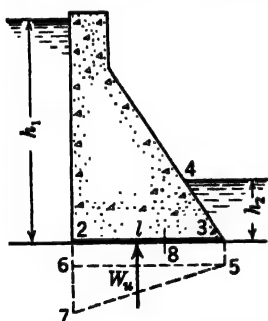


FIG. 8. Principles of uplift pressures.

(b) *Explanation of hydrostatic pressure.* The conception generally applied to hydrostatic-uplift pressure may be explained by a discussion of the hypothetical conditions illustrated in Fig. 8. This figure represents a dam with an upstream water depth of  $h_1$  and a tailwater depth of  $h_2$ . Consider the base as slightly raised from the foundation, permitting flow from the upper to the lower pool. Assuming that the width of crack is uniform, that the flow conforms to the laws governing flow in pipes, and neglecting loss at entrance, the pressure intensity will diminish uniformly from  $w_2h_1$  at point 2, to  $w_2h_2$  at point 3. Intermediate intensities are represented by the line 7-5.

If, without lowering the dam, the crack is closed at point 2, thus stopping the flow, the pressure becomes constant and equal to  $w_2h_2$ . If the closure is at point 3, the pressure is uniform at  $w_2h_1$ . If the closure is at some intermediate point, the intensity is  $w_2h_1$  upstream and  $w_2h_2$  downstream from the closure. If the obstruction at any of these points is partial, the effects noted will be partially attained.

Actually, the dam is not raised from its foundation but water is forced through the pores and cracks of the masonry and the foundation materials. Water flowing through such pores or cracks follows a similar law of decreasing pressures. However, the cracks or pores are not concentrated along a single line, nor are they always uniformly distributed. Consequently, the actual internal pressures may differ somewhat from those indicated in Fig. 8.

(c) *Simple ideal case.* Fig. 9 represents underflow conditions for a non-porous dam with a straight base on a homogeneous isotropic foundation of

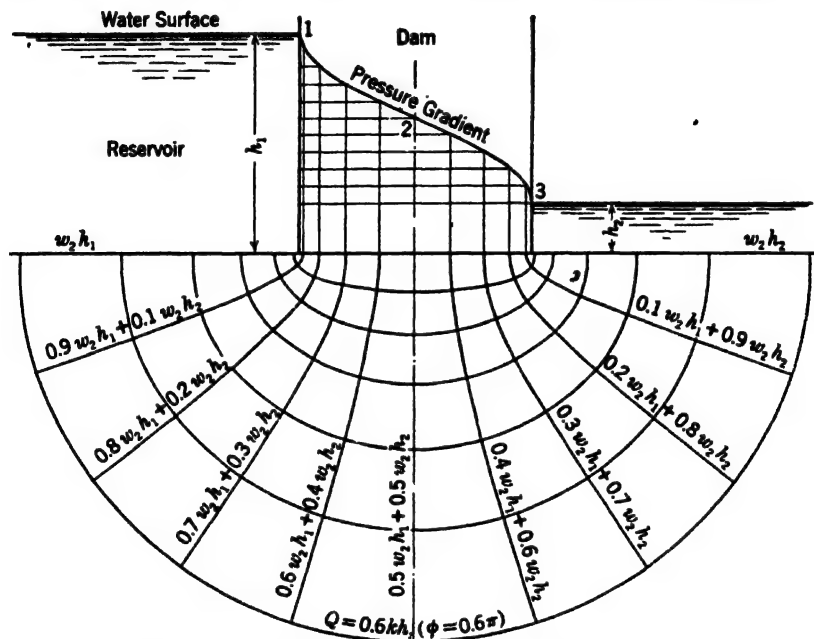


FIG. 9. Percolation of water under an impervious dam.

unlimited depth and horizontal extent. Headwater depths and tailwater depths are represented by  $h_1$  and  $h_2$ , respectively. The concentric semi-ellipses represent lines of flow for water passing through the foundation. The hyperbolas, drawn normal to the lines of flow at all points, represent lines of equal hydrostatic pressure within the foundation and at the base of the dam. The resultant hydrostatic pressures in water depths are represented by the S-curve 1-2-3.

This network of flow lines and pressure lines is called a flow net. For simple conditions, its form may be determined mathematically.<sup>9</sup> For more complicated conditions, other means of determination are available.<sup>10</sup> The construction of flow nets is discussed in Art. 14 of Chapter 3.

<sup>9</sup> WARREN WEAVER, "Uplift Pressures on Dams," *J. Math. Phys.*, June 1932.

<sup>10</sup> E. W. LANE, "Flow Net and Electric Analogy," *Civil Eng.*, October 1934; also L. F. HAEZL, "Uplift and Seepage under Dams on Sand," *Trans. Am. Soc. Civil Engrs.*, Vol 100, 1935, p. 1352.

(d) *Effect of porosity on flow net.* The form of the flow net is not affected by degree of porosity of the foundation. If the dam is also pervious, the pressure pattern is altered, but for practical conditions this is not likely to be important for masonry dams.

Most foundations are jointed. Resistance to flow through the cracks is less than through the pores of the rock, hence the cracks control both flow and pressure. If the cracks are uniformly distributed and the dam is relatively

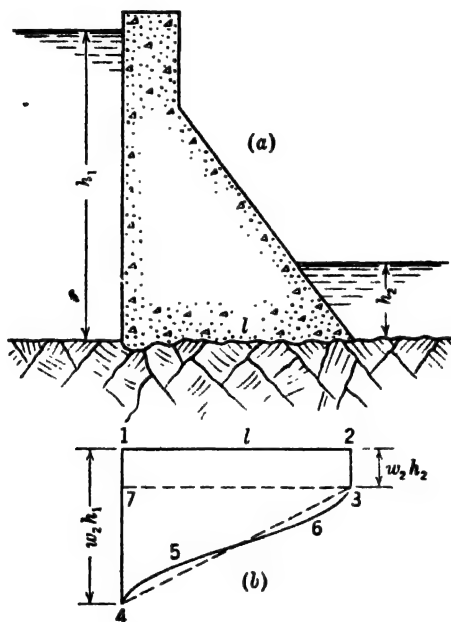


FIG. 10. Uplift pressure intensities without cutoff.

impervious to seepage, internal pressures may be assumed to approximate those for the homogeneous foundation.

(e) *Simplest practical case.* The simplest case of a masonry dam on a rock foundation is illustrated in Fig. 10. Pressure intensities are represented by the figure 1-2-3-6-5-4, Fig. 10b, where 1-4 and 2-3 represent  $w_2 h_1$  and  $w_2 h_2$ , respectively. If the straight line 4-3 is substituted for the curve, the average pressure is unchanged. Distribution is slightly altered, but considering the uncertainties involved, such a substitution is generally considered permissible, which justifies the use in practice of the simple pressure diagram of Fig. 8.

(f) *The control of pressure intensities.* Important dams are usually provided with cutoff walls or grout curtains to reduce underflow and with drains to relieve pressures downstream from the cutoff. Fig. 11 represents the idealized thin, tight cutoff, exactly at the upstream face, with a drain immediately back

of it. If the cutoff were perfectly tight, intensity of hydrostatic pressure would be reduced to the rectangle 1-2-3-7, in which the depth 2-3 represents pressure due to tailwater. Actually, a grout curtain is never perfectly tight, hence the cutoff alone produces a pressure diagram of some such form as 1-2-3-4, in which 7-4 represents the amount by which the cutoff fails to dissipate all of the head ( $h_1 - h_2$ ) on the dam.

The introduction of an adequate drain reduces the pressure to some line such as 3-5-6. The exact form of this line depends on the thoroughness with

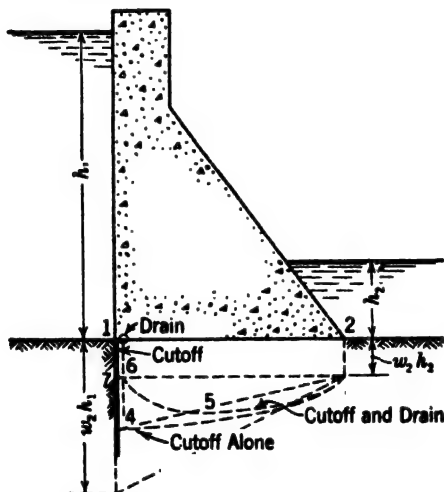


FIG. 11. Uplift pressure intensities with cutoff.

which the drainage is executed. Details of grout and drainage works are discussed in Chapter 3.

The greatest intensity of pressures does not necessarily go with the poorest foundation, particularly where the grouting is thorough. The effectiveness of a grout curtain depends on its tightness in relation to the remainder of the foundation. Water enters a thoroughly grouted fissured foundation with difficulty but escapes readily through the ungrouted rock downstream from the cutoff. This favors a low uplift.

Open horizontal seams in the foundations can be either quite beneficial or quite the reverse. If they have access to tailwater but not to headwater they act effectively as drains. If they are open to headwater but have little or no connection with tailwater near the dam, they greatly increase the pressure under the dam. For this reason, it is necessary to grout effectively foundations having horizontal stratification.

(g) *Influence of silt deposits.* The reservoir floor above a dam may sometimes become blanketed with silt. It has been claimed that silt deposits relieve the water pressure on the upstream face of the dam, but the amount of such reduction for dams on good rock foundations is small.



A silt deposit which has a tightness equal to or greater than that of the foundation will reduce the total forces acting on the dam,<sup>11</sup> because it causes a reduction in water pressure on the upstream face and the base, the effect of which is greater than the effect of the silt pressure itself.

However, in dams on tight rock foundations, the silt must be assumed to be much more permeable than the foundation, and its effect on upstream face water pressure and underpressure should be neglected.

(h) *Hydrostatic pressure within the foundation.* Hydrostatic pressures should be investigated not only at the junction of the dam and the foundation but also within the foundation itself. Stability should be investigated above any plane on which such pressures may exist. This is particularly important where the downstream toe does not abut against strong rock, or where the rock at the toe might be scoured away by overflowing water.

(i) *Pressure intensities within the dam.* Hydrostatic pressures exist within the body of the dam as well as under the foundation. It appears probable that intensities within the dam are less than for the foundation. However, it is not customary to take advantage of reduced pressure intensities within the dam, the same assumptions usually being used from top to bottom of a given section. This ordinarily involves no ineconomy, as weight in the upper portions contributes to stability at the base. (See discussion of top details, Art. 2b, Chapter 9.)

(j) *Uplift intensities in hollow dams.* For hollow dams without watertight floor slabs, spaces between the buttresses afford effective drainage above the foundation, reducing pressures at the base and in horizontal construction joints above the base to that due to tailwater. However, attention must be paid to possible horizontal seams in the foundation which may be subjected to hydrostatic pressures. Such conditions must be considered, and grouting and drainage provided where necessary. (See Art. 3 of Chapter 14.)

(k) *Observed hydrostatic-pressure intensities.* Fig. 12 shows a compilation of measured hydrostatic-pressure intensities at the base for a number of dams, platted on percentages rather than on actual distances and forces.<sup>12</sup> Pressures shown represent intensities and must be multiplied by the area factor to get net uplift forces. Note that the Oester Dam, the only one not grouted or drained, shows much greater pressures than the others. Hydrostatic-pressure observations are subject to many uncertainties. Observed pressures for the same headwater and tailwater levels may be different for rising and falling reservoir; proximity to a crack or fissure may cause a local variation; evaporation from a test well, a connecting crack in a tight area, variation in temperature, or faulty observation procedure may vitiate the results. Pressure intensity values to be used in design are discussed in Art. 5q.

(l) *Uplift areas.* The discussion thus far has related only to the *intensity* of internal hydrostatic pressures. The total uplift force involves also the *area*

<sup>11</sup> WILLIAM P. CREAGER, "Masonry Dams" [Discussion], *Trans. Am. Soc. Civil Engrs.*, Vol. 106, 1941, p. 1248.

<sup>12</sup> IVAN E. HOUX, "Uplift Pressures in Masonry Dams," *Civil Eng.*, September 1932.

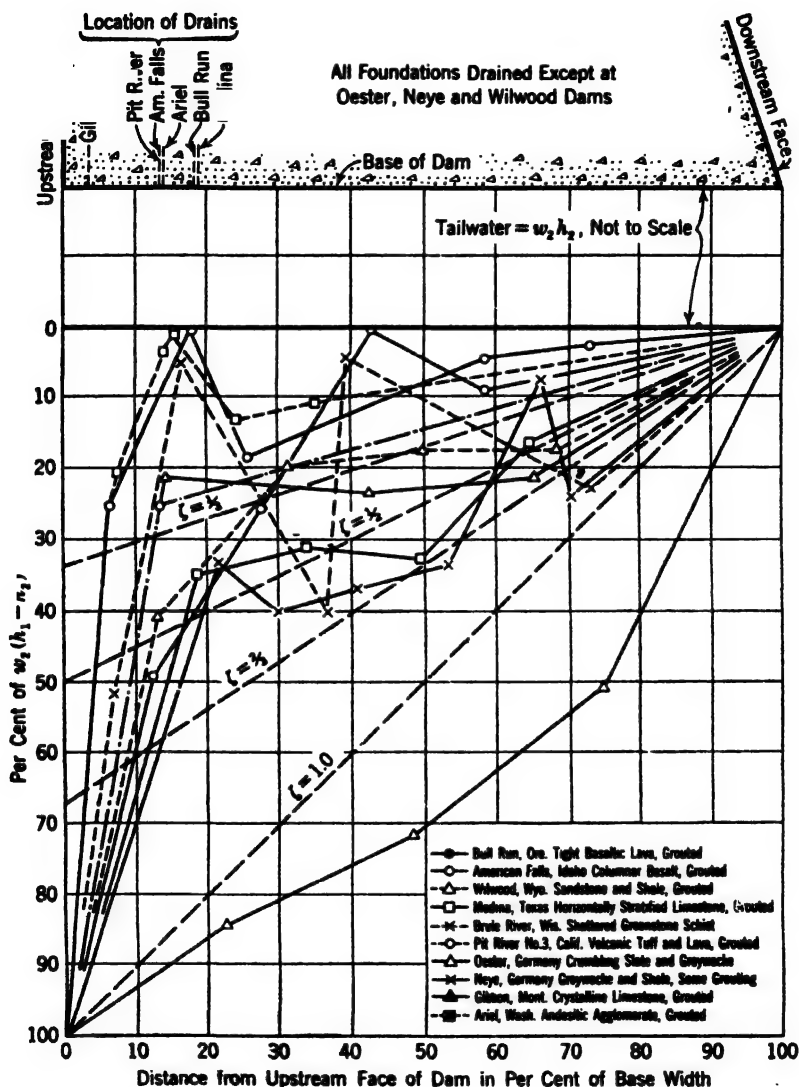


FIG. 12. Maximum observed hydrostatic pressure under existing gravity dams on rock foundations.

on which these intensities act. If the dam shown in Fig. 8 and discussed in Art. 5b is assumed to be supported clear of its base by some imaginary means, the pressures represented by 2-7-5-3 will act over the whole area and the uplift,  $W_u$ , and its line of action are readily computed. However, if it is assumed to be supported on blocks, the effective area may be reduced. Actual dams are always supported by material contacts, which leads to the conclusion that the uplift pressures may act on only a portion of the base having a ratio,  $c$ , to the total area.

Views on the value of  $c$  for rock or masonry are divergent. One theory is that actual molecular contact, capable of excluding water under pressure, must exist over a substantial portion of any joint capable of sustaining tension. Masonry and rock are looked upon as essentially solid materials permeated with small interconnected holes or pores. Barring faulty construction, uplift forces are assumed to act only within these voids. Volumetric voids, determined by the absorption of water, run from 4 per cent to 6 per cent for concrete. Ingenious mathematical devices have been developed for computing the projected area of these pores on which the uplift may act. These theories ignore the possibility of faulty foundation or construction joints.

Henny<sup>13</sup> reaches the conclusion that the value of  $c$  varies with stress in the concrete, a high compression being assumed to partially close the voids. He states that "nothing is known of effective uplift area at the base of a dam where concrete comes in contact with rock," but nevertheless he recommends average values of  $c$  ranging from 0.25 to 0.40.

Other writers have generally found theoretical uplift areas to be smaller than Henny's, but they usually recommend an allowance for uncertainties. Values of  $c$  ranging from  $\frac{1}{3}$  to  $\frac{2}{3}$  for rock foundations, depending on judgment and on the quality of the rock foundation treatment, are in use.

However, the acceptance of the pore-space theory is not universal. Levy,<sup>14</sup> one of the early advocates of an allowance for uplift, recommended that the vertical pressure at all points along the upstream face (computed without regard to uplift) exceed the hydrostatic pressure. This is equivalent to a value of unity for  $c$  and a uniform variation of hydrostatic pressure from head-water to tailwater. This criterion was accepted by some American engineers but was criticized by others as unduly severe.<sup>15</sup>

Terzaghi, as a result of tests made in Vienna,<sup>16</sup> claims to have found that the value of  $c$  for concrete is at least 0.95. Again, in 1936,<sup>17</sup> he found that for concrete and plastic clay the factor  $c$  is practically unity.

Uplift forces at the foundation joint and at horizontal construction joints within the dam depend on the perfection of bonding. (For a discussion of

<sup>13</sup> D. C. HENNY, "Stability of Straight Gravity Dams," *Trans. Am. Soc. Civil Engrs.*, Vol. 99, 1934, p. 1041.

<sup>14</sup> MAURICE LEVY, *Compt. rend. acad. sci.*, August 5, 1895.

<sup>15</sup> For summary of opinions see A. FLORIS, "Uplift Pressure in Gravity Dams," *Western Construction News*, January 25, 1928.

<sup>16</sup> K. TERZAGHI, "Stability of Straight Concrete Gravity Dams" [Discussion], *Trans. Am. Soc. Civil Engrs.*, Vol. 99, 1934, p. 1107.

<sup>17</sup> Idem, *Eng. News-Record*, June 18, 1936, p. 872.

bonding, see Art. 13, Chapter 15.) If the bonded area is incomplete or becomes so owing to shrinkage or other cause, the effective uplift area is increased.

The only conclusion that can be drawn from a study of available discussions on uplift is that the value of the area factor  $c$  for masonry and rock is uncertain. Values for use in design are discussed in Art. 5g.

(m) *Application to rock foundations.* The observed pressure diagrams shown in Fig. 12 are too complicated and variable for direct use in design. Their exact forms can be determined only approximately even for constructed dams; consequently it is permissible to resort to simplification.

Consider the conditions illustrated in Fig. 13. Without cutoff or drain the pressure-intensity diagram is represented approximately by 1-7-3-2. With the cutoff and drain, the pressure-intensity diagram would, ideally, take some such form as the curve 6-5-3. Fig. 11. Practically, it is likely to be of some more irregular form, as illustrated by the numerous curves of Fig. 12.

Considering the number of variables and unknowns involved, the pressure may be represented with all justified accuracy by the polygon 1-7-6-3-2 of Fig. 13. The triangle 4-7-6 results from the fact that in an actual dam the cutoff and grout curtain are of appreciable thickness and that the drains are some distance from the face. The line 3-6 being merely an approximation of some unknown more complicated pressure diagram, it is permissible to ignore the triangle 4-7-6. The resulting approximate pressure-intensity diagram is the trapezoid 1-4-3-2.

The total uplift force is obtained by applying this pressure-intensity diagram to that portion of the area of the base of the dam on which it is assumed to act. For a dam slice of uniform thickness, this total may be computed from the equation

$$W_u = cw_2[h_2 + \frac{1}{2}\zeta(h_1 - h_2)]A \quad [18]$$

where  $A$  is the area of the base,  $c$  is the proportion of that area on which the hydrostatic pressure acts, and  $\zeta$  is the proportion of the net head,  $(h_1 - h_2)$  remaining to be dissipated below the grout curtain. The line of application passes through the center of gravity of the trapezoid 1-4-3-2.

Uplift determined in this manner can never be exact. Closer approximation can be attained by continued experimentation and the further observations on constructed dams, but the need for careful judgment on the part of the

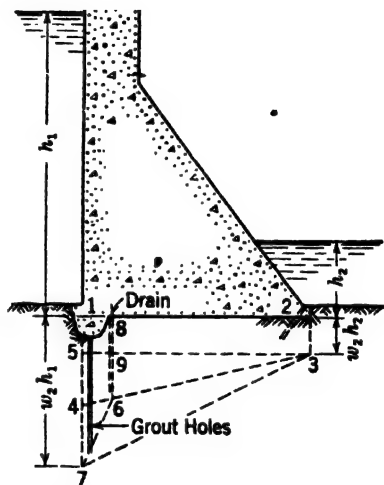


FIG. 13. Practical uplift pressure-intensity diagrams.

designer cannot be escaped. Variations in Eq. 18 for nonrectangular bases can be readily made.

(n) *Application to earth foundations.* For earth foundations, special methods are used to determine the hydrostatic pressure on the base of the dam, as discussed in Chapter 3.

(o) *Examples of uplift assumptions.* Table 1, Chapter 8, lists the uplift assumptions used on several important dams on rock foundations. Most of these dams are provided with some kind of protection against uplift, in the form of cutoffs, grout curtains, drainage systems, or other features. These dams are among the largest and most important built in this country, and failure would result in immense loss of life and property. Accordingly, it was the designers' intentions to provide an ample margin of safety, not only in the assumption of uplift but in other features.

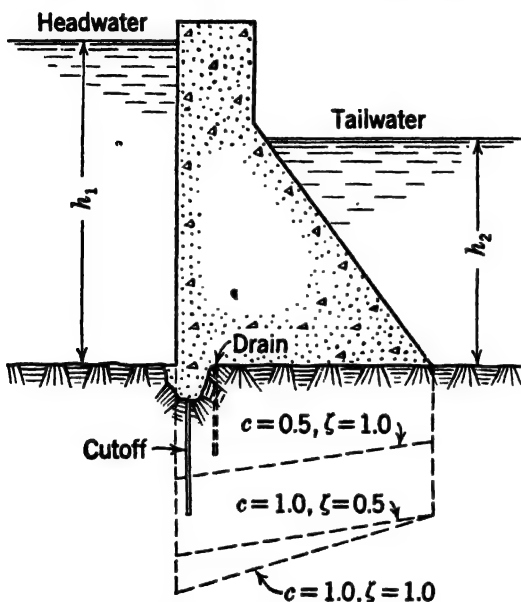


FIG. 14. Influence of  $c$  and  $\zeta$  on uplift.

and ( $c = \frac{2}{3}$ ,  $\zeta = 0.75$ ) are equivalent. When  $h_2$  is not equal to zero,  $c$  and  $\zeta$  are not interchangeable. Where the tailwater depth is great, the influence of these two factors is distinctly different, as illustrated in Fig. 14.

(q) *Values of  $\zeta$  and  $c$  for use in design.* The engineer may take into consideration the factors affecting uplift previously described; but if he departs materially from the most conservative precedents, he must be guided by mature experience, ample foundation explorations, well-directed and inspected construction work, and expert geological advice. So far as known to the authors, Eq. 18 has not heretofore been used widely. It was not used for the dams listed in Table 1 of Chapter 8, and values of  $\zeta$  are not generally available for constructed dams. Most modern designs are based on assumptions equivalent to a value of unity for  $\zeta$  and  $\frac{1}{3}$  to  $\frac{2}{3}$  for  $c$ . Considering the availability of data indicating clearly that  $\zeta$  is less than unity (Fig. 12) and the absence of any proof that  $c$  is less than unity, especially on joints where bond may be defective, this procedure seems illogical. Where there is little or no tailwater, the difference is immaterial (see Art. 5p). Consider, however, the conditions

at Parker Dam<sup>18</sup> with a maximum headwater depth of 310 ft and tailwater depth of about 260 ft. Referring to Fig. 14, there is obviously a great deal of difference between the uplift computed for  $c = 1.0$ ,  $\zeta = 0.5$ , and that for  $c = 0.5$ ,  $\zeta = 1.0$ . The latter pair of values would show only half flotation on a dam or a bridge pier completely immersed, which the authors believe to be unsound.

The fact that dams designed on the assumptions of uplift in current use have stood successfully is not positive proof that such assumptions are correct. Fortunately there is present in most rock foundations and even in poorly constructed horizontal joints in the dam a considerable amount of shearing and tensile strength which frequently is neglected in the design. This neglected strength adds materially to the stability of the dam and may be sufficient to counterbalance deficient uplift assumptions.

However, the total shearing and the total tensile strength vary as the first power of the height of the dam, whereas uplift varies as the square of the height.<sup>19</sup> Consequently, the authors desire to caution against the use of uplift assumptions which are not the most conservative, for dams greater in height than those for which such assumptions previously have been used.

The following values of uplift constants seem logical but are to be used with judgment and are subject to the aforementioned cautionary remarks:

For all conditions,  $c = 1.0$ .

For earth foundations,  $\zeta$  should be determined by a flow net<sup>1</sup> or special analysis as described in Chapter 3.

For rock foundations:

Height <sup>2</sup> of Dam	Type of Rock Foundation	Grouting <sup>3</sup> and Drainage	$\zeta$
Moderate	Horizontally stratified	None	1.00
Do.	Fair, horizontally stratified	Yes	0.67
High	do.	do.	0.75
Moderate	Good, horizontally stratified	do.	0.50
High	do.	do.	0.67
Moderate	Fair, massive	None	0.67
Do.	do.	Yes	0.50
High	do.	do.	0.67
Moderate	Good, massive	None	0.50
Do.	do.	Yes	0.50 <sup>4</sup>
High	do.	do.	0.50

<sup>1</sup> See footnote 10, Art. 5c.

<sup>2</sup> "Moderate" represents dams up to about 200 ft. "High" represents dams above about 200 ft.

<sup>3</sup> Assumed to be first-class.

<sup>4</sup> A minimum limit.

<sup>18</sup> This dam is an arch, but an alternative gravity section was included in preliminary studies.

<sup>19</sup> See discussion by CREAGER in *Trans. Am. Soc. Civil Engrs.*, Vol. 95, 1931, p. 197, and *Trans. Am. Soc. Civil Engrs.*, Vol. 99, 1934, p. 1086.

**6. Ice Pressure.** In common with other materials, ice expands and contracts with changes in temperature. In a reservoir completely frozen over, a decided drop in the temperature of the air may cause the opening up of cracks which subsequently fill with water and freeze solid. When the next rise in temperature occurs, the ice expands, and if restrained it exerts pressure on the dam. Little is known of the magnitude of this pressure, and allowances made in the past have been variable.

The thrust, of course, is limited to the crushing strength of ice, which is variously reported between 100 and 1000 lb per sq in. for quickly applied load. The latter value corresponds to the enormous amount of 144,000 lb per sq ft and, where ice attains a thickness of 4 ft, amounts to an absurd value of more than 500,000 lb per lin ft of dam.

That ice thrust under usual conditions can never approach such a value, is proved by the fact that a great many dams are standing today which otherwise would certainly have failed.

Experiments made at McGill University <sup>20</sup> in 1932 showed that ice expands with rise of temperature, and being plastic, it flows under sustained pressure. Consequently, the yield strength is far below the quick-crushing strength. The rate of rise of temperature and its probable duration are therefore important factors in determining the pressure exerted on a dam.

No general rule can be laid down for all conditions, but the paper referred to contains a curve showing the relation between the increase of pressure in pounds per square foot per hour and the hourly rate of increase of temperature of an experimental block of ice. This curve is reproduced, with permission of its authors, as Fig. 15. From this curve and other essential considerations, an estimate can be made of the probable pressure under given conditions.

Unfortunately, little is known about the rates of temperature rise in natural ice sheets. Fig. 15 was derived from tests on 3-in. cubes, so controlled that the ice temperature followed closely the air temperature. Data are lacking on the relation between rate of change of air temperature and reservoir ice temperature. It seems reasonable to expect that with a rapid change in air temperature, the ice temperature will lag, particularly for a thick covering. Also, because the bottom of the ice sheet is always in contact with water, it is unlikely that the average temperature of the ice reaches the lowest air temperature even for long exposure.

Usually, some idea of rates of change in air temperatures can be obtained from weather records.

A conservative design will probably result if the ice temperature is assumed to follow the average air temperature over a period of 12 to 24 hr. Actual variations in ice temperatures at the dam site may be observed, if time and facilities are available.

To illustrate the use of Fig. 15, suppose it is found that the ice temperature at a given dam site may rise from  $-20^{\circ}\text{F}$  to  $+32^{\circ}\text{F}$ , a total of  $52^{\circ}\text{F}$  in

<sup>20</sup> ERNEST BROWN and GEORGE C. CLARKE, "Ice Thrust in Connection with Hydroelectric Plant Design," *Eng. J.*, January 1932.

16 hr, or an average of  $3.25^{\circ}\text{F}$  per hr. From Fig. 15 a rate of rise of  $3.25^{\circ}\text{F}$  per hr corresponds to a pressure increase of 200 lb per sq ft per hr which, for a total period of 16 hr, results in a total ice pressure of  $16 \times 200 = 3200$  lb per sq ft.

If the rate of rise is increased for the same total rise, the pressure is increased. Also, a greater rise in the same time, or even a longer time, or a smaller rise in a very short time, may produce a greater total pressure. Thus it is necessary to investigate all possible combinations of total rise and time of rise to get the maximum possible ice pressure.

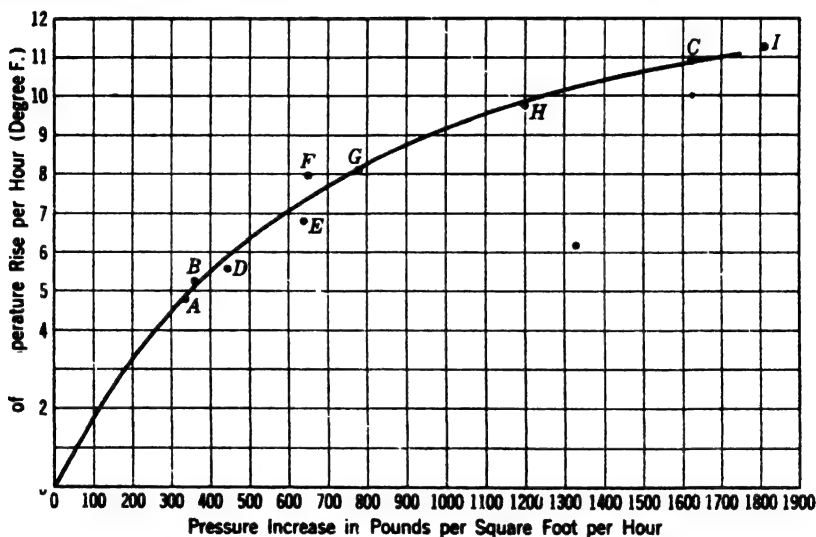


FIG. 15. Relation between temperature and pressure rise for ice.

The investigation above referred to was made primarily in connection with a power development in northern Saskatchewan, on the Churchill River, where the lowest temperature during construction was  $-50^{\circ}\text{F}$ , and an ice cover of 3 to 4 ft was expected. In the light of the tests, an ice pressure of 10,000 lb per lin ft of dam was adopted for this design. Earlier tests by Professor Brown<sup>21</sup> on the properties of ice have been published. As a result of these investigations, pressures of 3000 to 5000 lb per sq ft of expected ice thickness have been adopted generally in this country. Such pressures, and pressures computed on the foregoing basis, are smaller than values used in many existing dams. Ice pressures ranging from practically zero to 47,000 lb per lin ft have been used for dams in the vicinity of New York, where the maximum ice thickness is about 2 ft.<sup>22</sup>

<sup>21</sup> ERNEST BROWN, Report of the Joint Board of Engineers on St. Lawrence Waterways Project, Ottawa, November 1926, p. 406, Appendix E, "Ice Formation on the St. Lawrence and Other Rivers."

<sup>22</sup> HARRISON, *Trans. Am. Soc. Civil Engrs.*, Vol. 75, 1912, p. 142.



Where the dam is provided with an overflow spillway, the spillway crest is usually some distance below the maximum or design water level. The maximum water level occurs only at times of freshet, and a solidly frozen ice sheet at such time is improbable. It is usual to assume that the worst ice condition will occur only with water at the spillway lip.

Nothing is known of the action of ice during an earthquake, and its earthquake effect is ignored.

Ice floes are capable of exerting comparatively little pressure against a dam. If the velocity of the approaching water is high and the crest is not clear, the most that can be expected is a local thrust, and the ice in such cases is always soft. Possible ice thrust on the downstream side of the dam is usually neglected in the calculations.

**7. Earth and Silt Pressures.** (a) *Source.* Masonry dams are sometimes subjected to earth pressures on either the downstream or upstream face, where the foundation trench is backfilled. Such pressures usually have a minor effect on the stability of the structure, and may be ignored in design.

Practically all streams transport silt, particularly during floods, when the quantities may be enormous. Such materials are deposited in the reservoirs or slack water above the dam.

Quite often, sluices are constructed in the lower part of the dam which, if periodically flushed in the proper manner, limit the depth of such deposits adjacent to the dam. Because of this possibility, and the almost total absence of experimental data, the pressure exerted by silt on dams has been largely ignored. In fact, few examples of important dams designed for silt pressure can be cited. Few storage dams are subjected to silt pressure in appreciable amount. However, the basin above a diversion dam may be completely filled with silt. Also, some flood-control reservoirs are deliberately constructed for the retention of debris and may be filled to the top.

The determination of earth pressures involves many variable factors, such as the inclination of the ground surface, the inclination of the face of the retaining structure, the rigidity of the structure, the presence of vibratory loads, the angle of friction between wall and fill, the state of saturation or the moisture content of the fill, the manner of deposition, the age of the fill, the internal shearing strength or angle of internal friction, and perhaps other factors.

These factors are inherently subject to wide variation. Although many theories have been advanced and much experimentation done, the actual development of needed constants has lagged. Measurement of actual pressures on full-sized structures is lacking, as are also small-scale tests on water-deposited silts.

(b) *Theoretical pressure.* A widely used formula for earth pressure is that attributed to Rankine, as follows:

$$P_s = \frac{w_s h^2}{2} \left( \frac{1 - \sin \alpha}{1 + \sin \alpha} \right) \quad [19]$$

where  $w_s$  is the weight, in pounds per cubic foot, of the silt or earth, in the air or submerged, as the case may be;  $h$  is its depth; and  $\alpha$  is its angle of internal friction.

The force  $P_s$  is assumed to be located a distance,  $2h/3$  below the surface of the fill. This equation assumes a level fill, which is the usual condition for silt or water-borne detritus, and ignores the friction between the fill and the wall. Recent experiments indicate that  $\alpha$  is not changed materially by submergence; that earth pressure and water pressure exist coincidentally in a submerged fill;<sup>23</sup> and that the pressure exerted by the submerged fill, over and above water pressure, is reduced in the proportion that the weight of the fill is reduced by submergence.

Terzaghi found the Rankine formula (Eq. 19) somewhat inadequate for large retaining walls. However, it is generally considered satisfactory for computing silt pressures on dams.

Where silt pressures are considered at all, it is usual to assume that  $P_s$  acts horizontally. If the face against which the silt acts is inclined, as illustrated in Fig. 16, the submerged weight of the material within the area 1-2-3-5 may be included in the vertical forces acting on the dam.

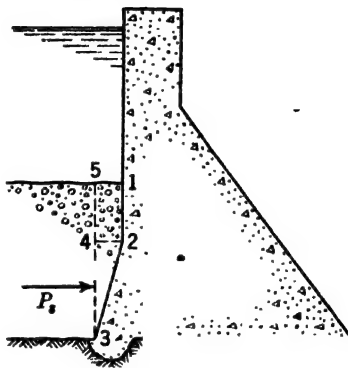


FIG. 16. Silt loads on a dam.

(c) *Computation of submerged weight.* If  $w'_s$  is the dry weight of the earth in a cubic foot of fill, and  $k$  is the percentage of voids, then in 1 cu ft of the fill there will be  $(1 - k)$  cu ft of solids, weighing  $w'_s$  lb. The weight of water displaced when this cubic foot of fill is submerged will be  $w_2(1 - k)$  lb. Therefore, the weight,  $w_s$ , of the submerged fill will be

$$w_s = w'_s - w_2(1 - k) \quad [20]$$

If the specific gravity of the solid particles of the fill,  $\lambda$ , rather than the percentage of voids, is known, the submerged weight may be expressed thus:

$$w_s = w'_s \left( \frac{\lambda - 1}{\lambda} \right) \quad [21]$$

The dry weight,  $w'_s$ , of the solid material in a cubic foot of fill, as it will be laid down in the reservoir, may be estimated from deposits of silt in neighboring reservoirs. A simple means for finding the dry density of soil in place has been

<sup>23</sup> K. TERZAGHI, "Retaining Wall Design for Fifteen-Mile Falls Dam," *Eng. News-Record*, May 17, 1934, p. 632.

developed by Proctor.<sup>24</sup> Values commonly used for the constants in Eqs. 20 and 21 are as follows:

$$w'_d = \text{dry weight} = 100 \text{ lb per cu ft}$$

$$k = \text{voids} = 40 \text{ per cent}$$

$$\lambda = \text{specific gravity} = 2.67$$

(d) *Angle of internal friction.* Experimental values for the angle of internal friction,  $\alpha$ , are scarce. Where earth or silt pressure is of primary importance in the design of a dam, a special study, including experimental work, may be required. For simple conditions, where earth or silt pressures require consideration but are not of such importance as to demand great accuracy, the value of  $\alpha$  may be taken as about  $30^\circ$  for sand and gravel, clay, or silt.

**8. Wind Pressure.** Wind pressure is seldom a factor in the design of a dam. Such structures are usually in sheltered locations. Even in exposed locations, the wind has access to only the downstream face of a loaded dam. The maximum possible pressures are small when compared to the loads for which the dam is designed, and it acts against the water load. An unloaded masonry dam is not subject to damage by wind. The superstructure of dams carrying very large sluice gates may need to be proportioned to resist wind loads of 20 to 30 lb per sq ft. Transverse wind pressure on the exposed buttresses of hollow dams may require consideration under some circumstances (see Art. 3, Chapter 14).

**9. Wave Pressures and Heights.** The upper portions of dams are subject to the impact of waves. The dimensions and force of waves depend on the extent of the water surface, the velocity of the wind, and other factors.

Knowledge of wave heights is important if overtopping by wave splash is to be avoided. Wave pressure against massive dams of appreciable height is usually of little consequence. Wave forces on sea walls and breakwaters are important, but such structures do not come within the scope of this book.

Formulas for wave heights proposed by Stevenson<sup>25</sup> have been widely used.

Molitor<sup>26</sup> proposes modifications of the Stevenson formulas to include the wind velocity, as follows:

$$h_w = 0.17\sqrt{VF} + 2.5 - \sqrt[4]{F} \quad [22]$$

where  $h_w$  is the height of the wave from trough to crest in feet,  $V$  is the wind velocity in miles per hour, and  $F$  is the "fetch" or straight length of water

<sup>24</sup> R. R. PROCTOR, "Design and Construction of Rolled Earth Dams," *Eng. News-Record*, August 31, September 7, 21, 28, 1933.

<sup>25</sup> THOMAS STEVENSON, *Design and Construction of Harbours: A Treatise on Maritime Engineering*, Ed. 2, Edinburgh, 1874.

<sup>26</sup> D. A. MOLITOR, "Wave Pressures on Sea Wall and Break Waters," *Trans. Am. Soc. Civil Engrs.*, Vol. 100, 1935, p. 984.

subject to wind action in statute miles. For  $F$  greater than 20 miles, this equation may be simplified thus:

$$h_w = 0.17\sqrt{VF} \quad [23]$$

Molitor develops empirical formulas for wave lengths, velocities, height of rise above still water level, height of rise against obstructions, force of impact, and other wave functions, suited particularly to the design of sea walls and breakwaters, having wave resistance as a primary function. Fig. 17 shows in simplified form functions applicable to the design of dams, where the water depth is relatively great and wave pressure is a minor part of the total load.

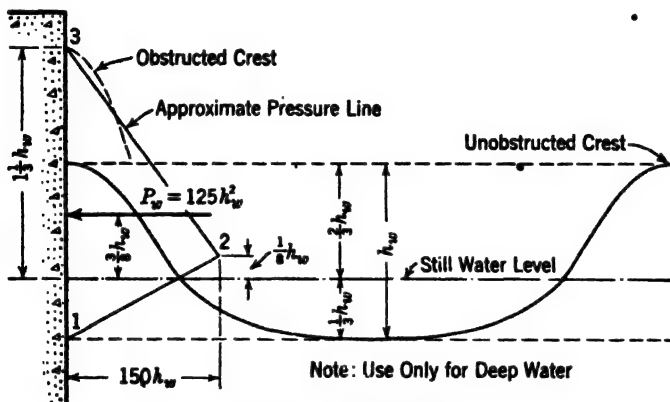


FIG. 17. Wave data.

The maximum unit pressure occurs about  $0.125h_w$  above the still water level and is approximately

$$p_w = 2.4w_2h_w = 150h_w \quad [24]$$

The wave-pressure diagram is of a curvilinear form which for present purposes may be approximately represented by the triangle 1-2-3 in Fig. 17. The area of the triangle represents the total force,

$$P_w = 2w_2h_w^2 = 125h_w^2 \quad [25]$$

The center of application is above the still water surface a height  $0.375h_w$ .

Eqs. 22 and 25 are solved diagrammatically in Fig. 18. Eq. 23 is used only to simplify numerical work where a diagram is not available.

As an example, assume a dam with vertical face, facing a 6.5-mile fetch of unobstructed water and subject to a wind velocity of 80 miles per hr. From Fig. 18,  $h_w$  is found to be 4.8 ft and  $P_w$  is 2.88 kips or 2880 lb. The center of action is  $0.375h_w$  or 1.80 ft above the still water level. The maximum unit pressure is  $150 \times 4.4 = 660$  lb per sq ft, 0.55 ft above the still water level. The vertical rise against the dam face is  $1.33 \times 4.8 = 6.4$  ft.

There is a popular belief that waves rise higher against an inclined wall, such as the face of a hollow dam, than against a vertical wall. The authors are not prepared to prove or disprove this belief. Unless the inclination is so flat as to cause the wave to break, any difference in height of rise is probably small.

For earth dams having flat slopes, it is variously assumed that the wave will ride up the slope a vertical distance above still water level equal to  $1.4h_w$  to  $1.5h_w$ , the higher value being for the smoothest slope.

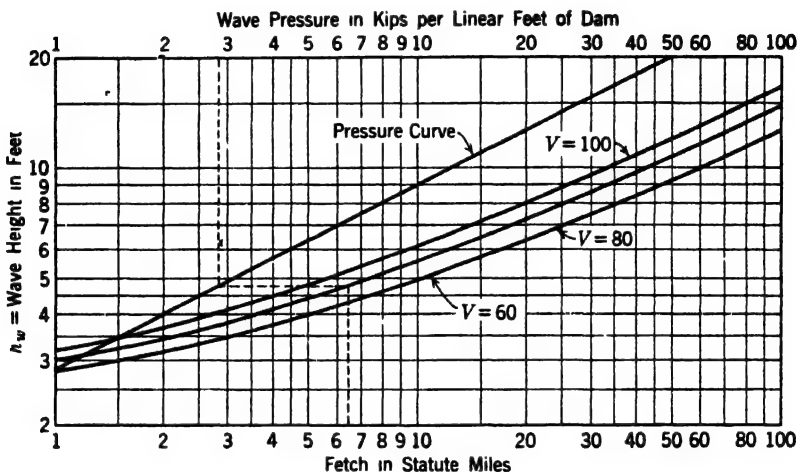


FIG. 18. Wave heights and pressures.

Eqs. 22 to 25 are purely empirical and should not be used outside the range for which they have been tested, i.e., for moderately deep water and winds of storm proportions. Eq. 22, for example, gives a wave height of 2.5 ft when the wind velocity and the fetch are zero, which is of course absurd. All equations and related functions in this article, and the functions shown on Fig. 17, should be considered as applying only to wind velocities in excess of 60 miles per hr. Even in this range the results are approximate only, but they are adequate for use in dam design where wave pressure is of secondary importance.

**10. Tides, Setup, and Seiches.** Tide movements are imperceptible in inland waters, the maximum for the Great Lakes being less than 1 in.<sup>27</sup> However, an appreciable piling up of water on one shore of a lake or reservoir may be caused by wind action, particularly in shallow water. The height of rise above the undisturbed lake level is called "setup." For deep water and small areas, this effect is small and may be considered to be included in the freeboard allowance. For wide, shallow reservoirs a special study may be

<sup>27</sup> PAUL S. WELCH, *Limnology*, McGraw-Hill Publishing Co., 1935, p. 38.

required. The Zuider Zee formula is the best available means for estimating "setup." It is as follows:

$$S = \frac{V^2 F}{1400 D} \cos A \quad [26]$$

where  $S$  = setup in feet above still pool level,  $V$  = wind velocity in miles per hour;  $F$  = fetch in miles,  $D$  = average depth of water in feet, and  $A$  = angle of wind and fetch.<sup>28</sup>

It is unfortunate that up to the present no formula has been devised that checks accurately the setups experienced at different localities. Therefore, conservatism is necessary in this respect.

Periodic undulations, called seiches, also occur. Seiches may be set in motion by intermittent wind action, variations in atmospheric pressures, earthquakes, or irregular inflow or outflow. They come and go at regular periods, which may vary from a few minutes to several hours. After the generating influence is removed, the oscillations gradually subside. In Lake Geneva, Switzerland, amplitudes in excess of 6 ft have been observed.<sup>29</sup> Amplitudes of 0.5 ft or more may readily occur in reservoirs of moderate size. These movements increase the pressure against a dam and may cause unexpected flow over a spillway. No information is available for computing their magnitude. The factor of safety used in computing freeboard should be sufficient to cover possible seiches.

**11. The Weight of the Dam.** The unit weight of concrete varies considerably, depending on the ingredients. Construction of any important concrete dam will involve a careful analysis of available concrete materials, which should be made in accordance with an adequate treatise on concrete. Such an analysis will include data on weights. It is frequently necessary to proceed with designs, at least in a preliminary manner, before a complete concrete analysis is available. The designer may then make his own determination of concrete weights, using a standard concrete text as a guide, or proceeding as follows:

1. Establish a cement-concrete ratio, expressed as pounds of cement per cubic yard of finished concrete.

2. Establish the probable water-cement ratio. This ratio is usually expressed in cubic feet of water per 94-lb bag of cement.

3. Determine the specific gravity of the aggregate and the cement. For approximate work, an average value of 2.65 may be used for the aggregate. The specific gravity of commercial portland cement is usually close to 3.10. Pozzolanic and other special cements may be appreciably lower.

4. Compute the solid volume of the aggregate in a cubic yard of concrete as follows:

$$V_a = 27 - V_c - V_m \quad [27]$$

<sup>28</sup> See also C. C. SCHRONTZ, *Hydraulics Bull.* 1, Vol. 2, February 1 1939, U. S. Waterways Experiment Station, Vicksburg, Miss.

<sup>29</sup> *Idem.*

where  $V_a$ ,  $V_c$ , and  $V_w$  are the solid volumes in cubic feet of aggregates, cement, and water, respectively, the whole being assumed free from air voids when mixed. This does not mean a void-free concrete, as some of the water eventually evaporates and is replaced by air. Values of  $V_c$  and  $V_w$  are found thus:

$$V_c = \frac{W_c}{62.5\lambda_c} \quad [28]$$

$$V_w = \frac{W_c r_{c-w}}{94} \quad [29]$$

where  $W_c$  is pounds of cement per cubic yard of concrete,  $\lambda_c$  is the specific gravity of cement,  $r_{c-w}$  is cubic feet of water per bag of cement, 62.5 is the weight in pounds of a cubic foot of water, and 94 is the weight in pounds of a bag of cement.

5. Compute the weight of a cubic yard of *saturated* concrete thus:

$$27w_1 = \lambda_a V_a + W_c + 62.5V_w \quad [30]$$

where  $w_1$  is the weight of 1 cu ft of saturated concrete,  $\lambda_a$  is the specific gravity of the aggregate, and other symbols are as above described,  $V_a$  being determined from Eq. 27.

6. To get the weight of a cubic yard of fully cured, air-dried concrete, substitute  $0.2W_c$ , the weight of the water of hydration, for  $62.5V_w$  in Eq. 29. Thus for *air-dried* concrete

$$27w_1 = \lambda_a V_a + 1.2W_c \quad [31]$$

Shrinkage of the concrete on drying out will slightly increase the weight, but this may be ignored.

7. In the interest of conservatism, it is usual to use  $w_1$ , from Eq. 31, for design purposes, although the loaded dam is likely to be partly or completely saturated.

8. In the absence of exact information, 150 lb per cu ft for the design weight of concrete will be found to conform to modern practice.

**12. The Weight of the Foundation.** Dams have sometimes been tied down to the rock foundation in order to increase their resistance to overturning, sliding, or both. Steel bars or cables are grouted into holes bored in the rock and extended into the dam near the upstream face. This practice has been criticised, on the ground that a satisfactory anchorage of the bars in the foundation is seldom possible.

As an example of such anchorage, a dam in Algeria, found to be weak, was tied to the bedrock with steel cables.<sup>30</sup> The cables were grouted into 10-in. holes, spaced about 13 ft centers. Each cable contained 630 galvanized high strength  $\frac{3}{16}$ -in. wires, laid parallel. The wires were highly prestressed and

<sup>30</sup> "Shaky Dam Tied Down with Steel Cables," *Eng. News-Record*, Feb. 20, 1936, p. 286.

anchored individually into a concrete bearing head on the top of the dam. In this manner, a stabilizing load of about 85 tons per lin ft of dam was provided.

**13. Earthquake Forces.** (a) *General statement.* In regions where earthquakes are possible or probable, dams must resist the inertia effects caused by the sudden movements of the earth's crust. If the foundation under a dam moves, the dam must move with it, if rupture is to be avoided. To produce such motion, forces must be applied to overcome the inertia of the structure. These forces are applied through the medium of stresses in the dam and its foundation. Their magnitude is primarily determined by the severity of the earthquake, the mass of the structure, its elasticity, and the earthquake effects on the water load.

The Engineering Foundation's Special Committee on Arch Dams, in 1927,<sup>31</sup> found that

The positive evidence as to the behavior of masonry dams is that they are not injured in any earthquake of the intensity of the 1906 California shock. The Crystal Springs Dam is built of concrete masonry of gravity section, but of an arch form. It is situated within a few hundred feet of an earthquake rift and must have been subjected to as severe shaking as it is possible for a structure to receive that is not situated directly over the rift. It was not damaged. In the Santa Barbara earthquake, the Gibraltar Dam, an arched structure, was so severely shaken that a watchman who was on the dam at the time had difficulty in standing up. The dam was not damaged by the shake. These are two major instances of dams passing through earthquake shocks without damage.

Notwithstanding this favorable record, it must be true that earthquake forces reduce the factor of safety, and conservatism demands their full consideration in seismically active regions. There are few if any regions where small earthquake disturbances certainly can be said to be unlikely.

Earthquake forces of course must be combined with other forces acting on the dam. Because of their short duration and infrequent occurrence, some concession in factor of safety is permissible for the condition of maximum earthquake and the most adverse combination of other conditions. For open-spillway dams, earthquake and maximum flood frequently are not assumed to occur simultaneously.

(b) *Acceleration.* The intensity of the inertia force depends on the acceleration, i.e., on the rate of change in the velocity of motion. This acceleration is usually designated by its ratio to  $g$ , the acceleration of gravity. According to Dewell,<sup>32</sup>

Accelerations ranging from  $0.0037g$  to  $g$  have been observed or estimated in earthquakes. An intensity of  $0.4g$ , or more than  $12 \text{ ft/sec}^2$ , is not uncommon in great shocks; but this, as well as the highest intensity just noted, is of such local occurrence that from the standpoint of general structural design it need not be considered.

<sup>31</sup> A. D. FLINN, *Arch Dam Investigation*, Vol. 1, *Am. Soc. Civil Engrs.*, 1927.

<sup>32</sup> See H. D. DEWELL, "Earthquake-Resistant Construction." *Eng. News-Record*, April 26, 1928, p. 650.



After discussing available records, Dewell concluded that

If historical records are to be followed, it would seem that for American conditions, in the case of buildings on firm soil, at a distance of several miles from the nearest fault plane likely to be active, the value of one-tenth gravity, or  $3.2 \text{ ft/sec}^2$ , as a design acceleration is a reasonable maximum, . . .

Fig. 19, compiled in the Pittsburgh office of the U. S. Engineers, gives a general idea of the intensity and general distribution of historic earthquakes in the

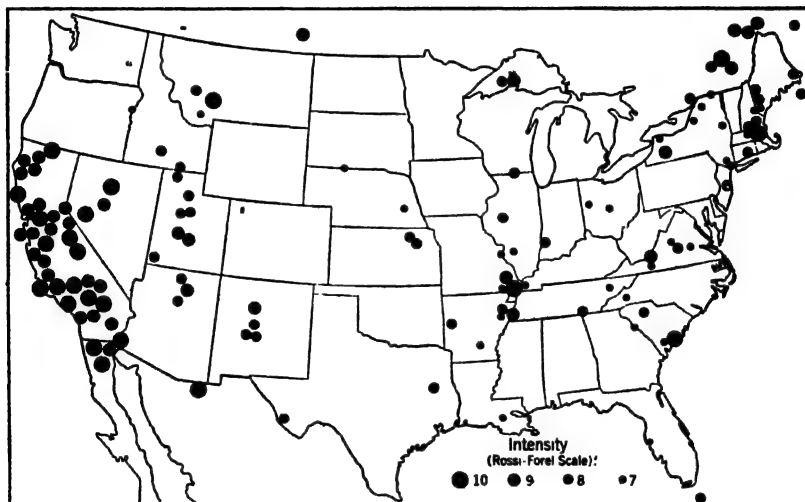


FIG. 19. Earthquake intensities in the United States.

United States. The rating on this figure is according to the Rossi-Forel scale, which has ten graduations based on observed effects on people and objects, or as has been said, on "wall-cracking and man-scaring" effects. Differences of opinion as to ratings are inevitable. Some of the earthquakes rated as 10 on Fig. 19 might be rated 9-10 by other writers.

The upper four of the Rossi-Forel ratings, the only ones involving structural damage, are described as follows:

7. *Strong shock.* Overthrow of movable objects; fall of plaster; ringing of church bells; general panic, without damage to buildings. (Max.  $\alpha = 0.02$  to  $0.04$ .)
8. *Very strong shock.* Fall of chimneys; cracks in the walls of buildings. (Max.  $\alpha = 0.05$  to  $0.10$ .)
9. *Extremely strong shock.* Partial or total destruction of some buildings. (Max.  $\alpha = 0.1$  to  $0.2$ .)
10. *Shock of extreme intensity.* Great disaster; ruins; disturbance of the strata, fissures in the ground; rock falls from mountains. (Max.  $\alpha = 0.25$  to  $0.30$ .)

There is no fixed relation between the Rossi-Forel scale and earthquake acceleration, and there is no way of extending acceleration data back to any except the most recent historical earthquakes. In fact "strong motion" seismographs are still in the development stage, and no such instrument has ever happened to be located in the destructive area of an important earthquake.

The parenthetic values of  $\alpha$  shown in the foregoing list are deduced from Freeman's interpretation<sup>23</sup> of the range of accelerations as proposed by a number of students of earthquake action. These figures indicate values estimated to have occurred over small areas of soft ground near the center of destructive activity. The acceleration range of  $0.25g$  to  $0.30g$ , shown for a scale value of 10, is higher than usually used for dams on rock foundations, even in seismically active areas, but is perhaps none too high for structures on alluvial foundations immediately adjacent to important live faults. Dams should not be built in such locations.

An acceleration of  $0.1g$  has been used in the design of a number of recent dams, as indicated in Table 1, Chapter 8. This value may be said to be tentatively standard for dams in seismically active regions. For sites close to known active faults, larger values should be adopted. In favorable locations, smaller values may be justified. The designer should carefully study local conditions, particularly the seismographical history of the region. For important structures, an investigation should be made by a competent geologist. Current earthquake data for the United States can be obtained from the Coast and Geodetic Survey, Washington, D. C.

(c) *Inertia of masonry.* The force required to accelerate a given mass, as the body of a dam, is found from the equation

$$P_e = Ma = \frac{W}{g} ag = \alpha W \quad [32]$$

where  $P_e$  is the horizontal earthquake force,  $M$  is the mass of the dam, or any portion of it under consideration,  $a$  is the earthquake acceleration,  $\alpha$  is the ratio of  $a$  to  $g$ , and  $W$  is the weight of the dam or block. Referring to Fig. 20, values of  $P_e$  may be determined separately for the blocks shown, by making  $P_{e1} = \alpha W_1$ ,  $P_{e2} = \alpha W_2$ , etc., each force acting horizontally through the center of gravity of its block. Planes 7-8, 6-9, and 10-11 represent intermediate heights at which the stability is to be figured.

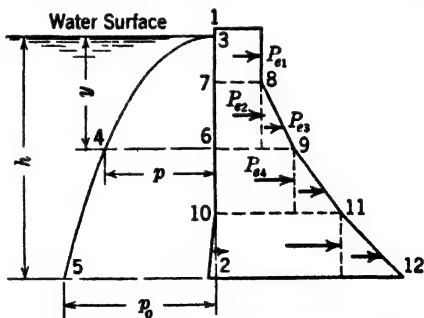


FIG. 20. Earthquake forces on a dam.

(d) *Resonance.* Eq. 32 is based on a single simple motion, with no recognition of the elasticity of the structure. Because of the yielding of the lower

<sup>23</sup> JOHN R. FREEMAN, *Earthquake Damage and Earthquake Insurance*, McGraw-Hill Book Co., 1932.

parts, the acceleration of the upper part of a tall structure, under such a simple movement, may be reduced. However, earthquake movements are reversed and repeated. Also, an elastic structure, given an impulse, tends to oscillate. Should the periods of oscillation for the structure and vibration period of the earth tremor coincide, a dangerous cumulative effect may be produced. Vibration periods for important earth shocks are generally of the order of 1 sec<sup>34</sup> or more, and the motions are inconstant in magnitude, period, and direction. Dewell's studies indicate that "long continued resonance between the structure and the earthquake wave, so feared by many writers, is not probable, but that any structure whose natural period of elastic vibration is in excess of one second, when subjected to an earthquake of major intensity, may suffer the effects of resonance for a few vibrations." Westergaard<sup>35</sup> finds the time of vibration for a concrete gravity dam of triangular section, reservoir empty, with a modulus of elasticity of 2,000,000 lb per sq in. to be

$$t_v = \frac{h^2}{2000l} \quad [33]$$

where  $t_v$  is the time of vibration in seconds,  $h$  is the height of the dam in feet, and  $l$  is the base length, in feet. For reasonable ratios of  $h$  to  $l$ ,  $t_v$  approaches 1 sec only for heights in excess of 1000 ft. The possibility of resonance for dams of usual heights need not be considered.

(e) *Increased water pressure.* The inertia of the water in the reservoir also produces a force on the dam, the determination of which is complicated. This problem was admirably treated by Westergaard in 1933.<sup>36</sup>

The increased water pressure caused by the earthquake may be represented by a diagram of the form 3-4-5-2, Fig. 20. The true equation of the curve 3-4-5 is complex, but an ellipse or parabola may be assumed without appreciable error. A parabola is simpler to use and gives values on the side of safety. The resulting equations are

$$p_e = C_e \alpha \sqrt{hy} \quad [34a]$$

$$p_0 = C_e \alpha h \quad [34b]$$

$$P_e = \frac{2}{3} C_e \alpha y \sqrt{hy} \quad [34c]$$

$$P_{e0} = \frac{2}{3} C_e \alpha h^2 \quad [34d]$$

$$P_e x = \frac{1}{15} C_e \alpha y^2 \sqrt{hy} \quad [34e]$$

$$P_{e0} x_0 = \frac{1}{15} C_e \alpha h^3 \quad [34f]$$

In these equations,  $p_e$  represents the additional unit water pressure caused by the earthquake at any depth  $y$ ;  $p_0$  the same at the base of the dam;  $P_e$  the

<sup>34</sup> *Handbuch der Physik*, Vol. 6, 1928, p. 596.

<sup>35</sup> H. M. WESTERGAARD, "Water Pressure on Dams during Earthquakes," *Trans. Am. Soc. Civil Engrs.*, Vol. 98, 1933, p. 418.

<sup>36</sup> *Idem*.

total pressure down to any depth  $y$ ;  $P_{e0}$  the same at the base of the dam;  $P_e x$  the moment to depth  $y$ , as the moment of 3-4-6, Fig. 20, about point 6;  $P_{e0} x_0$  the same for the bottom of the dam;  $\alpha$  is the ratio of the earthquake acceleration to  $g$ ;  $h$  is the total height of the dam; and  $C_e$  is a factor depending on physical conditions, principally the height of the dam,  $h$ , and the earthquake period,  $t_e$ .

Westergaard develops an approximate equation for  $C_e$  sufficiently accurate for all usual conditions, which may be written in pound-foot-second units as follows:

$$C_e = \frac{51}{\sqrt{1 - 0.72 \left( \frac{h}{1000 t_e} \right)^2}} \quad [35]$$

This equation should be used with caution for extremely high dams on very short vibration periods. Values of  $C_e$  for dams up to 500 ft in height may be taken from Fig. 21.

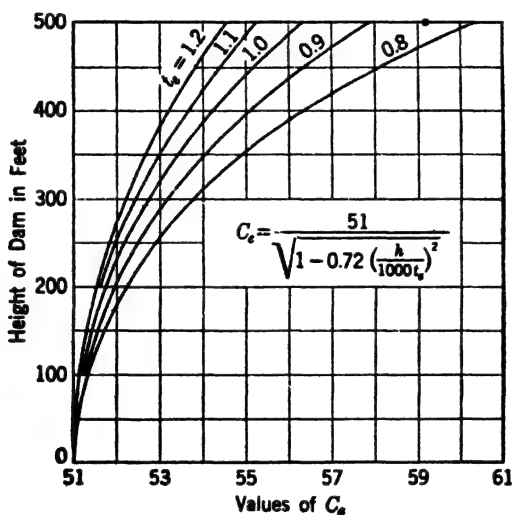


FIG. 21. Value of earthquake factor  $C_e$ .

Eqs. 34a to 34f assume the masonry face to be essentially vertical and normal to the direction of earthquake motion. This is the condition usually considered for straight gravity dams. If the water face is inclined, as in hollow dams, or curved, as in arched dams, it may be necessary to consider water pressure caused by earthquake accelerations inclined to the structural surface. Very little is known of the magnitude of such pressures.

It seems reasonable to start with the assumption that the pressure varies in some continuous manner from the full computed effect on a normal surface to

zero on a surface parallel to the earthquake motion. This condition may be met by inserting  $\cos \theta$  as a multiplier in Eqs. 34a to 34f, thus:

$$p_e = C_e \alpha \sqrt{hy} \cos \theta \quad [36a]$$

$$p_0 = C_e \alpha h \cos \theta \quad [36b]$$

$$P_e = \frac{2}{3} C_e \alpha y \sqrt{hy} \cos \theta \quad [36c]$$

$$P_{e0} = \frac{2}{3} C_e \alpha h^2 \cos \theta \quad [36d]$$

$$P_{ex} = \frac{1}{15} C_e \alpha y^2 \sqrt{hy} \cos \theta \quad [36e]$$

$$P_{e0x0} = \frac{1}{15} C_e \alpha h^3 \cos \theta \quad [36f]$$

where  $\theta$  is the angle between the direction of motion and a normal to the face at the point or on the line under consideration.

These equations also may be considered applicable to surfaces and accelerations inclined to the vertical, if  $\theta$  is taken as the smallest angle between the oblique direction of acceleration and the normal to the surface. In the case of slab and buttress dam (see Chapter 14) and a horizontal motion normal to the axis,  $\theta$  becomes equal to  $\phi''$ , the angle between the upstream face and the vertical.

This method of allowing for oblique pressures has no foundation other than the general statements made herein and should be considered tentative. It is believed to be more rational than the assumption of uniform normal pressures on curved faces.

(f) *Most unfavorable direction of earthquake movement.* An earthquake movement may take place in any direction. For a gravity dam, reservoir full, the most unfavorable direction is upstream normal to the axis. The corresponding force acts downstream. For reservoir empty, a downstream acceleration is more unfavorable. A vertical acceleration changes the weight of the masonry and the water in the same ratio. Considering these elements alone, the resultant is not displaced from the position it would occupy if there were no earthquake. However, the stresses are changed. If the acceleration is upward the stress is equal to the no-earthquake stress multiplied by  $(1 + \alpha)$ , which is generally less than the stress for an equal horizontal acceleration. If the acceleration is downward, the multiplier is  $(1 - \alpha)$ . For a direction of acceleration intermediate between horizontal and vertical, the situation is more complex. For small deviations from the horizontal, the maximum stress may be slightly greater than for a horizontal acceleration of equal value, but the difference is smaller than the uncertainties in the value of  $\alpha$ ; hence, deviation from the horizontal may be ignored for dams with straight vertical faces.

Uplift is usually assumed to be unaffected by earthquake.

For arch dams with appreciable rise, maximum stresses may be caused by cross-channel acceleration. The forces due to the inertia of the masonry are

easily deduced and act unsymmetrically (as to direction) on the two halves of the arch. The increased water pressure is assumed to act normally but with varying intensity. Because of the limited expanse of water in the direction of motion, the applicability of Eqs. 36a and 36b is subject to question, but they are probably on the side of safety and may be used in the absence of better data.

In the case of a vertical arch and upstream acceleration, the applicability of Eqs. 36a and 36b for reduction of earthquake effects near the ends is not entirely clear, particularly if the abutments and the arch form sharp re-entrant angles which prevent the lateral escape of the water. It is not uncommon in such cases to assume uniform loading, normal to all parts of the circular face, and to base computations on Eqs. 34a and 34b. This is not necessarily on the side of safety, as it is possible for a variable load to cause higher stresses than a larger constant one.

In the design of hollow dams, the most unfavorable direction of movement may be in a vertically inclined direction normal to the inclined water face. For the masonry mass, this involves no difficulty, but the effect of the water is uncertain. The usual procedure at the present time is to use a horizontal acceleration, the increased water unit load being computed from Eq. 36a. Eqs. 36c to 36f, if used, require alteration to allow for the fact that length of the area under pressure is not equal to depth below the surface. This procedure is believed conservative so far as the stability of the dam as a whole is concerned.

The load on the face slab, or arch, may be greater for an acceleration normal to the face, or inclined at some intermediate angle. Generally, it will be safe to allow any excess over pressures computed as above to be absorbed in the safety factor used in designing the face structure.

If desired, an approximate determination which will err on the side of safety, for slab or arch strength, can be made by assuming that the unit pressure caused by an inclined acceleration is the same as for a horizontal acceleration, being determined by Eqs. 34a and 36a for surfaces respectively normal and inclined to the direction of the acceleration. This involves the assumption of a considerable extent of water in the direction of acceleration. For an inclined acceleration this is not true, particularly near the top; hence actual unit pressures should be smaller than the pressures computed in this manner.

(g) *Inertia of ice and silt.* Nothing is known of the effect of earthquake movements on ice and silt pressures. It is the belief of the authors that ice pressures probably are not materially increased by earthquake movements and that any effect on silt pressures safely may be ignored.

(h) *Movements on faults.* A dam built across a fault on which slippage occurs may be subjected to an immeasurable force, and disruption can be avoided only by providing sufficient flexibility to absorb the motion without damage. Dam foundations crossed by active faults should be avoided. Fault movement is not necessarily confined to the fault on which the earthquake originates, but secondary movements may occur on any active fault in the disturbed area. It is not possible to insure that any prominent fault, although

apparently dead, may not be subjected to some movement during an earthquake; however, secondary fractures, bearing no evidence of movement in recent geologic times, involve little danger. Slight movements are not necessarily disastrous.

**14. Vertical Reaction of the Foundation.** (a) *Static requirements.* Let  $\Sigma(W)$  (Fig. 22) be the resultant<sup>37</sup> of all vertical forces acting on the dam above the foundation and  $\Sigma(P)$  the resultant of all horizontal forces. The resultant,  $R$ , of  $\Sigma(W)$  and  $\Sigma(P)$  will represent the resultant of all forces.

For the dam to be in static equilibrium, the resultant,  $R$ , must be balanced by an equal and opposite reaction of the foundation, consisting of the total vertical reaction, equal to  $\Sigma(W)$ , and the total horizontal shear or friction equal to  $\Sigma(P)$ .

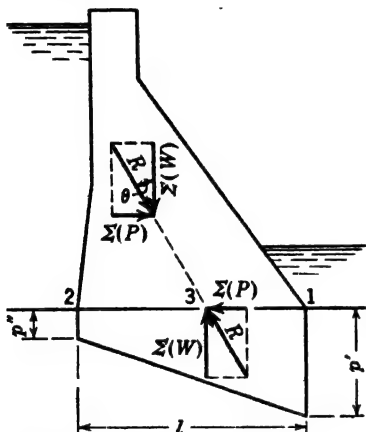


FIG. 22. Foundation reactions for gravity dam.

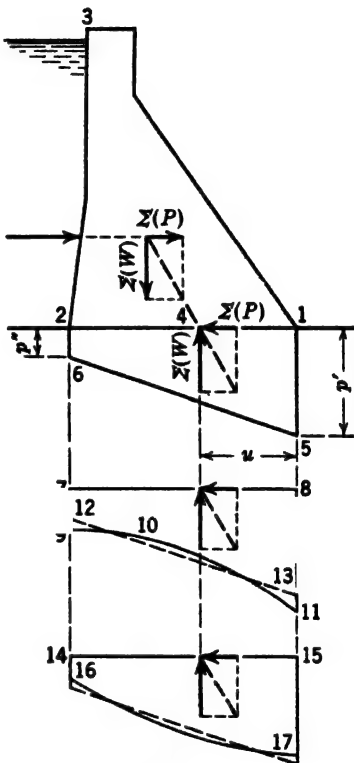


FIG. 23. Foundation pressure distribution possibilities.

(b) *Effects of elasticity.* Both masonry and foundation are elastic. The effect of such elasticity on the distribution of the foundation stresses is not exactly known. A simplified elementary idea is presented in Fig. 23. Assume 1-2-3 to be a perfectly rigid dam slice, having a uniform thickness of 1 ft, resting on an elastic foundation; and let the relation of  $\Sigma(P)$  and  $\Sigma(W)$  be such that  $R$  cuts the base, at some point, 4. If the foundation is assumed cut along the planes 1-5 and 2-6, and if the vertical reaction is considered alone, ignoring horizontal forces and all secondary effects, the unit vertical reaction

<sup>37</sup>  $\Sigma(W)$  and  $\Sigma(P)$  are here used to represent a general condition and may be applied to either full or empty reservoirs.

(by assumption) varies linearly from 1 to 2. The reaction diagram will have the form 2-6-5-1. The area of this trapezoid must equal the force  $\Sigma(W)$ , and its center of gravity must be vertically below the point 4.

If the foundation is not cut along the planes 1-5 and 2-6, the foundation deformation will spread outside of the prism between these two lines. Consequently, there will be shears across the planes 1-5 and 2-6, which will cause stress concentrations at 1 and 2. The vertical reaction diagram will be altered to some such form as 7-9-10-11-8. The area of this new diagram must equal  $\Sigma(W)$ , and its center of gravity must be vertically below the point 4.

Actually, the dam is not rigid, as assumed, but is elastic; hence, the reaction will cause it to change shape. Other things being equal, the yield is greatest where the stress is greatest; consequently, the maximum yielding will occur at the corner 1. This might be expected to result in an appreciable reduction of the ordinate 8-11 and a slight reduction of 7-9, with slight interior increases to preserve a balance, but this would displace the center of gravity of the reaction diagram. Consequently, the dam rotates until equilibrium is established. The result is a modification of the curve 9-10-11, bringing it closer to the straight line 12-13. Whether the new line will coincide with 12-13, fall a little short of it, or go slightly beyond, as indicated by 16-17, is not subject to simple determination.

The problem is complicated by the horizontal reaction,  $\Sigma(P)$ , the direct pressure of the water on the dam and foundation, internal stress relations, and other theoretical considerations. Solutions have been proposed for the relatively simple case of a homogeneous elastic dam on a similar foundation of infinite extent. Some attempts at experimentation have been made. (See Art. 14, Chapter 12.)

Practically, the foundation is never homogeneous but conforms to some condition such as that illustrated in Fig. 10. The interruption of tensile and shearing resistances at cracks and fissures may appreciably alter the result of theoretical computations and laboratory tests. Variation of the foundation texture with depth and the limitations resulting from a finite longitudinal profile of the dam introduce further complications.

The best evidence available to date indicates that a trapezoidal reaction diagram may be used without appreciable error for rock foundations, and for dam profiles of *usual form*. The words *usual form* are purposely emphasized. Consider the exaggerated condition illustrated in Fig. 24. Assuming straight line distribution of vertical pressures, the cantilever 1-2-3 is subjected to the heavy load 1-4-5-3, and tension is indicated on a vertical plane at point 1. Horizontal shear stresses on 1-3 tend to reduce or nullify this tension. Regardless of the extent of such reduction the elastic yielding of the portion 1-2-3 of the dam is relatively great, reducing the pressure on the downstream portion

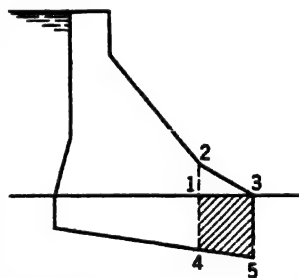


FIG. 24. Exaggerated toe detail.



of the foundation and upsetting the straight line distribution. For tension to actually exist in the masonry at point 1, it must also exist on a vertical plane in the foundation at the same point, which is difficult to conceive, or shear failure must occur along plane 1-3. A vertical shear failure is a possibility. Profiles tending toward the condition illustrated in Fig. 24 should be avoided.

(c) *Equations for distribution of vertical pressures.* Having accepted the theory of linear distribution, the unit vertical pressures at any point may be computed from simple rules of mechanics. Let 1-2 on Fig. 25 represent the

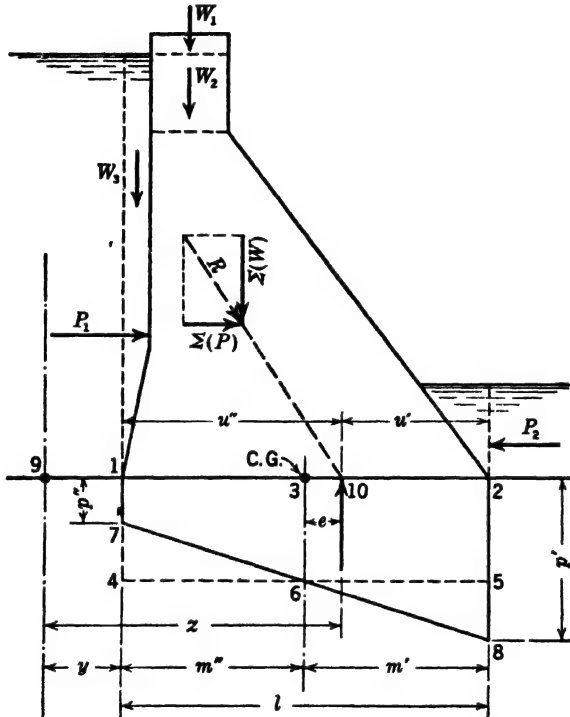


FIG. 25. Elements of foundation pressure distribution equations.

base of an elemental slice of a dam, the center of gravity of the area of the base being at point 3. The pressure on the base may be considered as a combination of direct pressure and flexural stress. These components are computed thus:

$$\text{Direct stress} = \frac{\Sigma(W)}{A} \quad [37]$$

$$\text{Flexural stress} = \frac{\Sigma(Px_0) + \Sigma(Wx_0)}{I} m \quad [38]$$

or, the alternative

$$\text{Flexural stress} = \frac{\Sigma(W)e}{I} m \quad [38a]$$

where  $A$  = area of the bases in square feet;

$\Sigma(W)$  = sum of all vertical forces, including uplift but excluding foundation reaction;

$\Sigma(Wx_0)$  = moment, about the center of gravity of the base, of all vertical forces, including uplift but excluding foundation reaction, positive if causing rotation downstream;

$\Sigma(Px_0)$  = moment of horizontal forces about the center of gravity of the base, positive if causing rotation downstream;

$x_0$  = moment arm to the center of gravity of the base;

$I$  = moment of inertia of the base about its center of gravity;

$m$  = distance from the center of gravity of the base to the point at which the pressure is desired;

$e$  = eccentricity of loading, or distance from the center of gravity of the base to the intersection of the resultant with the base.

Values of  $\Sigma(Wx_0)$  and  $\Sigma(Px_0)$  are found by taking the moments of component parts of the load,  $W_1, W_2, W_3$ , etc., including *uplift*, and  $P_1, P_2$ , etc., of Fig. 25 about the center of gravity of the base and summing. If alternate Eq. 37a is to be used, moments are taken about some arbitrary point, such as 9, and the position of the resultant and its distance from the center of gravity of the base are computed thus:

$$z = \frac{\Sigma(Px_9) + \Sigma(Wx_9)}{\Sigma(W)} \quad [39]$$

$$e = z - (y + m'') \quad [40]$$

where  $x_9$  designates a moment arm about point 9, and  $y, m''$ , and  $z$  have the significance indicated on Fig. 25.

Total vertical foundation pressures are found by combining Eqs. 37 and 38, or 37 and 38a, thus:

$$p = \frac{\Sigma(W)}{A} \pm \frac{\Sigma(Px_0) + \Sigma(Wx_0)}{I} m \quad [41]$$

or, alternative

$$p = \frac{\Sigma(W)}{A} \pm \frac{\Sigma(W)e}{I} m \quad [41a]$$

Substituting  $m'$  and  $m''$  for  $m$ , and selecting proper signs, the vertical pressures at the downstream and upstream faces are

$$p' = \frac{\Sigma(W)}{A} + \frac{\Sigma(Px_0) + \Sigma(Wx_0)}{I} m' \quad [42]$$

$$p'' = \frac{\Sigma(W)}{A} - \frac{\Sigma(Px_0) + \Sigma(Wx_0)}{I} m'' \quad [43]$$

or, the alternative,

$$p' = \frac{\Sigma(W)}{A} + \frac{\Sigma(W)e}{I} m' \quad [42a]$$

$$p'' = \frac{\Sigma(W)}{A} - \frac{\Sigma(W)e}{I} m'' \quad [43a]$$

In Fig. 25, the direct stress is represented by the rectangle 1-4-5-2, and the flexural stress by the negative triangle 7-4-6 and the positive one 6-5-8. The combined pressures are represented by the trapezoid 1-7-8-2. The lengths 2-8 and 1-7 represent, respectively, the values of  $p'$  and  $p''$ , as given by Eqs. 42 and 43.

Eqs. 37 to 43 are general and are independent of the shape of the base of the elemental slice of dam being analyzed. They apply equally to the rectangular base of a foot-thick slice of a straight gravity dam, the tapering base of a slice between radial planes of a curved dam, or the irregular base of the buttress of a hollow dam.

For a foot-thick slice from a straight gravity dam, certain simplifications are possible. For such a slice, the base is a rectangle, of 1-ft width, and length  $l$ . The center of gravity is at the midpoint, and  $m' = m'' = 0.5l$ . Also,  $I = \frac{l^3}{12}$ , and  $A = l$ . Substituting these values in Eqs. 42a and 43a gives:

For reservoir full—rectangular base

$$p' = \frac{\Sigma(W)}{l} \left( 1 + \frac{6e}{l} \right) \quad [42b]$$

$$p'' = \frac{\Sigma(W)}{l} \left( 1 - \frac{6e}{l} \right) \quad [43b]$$

For reservoir empty—rectangular base, if negative value of  $e$  is ignored

$$p' = \frac{\Sigma(W)}{l} \left( 1 - \frac{6e}{l} \right) \quad [42c]$$

$$p'' = \frac{\Sigma(W)}{l} \left( 1 + \frac{6e}{l} \right) \quad [43c]$$

(d) *Uplift and foundation reactions combined.* Where uplift exists the total upward reaction on the base of the dam is assumed to be divided into two parts, as illustrated in Fig. 26. The total reaction diagram 1-5-6-2 is divided into uplift 3-4-5-6 and net foundation reaction  $\Sigma(W)$ , 1-2-3-4. As uplift is included in  $\Sigma(W)$  and  $\Sigma(Wx)$ ,  $p'$  (Eq. 42) is represented by 2-3 and  $p''$  (Eq. 43) by 1-4. These values are designated as  $p'_r$  and  $p''_r$  in Fig. 26. Total terminal vertical unit forces may be found thus:

$$p'_v = p'_r + p'_u \quad [44]$$

$$p''_v = p''_r + p''_u \quad [45]$$

where symbols are used as in Fig. 26. Assuming that the uplift is distributed in accordance with line 4-3 of Fig. 13, as discussed in Art. 5*m*, the uplift terms may be computed thus:

$$p'_u = cw_2h_2 \quad [46]$$

and

$$p''_u = cw_2[h_2 + \frac{1}{2}(h_1 - h_2)] \quad [47]$$

If the uplift diagram is of irregular form, these values should be computed accordingly.

(e) *Requirements for stability.* It is a general rule that dams of masonry or unreinforced concrete shall be free from tensile stresses. This requires that

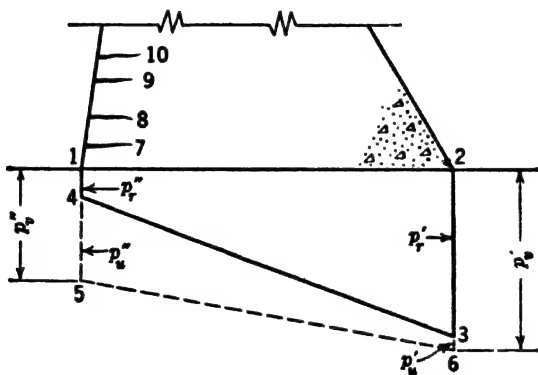


FIG. 26. Combined uplift and foundation pressures.

neither  $p'_r$  nor  $p''_r$ , Fig. 26, shall be negative. (See Art. 5, Chapter 8, for possible exceptions to this rule.)

It is also necessary to limit compressive stresses within the masonry and on the bases of high dams. These stresses are determined from the vertical pressures. It is probable that the water pressure against fully submerged rock or masonry is not injurious; hence if uplift could be depended on to always act to its full assumed extent, stresses at the corners of solid gravity dams might be computed from  $p'_r$  and  $p''_r$ . However, uplift is uncertain. It must be allowed for because it *may* exist, but its existence is never *assured*. It may require years for water under pressure to penetrate to all parts of a carefully constructed dam. The dam must be safe either with or without uplift. Consequently, stresses must always be computed on the basis of  $p'_r$  and  $p''_r$ , values of which may be determined from Eqs. 44 and 45, or they may be computed directly from Eqs. 42 and 43 by omitting uplift from the forces used in the computation.

(f) *Law of the middle third.* If the value of  $e$  in Eq. 42*b* is greater than  $l/6$ ,  $p''_r$  is negative, i.e., tension. Similarly,  $p'_r$  becomes negative for  $e$  greater than  $l/6$  in Eq. 42*c*.

If tension is not to be permitted, it follows that for a rectangular base the distance from the center of the base to the point at which the line of action of the resultant cuts the base cannot exceed one-sixth of the base length.

This leads to the well-known law of the middle third, which requires *for a dam slice having a rectangular base* the resultant for all conditions of loading shall fall within the middle third of the base.

This law is merely a means of determining that neither  $p'$  nor  $p''$  is negative, under the usual simple conditions of a solid dam with a rectangular base. If  $e$  is numerically exactly equal to one-sixth of  $l$ , either  $p'$  or  $p''$  will be zero, depending on the sign of  $e$ , and the other will be equal to twice the average pressure.

Special conditions under which tension (on inclined planes) may occur, with the resultant slightly within the middle third, are discussed in Art. 5, Chapter 8.

**15. Horizontal Foundation Reactions.** Many of the loads on the dam are horizontal or have horizontal components, which must be resisted by frictional or shearing forces along joints in the dam or the foundation. Until the last few years the general practice has been to consider sliding alone, on the theory that the bonding of construction joints is not dependable. In such case the distribution of frictional forces is not considered, but only the total force. Inasmuch as no masonry dam founded on ledge rock ever slid on its base until it had sheared through a portion of its foundation or masonry, and usually a substantial portion, it has become common practice to refer to the shear strength or shear resistance of the dam foundation. In gravity dams of moderate size, allowance for shearing strength may be made in accordance with Eq. 4 of Chapter 8.

In structures of magnitude, the actual distribution of shearing stresses and of other internal stresses may require consideration. This subject is treated in Chapter 12.

## CHAPTER 8

### REQUIREMENTS FOR STABILITY OF GRAVITY DAMS

**1. Causes of Failure.** There are two direct ways in which a gravity dam may fail:

1. By sliding (a) on a horizontal or nearly horizontal joint above the foundation, (b) on the foundation, or (c) on a horizontal or nearly horizontal seam in the foundation.

2. By overturning on a horizontal joint (a) within the dam, (b) at the base, or (c) at a plane below the base. •

The direct cause of sliding is the presence of horizontal forces greater than the combined shearing resistance of the joint or base and the static friction induced by the vertical forces.

The direct cause of pure overturning, not preceded by some other type of failure, if tension is ignored, is the presence of horizontal forces great enough in comparison with the vertical forces to cause the resultant of all forces acting on the dam above any horizontal plane, including uplift, to pass outside of the limits of the dam.

As the resultant approaches the face, the compressive stresses increase rapidly, hence overturning would be preceded and accelerated by a compression failure. In fact, a dam with the resultant well inside the joint may overturn if the toe of the dam fails by crushing or other causes so as to reduce the effective length of the joint or base sufficiently to cause the resultant to pass outside.

A dam may start to overturn but finally fail by sliding. If the resultant passes appreciably outside the middle third (or kern, if the base is of irregular form), a horizontal tension crack may occur, which reduces the shearing strength of the joint or base. Also, the admission of headwater pressure to the fissure increases the uplift, reducing the net reaction, and the frictional resistance to horizontal motion. As a result, sliding may occur.

The area of the foundation being of great extent, stability below the base is usually assured. Failures have resulted, however, from erosion of the foundation by water spilling over the crest. In this event, the dam may become undermined and eventually overturn, or the erosion may expose a horizontal seam filled with clay or other practically frictionless material, in which event, the supporting downstream ledge having been removed, the dam and that portion of the foundation above the exposed seam may slide.

The gradual disintegration of the dam by weathering and other causes will, of course, finally result in its failure. Modern masonry dams are practically indestructible if well built and composed of proper ingredients. However, if proper precautions are not observed in the choice of materials and methods of construction, rapid deterioration may occur.

**2. Location of the Resultant.** If the resultant of all forces acting on a dam above any horizontal joint, including uplift, passes outside that joint, the dam will overturn unless the joint is capable of resisting tensile stresses. The tensile strength is always disregarded as indeterminate and unreliable; hence, the resultant must intersect the joint. Also, for a conservative design, other restrictions are necessary.

It was shown in Art. 14, Chapter 7, that, when the resultant falls outside the middle third, for a rectangular base, or when either  $p'$  or  $p''$ , as determined by Eq. 41 or 42, Chapter 7, is negative, tensile stresses are set up. If the joint is incapable of resisting these tensile stresses, the elasticity of the masonry will cause a slight opening of the joint. Such an opening is particularly objectionable at the upstream side when the pond is full, as it may admit full head-water pressure over the entire area not in compression, a condition considerably more severe than usually assumed for uplift. This additional uplift would result in a movement of the resultant toward the toe of the joint, with a further opening of the joint in tension, and a further increase in uplift. The progression may be sufficient to cause failure.

Tension at the downstream face can occur only when the reservoir is empty. It is customary to prohibit such tension. The logic of this requirement is open to question as it is difficult to imagine a dam of the usual type overturning upstream before the water is let into the pond. Tension, reservoir empty, over as much as 10 per cent of the joint, does not necessarily mean a bad design. However, because specifications and codes for the design of dams usually prohibit such tension, the first designing rule may now be written thus:

#### **RULE 1, GOVERNING THE LOCATION OF THE RESULTANT:**

*Tension shall not exist in any joint of the dam, under any condition of loading. For dams with rectangular joints, this requirement is met if the resultant of all forces including uplift, acting on the dam above any horizontal joint, for full or empty reservoir, intersects the joint within the middle third. For irregular joints, neither  $p''$ , reservoir full, nor  $p'$ , reservoir empty, Eqs. 41 and 42, Chapter 7, shall be tension. (See also Rule 4.)*

**3. Resistance to Sliding.** (a) *Friction only.* The resultant,  $\Sigma(P)$ , of all the horizontal forces acting on the dam above any horizontal joint has a tendency to slide that part of the dam over the lower part. The planes of weakness are the necessary horizontal construction joints, including the joint at the base. The shearing and frictional resistance of the joint must be sufficient to withstand the tendency to slide. Until recent years, designers generally have relied wholly on frictional forces, shear resistance being considered

as adding to the factor of safety but too uncertain to be included in design computations. This procedure is still favored by many designers, particularly for gravity dams of moderate dimensions, and if properly used should produce safe and economical structures.

If  $f'$  represents the coefficient of static friction of the materials above and below the joint, then  $f'\Sigma(W)$  will be the frictional resistance to sliding.

For equilibrium, neglecting shear,  $f'\Sigma(W)$  must be equal to or greater than  $\Sigma(P)$ . This may be expressed thus:

$$f'\Sigma(W) = > \Sigma(P) \quad [1]$$

or,

$$\frac{\Sigma(P)}{\Sigma(W)} = \tan \theta = < f' \quad [2]$$

where  $\theta$  is the angle between the vertical and the resultant. This leads to

**RULE 2a, RESISTANCE TO SLIDING, SHEAR NEGLECTED:**

*The tangent of  $\theta$ , the angle between the vertical and the resultant of all forces, including uplift, acting on the dam above any horizontal plane, shall be less than the allowable coefficient of friction at that plane.*

The coefficient,  $f'$ , in carefully constructed dams on rock foundations, with particular attention paid to obtaining rough surfaces at the base and at construction joints, is usually considered to be at least twice as great as indicated by experiments on well-dressed specimens of the same materials. Therefore, if  $\tan \theta$  is made equal to or less than the coefficient of friction, as indicated by such tests, a factor of safety in this respect of at least two will be provided; and the neglect of the adhesion or shearing resistance at the joints and foundation will serve to increase further the factor of safety. Therefore, for horizontal joints and rock foundations, and neglecting shear, Eq. 2 may be modified for safe design thus:

$$\frac{\Sigma(P)}{\Sigma(W)} = \tan \theta = < f \quad [3]$$

where  $f$  is the coefficient of friction of the materials on each side of the joint or at the base, as indicated by tests on well-dressed specimens of the same materials.

Values of  $f$  for masonry on masonry and masonry on good rock foundations have been assumed variously between 0.6 and 0.75. In general, and for careful work, a value of 0.75 is not excessive. Proper allowance, however, should always be made where the rock foundation is poor, or where it contains nearly horizontal seams close to the finished surface of the foundation. Such seams are particularly dangerous if they contain clay or other unstable material. The allowance to be made will depend on the character of the seam and its contents, its inclination, and the ability of the rock above the seam to resist movement. Rock otherwise satisfactory may have to be removed in order to eliminate an objectionable seam below it.





and increase in the coefficient of friction obviously are ineffective. Eq. 3, therefore, should be rewritten for earth foundations thus:

$$\frac{\Sigma(P)}{\Sigma(W)} = \tan \theta = \frac{f}{S_f} \quad [3a]$$

where  $S_f$  is the factor of safety desired.

For masonry dams on gravel, sand, and clay, approximate values of  $f$  are 0.50, 0.40, and 0.30, respectively, but tests on the material should be made. In conservative designs the dam is usually anchored to deep cutoff walls or piles, as indicated in Chapter 3, or a factor of safety of three or more is adopted. The weight of the apron, which is an adjunct of every spillway dam on earth, will assist materially in reducing the tendency to slide.

(b) *Combined shear and friction.* The factor of safety introduced by the neglect of shear under Rule 2a is unknown and variable. Total horizontal and vertical forces vary (at least approximately) as the square of the height of the dam, while shear resistance varies as the first power of the height.<sup>1</sup> Consequently, relative safety decreases with increasing height. With increasing heights of structures and improvements in construction operations, there is a present tendency to include a definite allowance for shear. This subject was discussed in considerable detail by Henny in 1933.<sup>2</sup>

In considering horizontal joints, the force required to slide the dam, without shear, is added to the force required to shear it, without frictional resistance, and this sum is divided by the total horizontal load to get a factor of safety which must not be lower than a specified minimum. This leads to

**RULE 2b, RESISTANCE TO SLIDING, SHEAR INCLUDED:**

*The total frictional resistance to sliding on any joint, plus the ultimate shearing strength of the joint, must exceed the total horizontal force above the joint for all conditions of loading, by a safe margin.*

This relationship may be stated algebraically thus:

$$\Sigma(P) = < \frac{f\Sigma(W) + rs_aA}{S_{s-f}} \quad [4]$$

where  $s_a$  is the unit shearing strength of the material,  $S_{s-f}$  is the shear-friction factor of safety,  $A$  is the area of the joint,  $r$  is ratio of the average to the maximum shearing stress on the joint, and other symbols are as defined under Eqs. 1, 2, and 3. The friction factor is that for well-dressed specimens. The value of  $r$  may be determined from the principles explained in Chapter 12, but for practical purposes, with the relatively large factors of safety hereinafter recommended, a value of 0.5 may be assumed.

Shear strength may be determined by test if published data for the material involved are not available. It is necessary to know the shear strength of

<sup>1</sup> See discussion by CREAGER, *Trans. Am. Soc. Civil Engrs.*, Vol. 99, 1934, p. 1066.

<sup>2</sup> D. C. HENNY, "Stability of Straight Concrete Gravity Dams," *Trans. Am. Soc. Civil Engrs.*, Vol. 99, 1934, p. 1041.

both the foundation and the masonry, the smaller value being used. Houk<sup>3</sup> states that

The principal uncertainty involved in evaluating the shear-friction factor of safety is the determination of the average shearing strength of the material. Values of shearing strength [ $\tau_a$ ] used in calculating shear-friction factors of safety for dams built by the Bureau of Reclamation have varied from about 300 to 700 lb per sq in., depending upon the characteristics of concrete and rock specimens as determined by laboratory tests.

The influence of construction joints and of foundation jointing on shearing strength must be considered. Modern methods of construction insure that the shearing strength of construction joints above the base will be essentially that of the concrete. If the dam is resting on a rock surface which is essentially smooth, or if there is a possibility of a smooth plane in the foundation below the base which may be devoid of shearing strength, the value of  $s_a$  to be adopted must be zero.

The apparent factor of safety against sliding when friction alone is considered, as in Eqs. 1, 2, and 3, is usually relatively small. Low values are permissible because of the added safety due to the neglected shearing strength. In Eq. 4, the shear is included in the computations; hence the factor of safety,  $S_{s-f}$ , should approach values used in normal structural computations, say four or five.

According to Houk<sup>4</sup>

The aim of the Bureau of Reclamation has been to keep the minimum shear-friction factor of safety greater than 5 during the most severe condition of reservoir load combined with maximum horizontal and vertical earthquake accelerations. This is easily done in designing gravity dams of ordinary height but requires unusually careful planning in designing dams of unprecedented height, such as Shasta (in California) and Grand Coulee.

(c) *Alternative use of rules 2a and 2b.* As previously stated, Rule 2a was used exclusively until recently, and it is still preferred by some designers. Rule 2b is gaining in favor. Properly used, either should produce a safe design. The authors recommend that the value of  $\tan \theta$  (Rule 2a) always be computed. If the safe sliding factor is exceeded, Rule 2b should be applied and the design may be considered safe if  $S_{s-f}$  is equal to or exceeds the specified allowable value.

As a matter of precaution, it is recommended that  $S_{s-f}$  always be computed for the lower portion of very high dams, say at all joints more than 300 ft below the upstream water level. Joints within the dam as well as those at the base should be tested, also joints within the foundation if required.

Allowable friction and shear in the dam are not necessarily the same as in the foundation.

<sup>3</sup> IVAN E. HOUK, "Basic Design Assumptions, Masonry Dams," *Trans. Am. Soc. Civil Engrs.*, Vol. 106, 1941, p. 1115.

<sup>4</sup> *Idem.*

**4. Compressive Stresses.** Equations for the derivation of the vertical compressive stresses on the base and horizontal joints have been derived in Art. 14, Chapter 7. The maximum *vertical* compressive stresses are not the maximum stresses which occur in the structure. The maximum stresses occur at the ends of joints, on inclined planes, normal to the face of the dam.

Where there are no external forces acting against the faces, these maximum stresses are given by the equations

$$p'_i = p'_s \sec^2 \phi' \quad (\text{downstream face}) \quad [5]$$

and,

$$p''_i = p''_s \sec^2 \phi'' \quad (\text{upstream face}) \quad [6]$$

where  $\phi'$  is the angle between the downstream face and the vertical,  $\phi''$  the same for the upstream face. Values of the vertical pressures,  $p'_s$  and  $p''_s$ , are obtained from Eqs. 43 and 44, Chapter 7.

Eq. 5 applies only above tailwater level and Eq. 6 only to the condition of empty reservoir. Where external normal forces are involved, the corresponding inclined pressures are:

$$p'_i = p'_s \sec^2 \phi' - p'_n \tan^2 \phi' \quad [5a]$$

and,

$$p''_i = p''_s \sec^2 \phi'' - p''_n \tan^2 \phi'' \quad [6a]$$

where  $p'_n$  and  $p''_n$  are the external normal pressures at the downstream and upstream faces, respectively.

In making computations, the use of tables may be avoided by noting that  $\sec^2 \phi$  is equal to  $1 + \tan^2 \phi$ .

Inclined stresses determined in this manner may be inexact, not because of any deficiency in Eqs. 5 and 6 but because of uncertainties involved in the determination of the vertical pressures as discussed in Art. 14, Chapter 7. These uncertainties are amply offset by the safety factors commonly adopted for compressive stresses in dams.

Lack of information concerning inclined stresses led early designers to the rather general custom of considering vertical pressures only, which custom still has some following. Under this plan, the effect of inclination is allowed for by assuming different permissible stresses at the heel and toe. It is more rational to use the inclined stresses, which lead to the third stability requirement, viz.:

### RULE 3, GOVERNING COMPRESSIVE STRESSES:

*The unit inclined compressive stresses in the dam and the foundation shall not exceed certain prescribed values.*

No satisfactory tests have been made upon the strength of stone masonry under conditions similar to those actually encountered in dams. In fact, such tests would be very difficult to accomplish. Test data for the component parts, both the stone and the mortar, are readily made, but these can hardly

be assembled in a manner to reveal the strength of the whole, which depends on the combined action of the materials. In designing such dams, it is necessary to be guided by precedent and by the recommendations of authorities specially experienced in masonry construction. Baker <sup>5</sup> recommends allowable stresses "about as follows, *provided* each is the best of its class":

	Lb per sq ft
Rubble	20,000 to 30,000
Squared-stone	30,000 " 40,000
Limestone Ashlar	40,000 " 50,000
Granite Ashlar	50,000 " 60,000

Of the types listed, only rubble has been commonly used for dams, and this has now been supplanted by concrete.

The pressures actually used in a number of gravity dams are listed in Table 1 (see Art. 8).

Modern dams are constructed almost exclusively of concrete. It is not feasible, or necessary, to go into the details of concrete strength here. Any gravity dam of such magnitude that the unit pressures are of controlling importance demands a careful study of available concrete material to determine the economy and strength that may be attained, and a suitable text on concrete should be consulted. Crushing strengths up to 4000 lb per sq in. (576,000 lb per sq ft) in 28 days are obtainable, but usual limits for concrete used for gravity dams are from 2000 to 3000 lb per sq in. in 28 days.<sup>6</sup> The ultimate long-time strengths run higher, depending on the kind of cement used and other conditions. (See Art. 2, Chapter 15.) Because of its greater uniformity and dependability, concrete requires a smaller factor of safety than stone masonry. A working stress of one-sixth of the 28-day strength may be considered conservative for gravity dams. Approximately 110,000 lb including earthquake forces, and 78,000 lb excluding earthquake forces, were allowed in the Grand Coulee and Shasta Dams, as shown in Table 1. Allowable stress in buttressed dams is discussed in Chapter 14.

The strength of the foundations on which dams may be founded varies from rock which is much stronger than concrete, through all stages of decomposed and disintegrated rock, which may be very weak, poorly cemented, or lightly consolidated sedimentary rocks, down to gravel, silt, and clay deposits. Technical details of tests to determine the strength of rock and soils are beyond the scope of this book.

An entire rock foundation is never unbroken. Fractures are elements of weakness even though consolidated by grouting, the effects of which are difficult to determine. The testing of a rock foundation as a whole is impracticable, and tests on small areas are of no value. Therefore, laboratory tests on samples of the rock must be supplemented by mature judgment in con-

<sup>5</sup> IRA O. BAKER, *A Treatise on Masonry Construction*, John Wiley & Sons, 1910, p. 296.

<sup>6</sup> Standard test for low-heat cement requires a longer period than 28 days.

sidering the foundation as a whole. Permeability, solubility, and settlement also should receive attention.

The bearing strength of foundation materials is quite variable. Except for low dams on obviously strong rock and very low dams on obviously strong sand or gravel the bearing strength should be carefully investigated by field and laboratory tests. The use of building code or handbook values for foundation strength should be discouraged in important structures.

In the case of solid rock, the making of laboratory tests is simple. Suitable specimens are selected, dressed, and tested for crushing strength, modulus of elasticity, and such other qualities as may be desired. Unfortunately, no definite relationship has ever been established between the strength of laboratory samples and the strength of the foundation "en masse." It is doubtful if any constant relationship exists.

Laboratory tests are normally conducted on small unconfined specimens. Tests have shown that concrete test cylinders withstand greatly increased axial compression when subjected to circumferential pressures during test.<sup>7</sup> Similarly, the lateral pressure produced through the action of Poisson's ratio within a perfectly confined foundation material may be expected to increase ability to withstand vertical load. However, actual foundations even in "good rock" are likely to be cracked and fissured at least to a minor extent, and even minute openings may be sufficient to relieve lateral stresses caused by expansion under load. If the rock contains obviously open seams it probably can be strengthened by thorough grouting, not only at the upstream face for watertightness but also at other points of maximum stress. The efficiency of such grouting in the development of lateral restraint is not known.

Summarizing, in a foundation consisting of a single solid rock mass, free from any kind of jointing that could relieve lateral pressures caused by lateral expansion under vertical load, the bearing strength is no doubt considerably in excess of the laboratory strength and it may be permissible under favorable circumstances to permit the working stress to approach the laboratory breaking strength. However, this should be done only under the advice of experienced experts.

For a foundation of good, compact, but jointed rock, the conservative designer usually will consider that the ultimate strength of the rock "en masse" is not appreciably greater than the breaking strength of laboratory samples, and will apply a safety factor of from 4 to 7 in selecting an allowable working stress. Specimens selected for testing should be representative and should not consist entirely of either the best or the poorest materials. Allowance must be made for the fact that joint planes must necessarily be excluded from laboratory samples.

Whether the maximum pressure in the foundation is equal to the inclined pressure in the dam at the base or to the vertical pressure only is frequently the subject of debate. Undoubtedly, stress conditions change rapidly in the

<sup>7</sup> "A Study of the Failure of Concrete Under Combined Compressive Stresses," *University of Illinois Bull.* 185, 1928.

rock beneath the toe, but it seems rational and on the side of safety to assume that the maximum stress in the rock in immediate contact with the base of the dam equals the inclined toe stress in the dam. (See also Chapter 12.)

It is sometimes necessary to build masonry dams on other than rock foundations. The bearing and shearing strengths of such foundation materials are variable. Usually the dams are low, and provision against underflow (see Chapter 3) and sliding (Rules 2a and 2b, Art. 3) results in a width of base which is ample to provide bearing strength. Building codes may be used as a rough guide to bearing values in such cases. The "New York Building Code" allows the following for buildings:

	Lb per sq ft
Gravel	12,000
Coarse sand	8,000
Firm clay	4,000
Soft clay	2,000

If an important masonry structure involving large forces or any structure impounding much water is founded on other than rock, a careful investigation should be made by an expert in soil mechanics. It is not possible, at the present time, to write a simple specification for such an investigation. Foundation materials having a dry weight of less than 100 lb per cu ft should be looked on with grave suspicion. Such loose foundation materials generally should be removed.

Piling generally is undesirable for the support of dams on soft foundations and should be avoided or used with extreme care. The weight of the structure being supported on the piles, the foundation materials may remain or become soft and porous or may settle entirely away from contact with the base, with consequent danger of underflow or piping. Dams founded on piles should be provided with ample cutoffs, upstream aprons, drains, or other suitable means of controlling percolation and piping. Means for accomplishing these purposes are discussed in Chapter 3. Piling sometimes can be used to advantage under portions of a dam or under auxiliary structures where underflow is not a problem.

**5. Tension on Inclined or Vertical Planes.** Eqs. 5, 5a, 6, and 6a are applicable to either full or empty reservoir. If the location of the resultant is such that  $p'' \sec^2 \phi''$ , in Eq. 6a, is less than  $p''_n \tan^2 \phi''$ ,  $p''_i$  will be negative. Such a condition is possible but not usual. It might occur in the case of an inclined upstream face on a dam designed without uplift and where, as a consequence,  $p''_r$  approaches zero.

Tension from this cause at the downstream toe of an unloaded dam subject to tailwater pressure is not likely to be a cause for concern. Maximum and minimum stresses in the interior of the dam are also generally inclined. Under usual design assumptions the interior compressive stresses never exceed the maximum at the face. Also, usual standard computation procedures based on the assumption of linear distribution of vertical pressures do not

show tensile stresses at interior points of a simple gravity section unless tension also exists at some point on the face of the masonry. However, any unusual condition tending to develop tension at any point whatever should be avoided, which leads to

**RULE 4, GOVERNING INTERNAL TENSION:**

*The dam shall be designed and constructed in such manner as to avoid or adequately provide for tension on interior planes, inclined, vertical, or horizontal.*

The application of this rule is complicated and cannot readily be carried along in the step-by-step application of the other rules for the design of a dam. Ordinarily, it is not a determining factor in design. Hence, the normal procedure is to complete the design without regard to Rule 4 and then to test for internal tension. Rules for computing internal stresses are given in Chapter 12.

**6. Margin of Safety.** All design factors contributing to the permanent safety of a dam should be chosen with care and should be conservative. A careful estimate of the weight of the dam should not vary more than 1 or 2 per cent from the actual weight, and the weight and pressure of the water are closely known. The maximum depth of water should include liberal allowance for the highest possible flood, and waves and seiches should be provided for if required, in order that the assumed water load surely shall not be exceeded. Allowances for uplift, earthquake forces, silt, and ice pressures must be adequate. The assumed safe sliding factor, foundation strength, and concrete or masonry strength must be conservative. If all these factors are carefully chosen, the dam, if properly designed and constructed, will be safe. If the foundation is rock, there is an additional element of safety because of the adhesion of the concrete to the foundation. To this feature alone can be attributed the continued existence of a number of poorly designed dams. These considerations lead to

**RULE 5, GOVERNING THE MARGIN OF SAFETY:**

*All assumptions of forces acting on the dam shall be unquestionably on the safe side, all unit stresses adopted in design shall provide an ample margin against rupture, and the adopted safe sliding factor or shear-friction safety factor shall be conservative.*

The term "factor of safety" as used in structural design is directly applicable to hollow dams and arch dams through the stress equations, but the term is less directly applicable to gravity dams. It is sometimes said that a gravity dam, with the resultant, reservoir full, at the downstream middle third point has a factor of safety of two against overturning. This statement comes from the fact that doubling the active overturning moment in such a dam of triangular form with vertical upstream face will move the resultant out to the downstream face. Actually, failure by crushing would occur before the



resultant reached the face. On the other hand, the possibility of doubling the moment is nonexistent, hence a numerical factor of safety against overturning is meaningless. The same is true of sliding. The shear-friction safety factor and the safety factor against a compression failure have the ordinary structural significance.

The safety limits established in Chapter 7 are ample and conservative. They should never be reduced, and they need never be increased to produce a safe structure. The designer may occasionally find a more abundant conservatism desirable. No estimate can be placed on the value of human life and happiness. A dam impounding water above a populous community should be more than safe, for at least two reasons. First, the appalling loss of life that would be caused by failure justifies unusual conservatism. Second, there is a definite psychological problem involved—if those living below the dam are afraid of it, happiness and property values are affected. Public sentiment may cause the abandonment of the dam although it may, in fact, be perfectly safe. Freedom from questionable features subject to unfriendly attack is important.

**7. Details of Design and Methods of Construction.** The shape of the section of the dam having been determined in accordance with established rules, careful attention must be given to the details of the design and the methods of construction, in order that the structure may be satisfactory in every respect.

The location and extent of vertical building joints, passageways, and other planes of weakness must be within proper limits, in order that the stresses used in the design will not be seriously increased. Such features as drains and cutoffs, on which the assumption of uplift is based, must be carefully designed, and other matters of importance attended to. The masonry in the structure must be of a quality to withstand safely the working stresses adopted in the design, practically watertight, and durable. Outlet works and spillway must be designed to avoid overtopping or damage from overfalling water. Free-board must be provided to prevent overtopping by floods or waves. These considerations lead to

#### **RULE 6, GOVERNING DETAILS OF DESIGN AND METHODS OF CONSTRUCTION:**

*All details shall support and conform to the assumptions used in the design; the masonry shall be of a quality suited to the working stresses adopted, and shall be practically watertight and durable; protection against overflowing water shall be ample.*

**8. Comparison of Stresses and Assumptions, Existing Dams.** In Table 1 are given the pertinent assumptions used in the design and calculated stresses in a number of prominent dams, as well as those for the examples of design included hereinafter. References given do not include all the data contained in the table. Many data were obtained by direct contact with the designers.





The descriptive notes following and referred to in the table contain essential information required for a correct interpretation of the data. Some of these notes were required by those furnishing the data.

All stresses are calculated except those included in parentheses, which are maximum allowed stresses. Although some of the dams are curved, they have all been figured as gravity sections.

Table 17 of Chapter 10 shows the general characteristics of some of the highest concrete gravity dams.

## CHAPTER 9

### GENERAL PROCEDURE FOR THE DESIGN OF GRAVITY DAMS

**1. General Considerations.** A gravity dam must conform at all elevations to each of the rules established in Chapter 8. The relative influence of these rules on the design varies with height. Near the top all stability requirements are met if a reasonable top thickness is provided; next, compliance with Rule 1 assures compliance with all other rules; and proceeding downward the other rules come into ascendancy, in turn. The designer usually knows at least approximately which rules govern at a given elevation, and may prepare his design according to such rules, later checking for compliance with others, redesigning where found necessary.

Each of the design rules is simple and within limits may be expressed algebraically. However, because of the many variables involved and the necessity of changing from one governing rule to another at different heights, it is not practicable to write a set of equations from which all of the dimensions of a gravity dam may be directly determined. The only practicable solution is to design the dam, joint by joint, beginning at the top, making each joint conform to all rules.

This procedure results in a dam having polygonal faces which may be smoothed up for appearance with no appreciable change in stability or economy.

**2. Theoretical Cross-Sections.** (a) *Triangular sections.* If the loading on a gravity dam consists only of water pressure and triangular uplift, with no ice, tailwater, or other loads of special form, stability conditions can be satisfied down to the elevation at which pressures become excessive by a simple triangular section, with vertical upstream face and the vertex at the maximum water level. The inclination of the downstream face is given by the equation

$$\tan \phi' = \frac{w_2}{w_1 - 0.5c\zeta w_2} \quad [1]$$

where  $\phi'$  is the angle at the apex,  $w_2$  is the weight of a cubic unit of water,  $w_1$  is the weight of a cubic unit of masonry, and  $c$  and  $\zeta$  are uplift factors (Art. 5m, Chapter 7). A truly triangular section is not practical nor is it necessarily the most economical section, as will be shown subsequently.

(b) *Practical top details.* The crest of a dam must have a substantial thickness to resist the shock of floating objects, to afford a roadway, for appearance, and sometimes for other purposes. Also, some superelevation or freeboard is

usually required. Within limits, the masonry added for these purposes decreases rather than increases the total masonry volume in the dam. The influence of top width on net cross-section, for a simple case, is illustrated in Fig. 1. The increased masonry volume in the upper portion of the dam is

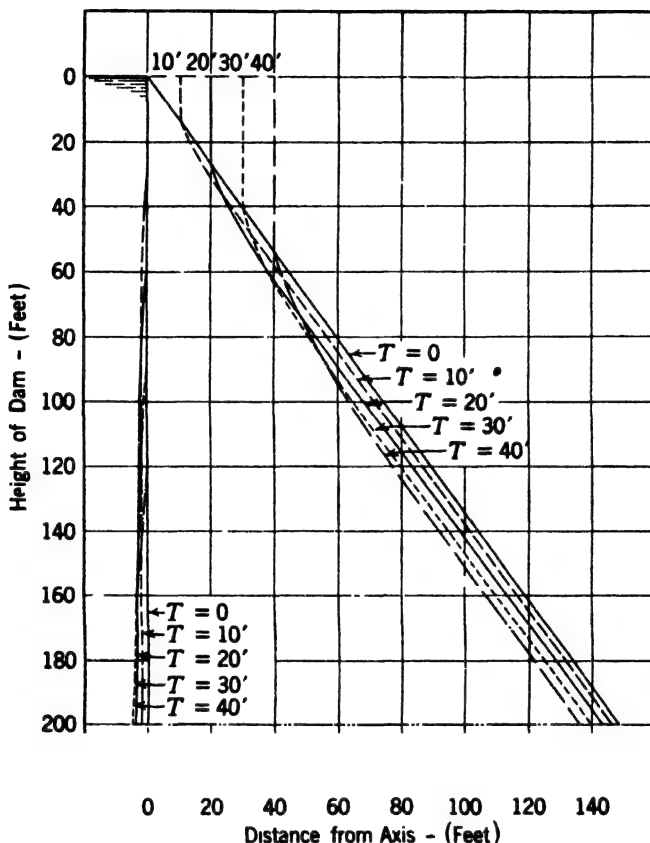


FIG. 1. Comparative effects of top width.

offset by savings at lower levels, hence the most economical top width is a function of the height. For nonoverflow gravity dams of fairly uniform moderate heights, and designed in accordance with usual assumptions but without allowance for earthquake forces, the most economical top width is about 14 per cent of the height.<sup>1</sup> For dams in "V" canyons, this figure should perhaps apply to the average height. Where earthquake forces are involved, a heavy top section is a disadvantage; however, an extremely thin top gives an incon-

<sup>1</sup> W. P. CREAGER, "The Economical Top Width of Non-Overflow Dams," *Trans Am. Soc. Civil Engrs.*, Vol. 80, 1916, p. 723.

gruous appearance. The top width of low dams is usually somewhat greater than that dictated by economy, as a roadway or passageway is often necessary, as well as sufficient width to withstand the shock of floating bodies.

Two devices commonly used for obtaining adequate top widths without material departure from the triangular section are shown in Fig. 2. The plan illustrated at (a) is applicable to low dams where the truly economic top width is too small to meet practical purposes. The plan shown at (b) is sometimes advantageously used in high dams. A notable example is Shasta.<sup>2</sup> In a very high dam it offers the advantage of a reduced toe angle,  $\phi$ , for a given masonry volume. It is not economical until stress values become critical. (See Exam-

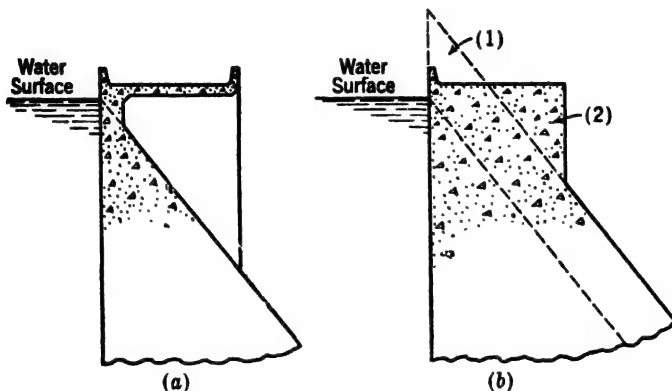


FIG. 2. Alternative top details.

ple 3, Chapter 10.) It has the incidental effect of increasing the depth to which the vertical upstream face may be carried.

A superelevation of the top above high water surface is usually desirable to get beyond the reach of waves, for appearance, and for other incidental purposes.

Although modern dams have not been provided with a freeboard exceeding 3 or 4 per cent of their height as a maximum, it is possible that a freeboard of 5 per cent or more might prove economical. If regulations require, as a precaution, that water pressure be assumed to top of dam regardless of computed maximum water levels, freeboard should not be applied extravagantly.

The crest of a dam usually serves as a passageway and must be provided with railings or parapets for safety. If the upstream parapet is a solid wall designed to resist wave forces, it may serve as a part of the freeboard.

**3. Division into Zones.** Before proceeding further, it is desirable to indicate the influence of each designing rule on the general shape of the section of the dam. In order to do this, reference is made to Figs. 3 and 4, which indicate typical sections of a solid, nonoverflow and spillway dam, respectively.

<sup>2</sup> U. S. Bur. Reclamation Spec. 780.

The section of the dam may be divided into a number of zones, as indicated, it being necessary to design each zone in accordance with a different rule or combination of rules.<sup>3</sup>

#### 4. Description of Zones, Nonoverflow Dams, Rectangular Bases. (a)

**Zone I.** Beginning at the top of the dam, Fig. 3, Zone I is that portion above the maximum water surface, or if there is ice, above the bottom of the ice sheet. When ice pressure occurs, the quantity of masonry in Zone I is fixed

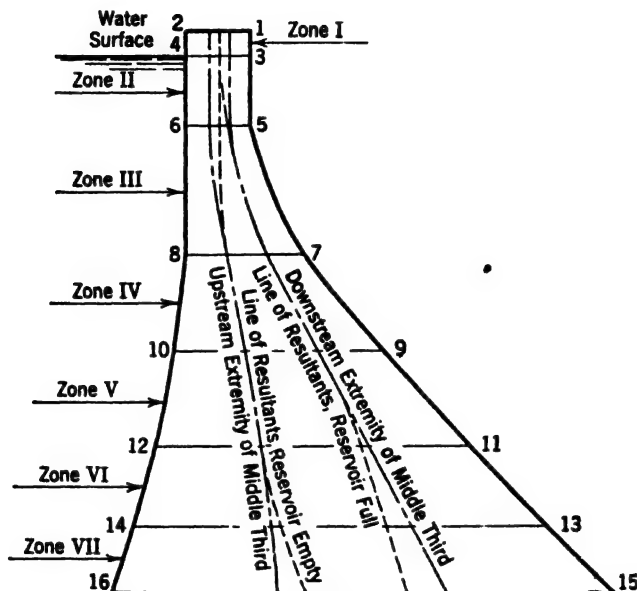


FIG. 3. Zoning for nonoverflow gravity dams.

by Rule 2a or 2b, as sufficient weight or strength must be provided to prevent the portion 1-2-3-4 from sliding. If there is no ice, the height of Zone I is controlled by freeboard requirements and the width is determined by practical consideration or economy for the section as a whole.

(b) **Zone II.** For a limited distance below the bottom of Zone I, the resultants, reservoir full and empty, lie well within the middle third (or kern), as the width of the top is always greater than necessary to conform to Rule 1. Both upstream and downstream faces, therefore, may remain vertical until, at some plane, 5-6, the resultant, reservoir full, intersects the joint at the exact extremity of the middle third. That portion of the dam between the bottom of Zone I and the plane 5-6 constitutes Zone II.

(c) **Zone III.** Below the bottom of Zone II, the downstream face must begin to batter to conform to Rule 1, reservoir full. The resultant, reservoir

<sup>3</sup> As far as the authors are aware, Wegmann was the first to use similar divisions of the section of the dam to explain the methods of design.



empty, still being within the middle third, the upstream face may remain vertical until at some plane, 7-8, the resultant, reservoir empty, intersects at the upstream extremity of the middle third. That portion of the dam between planes 5-6 and 7-8 in which dimensions are determined by Rule 1, reservoir full, constitutes Zone III.

(d) *Zone IV.* Below the plane 7-8 the upstream face must begin to batter to conform to Rule 1, reservoir empty, and for a distance the position of each

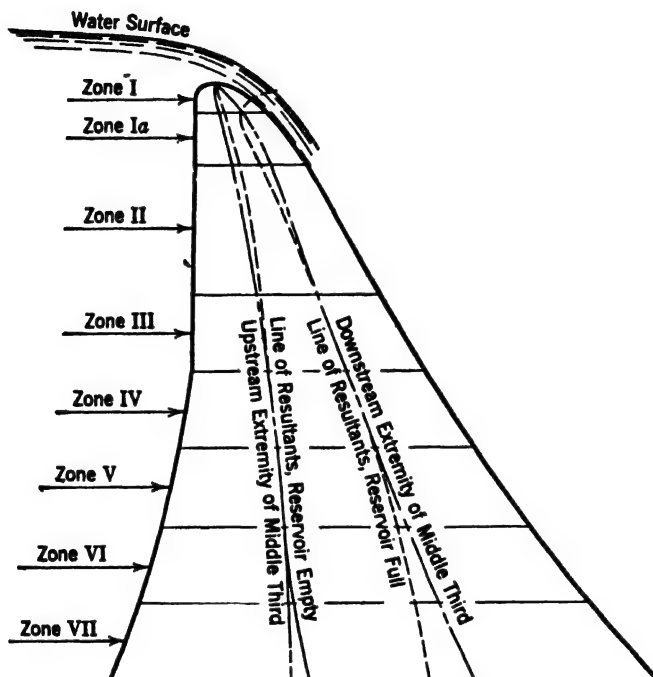


FIG. 4. Zoning for overflow gravity dams.

face is determined by the position of the resultant, reservoir full or empty as the case may be. This portion of the dam constitutes Zone IV.

(e) *Zone V.* The lower limit of Zone IV is fixed by the condition of limiting inclined pressures, Rule 3. Usually the maximum allowed unit pressure is reached at the downstream face first, and for a distance the length of the joints must be determined by Rule 3 for full reservoir and by Rule 1 for empty reservoir. This portion of the dam constitutes Zone V. In this zone the resultant, reservoir full, intersects well within the middle third and, for reservoir empty, the resultant continues to intersect at the upstream extremity of the middle third. (See Art. 4h for limitations of Zones V, VI, and VII.)

(f) *Zone VI.* The bottom of Zone V is fixed by the condition of limiting inclined pressure at the upstream face, below which level the slope of the

downstream face is determined by Rule 3, reservoir full, and the upstream face by Rule 3, reservoir empty. The portion of the dam thus controlled by these rules constitutes Zone VI. (See Art. 4*h* for limitations of Zones V, VI, and VII.)

(*g*) *Zone VII.* As the dam increases in height, the batters of both upstream and downstream faces increase. Consequently, at some elevation, the value of  $\sec^2 \phi'$  (for the downstream face, Eq. 5, Chapter 8) may become so great that conformity with Rule 3 is incompatible with the design assumptions. The portion of the dam in which this condition prevails constitutes Zone VII. It usually must be eliminated by revision of the entire design. (See Art. 4*h* for limitations of Zones V, VI, and VII.)

(*h*) *Limitations of Zones V, VI, and VII.* When division of the dam into zones was first suggested, it was usual to design for vertical pressures, the effect of face batters being recognized by prescribing a lower allowable vertical pressure at inclined faces. On this basis, Zones V and VI are subject to definite delineation. However, if inclined pressures are made the criterion, as is now recognized as more logical, these zones are complicated. Under some conditions, widening the base by a downstream extension may increase the value of  $\sec^2 \phi'$  more rapidly than it decreases  $p_v$  (see Eq. 5, Chapter 8). In such case, the whole design may need to be revised.

For very high dams, a special study looking beyond the simple stress distribution assumed in Chapter 7 may be justified. Particular attention should be given in such cases to stresses at points where face slopes change. This is discussed in Chapter 12.

**5. Description of Zones, Spillway Dams, Rectangular Bases.** It is usually impracticable to provide sufficient weight in the top few feet of an overflow dam, Fig. 4, to insure stability by simple gravity action, particularly if the horizontal loading is computed on the basis of the diagram 7-16-17-2 of Fig. 7, Chapter 7. If the true loading, 1-18-17-2 is used, the difficulty is reduced; but with an ice thrust at the crest, theoretical stability by gravity action alone is impossible, as there is little weight above the ice line. At the extreme top of the dam, the section is designed to conform to the shape of the jet of spilling water. Rule 1 must be violated and the concrete must be capable of resisting tension. The top lift of the dam should be thick enough to locate the top horizontal construction joint at an elevation where the computed tensile stress does not exceed 30 lb per sq in., or else vertical tensile reinforcement should be provided near the upstream face. The first section at which Rule 1 becomes applicable marks the bottom of Zone I.

Also, at the top of the dam, Rule 2*a* is violated and dependence must be placed on shearing resistance, Rule 2*b*. This condition may prevail to a depth greater than the bottom, Zone I, as determined by Rule 1. The portion of the dam conforming to Rule 1 but not to Rule 2*a* is designated as Zone I*a*.

Immediately below the bottom of Zone I*a*, stability requirements as dictated by Rules 1 and 2*a* are more than met by a vertical upstream face and a downstream face conforming to the required overflow shape. At some depth

the resultant for maximum load condition will fall exactly at the downstream middle third point (or  $p''$  will be zero, if base is not rectangular). The depth at which this occurs marks the bottom of Zone II, which corresponds to Zone II for nonoverflow dam, except that the predetermined slope of the downstream face is inclined rather than vertical.

The conditions fixing the limits of Zones III to VII, inclusive, for spillway dams are exactly as previously described for nonoverflow sections.

**6. Zones for Irregular Bases and Hollow Dams.** The arrangement of zones indicated in Figs. 3 and 4 represents the conditions met in the design of solid gravity dams, straight in plan. In a curved gravity dam, the arrangement is identical except that, sections being trapezoidal, the law of the middle third no longer applies, the limiting position of the resultant being such that  $p'$  or  $p''$  shall equal zero. The arrangement for the buttresses of hollow dams may be quite different, particularly if reinforcement is provided against tensile stresses, but the principles involved are the same.

**7. Expansion of Fundamental Equations.** Fundamental forms of the equations required in the design of gravity dams are derived in Chapters 7 and 8. It is possible to expand these equations into forms for the solution of particular problems by inserting forces and dimensions for such general terms as  $\Sigma(W)$ ,  $\Sigma(P)$ ,  $\Sigma(Wx)$ , and  $\Sigma(Px)$ . Theoretically, such expanded equations may be solved directly for the dimensions of each new joint in the dam. The equations are usually of the second or third degree, sometimes higher, and frequently require simultaneous solution. In all except the simplest cases, it is preferable to assume trial dimensions for each new joint and compute forces and moments by a tabular procedure to be illustrated in Chapters 10 and 11. This is particularly true if the base of the dam is not rectangular.

## CHAPTER 10

### THE DESIGN OF SOLID NONOVERFLOW GRAVITY DAMS

**1. Introduction.** The practical application of the principles developed in preceding chapters will be explained by examples. A moderately low non-overflow gravity dam, straight in plan and subject to water load only will be first considered, followed by examples of higher structures and more complicated loadings. Only nonoverflow dams are considered in this chapter.

#### EXAMPLE 1. 200-FOOT NONOVERFLOW DAM

**2. Data, Example 1.** Let it be required to design a cross-section for a non-overflow gravity dam 200 ft in height, conforming to all the rules of Chapter 8 and to the following specifications and conditions:

- $H$  = maximum depth of water to be retained = 200 ft,
- $h_2$  = depth of tailwater = 0,
- $L$  = top width = 24 ft,
- $h_c$  = spillway crest to maximum water surface = 10 ft,
- $w_1$  = weight of masonry = 150 lb per cu ft,
- $w_2$  = weight of water = 62.5 lb per cu ft,
- $c$  = uplift area factor = 1.0,
- $\zeta$  = uplift intensity factor = 0.5,
- $P_i$  = ice pressure, compute for ice 3.0 ft thick at top at spillway level, temperature rise 48° F in 12 hr,
- $V$  = wind velocity = 80 miles per hr,
- $F$  = fetch = 4.00 miles,
- $f$  = allowable coefficient of friction for joints and base, also value of  $k$  in shear-friction equation = 0.75,
- $s_a$  = ultimate shear resistance of the foundation = 800 lb per sq in. (use same for horizontal joints in dam),
- $S_{s-f}$  = minimum permissible shear-friction safety factor = 5.0 (investigation for shear required only when  $\tan \theta$  is greater than  $f = 0.75$ ),
- $p_i$  = maximum allowable inclined stress in dam or foundation = 60,000 lb per sq ft.

**3. Computation of Constants.** (a) *Freeboard.* The wave height corresponding to the specified wind velocity of 80 miles per hr, and the assumed reach of 4 miles, is found from Eq. 22 or from Fig. 18, Chapter 7, to be 4.1 ft

The theoretical rise above the still water level is  $1\frac{1}{3}h_w$  (see Fig. 17, Chapter 7); hence the required freeboard is approximately 5.5 ft or, say, 6.0 ft.

(b) *Wave pressure.* The wave pressure against the dam, from Eq. 25 or Fig. 18, Chapter 7, is 2100 lb per ft of dam. The center of action is  $0.375 \times 4.1 = 1.54$  ft above the still water level or, say, 1.5 ft.

(c) *Ice pressure.* The average rate of temperature rise is 48 divided by 12 =  $4^\circ$  per hr. The corresponding pressure rise per hr, from Fig. 15, Chapter 7, is 250 lb per sq ft, or a total of  $250 \times 12 \times 3 = 9000$  lb per lin ft of dam.

4. *Top Details.* The top width is specified at 24 ft, which with a little freeboard masonry will give a satisfactory section. The necessary freeboard was found in Art. 3a to be 6 ft. This will be assumed to consist of a 4-ft parapet wall and a 2-ft extension of the dam section above high water.

5. *Zone I, Example 1.* For the condition of water at flood level, Zone I consists of the masonry above Section 1-2, Fig. 1. It resists only wave action

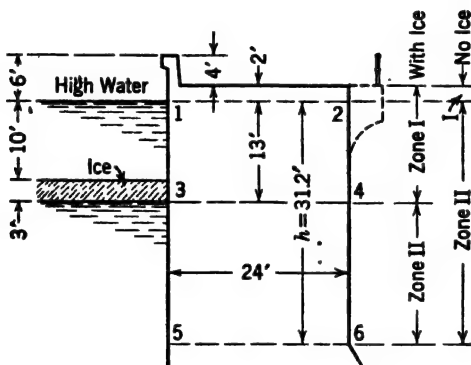


FIG. 1. Zones I and II, Example 1.

and requires no design computation. For the condition of ice at the spillway level, Zone I may conveniently be assumed at the bottom of the ice sheet, Section 3-4. Stability against sliding on 3-4, Rule 2a or 2b, is tested by Eq. 3, Chapter 8, thus:

$$\begin{aligned}
 W_1 &= \text{weight of masonry} = 24 \times 15 \times 150 = 54,000 \text{ lb,} \\
 W_u &= \text{uplift} = 0.25 \times 24 \times 3 \times 62.5 = -1125 \text{ lb,} \\
 \Sigma(W) &= 52,875 \text{ lb,} \\
 P_i &= \text{ice pressure (Art. 3e)} = 9000 \text{ lb,} \\
 \Sigma(P) &= 9000 \text{ lb,} \\
 \tan \theta &= \frac{9000}{54,000} = 0.167.
 \end{aligned}$$

$\tan \theta$  is far below the required value,  $f$ , hence shearing strength need not be investigated. The weight of the parapet wall and of any coping or ornamental work is neglected. The condition of high water and no ice is less severe.

**6. Zone II, Example 1.** (a) *Without ice.* For a straight gravity dam, a moment equation may be written about the downstream middle third involving known dimensions and forces and the unknown distance from high water to the bottom of Zone II. The elements of such an equation for the present example are shown in Table 1. The moments are assembled and equated thus:

$$10.42h^3 - 9300h = 26,700$$

Solving by trial,  $h$ , the depth to the bottom of Zone II, is found to be 31.2 ft.

TABLE 1  
DATA FOR ZONE II, EXAMPLE 1

Line	Item	Description and dimensions	Forces (lb)		Lever (ft)	Moment (ft-lb)
			Horiz.	Vert.		
1	$W_0$	Zone I, $24 \times 2 \times 150$		7,200	$\frac{1}{6} \times 24$	28,800
2	$W_1$	Zone II, $24 \times 150h$		$3,600h$	"	$14,400h$
3	$W_u$	Uplift, $0.25 \times 24 \times 62.5h$		$-375h$	$\frac{1}{3} \times 24$	$-3,000h$
4	$P$	Water, $0.5 \times 62.5h^2$	$31.25h^2$		$\frac{1}{3}h$	$-10.42h^3$
5	$P_w$	Waves (Art. 3b)	2,100		1.0	$-2,100$
6		Waves (Art. 3b)			$h$	$-2,100h$

Inserting this value of  $h$  in Table 1 and summing horizontal and vertical forces, the inclination of the resultant is found to be

$$\tan \theta = \frac{32,520}{107,820} = 0.301$$

which is far below the allowable. Also, with the resultant exactly at the third point,  $e$ , in Eq. 42b, Chapter 7, is  $\frac{1}{6}l$ , and with  $p'_u = 0$ , the maximum vertical pressure is

$$p'_v = 2 \frac{\Sigma(W)}{l} = \frac{2 \times 107,820}{24} = 8990 \text{ lb per sq ft}$$

which is small.

It is evident from inspection that the resultant, reservoir empty, is at the center of the block.

(b) *With ice.* The computation must be checked for the condition of ice at the spillway level. The required computations are shown in Table 1-A, which is similar to Table 1. Actual values of  $h$  are used and  $P$ , is substituted for  $P_w$  in line 5. Also, moments are computed to the center of the section

TABLE 1-A  
ZONE II, WITH ICE, EXAMPLE 1

Line	Item	Description and dimensions	Forces (lb)		Lever (ft)	Moment (ft-lb)
			Horiz.	Vert.		
1	$W_0$	Zone I, $24 \times 2 \times 150$		7,200	0	0
2	$W_1$	Zone II, $24 \times 31.2 \times 150$		112,320	0	0
3	$W_u$	Uplift, $0.25 \times 62.5 \times 24 \times 21.2$		-7,950	-4	31,800
4	$P$	Water = $0.5 \times 62.5 \times 21.2^2$	14,045		7.07	99,298
5	$P_i$	Ice	9,000		19.7	177,300
6	Total		23,045	111,570	(2.76)	308,398

$\tan \theta = 0.206$ .

instead of the downstream third point. Moments and forces are totaled in line 6. The lever arm of 2.76 ft, shown in parentheses, is obtained by dividing the total moment by the total vertical force. The resultant is 2.76 ft from the center of the section and hence is within the middle third.  $\tan \theta$  is 0.206. Therefore, ice at spillway level is less severe than water and waves at the flood level, and the depth of 31.2 ft is correct.

**7. Zone III, Example 1.** Below the 31.2-ft depth, the downstream face must be battered to keep the resultant, reservoir full, within the middle third, Rule 1, Chapter 8. The usual procedure is to choose increments of depth and compute the corresponding horizontal joint lengths. There is no fixed rule as to depth of increment. Increments approximately equal to 15 per cent of depth below the top of the dam, with a minimum of 10 ft, will be used in this example.<sup>1</sup> The depth of the first block will be made 8.8 ft to bring the joint to an even depth of 40 ft below the high water level.

Two methods of solving for the unknown joint length are available. One is an analytical solution in which an equation is produced that may be solved for the unknown dimension. In the other, a trial joint length is assumed and the resulting section is tested for position of the resultant. Successive trials are made until the resultant, reservoir full, falls at the middle third. Both methods will be illustrated.

**8. Block 1, Zone III, Analytical Solution.** The first block in Zone III is of the form shown in Fig. 2, all dimensions except  $\Delta l$ , or  $l$ , being known. Moments may be taken about point 1. The force  $W_0$ , the weight of the masonry above the top of the block, and the position of its concentrated resultant are

<sup>1</sup> Greater increments are permissible. See Arts. 18 and 19.

known from previous computations. This force is entered in the first line of Table 2 and its moment computed as shown. The weight and moment of the

TABLE 2  
BLOCK 1, ZONE III, BY EQUATION, EXAMPLE 1

Line	Item	Description and dimensions	Forces (lb)		Lever (ft)	Moment (ft-lb)
			Horiz.	Vert.		
1	$W_0$	Zones I and II, $33.2 \times 24 \times 150$		119,520	12	1,434,240
2	$W_1$	$24 \times 8.8 \times 150$		31,680	12	380,160
3	$W_2$	$0.5 \times 8.8 \times 150\Delta l$		$660\Delta l$	24	$15,840\Delta l$
4	$W_2$	$0.5 \times 8.8 \times 150\Delta l$			$\frac{1}{3}\Delta l$	$220\Delta l^2$
5	$W_u$	$0.25 \times 62.5 \times 40(24 + \Delta l)$		-15,000	8	-120,000
6	$W_u$			$-625\Delta l$	$\frac{2}{3} \times 24$	$-10,000\Delta l$
7	$W_u$				$\frac{1}{3}\Delta l$	$-208.33\Delta l^2$
8	$P$	$0.5 \times 62.5 \times 40 \times 40$	50,000		$\frac{1}{3} \times 40$	666,667
9	$P_w$	Waves (Art. 3b)	2,100		41.5	87,150

Data:  $h_0 = 31.2$  ft,  $h = 40$  ft,  $\Delta h = 8.8$  ft,  $l_0 = 24.0$  ft.

prism 1-3-4-5 are computed in line 2. The weight of the triangle 2-3-4 contains the unknown  $\Delta l$ , as shown in line 3. The lever arm is  $24 + \frac{1}{3}\Delta l$ . To avoid mixed values, this is written in two parts, lines 3 and 4. Two moment values result, one containing  $\Delta l$  and one  $\Delta l^2$ .

The uplift is represented by the triangle 1-2-6. For  $\zeta = 0.5$ ,  $c = 1.0$ ,  $h = 40$ , and  $w_2 = 62.5$ , the force  $W_u$  is  $0.5 \times 1250(24 + \Delta l)$ , with center of action  $\frac{1}{3}(24 + \Delta l)$  from the face. The moment is  $\frac{1}{6} \times 1250(24 + \Delta l)^2$ . To avoid mixed quantities, the force is written in two parts and the moment in three parts, lines 5, 6, and 7.

The horizontal water pressure and its moment, line 8, are computed from Eqs. 2 and 4, Chapter 7. The wave pressure,  $P_w$ , line 9, and its location, are taken from Art. 3b. The uplift forces and moments are opposite in direction to all the other forces and moments and are considered negative.

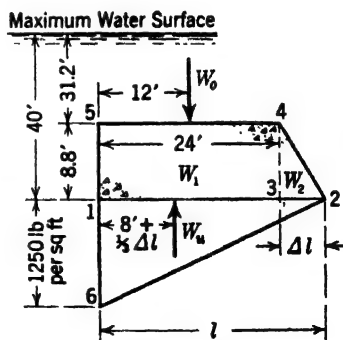


FIG. 2. Block 1, Zone III, Example 1.



If the vertical forces and all moments are summated, there results:

$$\Sigma(W) = 35\Delta l + 136,200$$

and

$$\Sigma(M) = 11.67\Delta l^2 + 5840\Delta l + 2,448,217$$

The distance from the center of moments (point 1) to the resultant is

$$x'' = \frac{\Sigma(M)}{\Sigma(W)}$$

which must equal  $\frac{2}{3}l$  or  $16 + \frac{2}{3}\Delta l$ , hence

$$\frac{11.67\Delta l^2 + 5840\Delta l + 2,448,217}{35\Delta l + 136,200} = 16 + \frac{2}{3}\Delta l$$

This expression simplifies into a quadratic equation giving a value of 3.14 ft for  $\Delta l$ , or  $l = 27.14$  ft.

It is necessary to insert these values in lines 1 to 4 of Table 2 to get the forces to be carried forward to the next block. The results, reservoir empty, are  $\Sigma(W) = 153,272$  lb and  $\Sigma(M) = 1,866,304$  ft-lb. Dividing  $\Sigma(M)$  by  $\Sigma(W)$  gives 12.26 ft, from the face to the resultant, which is greater than  $\frac{1}{3}l$ ; hence the resultant, reservoir empty, is within the middle third.

By making the remaining substitutions, data are obtained with which sliding factor and unit stresses may be computed, but this is usually unneces-

sary in Zone III. Table 2 should be repeated for the condition of ice loading in combination with water pressure to the spillway lip. Water at flood level without ice will be found to control in this example at  $h = 40$  ft, and at all greater depths.

**9. Block 2, Zone III, Trial Solution.** The value of  $\Delta l$  for block 2 will be found by trial. Computations are shown in Table 3. Conditions and dimensions are shown in Fig. 3, which is the same as Fig. 2 except that dimensions are generalized. A value of 10 ft is assumed for  $\Delta h$ .

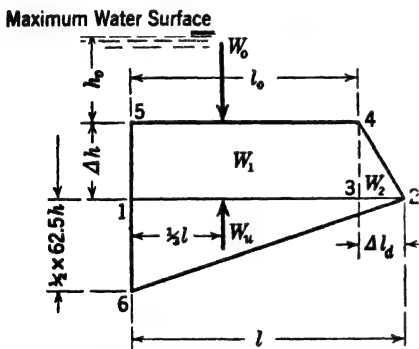


FIG. 3. General block form, Zone III, Example 1.

Weight and moment values for  $W_0$ , line 1, are taken from the computations for the block above. Values for  $W_1$ , line 2, are for the block 1-3-4-5 of known dimensions. In line 3 an estimate is made of the value of  $\Delta l_d$ , the downstream projection of the new joint. This first estimate need not be accurate. Experience shows that the face slopes flatten somewhat for the first few blocks of Zone III. A value of 4.6 ft for  $\Delta l_d$  is assumed, and corresponding values of  $l$ ,  $\frac{1}{3}l$ , and  $\frac{2}{3}l$ , are computed as shown.

TABLE 3  
BLOCK 2, ZONE III, EXAMPLE 1

Line	Item	Description and dimensions	Forces (lb)		Lever (ft)	Moment (ft-lb)
			Horiz.	Vert.		
1	$W_0$	Masonry above $h = 40$		153,273		1,866,304
2	$W_1$	$27.14 \times 10 \times 150$		40,710	13.57	552,435
3	Trial	$\Delta l_d = 4.6, l = 31.74, \frac{1}{3}l = 10.58, \frac{2}{3}l = 21.16$				
4	$W_2$	$0.5 \times 4.6 \times 10 \times 150$		3,450	28.67	98,912
5	Total	Reservoir empty		197,463	(12.75)	2,517,651
6	$W_u$	$0.25 \times 62.5 \times 31.74 \times 50$		-24,797	10.58	-262,352
7	$P$	Horiz. water = $0.5 \times 62.5 \times 50^2$	78,125		16.67	1,302,344
8	$P_w$	Waves (Art. 3b)	2,100		51.50	108,150
9	Total	Reservoir full	80,225	172,636	(21.23)	3,665,793
10	Trial	$\Delta l_d = 4.72, l = 31.86, \frac{1}{3}l = 10.62, \frac{2}{3}l = 21.24$				
11	$W_2$	$0.5 \times 4.72 \times 10 \times 150$		3,540	28.71	101,633
12	$W_u$	$0.25 \times 62.5 \times 31.86 \times 50$		-24,891	10.62	-264,342
13	Total	Reservoir empty		197,523	(12.76)	2,520,372
14	Total	Reservoir full		172,632	(21.24)	3,666,524

Data:  $h_0 = 40$  ft,  $h = 50$  ft,  $\Delta h = 10$  ft,  $l_0 = 27.14$  ft.

Values of  $W_2$  are computed in line 4, and totals, reservoir empty, are taken in line 5. Dividing the moment by the vertical force, the resultant, reservoir empty, is 12.75 ft from the face. This distance being greater than  $\frac{1}{3}l$  the base (line 3), the resultant, reservoir empty, is within the middle third.

Uplift, horizontal water pressure, and wave force are computed in lines 6, 7, and 8. Totals, reservoir full, are taken in line 9. The resultant is found to be 21.23 ft, which is slightly greater than  $\frac{2}{3}l$  the trial value of  $l$  (line 3); hence the resultant is outside the middle third by 0.07 ft. To get a new trial value of  $\Delta l_d$ , add  $1.5 \times 0.07$  or, say, 0.12 ft, to the previous value of 4.6 ft. The new trial data are shown in line 10.

New values of  $W_2$  and  $W_u$  are computed in lines 11 and 12, and new totals, reservoir empty and reservoir full, are taken in lines 13 and 14. The distance to the resultant, line 14, is the same as  $\frac{2}{3}l$ ; hence the trial values are correct. The distance from the face to the resultant, line 13, is 12.76 ft, which is more than  $\frac{1}{3}l$ ; hence the resultant, reservoir empty, is within the middle third. It is evident by inspection that  $\tan \theta$  is less than the allowable value of  $f$ .

The designer may make his choice between the methods illustrated in Tables 2 and 3. Table 3 is longer but it requires no outside computations and it supplies data, required in subsequent work, that can be obtained from Table 2 only by recomputation after  $\Delta l$  is found.

**10. Remainder of Zone III.** Succeeding blocks in Zone III are computed as illustrated for block 1 or block 2. Proceeding at 10-ft depth intervals, it is found that the resultant, reservoir empty, falls outside the middle third at  $h = 80$  ft, indicating that Zone IV has been reached.

The bottom of Zone III is found by interpolation, checked by trial, to be approximately at  $h = 75$  ft; hence the final block (No. 5) is given a 5.0-ft depth. Computations are shown in Table 4. Computations for the inter-

TABLE 4  
BLOCK 5, ZONE III, EXAMPLE 1

Line	Item	Description and dimensions	Forces (lb)		Lever (ft)	Moment (ft-lb)
			Horiz.	Vert.		
1	$W_0$	Masonry above $h = 75$		310,609		4,674,716
2	$W_1$	$5 \times 43.95 \times 150$		32,697	21.98	724,519
3	Trial	$\Delta l_d = 3.45$ , $l = 47.40$ , $\frac{1}{3}l = 15.80$ , $\frac{2}{3}l = 31.60$				
4	$W_2$	$0.5 \times 3.45 \times 5 \times 150$		1,294	45.10	58,359
5	Total	Reservoir empty		344,600	(15.84)	5,457,594
6	$W_u$	$0.25 \times 62.5 \times 47.40 \times 75$		-55,547	15.80	-877,643
7	$P$	Horiz. water = $0.5 \times 62.5 \times 75^2$	175,781		25.00	4,394,531
8	$P_w$	Waves (Art. 3b)	2,100		76.50	160,650
9	Total	Reservoir full	177,881	289,053	(31.60)	9,135,132

Data:  $h_0 = 70$  ft,  $h = 75$  ft,  $\Delta h = 5$  ft,  $l_0 = 43.95$  ft.

vening blocks (3 and 4) are not shown, but the essential results are shown in Table 8.

It is not necessary that the bottom of Zone III be exactly located. The first joint found in Zone IV (at  $h = 80$  ft in this example) may simply be designed for the conditions of that zone and connected by straight faces to the last computed joint in Zone III. Any ineconomy thus introduced is negligible. (See Arts. 17, 18, and 19.)

**11. Sliding Factor and Stresses, Base of Zone III.** As a precautionary measure, sliding factor and stresses should be computed before proceeding with Zone IV. From line 9, Table 4, the inclination of the resultant is

$$\tan \theta = \frac{177,881}{289,053} = 0.615$$

Although this factor is well below the stated allowable limit, the shear-friction factor of safety will be investigated for purposes of illustration.

By transposition, Eq. 4, Chapter 8, may be written

$$S_{s-f} = \frac{f\Sigma(W) + rs_a A}{\Sigma(P)}$$

Inserting values of  $f$  and  $s_a$  from Art. 2, other constants from Table 4, and assuming  $r = 0.5$ ,  $rs_a = 400$ ,

$$S_{s-f} = \frac{0.75 \times 289,053 + 400 \times 144 \times 47.40}{177,881} = 16.6$$

which is more than three times the required value of 5.0.

The resultant, reservoir full, being exactly at the third point,  $e$ , in Eq. 42b, Chapter 7, is  $\frac{1}{6}l$ . Therefore

$$p' = 2 \frac{\Sigma(W)}{l} = 12,330 \text{ lb per sq ft}$$

There being no tailwater, there is no uplift at the downstream face; hence,  $p'_u = 0$  in Eq. 44, Chapter 7, and  $p'$  as above computed may be taken as  $p'$  in Eq. 5, Chapter 8.

The angle between the downstream face and the vertical is such that

$$\tan \phi = \frac{\Delta l}{\Delta h} = \frac{3.42}{5.0} = 0.684$$

and

$$\sec^2 \phi' = 1 + \tan^2 \phi' = 1.468$$

Substituting in Eq. 5, Chapter 8, the inclined pressure is found to be

$$p'_i = 12,330 \times 1.468 = 18,100 \text{ lb per sq ft}$$

The maximum pressure at the vertical upstream face, reservoir empty, is

$$p'' = 2 \times \frac{344,584}{47.40} = 14,549 \text{ lb per sq ft}$$

All of these values are well within the prescribed limits.

**12. Zone IV, Example 1.** Below the bottom of Zone III the upstream face must be battered to keep the resultant, reservoir empty, within the middle third. Depth intervals are again assumed and the length and position of each new joint computed to cause the resultant for both reservoir empty and reservoir full to fall at the middle third points. It is possible to set up simultaneous equations which may be solved for the two unknowns, but such equations are complicated and solution by trial is preferable.

**13. Block 1, Zone IV.** Conditions for the first block of Zone IV are shown in Fig. 4. The projections 1-2 and 3-4 of the new base constitute the two unknowns. In Zone III, moment arms were measured to the upstream end of the joint. In Zone IV the position of this point is unknown, hence some

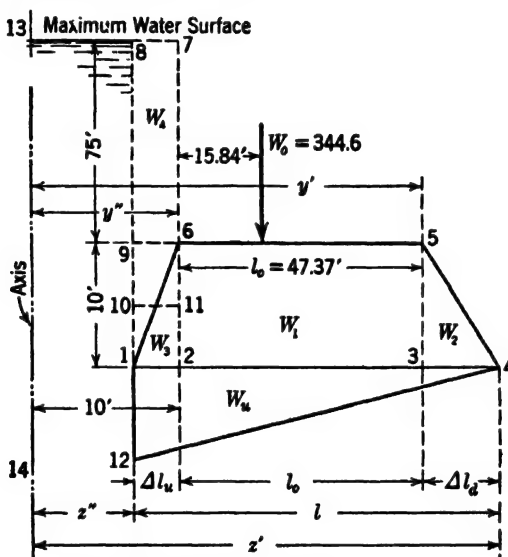


FIG. 4. Block 1, Zone IV, Example 1.

other center of moments is required. Any point may be chosen, but the handling of signs is simplified if the center is outside the dam. It is convenient to choose an axis that can be carried forward from block to block. The axis 13-14, 10 ft from the upstream face of Zone III, is chosen.

The computations are shown in Table 5. The weight of masonry above the top of the block, designated as  $W_0$ , and the distance from its line of action are transferred from line 5, Table 4, to line 1, Table 5. The force is changed from pounds to kips, and the lever arm is corrected to the new axis. The

TABLE 5  
BLOCK 1, ZONE IV, EXAMPLE 1

Line	Item	Description and dimensions	Forces (kips)		Lever (ft)	Moment (ft-kips)
			Horiz.	Vert.		
1	$W_0$			344.6	25.84	8,904
2	$W_1$	$10 \times 47.37 \times 150$		71.1	33.68	2,395
3	$W_2$	$0.5 \times 10 \times 7 \times 150$		5.2	59.70	310
4	Total	Partial, empty		420.9	(27.58)	11,609
5	Est.	$z' - 27.56 = \frac{2}{3}l = 36.81; \frac{1}{3}l = 18.405; l = 55.23; \Delta e_u = 0.86;$ $z'' + \frac{1}{3}l = 27.55; z'' + \frac{2}{3}l = 45.96$				
6	$W_3$	$0.5 \times 10 \times 0.86 \times 150$		0.6	9.71	6
7	Total	Empty		421.5	(27.56)	11,615
8	$W_4$	$62.5 \times 80 \times 0.86$		4.3	9.57	41
9	$W_u$	$1328 \times 55.23$		-73.3	27.55	-2,019
10	$P$		225.8			6,397
11	$P_u$		2.1		86.50	182
12	Total	Full	227.9	352.5	(46.00)	16,216
13	Check	Outside 0.04', try $\Delta l_d = 7.08; \Delta l_u = 0.90; l = 55.35; z'' = 9.1;$ $z'' + \frac{1}{3}l = 27.55; z'' + \frac{2}{3}l = 46.00$				
14	$W_2$	$0.750 \times 7.08$		5.3	59.73	317
15	$W_3$	$0.750 \times 0.90$		0.7	9.70	7
16	Total	Empty		421.7	27.56	11,623
17	$W_4$	$5 \times 0.9$		4.5	9.55	43
18	$W_u$	$1328 \times 55.35$		-73.5	27.55	-2,025
19	Total	Full		352.7	45.99	16,220

Data:  $h_0 = 75$  ft,  $h = 85$  ft,  $\Delta h = 10$  ft,  $l_0 = 47.37$  ft,  $y'' = 10$  ft,  $y' = 57.37$  ft.  
 Tan  $\theta = 0.646$ .

accuracy of basic data does not justify more than four or five significant figures; hence it is convenient to express all forces for the lower portions of the dam in kips. Data for the known central block 6-2-3-5 are shown in line 2. A trial value must be assumed for the base 3-4 =  $\Delta l_d$  of the triangular block  $W_2$ . It is known from experience that the inclination of the downstream face is somewhat greater in Zone IV than in Zone III. As a first trial,  $\Delta l_d$  may be made 7.00 ft. The corresponding weights and moments are shown in line 3.

Partial totals are cast in line 4, and the resultant of these three items is found to be 27.58 ft from the axis.

If the upstream addition 1-2-6 were weightless, the distance from the resultant, line 4, to the downstream end of the joint would equal two-thirds of the required joint length. Actually, the weight of this addition will cause a small change in the position of the resultant, reservoir empty. It will be tentatively assumed that the computed value of 27.58 will be reduced to 27.56.

The corresponding length of joint is estimated in line 5. The distance from the axis to the downstream end of the joint ( $z'$ , Fig. 4) is  $10 + 47.37 + 7.0 = 64.37$  ft. Subtracting 27.56 gives a value of 36.81 ft for  $\frac{2}{3}l$  or  $l = 55.23$  ft. Deducting  $\Delta l_d$  and  $l_0$  leaves 0.86 ft for  $\Delta l_u$ . Distances from the axis to the third points are 27.55 ft and 45.96 ft.

The weights and moments for 1-2-6 are computed in line 6 and added to the partial totals of line 4, giving the trial totals, reservoir empty, line 7. The lever arm computed in this line checks that assumed in line 5, hence  $\Delta l_u = 0.86$  ft is correct for  $\Delta l_d = 7.00$  ft, although the correctness of the latter length remains to be determined.

Water loads are next introduced. The weight of the water in the prism 8-1-6-7, Fig. 4, may be divided into the rectangle 8-9-6-7 and the triangle 9-1-6, but unless the triangular portion is relatively large, the rectangle 8-10-11-7 may be used with only a negligible error in moments. This plan is followed in line 8.

Uplift is computed in line 9. Because this force and its moment are opposed in direction to other forces and moments, they are shown as negative.

The horizontal water load, line 10, and the wave load, line 11, complete the forces acting on the dam. Totals in line 12 are used to compute the distance to the resultant, reservoir full. The computed distance is 46.00 ft, which is 0.04 ft greater than  $z'' + \frac{2}{3}l$ , line 5; hence the resultant is outside the middle third by this small amount.

Assuming that the small correction required will have no appreciable effect on the location of resultants, the previous trial value of  $\Delta l_d$  should be increased by twice the computed error, from 7.00 ft to 7.08 ft. A corresponding change of 0.04 ft is required in  $\Delta l_u$  to avoid moving the upstream third point.

New trial data are shown in line 13. New values for  $W_2$  and  $W_3$  are computed in lines 14 and 15. New totals for reservoir empty and a new distance to the resultant are computed in line 16. Comparison with the value of  $z'' + \frac{1}{3}l$  in line 13 shows the resultant to be inside the middle third by 0.01 ft, which is satisfactory.

New values of  $W_4$  and  $W_u$  are computed in lines 17 and 18. New totals and a new distance to the resultant for reservoir full are shown in line 19. Comparison with  $z'' + \frac{2}{3}l$ , line 13, shows this new resultant to be 0.01 ft inside the middle third, which is satisfactory; hence the value of 55.35 ft for  $l$ , as shown in line 13, may be taken as correct.

If the results had been unsatisfactory, a repetition of the trial computation, lines 13 to 19, would have been required. If the dam were being designed without uplift so that  $p_v''$ , Eq. 45, Chapter 7, reservoir full, might approach zero, it would be necessary at this point to check for inclined tension, using Eq. 6a, Chapter 8. In the present example, such tension will not occur at any point.

**14. Block 2, Zone IV.** As the depth is nearing 100 ft, the block height is increased to 15 ft. Otherwise, computations are made as for block 1. Assuming that the slope of the face will be about the same as in block 1,  $\Delta l_d$  for a 15-ft height is estimated at 10.65 ft.

The computations are shown in Table 6. Values of  $W_0$ , line 1, for weight of masonry above the top of the block, are taken from line 16, Table 5. The axis of moments being the same as in the previous block, the moment is transferred without change.

Lines 2 to 7 follow the procedure of Table 5. A value for "previous vertical water load,"  $W'_4$ , is introduced in line 8, being  $\Sigma(W_4)$  for preceding blocks. Lines 9 to 20 are exactly like lines 8 to 19 of Table 5. The final value of  $\Delta l_d$  is found to be 10.75 ft against a first trial of 10.65 ft.

From data in line 20, Table 6, the inclination of the resultant is

$$\tan \theta = \frac{314.6}{465.0} = 0.677$$

The face slope is

$$\tan \phi' = \frac{\Delta l_d}{\Delta h} = \frac{10.75}{15.00} = 0.71667$$

$$\sec^2 \phi' = 1 + \tan^2 \phi' = 1.5136$$

Vertical pressure at the downstream face is

$$p'_v = \frac{2\Sigma(W)}{l} = \frac{2 \times 465.0}{67.14} = 13.85 \text{ kips per sq ft}$$

The maximum inclined pressure is

$$p'_i = 13,850 \times 1.5136 = 20,966 \text{ lb per sq ft.}$$

These values are all far below the allowable limits.

**15. Remainder of Zone IV.** Computations proceed, block by block, until the computed inclined pressure exceeds the allowable limit, indicating that the bottom of Zone IV has been reached. In the present example, Zone IV



TABLE 6  
BLOCK 2, ZONE IV, EXAMPLE 1

Line	Item	Description and dimensions	Forces (kips)		Lever (ft)	Moment (ft-kips)
			Horiz.	Vert.		
1	$W_0$	Empty, line 16, Table 5		421.7		11,623
2	$W_1$	$15 \times 55.35 \times 150$		124.5	36.78	4,579
3	$W_2$	$0.5 \times 15 \times 10.65 \times 150 =$ $1.125 \times 10.65$		12.0	68.00	816
4	Total	Partial, empty		558.2	(30.49)	17,018
5	Est.	$z' - 30.44 = \frac{2}{3}l = 44.66; l = 66.99; \Delta L_u = 0.99; z'' + \frac{1}{3}l = 30.44;$ $z'' + \frac{2}{3}l = 52.77; z'' = 8.11$				
6	$W_3$	$1.125 \times 0.99$		1.1	8.77	10
7	Total	Empty		559.3	(30.45)	17,028
8	$W'_4$	$W_4$ , line 17, Table 5		4.5		43
9	$W_4$	$62.5 \times 92.5 \times 0.99 =$ $5.781 \times 0.99$		5.7	8.60	49
10	$W_u$	$1.5625 \times 66.99$		-104.8	30.44	-3,190
11	$P$	$0.5 \times 62.5 \times 100^2$	312.5			10,417
12	$P_w$		2.1		101.50	213
13	Total	Full	314.6	464.7	(52.85)	24,560
14	Check	Outside 0.08', try $\Delta L_d = 10.75; \Delta L_u = 1.04; l = 67.14; z'' = 8.06;$ $z'' + \frac{1}{3}l = 30.44; z'' + \frac{2}{3}l = 52.82$				
15	$W_2$	$1.125 \times 10.75$		12.1	68.03	823
16	$W_3$	$1.125 \times 1.04$		1.2	8.75	10
17	Total	Empty		459.5	(30.45)	17,035
18	$W_4$	$5.781 \times 1.04$		6.0	8.58	51
19	$W_u$	$1.5625 \times 67.15$		-105.0	30.44	-3,196
20	Total	Full	314.6	465.0	52.82	24,563

Data:  $h_0 = 85$  ft;  $h = 100$  ft;  $\Delta h = 15.0$  ft;  $h_0 = 55.35$  ft;  $y'' = 9.1$  ft;  $y' = 64.45$  ft.  $\tan \theta = 0.673$ .

extends to the bottom of the dam. Computations for block 7 at the bottom are shown in Table 7. The joint length is 143.10 ft, and the maximum inclined

TABLE 7  
BLOCK 7, ZONE IV, EXAMPLE 1

Line	Item	Description and dimensions	Forces (kips)		Lever (ft)	Moment (ft-kips)
			Horiz.	Vert.		
1	$W_0$	Concrete above		1,639.0		77,465
2	$W_1$	$25 \times 124.42 \times 150$		466.6	68.00	31,729
3	$W_2$	$0.5 \times 25 \times 18.40 \times 150$ ( $z = 148.61$ )		34.5	136.34	4,704
4	Total	Partial		2,140.1	(53.22)	113,898
5	Est.	$z' - 53.21 = 95.40 = \frac{2}{3}l; \frac{1}{3}l = 47.70; l = 143.10; \Delta l_u = 0.28; z'' = 5.51; z'' + \frac{1}{3}l = 53.21; z'' + \frac{2}{3}l = 100.91; z'' + l = 148.61$				
6	$W_3$	$0.5 \times 25 \times 0.28 \times 150$		0.5	5.70	3
7	Total	Empty		2,140.6	(53.21)	113,901
8	$W'_4$	(Water)		28.9		220
9	$W_4$	$62.5 \times 0.28 \times 187.5$		3.3	5.65	19
10	$W_u$	$0.25 \times 62.5 \times 143.10 \times 200$		-447.2	53.21	-23,796
11	$P$	$0.5 \times 62.5 \times 40,000$	1,250.0		66.67	83,338
12	$P_w$		2.1		201.50	423
13	Total	Full	1,252.1	1,725.6	100.90	174,105

Data:  $h_0 = 175$  ft,  $h = 200$  ft,  $l_0 = 124.42$  ft,  $y'' = 5.79$  ft,  $y' = 130.21$  ft.  $\tan \theta = 0.725$ .

pressure is 37,200 lb per sq ft. The sliding factor is 0.725, which is less than the allowable; hence the shear-friction factor of safety is not required but may be computed as a matter of interest, thus:

$$\begin{aligned}
 S_{s-f} &= \frac{f\Sigma(W) + r s_a A}{\Sigma(P)} \\
 &= \frac{0.75 \times 1,725,600 + 400 \times 144 \times 143.1}{1,252,100} = 7.6
 \end{aligned}$$

which is well above the allowable value of 5.0.

**16. The Completed Section.** Essential data for the completed section are shown in Table 8, and a scale drawing is shown in Fig. 5. The maximum stresses which occur at the downstream face, reservoir full, are far below the allowable limit of 60,000 lb per sq ft. The sliding factor reaches a maximum

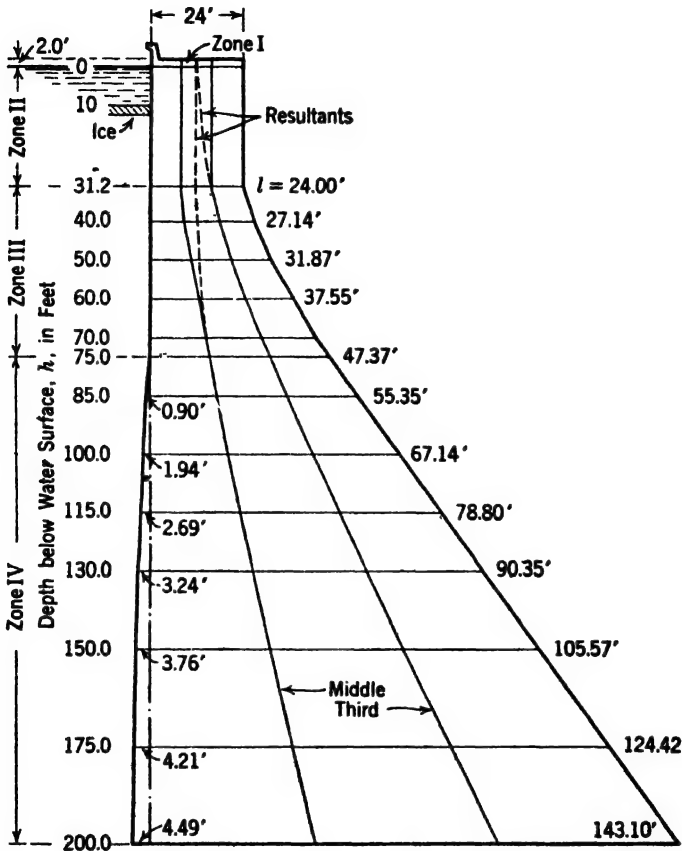


FIG. 5. Complete profile, Example 1.

of 0.725 against an allowable value of 0.75, and the shear-friction safety factors are well above the allowable value of 5.0.

**17. Required Precision.** In Example 1, joint lengths and the position of resultants are computed to the nearest 0.01 or 0.02 ft. Such precision is not justified by the accuracy of the basic data. The distance from the axis of moments to the resultant, reservoir full, at the base of the dam, is 100.90 ft on the basis of concrete weighing 150 lb per cu ft. If the actual weight of the concrete should be 150.25 lb per sq ft, this distance would be 100.80 ft. It is unlikely that the weight of the concrete can be foretold to within such accu-

**TABLE 8**  
**DIMENSIONS AND STRESSES, EXAMPLE 1**

Zone	Block	Depth $h$	$l$	$\Delta d$	$\Delta u$	$\Sigma \Delta u$	$p'$	$p'_1$	$p''$	$p''_1$	$\tan \theta$	$S_{s-f}$
I	1	-2 0	24 00	...	...	...	...	...	...	...	...	
	..	0 0	24 00	...	...	...	300	300	300	300	...	
II	1	31.2	24 00	...	...	...	8,990	8,990	4,980	4,980	0.301	
III	1	40 0	27.14	3 14	...	...	9,780	11,025	7,151	7,151	0.303	
	2	50 0	31.87	4 73	...	...	10,834	13,258	9,909	9,909	0.465	
	3	60 0	37.55	5 68	...	...	11,419	15,104	12,005	12,005	0.535	
	4	70 0	43.95	6 40	...	...	11,947	16,639	13,753	13,753	0.591	
	5	75 0	47.37	3 42	...	...	12,216	17,929	14,498	14,498	0.615	16.6
IV	1	85 0	55.35	7 08	0.90	0.90	12,744	19,133	15,238	15,364	0.646	
	2	100 0	67.14	10.75	1.04	1.94	13,852	20,969	16,667	16,749	0.673	
	3	115 0	78.80	10.91	0.75	2.69	15,168	23,194	18,368	18,447	0.697	
	4	130 0	90.35	11.00	0.55	3.24	16,607	25,546	20,232	20,255	0.707	
	5	150 0	105.57	14.70	0.52	3.76	18,655	28,733	22,882	22,898	0.716	
	6	175 0	124.42	18.40	0.45	4.21	21,342	32,900	26,346	26,354	0.722	
	7	200 0	143.10	18.40	0.28	4.49	24,120	37,180	29,918	29,922	0.725	7.6

NOTE: Units are ft and lb per sq ft.

racy. Uplift forces are even more uncertain; hence computations to the nearest 0.1 ft are amply close.

Beginning with block 1, Zone IV (Table 5), moments are shown in foot-kips and forces in kips and tenths of kips. This reduces the number of digits to be handled. Neither weight nor uplift are known to 0.1 of 1 per cent; hence four significant figures, at most five, give ample accuracy.

**18. Permissible Block Depths.** Block depths in Zones III and IV, Example 1, are approximately 15 per cent of the depth above the base of the block with a 10-ft minimum. Inspection of Table 8 and Fig. 5 shows that the precision requirements (Art. 17) would have been satisfied with a smaller number of blocks.

For Example 1, ample accuracy would be attained with joints at depths of 31.2, 40, 50, 60, 75, 100, 130, 160, and 200 ft.

**19. Practical Profile.** The profile of Fig. 5, with its continuously changing face slopes, is perfectly practical to construct and many dams have been built along these lines. However, so-called practical profiles, in which the face slopes are made continuous over appreciable depths, are sometimes used. This procedure is at a slight loss of economy except where, for high dams, it is found necessary to "redesign" to secure conformity with Rule 3 governing the design of Zones V, VI, and VII, as discussed in Art. 4*h*, Chapter 9. The need for the use of a practical profile for a high dam is shown hereinafter in Example 3, Arts. 34 and 35. Examples of "practical" profiles are shown in

Fig. 6. Such a profile can be fitted to the dam of Example 1 with little if any increase in masonry volume.

The more arbitrary forms with face slopes beginning at the top usually contain an excess of masonry in Zones II and III, but added weight in this region contributes to stability further down and is not necessarily an ineconomy.

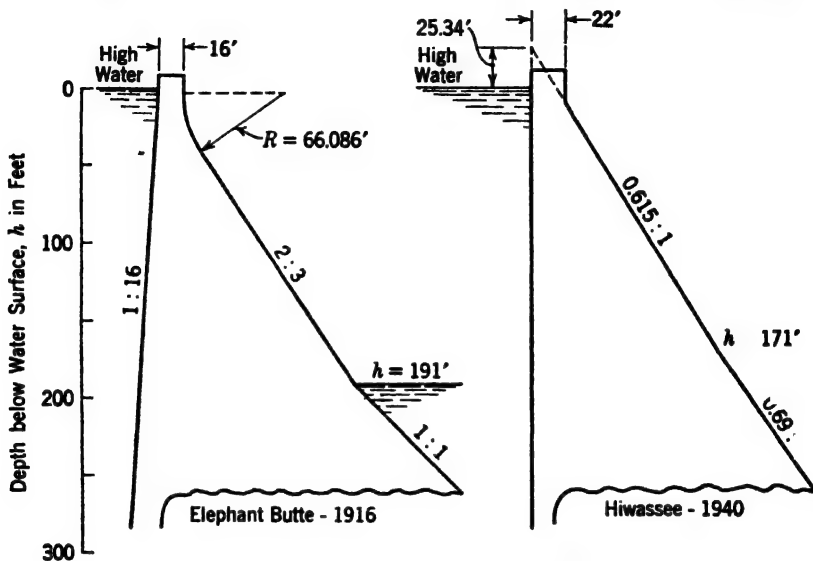


FIG. 6. Examples of "practical" profiles.

#### EXAMPLE 2. 200-FOOT NONOVERFLOW DAM WITH EARTHQUAKE ALLOWANCE

**20. Data, Example 2.** Let it be required to design a cross-section for a nonoverflow gravity dam conforming to all the requirements of Example 1, but with the added requirement that it must resist an earthquake acceleration of an intensity of  $0.1g$ , and a period of 1 second.

**21. Earthquake Forces.** (a) *Inertia of masonry.* An earthquake movement may be in any direction. The most severe direction for this type of dam is normal to the axis. The force due to the inertia of the masonry is found from Eq. 32, Chapter 7, which with  $\alpha = 0.1$  becomes

$$P_{em} = 0.1W \quad [1]$$

The letter "m" is added to the subscript to indicate that the force is derived from the masonry. The possibility of resonance and of inertial ice pressure are ignored.

(b) *Increased water pressure.* The increase in water pressure due to the assumed earthquake movement is determined in accordance with Art. 13e, Chapter 7. The coefficient  $C_e$  for a 200-ft dam, and a period  $t_e$  of 1 sec, from

Fig. 21, Chapter 7, is 51.7. Inserting this value in Eq. 34c, Art. 13e, Chapter 7, and making  $h = 200$  ft, the equation of total horizontal force is

$$\begin{aligned} P_{cw} &= \frac{2}{3} \times 51.7 \times 0.1y^{3/2} \sqrt{200} \\ &= 48.74y^{3/2} \end{aligned} \quad [2]$$

where  $y$  is depth below the surface. The letter "w" is added to the subscript to indicate that the force is derived from the water.

Making similar substitutions in Eq. 34e, Chapter 7, the moment equation is found to be

$$\begin{aligned} P_{cw}x &= \frac{1}{5} \times 51.7 \times 0.1y^{5/2} \sqrt{200} \\ &= 19.50y^{5/2} \end{aligned} \quad [3]$$

**22. Constants and Top Details.** Freeboard, wave pressure, and ice pressure are the same as for Example 1. The top width of 24 ft might be reduced to reduce earthquake effects, but for comparative purposes will be retained.

**23. Zone I, Example 2.** The influence of ice pressure will be found to be even less important than in Example 1 and therefore may be ignored. Hence, Zone I is merely the 2 top feet of the dam, so obviously stable as to require no investigation.

**24. Zone II, Example 2.** The depth of Zone II may be found as in Example 1, by adding items for  $P_{cm}$  and  $P_{cw}$  and their moments to Table 1. However, the fractional powers of  $y$ , in the earthquake force equations, ( $y$  being identical with  $h$  in Table 1), make solution by trial preferable.

The computations are shown in Table 9. From a preliminary trial, not shown, the value of  $h$  was estimated to be 20 ft. The governing stability requirement is that with reservoir full, and earthquake forces acting downstream, the resultant shall pass through the downstream third point. The solutions being by trial, the moments may as well be taken about the upstream end of the joint.

Trial data are set up in line 1. Line 2 is for  $W_0$ , the masonry of Zone I; and line 3 is for  $W_1$ , the masonry of Zone II, to the trial depth. Totals, reservoir empty, are taken in line 4. These totals are required for transfer to the computations for the next block. Values in line 5 represent earthquake effects for the two masonry blocks. The horizontal force is equal to  $0.1(W_0 + W_1)$ . The lever arm about the base is 11.0 ft, which is half the height of the two zones. If the location of the resultant, reservoir empty, earthquake force acting upstream, is desired, an additional total is required including earthquake moments considered as negative.

Values for  $W_u$ ,  $P$ , and  $P_w$ , lines 6, 7, and 9, are computed as for Example 1. Forces and moments for earthquake effect on water pressure, line 8, are computed from Eqs. 2 and 3.

Totals, reservoir full, are taken in line 10. The distance from the upstream face to the resultant is 15.92 ft, which is 0.08 ft less than  $\frac{2}{3}l$  (line 1); hence the zone depth could be made greater than 20 ft, but it cannot be 21 ft, and the trial depth is assumed correct.

TABLE 9  
DEPTH OF ZONE II, EXAMPLE 2

Line	Item	Description and dimensions	Forces (lb)		Lever (ft)	Moment (ft-lb)
			Horiz.	Vert.		
1	Trial	$h = 20, l = 24, \frac{1}{3}l = 8.0, \frac{2}{3}l = 16.0$				
2	$W_0$	$2 \times 24 \times 150$		7,200	12.00	86,400
3	$W_1$	$20 \times 24 \times 150$		72,000	12.00	864,000
4	Total	Empty, no earthquake		79,200		950,400
5	$P_{em}$	Earthquake, $W_0$ and $W_1$	7,920		11.00	87,120
6	$W_u$	Uplift, $0.25 \times 62.5 \times 24 \times 20$		-7,500	8.00	-60,000
7	$P$	Horiz. water, $0.5 \times 62.5 \times 20^2$	12,500		6.67	83,333
8	$P_{ew}$	Earthquake-water, Eqs. 2 and 3	4,359			34,889
9	$P_w$	Waves (Art. 3b)	2,100		21.50	45,150
10	Total	Reservoir full	26,879	71,700	(15.92)	1,140,892

**25. Block 1, Zone III.** Computations for Zone III proceed exactly as in the case of Example 1, except that the number of blocks will follow the suggestions of Art. 18.

Computations for block 1, with a depth of 10 ft, are shown on Table 10. This is a trial solution, following the form of Table 3 of Example 1, with such alterations as are required to include earthquake forces.

Line 1 is for masonry above the top of the block and is transferred from line 4 of Table 9. Line 2 is earthquake effect from this masonry, transferred from line 5, Table 9. The moment in line 2 is to the top of the block. It is transferred to the bottom by the correction in line 3.

Values in line 4 are for the rectangular portion of the new block and those in line 5 are the earthquake effects on the same. Moment arms are half the width and half the height of the rectangle.

Line 6 sets out the first trial value for  $\Delta l_d$  and the corresponding value of  $l$ .

Lines 7 and 8 are for vertical and earthquake effects from the downstream triangular portion of the block. Lever arms are  $l_0 + \frac{1}{3}\Delta l$  and  $\frac{1}{3}\Delta h$ , as indicated.

TABLE 10  
BLOCK 1, ZONE III, EXAMPLE 2

Line	Item	Description and dimensions	Forces (lb)		Arm (ft)	Moment (ft-lb)
			Horiz.	Vert.		
1	$W_0$	Masonry above $h = 0$		79,200	12.00	950,400
2	$P_{em}$	Earthquake, $W_0$ , above $h = 20$	7,920		11.00	87,120
3	$P_{em}$	Earthquake, $W_0$ correction			10.00	79,200
4	$W_1$	$10 \times 24 \times 150$		36,000	12.00	432,000
5	$P_{em}$	Earthquake, $W_1$	3,600		5.00	18,000
6	Trial	$\Delta l_d = 4.0, l = 28.0, \frac{1}{3}l = 9.33, \frac{2}{3}l = 18.67$				
7	$W_2$	$0.5 \times 4 \times 10 \times 150$		3,000	25.33	76,000
8	$P_{em}$	Earthquake, $W_2$	300		3.33	1,000
9	Total	Reservoir empty, no earthquake		118,200		1,458,400
10	Total	Earthquake on masonry	11,820			185,320
11	Total	Reservoir empty, negative earthquake	11,820	118,200	(10.77)	1,273,080
12	$W_u$	Uplift = $0.25 \times 62.5 \times 28 \times 30$		-13,125	9.33	-122,500
13	$P$	Horiz. water, $0.5 \times 62.5 \times 30 \times 30$	28,125		10.00	281,250
14	$P_{re}$	Earthquake on water, Eqs. 2 and 3	8,008			96,116
15	$P_w$	Waves (Art. 3b)	2,100		31.50	66,100
16	Total	Reservoir full, earthquake positive	50,053	105,075	(18.70)	1,964,686
17	Trial	$\Delta l_d = 4.05, l = 28.05, \frac{1}{3}l = 9.35, \frac{2}{3}l = 18.70$				
18	$W_2$	$0.5 \times 4.05 \times 10 \times 150$		3,038	25.35	77,013
19	$P_{em}$	Earthquake, $W_2$	304		3.33	1,012
20	$W_u$	Uplift = $0.25 \times 62.5 \times 28.05 \times 30$		-13,148	9.35	-122,934
21	Total	Reservoir empty, no earthquake		118,238		1,459,413
22	Total	Earthquake on masonry	11,824			185,332
23	Total	Reservoir empty, negative earthquake	11,824	118,238		1,274,081
24	Total	Reservoir full, earthquake positive	50,057	105,090	(18.70)	1,965,277

Data:  $h_0 = 20$  ft,  $h = 30$  ft,  $\Delta h = 10$  ft,  $l_0 = 24$  ft.



Line 9 contains totals, reservoir empty and earthquake items ignored. Line 10 contains totals of earthquake items only, and line 11 contains totals with reservoir empty and earthquake forces acting upstream.

Moments from vertical forces and from horizontal forces caused by earthquake action on the masonry must be summated separately as the latter must be considered as if acting upstream for reservoir empty and downstream for reservoir full.

The computed lever arm in line 11 exceeds  $\frac{1}{3}l$  (line 6); hence the resultant, reservoir empty, is within the middle third.

Lines 12, 13, and 15 are for uplift, horizontal water pressure, and wave pressure. Computations are the same as in Example 1.

Line 14 is for the horizontal effect of earthquake on the water in the reservoir. The force is computed from Eq. 2 and the moment from Eq. 3.

In the totals for reservoir full, line 16, all earthquake forces are assumed to be acting downstream; hence earthquake moments are taken as positive.

The computed lever arm in line 16 exceeds  $\frac{2}{3}l$  (line 6) by 0.03 ft; hence the resultant, reservoir full, is outside that small amount, which is negligible, but will be corrected to illustrate the procedure. A new trial value for  $\Delta l_d$  is obtained by adding  $1.5 \times 0.03$  to the previous trial value. The new data are recorded in line 17.

Values depending on  $\Delta l_d$  are recomputed in lines 18, 19, and 20, and new totals are taken in lines 21, 22, 23, and 24. These totals replace those of lines 9, 10, 11, and 16.

The computed lever arm in line 24 is identical with  $\frac{2}{3}l$  (line 17); hence the second trial value of  $\Delta l_d$  is correct.

**26. Remainder of Zone III.** Computations for other blocks in Zone III follow the pattern of Table 10 and need not be shown. Care is required to see that earthquake forces are properly carried forward. Because of the horizontal earthquake force on the masonry, the resultant, reservoir empty, reaches the upstream middle third much sooner than in Example 1. The bottom of Zone III is found to be at  $h = 40$  ft.

**27. Zone IV.** It is not necessary to show all the computations for Zone IV; but to illustrate the handling of earthquake items, computations for the last block are shown in Table 11. Because of the large number of items that must be recomputed for each new assumed value of  $\Delta l_d$  in Zone IV, the correction procedure of Table 10 (Zone III) is confusing. It is simpler to make a complete new tabulation for each trial, copying values that do not change. Table 11 represents the final result of a series of trials. (Usually two and seldom more than three trials are required.)

The construction of most of the lines in Table 11 is evident by comparison with Table 10. The trial value of  $\Delta l$ , line 6, is estimated from the slope of the downstream face on the block above, in the case of a first trial, or from the results of a previous trial.

The axis of moments is 20 ft upstream from the face of Zones I and II.

TABLE 11  
BLOCK 7, ZONE IV, EXAMPLE 2

Line	Item	Description and dimensions	Forces (kips)		Lever (ft)	Moment (ft-kips)
			Horiz.	Vert.		
1	$W_0$	Masonry above $h = 160$		1,684.5		91,826
2	$P_{em}$	Earthquake, $W_0$ (from previous computations)	168.4			9,601
3	$P_{em}$	Earthquake, $W_0$ correction			40.00	6,736
4	$W_1$	$40 \times 135 \times 0.150$		810.0	71.30	57,753
5	$P_{em}$	Earthquake for $W_1$	81.0		20.00	1,620
6	Trial	$\Delta l_d = 29.10, z' = 167.90$				
7	$W_2$	$0.5 \times 29.10 \times 40 \times 0.150$		87.3	148.50	12,964
8	$P_{em}$	Earthquake for $W_2$	8.7		13.33	116
9	Sub-total	Earthquake negative		2,581.8	(55.96)	144,470
10	Est.	$167.90 - 55.68 = 112.22 = \frac{2}{3}l, \frac{1}{3}l = 56.11, l = 168.33, \Delta l_u = 4.23, z'' = -0.43, \frac{2}{3}l + z'' = 111.79$				
11	$W_3$	$0.5 \times 4.23 \times 40 \times 0.150$		12.7	2.39	30
12	$P_{em}$	Earthquake for $W_3$	1.3		13.33	17
13	Total	Reservoir empty, no earthquake		2,594.5	(62.66)	162,573
14	Total	Earthquake on masonry	259.4			18,090
15	Total	Reservoir empty, earthquake negative		2,594.5	(55.69)	144,483
16	$W_{00}$	Vert. water on blocks above $h = 160$		95.2		972
17	$W_4$	Vert. water, block 7 = $0.0625 \times 4.23 \times 180$		47.6	1.68	80
18	$W_u$	Uplift = $0.25 \times 0.0625 \times 168.33 \times 200$		-526.0	55.68	-29,288
19	$P$	Horiz. water = $0.5 \times 0.0625 \times 200 \times 200$	1,250.0		66.67	83,333
20	$P_e$	Horiz. water, earthquake, Eqs. 2 and 3	137.8			11,029
21	$P_w$	Waves (Art. 3b)	2.1		201.50	423
22	Total	Reservoir full, earthquake positive	1,649.3	2,211.3	(111.79)	247,213

Data:  $h_0 = 160$  ft,  $h = 200$  ft,  $\Delta h = 40$  ft,  $l_0 = 135$  ft,  $y'' = 3.80$  ft,  $y' = 138.80$  ft.

The subtotal taken in line 9, earthquake moments considered negative, gives the approximate location of the resultant, reservoir empty. If the resultant, reservoir empty, is to be at the upstream third point, this distance subtracted from  $z'$  (line 6) gives  $\frac{2}{3}l$ . Experience with trials not shown indicates that the computed distance of 55.96 ft to the resultant should be shortened to 55.68 ft in estimating the joint length (line 10).

The distance,  $z''$ , from the axis of moments to the upstream face is found by subtracting  $\Delta l_u$  from  $y''$ , which is  $z''$  for the previous block. The value in this case is  $-0.43$  ft, showing that the joint crosses the axis. The desired distance from the axis to the resultant, found by adding  $z''$  (algebraically) to  $\frac{2}{3}l$ , is 111.79 ft.

Having obtained a value of  $\Delta l_u$  (line 10), the computation for reservoir empty is completed in lines 11 and 12, and three totals are taken in lines 13, 14, and 15, having the same significance as the totals in lines 9, 10, and 11, Table 10. Distance to the resultant, reservoir empty, line 15, is within 0.01 ft of the distance assumed in line 10, which is satisfactory.

Values in line 16 represent accumulated vertical water loads on the upstream faces of previous blocks. Line 17 is for vertical water loads on the present block. The significance of remaining lines can be seen by comparison with Table 10.

The distance of 111.79 ft from the axis to the resultant, reservoir full, line 22, is identical with  $\frac{2}{3}l + z''$ , line 10; hence, the resultant falls at the downstream third point.

Stresses and sliding factors are computed as for Example 1, with the following results:  $p'_i = 40,178$  lb per sq ft;  $p''_i = 31,171$  lb per sq ft;  $\tan \theta = 0.746$ ;  $S_{s-f} = 6.9$ .

TABLE 12  
DIMENSIONS AND STRESSES, EXAMPLE 2

Zone	Block	$h$	$l$	$\Delta l_d$	$\Delta l_u$	$\Sigma \Delta l_u$	$p'$	$p'_i$	$p''$	$p''_i$	$\tan \theta$	$S_{s-f}$
I	1	2.0	24.00	...	...	...	...	...	...	...	...	
	...	0.0	24.00	...	...	...	300	300	300	300	...	
II	1	20.0	24.00	...	...	...	...	...	...	...	0.374	25.3
III	1	25.0	25.74	0.75	...	...	...	...	...	...	0.426	
	2	30.0	28.02	2.28	...	...	...	...	...	...	0.477	
	3	40.0	33.60	5.58	...	...	...	...	...	...	0.561	
IV	1	50.0	42.12	6.57	1.95	1.95	...	...	...	...	0.617	12.3
	2	60.0	50.61	6.77	1.72	3.67	...	...	...	...	0.653	
	3	75.0	63.36	10.47	2.28	5.95	...	...	...	...	0.688	
	4	100.0	84.57	17.86	3.35	9.30	...	...	...	...	0.718	
	5	130.0	109.80	21.60	3.54	12.84	...	...	...	...	0.734	
	6	160.0	135.00	21.84	3.36	16.20	21,366	32,644	24,956	25,260	0.747	
	7	200.0	168.33	29.10	4.23	20.43	26,273	40,178	30,826	31,171	0.746	

NOTE: Units are ft and lb per sq ft.

**28. Comparison with Example 1.** Essential data for the entire section of Example 2 are shown in Table 12, and the section is plotted in Fig. 7. An outline of Example 1 is shown dotted for comparison. The earthquake forces

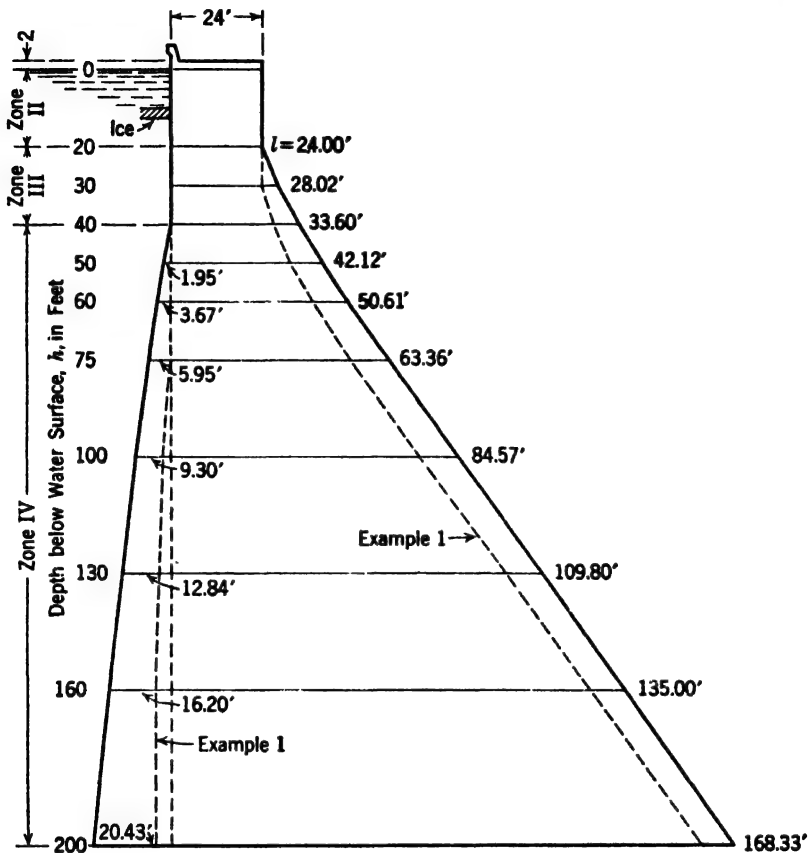


FIG. 7. Complete profile, Example 2.

cause a notable increase in section. Total cross-sectional areas are: Example 1, 14,271 sq ft; Example 2, 17,297 sq ft. The excess for Example 2 is about 21 per cent.

### EXAMPLE 3. 350-FOOT NONOVERFLOW DAM

**29. Effect in Lower Zones Shown.** Examples 1 and 2 illustrate all the principles involved in the design of straight gravity dams except that with the specified heights and stress limits they do not enter Zones V, VI, and VII. The treatment of these zones will be illustrated by designing a section similar to that of Example 1 but extending to a greater depth.

**30. Data, Example 3.** Design data will be assumed as follows:

- $H$  = maximum depth of water to be retained = 350 ft,  
 $h_2$  = depth of tailwater = 0,  
 $L$  = top width = 45 ft,  
 $w_1$  = weight of masonry = 150 lb per cu ft,  
 $w_2$  = weight of water = 62.5 lb per cu ft,  
 $c$  = uplift area factor = 1.0,  
 $\zeta$  = uplift intensity factor = 0.5,  
 $V$  = wind velocity = 80 miles per hr,  
 $F$  = fetch = 4.00 miles,  
 $f$  = allowable coefficient of friction on base = 0.70 (use same for horizontal joints in dam),  
 $s_a$  = ultimate shearing strength of the foundation = 800 lb per sq in. (use same for horizontal joints in dam),  
 $S_{s-f}$  = minimum permissible shear-friction safety factor = 5.0 (investigation for shear required only when  $\tan \theta$  is greater than  $f = 0.70$  or where depth exceeds 300 ft),  
 $p_i$  = maximum allowable inclined stress on dam or foundation = 50,000 lb per sq in.

**31. Discussion of Constants.** Although the wave conditions are the same as in Example 1, the freeboard will be increased to a total of 8 ft, because of the importance of the structure. A 4-ft parapet wall will again be assumed, making a height of 4 ft for Zone I. The top width is prescribed as 45 ft, about 13 per cent of the maximum height.

The wave pressure will be the same as for Example 1, Art. 3b. This force is frequently ignored, its relatively small effect being absorbed in a liberal estimate of the maximum water level. There are no special loadings, such as ice pressure or silt pressure.

The allowable sliding factor and inclined compressive stresses are somewhat less than in Example 1. This could be due to less favorable foundation conditions or to increased conservatism because of some special condition.

**32. Zones I to IV.** Assuming that the dam can be designed by the step-by-step process, computations for Zones I, II, III, and IV are of the same form as for Example 1 except that near the bottom of Zone IV,  $\tan \theta$  exceeds the allowable value of 0.70. This condition first occurs at  $h = 250$  ft. Trial computations which satisfy Rule 1 (position of the resultant) at this depth, for reservoir full or empty, are shown in Table 13.

The sliding factor, line 15, is 0.7123, which is slightly too high. However, the shear-friction safety factor is

$$\frac{0.7 \times 2,744,700 + 142.8 \times 144 \times 400}{1,953,100} = 5.2$$

hence the section is safe.

TABLE 13  
BLOCK 3, ZONE IV, EXAMPLE 3

[ $h = 210$  ft to  $h = 250$  ft]

Line	Item	Description and dimensions	Loads (kips)		Levers (ft)	Moment (ft-kips)
			Horiz.	Vert.		
1	$W_0$	Masonry above $h = 210$		2,396.1	82.40	197,447
2	$W_1$	Masonry $40 \times 142.81 \times 0.15$		856.8	106.21	91,007
3	Trial	$\Delta l_d = 29.50$ , $z' = 207.11$				
4	$W_2$	Masonry $0.5 \times 40 \times 29.5 \times 0.15$		88.5	187.44	16,588
5	Sub-total			3,341.4	(91.29)	305,042
6	Est.	$207.11 - 91.21 = 115.90 = \frac{2}{3}l$ , $\frac{1}{3}l = 57.95$ , $l = 173.85$ , $z'' = 33.26$ , $\Delta l_u = 1.54$				
7	$W_3$	Masonry $0.5 \times 40 \times 1.54 \times 0.15$		4.6	34.29	158
8	Total	Reservoir empty		3,346.0	91.21	305,200
9	$W'_4$	Vert. water above $h = 210$		55.7		2,075
10	$W_4$	Vert. water $230 \times 1.54 \times 0.0625$		22.1	34.03	753
11	$W_u$	Uplift $0.25 \times 250 \times 173.85 \times 0.0625$		-697.1	91.21	-61,941
12	$P$	Horiz water $0.5 \times 250 \times 250 \times 0.0625$	1,953.1		83.33	162,752
13	$P_w$	Waves (Art 3b)	2.1		251.50	528
14	Total	Reservoir full	1,955.2	2,744.7	149.15	409,367

Data:  $h_0 = 210$  ft,  $h = 250$  ft,  $l_0 = 142.81$  ft,  $y'' = 34.80$  ft,  $y' = 177.61$  ft  
 $\tan \theta = 1,955.2 \div 2,744.79 = 0.712$  (too high).

It happens that this is the only case in any example where the specified sliding factor is exceeded, and for the benefit of those who may be required to design strictly to a sliding factor, a means of correction will be illustrated. The most economical procedure is to extend the upstream face until the net vertical force, reservoir full, is equal to the horizontal force divided by the allowable sliding factor, i.e., until  $\Sigma(W)_F = 1955.2 \div 0.7 = 2793.14$  kips. The required increase in net weight is  $2793.14 - 2744.79 = 48.35$  kips.

If the upstream extension ( $\Delta l_u$ ) is increased by 1 ft, other dimensions remaining constant, the vertical force increments are as follows:

$$\begin{aligned}\text{Masonry, } W_3 &= 0.075 \times 1.00 \times 40 = 3.0 \text{ kips,} \\ \text{Water on upstream face, } W_4 &= 230 \times 1.0 \times 0.0625 = 14.38 \text{ kips,} \\ \text{Uplift, } W_u &= -0.015625 \times 1.0 \times 250 = -3.91 \text{ kips,} \\ \text{Total} &= 13.47 \text{ kips.}\end{aligned}$$

The required extension then is  $48.35$  divided by  $13.47 = 3.59$  ft. Adding this length to the value of  $1.54$  ft shown in Table 13 gives a new value of  $5.13$  ft for  $\Delta l_u$ .

To keep the resultant, reservoir full, at the third point,  $\Delta l_d$  must be changed from  $29.50$  ft to  $28.60$  ft, after which check computations show the sliding factor to be good and resultant within the middle third for reservoir full or empty.

**33. Bottom of Zone IV.** Proceeding by trial and checking stresses, the inclined stress at the downstream face reaches the allowable limit of  $50,000$  lb per sq ft at  $h = 264$  ft; hence this elevation marks the bottom of Zone IV. The final computations are shown in Table 14.

Here again the resultant, reservoir empty (line 6), is well within the middle third of the base, this being necessary in order that  $\tan \theta$ , line 13, shall not exceed  $0.70$ .

The resultant, reservoir full, with uplift, line 12, being very close to the downstream third point, the section being rectangular, and there being no tailwater, the vertical pressure at the downstream toe is twice the average pressure, as shown in line 14. The slope of the downstream face,  $\tan \phi'$ , line 15, is  $0.715$ , and  $\sec^2 \phi' = 1 + \tan^2 \phi' = 1.511$ ; hence the inclined pressure at the toe, line 16, is  $p'_t = 50.038$  kips per sq ft, which is sufficiently close to the specified limit.

The dimensions of the section thus computed from  $h = 0$  to  $h = 264$  ft are shown in Fig. 8.

**34. Zone V.** When division into zones and multiple-step design were originated, it was the general practice to limit vertical pressure rather than inclined pressure. Under that condition, limiting pressures in Zones V and VI were readily controlled by varying the upstream and downstream extensions of the base. However, with the present general practice of limiting inclined pressures, the design of the lower zones is more complicated.

Consider a block between  $h = 264$  ft and  $h = 300$  ft. If the joint length at  $h = 300$  ft is made just sufficient to satisfy Rules 1 and 2, the inclined stress at the downstream toe will exceed the limit of  $50,000$  lb per sq ft.

TABLE 14  
BOTTOM OF ZONE IV, EXAMPLE 3

[ $h = 250$  ft to  $h = 264$  ft]

Line	Item	Description and dimensions	Forces (kips)		Levers (ft)	Moment (ft-kips)
			Horiz.	Vert.		
1	Trial	$\Delta l_d = 10.01$ , $\Delta l_u = 1.80$ , $l = 188.35$ , $z' = 216.22$ , $z'' = 27.87$ , $\frac{1}{3}l + z'' = 90.65$ , $\frac{2}{3}l + z' = 153.44$				
2	$W_0$	Masonry above $h = 250$		3,354.13		305,020
3	$W'_1$	$14 \times 176.55 \times 0.15$		370.75	117.94	43,726
4	$W'_2$	$7 \times 10.01 \times 0.15$		10.51	209.55	2,202
5	$W'_3$	$7 \times 1.80 \times 0.15$		1.89	29.07	55
6	Total	Reservoir empty		3,737.28	(93.92)	351,003
7	$W'_4$	Vert. water above $h = 250$		129.43		4,452
8	$W_4$	Vert. water = $257.0 \times 1.80 \times 0.0625$		28.91	28.77	832
9	$W_u$	Uplift = $264 \times 188.35 \times 0.015625$		-776.94	90.65	-70,430
10	$P$	Horiz. water = $0.5 \times 264^2 \times 0.0625$	2,178.00		88.00	191,664
11	$P_w$	Waves (Art. 3b)	2 10		265.50	558
12	Total	Reservoir full	2,180.10	3,118.68	(153.30)	478,079
13	$\tan \theta$	Inclination of resultant = $2,180.1 \div 3,118.68 = 0.699$				
14	$p'_v$	= $2 \times 3,118.68 \div 188.35 = 33.116$ kips per sq ft				
15	$\tan \phi'$	Downstream face = $10.01 \div 14 = 0.715$ , $\sec^2 \phi' = 1.511$				
16	$p'_i$	= Inclined stress = $33.116 \times 1.511 = 50.038$ kips per sq ft				

Data:  $h_0 = 250$  ft,  $h = 264$  ft,  $\Delta h = 14$  ft,  $l_0 = 176.55$  ft,  $y'' = 29.67$  ft,  $y' = 206.21$  ft. Axis of moments, 40 ft upstream from face of Zone II.

The vertical pressure,  $p'_v$ , can be reduced by extending the downstream end of the joint, the upstream extension being changed only as required to maintain conformity with Rule 1, reservoir empty, or Rule 2a, reservoir full, whichever controls. However, in this particular case, increasing  $\Delta l_d$  increases  $\sec^2 \phi'$  more rapidly than it decreases  $p'_v$ , and  $p'_i$  is increased.



Tan  $\phi'$  immediately above  $h = 264$  ft is 0.715. If this value is continued for another block, the inclined pressure at the downstream face, at  $h = 300$  ft, can be brought within the prescribed limit by using an upstream extension of 53.4 ft, giving a total joint length of 267.5 ft. The value of  $\sec^2 \phi''$  for the upstream face is then so great that  $p_t''$ , reservoir empty, exceeds the allowable limit.

The step-by-step design can proceed below  $h = 264$  ft only by making the downstream face steeper than in the last block above. A value of  $l = 230$  ft,

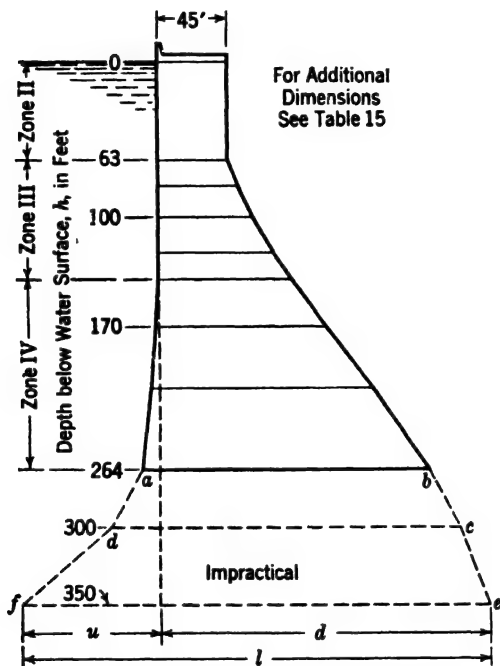


FIG. 8. Multiple-step design, Example 3.

with  $\Delta l_d = 21.0$  ft and  $\Delta l_u = 20.65$  ft, as represented by  $c-d$ , Fig. 8, gives about the best obtainable result.

In the next block, from  $h = 300$  ft to  $h = 350$  ft, still further steepening of the downstream slope is necessary, about the best obtainable base being represented by  $e-f$ . Dimensions of the section thus computed are shown in Table 15.

If the dam ended at  $h = 300$  ft, the base  $c-d$  might be accepted as satisfactory. However, the block  $c-d-f-e$  is of unusual form and would generally be considered undesirable. A convex face under compression, whether smoothly curved or polygonal, may be subject to tensile stresses on surfaces parallel to the face. The outer layer of such a section tends to buckle outward. Unless the buckling force is canceled by the weight component normal to the

TABLE 15  
DIMENSIONS AND STRESSES, MULTIPLE-STEP DESIGN,\* EXAMPLE 3

Line	$h$	$u^{**}$	$d^{**}$	$l$	$\frac{1}{6}l$	Reservoir empty			Reservoir full			
						$eE$	$p''_0$	$p''_1$	$eF$	$p'_0$	$p'_1$	$\tan \theta$
1	-4	0	45.00	45.00	7.50	0	...	...	0	...	...	...
2	0	0	45.00	45.00	7.50	0	...	...	0	...	...	...
3	63	0	45.00	45.00	7.50	0	...	...	7.50	...	...	0.279
4	80	0	51.54	51.54	8.59	2.91	...	...	8.58	...	...	0.308
5	100	0	61.53	61.53	10.26	6.66	...	...	10.26	...	...	0.485
6	120	0	73.53	73.53	12.26	10.58	...	...	12.25	...	...	0.558
7	140	0	86.97	86.97	14.50	14.46	...	...	14.50	...	...	0.616
8	170	2.77	108.41	111.18	18.53	18.52	...	...	18.52	...	...	0.663
9	210	5.20	137.61	142.81	23.80	23.66	...	...	23.80	...	...	0.696
10	250	10.33	166.21	176.54	29.42	27.00	...	...	29.42	31,651	47,650	0.700
11	264	12.13	176.22	188.35	31.39	28.12	37,616	38,238	31.26	33,116	50,038	0.699
12	300	32.78	197.22	230.00	38.33	21.75	33,168	44,080	38.31	37,447	50,229	0.653
13	350	90.78	215.22	306.00	51.00	1.54	21,792	51,115	59.55	45,366	51,245	0.555

\* Results show multiple-step design, not practicable for this example

\*\* See Fig. 8.

face, tension results. It cannot be said that such a section should never be used, but appreciable convexed curvature in regions of high compression should be permitted only after careful analysis of internal stress conditions.<sup>2</sup> Changes in face slope undoubtedly cause departure from the usually assumed straight line distribution of vertical pressures.

The difficulties enumerated can be eliminated only by alteration of the section above  $h = 264$  ft.

**35. Redesign.** To secure adequate joint length below  $h = 264$  ft, without reversed curvature or destructively large values of  $\sec^2 \phi'$ , widening must be begun at some elevation above  $h = 264$  ft. The simplest procedure is to begin at the top, converting the whole dam into a single block controlled by the rules for Zone VI.

The upstream face may be kept vertical to some depth to be determined by trial. Preliminary computations indicate a depth of about 100 ft, which may be used as a first assumption.

Solution is accomplished by trial. An arbitrarily assumed joint length may be placed in successive trial positions until that position is found which, without violating Rules 1 or 2, gives (if possible) satisfactory values for both  $p'_1$ , reservoir full, and  $p''_1$ , reservoir empty. If this cannot be accomplished with a given trial length, a longer length is assumed and the trial is repeated. If there is strength to spare, a shorter length may be tried, continuing until a

<sup>2</sup> Convexed profiles are used without question in the upper portions of overflow dams where compressive stresses are low.

TABLE 16  
SINGLE-STEP DESIGN, EXAMPLE 3

Line	Item	Description and dimensions	Forces (kips)		Levers (ft)	Moment (ft-kips)
			Horiz.	Vert.		
1	$W_0$	Masonry $4 \times 45 \times 0.15$		27.0	22.50	608
2	$W_1$	Masonry $0.5 \times 53.94 \times 45 \times 0.15$		182.0	30.00	5,460
3	$W_2$	Masonry $0.5 \times 350 \times 292 \times 0.15$		7,665.0	97.33	746,034
4	$W_3$	Masonry $0.5 \times 250 \times 18.5 \times 0.15$		346.9	-6.17	-2,140
5	Total	Reservoir empty		8,220.9	(91.23)	749,962
6	$W_4$	Vert. water $100 \times 18.5 \times 0.0625$		115.6	-9.25	-1,069
7	$W_5$	Vert. water $0.5 \times 250 \times 18.5 \times 0.0625$		144.5	-12.33	-1,782
8	$W_u$	Uplift $0.25 \times 350 \times 310.5 \times 0.0625$		-1,698.0	85.00	-144,330
9	$P$	Horiz. water $0.5 \times 350 \times 350 \times 0.0625$	3,828.1		116.67	446,615
10	$P_w$	Waves (Art. 3b)	2.1		351.50	738
11	Total	Reservoir full	3,830.2	6,783.0	(154.82)	1,050,134
12	$x_a$	Distance, axis to c.l. of base			136.75	
13	$M_F$	Moment about c.l. of base, reservoir full			18.07	122,569
14	$M_E$	Moment about c.l. of base, reservoir empty			45.52	374,215
15	Stresses, reservoir full, lb per sq ft			Stresses, reservoir empty, lb per sq ft		
16	$\Sigma(W) \div l = 6,783.0 \div 310.5 = 21,845$			$\Sigma(W) \div l = 8,220.9 \div 310.5 = 26,476$		
17	$6M_F \div l^2 = 6 \times 122,569 \div 96,410 = 7,628$			$6M_F \div l^2 = 6 \times 374,215 \div 96,410 = 23,289$		
18	Total $= p'_0$ 29,473			Total $= p''_0$ 49,765		
19	Inclined stress $= p'_0 \sec^2 \phi' = 49,987$			Inclined stress $= p''_0 \sec^2 \phi'' = 50,038$		

Data: Upstream face vertical above  $h = 100$  ft,  $\Delta l_u = 18.5$  ft,  $\Delta l_d = 292$  ft,  $l = 310.5$  ft.  $\tan \phi' = 0.83429$ ,  $\sec^2 \phi' = 1.696$ ,  $\tan \phi'' = 0.074$ ,  $\sec^2 \phi'' = 1.00548$ .  $\tan \theta$  reservoir full  $= 3,830.2 \div 6,783.0 = 0.565$ .

joint length is found which at its best position gives the allowable inclined stresses at the two faces simultaneously.

Computations for a trial joint length of 310.5 ft, with  $\Delta L_u = 18.5$  ft and  $\Delta L_d = 292$  ft, are shown in Table 16. As an aid to computations, the masonry section and vertical water areas are divided into rectangles and triangles as shown in Fig. 9. Moments are computed to a vertical extension of the upstream face at the top.

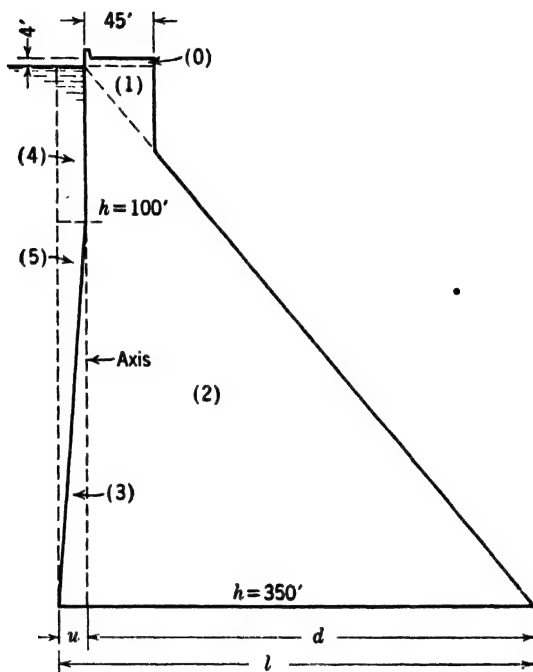


FIG. 9. Single-step design, Example 3.

The computed upstream and downstream inclined stresses at the base are, respectively, 49,987 and 50,038 lb per sq ft.  $\tan \theta$  is 0.565, which is safe. The depth below water surface being in excess of 300 ft, the shear-friction factor is computed as an added precaution. Its value is 5.9, which again is safe.

The resultant, reservoir full or empty, is well within the middle third. Check computations show that all stability requirements for the reservoir full or empty are more than satisfied at all joints above the base.

**36. Comparison of Sections.** The multiple-step design (Table 15) and the single-step design (Table 16) for Example 3 are platted together in Fig. 10. A section of Shasta Dam<sup>3</sup> is also shown, for comparison.

<sup>3</sup> U. S. Bur. Reclamation Spec. 780.

The multiple-step design is much the more economical for the upper portions of the dam, where it is practicable. The single-step design is, of course, understressed at all points except the base. Where a considerable portion of the dam is of less depth than sections  $a-b$  or  $c-d$ , Fig. 8, a substantial saving may be made by using a different section, based on the step-by-step design

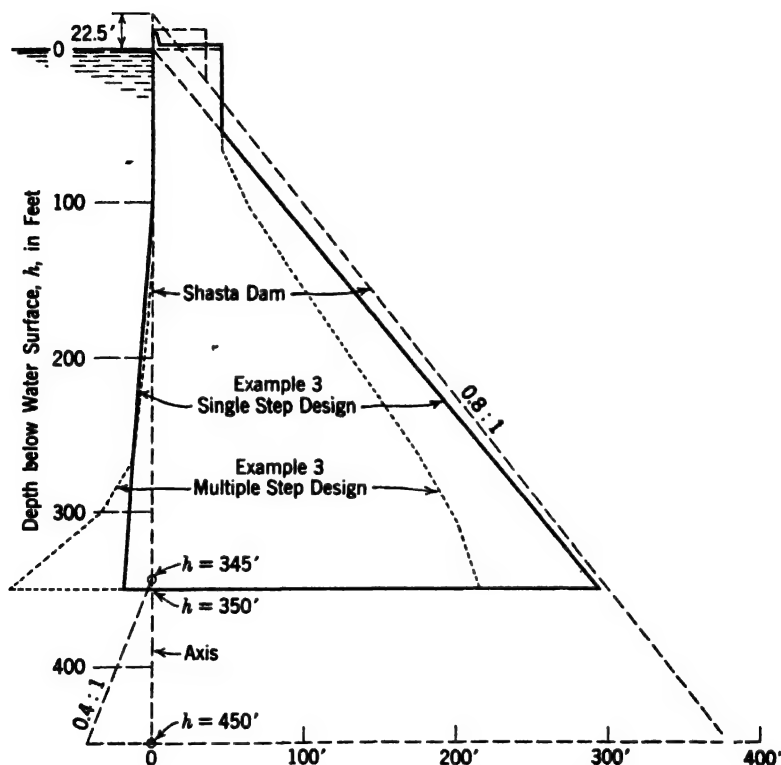


FIG. 10. Comparative sections, Example 3.

for such portions. In a possible case, the maximum section, requiring the full section of Fig. 9, may apply to only a short length of the central portion of the dam.

This example leads to the indication which may be proved, that for any specified stress there is a definite limit beyond which it is impracticable to go. However, for good foundations, and carefully planned and constructed masonry, stresses considerably above the value of 50,000 lb per sq ft here used may be permitted.

If the masonry stress rather than the strength of the foundation is controlling, it may be economical to increase the masonry strength through the use of more expensive materials, thus keeping out of Zones V and VI.

## COMPARISON OF NONOVERFLOW DAMS

**37. Comparison of Nonoverflow Dams.** A comparison of the sections of representative solid nonoverflow dams is given in Figs. 11 to 13, which also include for comparison the authors' examples. Comparisons of assumptions used and calculated stresses in these dams are given in Table 1, Chapter 8.

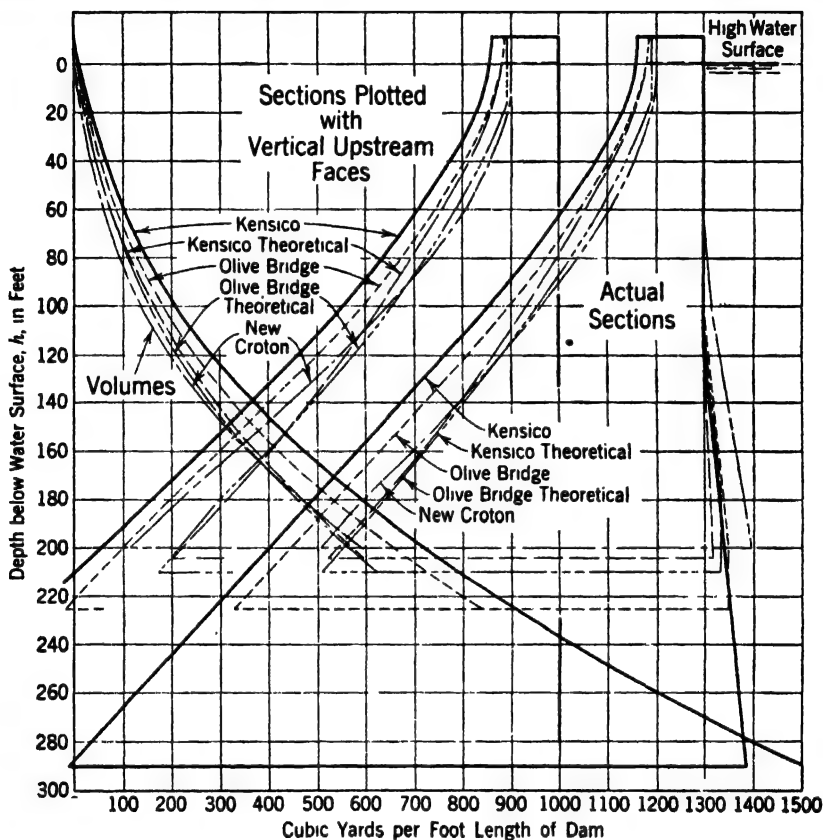


FIG. 11. Data on New York Board of Water Supply dams.

Differences in shape of these sections are due to differences in assumptions and also to the different factors of safety adopted. For instance, both the theoretical and adopted sections of the Olive Bridge and Kensico Dams are shown in Fig. 11. The theoretical sections agree very well with the authors' example, but the actual sections exceed the theoretical sections by a large margin. It has been stated that the increase was an arbitrary one to conform to the importance of the project. In order to assist in the comparison of these sections, they have also been plotted with vertical upstream faces. Cubic yards per foot of length for different heights of dam are also given.

The Tygart Dam, Fig. 13, is quite thick on account of a weak foundation. Some of the other dams shown on Figs. 12 and 13 adhere more closely to theoretical principles, as will be seen by a comparison of the authors' examples with the dams shown in the figures.

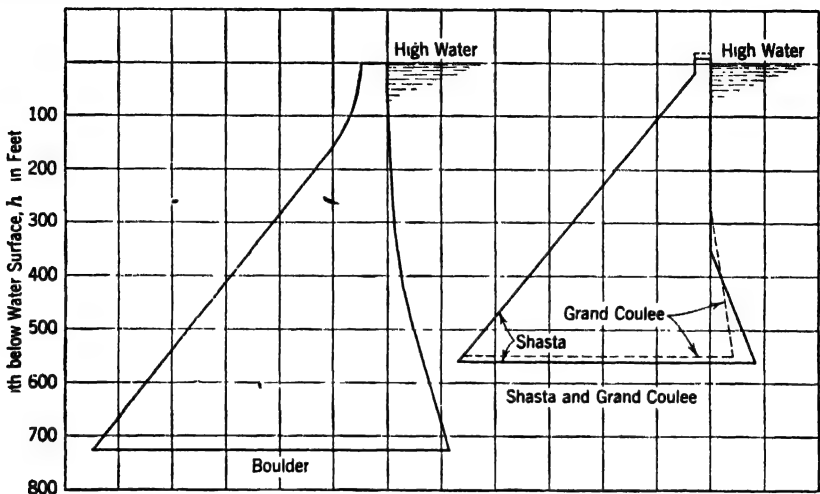


FIG. 12. Profiles of Shasta, Grand Coulee, and Boulder Dams.

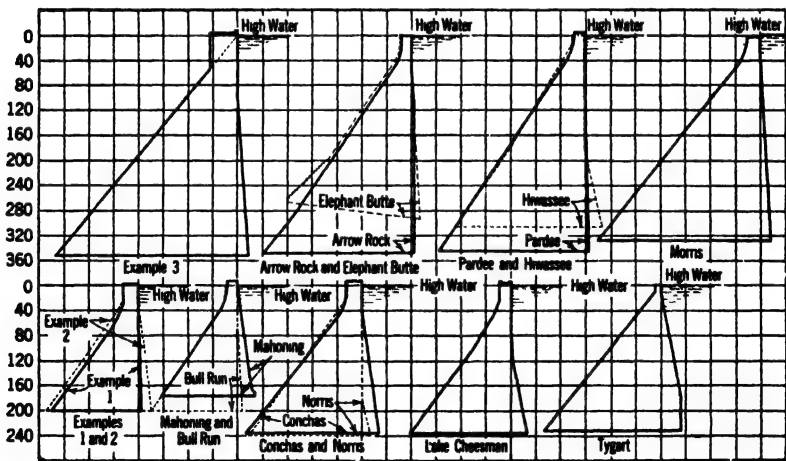


FIG. 13. Profiles of notable nonoverflow gravity dams.

Curves of quantities in nonoverflow dams, designed in accordance with stated assumptions, are indicated in Fig. 14. These are worked up with 140 lb per cu ft concrete for use in conservative preliminary estimates.

Table 17, compiled by Robert A. Sutherland in 1940, gives a list of representative solid gravity dams in this country and a few high foreign dams.

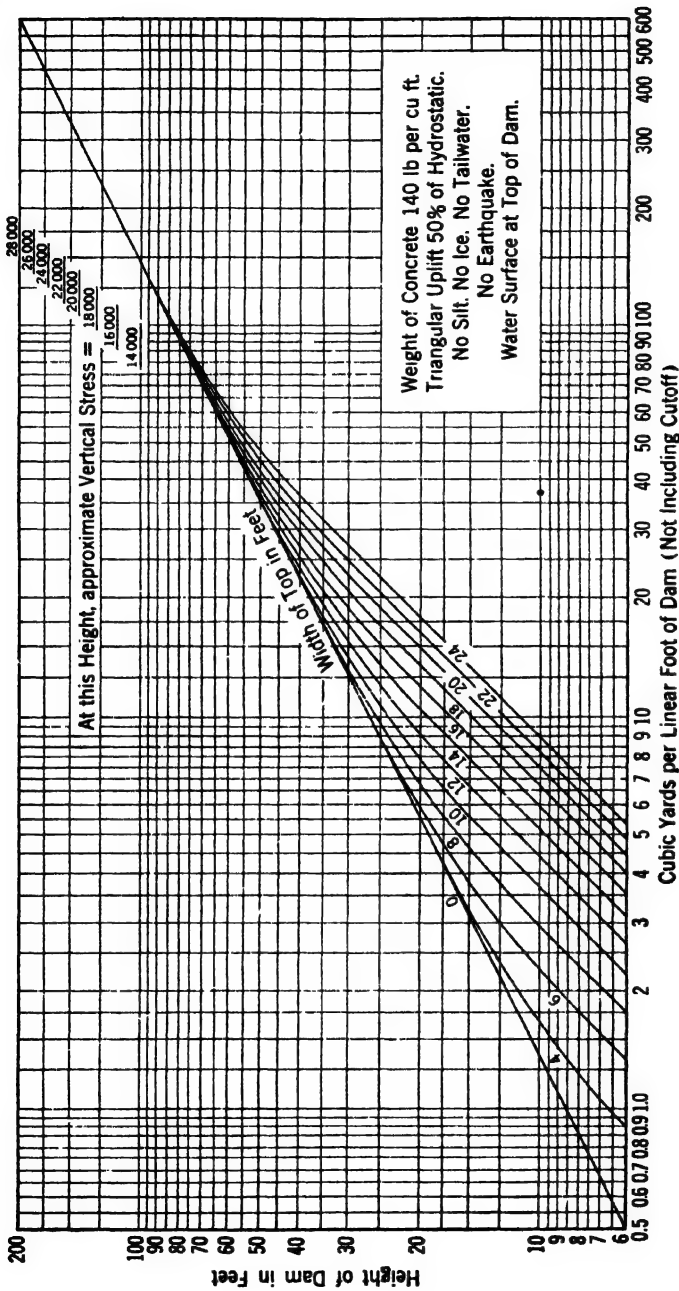


FIG. 14. Contents of solid nonoverflow dams.



TABLE 17  
REPRESENTATIVE LIST OF SOLID GRAVITY DAMS <sup>1</sup>

[Dates in parentheses indicate raising. Types: O = overflow; NO = nonoverflow; C = curved in plan]

No.	Name	Location	Height (ft.)	Date com- pleted	Foundation	Base width (ft.)	Type	References
								NOTE: Numbers in parentheses are dates of publication.
1	Alpine	Calif.	131	1918 (1941)	.....	...	...	26, 14 (12/41)
2	Arnold		110	1930?	.....	...	...	.....
3	Arrowrock	Idaho	348	1915	granite	238	NO, C	17, 20, 25, 23
4	Ashokan (Olive Bridge)	N. Y.	252	1911	slate, shale	190	NO	26, 20, 23, 17, 25, 1 (7/36)
5	Barker	Colo.	172	1909	granite	123	NO	20, 25, 18
6	Barrett	Calif.	192	1922	.....	...	...	28, 6 (10/27/21) (7/27/22)
7	Bartlett's Ferry	Ga.-Ala.	145	1925	.....	...	O	26
8	Big Creek #1	Calif.	132	1913	.....	...	...	26
9	Blackbrook		108	1905	.....	...	...	.....
10	Black Canyon	Idaho	184	1924	shale, basalt	130	O	6 (11/20/24), 9 (2/28) (8/28)
11	Boonton	N. J.	114	1905	sandstone, shale	77	NO	20, 26, 27, 25, 18
12	Boulder (gravity-arch)	Nev.-Ariz.	726	1935	andesite breccia	660	C	16, 9 (7/38)
13	Bull Run	Oreg.	200	1928	basaltic lava	...	...	.....
14	Butte City	Mont.	120	1892	.....	83	C	18, 26
15	Carpenter	Ark.	115	1931	.....	...	O	6 (2/5/31)
16	Cedar R.	Wash.	200	1915	.....	...	...	5 (4/10/15), 6 (7/12/28)
17	Cheat Haven	Pa.	100	1920?	.....	...	O	.....
18	Cheesman	Colo.	236	1904	granite	176	NO, C	18, 20, 26, 25
19	Cheoah	N. C.	230	1919	.....	...	...	.....

20	Claytor	Va.	123	1939	.....	108	...	...	7 (1/40), 6 (2/15/40)
21	Conchas	N. Mex.	235	1939	sandstone, shale	...	O	O	6 (5/28/36) (6/15/37) (6/9/38) (2/10/38), 9 (6/39), 1 (7/36)
22	Conowingo	Md.	100	1927	.....	...	O	O	6 (12/23/26) (1/28/32)
23	Copco #1	Oreg.	257	1922	.....	...	NO	NO	18, 20, 25, 26, 27
24	Cross River	N. Y.	170	1908	gneiss	116	NO	NO	18, 20, 25, 26
25	Croton Falls	N. Y.	167	1911	granite	128	NO	NO	26, 6 (5/11/22)
26	Devil's Gate	Calif.	140	1920	.....	98	NO, C	NO, C	23, 26, 28, 6 (6/1/23), 8 (7/27), 11 (4/23)
27	Don Pedro	Calif.	284	1923	.....	176	NO, C	NO, C	1 (1/36) (5/36)
28	Dover	Ohio	100	1937	limestone	...	O	O	.....
29	East Park	Calif.	139	1911	.....	...	...	...	28, 6 (5/5/21)
30	Eel River (Scott)	Calif.	135	1921	.....	...	...	...	16, 20, 23, 25, 8 (3/27)
31	Elephant Butte	N. Mex.	306	1916	sandstone	234	NO	NO	26, 28, 6 (5/28/25)
32	Exchequer (L. McClure)	Calif.	326	1926	greenstone	208	O, C	O, C	(8/26/26)
33	Fifteen Mile Falls	N. H.-Vt.	117	1930	schist	...	O	O	1 (1/34), 6 (9/29/32)
34	Friant	Calif.	290	1942	mica-schist	...	O	O	6 (8/26/37) (6/20/40), 14 (7/39) (8/39)
35	Gilboa	N. Y.	160	1927	.....	158	O	O	26, 6 (10/5/22)
36	Grand Coulee	Wash.	550	1942	granite	520	O	O	16, 1 (2/35), 6 (8/1/35) (12/23/37), 9 (7/38), 14 (12/37) (7/38)
37	Gravelly Valley	Calif.	106	1920	.....	...	...	...	.....
38	Gulf Island	Maine	110	1925	.....	...	...	...	.....
39	Hauser Lake	Mont.	132	1912	.....	...	...	...	20
40	Hemet	Calif.	135	1895	granite	100	O, C	O, C	18, 26, 28

<sup>1</sup> Compiled by Robert A. Sutherland, 1940.

TABLE 17—*Continued*  
REPRESENTATIVE LIST OF SOLID GRAVITY DAMS

No.	Name	Location	Height (ft)	Date com- pleted	Foundation	Base width (ft)	Type	References
41	Hiwassee	N. C.	307	1940	graywacke	235	O	1 (6/40), 6 (7/21/38) (9/14/39)
42	Holter	Mont.	110	1910	.....	...	...	2 (4/33)
43	Hoopes	Calif.	135	1934	.....	...	...	28
44	Huntington	Calif.	169	1912 (1917)	.....	...	...	6 (5/14/31)
45	Jordan	Ala.	125	1929	.....	...	O, C	18, 20, 25, 26, 1 (7/36)
46	Kensico	N. Y.	307	1916	schist, lime- stone, gneiss	230	NO	9 (1/30) 6 (12/31/31)
47	Koon	Pa.	108	1932	.....	...	O	20, 25, 26
48	La Grange (Turlock)	Calif.	127	1894	.....	90	O, C	.....
49	Loch Raven	Md.	103	1914	.....	...	...	6 (12/23/37) (12/1/38)
50	Mahoning	Pa.	160	1941	.....	...	O	(4/27/39)
51	Marshall Ford	Tex.	268	1941	limestone, shale	...	O	16, 9 (4/38) (2/40), 6 (5/13/37) (8/12/37)
52	Martin (Cherokee Bluffs)	Ala.	145	1926	.....	...	O, C	(8/24/39)
53	Medina	Tex.	178	1913	limestone	128	NO	6 (8/23/23) (12/30/26)
54	Mitchell	Ala.	105	1924?	.....	...	O	19, 20, 25, 26 15, 6 (9/27/23)

55	Morris (Pine Canyon)	Calif.	328	1934	grano-diorite gneiss	280	NO, C	1 (6/35) (9/35) (12/35), 6 (5/25/33) (12/27/34)
56	Mulholland	Calif.	204	1925	.....	175	NO, C	6 (5/3/34)
57	Narrows (Yadkin)	N. C.	216	1917	.....	185	O, C	20, 1 (5/31)
58	New Croton (Quaker Bridge)	N. Y.	238	1907	limestone	185	NO	17, 18, 21, 25, 26, 1 (7/36), 9 (1/36)
59	Norris (Cove Creek)	Tenn.	240	1935	dolomite	185	O	1 (6/33) (4/35) (12/35), 6 (5/25/33) (7/12/34) (12/6/34) (12/13/34)
60	Ocmulgee R.	Ga.	112	1915	.....	93	O	6 (11/27/30) (3/26/31), 7 (1931)
61	Osage (Bagnell)	Mo.	148	1931	dolomite and sandstone	298	C	26, 28, 3 (7/16/26), 6 (5/25/39), 14 (12/36)
62	O'Shaughnessy (Hetch Hetchy)	Calif.	430	1925 (1937)	granite	265	NO, C	6 (3/22/28)
63	Otay (lower)	Calif.	175	1919	.....	246	NO, C	16 (1938)
63a	Owyhee	Oreg.	405	1932	rhyolite	246	NO, C	28, 6 (2/14/29) (10/13/32)
64	Pardee (Lancha Plana)	Calif.	345	1929	.....	158	NO, C	6 (1/28/26)
65	Pit River No. 3	Calif.	112	1925	volcanic tuff and lava	158	O	6 (7/20/33)
66	Prettyboy	Md.	147	1934	schist	158	O	6 (4/30/31)
67	Rio Fuego	Tex.	125	1936?	.....	158	NO, C	16, 18, 20, 25
68	Rock Island	Wash.	108	1932	sandstone	158	NO, C	6 (1/11/34)
69	Roosevelt	Ariz.	285	1911	.....	158	NO, C	.....
70	Round Hill	Pa.	114	1901	.....	158	NO, C	.....
71	Safe Harbor	Pa.	106	1932	.....	158	O	.....
72	San Dimas	Calif.	130	1922	.....	158	NO, C	.....
73	San Mateo (Crystal Springs)	Calif.	154	1889	argillo calcareous limestone	176	NO, C	18, 20, 25, 26, 28

TABLE 17—Continued  
REPRESENTATIVE LIST OF SOLID GRAVITY DAMS

No.	Name	Location	Height (ft)	Date com- pleted	Foundation	Base width (ft)	Type	References
74	Savage	Calif.	167	1930	.....	...	...	28
75	Shasta	Calif.	560	1944	metamorphosed andesite	580	O, C	16, 6 (8/26/37) (11/18/37) (5/5/38), 14 (1/38) (4/38) (5/38) (6/38)
76	Shaver Lake	Calif.	173	1927	.....	...	...	28
77	Spiers Falls	N. Y.	154	1903	granite	113	NO	18, 20, 25, 26
78	St. Francis (Failed)	Calif.	205	1926	schist and conglomerate	176	NO, C	6 (3/22/28) (5/5/28), 9 (5/28)
79	Stevenson	Conn.	120	1919	.....	...	O, C	6 (8/17/39)
80	Sturgeon Pool	N. Y.	108	1920?	.....	...	O	15
81	Sweetwater	Calif.	129	1888 (1916)	porphyry	76 <sup>1</sup>	O, C	20, 26, 6 (8/3/22), 14 (3/40)
82	Tallulah (Burton)	Ga.	116	(1940)	.....	...	O	.....
83	Titicus	N. Y.	135	1895	granite	81	O	18, 20, 25, 26
84	Twin Falls	Idaho	137	1912	.....	...	...	.....

	Tygart	W. Va.	240	1938	sandstone and shale	195	O	
85								1 (6/35), 2 (11/35), 6 (2/6/36) (5/21/36)
86	Wachusset	Mass.	228	1906	granite, schist	187	NO	18, 20, 25, 26
87	White Salmon	Oreg.	125	1912	.....	...	O	26
88	Wilson (Muscle Shoals)	Ala.	140	1926	limestone	101	O	26, 6 (3/31/21) (4/23/25) (2/3/27)
89	Wolf Creek		130	1918?	.....	...	...	.....
	<b>Foreign Dams</b>							
90	Camarasa	Spain	333	1920	limestone	250	NO, C	22, 23, 26, 6 (8/17/22), 9 (1/30)
91	Chambon	France	450	1935	gneiss, schist, limestone	230	NO	22, 6 (12/26/35), 7 (1932), 10 (1, 2/35), 12 (7, 8/35) 6 (10/1/36)
92	El Fuerte	Mexico	300	1940?	.....	...	...	4 (12/30/38), 6 (10/20/38)
93	Genissiat	France	360	1942?	.....	230	NO	22, 23, 26, 27, 7 (1931) 6 (3/28/35)
94	Grimsef (Aare, Spitalamm)	Switzerland	377	1931	granite	320	NO, C	22
95	Ricobaya	Spain	326	1935	.....	251	...	13 (5/37)
96	Sarrans	France	360	1930	granite	...	...	6 (3/28/35)
97	Shing Mun	Hong Kong	300	1940?	granite	...	...	23, 26, 27, 1 (8/32), 6 (8/28/24) (9/9/26)
98	Tranco de Beas	Spain	295	1935?	.....	220	...	
99	Truyere	France	315	1933	.....	..	...	
100	Waggital (Schraeh)	Switzerland	366	1925	.....	246	NO	

TABLE 17—*Continued*

## REFERENCES

**Magazines**

1. Civil Engineering, New York.
2. Construction Methods, New York.
3. Engineering, London.
4. The Engineer, London.
5. Engineering Record, New York.
6. Engineering News-Record, New York.
7. Journal American Concrete Institute, New York.
8. Modern Irrigation, Los Angeles, Calif.
9. New Reclamation Era (now "Reclamation Era"), Washington, D. C.
10. Revue Generale de l'Hydraulique, Paris, France.
11. Successful Methods.
12. Travaux, Paris, France.
13. Water and Water Engineering, London, England.
14. Western Construction News, San Francisco, Calif.

**Books**

<i>Author</i>	<i>Book</i>
15. Creager and Justin	"Hydro-Electric Handbook," 1927.
16. U. S. Bureau of Reclamation	"Dams and Control Works," 1927 and 1938.
17. Seimemi	"Dighe."
18. Flinn, Weston, and Bogert	"Waterworks Handbook," 1918.
19. Hanna and Kennedy	"Design and Construction of Dams."
20. Davis and Wilson	"Irrigation Engineering," 1919.
21. Koechlin	"Mecanisme de l'Eau."
22. Lugeon	"Barrages et Geologie."
23. Schoklitsch	"Hydraulic Structures."
24. Scripps	"Yearbook."
25. Smith	"Construction of Masonry Dams."
26. Wegmann	"The Design and Construction of Dams," 1927.
27. Ziegler	"Der Talsperrenbau," Band II, 1927.

**Other References**

28. Hawley, "900 Dams Inspected," *Eng. News-Record*, 7/16/36.

## CHAPTER 11

### THE DESIGN OF SOLID SPILLWAY GRAVITY DAMS

**1. Methods of Design.** The general method of determining the stability of solid spillway dams differs in no way from that previously described for solid nonoverflow dams, except in the vicinity of the crest where, as previously mentioned, the section should be proportioned to fit the lower nappe of the sheet of water spilling over the dam during maximum flood. Principles of design developed in Chapter 10 will be supplemented as required but will not be repeated in this chapter.

**2. The Shape of the Crest.** (a) *Controlling factors.* It was pointed out in Art. 4 of Chapter 7 that if the sheet of water spilling over the dam leaves the face of the dam there is danger of the formation of a partial vacuum under the sheet with a resultant additional overturning force on the dam. Therefore, except for special conditions mentioned subsequently, it is desirable to shape the crest and the downstream face to completely fill the space under a freely discharging jet corresponding to the maximum flood to be expected.

Experiments have been made to determine the shape of the sheet of water flowing over aerated sharp-crested weirs. The general form of the sheet is

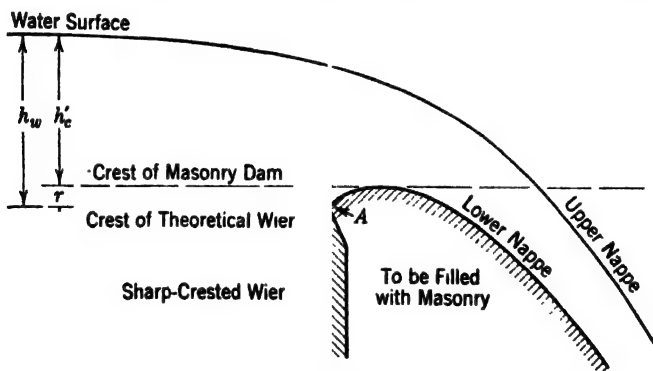


FIG. 1. Nappe for sharp-crested weir with vertical upstream face.

indicated in Fig. 1. If the area below the lower nappe is filled with masonry, the shape of the sheet and the discharge will not be changed appreciably.

This shape of crest has become standard in modern designs except for special considerations. For reference, therefore, it will be designated the "standard dam crest" and the head on the crest, used in establishing it, will be termed the "design head."



The designer is interested in both the shape of the standard dam crest and the discharge coefficient for the following types:

- Type 1. Straight dams with no velocity of approach.
  - (a) Vertical upstream face.
  - (b) Inclined upstream face.
- Type 2. Straight dams with appreciable velocity of approach.
  - (a) Vertical upstream face.
  - (b) Inclined upstream face.
- Type 3. Curved dams with no velocity of approach.
  - (a) Vertical upstream face.
  - (b) Inclined upstream face.
- Type 4. Curved dams with appreciable velocity of approach.
  - (a) Vertical upstream face.
  - (b) Inclined upstream face.

The shape of the crest for these types of dams will be covered in this article and the corresponding coefficients of discharge in Art. 3.

(b) *Types 1a and 1b. Straight dams—no velocity of approach.* Experiments by Bazin for the shape of the sheet of water flowing over a sharp-crested weir have been translated by Arthur Marichal and John C. Trautwine, Jr.<sup>1</sup> The experiments for weirs with vertical water faces, and those with water faces inclined 45°, apply directly to the determination of the shape of the crest of the ordinary types of solid and hollow dams, respectively. The curves indicated in Fig. 2 and Fig. 3 to about  $y = +0.12$  for the upper nappe and  $y = +0.65$  for the lower nappe are plotted directly from the experiments.

A mathematical extension of Bazin's experimental data made by Creager<sup>2</sup> was used in the completion of these figures. At the time of the first publication of Creager's data there were no experimental verifications of his mathematical extensions and he therefore recommended the use of a "masonry line," slightly beyond the computed lower nappe line. However, since then the accuracy of the extensions has been substantiated by experiments<sup>3</sup> and it is now considered permissible to limit the masonry to the computed lower nappe line.

(c) *Type 2a. Straight dams—appreciable velocity of approach—vertical upstream face.* The coordinates shown on Figs. 2 and 3 are for a zero or negligible velocity of approach. If the velocity of approach is appreciable, a wider path is followed by the jet. Coordinates for the lower nappe, with a vertical

<sup>1</sup> *Proc. Engs. Club of Philadelphia*, April 1893.

<sup>2</sup> WILLIAM P. CREAGER, *Engineering for Masonry Dams*, John Wiley & Sons, 1929, p. 106.

<sup>3</sup> Experiments by Ettore Scimemi, Figs. 22 and 23, p. 1114, *Trans. Am. Soc. Civil Engrs.*, Vol. 103, 1938, to a distance below the crest equal to  $6\frac{1}{2}$  times the head on the crest. Creager's "masonry line" is shown in the figures but the upper and lower nappes check his extensions. "Model Research on Spillway Crests," by Houser and Reid, *Civil Eng.*, January 1935, p. 10, to a distance below the crest equal to about four times the head on the crest.

upstream face, and appreciable velocities of approach are given in Table 1, which is based on experiments by Warnock.<sup>4</sup>

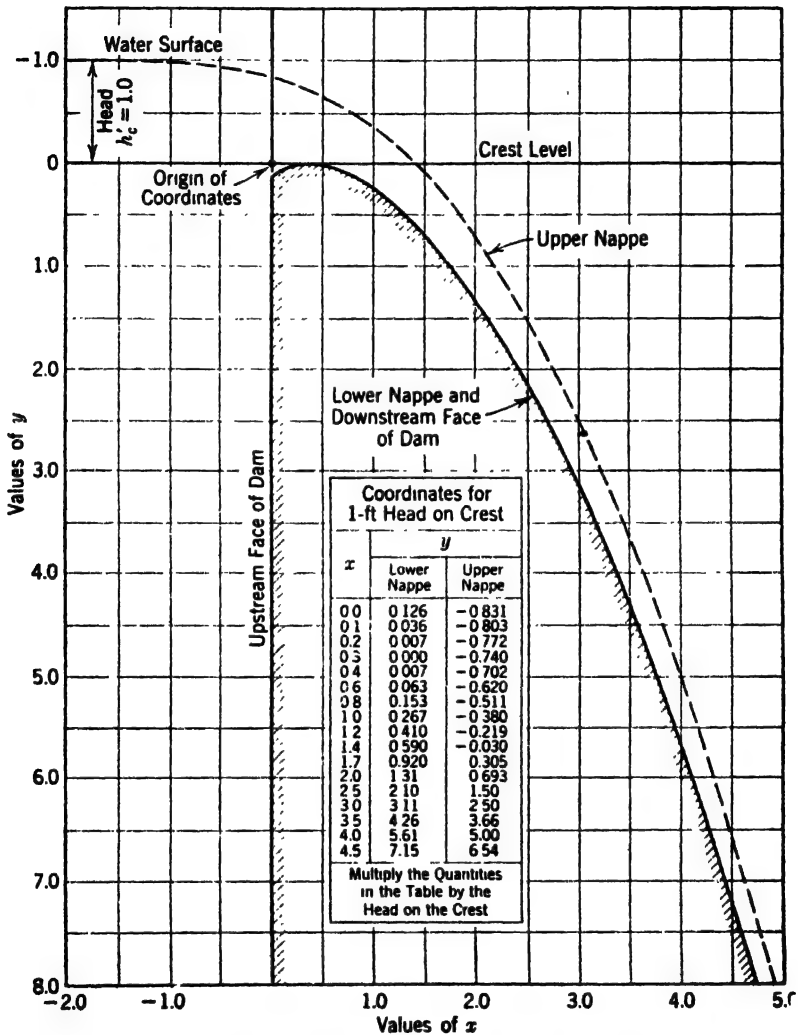


FIG. 2. Standard crest, upstream face vertical.

Values of  $x$  and  $y$  in Table 1 correspond to a value of unity for  $(h_w + h_v)$ ,  $h_w$  being the head on the theoretical crest of the sharp-crested weir (see Fig. 1) and  $h_v$  the head corresponding to the velocity of approach (see Figs. 5, 6,

<sup>4</sup> J. E. WARNOCK, *A Study for the Design of Crests for Overfall Dams*, thesis submitted to the faculty of the Graduate School of the University of Colorado, 1930; laboratory work by the U. S. Bur. of Reclam., Denver, Colo.

and 7, Chapter 7). To obtain true coordinates, multiply tabular values by the required value of  $(h_w + h_v)$ , determined as described in Art. 19. It should

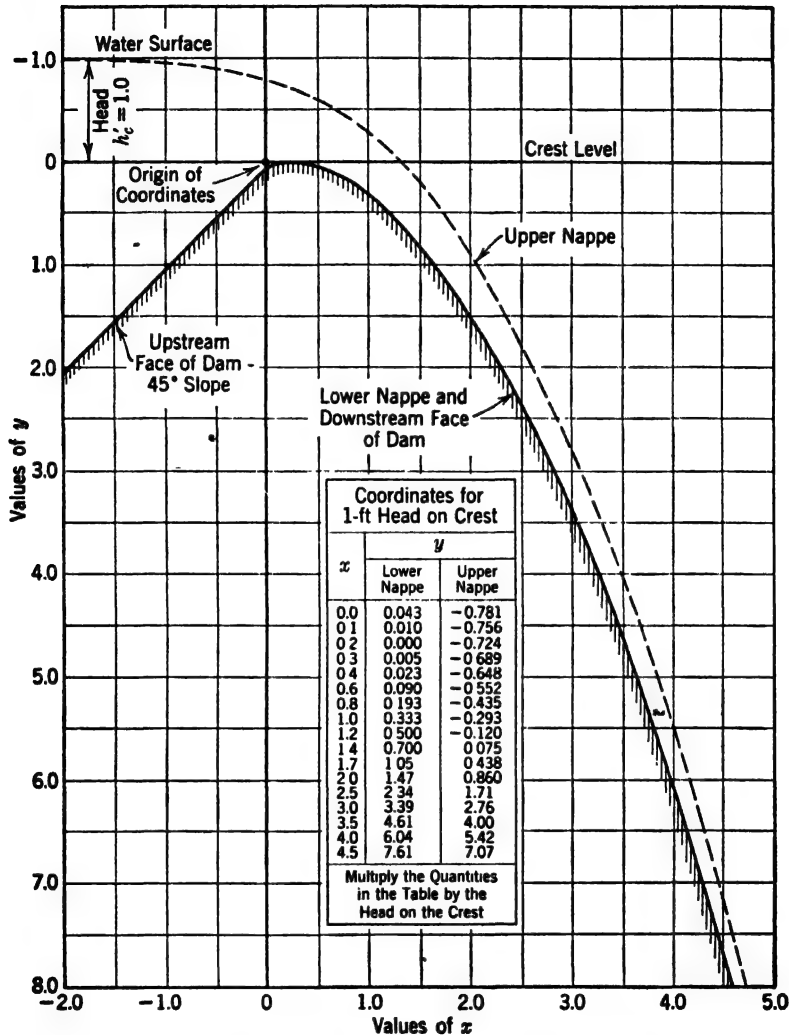


FIG. 3. Standard crest, upstream face inclined 45°.

be carefully noted that Table 1 is based on  $h_w$ , Fig. 1, and not on  $h'_c$ , as are the tables in Figs. 2 and 3.

Values in Table 1 for the almost negligible velocity of approach corresponding to  $\frac{h_v}{h_w + h_v} = 0.002$  will give a shape of crest which will agree almost exactly with the shape obtained from Fig. 2.

(d) *Type 2b. Straight dams—appreciable velocity of approach—inclined upstream face.* No data are available for this type. For such cases, experiments are necessary.

(e) *Type 3a. Curved dams—no velocity of approach—vertical upstream face.* The shape of crest for dams of this type is discussed in Shaft Spillways, Art. 3 of Chapter 6.

(f) *Types 3b, 4a, and 4b. Curved dams with inclined upstream face and curved dams with appreciable velocity of approach.* No data are available for these types. For such cases, experiments are necessary.

(g) *Influence of special details.* Experiments by Rouse and Reid <sup>5</sup> indicate that the shape of the crest will not be affected materially by details shown in Figs. 4a and 4b, provided the distance,  $d$ , is equal to at least one-half the sum

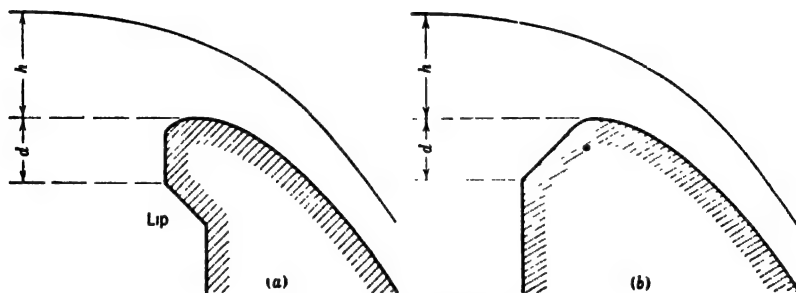


FIG. 4. Special crest details.

of the head on the crest and the head corresponding to the velocity of approach. This is because vertical velocities are small below such depth.

(h) *Adherence of jet.* Experiments <sup>6</sup> on models of standard dam crests have shown that the jet adheres to the concrete for heads on the crest up to 2 or 3 times the design head, even though the most effective practical means for admitting air is provided. Although it is not certain that the relationship will hold directly between model and prototype, adherence of the jet to accurately designed crests may be expected for heads considerably higher than the design head.

Should any irregularities exist in the crest which would cause eddies, or should the crest not correspond to the shape of the jet for appreciable velocities of approach, as previously explained, negative pressures may be set up on the face of the dam or the jet may jump clear if there are piers on the crest or other means of aeration.

Since the adhering nappe, with resulting partial vacuum under it, increases the coefficient of discharge, the crest, in special cases, has been shaped for a design head somewhat less than that for the expected flood, in order to increase the spillway capacity, making provisions at the same time for resisting the

<sup>5</sup> Rouse and Reid, op. cit.

<sup>6</sup> Idem.

TABLE 1  
COORDINATES OF LOWER NAPPE WITH VELOCITY OF APPROACH

$\frac{h_r}{h_w + h_v}$	0.002	0.020	0.040	0.060	0.080	0.100	0.120	0.140	0.160	0.180	0.200	0.220
$\frac{z}{h_w + h_v}$	$\frac{y}{h_w + h_v}$											
0.000	0.0000	0.0000	0.0000	0.0000	0.0000	0.0000	0.0000	0.0000	0.0000	0.0000	0.0000	0.0000
0.020	0.0280	0.0265	0.0250	0.0235	0.0220	0.0210	0.0200	0.0195	0.0190	0.0175	0.0160	0.0150
0.040	0.0490	0.0460	0.0440	0.0400	0.0380	0.0355	0.0340	0.0320	0.0310	0.0295	0.0280	0.0265
0.060	0.0650	0.0605	0.0570	0.0530	0.0500	0.0465	0.0440	0.0420	0.0405	0.0390	0.0365	0.0355
0.080	0.0765	0.0720	0.0670	0.0630	0.0585	0.0555	0.0520	0.0500	0.0480	0.0455	0.0430	0.0415
0.100	0.0860	0.0810	0.0760	0.0710	0.0655	0.0615	0.0580	0.0550	0.0525	0.0500	0.0480	0.0450
0.120	0.0940	0.0880	0.0825	0.0770	0.0715	0.0665	0.0625	0.0595	0.0560	0.0535	0.0505	0.0475
0.140	0.1000	0.0940	0.0880	0.0820	0.0755	0.0700	0.0655	0.0620	0.0580	0.0555	0.0515	0.0485
0.160	0.1045	0.0980	0.0920	0.0845	0.0780	0.0725	0.0675	0.0635	0.0595	0.0560	0.0525	0.0490
0.180	0.1080	0.1010	0.0945	0.0870	0.0800	0.0740	0.0685	0.0640	0.0600	0.0560	0.0530	0.0485
0.200	0.1105	0.1030	0.0965	0.0890	0.0815	0.0750	0.0695	0.0645	0.0595	0.0560	0.0520	0.0480
0.220	0.1120	0.1040	0.0975	0.0895	0.0820	0.0745	0.0690	0.0640	0.0590	0.0550	0.0510	0.0465
0.240	0.1120	0.1050	0.0980	0.0890	0.0815	0.0745	0.0680	0.0630	0.0575	0.0535	0.0490	0.0450
0.260	0.1120	0.1045	0.0975	0.0875	0.0800	0.0730	0.0665	0.0610	0.0560	0.0510	0.0465	0.0425
0.280	0.1115	0.1040	0.0960	0.0860	0.0780	0.0710	0.0645	0.0590	0.0535	0.0490	0.0445	0.0400

2.300	0.1105	0.1020	0.0940	0.0845	0.0760	0.0690	0.0620	0.0560	0.0505	0.0460	0.0415	0.0365
0.320	0.1090	0.1005	0.0920	0.0820	0.0735	0.0660	0.0590	0.0525	0.0480	0.0430	0.0380	0.0330
0.340	0.1070	0.0980	0.0885	0.0785	0.0700	0.0630	0.0555	0.0490	0.0440	0.0390	0.0340	0.0290
0.360	0.1040	0.0950	0.0855	0.0750	0.0670	0.0590	0.0515	0.0450	0.0400	0.0350	0.0300	0.0250
0.380	0.1010	0.0910	0.0815	0.0710	0.0625	0.0550	0.0475	0.0415	0.0360	0.0305	0.0255	0.0200
0.400	0.0970	0.0870	0.0770	0.0670	0.0580	0.0500	0.0425	0.0360	0.0310	0.0260	0.0200	0.0150
0.450	0.0845	0.0745	0.0650	0.0540	0.0450	0.0365	0.0290	0.0220	0.0165	0.0110	0.0060	0.0000
0.500	0.070	0.060	0.050	0.039	0.030	0.020	0.013	0.006	0.000	0.006	0.012	0.018
0.600	0.032	0.022	0.012	0.000	0.010	0.020	0.028	0.035	0.042	0.048	0.054	0.059
0.700	0.016	0.028	0.038	0.049	0.059	0.068	0.076	0.084	0.091	0.098	0.104	0.108
0.800	0.074	0.084	0.095	0.108	0.117	0.126	0.134	0.142	0.149	0.156	0.160	0.164
0.900	0.138	0.150	0.162	0.173	0.183	0.192	0.201	0.208	0.215	0.222	0.226	0.228
1.00	0.214	0.224	0.236	0.247	0.258	0.266	0.276	0.282	0.290	0.297	0.300	0.298
1.20	0.393	0.402	0.412	0.422	0.432	0.440	0.448	0.455	0.463	0.470	0.473	0.466
1.40	0.606	0.614	0.623	0.632	0.641	0.650	0.657	0.664	0.670	0.672	0.670	0.661
1.60	0.850	0.860	0.867	0.874	0.883	0.890	0.896	0.904	0.905	0.900	0.893	0.886
1.80	1.132	1.140	1.147	1.155	1.164	1.170	1.175	1.180	1.173	1.166	1.156	1.146
2.00	1.451	1.460	1.467	1.476	1.485	1.490	1.494	1.496	1.476	1.464	1.454	1.440
2.20	1.798	1.807	1.816	1.825	1.834	1.839	1.841	1.834	1.818	1.801	1.785	1.767
2.40	2.179	2.188	2.198	2.206	2.212	2.213	2.212	2.198	2.179	2.164	2.147	2.125
2.60	2.602	2.611	2.622	2.621	2.620	2.618	2.604	2.591	2.568	2.548	2.526	2.504
2.80	3.048	3.060	3.068	3.062	3.055	3.036	3.014	3.000	2.976	2.953	2.916	2.893

NOTE: Values above stepped line are measured upward from origin, values below are measured downward. Origin is at top of theoretical sharp-crested weir, point A, Fig. 1.

vacuum load on the dam. The difference in the discharge coefficient with and without adhering jets is shown in Fig. 7 and described in Art. 3.

When lift gates on the crest of a dam are being opened, the jet will at first shoot clear of the downstream face of a standard crest and there will be no vacuum under the jet. However, when the gate is nearly open, the air may not be admitted freely enough and the jet may become depressed and adhere to the face.

When the gate has been completely opened and is being closed, the jet will adhere to the face to a much lower elevation than that at which depression occurred while the gate was being opened, because for gate closure, a free air passage is not present at the start.

The stability of the dam is of course determined for the condition of full reservoir and crest gates closed. When the gates are partly open, the water pressure above the crest is reduced and this reduction is considered ample compensation for any possible partial vacuum under the jet.

(i) *Jet velocities.* Application of the equations of Art. 4, Chapter 7, requires a knowledge of the velocity of the overflowing jet, particularly its horizontal component,  $V_h$ , which for the standard crest is constant after the influence of contraction is passed. In the deriving of his shape of crest, Creager<sup>7</sup> found values of  $V_h$  as follows:

Vertical upstream face, zero velocity of approach,  $V_h = 6.63\sqrt{h_c}$

Upstream face inclined at  $45^\circ$ , zero velocity of approach,  $V_h = 6.52\sqrt{h_c}$

Values for other inclinations for zero velocity of approach may be obtained by interpolation. These values apply only to *standard* conditions, i.e., where the head exactly conforms to the design head. Data for higher or lower heads and for appreciable velocities of approach are not available. However, should occasion arise where such velocities are required, they may be estimated thus:

1. Using principles discussed in Art. 3, compute the required head or the discharge, whichever is unknown.

2. Choose a point well beyond the crest and compute by trial the thickness of sheet corresponding to the discharge, assuming the velocity head to equal the vertical fall from the energy gradient in the pond to the lower third line of the jet, and assuming the jet to be in contact with the masonry. Allowance for losses may be made according to judgment.

3. Assume the jet to be parallel to the face of the dam and resolve the velocity into components.

4. A more accurate determination may be made experimentally.

**3. Discharge Capacity.** (a) *Fundamental formula.*<sup>8</sup> Francis has determined that the discharge of water over dams may be expressed by the equation

$$Q = ql_n = Cl_n[(h_c + h_o)^{1.5} - h_o^{1.5}] \quad [1]$$

<sup>7</sup> WILLIAM P. CREAGER, *Masonry Dams*, New York, John Wiley & Sons, 1929, p. 107.

<sup>8</sup> A very complete discussion of the theory and experiments relating to the discharge of water over dams with various-shaped crests may be found in *U. S. Geol. Survey Water-Supply Paper* 200, by R. E. Horton.

where  $Q$  = the total discharge, in cubic feet per second;  $q$  = the discharge per linear foot of effective crest;  $l_n$  = the net or effective length of crest, i.e., the total length of crest corrected for end contractions due to piers and sharp-cornered abutments;  $h_c$  = the actual or measured head on the crest taken at a point sufficiently remote from the dam to avoid the surface curve;  $h_v$  = the head corresponding to the velocity of approach (see Art. 3c); and  $C$  = a coefficient which depends on the shape of the crest and the head on the crest.

An approximate form of Francis's equation is

$$Q = ql_n = Cl_n(h_c + h_v)^{1.5} \quad [2]$$

For the same values of  $C$ , Eq. 2 gives values of  $Q$  in excess of those from Eq. 1, not exceeding about 1 per cent for depths of channel of approach not less than twice the head on the crest.

(b) *End contractions.* Francis's equation for the necessary correction due to complete end contractions is

$$l_n = l_t - 0.1n(h_c + h_v) \quad [3]$$

where  $l_t$  = the total clear length of crest between abutments and piers and  $n$  = the number of complete contractions.

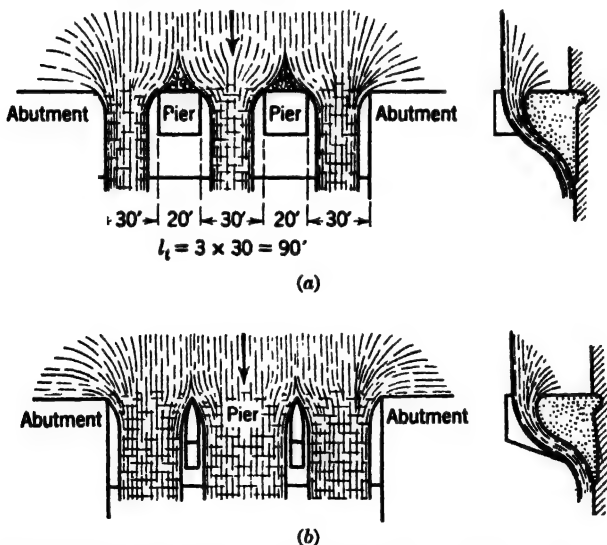


FIG. 5. (a), Complete contractions due to abutments and large piers. (b), Partial contractions due to sharp piers.

If the crest is obstructed by piers having considerable widths and sharp corners, as indicated in Fig. 5a,  $n$  represents the number of corners which serve to deflect the water, there being six complete contractions in this instance, two for each pier and one for each abutment. Usually, however, the piers are relatively thin and are provided with rounded corners or sharp



upstream ends, as indicated in Figs. 5b and 6. In such cases the contractions for the piers are not complete, and Francis's equation would give values of  $l_n$  too small. Francis's equation then may be written

$$l_n = l_i - (h_c + h_v)(K_a n_a + K_b n_b \cdots K_n n_n) \quad [4]$$

where  $K_a$ ,  $K_b$ , etc., represent the contraction coefficients applicable to the several different contractions which may be expected, and  $n_a$ ,  $n_b$ , etc., the number of contractions having contraction coefficients,  $K_a$ ,  $K_b$ , etc., respectively.

From a study of the data contained in the published experiments of the discharge capacity of the Wilson and Keokuk dams <sup>9, 10</sup> and other considerations, the authors have derived the approximate values of the coefficient of contraction,  $K$ , shown in Fig. 6, for piers having a thickness equal to about one-third the head on the crest. Exact values can be found only by experimentation.

For the case of one gate open and adjacent gates closed, each of the two end contractions may have a value of  $K$  equal roughly to about 2.5 times that when all gates are open.

When the length of the weir between end contractions becomes short relative to the head on the crest, the flow approaches that of discharge through an orifice and the principles of the weir no longer apply. In addition, the trajectory of the jet, fixing the shape of the crest of the dam, changes considerably. Therefore, when the length of crest between complete end contractions becomes less than about three times the head on the dam, or when the length of crest between piers of the usual type becomes less than about two times the head on the dam, the trajectory of the jet and discharge should be found by model experiments.

(c) *Velocity head correction.* The velocity head,  $h_v$ , introduced into Eqs. 1 and 2 to compensate for the motion of the water toward the weir, is found from the equation

$$h_v = \frac{V_a^2}{2g} \quad [5]$$

where  $V_a$  is the *effective* velocity of approach and  $g$  is the acceleration of gravity. The velocity in the channel of approach is not uniform. The filaments above the elevation of the crest sometimes have a velocity considerably

<sup>9</sup> L. G. PULS, "Spillway Discharge Capacity of Wilson Dam," *Trans. Am. Soc. Civil Engrs.*, Vol. 95, 1931, p. 316.

<sup>10</sup> NAGLER and DAVIS, "Experiments on Discharge over Spillways and Models, Keokuk Dam," *Trans. Am. Soc. Civil Engrs.*, Vol. 94, 1930, p. 777.

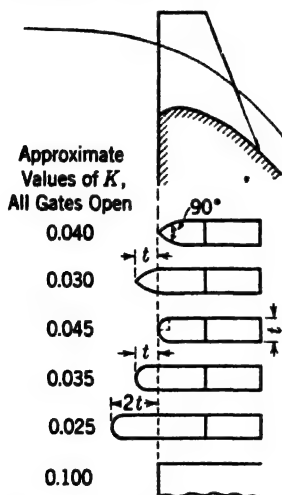


FIG. 6. Approximate contraction coefficients.

greater than the mean, depending on the depth and width of the channel and its surface conditions. The energy of the filaments above the elevation of the crest has a proportionately greater effect in increasing the discharge. The true value of  $V_a$  depends on too many variables to permit general determination. It may vary from 1.00 to 1.25 times the mean velocity.

In view of the fact that the velocity of approach above the elevation of the crest may be materially affected by wind, ice, and other conditions, it is usual

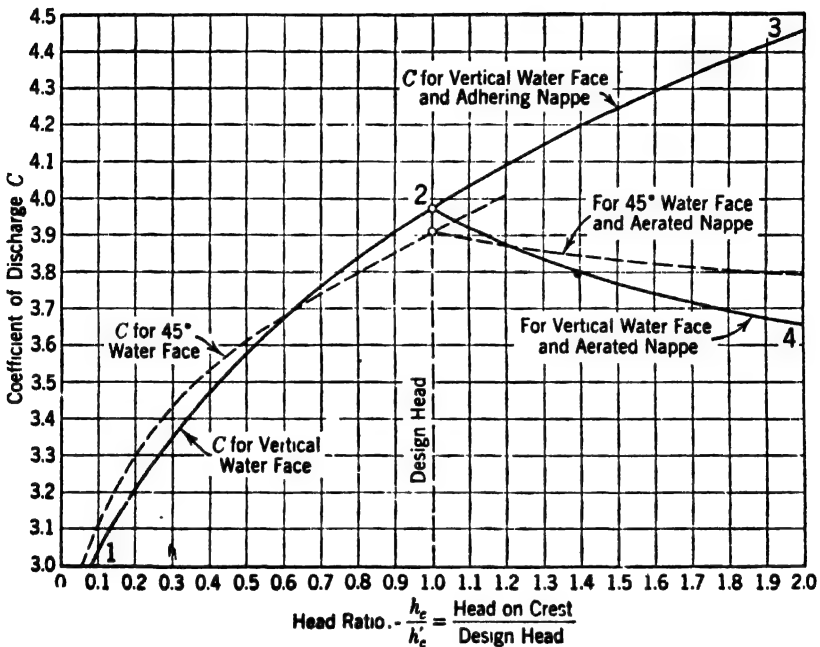


FIG. 7. Coefficients of discharge for straight standard dam crests with no velocity of approach.

to assume the velocity of approach equal to the mean velocity. Such an assumption is on the safe side when determining the capacity of the dam to pass the maximum flood.

If the spillway is to be used as a measuring weir, it may be desirable to make a more careful estimate of the velocity of approach, by study of experimental data for comparable installations, or by a model test.

If  $h_c$  is measured to a large pond,  $h_v$  may be neglected.

(d) *Coefficients for standard crests.* The designer is interested in the coefficient of discharge for the eight types of standard dam crests listed in Art. 2a.

(e) *Type 1a. Straight dams—no velocity of approach—vertical upstream face.* Values of  $C$  for Eqs. 1 and 2, applicable to this type of crest, can be obtained from the "vertical water face" curve of Fig. 7. The "design head,"  $h'_c$ , used in this figure is the head used in determining the shape of the crest as previ-

ously described. The first step in the determination of this curve is to find the coefficient of discharge  $C'$  for the design head  $h'_c$  as follows:

It will be remembered that the method of construction of the standard dam crest corresponds to the shape of the jet from a theoretical sharp-crested weir as shown in Fig. 1. Thus, for the design head, the discharge over the standard dam crest is the same as the discharge over the theoretical sharp-crested weir for the same elevation of water surface.

Francis's Eq. 1 was deduced from experiments on sharp-crested weirs, and the value of  $C$  was assumed to be constant at about 3.33 when the head was measured from the sharp crest, i.e.,  $h_w$  in Fig. 1.

From Fig. 1 and Art. 2, also tabulation in Fig. 2, for a vertical face and zero velocity of approach

$$h_w = h'_c + r = 1.126h'_c \quad [6]$$

where  $r$  is  $h'_c$  times the initial value of  $y$  in the table in Fig. 2, and  $h_w$  is the depth of the theoretical sharp crest below the design water depth.

Consequently, to obtain the coefficient,  $C'$ , applicable to the design head,  $h'_c$ , on the concrete crest, Francis's coefficient must be increased for use in Eqs. 1 or 2 thus:

$$C' = (1.126)^{1.5}C_w = 3.33(1.126)^{1.5} = 3.98 \quad [7]$$

The value of 3.98 for  $C'$  (or of  $C$ , Eqs. 1 and 2) is good only for flow at the design depth. In studying the performance of spillways, it is necessary to estimate discharges for all depths, and in such investigations,  $C$  must be treated as a variable. Discharge coefficients for standard crests for all ratios of actual head  $h_c$  to design head  $h'_c$ , up to 2.0, may be taken from Fig. 7. Point 2 on this diagram corresponds to a head ratio of 1.0, i.e., the actual discharge head is equal to the design head. The discharge coefficient is 3.98, as computed above. For actual heads smaller than the design head, the discharge coefficient is reduced, as indicated by the curve 1-2. For actual heads greater than the design head, there are two possibilities. If the overfalling stream adheres to the face of the dam, the value of  $C$  increases as indicated by the curve 2-3. If the overfalling stream leaps clear of the dam and if the space between the dam and the lower nappe is fully aerated, there will be a decrease in the value of  $C$  as indicated by the curve 2-4. It is only  $C$  and not the unit discharge,  $Ch_c^{1.5}$  that decreases with increasing values of  $h_c$  above the design head. As described heretofore, aeration is difficult if not impossible to obtain for standard dam crests.

Values of  $C$  for heads less than the design head, as shown in Fig. 7, for a vertical-face dam, were deduced from a study of a number of experiments on many types of crests. The curve for values of  $C$  greater than the design head was simply extrapolated. The curve for values of  $C$  greater than the design head, for the aerated nappe, was determined theoretically in the same manner as that previously used for determining  $C'$  for the design head.

Comparisons with the model experiments of Rouse and Reid <sup>11</sup> and those of Dr. Thoma in Munich <sup>12</sup> show that the curve agrees closely with experiment for values of  $\frac{h_o}{h_c}$  from about 0.1 to 0.3 and that it shows values of  $C$  about 2 per cent lower for values of  $\frac{h_o}{h_c}$  of 1.0 (design head) and about 3 per cent lower for values of  $\frac{h_o}{h_c}$  of about 2.0. Thus the curves are comparatively conservative and within the accuracy obtainable in actual dams.

(f) *Type 1b. Straight dams—no velocity of approach—inclined upstream face.* For this type, with a 45° upstream face, the coefficient of discharge,  $C'$ , for the design head in Fig. 7, was obtained in exactly the same manner as described in the previous item for Type 1b (vertical upstream face), except that  $r$  was taken as 0.043 and  $C_w$  as 3.66, resulting in a coefficient,  $C'$ , of

$$C' = (1.043)^{1.5} C_w = 3.66(1.043)^{1.5} = 3.91 \quad [7a]$$

There is evidence to indicate that when  $\frac{h_c}{h_o}$  is less than about 0.6, the values of  $C$  for a 45° water face are slightly greater than for a vertical face. No attempt was made to extrapolate the curve for a 45° face beyond the design head for the case of adhering jet, since no verification was available.

(g) *Type 2a. Straight dams—appreciable velocity of approach—vertical upstream face.* The curves of Fig. 7 apply to zero velocity of approach only. Since it has been shown in Art. 2c that the shape of the standard crest changes with the velocity of approach, it is evident that the coefficients of discharge also change.

The discharge may be computed by making  $C = 3.33$  in Eq. 1 or 2, and making  $h_c = h_w$  the depth to the theoretical sharp crest for the design depth. A coefficient applicable to the head on the actual crest, i.e., the design head  $h'_c$ , may be developed by following the procedure of Eqs. 6 and 7, the value of  $r$  being the maximum positive value of  $y$  computed from the appropriate coefficient from Table 1.

Also, in this manner values of  $C$  for heads greater than the design head, when fully aerated, can be obtained. However, as explained before, such aeration is difficult if not impossible to obtain for standard dam crests. There are no data for the value of  $C$  for heads less than the design head, nor for heads greater than the design head when not aerated. For such cases experiments are necessary.

(h) *Type 2b. Straight dams—appreciable velocity of approach—inclined upstream face.* No data are available for this type. For such cases, experiments are necessary.

<sup>11</sup> Op. cit.

<sup>12</sup> Reported by O. Dillman in "Untersuchungen an Überfällen," *Mitt. Hydraul. Inst. Tech. Hochs. München*, Heft 7 (Oldenbourg, Munich, 1933).

(i) *Types 3 and 4. Curved dams.* The correct shape of the crest of the dam, when curved and with zero velocity of approach and vertical upstream face, is described in Art. 3 of Chapter 6. For such dams with crests shaped in accordance therewith, the coefficient of discharge for the design head can be obtained from Fig. 7a.

(j) *Influence of special details.* For reasons explained in Art. 2e, the discharge coefficient is not appreciably altered by a re-entrance or lip as shown in Fig. 4a, or a change in the 45° water face as shown in Fig. 4b, provided the

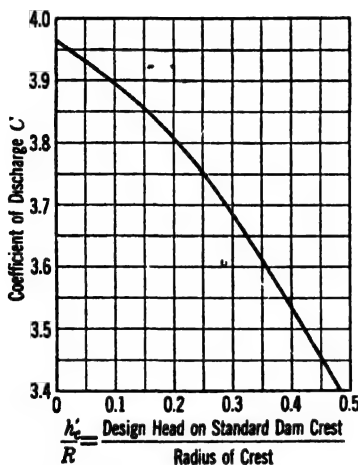


Fig. 7a. Coefficients of discharge for curved standard dam crests with vertical upstream faces, operating at design head, no velocity of approach.

distance  $d$  in both cases is equal to or greater than one-half the sum of the head on the crest and the head corresponding to the velocity of approach.

(k) *Special spillway types.* Certain types of collapsible dams, intakes of chute spillways (Art. 1, Chapter 6), and other wide flat intakes, require special formulas.

It is not always possible to use the standard crest form for a spillway. Certain types of dam crests require crest forms of other kinds. Also, crests of many forms will be found on existing dams which the engineer is frequently called upon to analyze. In many cases no experiments have been made on such types of crests and approximations must be made from data on the nearest type. Horton<sup>13</sup> has analyzed tests on a number of different types of dam

crests, and these will be found very useful in such cases. However, the "broad-crested" weir, a type most frequently substituted for the standard crest, will be described in the next section.

If Fig. 8a represents the upstream portion of a flat-top dam of appreciable width, or the intake to a chute spillway (Art. 1, Chapter 6), or similar conduit, the velocity at any point where the depth is  $d$  may be computed from the equation

$$V = \sqrt{2g(h_c + h_v - d - h_f)} \quad [8]$$

where  $h_f$  is the total head loss due to contraction and friction between the pond level and the point at which  $d$  is measured, other symbols being as shown in the figure.

The corresponding discharge is

$$Q = AV = ld\sqrt{2g(h_c + h_v - d - h_f)} \quad [8a]$$

<sup>13</sup> R. E. HORTON, "Weir Experiments, Coefficients, and Formulas," U. S. Geol. Survey Water-Supply Paper 200, 1907.

If the corner is well rounded to eliminate contraction and if the top of the dam is frictionless (or if friction is ignored),  $h_f$  is zero and Eq. 8 becomes

$$V = \sqrt{2g(h_c + h_v - d)} \quad [9]$$

Eq. 8a likewise becomes

$$Q = AV = ld\sqrt{2g(h_c + h_v - d)} \quad [9a]$$

If the top of the frictionless well-rounded dam is level, and if there is no obstruction to artificially hold up the water depth on the crest, the depth  $d$  will assume the minimum or critical value of

$$d = \frac{2}{3}(h_c + h_v) \quad [10]$$

which may be substituted in Eq. 9a to give

$$Q = 3.087l(h_c + h_v)^{1.5} \quad [11]$$

Of course, no dam top or spillway channel floor is frictionless; hence if the floor is level, as indicated in Fig. 8a, for any considerable distance, the depth

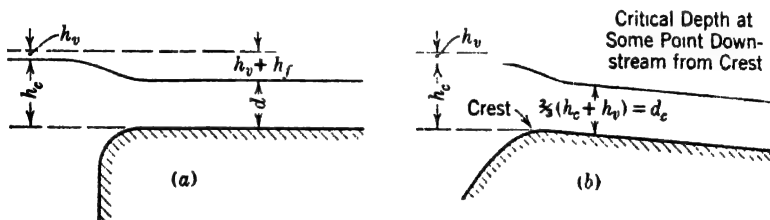


FIG. 8. Spillway intakes.

near the upstream edge of the crest will exceed the critical depth (Eq. 10), and resort must be had to Eq. 9a, the value of  $d$  being determined by means beyond the scope of this book. The usual procedure is to give the crest, or channel floor, a slope, as indicated in Fig. 8b, sufficient to balance the friction loss. The condition of frictionless flow is thus simulated and Eq. 11 becomes applicable, provided the depth is not held up by some constriction further downstream. If the slope *immediately* below the crest is greater than required to compensate for losses, the discharge may be increased.

Eq. 11 is usually used to compute the discharge of broad intakes for chute spillways. A small allowance for "entrance loss" may be made as a matter of safety. If the inlet is carefully designed, such loss will be small. Eq. 11 applies only to channel entrances, or to structures where the upstream and downstream length is several times the head  $h_c$ .

Eq. 8a is applicable to the discharge through restricted channels such as occur when cofferdams are built part way across a stream, and to temporary openings in dams to pass the stream during construction, as indicated in Fig. 9.

If  $h_f$  is negligible, use Eq. 9a. If the depth of water below the restriction is less than  $\frac{2}{3}(h_c + h_v)$ , the value of  $d$  for use in Eq. 9a should be made equal to  $\frac{2}{3}(h_c + h_v)$ <sup>14</sup> because the water surface through the restriction will be at that depth as hereinbefore explained. The value of  $l$ , in Eq. 11, as in all other cases, should be taken from Eq. 3 or 4.

(l) *Broad-crested weirs.* Flat-topped dams with square upstream corners (Fig. 10) are sometimes referred to as "broad-crested weirs." Discharge coef-

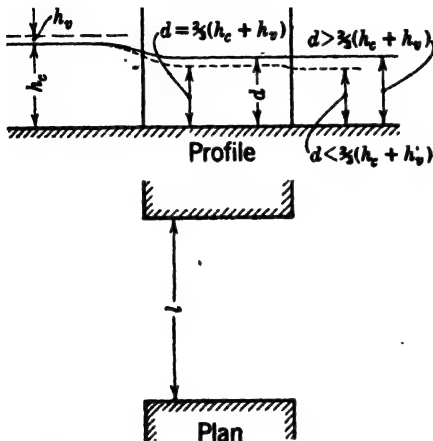


FIG. 9. Flow through restricted openings.

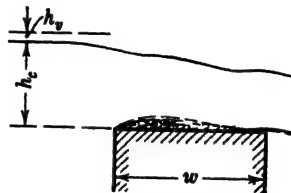


FIG. 10. Broad-crested weir not rounded.

ficients for such crests are irregular. If the head exceeds 1.5 to 2.0 times the crest width, the jet may jump clear of the crest, in which event the action is essentially that of a sharp-crested weir. Approximate coefficients for such weirs, based on available experimental data, are shown in Table 2.<sup>15, 16</sup> These coefficients are for use in the approximate equation

$$Q = C_b l n h_c^{1.1} \quad [11a]$$

(m) *Submerged spillways.* If the crest of the dam is submerged, as in Fig. 11a, the discharge coefficient, for use in Eqs. 1 and 2, should be modified according to the degree of submergence, as indicated in Table 2a.<sup>17</sup> In this table,  $C$  is

<sup>14</sup> Or Eq. 11 may be used, as it is the equivalent of Eq. 9a for  $d = \frac{2}{3}(h_c + h_v)$ .

<sup>15</sup> Computed from Bazin's experiments in *U. S. Geol. Survey Water-Supply Paper* 200, by R. E. Horton. Horton says these experiments apply to rising water surface only. Without aeration on top of the dam, the jet clears the crest at different heads for lowering water surface.

<sup>16</sup> Table is reproduced by permission from HORACE KING, *Handbook of Hydraulics*, McGraw-Hill Book Co., Inc., 1939, p. 164.

<sup>17</sup> From U. S. Deep Waterways experiments. See *U. S. Geol. Survey Water-Supply Paper* 200, p. 146. These experiments were made on a model having a rounded crest, approximating more closely than any of the others to the shape of a standard dam crest.

TABLE 2

VALUES OF  $C_b$  IN THE FORMULA,  $Q = C_b L_w h_c^{1.5}$  FOR BROAD-CRESTED WEIRS

[Applicable to rising water surface only]

Measured head in feet, $h_c$	Breadth of crest of weir (ft)										
	0.50	0.75	1.00	1.50	2.00	2.50	3.00	4.00	5.00	10.00	15.00
0.2	2.80	2.75	2.69	2.62	2.54	2.48	2.44	2.38	2.34	2.49	2.68
0.4	2.92	2.80	2.72	2.64	2.61	2.60	2.58	2.54	2.50	2.56	2.70
0.6	3.08	2.89	2.75	2.64	2.61	2.60	2.68	2.69	2.70	2.70	2.70
0.8	3.30	3.04	2.85	2.68	2.60	2.60	2.67	2.68	2.68	2.69	2.64
1.0	3.32	3.14	2.98	2.75	2.66	2.64	2.65	2.67	2.68	2.68	2.63
1.2	3.32	3.20	3.08	2.86	2.70	2.65	2.64	2.67	2.66	2.69	2.64
1.4	3.32	3.26	3.20	2.92	2.77	2.68	2.64	2.65	2.65	2.67	2.64
1.6	3.32	3.29	3.28	3.07	2.89	2.75	2.68	2.66	2.65	2.64	2.63
1.8	3.32	3.32	3.31	3.07	2.88	2.74	2.68	2.66	2.65	2.64	2.63
2.0	3.32	3.31	3.30	3.03	2.85	2.76	2.72	2.68	2.65	2.64	2.63
2.5	3.32	3.32	3.31	3.28	3.07	2.89	2.81	2.72	2.67	2.64	2.63
3.0	3.32	3.32	3.32	3.32	3.20	3.05	2.92	2.73	2.66	2.64	2.63
3.5	3.32	3.32	3.32	3.32	3.32	3.19	2.97	2.76	2.68	2.64	2.63
4.0	3.32	3.32	3.32	3.32	3.32	3.32	3.07	2.79	2.70	2.64	2.63
4.5	3.32	3.32	3.32	3.32	3.32	3.32	3.32	2.88	2.74	2.64	2.63
5.0	3.32	3.32	3.32	3.32	3.32	3.32	3.32	3.07	2.79	2.64	2.63
5.5	3.32	3.32	3.32	3.32	3.32	3.32	3.32	3.32	2.88	2.64	2.63

TABLE 2a

RELATIVE COEFFICIENTS, SUBMERGED CREST AND FREE CREST

$\frac{h_s}{h_c}$	$\frac{C_s}{C}$	$\frac{h_s}{h_c}$	$\frac{C_s}{C}$
0.0	1.000	0.6	0.907
0.1	0.991	0.7	0.856
0.2	0.983	0.8	0.778
0.3	0.972	0.9	0.621
0.4	0.956	1.0	0.000
0.5	0.937		



the coefficient for *free* discharge over a similar crest under the same head, and  $C_s$  is the modified coefficient due to the submergence. The heads are  $h_s$  and  $h_r$ , as in Fig. 11a.

It will be noted that, for values of  $h_s/h_c$  less than 0.30, the reduction in discharge is less than 3 per cent.

If a standing wave occurs below the crest, as indicated in Fig. 11b, the effect of submergence is lost and the discharge is the same as for a free crest.

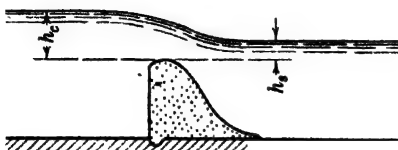


Fig. 11a. Submerged crest.

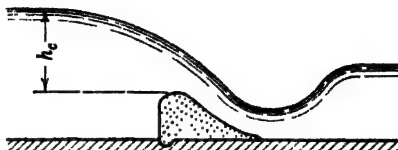


Fig. 11b. Submerged crest with standing wave.

(n) *Discharge through partly open crest gates.* It is not possible, within the scope of this book, to give data on the discharge through partly open crest gates, since the varied details of gates and supporting structures affect conditions materially. The reader is referred to the following publications:

Experiments on Wilson and Keokuk Dams, op. cit.

ROBERT E. HORTON, "Discharge Coefficients for Taintor Gates," *Eng. News-Record*, Jan. 4, 1934, p. 10.

THERON M. RIPLEY, "Discharge Through Taintor Gate Openings," *Civil Eng.*, August 1933, p. 386; BEN GUMENSKY, idem, November 1933, p. 627.

JULIAN HINDS, "Rating Curves for Canal Headgates," *Reclamation Record*, May 1922.

JULIAN HINDS, "Discharge Coefficients for Canal Headgates," *Reclamation Record*, October 1919.

**4. The Bucket.** Except for low dams, small maximum discharges, and the best rock foundations, a fillet or "bucket" should be provided at the toe of the spillway dam to deflect the sheet of water to a horizontal direction. A usual type of bucket is indicated in Fig. 22. Its use is obviously to prevent the impact of the falling water from scouring the foundation at the toe of the dam. Suggested dimensions are shown in Fig. 12.

Should the foundation be of such a character that, even with a bucket, some scour from the spilling water may be expected, more extensive provisions to prevent such scour must be made. These provisions are described in Part IV of Chapter 3.

The bucket, to be thoroughly effective, should be tangent to the foundation, or nearly so. A sudden enlargement where it joins the foundation will cause an eddy which, under the high velocity of the jet, will erode a stratified or soft foundation. The bucket is not considered in computing stability of the dam.

**5. Backwater Curves.** The flow in rivers having a variable cross-section or slope is known as varied flow. The backwater curve, upstream from a dam, as indicated in Fig. 13, is a typical example of varied flow.

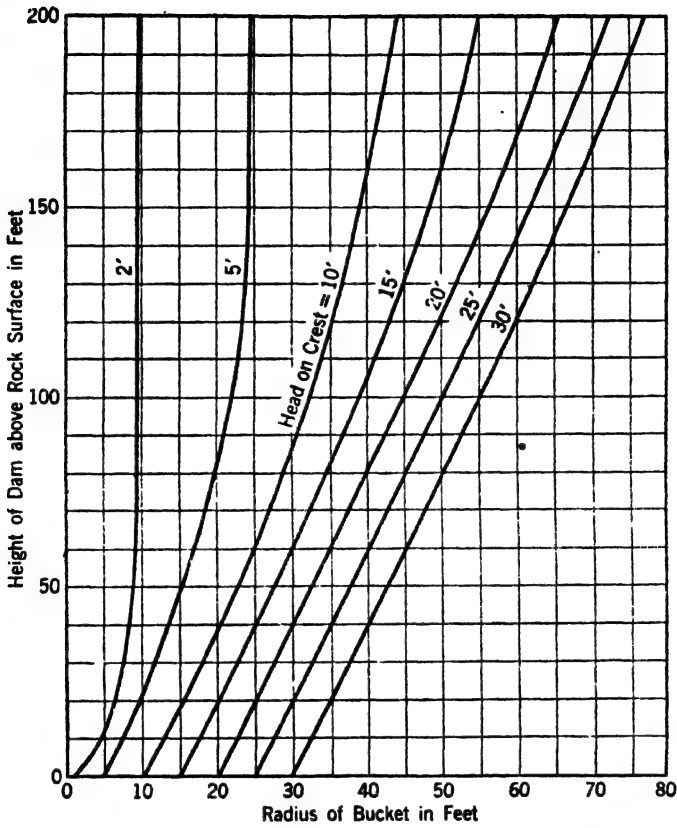


FIG. 12. Recommended radius of bucket for spillway dams with no tailwater.

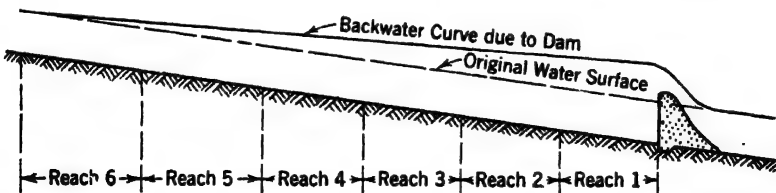


FIG. 13. Backwater curve.

Varied-flow problems can be approached most readily by the use of Bernoulli's theorem which, for open-water conditions, can be written

$$h'_e - h_e = h_w - h'_w + h_f \quad [12]$$

where the letters are as indicated in Fig. 14.

The river is divided into a number of reaches as shown in Fig. 13, although the reaches are usually more numerous than there indicated. Each reach should include a length that is reasonably uniform in section and slope. Each reach is investigated separately. The more numerous the reaches the more accurate will be the determination of the slope.

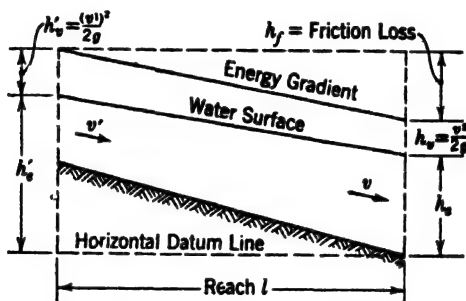


FIG. 14. Elements of backwater computations.

Let Fig. 14 indicate a typical reach. The first reach to be investigated is that adjacent to the controlling section, which is the section next to the dam for backwater curves. In Eq. 12,  $h_e$  and  $V^2/2g$  at the dam can be determined for any given flow. A trial value for  $h'_e$  is assumed and  $h'_w = V'^2/2g$  calculated.

With the trial value of  $h'_e$  and the known value of  $h_e$ , values of the hydraulic radius and velocity at each end of the reach are calculated and averaged. With these average values, and the coefficient of friction applicable to the channel, the slope, and hence the total trial friction loss for the length,  $l$ , of the reach are calculated.<sup>18</sup>

If this value of  $h_f$  does not give equality in the two sides of Eq. 12, new assumptions of  $h'_e$  must be made and the calculations repeated until an agreement is reached.

Values thus determined for the upper end of the first reach are to be used for the lower end of the second reach.

The foregoing discussion assumes that the reduction in velocity, as the water flows toward the dam, is very gradual. Should there be a sudden decrease in velocity, there should be added to  $h_f$  the corresponding loss due to sudden enlargement according to the principles of hydraulics.

When a reservoir is created on a flat, silt-laden stream, silt not only deposits in the reservoir but also in the river upstream from the reservoir. As a result,

<sup>18</sup> This should include the loss for obstructions, such as bridge piers, and for sudden enlargements and contractions.

the river bed upstream from the reservoir may be raised so high that high water is increased far beyond the backwater curve as computed for the unsilted condition. This condition is controlled by many variables, and rules for its general solution are not available.

### EXAMPLE 1. SOLID OVERFLOW DAM

**6. Data for Example 1.** The design of a straight, solid overflow dam will be illustrated by an example based on the following data:

$H$ = maximum depth of water to be retained	= 110 ft
$h_t$ = depth of tailwater	= 40 ft
$h_s$ = depth of silt against upstream face	= 60 ft
$h'_c$ = height from spillway crest to maximum water level	= 10 ft
$w_1$ = weight of masonry	= 150 lb/cu ft
$w_2$ = weight of water	= 62.5 lb/cu ft
$w'_s$ = dry weight of silt	= 100 lb/cu ft
$\lambda$ = specific gravity of silt particles	= 2.65
$\alpha$ = angle of internal friction for silt	= 30°
$c$ = uplift area factor <sup>19</sup>	= 0.75
$\zeta$ = uplift intensity factor	= 0.50
$f$ = allowable coefficient of friction for joints and base	= 0.75
$S_{s-f}$ = minimum allowable shear-friction safety factor.	
Required to be used only where $\tan \theta$ exceeds 0.75 = 0.75	
$p_i$ = maximum allowable inclined stress in dam and foundation	= 50,000 lb/sq ft

**7. Shape and Dimensions of Crest.** Crest dimensions may be computed from the tabular data for the lower nappe, Fig. 2, or if desired, a series of circular arcs may be substituted. It is desirable that the theoretical shape be closely followed, and abrupt changes should be avoided. The theoretical crest will be used in this example.

The computations will be made by the step-by-step procedure, with a resulting broken profile, and then compared with a straight-face design.

**8. Water and Silt Pressures.** Assuming no end contractions and ignoring velocity of approach in a first trial, the maximum discharge from Eq. 1 is 125.8 cu ft per sec per linear ft of crest. With a water depth of 50 ft above the silt bed, the velocity of approach is 2.52 ft per sec,  $h_a$  being 0.08 ft, which is negligible for this example. The water pressure on the face of the dam safely may be represented by the trapezoid 1-2-3-4, Fig. 15a. (See also Fig. 7, Chapter 7.)

<sup>19</sup> A value less than unity is introduced to illustrate procedure, although, as previously explained, the authors recommend  $c = 1.0$ .

The silt pressure is computed in accordance with Art. 7, Chapter 7. The submerged weight of the silt is found from Eq. 21, Chapter 7, thus:

$$w_s = 100 \cdot \frac{2.65 - 1}{2.65} = 62.3 \text{ lb/cu ft} \quad [13]$$

Inserting this value in Eq. 19, Chapter 7, and taking  $\sin \alpha$  as 0.5, the silt pressure is

$$P_s = 0.5 \times 62.3 \left( \frac{1 - 0.5}{1 + 0.5} \right) h_s^2 = 10.4 h_s^2 \text{ lb} \quad [14]$$

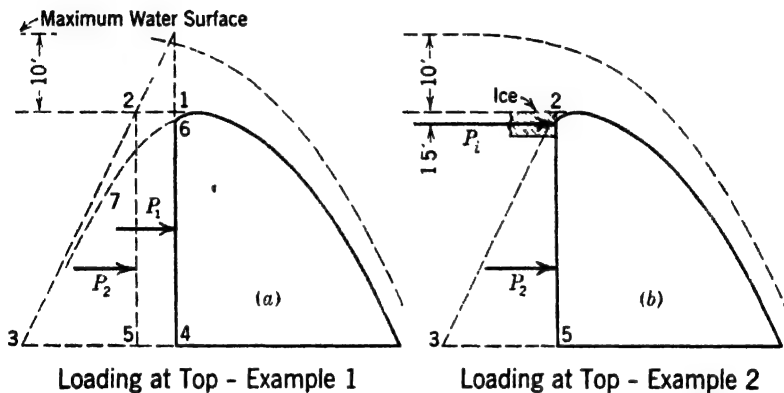


FIG. 15. Top loadings, Examples 1 and 2.

**9. Zones I and Ia, Example 1.** As stated in Art. 5, Chapter 9, Zone I is that portion of the top of the overflow dam in which both rules 1 and 2a are necessarily violated. Zone Ia is the next lower portion which complies with rule 1 but not with rule 2a. Any unfavorable conditions in these two zones are met by means other than changing the dimensions of the dam; hence they may be temporarily ignored. (Sec Art. 13.)

**10. Zone II.** For a limited distance below the bottom of Zone Ia, a section with a vertical upstream face and following the overflow curve more than fulfills stability requirements. This distance constitutes Zone II. The depth of Zone II is found by trial.

The top of the dam is drawn to large scale (say 0.5 in. = 1.0 ft), and divided into horizontal slices as indicated in Fig. 16. The lengths of the joints are found by multiplying tabular values from Fig. 2 by the value of  $h'_c$ , which is 10 in this example. Each slice, except the top one, is divided into a rectangle and an approximate triangle, and weights and moments about the upstream face are computed in Table 3, which extends down to  $h_d = 3h'_c = 30$  ft.

Stability computations at  $h_d = 30$  are shown in Table 4, which is similar to tables described for nonoverflow dams in Chapter 10. Moments and forces

TABLE 3  
UPPER PORTION OF EXAMPLE 1

$h_d$ (ft)	Item *	Description and dimensions	Weight (lb)	Lever (ft)	Moment (ft-lb)
1.26	(1)	$6.23 \times 150$	935	3.25	3,039
2.0	(2)	$0.74 \times 7.40 \times 150$	822	3.70	3,041
2.0	(3)	$0.5 \times 0.74 \times 1.45 \times 150$	81	7.88	638
4.0	(4)	$2.00 \times 8.85 \times 150$	2,655	4.42	11,735
4.0	(5)	$0.5 \times 2.00 \times 3.00 \times 150$	450	9.85	4,432
6.0	(6)	$2.00 \times 11.85 \times 150$	3,555	5.92	21,046
6.0	(7)	$0.5 \times 2.00 \times 2.25 \times 150$	338*	12.55	4,242
8.0	(8)	$2.00 \times 14.08 \times 150$	4,224	7.04	29,737
8.0	(9)	$0.5 \times 2.00 \times 1.83 \times 150$	274	14.69	4,025
10.0	(10)	$2.00 \times 15.95 \times 150$	4,785	7.98	38,184
10.0	(11)	$0.5 \times 2.00 \times 1.66 \times 150$	249	16.50	4,108
15.0	(12)	$5.00 \times 17.65 \times 150$	13,238	8.82	116,759
15.0	(13)	$0.5 \times 5.00 \times 3.65 \times 150$	1,368	18.87	25,814
20.0	(14)	$5.00 \times 21.30 \times 150$	15,975	10.65	170,134
20.0	(15)	$0.5 \times 5.00 \times 3.10 \times 150$	1,162	22.33	25,947
30.0	(16)	$10.00 \times 24.40 \times 150$	36,600	12.20	446,520
30.0	(17)	$0.5 \times 10.00 \times 5.20 \times 150$	3,090	26.13	101,907
30.0	Total		89,801	11.26	1,011,308

\* See Fig. 16.

for the masonry, line 1, are transferred from Table 3. The uplift,  $W_u$ , line 2, is based on Eq. 18, Chapter 7. For convenience, the horizontal water pressure is divided into a rectangle and a triangle, as illustrated in Fig. 15a.

Tan  $\theta$  is found to be 0.53, and the resultant, reservoir full, is inside the middle third by 1.47 ft; hence the bottom of Zone II has not been reached.

From a new trial (computations not shown) the resultant, reservoir full, is found to be exactly at the downstream middle third at 40 ft below the crest,  $h_2 = 40$ ,  $h_1 = 50$ .

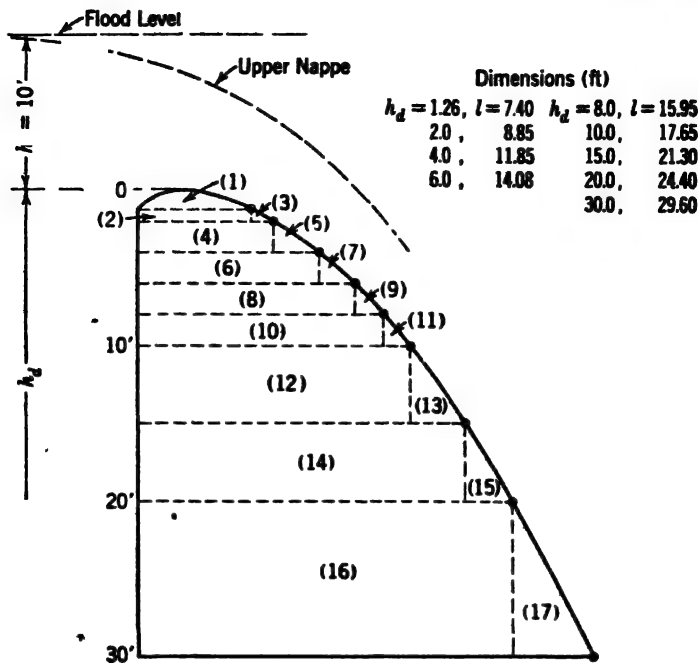


FIG. 16. Top details, Example 1.

TABLE 4  
STABILITY AT  $h_d = 30$  FT, EXAMPLE 1

Line	Item	Description and dimensions	Forces (lb)		Lever (ft)	Moment (ft-lb)
			Horiz.	Vert.		
1	$W_1$	From Table 3		89,801	11.26	1,011,308
2	$W_u$	$40 \times 62.5 \times 0.5 \times 0.75$ $\times 0.5 \times 29.70$		-13,922	9.90	-137,828
3	$P_1$	$10 \times 62.5 \times 30$	18,750		15.00	281,250
4	$P_2$	$0.5 \times 62.5 \times 30^2$	23,625		10.00	236,250
5	Total		42,375	75,879	(18.33)	1,390,980

Data:  $h_1$  = water depth = 40 ft,  $h_d$  = depth below crest = 30 ft,  $l$  = length of joint = 29.7 ft,  $\frac{2}{3}l$  = 19.8 ft.  
Results:  $\tan \theta = 0.53$ , resultant inside by 1.47 ft.

TABLE 5  
BLOCK 1, ZONE III, EXAMPLE 1, FINAL TRIAL

Line	Item	Description and dimensions	Forces (lb)		Lever (ft)	Moment (ft-lb)
			Horiz.	Vert.		
1	$W_0$	Masonry above $h_d = 40$		137,989		1,786,917
2	$W_1$	$34.65 \times 10 \times 150$		51,975	17.32	900,207
3	$W_2$	$0.5 \times 6.55 \times 10 \times 150$		4,912	36.83	180,909
4	Total	Reservoir empty				
5	$W_u$	Uplift = $50 \times 62.5 \times 0.5$ $\times 0.75 \times 0.5 \times 41.20$		-28,969	(13.73)	-397,744
6	$P_1$	$10 \times 62.5 \times 50$	31,250		25.00	781,250
7	$P_2$	$0.5 \times 62.5 \times 50^2$	78,125		16.67	1,302,083
8	$P_s$	Silt = $10.4 \times 10^2$	1,040	.	3.33	3,467
9	Total	Reservoir full	110,415	165,907	(27.47)	4,557,089

Data:  $h_1$  = water depth = 60 ft,  $h_d$  = depth below crest = 50 ft,  $h_s$  = silt depth = 10 ft,  $l_0$  = length of top joint = 34.65 ft.  
Results:  $l = 41.2$ ,  $\frac{2}{3}l = 27.45$ ,  $\tan \theta = 0.665$ .

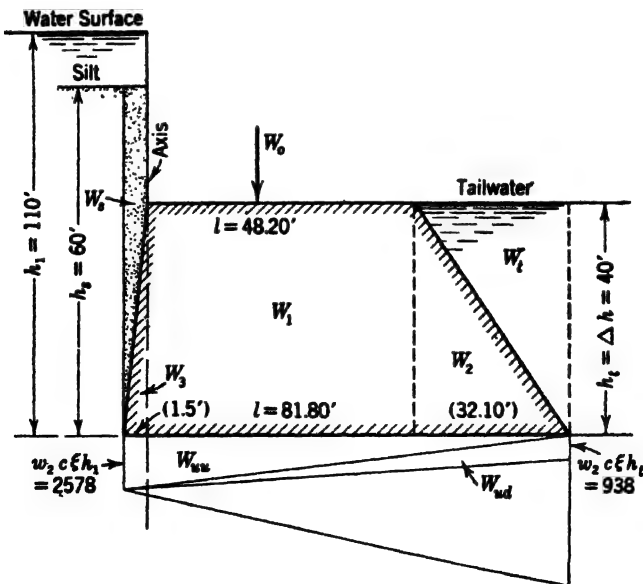


FIG. 17. Final block, Example 1.



**11. Lower Zones.** Below  $h_d = 40$  ft the procedure is exactly the same as for nonoverflow dams, as described in Chapter 10. Two sets of computations will be shown to illustrate the handling of silt and tailwater loads, which were not included in any of the examples of Chapter 10.

Table 5 is for the final trial for the first block in Zone III. The totals for reservoir empty are taken without silt pressure, as the silt increases stability against overturning upstream. Computations for silt shown in line 9 are according to Eq. 14. Table 5 requires no further explanation.

Computations for the last block in the dam are shown in Table 6. A few new steps, applicable to either overflow or nonoverflow dams and not previously illustrated, are introduced.

TABLE 6  
LAST BLOCK, EXAMPLE 1, FINAL TRIAL

Line	Item	Description and dimensions	Forces (lb)		Lever (ft)	Moment (ft-lb)
			Horiz.	Vert.		
1	$W_0$	Masonry above $h_d = 60$		261,900		4,375,000
2	$W_1$	Masonry, $48 \times 2 \times 140 \times 150$		289,200	24.10	6,970,000
3	$W_2$	Masonry, $0.5 \times 30 \times 40 \times 150$		90,000	58.20	5,238,000
4	Total	Reservoir empty		641,100	(25.87)	16,583,000
5	$W_{uu}$	Upstream uplift = $11.72 \times 110 \times 78.2$		-100,800	26.07	-2,628,000
6	$W_{ud}$	Downstream uplift = $11.72 \times 40 \times 78.2$		-36,700	52.13	-1,913,000
7	$W_t$	Wt. tailwater = $0.5 \times 30 \times 40 \times 62.5$		37,500	68.20	2,558,000
8	$P_1$	$625 \times 100$	62,500		50.00	3,125,000
9	$P_2$	$0.5 \times 62.5 \times 100^2$	312,500		33.33	10,417,000
10	$P_s$	Silt = $10.4 \times 60^2$	37,400		20.00	748,000
11	$P_t$	Tailwater	-50,000		13.33	-667,000
12	Total	Reservoir full	362,400	541,100	(52.16)	28,223,000

Data:  $h_1$  = water depth = 110 ft,  $h_d$  = depth below crest = 100 ft,  $h_2$  = tailwater depth = 40 ft,  $h_s$  = silt depth = 60 ft.

Results:  $l = 78.2$ ,  $\frac{1}{3}l = 26.07$ ,  $\frac{2}{3}l = 52.13$ ,  $\tan \theta = 0.67$ ,

For convenience in computing moments, the uplift is divided into two triangles, as illustrated in Fig. 17. The two values appear in lines 5 and 6.

Line 7 introduces  $W_t$ , the vertical weight of the tailwater. The tailwater is too deep to be pushed away by a hydraulic jump; hence static tailwater is used rather than the dynamic forces discussed in Art. 4d, Chapter 7. This load is triangular and its lever arm is measured to the center of gravity of the triangle.

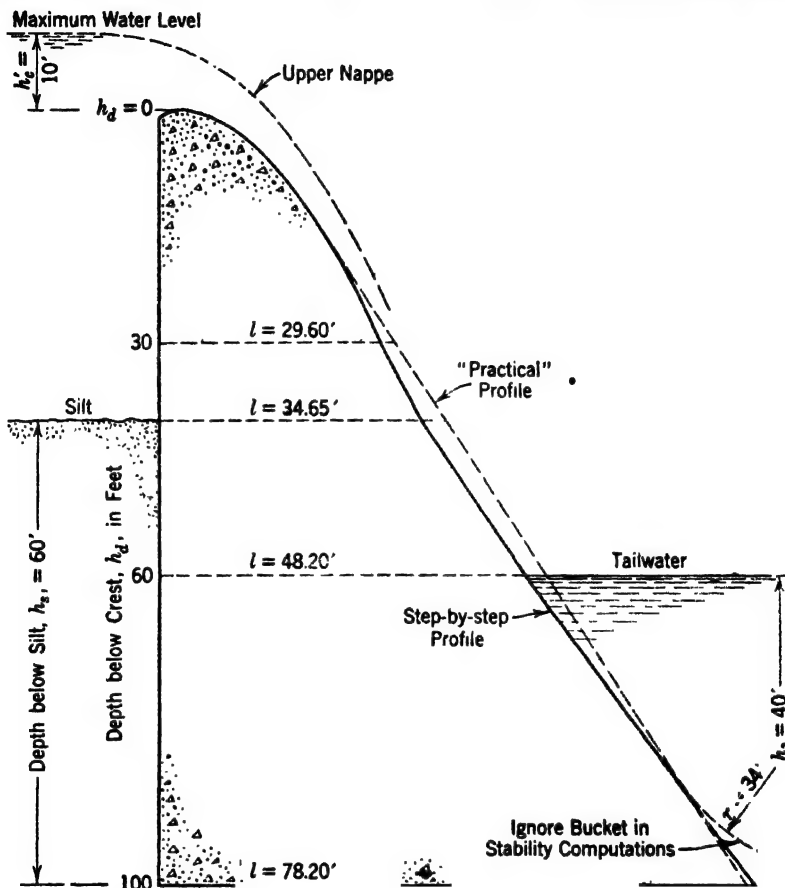


FIG. 18. Final dimensions, Example 1.

The horizontal pressure of the silt,  $P_s$ , line 10, corresponds to line 8, Table 5, already explained.

As in Table 5, the horizontal water load is divided into a rectangle and a triangle, with values shown in lines 8 and 9. The horizontal tailwater pressure,  $P_t$ , line 11, is negative, both as to force and as to moment. It is of triangular form with center of action one-third  $h_t$  from the base.

Sliding factor and stresses are well within allowable limits.

Dimensions resulting from the complete step-by-step analysis are tabulated and drawn to scale on Fig. 18. The bucket radius is taken from Fig. 12.

**12. Practical Profile.** As in the case of the nonoverflow dam, there is nothing impractical about the step-by-step profile. However, a straight downstream face or "practical profile" has been used as shown by the dotted line for Example 1 in Fig. 18. But in such cases this is at a loss of economy except for high dams, as explained in Art. 19 of Chapter 10. The practical profile of Fig. 18 contains 4414 cu ft of concrete per foot of dam, compared to 4274 cu ft for the step-by-step section. This relationship for the whole dam varies with height, depth of overflow, uplift, cross-section of stream, and other conditions.

**13. Stress Conditions near Crest.** By combining horizontal forces and uplifts with weights for the upper portion of the dam, as shown in Table 3, it is possible to find  $\tan \theta$  and the location of the resultant for closely spaced intervals. Such values, without their computations, are shown in Table 7.

TABLE 7  
STABILITY FACTORS NEAR TOP, NO ICE, EXAMPLE 1

Column no.	With uplift				No uplift	
	1	2	3	4	5	6
$h_d$	$\tan \theta$	$S_f$	$x_r$ (ft)	$\frac{2}{3}l$ (ft)	$\tan \theta$	$x_r$ (ft)
1.28		575		4.93	0.80	3.74
2.00	2.29	401	7.35	5.90	0.75	4.38
4.00	1.00	228	7.00	7.90	0.61	
6.00	0.79	167	7.95	9.39		
8.00	0.70	132	8.96	10.65		
10.00	0.66	110	9.94	11.8		
15.00	0.61	76	12.2	14.2		
20.00	0.60	58	14.5	16.3		
30.00	0.61	38	17.6	19.8		

Values of  $\tan \theta$  shown in column 1 of this table are in excess of the specified limit of 0.75 from the crest to  $h_d = 6$  ft.

That this is not significant is shown by the shear-friction safety factors of column 2, which are greatly in excess of the specified minimum of 5. This factor is computed from a transposition of Eq. 4, Art. 3b, Chapter 8. Actual average shears run from 1 to 11 lb per sq in.; hence there is no danger of failure by sliding near the crest.

Values of  $x_r$ , the distance from the vertical upstream face to the resultant, are shown in column 3, and values of  $\frac{2}{3}l$  in column 4. The resultant is within

the middle third at  $h_d = 4$  and all sections below. It is unlikely that the top 2 or 3 ft of the dam will overturn or even crack. The tensile stresses, if computed, will be found very low. If the true pressure curve, 6-7, Fig. 15, were used, there might be no tension at all.

If uplift is neglected,  $\tan \theta$  and  $x_r$  have the values shown in columns 5 and 6, and the resultant is within the middle third at all points. It is unlikely that appreciable uplift will occur in the upper 4 ft of a carefully constructed dam. Hence it may be concluded that the design is adequate.

#### EXAMPLE 2. SOLID OVERFLOW DAM WITH ICE PRESSURE

**14. Data for Example 2.** To illustrate the effect of ice pressure, let it be required to design an overflow dam, identical in all respects with that of Example 1 except that an ice pressure of 10,000 lb per linear ft of crest may be expected, the top of the ice at the level of the crest, and center of pressure down 1.5 ft.

**15. Alternative Loadings.** The dam must be safe against either of two loadings: viz., reservoir at flood level, with no ice; and ice and water at the crest. The design may be prepared for one of these conditions and then tested for the other; or, if the controlling condition changes with depth, the basis of design may be likewise changed.

Referring to Fig. 15a, the water load for flood condition is represented by the trapezoid 1-2-3-4, which may be divided into 1-2-5-4 and 2-3-5. In Fig. 15b, the total load is 2-3-5 plus a concentrated ice load of 10,000 lb, 1.5 ft below the crest. Shearing forces, near the crest, are higher for (b) than for (a). Triangle 2-3-5 being identical for the two cases, horizontal forces will be equal when

$$625h_d = 10,000$$

hence, at

$$h_d = 16 \text{ ft}$$

Moments due to horizontal forces will be equal when

$$0.5 \times 625h_d^2 = 10,000(h_d - 1.5)$$

or when

$$h_d = 30.4 \text{ ft}$$

Therefore, except for change in uplift, the condition of ice pressure will control for sliding down to  $h_d = 16$  ft and for overturning down to  $h_d = 30.4$  ft. Below these levels the condition of flood flow will control. Uplift is less for ice and water at the crest; hence the actual control depths will be somewhat less than 16 ft and 30 ft.

**16. Alternative Designs.** Stresses due to ice pressure may be controlled by adding reinforcement to a section computed for flood waters without ice, or by increasing the thickness of the upper portions of the dam. If the dam is low, reinforcement is likely to be the more economical. For dams of considerable height and within reasonable limits, the addition of masonry near

the top may actually result in economy because of beneficial effects below. (See "Practical top details," Art. 2b, Chapter 9.) For comparison, three alternative methods of treatment, designated as (a), (b), and (c), will be investigated.

(a) *Reinforcement for ice pressure.* If reinforcement is to be provided against ice thrust, the section is first designed for flood flow, without ice, and then investigated under ice load. In the present example, the first analysis may be copied from Example 1. As shown above, the investigation for ice load need extend only to  $h_d = 30$  ft.

Stability at  $h_d = 30$  ft may be found by eliminating  $P_1$  from Table 4, Example 1, and substituting a 10,000-lb ice thrust, 1.5 ft down from the crest. The uplift is also revised to conform to the reduced static pressure. Similar computations are made for other depths, yielding the final results shown in Table 8.

TABLE 8  
STABILITY FACTORS NEAR TOP, WITH ICE,  $h'_c = 10$  FT, EXAMPLE 2a  
(SECTION SAME AS IN EXAMPLE 1)

Column no.	With uplift—Ice and water at crest				
	1	2	3	4	5
$h_d$	$\tan \theta$	$S_{a-f}$	$x_r$ (ft)	$\frac{2}{3}l$ (ft)	$*p''_o$
1.26	12.2	42	3.39	4.93	
2.00	6.2	50	6.85	5.90	-144
4.00	2.4	65	10.56	7.90	-398
6.00	1.4	73	11.57	9.39	-485
8.00	1.01	77	12.20	10.65	-434
10.00	.80	78	12.73	11.77	-301
15.00	.58	74	14.00	14.20	
20.00	.51	64	15.42	16.27	
30.00	.35	46	18.58	19.75	

\* Tension, lb per sq in.

Values of  $\tan \theta$ , column 1, are very high near the top and exceed the specified minimum down to  $h_d = 10$  ft, but the shear-friction factors, column 2, are greatly in excess of the specified minimum. The maximum average shear (not shown) is less than 10 lb per sq in. Failure by sliding is not likely.

Comparing columns 3 and 4, the resultant is outside the middle third at all depths down to  $h_d = 15$  ft, the maximum being 2.66 ft at  $h_d = 4.0$  ft.

Tensile stresses, computed by Eq. 43a, Chapter 7, are shown in column 5. They are too high and persist for too great a depth to be ignored; hence reinforcement is required if the section is to be used.

Computations for the amount of reinforcement may be made at depths of 4 ft, 6 ft, and 8 ft and the greater computed amount used. Because of the small percentages of steel required, the computations usually fall outside the range of available charts and must be made by equations, which will be found in any recent book on reinforced concrete design. In the present example, 0.25 sq in. of steel per ft of crest is about sufficient. However, reinforcement placed in the ordinary manner does not prevent cracking, which no doubt affects uplift. In fact, it is usual to refigure stability for portions of the dam under tension on the basis of 100 per cent uplift. For this reason and from practical considerations, about 1.00 sq in. per ft of crest, placed about 6 in. from the upstream face, is recommended. The reinforcing bars must be anchored below the deepest zone of tensile stress.

(b) *Increase in downstream thickness.* The use of reinforcement may be avoided by increasing the thickness of the upper portion of the dam. Thickening may be accomplished in any desired manner. A simple plan is to proportion the crest for a value of  $h'_c$  greater than that expected at maximum flood. The arbitrary head used for this purpose is found by trial. Assume a trial value of 15 ft for the dam of Example 2. The resulting dimensions, down to  $h_d = 45$  ft, are shown on Fig. 19. The complete section is shown on Fig. 20. The "practical" section of Example 1 is superimposed for comparison.

TABLE 9

STABILITY FACTORS NEAR TOP, WITH ICE,  $h'_c = 15$  FT, EXAMPLE 2b

[Section Thickened Downstream]

Column no.	1	2	3	4
$h_d$	$\tan \theta$	$S_{s-f}$	$x_r$ (ft)	$\frac{2}{3}x_r$ (ft)
1.89	5.45	63	7.2	7.4
3.0	2.79	72	9.8	8.9
6.0	1.25	93	11.9	11.9
9.0	0.71	98	12.8	14.2
12.0	0.54	96	13.9	16.0
15.0	0.46	91	15.1	17.7

Computations for the dam as a whole, not shown, follow the form used for Example 1. Results of stability computations for the top 15 ft are shown in Table 9. The sliding factor is too great down to  $h_d = 9$  ft, but shear-friction

factors are safe at all depths. The resultant is within the middle third except at  $h_d = 3$  ft, where it is out only slightly. The section is amply safe.

The thickening of the downstream face, to resist ice thrust as in Fig. 20, has the disadvantage of decreasing the coefficient of discharge, as the flood

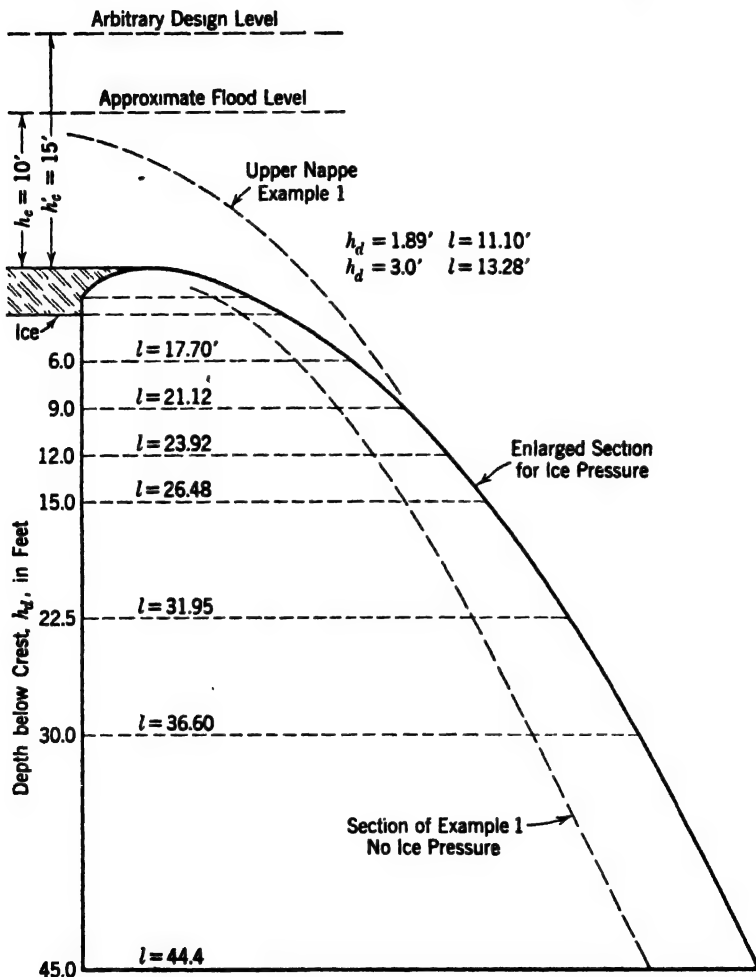


FIG. 19. Top details, Example 2b.

depth does not reach the "design depth." With a designed head of 15 ft, the coefficient of discharge at 10 ft, from Fig. 7, is about 3.74, against 3.98 if the crest were proportioned for 10 ft. Unless the spillway is lengthened, the flood depth and the load on the dam will be somewhat increased.

(c) *Increase in upstream thickness.* A third alternative method of securing stability against ice thrust is illustrated in Fig. 21, where the additional

masonry is added at the upstream face, using a beveled crest approach. The crest is shaped in accordance with Fig. 3. The curve of Fig. 3 is not affected if the depth of the bevel exceeds  $0.5h'_c$ , as explained in Art. 2g. The beveled thickness, 5.0 ft, in Fig. 21, is found by trial to provide sufficient thickness in

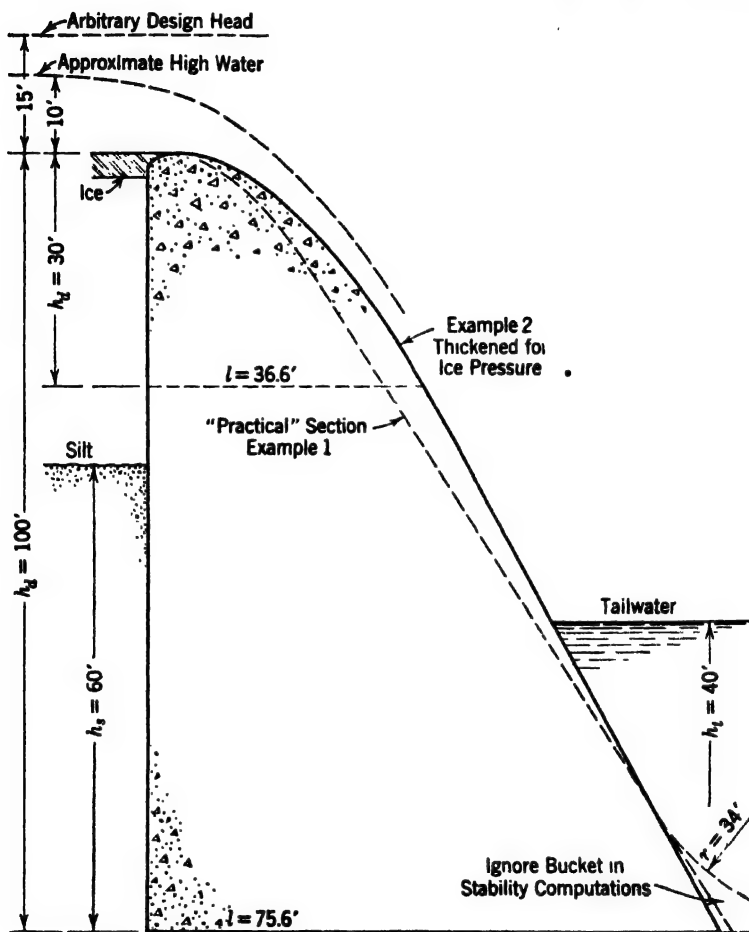


FIG. 20. Example 2b, thickened downstream for ice pressure.

the upper portions of the dam for the condition of ice and water at the crest. The total thickness at the base is made sufficient to insure stability under whatever loading is critical—in this case, water at flood level.

The computed dimensions are tabulated on Fig. 21, and stability factors near the top are shown in Table 10. From column 1 the friction factor is seen to be excessive above  $h_d = 8.0$  ft, but the shear-friction safety factor, column 2, is far above its required value at all depths. Comparing columns 3 and 4,



the resultant is seen to be in the middle third at all depths below  $h_d = 4.0$  ft, and not seriously out at any point.

At  $h_d = 100$  ft the resultant for the condition of flood flow without ice is at the downstream third point for a thickness of 75.4 ft. Consequently,

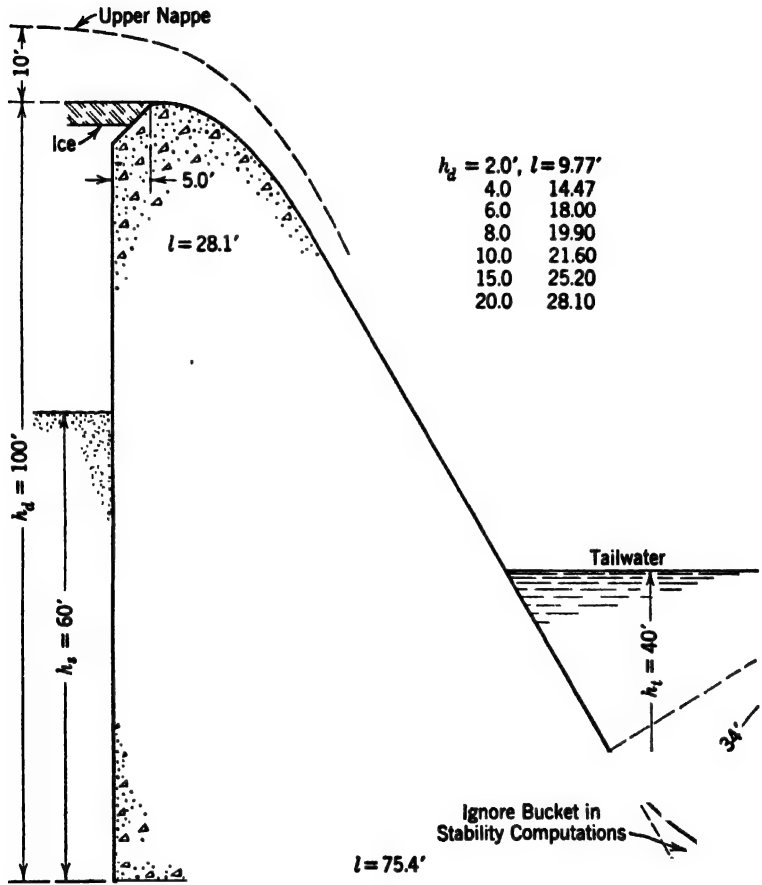


FIG. 21. Example 2c, thickened upstream for ice pressure.

the section shown on Fig. 21 may be considered safe for either of the specified conditions of loading.

(d) *Relative advantages of alternative sections.* The cross-sectional areas of these three alternative sections for Example 2 are as follows:

Example 2a, reinforced	4414 sq ft
Example 2b, thickened downstream	4680 sq ft
Example 2c, thickened upstream	4537 sq ft

**TABLE 10**  
**STABILITY FACTORS NEAR TOP, WITH ICE,  $h'_c = 10$  Ft, EXAMPLE 2c**  
**[Section Thickened Upstream]**

Column no.	1	2	3	4
$h_d$	$\tan \theta$	$S_{s-f}$	$x_r$ (ft)	$\frac{2}{3}l$ (ft)
2.0	5.7	56	11.1	10.0*
4.0	2.0	81	10.7	10.9*
6.0	1.1	101	11.2	12.0
8.0	0.80	96	11.2	13.2
10.0	0.64	96	11.8	14.4
15.0	0.47	78	13.2	16.8

\* Plus distance upstream face to axis.

Section 2c with beveled upstream face is more economical than section 2b and in addition has a higher discharge coefficient. As would be expected, the reinforced section, 2a, contains the smallest amount of concrete but requires about 50 lb of steel per ft of crest. The reinforced section is the most economical.

The relationships noted hold for this case but not necessarily for all cases. For example, if the actual depth of overflow were 15 ft, the three sections would be identical. That is, for a 15-ft flood depth, a 10,000-lb ice load at the crest is not controlling at any level. For an overflow less than 10 ft, or for an ice load in excess of 10,000 lb per linear ft of crest, the condition of ice at the crest will have a greater effect, which will extend to greater depth.

In Fig. 20, the downstream face of the section for Example 1, which is the same as that for Example 2a, crosses that for Example 2b at about  $h_d = 82$  ft. If the dam were of greater height there would be a saving below this depth to offset all or part of the excess masonry above. In other words, the "best section" for a given case depends on all the conditions of design and, in general, can be found only by trial.

The ice load of 10,000 lb per ft of crest used in these examples is in conformity with Art. 6, Chapter 7, which is believed by the authors to give reasonable results in cold climates. However, the designer may encounter specifications or building codes which require much higher values, in which event ice pressure will exert a more profound influence on the dimensions of the dam. The design procedure will not be changed.

### EXAMPLE 3. THIRTY-FOOT OVERFLOW DAM WITH HYDRAULIC JUMP

**17. Data, Example 3.** In Examples 1 and 2 the depth of overflow is given. Usually the designer must figure this depth from given flow data. Also in

Examples 1 and 2 velocity of approach and tailwater were of negligible proportions. The effect of these additional items will be illustrated by the analysis of a low dam with a considerable accumulation of debris in the upstream channel. The data are as follows:

$h_d$ = maximum height of dam above good rock	= 30 ft
$h_t$ = depth of tailwater	= 20 ft
$h_a$ = depth of debris against upstream face	= 20 ft
$w_1$ = weight of masonry	= 150 lb/cu ft
$w_2$ = weight of water	= 62.5 lb/cu ft
$w_s$ = dry weight of debris	= 110 lb/cu ft
$\lambda$ = specific gravity of debris particles	= 2.65
$\alpha$ = angle of internal friction for debris fill	= $35^\circ$
$c$ = uplift area factor	= 1.00
$\zeta$ = uplift intensity factor	= 0.50
$Q_m$ = maximum flood flow	= 50,000 cu ft/sec
$l_t$ = total clear length of crest	= 200 ft
$n$ = number of end contractions for two partly rounded abutments	= 2
$l_c$ = width of approach channel	= 210 ft
$K$ = coefficient of end contraction for each end	= 0.04
$f$ = allowable coefficient of friction for joints and base	= 0.75
$S_{s-f}$ = minimum allowable shear-friction safety factor.	
(Required to be used only where $\tan \theta$ exceeds 0.75)	= 5.0

The upstream fill is assumed to be composed of relatively coarse particles designated as "debris," as silt would not withstand the velocity that will prevail under the assumed flow conditions. The spillway is assumed to have an unobstructed width of 200 ft, the abutment corners being rounded sufficiently to give a contraction coefficient,  $K$ , of 0.04 (for each corner).

**18. Depth of Overflow.** The depth of overflow is computed from Equation 1,  $h'_c$  being the unknown. Values of  $l_n$  and  $h_v$  are also unknown but are determined when  $h'_c$  is found or assumed. The solution is made by trial, thus:

Try $h'_c$ = 15 ft	
$d_a$ = approach depth	= 15 + 10 = 25 ft
$A_a$ = approach area	= 25 $\times$ 210 = 5250 sq ft
$V_a$ = approach velocity	= $\frac{50,000}{5250}$ = 9.53 ft/sec
$h_v$ = $V_a^2/2g$	= 1.41 ft
$(h'_c + h_v)^{1.5}$ (see Eq. 1)	= 66.48
$h_v^{1.5}$ (see Eq. 1)	= 1.67
$(h'_c + h_v)^{1.5} - h_v^{1.5}$	= 64.81
$l_n$ (Eq. 4) = 200 - 2 $\times$ 0.04 $\times$ (15 + 1.41)	= 198.8 ft
$Q$ = 3.98 $\times$ 198.8 $\times$ 64.81	= 51,400 cu ft/sec

where 3.98 is the discharge coefficient from Fig. 7. The computed discharge is higher than required; hence a new trial is made. A depth of 14.8 ft gives a discharge of 50,200 cu ft per sec, which is close enough to the required flow; hence the depth of overflow is taken as 14.8 ft, which corresponds to an approach velocity of 9.60 ft per sec and a velocity head of 1.43 ft.

**19. Shape of Crest.** Because of the low height of the dam above the contemplated debris level, the velocity of approach will be appreciable and the crest dimensions must be based on Table 1 rather than on Fig. 2. (See Art. 2c.)

The coordinates of Table 1 are in terms of  $(h_w + h_v)$  (see Fig. 1 for  $h_w$ ). The value of  $h_w$  is found by trial. Using values of  $h'_c$  and  $h_v$  from the preceding article,

$$\frac{h_v}{h'_c + h_v} = \frac{1.43}{16.23} = 0.088$$

The value of  $h_v/(h_w + h_v)$  will be somewhat less than this. Assume a trial value of 0.08. Following down the column of Table 1 headed 0.08, the maximum rise of crest above the theoretical sharp crest is found to be  $0.082(h_w + h_v)$ . Therefore,

$$h'_c + h_v = h_w + h_v - 0.082(h_w + h_v)$$

from which

$$h_w + h_v = 1.089(h'_c + h_v) = 17.67$$

and

$$\frac{h_v}{h_w + h_v} = \frac{1.43}{17.67} = 0.0809$$

which is sufficiently close to the trial value of 0.08. Therefore, the shape of the crest may be computed from values of  $y/(h_w + h_v)$  taken from the 0.08 column of Table 1. This computation is performed in columns 1 to 4 of Table 11. Values in columns 1 and 2 are read directly from Table 1. Corresponding values in columns 3 and 4 are obtained by multiplying by  $17.67 = (h_w + h_v)$ . Values from Table 1 are selected at intervals required for accuracy of computation.

These coordinates are used to plot the face curve 2-10-13, Fig. 22. The  $y$  distances are measured from point 2 rather than from the crest level 8, as when data of Fig. 2 are used.

The radius of 22 ft for the bucket is taken from Fig. 12. The point of reverse curve between ogee and the bucket is above the joint corresponding to  $x/17.67 = 1.80$ , column 1, Table 11; hence the lowest section is assumed to be triangular with a back slope of 0.66 to 1, as shown.

**20. Stability Computations.** Weights and moments for the masonry are computed in columns 5 to 9, Table 11, which follows the procedure for the upper curved portion of Example 1. In this case all the downstream face is curved; hence all masonry weight computations are made in this one table.

**TABLE 11**  
**DIMENSIONS AND FORCES, RESERVOIR EMPTY, EXAMPLE 3**

1	2	3	4	5	6	7	8	9
$\frac{x}{17.67}$	$\frac{y}{17.67}$	$x$ (ft)	$y$ (ft)	Wt * Items	Dimensions	Weight (lb)	Arm (ft)	Moment (ft-lb)
0	0	0	0	(1)	0.5×0.88×1.06×150	70	0.70	49
0.06	0.0500	1.06	0.88	(2)	0.88×1.06×150	140	1.59	223
				(3)	0.5×0.38×1.06×150	30	1.76	53
0.12	0.0715	2.12	1.26	(4)	1.26×1.06×150	201	2.15	430
				(5)	0.5×0.15×1.06×150	12	2.82	34
0.18	0.0800	3.18	1.41	(6)	1.41×0.71×150	150	3.54	531
				(7)	0.5×0.06×0.71×150	3	3.65	11
0.22	0.0820	3.89	1.45	(8)	1.34×1.41×150	183	4.60	842
				(9)	0.5×0.11×1.41×150	12	4.36	52
0.30	0.0760	5.30	1.34	(10)	1.02×1.76×150	169	6.18	1,043
				(11)	0.5×0.32×1.76×150	42	5.89	247
0.40	0.058	7.06	1.02	(12)	0.53×1.77×150	153	7.95	1,215
				(13)	0.5×0.69×1.77×150	91	7.65	695
0.50	0.030	8.83	0.53	(14)	8.83×0.18×150	224	4.42	990
				(15)	0.5×0.71×1.77×150	94	9.42	885
0.60	-0.010	10.60	-0.18	(16)	1.89×10.60×150	3,005	5.30	15,930
				(17)	0.5×1.89×3.53×150	501	11.78	5,910
0.80	-0.117	14.13	-2.07	(18)	2.48×14.13×150	5,260	7.06	37,100
				(19)	0.5×2.48×3.54×150	658	15.31	10,070
1.00	-0.258	17.67	-4.55	(20)	3.09×17.67×150	8,180	8.84	72,300
				(21)	0.5×3.09×3.53×150	817	18.85	15,400
1.20	-0.432	21.20	-7.64	(22)	3.68×21.20×150	11,680	10.60	123,800
				(23)	0.5×3.68×3.53×150	975	22.38	21,900
1.40	-0.641	24.73	-11.32	(24)	4.28×24.73×150	15,880	12.36	196,400
				(25)	0.5×4.28×3.53×150	1,082	25.91	28,000
1.60	-0.883	28.27	-15.60	(26)	4.98×28.27×150	21,100	14.14	298,500
				(27)	0.5×4.98×3.53×150	1,315	29.45	38,700
1.80	-1.164	31.80	-20.58	(28)	7.98×31.80×150	38,050	15.90	602,500
				(29)	0.5×7.98×5.26×150	3,142	33.55	105,500
		37.06	-28.55					
Total						113,219	(13.95)	1,579,309

\* Item designations to (19) shown in Fig. 23; remainder follow similar pattern.

The method of computation is illustrated in Fig. 23, which shows the upper part of the crest divided into computation areas. The partial areas are marked with numerals (1), (2), (3), etc., for identification by corresponding numerals in column 5, Table 11.

Stability computations for flood stage are completed in Table 12. Weights and moments for the masonry shown in line 1 are transferred from the totals of Table 11, and other forces are computed as indicated.

As stated near the end of Art. 4d, Chapter 7, bucket reaction is usually ignored unless the depth of overflow is great. In the present case it is computed to illustrate its importance and the procedure.

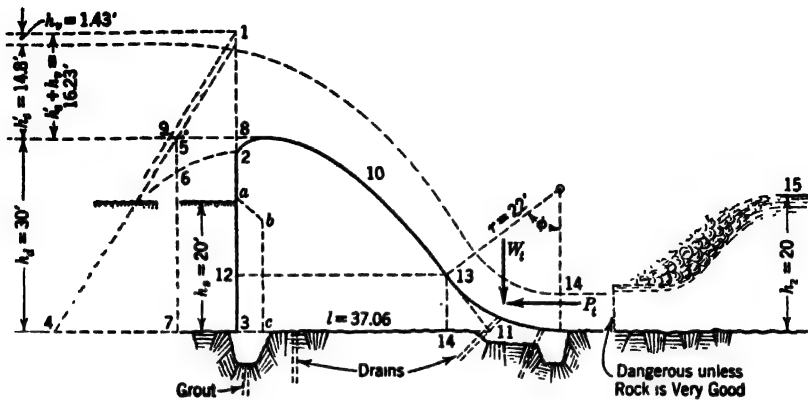


FIG. 22. Dimensions and loading, Example 3.

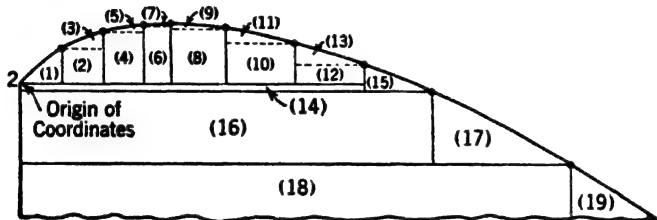


FIG. 23. Top details, Example 3.

TABLE 12  
STABILITY AT BASE, EXAMPLE 3

Line	Item	Description and dimensions	Forces (lb)		Lever (ft)	Moment (ft-lb)
			Horiz.	Vert.		
1	$W_1$	Masonry, from Table 11		113,200	13.95	1,579,200
2	$W_{uu}$	$0.25 \times 62.5 \times 44.8 \times 37.06$		-25,940	12.35	-320,000
3	$W_{ud}$	$0.25 \times 62.5 \times 4.8 \times 37.06$		- 2,780	24.70	- 68,500
4	$W_t$	Ignore				
5	$P_1$	$925 \times 30$	27,750		15.00	416,250
6	$P_2$	$0.5 \times 62.5 \times 30 \times 30$	28,120		10.00	281,200
7	$P_s$	$9.25 \times 20 \times 20$	3,680		6.67	24,500
8	$P_t$	Eq. 16, Art. 4, Chapter 7	-11,200		5.00	- 56,000
9	Total	Flood stage	48,350	85,220	(21.8)	1,856,650

First, it must be determined whether the hydraulic jump will be drowned out, producing the condition illustrated in Fig. 21, or whether it will occur on or below the apron, causing the condition shown in Fig. 22. Ignoring losses, the total energy head at the downstream end of the bucket, point 14, Fig. 22, is equal to  $h'_c + h_a$  above the crest, plus the height of the dam, which is  $14.8 + 1.43 + 30.0 = 46.23$  ft. It is found by trial that this corresponds to a depth of 4.8 ft and a velocity head of 41.4 ft. The corresponding velocity is 51.6 ft per sec.

The tailwater channel is of such width (200 ft) that each unit length may be considered separately; hence, whether the hydraulic jump will occur may be determined by the equation

$$\frac{q}{g} V_1 + p_1 = > \frac{q}{g} V_2 + p_2 \quad [15]$$

where  $q$  is the discharge per foot of crest ( $50,000 \div 200 = 250$ ),  $V_1$  is the velocity at the downstream end of the bucket ( $= 51.6$  ft per sec, see above),  $p_1$  is the hydrostatic pressure at the same point in units of  $w_2$  (62.5 lb). Values of  $V_2$  and  $p_2$  apply similarly downstream from the jump.

Taking the upstream and downstream depths as 4.8 ft and 20.0 ft, respectively, Eq. 15 is evaluated thus:

$$\frac{250}{32.2} \times 51.6 + 0.5 \times 4.8^2 = > \frac{250}{32.2} \times 12.5 + 0.5 \times 20^2$$

$$413 = > 297$$

Consequently the jump will occur downstream from point 14 and conditions illustrated may be used in computing stability.

Proceeding with Table 12, the upstream uplift triangle is computed in line 2, as for other examples, the head being  $h'_c + h_a = 14.8 + 30 = 44.8$  ft. The downstream triangle is computed in line 3 for a tailwater depth of 4.8 ft as previously found. Both are applied only to the portion 3-11 of the base on the assumption that uplift under the bucket extension is relieved by drainage. The vertical component of the jet reaction,  $W_i$ , is ignored as it falls largely downstream from point 11.

Values of  $P_1$  and  $P_2$ , lines 8 and 9, are computed from the trapezoid 8-5-4-3, where point 1 on the extension of 4-5 is at the level of the upstream water surface. The use of a trapezoid with top at 8-9 as suggested in Art. 4a, Chapter 7, is not required in the present example because the debris fill shields much of the dam from pressures due to velocity of approach and, moreover, the pressures near the crest are known to follow some such line as 2-6.

The submerged weight of the debris fill, from Eq. 21, Chapter 7, is 68.4 lb per cu ft. The pressure, from Eq. 19, Chapter 7, is  $9.25h_s^2$ , which gives the forces and moments shown in line 10. The back reaction of the tailwater jet is computed from Eq. 15, Art. 4, Chapter 7.

From data previously given,  $\tan \phi = 0.66$ ; hence,  $\phi = 33^\circ 30'$ ,  $\sin \phi = 0.552$ ,  $1 - \sin \phi = 0.448$ . Also,  $V$  at point 14 has been estimated to be 51.6 ft per sec. Therefore,

$$P_t = 62.5 \times \frac{250}{32.2} \times 51.6 \times 0.448 = 11,200 \text{ lb}$$

This force is assumed to act about halfway, vertically, from point 11 to 13, Fig. 22. This distance is found to be about 5.0 ft by scaling. The computation is completed in line 8, Table 12. It is seen by inspection that  $P_t$  has an appreciable influence on sliding but relatively little on overturning. As it is a stabilizing factor, the usual practice of omitting it is on the side of safety.

Totals for the fully loaded dam are shown in line 9. The section is stable in all respects, including  $\tan \theta$ , which is 0.57. Stability at higher points should be computed as for Example 1. The computations need not be shown here.

The tailwater condition illustrated is dangerous except for very good rock; and unless the submergence can be increased, additional paving or other treatment may be required to prevent erosion. This subject is treated in Part IV of Chapter 3.

**21. Possible Undercut Section.** Comparison of lever arms in lines 1 and 9 of Table 12 with the dimensions of Fig. 22 shows that the resultant is within the middle third for both full and empty reservoir; also the sliding factor is more than safe. It is evident, therefore, that except for the required dimensions of the overflow curve, the masonry volume can be reduced. This condition can be met by undercutting the upstream face, as illustrated in Fig. 4a, or as indicated by the dotted lines  $a-b-c$  of Fig. 22. The point  $a$  should be far enough below the crest to avoid interference with the discharge (see Art. 2g), and the undercut section must be stable at  $b$ . Subject to these limitations, the width of undercutting,  $3-a$ , Fig. 22, is found by trial.

The advantage of the undercut section is principally with dams with bases above the bottom of Zone II. For higher dams, any saving near the top must be offset by a greater base width at lower elevations.

## DETAILS

**22. Controlled Crests.** Overflow dams are frequently provided with flashboards, gates, or other devices for backing up the water above the fixed crest level at times of low flow but capable of being opened or removed during floods. The design and use of such devices are discussed in Chapter 24. The effect of these devices on the stability of the dam must be considered. Crest controls may be attached directly to the crest or they may be supported by piers.

The simplest control attached directly to the crest is the flashboard arrangement illustrated in Fig. 24. The stability of the dam must be checked for water at the top of the flashboards, the force against the boards being included. If the flashboards reach entirely to the flood water level, the overturning



force of the water is the same as for a nonoverflow dam, but the stability factors near the top are different. The method of analysis is similar to that for the upper portions of Example 1.

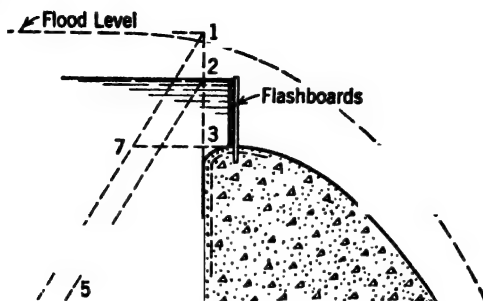


FIG. 24. Flashboard loading.

Usually the flashboards reach only part way to the flood level, as illustrated in Fig. 24. In such case, loading 2-5-4 is likely to control near the crest. At greater depth, loading 3-7-6-4, for flood conditions flashboards removed, controls. In case of doubt, both conditions should be checked. The weight of the water between the line 2-3 and the flashboards may be included as a

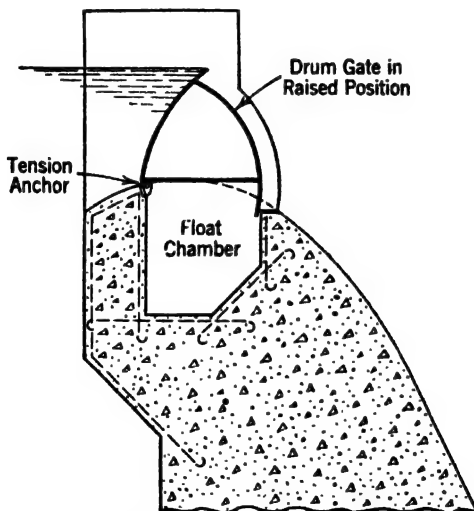


FIG. 25. Drum gate crest.

stability force. If there is any likelihood that the flashboards may be overtopped, a test should be made on such basis.

The drum gate, shown in Fig. 25, usually rises entirely to the flood level; hence the general stability is computed as for a nonoverflow dam. The top details require special attention. The use of reinforcement is essential.

Other types of controls supported directly from the crest are illustrated in Chapter 24.

Radial gates, Stoney gates, and roller-crests are supported by piers. The piers usually are reinforced and must be anchored to a depth where the combination of pier, gate, and dam is stable as a nonoverflow section. The piers resemble in some respects the buttresses of hollow dams, discussed in Chapter 14.

**23. Ice on Controlled Crests.** If crest gates are likely to be closed and the reservoir full to flood level during very cold weather, the importance of ice pressure may be greatly increased. The gates themselves are subject to damage and the ice thrust is raised to a higher level, increasing the overturning effect on the dam if the gates are sufficiently strong to transmit the thrust.

A sudden flood which might thaw or break up the ice in the reservoir might find the gates so incrustated with ice as to be inoperative, thus creating a serious flood hazard.

The effect of ice under proper or improper operation should be carefully considered wherever crest devices are installed in extremely cold climates. Some controls, as for example the flashboards illustrated in Fig. 24, can be designed to fail under ice thrust; but this is not practical for some of the more elaborate and expensive controls.

**24. Comparison of Solid Spillway Dams.** The fundamental theory of design, for solid spillway and nonoverflow dams, differs only in the upper part which, in the former, is proportioned to conform to the shape of the sheet of water spilling over the top.

The "standard" dam crest, described in Art. 2, has become generally recognized, and deviation from that shape is made usually only because of special reasons, including space required for drop crest gates.

Curves of quantities in spillway dams, adaptable to preliminary estimates, are given in Fig. 26. To insure conservatism, a low value of 140 lb per cu ft of concrete was used in the computation of this table. A list of representative solid gravity dams, which includes overflow dams, is given in Table 17 of Chapter 10.

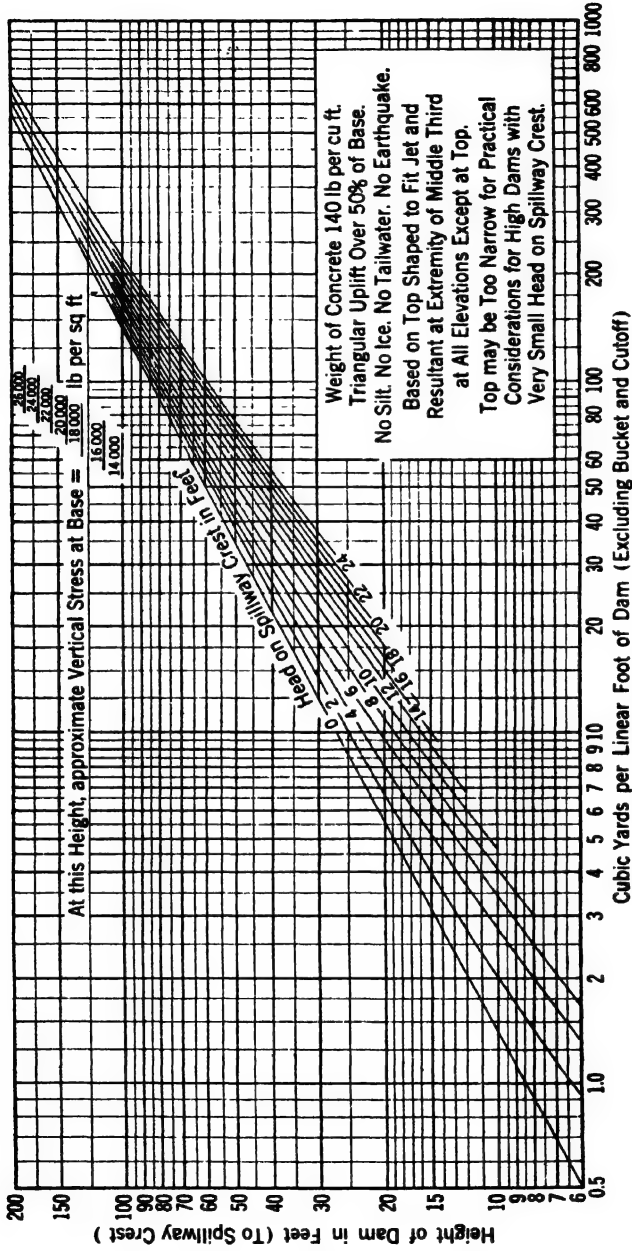


FIG. 26. Contents of solid gravity spillway dam.

## CHAPTER 12

### INTERNAL STRESSES AND STRESS CONCENTRATIONS IN GRAVITY DAMS

**1. Discussion of Secondary Stresses.** The assumptions ordinarily used in the design of dams do not reveal the concentrations of stresses found at corners, at the junction with the foundation, around openings, and at other points of structural discontinuity. Recently, considerable attention has been paid to these stresses and some progress has been made toward their solution.

These stress concentrations are not peculiar to dams but are merely special cases of the secondary stresses found in practically all structural members. Consider, for example, the simple case illustrated in Fig. 1. Neglect the

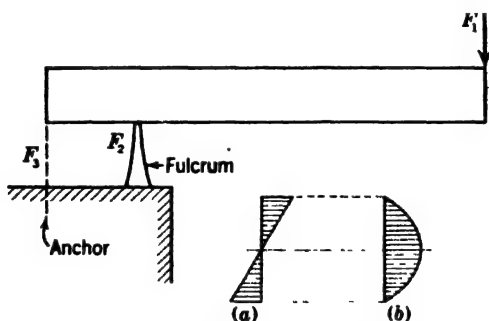


FIG. 1. Stress distribution in a beam.

weight of the beam itself. It is usual to assume that direct stresses and shears in such a beam are distributed according to diagrams *a* and *b*. Unless the forces  $F_1$ ,  $F_2$ , and  $F_3$  are applied to the beam in accordance with diagram *b*, this assumption does not hold, particularly near the ends and near the fulcrum. Secondary stresses exist at these points. These effects are local and for a moderately long beam are usually neglected.

There are, of course, many more complicated cases of secondary stress, some of which assume great importance but many of which can safely be ignored. It is important that the designer know when a special investigation is necessary.

The principles governing secondary stresses in dams are the same as for other structural elements, but the influence on safety is sometimes more important. Uncertainties in regard to foundation reactions were discussed in

Art. 14, Chapter 7. As stated there, these uncertainties ordinarily may be ignored, but as dams are extended to unprecedented heights and ever higher working stresses are adopted, caution dictates that at least the order of these secondary stresses be known.

**2. Need for Knowledge of Internal Stresses.** Under ordinary circumstances it is probable that the maximum compression or maximum tension in a dam occurs at a face; consequently internal stresses are not required in testing for the design rules of Chapter 8. However, a knowledge of internal stresses is a necessary preliminary to the study of secondary stresses. Also, internal cracks sometimes appear in gravity dams and in the buttresses of hollow dams, indicating the presence of tensile stresses although the usual computations indicate that no tension should be present.

When the concrete in a massive dam or a buttress sets and cools, it shrinks, thus tending to become shorter in all directions than the rock on which it is founded. Cross-stream shrinkage is of no importance in buttresses and can be allowed for by frequent contraction joints in gravity dams. Upstream and downstream shrinkage presents a more difficult problem, particularly in dams of appreciable upstream and downstream extent. To meet this condition it may be desirable to insert longitudinal as well as transverse joints into gravity dams, or to provide joints or reinforcement in buttresses. These joints should be of special design. (See Art. 1, Chapter 23.) Their relationship to the internal stress pattern should be known, and their design requires a knowledge of the shears which they must transmit. The computation of internal stresses in such dams thus becomes important.

**3. Principal Stresses.** Through every point in a structure such as a gravity dam, which is subject to forces parallel to a single plane, it is possible to draw a plane on which there is no shear and on which the normal stress is higher than on any other plane that can be drawn through the point. This maximum normal stress is called the "first principal stress" at the specified point. A second plane, at right angles to the first, also has no shear, and the normal stress is less than on any other plane. This minimum normal stress is called the "second principal stress."

**4. Stresses on Oblique Planes.** If the two principal stresses and the direction of either of them are known, the normal pressure and shear on any other given plane may be computed from the equations

$$p_{\beta} = p_1 \cos^2 \beta + p_2 \sin^2 \beta \quad [1]$$

and

$$s_{\beta} = 0.5(p_1 - p_2) \sin 2\beta \quad [2]$$

where  $\beta$  is the angle between the given plane and the plane on which the first principal stress acts,  $p_{\beta}$  and  $s_{\beta}$  are the normal pressure and shear on the given plane, and  $p_1$  and  $p_2$  are, respectively, the first and second principal stresses.

Eq. 2 conforms to the law, known from mechanics, that shears on mutually perpendicular planes are equal. Also, for  $\beta = 0, 90^\circ, 180^\circ$ , etc., the shear is

zero, which conforms to the requirement of no shear on the planes of principal stresses. The maximum shear which occurs for  $\beta = 45^\circ$  is  $0.5(p_1 - p_2)$ .

Eqs. 1 and 2 may be solved graphically by Mohr's circle,<sup>1</sup> as illustrated in Fig. 2. From any point,  $O'$ , lay off the first and second principal stresses,  $O'-g$  and  $O'-f$ . On  $f-g$  as a diameter draw the circle,  $f-e-g-d$ , with center at  $O$ . Draw the radius  $e-O$  in such position that the angle  $e-O-g$  is equal to  $2\beta$ , and draw  $e-c$  perpendicular to  $f-g$ . Then,  $O'-c$  and  $c-e$ , respectively, represent  $p_\beta$  and  $s_\beta$ , Eqs. 1 and 2.

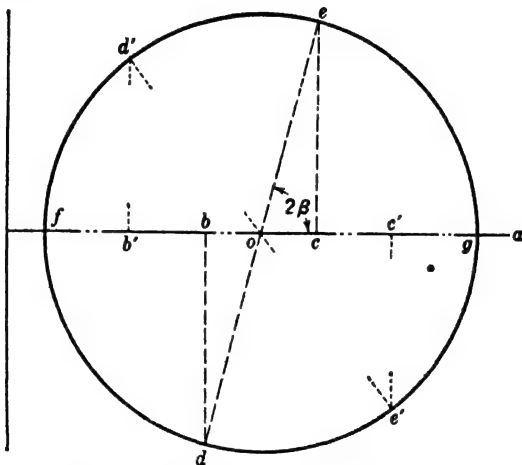


FIG. 2. Principal stresses by Mohr's circle.

If  $e-O$  is extended to  $d$ , and  $d-b$  drawn perpendicular to  $f-g$ , then  $O'-b$  and  $b-d (= c-e)$  represent normal stress and shear for  $\beta + 90^\circ$ .

**5. Determination of Principal Stresses.** Usually the principal stresses within a dam cannot be determined directly but must be computed from ascertainable values of stresses on other planes, i.e., by a reversal of the procedure of Art. 4. The Mohr's circle is particularly useful in such a case. Suppose that instead of the principal stresses, the normal stresses  $O'-b$  and  $O'-c$  and the corresponding shears,  $c-e = b-d$ , are known. Points  $e$  and  $d$  are at once plotted,  $e-d$  is drawn, locating  $O$ , and the circle completed, giving  $O'-f$  and  $O'-g$ , and the value of  $2\beta$ . Stresses on any other plane are at once determinable.

If the known stresses and shears are on planes not mutually perpendicular, such as  $O'-b'$ ,  $b'-d'$ , and  $O'-c$ ,  $c-e$ , the center is located by drawing the perpendicular bisector to the chord  $d'-e$ .

In general, something must be known about stress conditions on two planes. Six variables are involved: viz.,  $p_1$ ,  $p_2$ ,  $s_1$ ,  $s_2$ ,  $\beta_1$ , and  $\beta_2$ . If any four of these are known, the circle can be drawn. If a plane of principal stress is involved, advantage may be taken of the zero value of  $s$ .

<sup>1</sup> See any recent book on mechanics of materials.

The same results may be obtained analytically by proper transformation of Eqs. 1 and 2. For known stresses on two mutually perpendicular planes, the transformations are as follows:

$$\tan 2\beta = \frac{2s_v}{p_v - p_h} \quad [2a]$$

$$p_1 = \frac{p_v \cos^2 \beta - p_h \sin^2 \beta}{\cos^2 \beta - \sin^2 \beta} \quad [1a]$$

$$p_2 = p_v + p_h - p_1 \quad [1b]$$

where  $p_v$  and  $p_h$  are unit pressures on horizontal and vertical planes (or other mutually perpendicular planes),  $s_v$  is the unit shear on these planes, and other symbols are as stated in Art. 4.

**6. Stress Conditions at the Faces.** Stress conditions are more easily determined at the two faces of the dam than in the interior. The faces, being free from shear, are planes of principal stress. One of the principal stresses, the normal external loading, is known, as is also its direction of action. If  $\beta$  is made equal to  $\phi$ , the angle between the face and the vertical, and  $p_2$  is replaced with  $p_n$ , Eq. 1 becomes

$$p_v = p_1 \cos^2 \phi + p_n \sin^2 \phi \quad [3]$$

from which

$$p_1 = p_v \sec^2 \phi - p_n \tan^2 \phi \quad [4]$$

With proper substitutions, Eq. 4 may be converted into Eq. 5a or 6a, Chapter 8.

After  $p_1$  is known, horizontal pressures may be found from Eq. 1 by replacing  $\beta$  with  $(90^\circ + \phi)$  thus:

$$p_h = p_1 \sin^2 \phi + p_n \cos^2 \phi \quad [5]$$

Inserting the value of  $p_1$  from Eq. 4, and writing for both faces,

$$p'_h = p'_v + (p'_v - p'_n) \tan^2 \phi' \quad [6]$$

and

$$p''_h = p''_v + (p''_v - p''_n) \tan^2 \phi'' \quad [7]$$

where '' and ' designate, respectively, upstream and downstream face functions.

Exchanging  $\phi'$  and  $\phi''$  for  $\beta$  in Eq. 2, substituting for  $p_1$  from Eq. 4 and reducing gives shear equations for the two faces, for horizontal and vertical planes, as follows:

$$s' = (p'_v - p'_n) \tan \phi' \quad [8]$$

and

$$s'' = (p''_v - p''_n) \tan \phi'' \quad [9]$$

**7. Analysis at Interior Points.** The functions generally used in the computation of principal stresses at interior points are the vertical unit pressure,  $p_v$ , the horizontal unit pressure,  $p_h$ , and the vertical (or horizontal) shear,  $s_v$ . Of these three,  $p_v$  is available from the dam analysis and Eq. 41, Chapter 7. The other two must be specially computed.

The fundamental equations for these functions are

$$\frac{\partial p_v}{\partial y} + \frac{\partial s}{\partial x} + k_1 = 0 \quad [10]$$

and

$$\frac{\partial p_h}{\partial x} + \frac{\partial s}{\partial y} + k_2 = 0 \quad [11]$$

where  $x$  and  $y$  denote horizontal and vertical distance and  $k_1$  and  $k_2$  are constants depending, respectively, on weight and earthquake inertia of the masonry.

If general algebraic expressions for the functions of these equations are available, direct solution for internal stresses in the entire dam may be possible.<sup>2</sup>

For dams of practical form, it is necessary to develop special equations or to resort to geometric methods. The geometric method aids in the understanding of the problem, hence it will be described first. To facilitate comparisons, it will be applied to a problem which can also be solved by equation, perhaps with less labor.

**8. Geometric Analysis of Shears.** (a) *Description of method.* The geometric method of analysis was described by the late William Cain in 1909.<sup>3</sup>

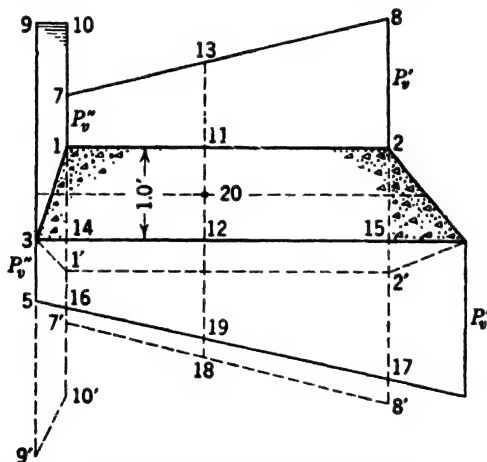


FIG. 3. Vertical loads on a block of unit height.

The fundamental principles involved are illustrated in Fig. 3. Vertical pressures are computed on two horizontal planes usually a unit distance apart. Two such planes are represented by 1-2 and 3-4 in the figure. For present purposes the masonry prism between these two planes will be assumed to be of uniform unit thickness perpendicular to the page. Vertical unit pressures at

<sup>2</sup> See several discussions, "Determination of Principal Stresses in Buttresses and Gravity Dams," *Trans. Am. Soc. Civil Engrs.*, Vol. 98, 1933, pp. 971-1038.

<sup>3</sup> "Stresses in Masonry Dams," *Trans. Am. Soc. Civil Engrs.*, Vol. 64, 1909, p. 208.



the four corners are platted as 1-7, 2-8, 3-5, and 4-6. These values include uplift, if any exists. The trapezoid 1-7-8-2 thus represents the downward pressure on the top of the block. Additional downward forces are the weight of the block itself and the vertical water pressure on the upstream face represented by 3-9-10-1; also vertical tailwater pressure on 2-4 if any exists. Considering the whole block, these downward forces are balanced by an upward force represented by the trapezoid 3-5-6-4.

If any portion other than all of the block is considered, the "external" forces are not in balance, which gives rise to shear. At the plane 2-15, for example, there is a shearing force equal to the area of 15-17-6-4 less the weight of 2-15-4. At an interior plane such as 11-12, the shear is equal to the area of 12-19-6-4, less the area of 11-13-8-2 and less the weight of the block 11-2-4-12. This is the essence of the two-plane geometric method.

(b) *Computation procedure.* Shear values are usually required at a number of points and each computation requires the determination of two areas, the weight of a partial block and the finding of differences, as previously explained. Effort can be reduced by computing the differences directly. If a diagram for the weight of the masonry is platted within the lower diagram as at 3-1'-2'-4, and if the diagram 1-7-8-2 is platted in the reversed position, 1'-7'-8'-2', then the shear at 11-12 is equal to the area of 2'-17-6-4, minus 17-19-18-8', the latter area being the only variable.

If the vertical water load is inverted into the position 3-9'-10'-1', the shear at 11-12 is also equal to the area of 5-9'-10'-7'-18-19. The two values must check.

(c) *Required precision of computations.* Since the difference in the vertical pressure diagrams on the upper and lower planes is very small compared to that of either of the diagrams, it is necessary to take special precautions to insure sufficient accuracy in the differential pressures. This is accomplished by preserving consistency between computations for the upper and lower planes. It is not necessary to alter the precision of the primary dam computations which are required for the upper plane. However, for the lower plane, one should start with the moments and forces applicable to the upper plane, computed with normal accuracy, and, by combining *very accurately* the forces and moments of the block between the planes, find the toe and heel pressures on the lower plane.

(d) *Interpretation of results.* The computed shear across any section, as 11-12, rigidly represents the total shear across the prism at that point if the design assumptions hold. However, the shear is not constant from 11 to 12, hence the computed value will not be exact for either of these points but will approximate the shear at the midpoint 20.

Unit shearing stresses on mutually perpendicular planes being equal, the computed values may also be taken as the horizontal shearing stresses along the middle line of the block.

**9. Geometric Analysis of Horizontal Stresses.** Variation of horizontal stresses along a horizontal section depends on the vertical variation in unit

shears. To find this variation requires the repetition of the shear computation for a second unit-height block. A set of three planes, bounding the necessary two blocks, are represented by 1-2, 3-4, and 5-6, in Fig. 4.

Shears are computed along both of the center lines 7-8 and 9-10, following the procedure of Art. 8. Consider the prism 8-11-12-10. The total shearing force from 10 to 12 will be greater than from 8 to 11, hence there must be a balancing normal pressure on plane 11-12. If there is an external pressure on the face 8-10, an internal inertia force due to earthquake, or any forces other than those named, their horizontal components must be taken into account.

Instead of integrating two sets of shears and finding differences, it is convenient to integrate differences, following the idea used in computing the shears, Art. 8.

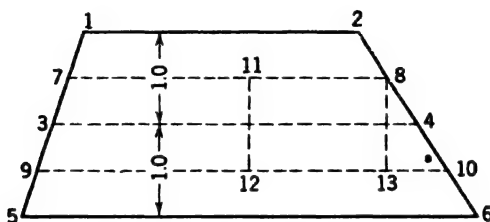


FIG. 4. Adjacent unit-height blocks.

**10. Numerical Example of Geometric Method.** Let  $a-b$ , Fig. 5, represent (not to scale) a horizontal section of the dam of Example 2, Chapter 10, at a depth of 190 ft below the maximum water level. Consider the dam fully loaded, subject to the specified earthquake effect, and for the moment ignore uplift. Computations (not shown) made to usual accuracy yield data as follows:

$$\Sigma(P) = 1,492,600 \text{ lb}$$

$$\Sigma(W) = 2,478,100 \text{ lb}$$

$$M_c = 40,740,000 \text{ ft-lb}$$

where  $\Sigma(P)$  is the sum of all horizontal forces above the plane,  $\Sigma(W)$  is the sum of vertical forces exclusive of uplift, and  $M_c$  is the corresponding moment about the center of the section. The section is assumed 1.0 ft thick normal to the paper.

It is also known from the dimensions of the dam, Fig. 7, Chapter 10, that

$$l = a-b = 160 \text{ ft}$$

$$\tan \phi' = 0.7275$$

$$\tan \phi'' = 0.1058$$

where  $l$  is the length of joint at  $h = 190$ ,  $\tan \phi'$  is the downstream face slope, and  $\tan \phi''$  is the upstream face slope.

Values of  $p'_v$  and  $p''_v$  for  $h = 190$  are computed from Eqs. 42 and 43, Chapter 7, and recorded on Fig. 5. Computations are carried to four decimal places, which is in excess of requirements.

Next, differential forces and moments are computed and combined with those for plane  $a-b$  to give new values for planes  $e-f$  and  $c-d$ , respectively 1 ft above and 1 ft below  $a-b$ . Computations for plane  $c-d$  are shown in Table 1. As previously explained, these computations are carried to fictitious precision, to insure consistency in differential results.

Computations for plane  $c-f$  are made in a similar manner, after which vertical reactions are computed at the ends of each of the sections. The computed values are recorded on Fig. 5.

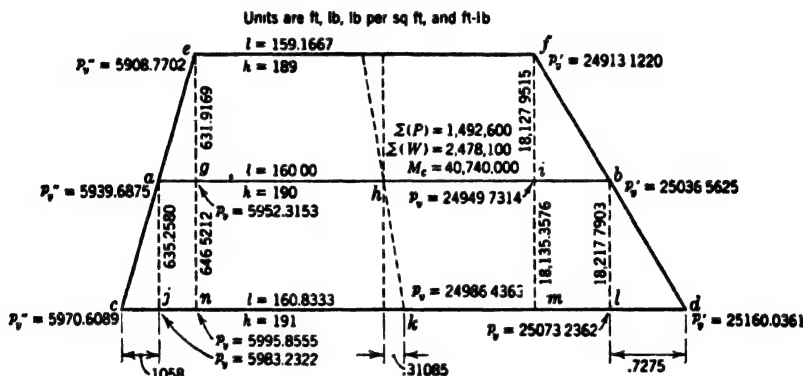


FIG. 5. Data for a numerical example.

The prisms  $e-f-b-a$  and  $a-b-d-c$  may now be analyzed for internal stresses. Vertical pressures at  $a$  and  $b$  being known, values at  $g$  and  $i$  are easily found by proportion. The total upward force on  $i-b$ , corresponding to the area 2'-17-6-4 of Fig. 3, is computed, and the weight of the triangle  $f-i-b$  is subtracted to give the shear on the plane  $f-i$ . The result is recorded on the diagram.

Shear on the plane  $e-g$  is found in the same way except that the vertical water load, corresponding to the area 3-9-10-1 on Fig. 3, must be taken into account. Using dimensions and pressures shown on Fig. 5, the computation is made thus:

$$\begin{array}{rcl}
 \text{Upward force on } a-g & = 0.5(5939.6875 + 5952.3153) \times 0.1058 & = 629.0869 \text{ lb} \\
 \text{Weight of } e-g-a & = 0.5 \times 1.00 \times 0.1058 \times 150 & = -7.9350 \text{ lb} \\
 \text{Vertical water load on } e-a & = 62.5 \times 189.5 \times 0.1058 & = -1253.0688 \text{ lb} \\
 \text{Total} & & = -631.9169 \text{ lb}
 \end{array}$$

Although the sign of the total as thus computed is minus, the shear on  $e-g$  is of the same sense as on  $f-i$ , and is considered positive.

Subtracting the vertical unit pressure at  $e$  from that at  $g$  leaves a remainder of 43.545 lb (for the 1 sq ft of intervening section). The corresponding remain-

TABLE 1  
MOMENTS AND FORCES AT  $h = 191$  Ft

Line	Description of items	Forces (lb)		Lever (ft)	Moment (ft-lb)
		Horiz.	Vert.		
1	Moments and forces at $h = 190$ ft	1,492,600.00	2,478,100.00		40,740,000
2	Moment correction to new center line, vertical forces			0.31085	-770,317
3	Moment correction to base, horizontal forces			1.00	1,492,600
4	Added masonry, rectangle		24,000.00	0.31085	-7,460
5	Added masonry, downstream triangle		54.56	79.9317	4,361
6	Added masonry, upstream triangle		7.94	80.3461	-638
7	Earthquake on added masonry, rectangle	2,400.00		0.5	1,200
8	Earthquake on added masonry, 2 triangles	6.25		0.3333	2
9	Vertical water on upstream face of block		1,259.69	80.3638	-101,233
10	Horizontal water (rectangle)	11,875.00		0.5	5,938
11	Horizontal water (triangle)	31.25		0.3333	10
12	Additional earthquake on water	1,014.64		0.5	507
13	Total at $h = 191$ ft	1,507,927.14	2,503,422.19	(16.52)	41,364,970

der for  $f-i$  is 36.6094 lb. Subtracting 150 lb, the weight of masonry per unit length, the remainders become -106.45 lb and -113.3906 lb. These values represent the net end dimensions of a differential shear diagram, similar to 7'-8'-17-16 of Fig. 3, which may be used for computing shears in the upper block, columns 1 and 2 of Table 2. Computations are begun at  $g$  (or at  $i$ , if desired) and stations are designated by distances from that point. Areas of the differential trapezoid corresponding to 7'-8'-17-16 of Fig. 3 are computed

**TABLE 2**  
**SHEAR AND HORIZONTAL STRESS COMPUTATIONS**

[All forces are in pounds.]

Stations	1	2	3	4	5	6	7	8	9
	$\lambda = 189 \text{ ft to } \lambda = 190 \text{ ft}$		$\lambda = 190 \text{ ft to } \lambda = 191 \text{ ft}$		Average shears	Col. 4 - col. 2	Net differential 15.00 - col. 4 + col. 2	$\Delta p_h$ Average col. $7 \times \Delta l$	$p_h$
	Areas of differential trapezoid	Total shear	Areas of differential trapezoid	Total shear					
<i>a</i>					* 627.957	* 14.602	* 0.398		12,816.44
<i>g</i>	0	631.917	0	646.521	639.219	14.604	0.396	0.04	12,816.48
<i>g</i> + 10	1,066.728	1,698.645	1,066.745	1,713.266	1,705.956	14.621	0.379	3.88	12,820.36
+ 20	2,137.813	2,769.730	2,137.785	2,784.306	2,777.018	14.576	0.424	4.02	12,824.38
+ 30	3,213.256	3,845.173	3,213.119	3,859.640	3,852.406	14.467	0.533	4.78	12,829.16
+ 40	4,293.056	4,924.973	4,292.747	4,939.268	4,932.120	14.295	0.705	6.19	12,835.35
+ 50	5,377.214	6,009.131	5,376.670	6,023.191	6,016.161	14.060	0.940	8.22	12,843.57
+ 60	6,465.729	7,079.646	6,464.888	7,111.409	7,104.528	13.763	1.237	10.88	12,854.45
+ 70	7,558.602	8,190.519	7,557.399	8,203.920	8,197.220	13.401	1.599	14.18	12,868.63
+ 80	8,655.832	9,287.747	8,654.206	9,300.727	9,294.238	12.978	2.022	18.10	12,886.73
+ 90	9,757.420	10,380.337	9,755.306	10,401.827	10,395.582	12.490	2.510	22.66	12,900.39
+ 100	10,863.365	11,495.282	10,860.706	11,507.227	11,501.252	11.940	3.060	27.85	12,937.24
+ 110	11,973.668	12,605.585	11,970.391	12,616.912	12,611.248	11.397	3.676	33.66	12,970.90
+ 120	13,088.328	13,720.245	13,084.375	13,730.896	13,725.570	10.651	4.349	40.11	13,011.01
+ 130	14,207.346	14,839.263	14,202.653	14,849.174	14,844.218	9.911	5.089	47.19	13,058.20
+ 140	15,330.721	15,962.638	15,325.226	15,971.747	15,967.192	9.109	5.891	54.90	13,113.10
+ 150	16,458.454	17,090.371	16,452.093	17,098.614	17,094.492	8.243	6.757	63.24	13,176.34
<i>i</i>	17,496.041	18,127.958	17,488.831	18,135.352	18,131.655	7.394	7.606	68.83	13,242.17
<i>b</i>					* 18,214.132	* 7.327	* 7.673	5.58	13,247.75

\* Values for stations *a* and *b* are found by extrapolation.

and recorded in column 1. The shear on  $e-g$  from Fig. 5 is recorded opposite  $g$  in column 2. Items in column 1 are added in turn (not cumulatively) to this value to give corresponding shear values in column 2. The end value, opposite point  $i$ , is 18,127.958 lb per sq ft, which checks the value of 18,127.9515 lb per sq ft found in advance and recorded on Fig. 5.

Shears in the lower block are similarly computed in columns 3 and 4. In order that computed shears in the two blocks may be opposite each other, computations in the lower block are started at  $g$  and ended at  $i$ . Values of the shear at these end points are found by preliminary computations and recorded on Fig. 5.

Values in columns 2 and 4 are averaged in column 5 to give vertical shear intensities along the section  $a-b$ . These values also represent horizontal shears at the stated stations along this section.

Horizontal and vertical shearing stresses being equal at any given point, values in columns 2 and 4 may be considered as unit horizontal shears at the mid-height of the upper and lower blocks. Their differences, column 6, represent net shear pulls on units of masonry between these planes.

Each cubic unit of masonry is also subjected to an earthquake force, acting downstream, which is 15 lb for this example. Subtracting values in column 6 from 15 lb gives the final differential forces of column 7, which act upstream. Values for points  $a$  and  $b$  are extrapolated. Adjacent values in column 7 are averaged and multiplied by their respective station lengths and recorded in column 8. These values must be balanced by changes in horizontal pressures.

Horizontal pressures at  $a$  and  $b$  may be computed from Eqs. 6 and 7 except that for this particular example, Eq. 7 must be slightly altered thus:

$$p''_h = p''_v + (p''_v - p''_h) \tan^2 \phi'' + p''_e \quad [12]$$

the difference being the addition of  $p''_e$ , the unit horizontal earthquake water pressure at the upstream face. In this example any possible vertical component of this force was ignored in the dam analysis; hence  $p''_e$  cannot be included as a part of  $p''_h$  without throwing the computations out of balance.

Both  $p'_v$  and  $p'_h$  are zero at the downstream face, hence  $p''_h = 12,816.44$  lb per sq ft at  $a$  and  $p''_h = 13,245.29$  lb per sq ft at  $b$ . The first of these values is entered in column 9, Table 2, opposite station  $a$ , and values in column 8 are added cumulatively to give horizontal compressive stresses at the various stations. The end result for station  $b$  is 13,247.77 lb per sq ft, 2.48 lb per sq ft less than the independently computed value, a discrepancy of about 0.02 of 1 per cent. No stress in the dam is known to this accuracy.

**11. Algebraic Determination of Shears.** The differential trapezoid 7'-8'-17-16 of Fig. 3 may be divided into a rectangle and a triangle; hence its partial area over a length,  $x$ , is a combined function of  $x$  and  $x^2$ , and the shear at  $x$  may be expressed by an equation of the form

$$s_x = A + Bx + Cx^2 \quad [13]$$

where  $A$ ,  $B$ , and  $C$  are constants. Their values may be determined from  $s'$  and

$s''$  at the ends of the section, and from the fact that  $\int s dx$  must equal the total horizontal shear, which is  $\Sigma(P)$ .

From the latter relationship we may write

$$\Sigma(P) = Ax + \frac{1}{2}Bx^2 + \frac{1}{3}Cx^3 \quad [14]$$

Also, need will later be found for the first derivative of Eq. 13, which is

$$\frac{ds}{dx} = B + 2Cx \quad [15]$$

Assuming the origin at the upstream end of the joint, values of  $A$ ,  $B$ , and  $C$  are as follows:

$$A = s'' \quad [16]$$

$$B = \frac{2}{l} \left( \frac{3\Sigma(P)}{l} - s' - 2s'' \right) \quad [17]$$

$$C = \frac{3}{l^2} \left( s'' + s' - \frac{2\Sigma(P)}{l} \right) \quad [18]$$

Values of  $s'$  and  $s''$  are determined from Eqs. 1 and 2,  $l$  is the known length of the joint, and  $\Sigma(P)$  is available from the dam computation.

**12. Algebraic Determination of Horizontal Stress.** Values in column 6, Table 2, represent  $\Delta s/\Delta h$ . Values in column 7 represent  $\Delta s/\Delta h + k_2$ ,  $k_2$  being the earthquake inertial force on a unit weight of masonry.

The numbers in column 6 represent a constant plus or minus the difference of two trapezoids. If these two trapezoids are superimposed, their differences will be represented by a third trapezoid and may be written

$$\frac{\Delta s}{\Delta h} + k_2 = E + Fx + Gx^2$$

If  $\Delta h$  is made very small and written as  $dy$ ,

$$\frac{ds}{dy} + k_2 = E + Fx + Gx^2$$

From Eq. 11,

$$\frac{ds}{dy} + k_2 = -\frac{dp_h}{dx}$$

As  $E$ ,  $F$ , and  $G$  are unknown as to sign as well as value, the minus sign may be ignored and we may write

$$\frac{dp_h}{dx} = E + Fx + Gx^2 \quad [19]$$

integrating,

$$p_h = D + Ex + \frac{1}{2}Fx^2 + \frac{1}{3}Gx^3 \quad [20]$$

Both  $(dp_h)/dx$  and  $p_h$  are determinable at  $x = 0$  and  $x = l$ , and the values thus obtained may be inserted in Eqs. 19 and 20 to form four simultaneous equations which may be solved for the unknown constants,  $D$ ,  $E$ ,  $F$ , and  $G$ . If desired, general solutions, similar to Eqs. 16, 17, and 18, may be written, or the solutions may be made directly after Eqs. 19 and 20 are put into numerical form.

**13. Numerical Computation of Principal Stress.** Let it be required to find the principal stresses at station  $g + 120$  for  $h = 190$  in Fig. 5, using shear and horizontal stress from Table 2. The vertical pressure at this station, found by interpolation from values shown on Fig. 5 or from Eq. 41, Chapter 7, is 20,275 lb per sq ft. The known constants, then, are as follows:

$$p_v = 20,275 \text{ lb per sq ft (by proportion)}$$

$$p_h = 13,011 \text{ lb per sq ft (from Table 2, column 9)}$$

$$s_v = 13,726 \text{ lb per sq ft (from Table 2, column 5)}$$

From Eq. 2a

$$\tan 2\beta = \frac{2s_v}{p_v - p_h} = \frac{2 \times 13,726}{7264} = 3.7792$$

$$\beta = 37^\circ - 35'$$

From Eq. 1a

$$p_1 = \frac{p_v \cos^2 \beta - p_h \sin^2 \beta}{\cos^2 \beta - \sin^2 \beta}$$

$$= 30,450 \text{ lb per sq ft}$$

From Eq. 1b

$$p_2 = p_v + p_h - p_1$$

$$= 2836 \text{ lb per sq ft}$$

The same result may be obtained graphically by means of Mohr's circle as explained in Art. 5, and once the principal stresses are known all stresses may be determined.

**14. Heel and Toe Stresses at the Base.** Concentrations of stress occur at abrupt changes in shape in all structural elements; consequently the generally used theory of straight-line distribution of vertical stress is not strictly applicable at changes in the profile of a dam. Except near the top, where the stresses are low, profile changes in dams usually are not abrupt, but distinct changes occur at the junction of the dam and the foundation. A brief discussion of this situation in Art. 14, Chapter 7, led to the conclusion that the theory of linear distribution of vertical reactions is a fair approximation of the actual distribution.

By a proper extension of the theory of internal stresses, an estimate can be made of the actual distribution of reactions between the dam and its base. Equations heretofore given in this chapter are not adequate for this purpose as



they are based on boundary conditions derived from the straight-line theory. A more general approach is needed.

A discussion of this subject will be found in a paper by Brahtz,<sup>4</sup> in which equations are developed and computed results are compared with results of photoelastic stress determinations. The equations are derived through the use of the Airy stress function and appear rather formidable to engineers of average mathematical ability. They are based on the assumption of an elastic homogeneous isotropic semi-infinite foundation. Such a foundation never exists, and it is impossible to determine the variable elastic properties of any rock foundation "en masse." Consequently, general equations for the determination of stress distribution in actual foundations cannot be precise. However, an analytical study such as that proposed by Brahtz, or a test by photoelastic means, affords a valuable insight to the problem, and study by these means may be justified on structures of magnitude.

The uncertainties involved are of the same nature as those encountered in the computation of foundation yielding (see Art. 10, Chapter 13), and the problems of computation are perhaps no more complicated. However, in the opinion of the authors, the process of analysis has not developed to a point which justifies its inclusion here.

The usual assumption of straight-line distribution may be used for all ordinary cases. If a case of unusual importance is encountered, the designer should make a complete review of published literature on the subject, and he may find it desirable to consult someone skilled in this type of computation and in photoelastic testing. The same comments apply to dam sections of special form, particularly those tending toward the condition illustrated in Fig. 24 of Chapter 7.

The designer must use his judgment as to what constitutes a case of "unusual importance." A good criterion for compressive stresses is the relationship of working stresses to ultimate strength. In gravity dams of moderate height, *computed* compressive stresses usually can be limited to 20 to 25 tons per sq ft. If the rock is good, *actual* stresses may overrun these values by an appreciable margin without danger. As the height increases, higher working stresses become necessary. For very high dams, working pressures may reach 30 or 40 tons or more per sq ft, and an appreciable overrun is of more importance.

Writers on foundation stresses attach considerable importance to the possibility that tension, not revealed by the equations of Chapters 7 and 8, may occur at the upstream end of the base, reservoir full. This possibility is usually ignored in structures of moderate proportions.

**15. Fillets in Corners.** It is well known in mechanics that the introduction of a fillet in a reentrant corner increases the strength of a structural member. This is no doubt also true in dams. Brahtz<sup>5</sup> treats this subject at some length and develops formulas for the relationship of fillet radius to stress.

<sup>4</sup> "The Stress Function and Photo-Elasticity Applied to Dams," *Trans. Am. Soc. Civil Engrs.*, Vol. 101, 1936, p. 1240.

<sup>5</sup> *Idem*, p. 1254.

The use of fillets at the junction of the dam and the foundation has not heretofore been common practice, but it has been recently adopted for such important structures as Shasta and Friant. The increased stresses (theoretically infinite) at corners without fillets apply to very short distances and doubtless tend to adjust themselves by superelastic yielding.

**16. Illustration of Foundation Stress Concentrations.** Computations made by Brahtz <sup>6</sup> for the Morris Dam for hydraulic load alone, and for the weight of the dam alone, are shown in Fig. 6.<sup>7</sup> Photoelastic stress curves are also shown for comparison. The sharp increase in stress at the corners is apparent.

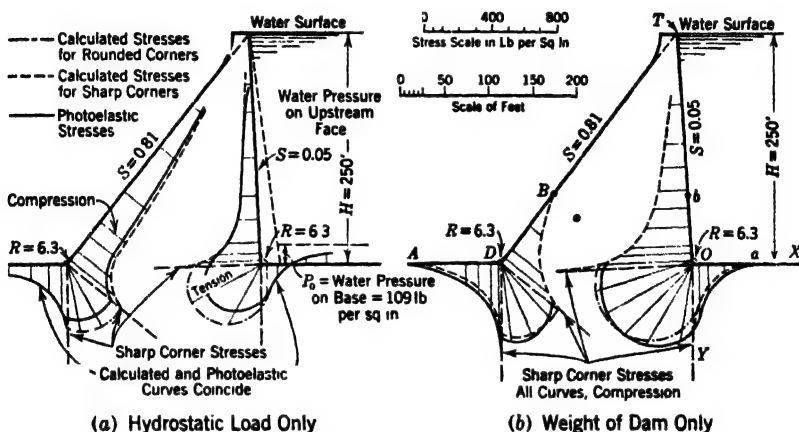


FIG. 6. Principal stresses along boundaries.

Stress computations in a preliminary study by Brahtz <sup>8</sup> for the Grand Coulee Dam are shown in Figs. 7 and 8.<sup>9</sup> Brahtz comments on these figures as follows:<sup>10</sup>

It will be seen that all stresses are compressive and tend to become infinite at the heel and toe. Of course, this is not possible because the material will become plastic before such magnitudes are reached and redistributions will occur near the corners, which must be considered as singular points where the elastic assumptions do not hold. The redistribution cannot be computed by the elastic theory, but it is evident that, after the plastic flow takes place, the stresses will be decreased near the corner and slightly increased a short distance from the corner. It will be noticed that the theoretical stresses are extremely high over only a minute distance so that the actual forces involved are very small. The effect of a redistribution, therefore, can only be slight.

<sup>6</sup> Idem.

<sup>7</sup> Reproduced from original paper by permission.

<sup>8</sup> BRAHTZ, op. cit.

<sup>9</sup> Reproduced from original paper by permission.

<sup>10</sup> BRAHTZ, op. cit., p. 1260.

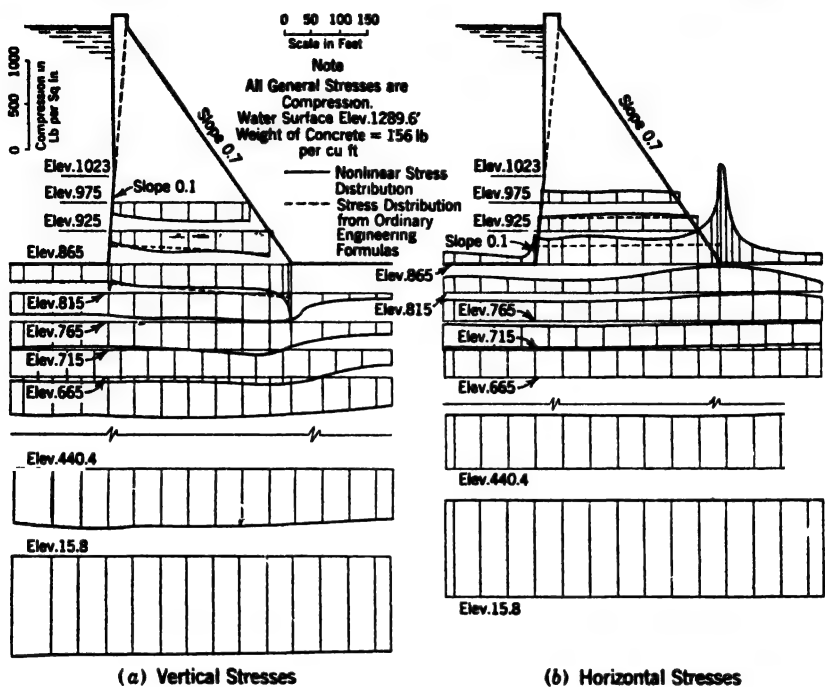


FIG. 7. Vertical and horizontal stresses at and near foundation plane.

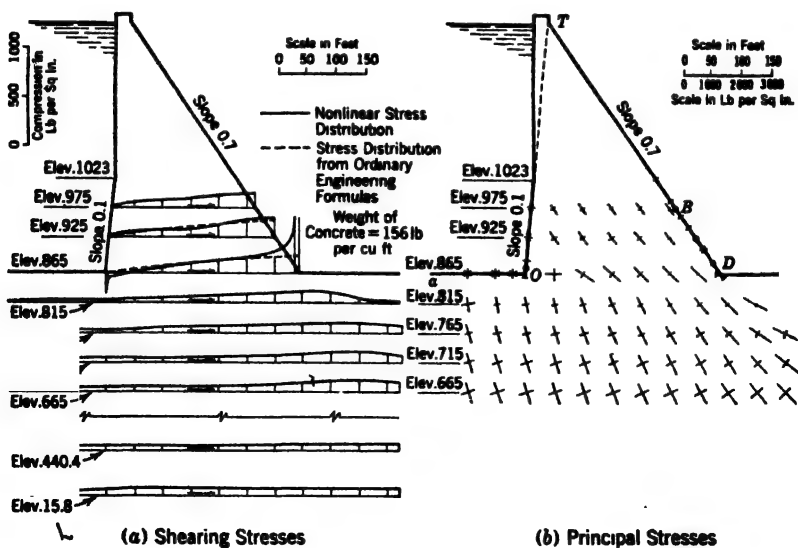


FIG. 8. Shear and principal stresses at and near foundation plane.

**17. Stress Concentration at Holes.** (a) *In plates.* If a thin plate subject to a uniform unidirectional primary stress is pierced by a hole, concentrations of unit stresses will occur at the sides of the hole parallel to the primary stress; and a transverse stress, of opposite sign, will occur at the opposite side. For

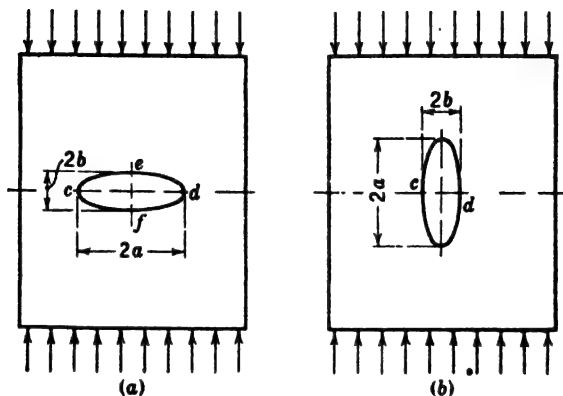


FIG. 9. Elliptical holes in stressed plates.

an elliptical hole laid flat to the direction of primary stress, as indicated at *a*, Fig. 9, Timoshenko gives the equations <sup>11</sup>

$$p_{c-d} = p_1 \left( 1 + 2 \frac{a}{b} \right) \quad [21]$$

and

$$p_{e-f} = -p_1 \quad [22]$$

where  $p_{c-d}$  is the unit stress at *c* or *d*,  $p_{e-f}$  is the unit stress at *e* or *f*,  $p_1$  is the unit stress if there were no hole, and  $2a$  and  $2b$  are diameters of the ellipse, normal and parallel, respectively, to the direction of stress.

If the ellipse is inverted, as in Fig. 9*b*, Eq. 21 becomes

$$p_{c-d} = p_1 \left( 1 + 2 \frac{b}{a} \right) \quad [23]$$

If the hole is circular,  $a$  and  $b$  are equal and  $p_{c-d}$  is  $3p_1$ .

These stress concentrations are purely local and reduce rapidly with increasing distance from the face of the hole. The distribution of the side stress for a circular hole in an infinite plate is <sup>12</sup>

$$p_x = \frac{1}{2} p_1 \left( 2 + \frac{r^2}{x^2} + 3 \frac{r^4}{x^4} \right) \quad [24]$$

<sup>11</sup> TIMOSHENKO, *Theory of Elasticity*, McGraw-Hill Book Co., 1934, p. 75 et seq.; also p. 175 et seq.

<sup>12</sup> Idem, p. 78.

where  $r$  is the radius of the hole and  $x$  is distance from the center of the hole. The value of  $p_x$  remains greater than  $p_1$  to an infinite distance, but beyond

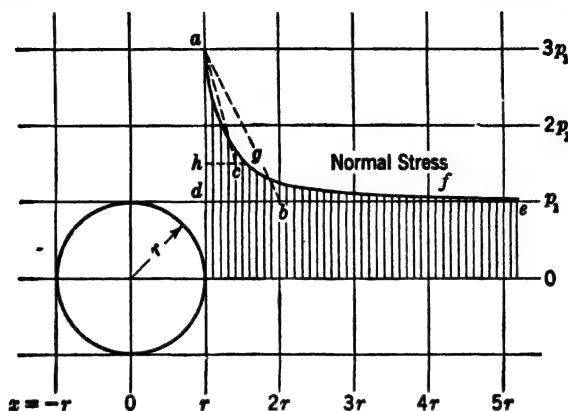


FIG. 10. Stress variation near an opening.

$x = 2r$  the difference is small. Eq. 24 is plotted to scale in Fig. 10. The area between the stress curve  $a-f$  and the line  $d-e$  must equal  $p_1 r$ .

The distribution of the transverse stress for a circular hole in an infinite plate is given by the equation<sup>13</sup>

$$p'_x = 0.5p_1 \left( \frac{r^2}{y^2} - 3 \frac{r^4}{y^4} \right) \quad [25]$$

where  $y$  is the vertical distance from the center of the circle. Eq. 25 is plotted to scale in Fig. 11. The stress reverses at about  $y = 1.7r$ . If point  $b$  represents  $y = 1.5r$ , the line  $a-b$  is a good practical approximation of the stress diagram. For this case, the stress at the surface is of opposite sign from the primary stress.

If the hole is rectangular, sharp local stresses occur at the corners.

(b) *In dams.* Openings of many kinds are required in dams. Stress conditions around such openings are usually more complicated than around openings in the idealized plates discussed in the preceding subsection. The dam slice through which

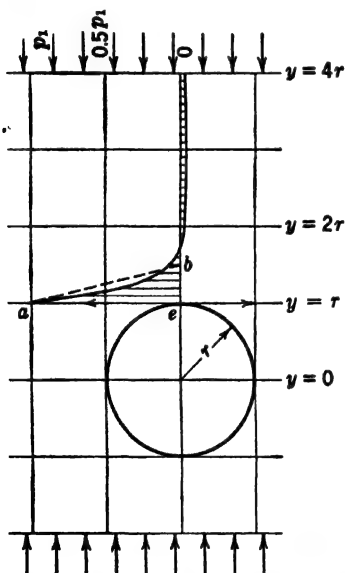


FIG. 11. Transverse stress near a circular opening.

the hole passes is never of infinite extent and the stress condition is usually complex. Rules derived for a single uniformly distributed stress in a plate of

<sup>13</sup> *Idem*, p. 77; Eq. 58,  $\theta = 0$ .

infinite extent are not strictly applicable to dam slices but, if properly used, may serve as a general guide to stress magnitudes.

Fig. 12 represents a slice from a gravity dam pierced by a circular drainage gallery at  $g$ . Fig. 12a shows an enlargement of a rectangular block cut from the slice containing the hole oriented with the directions of principal stresses at the position of the center of the hole if the hole did not exist. Two systems of transverse principal stresses are indicated. If these stresses are assumed to be uniform for indefinite distances away from the opening, two sets of opposing

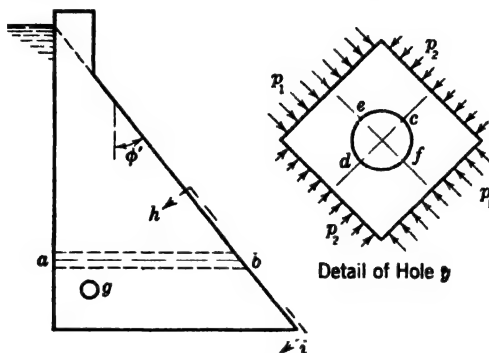


FIG. 12. Typical openings through dam.

stresses similar to the theoretical stresses in the thin plate, discussed above, will result. Thus unit compressions at  $c$  and  $d$  will be approximately

$$p_{c-d} = 3p_1 - p_2 \quad [26]$$

where  $p_1$  and  $p_2$  represent the first and second principal stresses. At  $e$  and  $f$  the stress will be

$$p_{e-f} = 3p_2 - p_1 \quad [27]$$

which becomes tension when  $p_1$  is greater than  $3p_2$ .

Eqs. 26 and 27 are merely convenient approximations of the true stress condition and apply approximately only to circular holes a considerable distance from a boundary. More complete equations for the solution of problems of this type have been derived by I. K. Silverman.<sup>14</sup>

Openings parallel to the dam axis, like the opening illustrated at  $g$ , Fig. 12, are of frequent occurrence. They usually are rectangular rather than circular. Frequently they are relatively close to the face of the dam or to the foundation. Principal stresses across them are not constant. No known equations can be expected to give accurately the stress concentrations around them. If these stresses are important, resort may be had to photoelastic analysis. The corners of such holes should be provided with fillets.

Openings transverse to the axis are also required. These may be inspection galleries, usually rectangular, or outlet tubes, usually circular. These are

<sup>14</sup> "Stresses Around Circular Holes in Dams and Buttresses," *Trans. Am. Soc. Civil Engrs.*, Vol. 103, 1938, p. 133.

studied by considering longitudinal slices of the dam parallel to the first principal stresses.

Referring again to Fig. 12, let  $a-b$  represent a circular outlet opening and let a view  $h-i$  of a portion of the face containing the opening be represented by Fig. 13. The opening will be elliptical in this view. Consider a slab of unit thickness. The only stress is  $p_x$ , acting as shown. Stresses at  $c$  and  $d$  are computed from Eq. 21 and at  $e$  and  $f$  from Eq. 22.

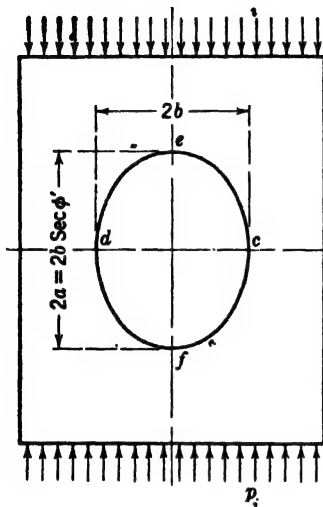


FIG. 13. Downstream face view of circular opening through dam.

The total tension may be approximated by assuming the surface intensity, Eq. 22 or 27, to reduce to zero in a distance equal to one-fourth the width of the opening (see discussion of Fig. 11). On this basis the total tension is

$$T = 0.25rp_{x-f} \quad [28]$$

where  $r$  is the radius of the circle or the half-width of the ellipse.

(d) *Reinforcement for compression.* The localized compressive stresses at the sides of circular or elliptical openings in dams are frequently ignored. However, where the principal stresses are high, as around an outlet tube at the face of a high dam, reinforcement may be desirable. If it is assumed that steel used for this purpose cannot be strained beyond the permissible strain limit for concrete in compression, the working unit stress cannot exceed  $n$  times the working stress of the concrete, where  $n$  is the ratio of the modulus of elasticity for steel to that for concrete. Experience indicates that shrinkage and "flow" of concrete appreciably increase the stress in the steel, and current specifications allow full stress value in longitudinal bars in columns.<sup>15</sup> It may therefore be assumed permissible to use normal working stresses in compressive reinforcement around holes in dams.

<sup>15</sup> Joint Committee Report, *Proc. Am. Soc. Civil Engrs.*, June 1940, p. 71 (Sec. 857)

In Fig. 10 the total excess compression is represented by the area between the curve  $a-g-f$ , and the line  $d-e$ . Its total amount is

$$T = rp_1 \quad [29]$$

where  $r$  is the radius of the circular hole. Eq. 29 holds for any shape of hole if  $r$  is taken as the half-width transverse to  $p_1$ . The distribution shown in Fig. 10 is for a circular hole only, without reinforcement. In any event, most of the excess compression is concentrated near the face of the hole.

An appreciable reduction in the amount of compression reinforcement is effected if an overstress is permitted in the concrete adjacent to the opening. In Fig. 10 the total value of  $T$  is equal to the area of the triangle  $a-d-b$ , which is  $1.00p_1r$ . Allowing a 50 per cent overstress, the value of  $t$  is the area between the curve  $a-g$  and the line  $h-g$ , or approximately the area of the triangle  $a-h-c$ , which is  $0.3p_1r$ .

**18. Numerical Examples of Circular Outlet.** Consider the circular outlet tube  $a-b$ , Fig. 12, with numerical data as follows:

Diameter of opening	= 8.00 ft
$\tan \phi'$	= 0.80
$p_i$ , inclined stress, without opening	= 50,000 lb/sq ft
Allowable overstress in concrete at the edge of opening	= 50 per cent
Allowable tensile stress in steel	= 16,000 lb/sq in.

Consider again an outside layer of unit thickness as in Fig. 13. Ignore the fact that the elliptical opening passes obliquely through the layer. The width of the opening is 8.00 ft and its height is  $8.00 \sec \phi' = 8\sqrt{1.64} = 10.24$  ft. From Eq. 22,

$$p_{c-f} = -p_1 = -p_i = -50,000 \text{ lb per sq ft}$$

From Eq. 28, at  $e$ , Fig. 13,

$$\begin{aligned} T &= 0.25 \times 4.0 \times 50,000 \\ &= 50,000 \text{ lb per lin ft} \end{aligned}$$

With an allowable stress of 16,000 lb per sq in., this requires 3.12 sq in. of steel per ft of opening, which is satisfied by  $1\frac{1}{2}$ -in. square bars, spaced 8.5-in. centers. These bars should extend beyond the tension limit sufficiently for adequate bond. A total length of twice the width of the hole will be adequate. The same reinforcement is required at  $f$ .

From Eq. 21, the estimated maximum compressive stress at the side of the opening is

$$\begin{aligned} p_{c-d} &= 50,000 \left( 1 + 2 \times \frac{4}{5.12} \right) \\ &= 128,000 \text{ lb per sq ft} \end{aligned}$$

The maximum excess over the allowable unit compression (with 50 per cent overstress) is  $128,000 - 75,000 = 53,000$  lb per sq ft. In Fig. 10 it is shown



that with a 50 per cent overstress the excess reduces to zero in a distance of about 0.4 of the radius of the opening. A similar curve may be constructed for an ellipse, but because of the approximate nature of the whole computation, it will be assumed that this excess will disappear in 0.5r, or 2 ft. Hence the excess total stress to be reinforced for is  $0.5 \times 2 \times 53,000 = 53,000$  lb per lin ft.

With a working stress of 16,000 lb per sq in., it is necessary to use 3.31 sq in. per ft of hole, which requires  $1\frac{1}{2}$ -in. square bars, spaced 8 in., or some equivalent arrangement.

Because of reducing compression, the effective working stress of the bars decreases with increasing distance from the face; hence large bars as close to the face as permissible are preferable.

The compression bars should be laid parallel to the direction of principal stress. They should extend beyond the compression area sufficiently to develop bond. For this example, 18-ft bars will be assumed.

Without the allowance for overstress, the total excess compression is

$$T = 4 \times 50,000 = 200,000 \text{ lb per ft}$$

and the required steel area is 12.5 sq in. per ft of opening, which requires three rows of  $1\frac{1}{2}$ -in. square bars, spaced about 6 in.

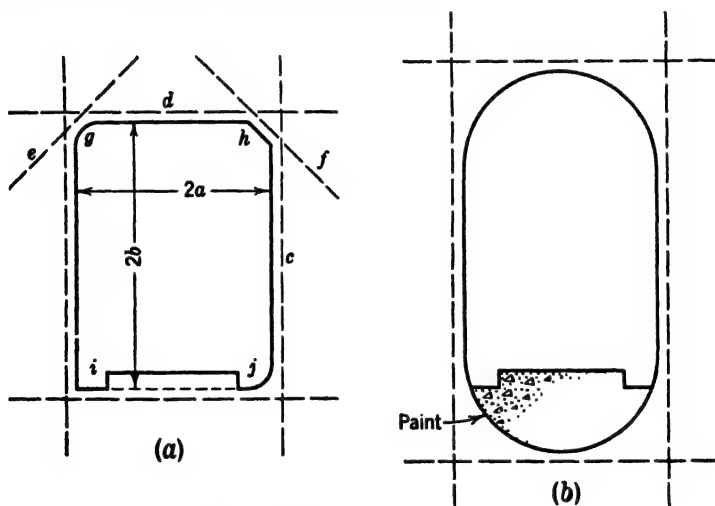


FIG. 14. Typical gallery details.

**19. Rectangular Gallery.** Let Fig. 14 represent a drainage gallery running parallel to the axis of the dam in about the position of opening *g*, Fig. 12. The critical stress condition will occur with reservoir empty. The first principal stress (without the opening) will not be parallel to the sides of the gallery but for the empty reservoir this usually may be ignored.

The distribution of stresses around such an opening is unknown. Concentrations at the corners will be sharp and will be influenced by the shape of the

corners. Fillets or chamfers as shown at *g* or *h* reduce these concentrations. The corner shown at *i* is often used where a drainage trough is required. The arrangement at *j* is better.

The total "excess" compression on one vertical side may be computed from Eq. 29 by making  $2a$  equal the width of the gallery. The amount of steel required in bars *c* may be computed as explained for vertical compression reinforcement in Art. 17, remembering that the results are only approximate.

The amount of tension along the top and bottom is unknown. As an approximation, the total tension may be assumed the same as for an ellipse of dimensions  $2a$  and  $2b$ , and the area of bars *d*, Fig. 14, may be computed as recommended for tension steel in Art. 17.

The corner bars, *e* and *f*, are optional. If used, their areas are determined arbitrarily. Where the gallery runs transverse to the axis and pierces the downstream face, a slab parallel to the face is considered as in the case of a circular hole.

The above treatment of a rectangular hole is no more than a rough approximation. If an exact analysis is required, resort must be had to detailed stress-function analysis or to a photoelastic test.

An alternative gallery design in which stress concentrations will more nearly approach those for an elliptical hole is shown in Fig. 14*b*. To provide a walkway, the semicircular bottom is filled in with an unbonded floor slab.

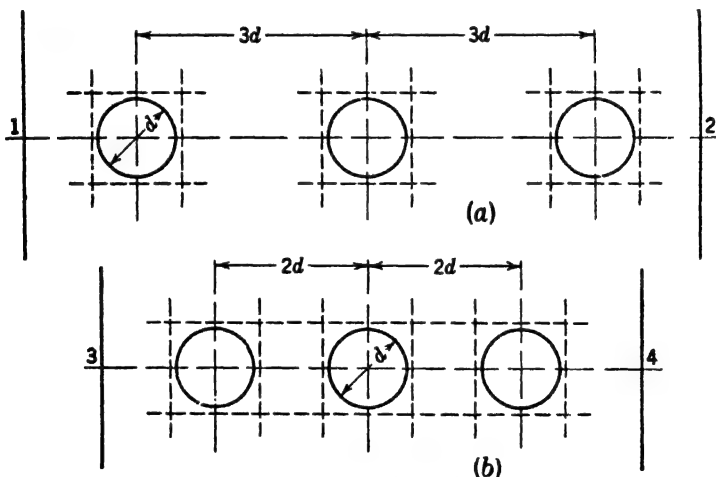


FIG. 15. Multiple openings through dam.

**20. Multiple Openings.** It is frequently necessary to provide a number of separate outlet tubes through a dam. In Fig. 15 a series of three such openings in a single horizontal plane is illustrated at *a* and a similar series, more closely spaced, at *b*.

If 1 and 2 represent vertical construction joints, the average compression on the unbroken portions of a section along 1-2 is equal to the total force on this

section, divided by the net area. The distribution of this stress is unknown. A safe design should result if the average compression does not exceed the allowable compressive stress and if compression steel is provided about as for a single hole (Art. 17).

If the holes are as close together as 2 diameters, the horizontal reinforcement may be made continuous. Such close spacing should be avoided if possible. For high dams, with high working compressive stresses, the widest practicable spacing of openings is desirable.

## CHAPTER 13

### ARCH DAMS <sup>1</sup>

**1. Classification of Arch Dams.** In a gravity dam the force of the water is held back by the weight of the masonry, with some assistance from shearing resistance and bond. The crushing strength of the masonry is important only in high dams. In arched dams the strength of the material is more fully developed.

Arch dams may be divided into two types: viz., the massive arch, where a single curved wall, usually vertical or nearly so, spans the full width between abutments; and the multiple arch, consisting of a number of smaller arches, usually inclined, supported on piers or buttresses. The present chapter deals only with massive arches. Multiple arches are discussed in Chapter 14.

Massive arch dams may be further divided, according to the theory used in the computation of stresses, into cylinder-theory and elastic-theory dams. Each of these types may be divided into constant-radius, constant-angle, and variable-radius sub-types, and elastic-theory arches are subject to further classification based on the completeness of the stress analysis.

#### CYLINDER THEORY OF DESIGN

**2. Theory of Cylinder Action.** In the cylinder theory for arch dams, the stresses are assumed to be approximately the same as in a thin cylinder of equal outside radius. Consider a ring 1-2 of unit height in the vertical submerged vessel of Fig. 1. The total load normal to a diameter is  $2w_2hr_e$ , where  $r_e$  is the outside radius of the ring,  $w_2$  is the unit weight of water, and  $h$  is the depth of the ring below the water surface. The resulting ring thrust is

$$T = w_2hr_e \quad [1]$$

and the average unit thrust,  $f$ , is

$$f = \frac{T}{t} = \frac{w_2hr_e}{t} \quad [2]$$

where  $t$  is ring thickness.

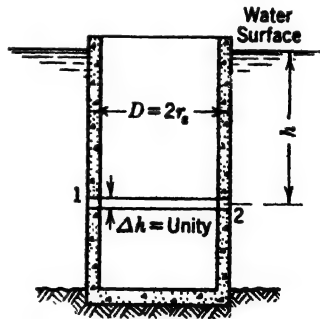


FIG. 1. Submerged cylinder.

<sup>1</sup> D. B. GUMENSKY, CARL H. HEILBRON, JR., WILLIAM H. SAYLOR, and other members of the staff of The Metropolitan Water District of Southern California rendered valuable assistance in the preparation of this chapter.

If  $t$  is small compared to  $r_e$ , the *maximum* unit stress will differ little from the *average* stress, as given by Eq. 2. If the cylinder wall is relatively thick, the stress distribution is not uniform. For great thicknesses, the difference between the maximum stress and the average stress may be appreciable. Formulas for thick cylinders may be found in standard works on mechanics.

For use in design, where the average allowable stress is prescribed and where the thickness is sought, Eq. 2 may be written

$$t = \frac{w_2 h r_e}{f} \quad [3]$$

which may be transformed to

$$t = \frac{w_2 h r_e}{f - 0.5 w_2 h} \quad [3a]$$

or

$$t = \frac{w_2 h r_i}{f - w_2 h} \quad [3b]$$

where  $r_e$  is the radius to the center line and  $r_i$  is the radius of the intrados of the ring.

An arch dam is never a complete cylinder, and stresses and dimensions computed by Eqs. 2 and 3 are only approximately correct. However, many

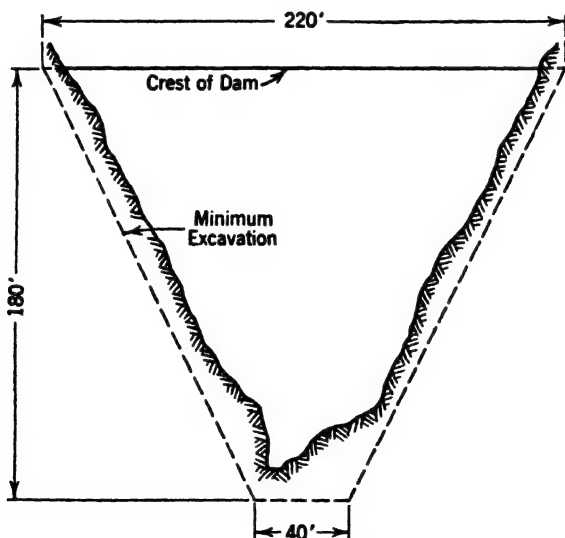


FIG. 2. Canyon cross-section, Examples 1, 2, and 3.

successful dams have been designed on this simple theory. Its use is still permissible for small dams in simple settings, provided a large allowance for stress uncertainties is made in choosing a factor of safety. Also, the cylinder theory is useful in preliminary studies. Examples of thin cylinder designs are

presented with the understanding that they are to be used only after the designer has gained an idea of the degree of approximation involved. Comparative designs for each of the sub-types, constant-radius, constant-angle, and variable-radius, will be prepared for the simple profile of Fig. 2.

**3. Example 1, Constant Radius.** (a) *Physical data.* In the simplest type of arch dam the radius to some feature, such as the upstream face, the downstream face, or the arch axis, is constant. An example will be worked out for the following data:

Dimensions of site, profile of Fig. 2.

Type of dam, constant radius to upstream face. Thin cylinder theory.

Material, concrete, ultimate strength at 28 days, 3000 lb/sq in.

Compressive working stress, 40,000 lb/sq ft.

Top thickness, min. 5 ft, which is approximately 1/40th of the top span.

(b) *Best central angle.* The masonry volume of any given arch is proportional to the product of the arch thickness and the length of the center line arc. For a fixed combination of span, loading, and permissible cylinder-theory stress, it can be shown that the area of the arch, in plan, is a minimum when

$$2\alpha = 133^{\circ}34' \quad [4]$$

or when

$$r = 0.544l \quad [5]$$

where  $2\alpha$  is the total angle subtended by the arc of the arch and  $l$  is the arch span. The radius may be  $r_e$ ,  $r_r$ , or  $r$ , if  $l$  is the corresponding span.

In a site with a variable span length, a constant-radius dam can have the correct central angle only at one elevation. However, an appreciable departure from the best angle makes only a small change in the volume of masonry. Eqs. 4 and 5 are applicable only to dams designed on the cylinder theory.

(c) *Laying out the dam.* The smallest masonry volume for the whole dam, with constant radius, is obtained by increasing the top angle to get the best average angle. For a given site, the top angle which gives the best average can be found by trial but it is usually impracticably large. Topography seldom permits a value as great as  $150^{\circ}$  for  $2\alpha$  at the top of the dam.

In the present example, a maximum value of  $150^{\circ}$  will be assumed. The corresponding value of the downstream radius,  $r_1$ , for the clear top width of 220 ft (Fig. 2) is 113.88 ft. The minimum top thickness being fixed at 5.00 ft,  $r_e$  is 118.88 ft. The theoretical thickness, below the top, is

$$t = \frac{w_2 h r_e}{40,000} = 0.186h$$

which varies as a straight line from zero at the top to 33.44 ft at the bottom.

The dam is laid out as follows:

(1) Draw the excavated rock contours, as shown on Fig. 3.

(2) Draw the center line 0-6 and locate the arch center 0. In an actual case, with irregular topography, 0 is located by trial.



(5) With center at 0, draw arcs through these points to the respective contours, which completes the plan of the dam.

(6) The cross-section 16-17-18 may be constructed before or after the plan is drawn.

All the dimensions and the stresses being thus determined, the design is complete.

(d) *Departure from best shape.* The relatively thin, wide-angled arches near the top of the dam conform with reasonable accuracy to the economic section. The bottom arch 11-7-14-13-6-12 is far from the best shape. The small arch 11-15-14 with a downstream radius of 21.76 ft and a thickness of 8.52 ft is equally strong, by the cylinder theory. This indicates that a constant-radius dam is not the most desirable type.

**4. Example 2, Constant Angle.** (a) *Constant-angle theory.* In Fig. 3 one arch somewhere near the top is of correct shape. For all others, the central angle is either too large or too small. It is theoretically possible to draw correct arches for each contour level and to place these on top of each other to form a dam. Such a procedure will be illustrated by an example, using the same data as for Fig. 3, except that the central angle rather than the upstream radius will be held constant.

TABLE 1  
COMPUTATIONS FOR EXAMPLE 2  
CONSTANT-ANGLE CYLINDER-THEORY DAM  
[Units are feet and pounds.]

1	2	3	4	5	6	7
$h$	$w_2h$	$f - w_2h$	$l_i$	$r_i = 0.544l_i$	$w_2hr_i$	$t = \frac{w_2hr_i}{f - w_2h}$
0	0	40,000	220	119.68	0	0.000
20	1,250	38,750	200	108.80	136,000	3.510
40	2,500	37,500	180	97.92	244,800	6.528
60	3,750	36,250	160	87.04	326,400	9.004
80	5,000	35,000	140	76.16	380,800	10.880
100	6,250	33,750	120	65.28	408,000	12.089
120	7,500	32,500	100	54.40	408,000	12.554
140	8,750	31,250	80	43.52	380,800	12.186
160	10,000	30,000	60	32.64	326,400	10.880
180	11,250	28,750	40	21.76	244,800	8.515

(b) *Laying out the dam.* The dimensions of the dam are computed and listed in Table 1. The span at the downstream face and the central angle for



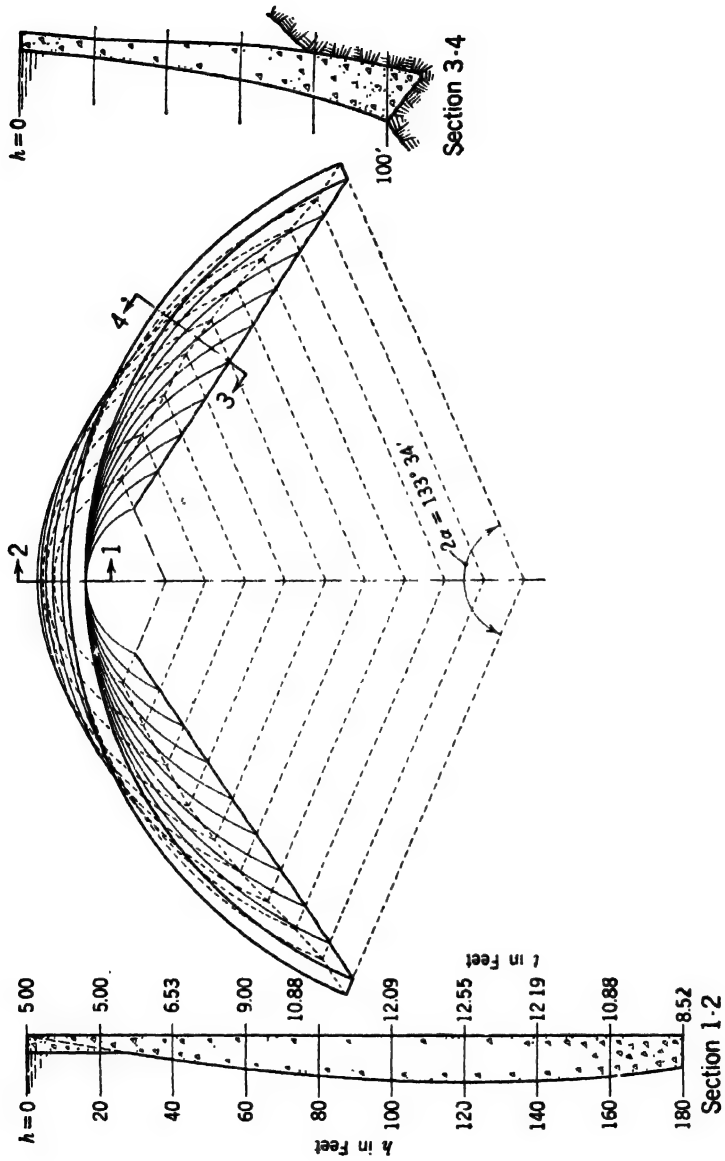


FIG. 4. Constant-angle arch dam, Example 2.

each arch being known, values of  $r_i$  are computed from Eq. 5 and recorded in column 5. Component parts of Eq. 3b are recorded in columns 2, 3, and 6, and  $t$  is computed in column 7. Arches laid out to these dimensions will be of correct theoretical shape. They may be superimposed in a number of ways, one of which is illustrated in Fig. 4. All possible arrangements require "overhang" upstream, downstream, or both. Excessive overhang for massive arch dams involves construction difficulties. However, dams with appreciable downstream overhang are now being built. The Calles dam (page 557) has a slight overhang. The Sweetwater Falls dam recently constructed near San Diego, California, by the California Water & Telephone Co., has a downstream overhang of approximately 32 ft. The dam of Fig. 4 contains about 70 per cent as much masonry as that shown in Fig. 3.

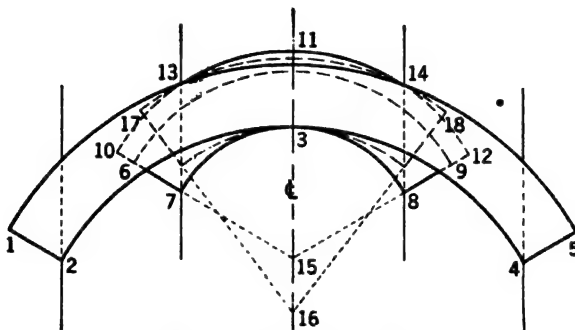


FIG. 5. Overhang of arches.

**5. Example 3, Variable Radius.** (a) *Variable-radius theory.* The so-called variable-radius dam is a compromise between the dams of Figs. 3 and 4. Neither the radius nor the central angle is constant. The design is begun at the top, the central angle for the first arch being made as wide as practicable. In Fig. 5 let 1-2-3-4-5 represent the top arch, or any other arch the dimensions of which have already been determined; and 6-7-3-8-9 the constant-angle design for the next contour interval below. Overhang can be eliminated by thickening the arch to 10-11-12. The undercutting from 13 to 10 and from 14 to 12 is permissible if the foundation rock is left in place to support the overhang; otherwise, point 10 must be moved all the way out to the face.

If the arch 6-7-3-8-9 fulfills the requirements of Eq. 3, 10-7-3-8-12 is thicker than necessary. Hence, the radius can be lengthened, and with a longer radius a smaller thickness is required to avoid overhang. By trial, an arch 16-17-18 is found which just avoids overhang and just fulfills the requirements of Eq. 3.

The dimensions of successive arches, proceeding downward, are determined in the same manner. If the contour intervals adopted for design are wide, as the 20-ft intervals of Figs. 2 and 3, points 13 and 14, Fig. 5, should be a little outside of the face 1-5 to avoid irregularity at intervening levels.

(b) *Laying out the dam.* The variable-radius principle will be illustrated for the identical data used for Figs. 3 and 4, except that both the radius and the central angle will be varied. The top angle should be made as large as convenient, which in the example will be assumed to be  $133^{\circ}34'$  (same as Fig. 4). From Eq. 5,  $r_c$  at the top of the dam is 124.68 ft. The top arch is laid out from the arch center, O, Fig. 6. The same radius and the minimum top thickness of 5 ft are good at the next depth interval.

At  $h = 40$  ft a greater thickness and a shorter radius are required. Choose a trial radius of 120.00 ft and compute the corresponding thickness 7.50 ft from Eq. 3, as indicated in Table 2. Lay this thickness from 1 to 2, Fig. 6.

TABLE 2  
COMPUTATIONS FOR EXAMPLE 3  
VARIABLE-RADIUS CYLINDER-THEORY DAM

[Dimensions in feet.]

$h$	$\frac{w_2 h}{f}$	$r_c$	$t = \frac{w_2 h r_c}{f}$
0	0.00	124.68	0.00
20	0.03125	124.68	3.90
40	0.06250	120.00	7.50
"	"	119.00	7.44
"	"	119.40	7.46
60	0.09357	113.00	10.59
"	"	112.00	10.50
80	0.12500	106.00	13.25
"	"	105.00	13.12
"	"	104.00	13.00
"	"	104.20	13.02
100	0.15625	98.00	15.31
"	"	96.00	15.00
120	0.18750	88.00	16.50
"	"	88.20	16.54
140	0.21875	80.00	17.50
"	"	80.50	17.61
160	0.25000	73.00	18.25
180	0.28125	66.50	18.70
"	"	66.00	18.56

Lay off the radius 120 ft from 2 to 3. An arc swung from point 3 through point 2 fails to cut the previous face at the  $h = 40$  ft contours, points 4 and 7; hence the assumed radius is incorrect. A second trial of  $r_c = 119.0$  ft was short

a value of 119.4 ft being found correct on the third trial. This procedure is continued to the bottom of the dam, the results being as shown in Table 2 and Fig. 6.

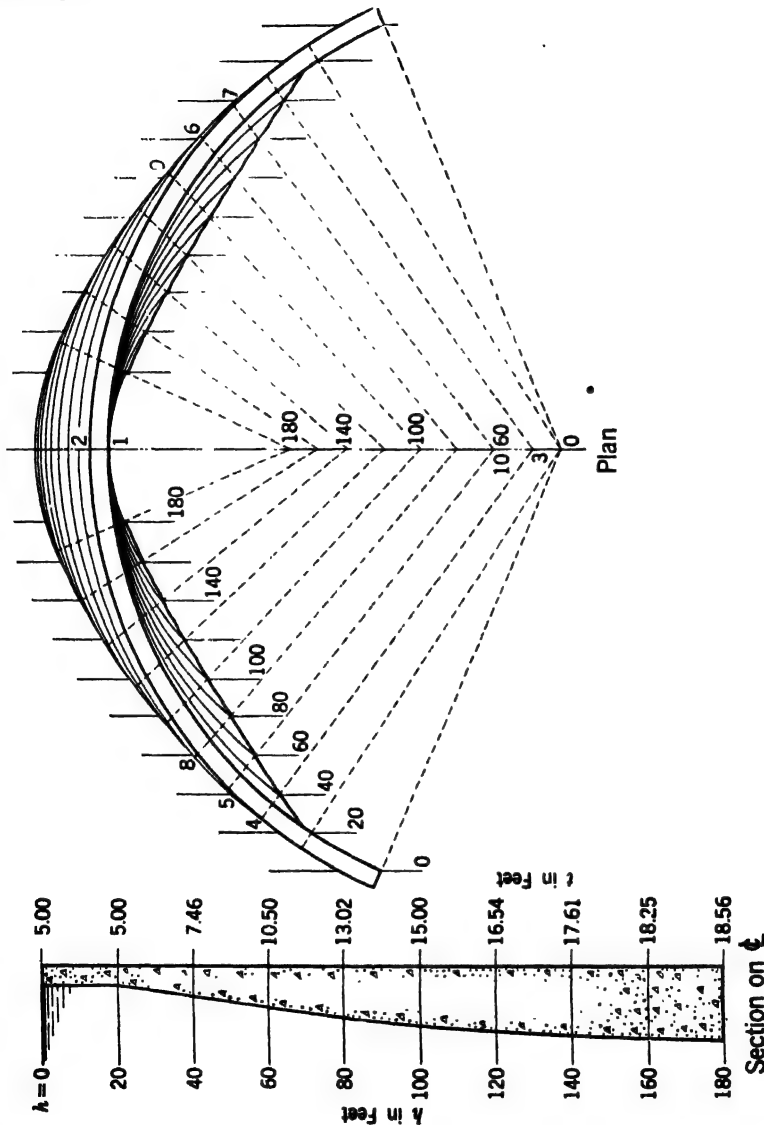


FIG. 6. Variable-radius arch dam, Example 3.

The masonry volume for Fig. 6 is about 82 per cent of that of the constant-radius dam of Fig. 3. This type of arch dam is widely used for both cylinder-theory and elastic-theory dams.

## ELASTIC THEORY OF DESIGN

**6. Need for Elastic Analysis.** (a) *Elastic deformations.* Because an arch slice from a dam is not a complete ring, stresses computed in accordance with the cylinder theory are only approximate. A complete ring under a uniform external load is shortened. Because the shortening is uniform, the shape of every portion of the ring must remain constant. In a segmental arch, such as any of the arches of Figs. 3, 4, and 6, the arch length is shortened by the load but the span is constant.<sup>1a</sup> Thus the loaded dam is deformed and moments and shears are introduced in addition to the normal-arch loads. Stresses produced in this manner are called rib-shortening stresses. If the arch is long and thin, with a large central angle, these stresses are small; but in thick, small-angle arches they are important.

(b) *Temperature change and shrinkage.* A drop in temperature causes a shortening of the arch length. Shrinkage also results from drying out of the concrete. These effects produce moments which are additional to those caused by elastic deformations. A rise in temperature has an opposite effect. These influences are small in flexible arches but are important in flat, thick ones. Both temperature and shrinkage effects may be variable throughout the thickness of the arch ring. (See Art. 9e.)

(c) *Abutment yielding.* In discussing elastic deformation, the abutment span was assumed fixed. Actually, the abutments are elastic and are slightly spread apart by the thrust of the arch. Such spreading adds to the rib-shortening effect. Also, if there are moments at the ends of the arch, the abutment faces will rotate slightly, which introduces further elastic forces. (See Art. 10a.)

(d) *Variable loads and arch forms.* The cylinder theory can be applied only to a simple concentric circular ring subject to a uniform radial loading. These restrictions do not apply to an elastic arch. The elastic theory is essential where inclined or irregularly shaped arches, earthquake loading, variable silt pressure, and other loading irregularities must be considered.

**7. Fundamentals of Elastic Theory.** The theory of elastic arches is amply covered in treatises on mechanics, masonry construction, and continuous structures. Reference should be made to a good text on mechanics for a complete discussion of fundamental principles, knowledge of which will be assumed in the following presentation.

**8. Statically Indeterminate Reactions.** Consider the arch of Fig. 7 and for the moment ignore foundation movement. Assume that the arch is rigidly attached to the abutment 1-2 and that the abutment 4-5 is removed and replaced by a resultant  $R$  having such *magnitude, direction, and position* that the end of the arch will not be rotated or displaced. It is convenient to resolve  $R$  into two unknown components, parallel to the  $x$  and  $y$  axes (see Fig. 8), and to assume that these act at the neutral axis of the arch. Actually, the point of application is unknown. An unknown moment  $M_R$  is introduced

<sup>1a</sup> Actually the span is slightly lengthened from foundation yielding. See Art. 10.

to account for this uncertainty. It is then possible to set up equations for the  $x$ ,  $y$ , and angular deflection of point 9, in terms of the known loads and these unknown elements of  $R$ . These deflections must separately equal zero; hence three equations are obtained which may be combined with the statical controls for the complete determination of the reactions.

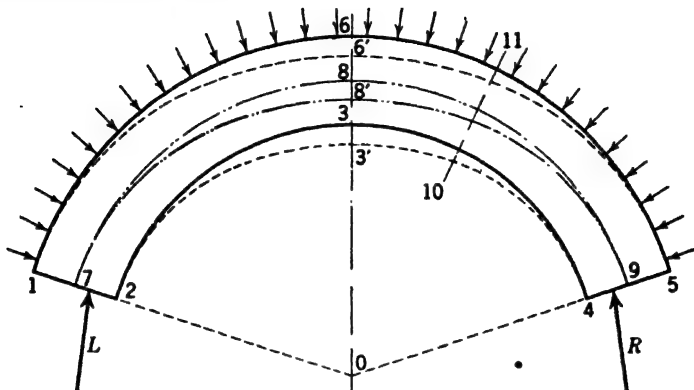


FIG. 7. Elastic deformation of arches.

If desired, instead of removing one of the abutments the arch may be assumed cut at some section as 10-11, usually at the crown, and first one and then the other of the resulting curved cantilevers removed and replaced with a thrust,  $T$ , unknown in magnitude, direction, and position. Resorting again to unknown  $x$  and  $y$  components, or to unknown thrust and shear compo-

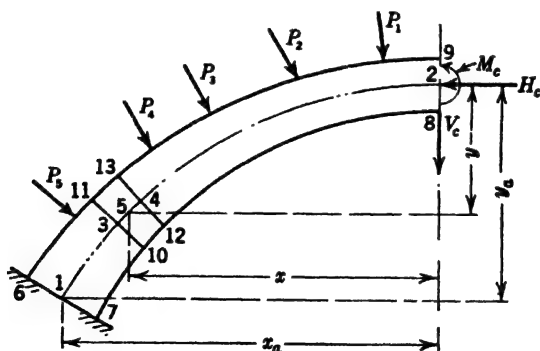


FIG. 8. Free half-arch.

nents, and an unknown moment, the  $x$ ,  $y$ , and  $\alpha$  deflections of each cantilever can be computed. These deflections no longer need be equal to zero but the respective deflections are numerically equal for the two parts of the arch.

If the arch and its loading are symmetrical about the center line 0-6, the analysis is simplified by dividing the arch into two equal halves. It makes

little difference whether an unsymmetrical arch is analyzed as a whole or as two approximately equal parts.

**9. Equations for Crown Deflections.** (a) *Loads and forces.* In Fig. 8, 6-7-8-9 represents the left portion of an arch, the right portion being replaced by its unknown reaction. This reaction is represented by a shear  $V_c$ , a thrust  $H_c$  acting at the neutral axis, and a moment  $M_c$ , all of unknown magnitude. The arch is subjected to known external loads  $P_1, P_2, P_3$ , etc., of any magnitude, which may be concentrated or distributed and which may act in any direction. Point 2 is taken as the origin of coordinates,  $x$  being positive to the left and  $y$  positive downward. The curve 1-2 represents the arch axis.

Consider an elemental voussoir, with center at point 5 and bounded by the radial planes 10-11 and 12-13. This element is subject to shear, thrust, and moment, resulting from combined action of the crown forces and external loads between point 5 and the crown. These forces produce deformations.

(b) *Moment deformations.* A moment acting on such a voussoir produces an angular deflection

$$\partial\alpha = \frac{M\Delta s}{EI} \quad [6]$$

where  $\partial\alpha$  is the change produced by the moment in the angle between planes 10-11 and 12-13,  $M$  is the moment,  $\Delta s$  is the length of the voussoir at the axis,  $E$  is the modulus of elasticity of the material of the arch, and  $I$  is the moment of inertia of the arch cross-section.

Eq. 6 is of the form generally used for flexure in straight beams. Flexure in curved beams is much more complicated, particularly where the ratio of thickness to radius of curvature is large. However, the same form of equation may be used with sufficient accuracy if all computations are referred to the neutral axis, which is displaced from the gravity axis toward the center of curvature<sup>2</sup> a distance

$$e = r - \frac{t}{1 + \frac{0.5t}{r} \operatorname{Log}_e \frac{1 - \frac{0.5t}{r}}{1 + \frac{0.5t}{r}}} \quad [7]$$

where  $r$  is the radius to the center line, or gravity axis, and logarithms are to the Napierian base. The last term of this equation represents  $r_n$ , the radius of the neutral axis.

Values of  $e/t$  for values of  $t/r$  from zero to unity are:

$t/r = 0.00$	0.10	0.20	0.30	0.40	0.50
$e/t = 0.0000$	0.0083	0.0167	0.0254	0.0337	0.0424
$t/r = 0.60$	0.70	0.80	0.90	1.00	
$e/t = 0.0513$	0.0604	0.0698	0.0796	0.0898	

<sup>2</sup> TIMOSHENKO, *Strength of Materials*, 1930, Part 2, p. 428.

Interpolations between these values are sufficiently accurate for all practical purposes. For a variable-thickness arch, the value of  $\epsilon$  is assumed proportional at each point to the radius of curvature of the center line at that point.

For ratios of  $r/t$  up to 0.25, the eccentricity of the neutral axis is frequently ignored. An occasional test for accuracy will enable the designer to decide when this refinement should be introduced.

The moment of inertia for straight, rectangular beams of unit thickness is

$$I = \frac{1}{12}t^3 \quad [8]$$

The corresponding value for a curved beam is

$$I_n = \epsilon r_n t^3 \quad [9]^3$$

which differs from  $\frac{1}{12}t^3$  by only 2 per cent for ratios of  $t/r$  as great as unity. Hence Eq. 8 may be used in all computations for arch dams.

Eq. 6 is applied to each of the elemental voussoirs making up the half-arch ring from 6-7 to 8-9, Fig. 8. The total rotation of the plane 8-9 with respect to the fixed plane 6-7 is

$$\Sigma_M \partial \alpha = \Sigma \frac{M \Delta s}{EI} \quad [10]$$

The summations are for the left half of the arch.

The moment  $M$  at any voussoir center is made up of component parts as follows:

$$M = M_E + M_c + H_c y + V_c x \quad [11]$$

where  $M_E$  is the moment of external forces between voussoir center and the crown about the voussoir center. Inserting this value in Eq. 10

$$\Sigma_M \partial \alpha = \Sigma \frac{M_E \Delta s}{EI} + \Sigma \frac{M_c \Delta s}{EI} + \Sigma \frac{H_c y \Delta s}{EI} + \Sigma \frac{V_c \Delta s}{EI} \quad [12]$$

This angular deflection, being for only a portion of the arch, is not necessarily equal to zero but must be equal to the deflection computed in the same manner for the remaining portion.

The moment,  $M$ , acting on the voussoir 10-11-12-13 also causes a displacement in space of the crown point 2. If the remainder of the half-arch is momentarily considered rigid, the hinge action at point 5 causes displacements at point 2 as follows:

$$\partial x = \frac{M \Delta s y}{EI} \quad [13]$$

$$\partial y = \frac{M \Delta s x}{EI} \quad [14]$$

<sup>3</sup>B. F. JAKOBSEN, "Stresses in Thick Arches of Dams," *Trans. Am. Soc. Civil Engrs.* Vol. 90, 1927, p. 484.



where  $\partial x$  and  $\partial y$  are the  $x$  and  $y$  components, respectively, of the displacement of point 2 by the rotation in the elemental voussoir.

Summating and substituting for  $M$  from Eq. 11, the total  $x$  and  $y$  movements at the crown, caused by moment, are

$$\Sigma_M \partial x = \sum \frac{M_E \Delta s y}{EI} + \sum \frac{M_C \Delta s y}{EI} + \sum \frac{H_c \Delta s y^2}{EI} + \sum \frac{V_c \Delta s x y}{EI} \quad [15]$$

$$\Sigma_M \partial y = \sum \frac{M_E \Delta s x}{EI} + \sum \frac{M_C \Delta s x}{EI} + \sum \frac{H_c \Delta s x y}{EI} + \sum \frac{V_c \Delta s x^2}{EI} \quad [16]$$

(c) *Thrust deformations.* The resultant of the crown forces and the external forces between point 5 and the crown produces a thrust on each elemental voussoir. This thrust causes a shortening of the voussoir, given by the equation

$$\partial s = \frac{T \Delta s}{AE} \quad [17]$$

where  $\partial s$  is the shortening of  $\Delta s$  by the thrust  $T$ , and  $A$  is the cross-sectional area of the arch ring.

These axial deformations are in different directions for the various blocks and must be resolved into  $x$  and  $y$  components for arithmetical summation, thus:

$$\partial x = \frac{T \Delta s}{AE} \cos \alpha \quad [18]$$

$$\partial y = \frac{T \Delta s}{AE} \sin \alpha \quad [19]$$

where  $\alpha$  is the angle between the  $y$  axis and the radii at the various voussoir centers.

The value of  $T$  is derived thus:

$$T = T_E + H_c \cos \alpha + V_c \sin \alpha \quad [20]$$

where  $T_E$  is the thrust at point 5, Fig. 8, caused by external loads between 2 and 5. Substituting into Eqs. 18 and 19 and summating, the total crown movements are

$$\Sigma_T \partial x = \sum \frac{T_E \Delta s}{AE} \cos \alpha + \sum \frac{H_c \Delta s}{AE} \cos^2 \alpha + \sum \frac{V_c \Delta s}{AE} \sin \alpha \cos \alpha \quad [21]$$

$$\Sigma_T \partial y = \sum \frac{T_E \Delta s}{AE} \sin \alpha + \sum \frac{H_c \Delta s}{AE} \sin \alpha \cos \alpha + \sum \frac{V_c \Delta s}{AE} \sin^2 \alpha \quad [22]$$

(d) *Shear deformations.* The resultant external and crown forces likewise produce a shear,  $S$ , at point 5, Fig. 8, which causes a displacement normal to the axis, given by

$$\partial n = \frac{kS\Delta s}{AG} \quad [23]$$

where  $\partial n$  is the shear displacement in the voussoir,  $k$  is the ratio of maximum unit shear to average unit shear,  $S$  is the shear, and  $G$  is the modulus of elasticity in shear. No serious error will result from assuming  $k = 1.2$  for arch dam design.<sup>4</sup> Actual shear distribution in curved beams is complicated.

These radial deformations are in different directions for the various blocks and must be resolved into  $x$  and  $y$  components for arithmetical summation, thus:

$$\partial x = \frac{kS\Delta s}{AG} \sin \alpha \quad [24]$$

$$\partial y = \frac{kS\Delta s}{AG} \cos \alpha \quad [25]$$

The value of  $S$  is given by the equation

$$S = S_E + H_c \sin \alpha + V_c \cos \alpha \quad [26]$$

where  $S_E$  is the shear at point 5 due to external loads between 2 and 5.

Summating Eqs. 24 and 25 and substituting from Eq. 26, the total crown deflections due to shear are

$$\Sigma \partial x = \sum \frac{kS_E \Delta s}{AG} \sin \alpha + \sum \frac{kH_c \Delta s}{AG} \sin^2 \alpha + \sum \frac{kV_c \Delta s}{AG} \sin \alpha \cos \alpha \quad [27]$$

$$\Sigma \partial y = \sum \frac{kS_E \Delta s}{AG} \cos \alpha + \sum \frac{kH_c \Delta s}{AG} \sin \alpha \cos \alpha + \sum \frac{kV_c \Delta s}{AG} \cos^2 \alpha \quad [28]$$

(e) *Effect of temperature change.* The crown is also subject to displacement by temperature change and shrinkage. Shrinkage of saturated concrete, except for temperature change, is small, and a loaded dam is wet. The total volume change effect is usually included in an assumed temperature range.

Referring again to the elemental voussoir, Fig. 8, a temperature change causes a change in the center line length given by the equation

$$\partial s = \Delta s C_F F \quad [29]$$

where  $C_F$  is the coefficient of thermal expansion and  $F$  is the average temperature change in the voussoir. Resolving into components and adding, the crown movements are

$$\Sigma_F \partial x = \Sigma \Delta s C_F F \cos \alpha \quad [30]$$

and

$$\Sigma_F \partial y = \Sigma \Delta s C_F F \sin \alpha \quad [31]$$

<sup>4</sup> PARCEL and MANEY, *Statically Indeterminate Stresses*, 2nd Ed., John Wiley & Sons, p. 27. VAN DEN BROEK, *Elastic Energy Theory*, John Wiley & Sons, p. 164.

If the average voussoir temperature change is constant from abutment to crown, Eqs. 30 and 31 simplify to

$$\Sigma_F \partial x = C_F F x_a \quad [32]$$

and

$$\Sigma_F \partial y = C_F F y_a \quad [33]$$

where  $x_a$  and  $y_a$  represent the coordinates of the arch center line at the abutment.

If the temperature varies in an upstream-downstream direction, a rotation is produced.<sup>5</sup> The exact law of radial temperature variation depends on many local conditions and is not readily predictable, nor is it constant from time to time at a given structure (see Art. 13c). Even for uniform variation from face to face, the deformation would be curvilinear if not restrained, and the restraint exerts an influence on stresses and deformation, particularly for thick short radius arches. An exact curvature formula is not available but the following approximation is suggested:

$$\partial \alpha = C_F \Delta F (1 - 0.5t/r) \Delta s/t \quad [34]$$

where  $\partial \alpha$  is total angular deformation in a voussoir and  $\Delta F$  is the total temperature difference from face to face. The total angular deflection is

$$\Sigma_{\Delta F} \partial \alpha = \Sigma C_F \Delta F (1 - 0.5t/r) \Delta s/t \quad [35]$$

The angular deflection causes displacements at the crown given by

$$\Sigma_{\Delta F} \partial x = \Sigma y C_F \Delta F (1 - 0.5t/r) \Delta s/t \quad [36]$$

and

$$\Sigma_{\Delta F} \partial y = \Sigma x C_F \Delta F (1 - 0.5t/r) \Delta s/t \quad [37]$$

Because of uncertainty in the value of  $\Delta F$ , and its internal distribution, the term  $(1 - 0.5t/r)$  may be taken as unity in thin arches.

Radial temperature increases in either direction according to the relative temperatures of air and water. A "cold" downstream face increases the moment at the crown, and a "hot" downstream face at the abutment. The designer should assume the most disadvantageous condition, or first one and then the other if uncertain.

**10. Foundation Deformations.** (a) *Fundamentals.* The foundations supporting the arches of a dam yield and turn under the action of thrust, shear, and moment. The prism 1 2, Fig. 9, of thickness  $\Delta b$  and width  $a$ , under a downward force, causes a depression of the underlying foundation material. If the foundation is isotropic, this deformation spreads to the sides and ends and the surrounding materials help support the prism. If two such prisms are placed side by side, the side support is reduced and the deformation increased. If many elemental slices are assembled to completely cover the rectangular area 5-4, the influence of side support becomes negligible for a

<sup>5</sup> See CLARENCE RAWHOUSER, *Temperature Control of Mass Concrete in Large Dams*, from "Dams and Control Works," U. S. Bur. Reclam., 1938, p. 243.

center slice. If the slices are independent of each other, deformation will vary with distance from the ends. If the prism is a solid unit, deformations will vary only as permitted by elastic yielding. The same reasoning applies to shear and moment deformation. The loaded area may be horizontal, vertical, or inclined.

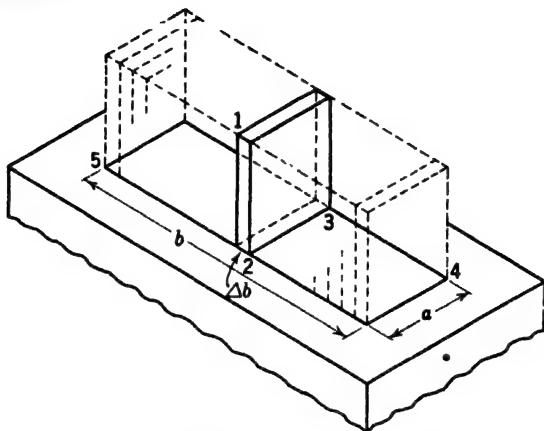


FIG. 9. Illustration of a loaded foundation.

(b) *Equations for normal reactions.* Fredrik Vogt <sup>6</sup> has derived equations for *average* deformation due to a *uniform* load on a plane rectangular *isotropic* foundation of *infinite extent*. These equations are involved algebraic expressions containing the variables  $a$ ,  $b$ ,  $E$ ,  $\mu$ , and the loads. By using diagrams for partial solution, they may be simplified to the following forms:

$$\partial'\alpha = \frac{Mk_1}{E_F a^2} \quad [38]$$

$$\partial's = \frac{Tk_2}{E_F} \quad [39]$$

$$\partial'n = \frac{Sk_3}{E_F} \quad [40]$$

$$\partial'\tau = \frac{Mk_4}{E_F a^2} \quad [41]$$

$$\partial''\alpha = \frac{Sk_5}{E_F a} \quad [42]$$

$$\partial''n = \frac{Mk_5}{E_F a} \quad [43]$$

<sup>6</sup> "Über die Berechnung der Fundamentdeformation," *Norske Videnskaps-Akad.*, Oslo, 1925.

Letters and symbols in these equations have the following significance, applied to a unit width foundation strip:

$M$  represents a moment acting normal to the foundation surface;

$T$  represents a thrust normal to the foundation surface;

$S$  represents shear, or tractive force, in the plane of the foundation;

$\bar{M}$  represents a twisting moment, acting in the plane of the foundation;

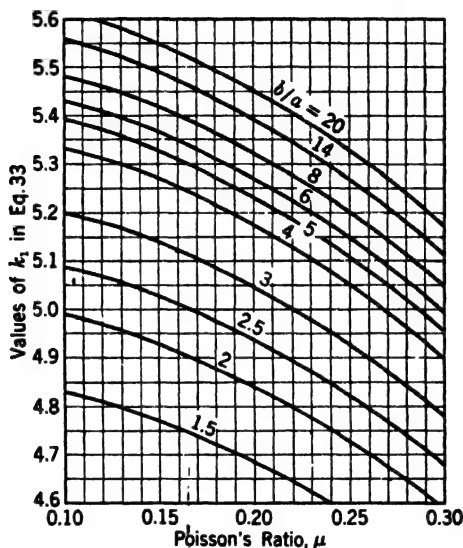


FIG. 10. Foundation deformation factor  $k_1$ .

$E_F$  represents Young's modulus for the foundation materials;

$a$  represents the length of a unit width element, as 2-3, Fig. 9;

$k_1, k_2, k_3, k_4$ , and  $k_5$  represent constants derived from the Vogt equations.

Their values are given in Figs. 10, 11, 12, 13, and 14;

$\partial/\alpha$  represents rotation or turning normal to the foundation surface from  $M$ ;

$\partial's$  represents the displacement of the foundation normal to its surface from  $T$ ;

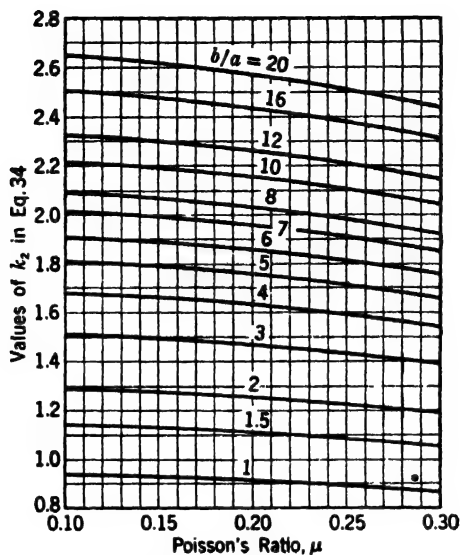
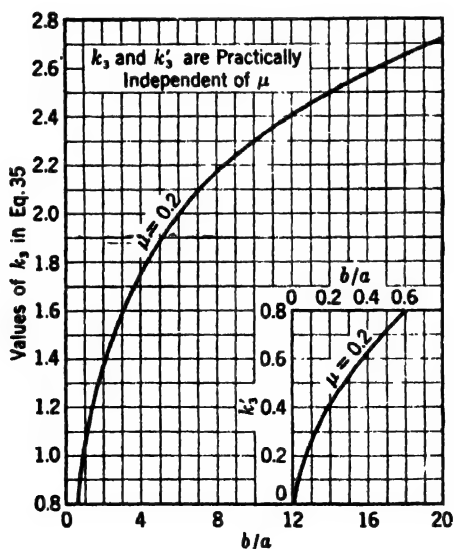
$\partial'n$  represents the displacement in the plane of the foundation from  $S$ ;

$\partial'\tau$  represents an angular twist of the foundation caused by a twist moment,  $\bar{M}$ . This effect is important only where the unit elements and forces are inclined to the foundation surface.

$\partial''\alpha$  represents the rotation normal to the foundation from  $S$ ;

$\partial''n$  represents the flexural displacement in the plane of the foundation from  $M$ .

(c) *Determining  $a/b$  for dam foundation.* A dam foundation is never of simple rectangular form, and the loading is irregular. No accurate means of

FIG. 11. Foundation deformation factor  $k_2$ .FIG. 12. Foundation deformation factors  $k_3$  and  $k'_3$ .

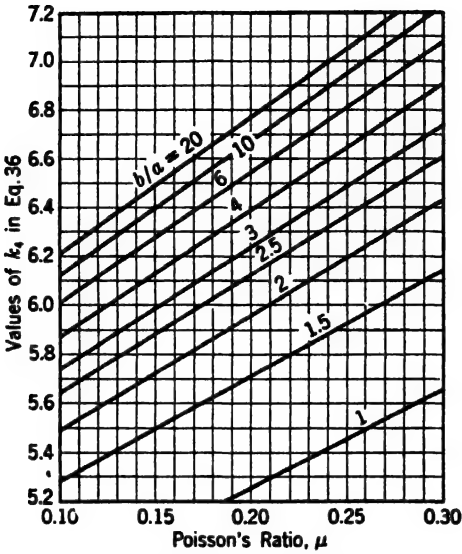


FIG. 13. Foundation deformation factor  $k_4$ .

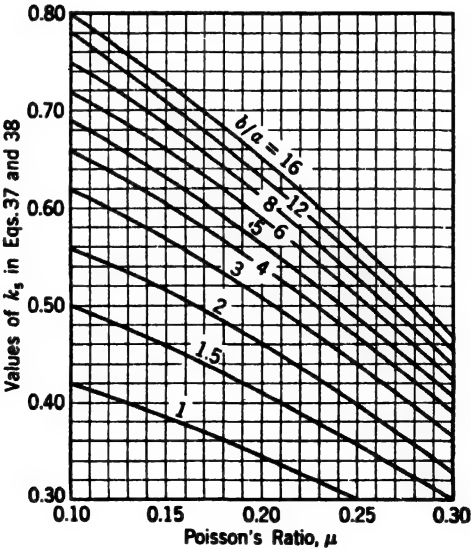


FIG. 14. Foundation deformation factor  $k_5$ .

providing for the size-shape factor is available. An approximation is illustrated in Fig. 15.

The actual plan of a curved dam is shown at the top of the figure, with a development of the abutment area below. This area is both straightened and flattened. A rectangle, 1-2-3-4, is drawn having about the same area as the developed surface. No definite rules are available for determining the length or width of this rectangle; hence it may as well be drawn by eye.

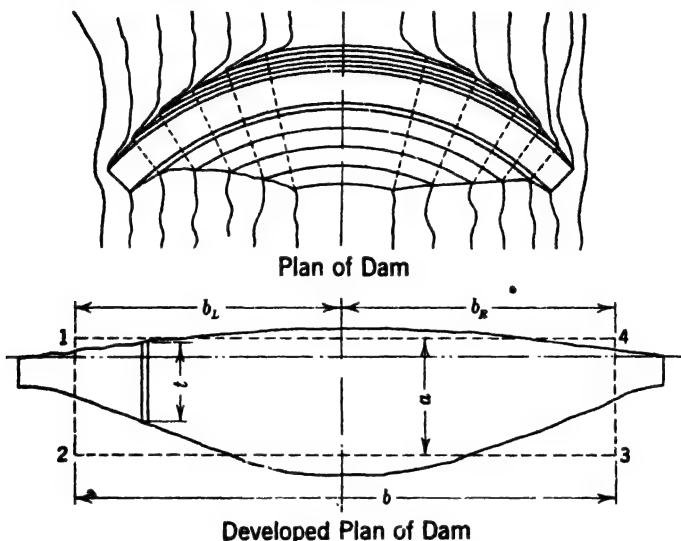


FIG. 15. Foundation dimension factors  $a$  and  $b$ .

Dimensions of the equivalent rectangle are used for finding values  $k_1$ ,  $k_2$ , etc. Opinion is divided as to whether the length  $b$  should be taken for the whole dam or half of it. In case of a narrow arch site with steep abutments, the reactions on the two sides are opposed and it is logical to consider each end separately, i.e., to use  $b_L$  and  $b_R$ , Fig. 15. If the dam site is wide with relatively flat abutment slopes, the angular and transverse shear deflection may be assumed to depend more nearly on the entire length  $b$ .

In Fig. 9, the dimension  $a$  of the foundation is also the length of the unit elements, and values of  $a$  and  $a^2$  appear in the deformation equations as structural elements. In Fig. 15, the structural width is no longer equal to the average width  $a$  but is a variable. The ratio  $b/a$  is still used in evaluating  $k_1$ ,  $k_2$ , etc. but  $t$  and  $t^2$  replace  $a$  and  $a^2$  in the deformation equations. This procedure is entirely empirical.

(d) *Equations for inclined reactions.* The arches of a dam are usually inclined to the abutment surfaces, which makes it necessary to alter Eqs. 38 to 43. In Fig. 16, let 1-2 represent the magnitude of a moment,  $M$ , acting in the center plane of a horizontal arch element of unit thickness, the abut-



ment surface being inclined to the plane of the arch by an angle  $\psi$ . The moment 1-2 can be resolved into two components 1-3 and 3-2 respectively parallel and normal to the foundation surface. The normal component  $M \sin \psi$  is spread over the slant width of the inclined abutment. The normal moment on a unit width of abutment is  $M \sin^2 \psi$ , which replaces  $M$  in Eq. 38.

Multiplying again by  $\sin \psi$ , the component motion in the plane of the arch is

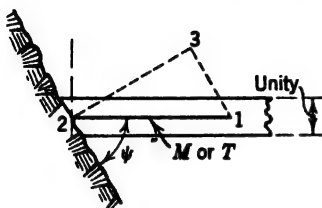


FIG. 16. Arch abutment angle.

$$\partial' \alpha = \frac{M k_1}{E_F t^2} \quad [44]$$

where  $t^2$  replaces  $a^2$  of Eq. 38.

The parallel component of the moment,  $M \cos \psi$ , or  $M \sin \psi \cos \psi$  per unit width foundation strip, produces a twisting deformation in the plane of the foundation which may be computed from Eq. 41. The twisting deformation has a component in the plane of the arch, given by the equation

$$\partial'' \alpha = \frac{M k_4}{E_F t^2} \sin \psi \cos^2 \psi \quad [45]$$

The thrust,  $T$ , similarly resolved, produces a direct deformation,

$$\partial' s = \frac{T k_2}{E_F} \sin^3 \psi \quad [46]$$

The parallel component,  $T \cos \psi$ , acts *up the abutment*, as a shear, producing a displacement which may be computed from a modification of Eq. 40 as follows:

$$\partial'' s = \frac{T k'_3}{E_F} \sin \psi \cos \psi \quad [47]$$

The value of  $k'_3$  is identical with  $k_3$ , except that the shear causing it acts in the direction of the long dimension of the dam and  $a/b$  must be substituted for  $b/a$  in entering the diagram, Fig. 12.

The direct shear effect is reduced only by the slant area of the foundation strip, altering Eq. 40 to the form

$$\partial' n = \frac{S k_3}{E_F} \sin \psi \quad [48]$$

Eqs. 42 and 43 take the respective forms

$$\partial'' \alpha = \frac{S k_5}{E_F t} \sin^2 \psi \quad [49]$$

and

$$\partial'' n = \frac{M k_5}{E_F t} \sin^2 \psi \quad [50]$$

(e) *Transverse components of deformations.* It is apparent from the preceding section that Eqs. 44 to 50 represent, in general, horizontal components of inclined deformations. These deformations likewise have vertical components. These vertical components do not affect the arch computation but are important in subsequent operations involving vertical elements of the dam. (See Arts. 24, 27, and 28.)

For Eqs. 44 and 45, the vertical components are

$$|\underline{\partial'\alpha} = \frac{Mk_1}{Eft^2} \sin^2 \psi \cos \psi \quad [44a]$$

and

$$|\underline{\partial''\alpha} = \frac{Mk_4}{Eft^2} \sin^2 \psi \cos \psi \quad [45a]$$

where the symbol  $|\underline{\quad}$  indicates that the movement is at right angles to the original force.

The equations for thrust deformation similarly become

$$|\underline{\partial's} = \frac{Tk_2}{E_f} \sin^2 \psi \cos \psi \quad [46a]$$

and

$$|\underline{\partial''s} = \frac{Tk'_3}{E_f} \sin^2 \psi \cos \psi \quad [47a]$$

The radial deformations of Eqs. 48 and 50 have no vertical components. They are also introduced into the cantilever computations (see Art. 35i) but without change.

Eq. 49 takes the form

$$|\underline{\partial''\alpha} = \frac{Sk_5}{Eft} \sin \psi \cos \psi \quad [49a]$$

(f) *Assembly of foundation equations.* Total foundation deformations for the arch are obtained by assembling Eqs. 44 to 50 as follows:

$$\partial_a \alpha = \frac{Mk_1}{Eft^2} \sin^3 \psi + \frac{Mk_4}{Eft^2} \sin \psi \cos^2 \psi + \frac{Sk_5}{E-t} \sin^2 \psi \quad [51]$$

$$\partial_a s = \frac{Tk_2}{E_f} \sin^3 \psi + \frac{Tk'_3}{E_f} \sin \psi \cos^2 \psi \quad [52]$$

$$\partial_a n = \frac{Sk_3}{E_f} \sin \psi + \frac{Mk_5}{Eft} \sin^2 \psi \quad [53]$$

where the subscript  $a$  identifies the deformation as due to abutment yielding and where  $M$ ,  $T$ , and  $S$  are end values for the arch given by Eqs. 11, 20, and 26, respectively. When full substitutions are made, these equations assume greatly extended forms which need not be written here. Some of the resultant

items are of minor importance and may frequently be neglected. (See Arts. 14j, 16c, and 16d.)

Corresponding equations for the transverse effects are .

$$\underline{\partial_a \alpha} = \frac{M}{E_r t^2} (k_1 + k_1') \sin^2 \psi \cos \psi + \frac{S k_5}{E_r t} \sin \psi \cos \psi \quad [51a]$$

$$\underline{\partial_a s} = \frac{T}{E_r} (k_2 - k_2') \sin^2 \psi \cos \psi \quad [52a]$$

$$\underline{\partial_a n} = \frac{S k_3}{E_r} \sin \psi + \frac{M k_5}{E_r t} \sin^2 \psi \quad [53a]$$

where the symbol  $\underline{\quad}$  indicates that the function acts at right angles to the plane of the element being analyzed. Eq. 53a is identical with Eq. 53.

It is convenient to rewrite Eqs. 51, 52, and 53, respectively, in the forms

$$\partial_a \alpha = M(E) + S(F) \quad [54]$$

$$\partial_a s = T(G) \quad [55]$$

$$\partial_a n = S(H) + M(F) \quad [56]$$

The significance of the symbols in parentheses is apparent by comparison with Eqs. 51, 52, and 53. The alternative transverse equations likewise may be abbreviated, thus:

$$\partial_a \alpha = M \underline{E} + S \underline{F} \quad [54a]$$

$$\partial_a s = T \underline{G} \quad [55a]$$

$$\partial_a n = S(H) + M(F) \quad [56a]$$

The significance of the terms  $\underline{E}$ ,  $\underline{F}$ , and  $\underline{G}$  is apparent by comparison with Eqs. 51a and 52a. Values of  $(H)$  and  $(F)$  are the same as in Eq. 56. Note that  $\underline{F}$  and  $(F)$  are not the same.

(g) *Crown displacements.* The angular displacement  $\partial_a \alpha$ , Eq. 51, causes an equal angular displacement at the crown. It also causes  $x$  and  $y$  displacements at the crown equal, respectively, to  $y \partial_a \alpha$  and  $x \partial_a \alpha$ . The  $\partial_a s$  and  $\partial_a n$  movements may be translated bodily to the center of coordinates and may be resolved into  $x$  and  $y$  components as required.

(h) *Limitation of accuracy.* The basic equations from which the factors  $k_1$  to  $k_5$  are computed assume an isotropic foundation material of infinite extent in the plane of the foundation and below it.

Even the best foundation is jointed and the foundation surface never approximates a plane. The determination of the dimensions  $a$  and  $b$ , Fig. 15, is not precise. The theory makes no allowance for these irregularities. The procedure outlined is the best so far proposed but its limitations must be recognized. Additional observations on actual dams are needed.

**11. Summary of Arch Equations.** The total displacements at the crown, obtained by the addition of the equations thus far deduced, are as follows:

$$\Sigma \partial \alpha = \Sigma_M \partial \alpha + \Sigma_{\Delta F} \partial \alpha + \partial_a \alpha \quad [57]$$

$$\begin{aligned} \Sigma \partial x = \Sigma_M \partial x + \Sigma_T \partial x + \Sigma_S \partial x + \Sigma_F \partial x + \Sigma_{\Delta F} \partial x + y \partial_a \alpha + \partial_a S \cos \alpha \\ + \partial_a n \sin \alpha \quad [58] \end{aligned}$$

$$\begin{aligned} \Sigma \partial y = \Sigma_M \partial y + \Sigma_T \partial y + \Sigma_S \partial y + \Sigma_F \partial y + \Sigma_{\Delta F} \partial y + x \partial_a \alpha + \partial_a S \sin \alpha \\ + \partial_a n \cos \alpha \quad [59] \end{aligned}$$

All summation equations may be written in differential form and integrated if the variables are expressible in simple algebraic terms. When full substitutions are made, Eqs. 57, 58, and 59 assume a greatly expanded form.

These equations for the left portion of the arch, equated each with its counterpart for the right portion, may be reduced, respectively, by transposition and combination to the forms

$$A_\alpha H_c + B_\alpha V_c + C_\alpha M_c + D_\alpha = 0 \quad [60]$$

$$A_x H_c + B_x V_c + C_x M_c + D_x = 0 \quad [61]$$

$$A_y H_c + B_y V_c + C_y M_c + D_y = 0 \quad [62]$$

The subscripts  $\alpha$ ,  $x$ , and  $y$  indicate respectively equations based on angular,  $x$ , and  $y$  deflections. The term  $A_\alpha$  is the algebraic sum of all of the coefficients of  $H_c$  in the expanded form of Eq. 57, the results for the right and left sides of the arch being combined. Similarly,  $B_\alpha$  is the sum of the coefficients of  $V_c$ , and so on. Values of  $H_c$ ,  $V_c$ , and  $M_c$  are found by the simultaneous solution of these equations.

**12. Cancellation of Factor  $1/E$ .** If Eqs. 57, 58, and 59 are fully expanded, each term except those dealing with temperature deformations will contain either  $1/E_M$ ,  $1/E_F$ , or  $k/G$ . The factor  $1/E_M$  may be introduced into the foundation equations by multiplying by  $E_M/E_F$ , a known ratio. The shear modulus may be expressed in terms of  $E$ , thus <sup>7</sup>

$$G = \frac{E}{2(1 + \mu)} \quad [63]$$

where  $\mu$  is Poisson's ratio. Hence

$$\frac{k}{G} = \frac{2k(1 + \mu)}{E} = \frac{n}{E} \quad [64]$$

where  $n$  represents the expression  $2k(1 + \mu)$ .

<sup>7</sup> TIMOSHENKO, *Strength of Materials* Vol. 1, 1930, p. 62.

By inserting a factor  $E_M/E_F$  in the foundation terms, substituting  $n/E$  for  $k/G$  in the shear terms, and multiplying the temperature terms by  $E_M$ , every term will contain the factor  $1/E_M$ , which may be eliminated. The resulting computed deflections will be  $E_M$  times the real deflections, but computed forces, moments, and stresses will be correct.

**13. Physical Constants.** (a) *Temperatures.* Concrete generates heat during hardening so that the temperature at some time during the hardening process is higher than at any subsequent time.<sup>8</sup> After the setting heat is lost, a routine seasonal temperature variation is established which depends on climate, weather, exposure, and concrete conductivity. The law of change is complex.<sup>9</sup> The temperature at the time of greatest deviation from the mean is never constant throughout the thickness or the length of the dam. In Eqs. 30 and 31,  $F$  is assumed to represent the departure from the mean, averaged for each voussoir. In Eqs. 32 and 33,  $F$  is averaged for the entire arch. In Eqs. 34, 35, 36, and 37,  $\Delta F$  represents the upstream-downstream variation, averaged for each voussoir, or for the entire arch, as desired. Available data seldom justify the assumption of variable values for  $F$  and  $\Delta F$ .

(b) *Value of  $F$ .* The stresses caused by a temperature rise are opposed to the load stresses; hence it is usual to consider only temperature drop. If an arch dam were poured quickly and completely, the value of  $F$  would be the difference between the maximum setting temperature and the ultimate minimum. Such a temperature drop would produce excessive stresses. Actually, much of the setting heat is lost during construction. Closing plugs, or contraction joints, should be left, to be filled or grouted after the setting heat has been dissipated. If the dam can be left out of service until it reaches its lowest ultimate temperature, and the joints filled at that time,  $F$  becomes zero, unless temperature rise is to be considered.

After carefully considering available data, the U. S. Bureau of Reclamation has adopted a temperature variation curve for arch dams<sup>10</sup> which is closely approximated by the empirical equation

$$F' = \frac{680}{t + 8} \text{ (usually use } 0.5 F') \quad [65]$$

where  $F'$  represents the total annual variation in temperature. If the joints are filled while the dam is at its mean annual temperature, then  $F$  may be taken as  $0.5F'$ .

In a thick arch dam, the time required for the dissipation of the heat of setting is excessive. This has led to the use of artificial cooling, by which

<sup>8</sup> IVAN E. HOUK, "Setting Heat and Concrete Temperatures," *Western Construction News*, Aug. 10, 1931, p. 411.

<sup>9</sup> R. E. GLOVER, "Flow of Heat in Dams," *J. Am. Concrete Inst.*, Proc., Nov.-Dec. 1934, p. 113.

<sup>10</sup> IVAN E. HOUK, "Temperature Variations in Concrete Dams," *Western Construction News*, Dec. 10, 1930, pp. 601-608.

means the final temperature may be achieved in a relatively short time. Such cooling has recently been successfully applied to a number of arch dams, a notable example being Boulder Dam.<sup>11</sup> The cost is moderate and more than justified by the benefits derived. With artificial cooling,  $F$  depends on the degree to which the ultimate low temperature is approximated.

(c) *Value of  $\Delta F$ .* The two faces of a loaded dam are not equally exposed. The temperature at the upstream face is controlled by the temperature of the water, which is more constant than air temperatures at the downstream face.

Daily and average air temperatures are generally known. Water temperatures may be approximated from measurements in similarly situated reservoirs. The U. S. Bureau of Reclamation has accumulated records of reservoir temperatures in the southwestern United States<sup>12</sup> which indicate, among other things, that (1) the lowest temperature will be about 40° F, which will not be limited to certain depths but will be general throughout the reservoir; (2) the highest temperature will be about 90° F, limited to water near the surface; (3) temperatures above 80° F will not extend to a depth greater than 40 ft; (4) the annual water temperature fluctuation has a range of about 15° F at the bottom and about 45° F at the surface; (5) the low limit of 40° F, being just above maximum density, may be assumed for most climates. The air face of the dam may drop below this but temperatures below 32° F probably do not exist at great distances below the surface. Also, it is doubtful if a slight drop below freezing would cause further shrinkage, particularly if the masonry is moist.

If  $\Delta F$  is considered at all, it is usual to assume one value for the entire dam, or  $\Delta F/t$  may be taken as a constant.

(d) *Thermal expansion coefficient for concrete.* The coefficient of thermal expansion (or contraction)  $C_F$  for concrete varies with composition. The usual range is from 0.000005 to 0.000007 per °F. Because  $F$  and  $\Delta F$  usually are not exactly known, a precise determination of  $C_F$  is not essential. A value of 0.000006 is frequently used. A more exact figure for any given concrete may be determined by test.

(e) *Setting shrinkage.* When concrete hardens in air, it is subject to shrinkage in addition to that caused by the loss of the heat of setting. The amount of setting shrinkage varies materially with the nature of cement and aggregates, the proportions, and the details of manufacture and curing. Shrinkage may disappear when the concrete is saturated. A loaded dam is usually wet; hence setting shrinkage is frequently ignored or allowed for by an arbitrary increase in the values of  $F$  and  $\Delta F$ . If the filling of closing plugs or contraction joints is delayed until after setting and drying out are complete, the effect of setting shrinkage is eliminated.

<sup>11</sup> B. W. STEELE, "Cooling Boulder Dam Concrete," *Eng. News-Record*, October 11, 1934.

<sup>12</sup> W. E. GREEN, "Measurement of Reservoir Water Temperatures in Southwestern U. S.," *U. S. Bur. Reclam. Tech. Mem.* 379, April 1934.

(f) *Young's modulus for concrete.* The joint Committee on Standard Specifications for Concrete and Reinforced Concrete<sup>13</sup> recommend values of  $E$  for concrete, for use in design, equivalent to the following:

$$f'_c = 2000 \text{ to } 2400, E = 2,000,000 \text{ lb/sq in.}$$

$$f'_c = 2500 \text{ to } 2900, E = 2,500,000 \text{ lb/sq in.}$$

$$f'_c = 3000 \text{ to } 3900, E = 3,000,000 \text{ lb/sq in.}$$

$$f'_c = 4000 \text{ to } 4900, E = 3,700,000 \text{ lb/sq in.}$$

$$f'_c = 5000 \text{ or more, } E = 5,000,000 \text{ lb/sq in.}$$

where  $f'_c$  is the compressive strength at 28 days.

The modulus varies with intensity and the duration of loading, as well as with the proportions of the concrete and the nature of its ingredients. Where the value of  $E$  is an important factor, a special study may be made.

(g) *Plastic flow.* The deformation of a concrete member under sustained stress slowly increases with time. This slow yielding, which is inelastic, is called "flow," and may be allowed for by using a reduced or "sustained" modulus of elasticity. Quantitatively, flow depends on the age of the concrete when loaded, duration of the load, and other factors. The "sustained" modulus varies with the stress throughout the length and thickness of the arch. Accurate allowance for it is impracticable at the present time. An approximate allowance can be made by an arbitrary reduction of  $E$ . Flow reduces stresses (but not deformation) due to temperature and shrinkage. However, this reduction takes place slowly after the load is applied; hence unless the application is very slow, early stresses will correspond to the normal modulus. It is usually on the safe side to ignore flow.

(h) *Poisson's ratio for concrete.* Poisson's ratio for concrete varies with the details of composition and manufacture, and with age. Values for working stresses usually run from 0.10 at early ages to 0.20 or a little more after 6 months or a year. Values of  $\frac{1}{6}$  and  $\frac{1}{5}$  are frequently used where specific determinations are lacking. Precision in choosing  $\mu$  is not essential.

(i) *Properties of stones.* The elastic properties of foundation rocks and stone masonry are widely variable and can be determined accurately only by individual tests. The properties listed in Table 3<sup>14</sup> show the impracticability of generalization.

The physical properties of a stone masonry arch dam are not necessarily the same as for the stones themselves, but with closely laid and well-filled joints may be assumed to be approximately the same. Jointing may similarly affect foundation constants. The designer cannot be relieved from a certain amount of judgment.

(j) *Earthquake loading.* Earthquake forces derived from the inertia of the masonry are computed as for other dams, Art. 13c, Chapter 7, except that

<sup>13</sup> Progress Report, January 1937, p. 44.

<sup>14</sup> J. B. JOHNSON, *Materials of Construction*, 8th Ed., John Wiley & Sons, 1939, p. 255

TABLE 3

## TESTS OF AMERICAN BUILDING STONE MADE AT THE WATERTOWN ARSENAL

Name of stone	Weight in lb per cu ft	Compression tests		Ratio of lateral expansion to longi- tudinal compression *	Shearing strength (lb)	Coefficient of expansion in water per °F
		Strength in lb per sq in.	Modulus of elasticity for working loads in lb per sq in.			
Brandford granite (Conn.)	162.0	15,707	8,333,200	0.250	1833	0.00000398
Milford granite (Mass.)	162.5	23,775	6,663,000	0.172	2554	0.00000418
Milford granite (Mass.)	..	..	..	..	..	0.00000415
Troy granite (N. H.)	164.7	26,174	4,545,400	0.196	2214	0.00000337
Milford pink granite (Mass.)	161.9	18,988	5,128,000	..	1825	..
Pigeon Hill granite (Mass.)	161.5	19,670	6,666,700	..	1550	..
Creole marble (Ga.)	170.0	13,466	6,806,500	0.345	1369	..
Cherokee marble (Ga.)	167.8	12,618	9,090,900	0.270	1237	0.00000441
Etowah marble (Ga.)	169.8	14,052	7,843,100	0.278	1411	..
Kennesaw marble (Ga.)	168.1	9,562	7,547,100	0.256	1242	..
Lee marble (Mass.)	..	..	..	..	..	0.00000454
Marble Hill marble (Ga.)	168.6	11,505	9,090,900	0.294	1332	0.00000194
Tuckahoe marble (N. Y.)	178.0	16,203	13,563,200	0.222	1490	0.00000441
Mt. Vernon limestone (Ky.)	139.1	7,647	3,200,200	0.250	1705	0.00000464
Bedford blue limestone (O.)	..	10,823	7,250,000	0.270	1017	0.00000380
North River bluestone (N. Y.)	..	22,947	5,268,800	..	..	..
Monson slate (Maine)	..	..	..	..	..	0.00000519
Cooper sandstone (Ore.)	159.8	15,163	2,816,900	0.091	1831	0.00000177
Sandstone, Cromwell (Conn.)	..	10,780	..	..	..	..
Maynard sandstone (Mass.)	133.5	9,880	1,941,700	0.333	1204	0.00000567
Kibbe sandstone (Mass.)	133.4	10,363	1,834,900	0.300	1150	0.00000577
Worcester sandstone (Mass.)	136.6	9,762	2,439,000	0.227	1242	0.00000517
Potomac sandstone (Md.)	..	..	..	..	..	0.00000500
Olympia sandstone (Oreg.)	..	12,665	..	..	..	0.00000320
Chuckanut sandstone (Wash.)	..	11,389	..	..	1352	..
Dyckerhoff Portland cement, neat	..	..	..	..	..	0.00000578

\* Poisson's ratio.

direction of motion plays a more important role. The inertial forces are not radial but are parallel to the axis of motion, and their effect may be greatest for cross-stream motion.

The influence of the curvature of the dam on the inertial effect of the water during an earthquake is uncertain but may be approximated in accordance with the tentative rules developed in Arts. 13e and 13f, Chapter 7. In cross-stream movement, the inclination on the receding side exceeds 90°, and the force is negative.

(k) *Water loads.* Water loads on arches are computed as for gravity dams, Art. 3, Chapter 7. If the dam is essentially vertical, it may be treated as if composed of a series of horizontal slices with stepped, vertical faces, and the



loads may be assumed normal to the upstream faces of these steps. If the structure is distinctly inclined so that it must be considered to be composed of inclined slices, then inclined pressures must be considered.

(l) *Weight of masonry.* The weight of the masonry of the arch is determined as for gravity dams, Art. 11, Chapter 7. If the arch is essentially vertical this weight is ignored in computing arch stresses except as it may indirectly influence interaction between adjacent arches (see Art. 28). If the unit arch slices are inclined, the component of the weight acting parallel to the arch slice is considered as a part of the arch loading.

### EXAMPLES OF ELASTIC ANALYSES

**14. Example 4, Analytical Analysis.** (a) *Selection of data.* An arch dam designed by the elastic theory may be of the constant-radius, constant-angle, or variable-radius type. The individual arches may be cylindrical rings under uniform normal loads or they may be of irregular form. For circular rings under uniform normal loads, the arch equations may be greatly simplified.

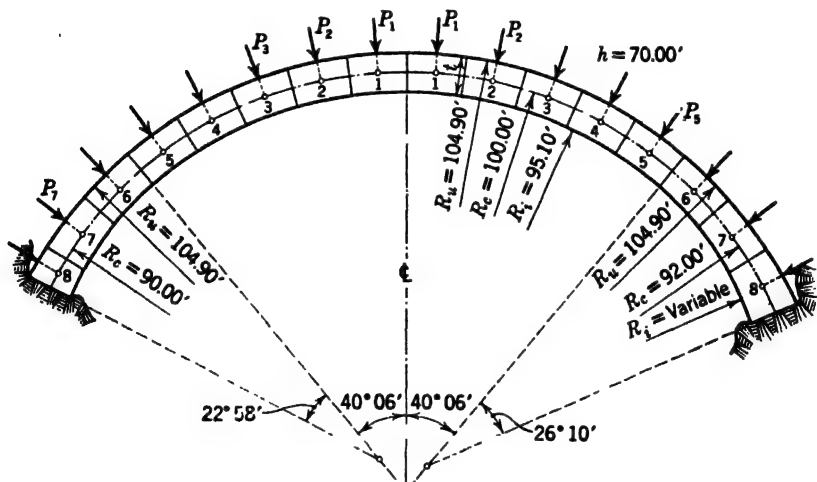


FIG. 17. Elastic arch, general case, Example 4.

Such arches are frequently assumed, particularly in preliminary studies, but more general shapes are also frequently encountered. It is desirable to illustrate the analysis of both types. This is best accomplished by beginning with a general case and simplifying for other forms. The arch of Fig. 17, with uniform normal loads, is chosen as an example.

In practice, this arch would be analyzed by some one of the simplified procedures to be subsequently developed, the general analysis being reserved for more complicated problems. However, this simple example is useful for

present purposes, as it involves no distracting complications, thus permitting attention to be concentrated on the method of analysis.

Data not shown on Fig. 17 are as follows:

*Arch Example No. 4*

*Unsymmetrical Elastic Arch Ring*

Dimensions as shown in Fig. 17,	
Abutment angle $\psi$ , left side,	60°
Abutment angle $\psi$ , right side,	65°
Depth below water surface, $h$ ,	70 ft
Water load = $62.5h$ ,	4375 lb/sq ft
Average temperature drop, $F$ ,	20° F
Radial temperature variation, $\Delta F$ ,	8° F
Temperature coefficient, $C_F$ ,	0.000006
Modulus of elasticity, arch,	3,000,000 lb/sq in.
Modulus of elasticity, foundation,	4,000,000 lb/sq in.
Poisson's ratio, arch,	$\frac{1}{6}$
Poisson's ratio, foundation,	0.20
Shear factor, $k$ ,	1.20
Shear modulus ratio, $n$ ,	2.80
Foundation ratio $b/a = 10$ but narrow site (assumed), hence use 5 (see Art. 10c)	

(b) *Laying out the arch* The arch is laid out to the given dimensions and divided into a convenient number of voussoirs. Because of the slenderness of the arch, the eccentricity of the neutral axis may be ignored (see Art. 9b). The center line lengths for the left and right sides, respectively, are 106.06 ft and 112.00 ft. A length of 14 ft for  $\Delta s$  will give seven full-length voussoirs and one short one on the left, and eight of full length on the right, which is satisfactory for an average arch.

(c) *Computation of constants.* The items required to build up Eqs. 60, 61, and 62, exclusive of foundation and temperature effects, are developed in Table 4. In the left-hand vertical column, the voussoirs are numbered consecutively from the crown to the abutment for both sides of the arch. The numbers refer to the voussoir midpoints. Column 1 contains values of the angle  $\alpha$ , between the  $y$  axis and radii to the various voussoir centers. These values are computed from the known values of  $\Delta s$  and  $r$ , or they may be measured from a carefully made drawing. The corresponding sines and cosines are shown in columns 2 and 3. Values of  $x$  and  $y$ , columns 4 and 6, are computed from the angular functions and the radii, or measured. Values of  $\Delta x$  and  $\Delta y$  represent differences between adjacent values of  $x$  and  $y$ , respectively. They are useful in the computation of  $M_g$ . Values of  $\Delta s$  are shown in column 8. Values of  $t$ , shown in column 9, may be computed or scaled. The arch slice being assumed 1 ft thick, the cross-sectional area  $A$  is equal to  $t$ , and values of  $\Delta s/t$  in column 10 may be substituted for  $\Delta s/A$  in the arch equations.

TABLE 4

## ARCH COMPUTATIONS, EXAMPLE 4

[Units are ft, lb and ft-lb;  $P$  is in pounds per panel.]

Point	1	2	3	4	5	6	7	8	9	10	10a	10b	11	12
Crown									9.80					
1	4° 01'	0.07005	0.99754	7.00	7.00	0.25	0.25	14.00	"	1.42857	10.00	0.36	0.17850	1.24950
2	12° 02'	0.20848	0.97903	20.85	13.85	0.25	1.95	"	"	"	29.79	3.14	"	3.72172
3	20° 03'	0.34284	0.93939	34.28	13.43	2.20	3.86	"	"	"	48.97	8.66	"	6.11898
4	28° 04'	0.47050	0.88240	47.05	12.77	6.06	5.70	"	"	"	67.22	16.80	"	8.39842
5	36° 06'	0.58920	0.80799	58.92	11.87	11.76	7.44	"	"	"	84.19	27.43	"	10.51722
6	44° 34'	0.70174	0.71243	69.60	10.08	19.20	9.03	"	9.85	1.42132	98.92	40.12	0.17580	12.23598
7	53° 29'	0.80368	0.59506	78.77	9.17	28.23	10.57	"	10.29	1.36054	107.17	52.79	0.15420	12.14633
8	60° 30'	0.87086	0.49242	84.77	6.00	38.80	9.23	8.06	10.93	0.73742	62.51	35.42	0.07408	6.27976
Abut.	63° 04'	0.89153	0.45295	86.68	1.91	48.03	3.56	"	11.23	"	"	"	"	"
Total						51.59				10.66213	508.77	184.72	1.29658	60.66761
Crown									9.80					
1	4° 01'	0.07005	0.99754	7.00	7.00	0.25	0.25	14.00	"	1.42857	10.00	0.36	0.17850	1.24950
2	12° 02'	0.20848	0.97903	20.85	13.85	2.20	1.95	"	"	"	29.79	3.14	"	3.72172
3	20° 03'	0.34284	0.93939	34.28	13.43	6.06	3.86	"	"	"	48.97	8.66	"	6.11898
4	28° 04'	0.47050	0.88240	47.05	12.77	11.76	5.70	"	"	"	67.22	16.80	"	8.39842
5	36° 06'	0.58920	0.80799	58.92	11.87	19.20	7.44	"	"	"	84.19	27.43	"	10.51722
6	44° 28'	0.70049	0.71366	69.60	10.68	28.22	9.02	"	9.84	1.42277	99.03	40.15	0.17633	12.27257
7	53° 11'	0.80056	0.59926	78.81	9.21	38.75	10.53	"	10.18	1.37525	108.38	53.29	0.15925	12.55048
8	61° 54'	0.88213	0.47101	86.31	7.50	50.55	11.80	"	10.35	1.29032	111.37	65.22	0.13154	11.33523
Abut.	66° 16'	0.91543	0.40246	89.37	3.06	56.85	6.30	"	11.31	"	"	"	"	"
Total										11.23119	558.95	215.05	1.35962	66.18212

Left Side

Right Side

Point	13	14	15	16	17	18	19	20	21	22	23	24
	$\frac{\Delta \alpha^2}{I}$	$\frac{\Delta \gamma}{I}$	$\frac{\Delta \gamma^2}{I}$	$\frac{\Delta \gamma \gamma}{I}$	$\frac{\Delta \gamma \sin^2 \alpha}{I}$	$\frac{\Delta \gamma \cos^2 \alpha}{I}$	$\frac{\Delta \gamma \sin \alpha \cos \alpha}{I}$	$P$	$\frac{P \gamma}{P \cos \alpha}$	$\frac{P \gamma}{P \sin \alpha}$	$\Sigma P \gamma$	$\Sigma \alpha \Sigma P \gamma$
Crown	.....	.....	.....	.....	.....	.....	.....	.....	.....	437.500	.....	.....
1	8.75	0.04462	0.01	0.31	0.00701	1.42155	0.09983	64.250	64.090	4.502	.....	.....
2	77.60	0.39270	0.86	8.19	0.06209	1.36649	0.29128	"	62.840	13.390	64.090	887.600
3	209.76	1.08171	6.56	37.08	0.16791	1.26065	0.46009	"	60.360	22.030	126.930	1,704.700
4	395.15	2.09916	24.69	98.77	0.31624	1.11233	0.59310	"	56.690	30.230	187.290	2,391.700
5	619.67	3.42720	65.80	201.93	0.49594	0.93264	0.68010	"	51.910	37.860	243.980	2,896.000
6	851.60	4.90283	140.10	345.41	0.69091	0.72140	0.71058	64.270	45.790	45.100	205.890	3,160.100
7	950.77	5.18296	232.14	471.28	0.87877	0.48176	0.65066	64.410	38.330	51.770	341.680	3,133.200
8	532.34	3.55846	170.80	301.62	0.55822	0.17881	0.31615	37.200	18.320	32.380	380.010	2,280.100
Abut	.....	.....	.....	.....	.....	.....	.....	.....	.....	.....	398.330	760.800
Total	3,651.64	21,54924	641.05	1,404.59	3,18649	7,47563	3,8169	.....	.....	.....	.....	.....
Crown	.....	.....	.....	.....	.....	.....	.....	.....	.....	437.500	.....	.....
1	8.75	0.04462	0.01	0.31	0.00701	1.42155	0.09983	64.250	64.090	4.502	.....	.....
2	77.60	0.39270	0.86	8.19	0.06209	1.36649	0.29128	"	62.840	13.390	64.090	887.600
3	209.76	1.08171	6.56	37.08	0.16791	1.26065	0.46009	"	60.360	22.030	126.930	1,704.700
4	395.15	2.09916	24.69	98.77	0.31624	1.11233	0.59310	"	56.690	30.230	187.290	2,391.700
5	619.67	3.42720	65.80	201.93	0.49594	0.93264	0.68010	"	51.910	37.860	243.980	2,896.000
6	851.17	4.97603	140.42	346.33	0.69813	0.72463	0.71129	64.260	45.860	45.010	295.890	3,160.100
7	989.10	6.17094	239.12	486.33	0.88139	0.49387	0.65977	64.370	38.570	51.530	341.750	3,147.500
8	979.90	6.64935	336.12	573.91	1.00407	0.28626	0.53612	64.590	30.420	56.980	380.320	2,852.400
Abut.	.....	.....	.....	.....	.....	.....	.....	.....	.....	.....	410.740	1,256.700
Total	4,134.10	24,84171	813.58	1,752.85	3,63278	7,50842	4,03155	.....	.....	.....	.....	.....

TABLE 4—Continued  
ARCH COMPUTATIONS, EXAMPLE 4

Point	25	26	27	28	29	29a	30	31	32	33
	$\Sigma(\Delta x \Sigma P_y)$	$\Sigma P_z$	$\Delta y \Sigma P_z$	$\Sigma(\Delta y \Sigma P_z)$	$\Delta y P$	$\frac{M}{I}$ from Col. 4 Table 28	$\frac{M}{I} = \frac{\Sigma(\Delta x \Sigma P_z) - \Sigma(\Delta y \Sigma P_z)}{\Delta y P + \frac{M}{I}}$	$\frac{\Delta x}{I} M$	$\frac{\Delta x}{I} M$	$\frac{\Delta y}{I} M$
<b>Left Side</b>										
Crown	.....									
1	.....	437,500	109,400	109,400	112,400		3,000	536	3,700	100
2	887,600	433,000	844,400	953,800	"		46,200	8,247	171,900	18,100
3	2,592,300	419,610	1,619,700	2,573,500	"		131,200	23,419	802,800	141,900
4	4,984,000	397,580	2,266,200	4,839,700	"		256,700	45,821	2,155,900	538,900
5	7,880,000	367,350	2,733,100	7,572,800	"		419,600	74,869	4,413,000	1,438,100
6	11,040,100	329,490	2,975,300	10,548,100	112,500		604,560	106,271	7,396,500	3,000,000
7	14,173,300	284,390	3,006,000	13,554,100	112,700		731,900	112,859	8,889,900	4,378,900
8	16,453,400	232,620	2,146,900	15,701,000	37,500		789,900	58,516	4,960,400	2,810,800
Abut	17,214,200	200,240	712,900	16,413,900			800,300			
Total								430,568	28,794,100	12,328,500
<b>Right Side</b>										
Crown	.....									
1	.....	437,500	109,400	109,400	112,400		3,000	536	3,700	100
2	887,600	433,000	844,400	953,800	"		46,200	8,247	171,900	18,100
3	2,592,300	419,610	1,619,700	2,573,500	"		131,200	23,419	802,800	141,900
4	4,984,000	397,580	2,266,200	4,839,700	"		256,700	45,821	2,155,900	538,900
5	7,880,000	367,350	2,733,100	7,572,800	"		419,600	74,869	4,413,000	1,438,100
6	11,040,100	329,490	2,972,000	10,544,800	112,500		607,800	107,173	7,459,300	3,024,400
7	14,187,600	284,480	2,995,600	13,540,400	112,600		759,800	120,998	9,535,900	4,688,700
8	17,040,000	232,950	2,748,800	16,289,200	113,000		863,800	113,624	9,806,900	5,748,700
Abut.	18,296,700	175,970	1,108,600	17,367,800			898,900			
Total								494,717	34,349,400	15,569,900



The values in columns 10a and 10b are for use in the variable temperature Eqs. 36 and 37.<sup>15</sup> Values of  $I$  needed for constructing column 11 are computed from Eq. 8.

The values in columns 12 to 19 all appear in the arch equations. Their derivation is evident. Each item of column 18, including the total, is equal to the difference between the corresponding items of columns 10 and 17; hence column 18 may be omitted if desired. Values in column 20 represent voussoir water loads and are obtained by multiplying scaled values of the voussoir lengths *at the upstream face* by the unit water load. These loads are represented on the drawing by their concentrated resultants, but in computing moments and forces, their distributed nature is considered.

The water loads must be resolved into  $x$  and  $y$  components for arithmetical summation. The water pressure is normal to the upstream face. The slight angle between this face and the axis near the abutments is ignored and the components  $P_y$  and  $P_x$ , columns 21 and 22, are computed as though the water forces were radial to the arch axis curve. If the arch thickness varies rapidly, the *actual angles of the forces* should be used. If there are other loads in addition to the normal water loads, their components are included in columns 21 and 22.

An arbitrary horizontal load, designated as  $H_1$  and applied at the crown, may be included in column 22 to keep the computed cantilever moments, due to external loads, as small as practicable. This reduces the number of significant figures required in terms involving moments and is particularly helpful where computations are made by slide rule or graphically. If the arch is circular, or nearly so, an approximate value for  $H_1$  may be obtained from Eq. 1. If the arch is not circular, an approximate value of  $H_1$  may be assumed or determined graphically. (See Art. 23g.)

For the present example  $H_1$  will be computed by inserting  $r_c$  in Eq. 1, thus

$$H_1 = 62.5 \times 70 \times 100 = 437,500 \text{ lb}$$

This value is entered in column 22 as a horizontal crown force.

Values of  $P_y$  are summated in column 23. These summations represent accumulated  $y$  components of the water load to the ends of the voussoirs and are recorded in the intermediate spaces.

Values of  $P_x$  are similarly summated in column 26. The  $x$  components of  $P$  (in this example) are opposed in direction to  $H_1$  and must be subtracted. (See Art. 14e for a system of algebraic signs.)

Values of  $M_E$  are computed by the theorem that *the moment at any point in a beam is equal to the moment at a previous point, plus the shear at the previous point times the distance between the points, plus the moment of intervening loads*. This theorem can be applied to the accumulated load components separately by using  $\Delta x$  and  $\Delta y$  as distances. Values of  $\Sigma P_y$  in column 23 are multiplied by  $\Delta x$  and recorded in column 24, giving moment increments for  $\Sigma P_y$ . The summations of these values, column 25, represent moments at various voussoir centers due to  $P_y$ . Values of  $\Delta y \Sigma P_x$  are similarly recorded in column 27 and summated in column 28. The total moment at the center of any voussoir, due

<sup>15</sup> The variable term  $(1 - 0.5 t/r)$  is taken as unity in this example.

to the concentrated resultants of the water loads, is equal to the algebraic sum of the items in columns 25 and 28 for that voussoir.

Because the loads are not actually concentrated, these moments are in error by an amount approximately equal to  $\frac{1}{8}\Delta sP$  in each case for uniform normal loads. These corrections are recorded in column 29. Column 29a represents the twist moment derived from the cantilever computations in a trial load analysis and hence is not involved in this example. The blank column is included to complete the computation form. The values of columns 25, 28, and 29, combined horizontally, give values of  $M_E$  as recorded in column 30. For the present example, the moment fractions in column 28 are opposed in direction to those of columns 25 and 29 and are accordingly subtracted. This is not always the case. The moments at the centers of voussoirs are assumed to be sufficiently near to the average values required for the arch equations. Columns 31, 32, and 33 give the combinations in which  $M_E$  appears in the arch equations.

As previously stated, values of  $\Sigma P_y$  and  $\Sigma P_x$  shown in columns 23 and 26 are correct at the ends of the voussoirs but not at the centers. The values needed in the thrust and shear equations are the averages of the end values; hence columns 23 and 26 are averaged in columns 34 and 35, respectively.

These columns serve as a basis for the computation of the  $T_E$  terms of Eqs. 21 and 22, and the  $S_E$  terms of Eqs. 27 and 28. Values of  $T_E$  and  $S_E$  are given by the equations

$$T_E = \Sigma P_x \cos \alpha + \Sigma P_y \sin \alpha \quad [66]$$

$$S_E = \Sigma P_x \sin \alpha + \Sigma P_y \cos \alpha \quad [67]$$

Substituting these values and making other permissible changes, the thrust and shear terms of Eqs. 21, 22, 27, and 28 are expanded as follows:

In Eq. 21

$$\sum \frac{T\Delta s}{AE} \cos \alpha = \frac{1}{E} \sum \left( \frac{\Delta s}{t} \cos^2 \alpha \Sigma P_x \right) + \frac{1}{E} \sum \left( \frac{\Delta s}{t} \sin \alpha \cos \alpha \Sigma P_y \right) \quad [68]$$

In Eq. 22

$$\sum \frac{T\Delta s}{AE} \sin \alpha = \frac{1}{E} \sum \left( \frac{\Delta s}{t} \sin \alpha \cos \alpha \Sigma P_x \right) + \frac{1}{E} \sum \left( \frac{\Delta s}{t} \sin^2 \alpha \Sigma P_y \right) \quad [69]$$

In Eq. 27

$$\sum \frac{kS\Delta s}{AG} \sin \alpha = \frac{n}{E} \sum \left( \frac{\Delta s}{t} \sin^2 \alpha \Sigma P_x \right) + \frac{n}{E} \sum \left( \frac{\Delta s}{t} \sin \alpha \cos \alpha \Sigma P_y \right) \quad [70]$$

In Eq. 28

$$\sum \frac{kS\Delta s}{AG} \cos \alpha = \frac{n}{E} \sum \left( \frac{\Delta s}{t} \sin \alpha \cos \alpha \Sigma P_x \right) + \frac{n}{E} \sum \left( \frac{\Delta s}{t} \cos^2 \alpha \Sigma P_y \right) \quad [71]$$

Values for the terms of these expanded equations are developed in columns 36 to 41.



(d) *Foundation constants.* The effects of foundation movement are computed in Tables 5 and 6. The first step is the evaluation of the factors in Eqs. 51, 52, and 53, which depend on the foundation alone.

TABLE 5  
FOUNDATION CONSTANTS, EXAMPLE 4

$$[E_M \div E_F = J : 0.75, \mu = 0.20, b \div a = 5, k_1 = 5.23, k_2 = 1.76, k_3 = 1.89, \\ k'_3 = 0.41, k_4 = 6.45, k_5 = 0.562.]$$

No.	Function	Symbol	Left	Right
1	$l$		11.23	11.31
2	$l^2$		126.11	127.92
3	$\psi$		60°	65°
4	$\cos \psi$		0.50000	0.42262
5	$\cos^2 \psi$		0.25000	0.17861
6	$\sin \psi$		0.86603	0.90631
7	$\sin^2 \psi$		0.75000	0.82139
8	$Jk_1 \sin^3 \psi \div l^2$		0.02020	0.02283
9	$Jk_4 \sin \psi \cos^2 \psi \div l^2$		0.00831	0.00612
10	(8) + (9)	(E)	0.02851	0.02895
11	$Jk_5 \sin^2 \psi \div l$	(F)	0.02815	0.03061
12	$Jk_2 \sin^3 \psi$		0.85737	0.98265
13	$Jk_3 \sin \psi \cos^2 \psi$		0.06658	0.04978
14	(12) + (13)	(G)	0.92395	1.03243
15	$Jk_3 \sin \psi$	(H)	1.2276	1.2847

Values of  $k_1$  to  $k_5$  are read from Figs. 10 to 14. To permit the cancellation of the factor  $1/E$ , as suggested in Art. 12, each term of the foundation equation is multiplied by  $E_M/E_F$ , which for convenience is represented by  $J$ .

The derivation of the first seven numbered items of Table 5 is obvious. Items 8 and 9 represent the constant portions of the first two terms of Eq. 51 and their sum, item 10, represents the constant ( $E$ ) of Eq. 54. Item 11 represents the constant in the last terms of Eqs. 51 and 53, or ( $F$ ), Eqs. 54 and 56. Items 12 and 13 are added together in item 14 to give the constant ( $G$ ), Eq. 55. Item 15 represents ( $H$ ), Eq. 56.

The introduction of the four foundation constants from Table 5 into the moment thrust and shear equations for the unknown crown forces and the known external loads is a complex operation. The computations are performed in Table 6. Items to be used in the computation of other items are recorded to four or five significant figures; others are shortened as permitted by subsequent operations. The need for the computed functions is developed in Art. 14f. Many of these functions frequently can be omitted (see Arts. 14j, 16c, and 16d).

(e) *Plus and minus signs.* Before proceeding further, it is necessary to establish a system of plus and minus signs. The crown point on the arch axis,

TABLE 6  
CROWN DEFORMATION CONSTANTS FOR FOUNDATION DEFORMATIONS, EXAMPLE 4

[Values of  $x$  and  $y$  are abutment values.  $J = 0.75$ ,  $\mu = 0.20$ ,  $b/a = 5$ .]

Item	Left	Right	Item	Left	Right	Item	Left	Right
$(E)$	0.02851	0.02895	$(F)$	0.02815	0.03061	$(F)$	0.02815	0.03061
$y(E)$	1.471	1.646	$(F) \sin \alpha$	0.02510	0.02802	$(F) \cos \alpha$	0.01275	0.01232
$x(E)$	2.471	2.587	$y(F) \sin \alpha$	1.3	1.8	$y(F) \cos \alpha$	0.7	0.7
$y^2(E)$	76.9	93.6	$x(F) \sin \alpha$	2.2	2.5	$x(F) \cos \alpha$	1.1	1.1
$x^2(E)$	214.2	231.2	$M_a(F) \sin \alpha$	20	25	$M_a(F) \cos \alpha$	10	11
$xy(E)$	127.5	147.1	$(F) \sin \alpha \Sigma P_z$	5.0260	4.9307	$(F) \cos \alpha \Sigma P_y$	5.0787	5.0603
$M_a(E)$	22.817	26.023	$y(F) \sin \alpha \Sigma P_z$	259	280	$y(F) \cos \alpha \Sigma P_y$	262	288
$yM_a(E)$	1,177	1,479	$x(F) \sin \alpha \Sigma P_z$	436	441	$x(F) \cos \alpha \Sigma F_y$	440	452
$xM_a(E)$	1,978	2,326						
Item	Left	Right	Item	Left	Right	Item	Left	Right
$(G)$			$(H)$			$(H)$		
$(G) \sin^2 \alpha$	0.92395	1.03243	$(H) \sin^2 \alpha$			$(H) \sin^2 \alpha$	1.2276	1.2847
$(G) \cos^2 \alpha$	0.73438	0.86519	$(H) \cos^2 \alpha$			$(H) \cos^2 \alpha$	0.9757	1.0766
$(G) \sin \alpha \cos \alpha$	0.19856	0.16724	$(H) \sin \alpha \cos \alpha$			$(H) \sin \alpha \cos \alpha$	0.25185	0.20811
$(G) \sin^2 \alpha \Sigma P_y$	0.37311	0.38039	$(H) \sin^2 \alpha \Sigma P_z$			$(H) \sin^2 \alpha \Sigma P_z$	0.49573	0.47334
$(G) \cos^2 \alpha \Sigma P_y$	293	355	$(H) \cos^2 \alpha \Sigma P_y$			$(H) \cos^2 \alpha \Sigma P_y$	195	189
$(G) \sin \alpha \cos \alpha \Sigma P_y$	38	29	$(H) \sin \alpha \cos \alpha \Sigma P_z$			$(H) \sin \alpha \cos \alpha \Sigma P_z$	100	85
$(G) \sin \alpha \cos \alpha \Sigma P_z$	149	156	$(H) \sin \alpha \cos \alpha \Sigma P_y$			$(H) \sin \alpha \cos \alpha \Sigma P_y$	99	83
	75	67					197	194

point 2, Fig. 8, is chosen as the center of coordinates,  $x$  being positive to the left and  $y$  positive downward. Deflection components  $\partial x$  and  $\partial y$  are positive to the left and downward, respectively. Angular deflections are positive when counterclockwise. Thrusts, shears, and loads are positive if causing compression in the arch. Moments are positive when producing tension at the intrados. A temperature drop is positive.

(f) *Assembly of coefficients.* The values computed in Tables 4 and 6 are assembled in Table 7 and combined to build up the coefficients of Eqs. 60, 61, and 62. Beginning with  $A_\alpha$ , the angular deformation due to a unit value of  $H_c$ , the third term of Eq. 12 gives  $\Sigma y(\Delta s/I)$  as the arch contribution. (Factor  $1/E$  omitted; see Art. 12.) For the left half of the arch, a positive  $H_c$  produces a positive rotation; hence the item carries a plus sign. The reaction causes a negative rotation in the right half of the arch, which becomes positive when the deflections for the two halves are equated and then transposed to form Eq. 60. The values shown are the totals from the upper and lower portions of column 14, Table 4.

To these values must be added the foundation deformation effects from Eq. 54. This is accomplished by substituting  $H_c y$  for  $M_x$  and  $H_c \sin \alpha$  for  $S$ . Values of  $y_u(E)$  and  $(F) \sin \alpha$  are taken from Table 6. The abutment turnings are in the same direction as the angular movements in the arch.

The coefficient  $A_x$  for  $H_c$  in the  $x$  deflection, Eq. 61, involves moment, thrust, and shear and is made up of the third term of Eq. 15, the second term of Eq. 21, and the second term of Eq. 27, plus contributions from foundation movements. The turning effect of a positive  $H_c$  produces a positive  $x$  deflection in the left half of the arch; hence the  $(\Delta sy^2)/I$  term is positive. The  $x$  deflection on the right side of the arch is negative but becomes positive by transposition. For similar reasons, the  $\Sigma(\Delta s \cos^2 \alpha)/t$  and  $n\Sigma(\Delta s \sin^2 \alpha)/t$  terms are positive.

The angular deflection caused by abutment rotation due to  $H_c$  produces an  $x$  deflection, which is found by multiplying the second and third items of  $A_\alpha$ , Table 7, by  $y$ , giving  $y_u^2(E)$  and  $y_u(F) \sin \alpha$ . The results, recorded as items 8 and 9, are taken from Table 6. The  $y_u(F) \sin \alpha$  item is doubled to take care of the last term of Eq. 56.

The abutment thrust deformation due to  $H_c$  from Eq. 55 is

$$\partial_a s = T(G) = H_c \cos \alpha (G)$$

The  $x$  component of this axial deformation is

$$\partial_a s \cos \alpha = T(G) \cos \alpha = H_c (G) \cos^2 \alpha$$

This component appears as the sixth term of  $A_x$ .

The abutment shear deformation due to  $H_c$ , from Eq. 56, is

$$\begin{aligned} \partial_a n &= S(H) + M(F) \\ &= H_c \sin \alpha (H) + H_c y_u(F) \end{aligned}$$

The  $x$  component is

$$\partial_a n \sin \alpha = H_c (H) \sin^2 \alpha + H_c y_u(F) \sin \alpha$$

TABLE 7

## ARCH EQUATION CONSTANTS, EXAMPLE 4

[Data:  $n = 2.80$ ,  $F = 20^\circ$ ,  $\Delta F = 8^\circ$ ,  $E = 3,000,000$  lb per sq in. = 432,000,000 lb per sq ft.]

Item	Terms	Functions	Left	Right
1	$A_\alpha$	$\Sigma y \frac{\Delta s}{l}$	+ 21.55	+ 24.84
2		$y_a(E)$	+ 1.47	+ 1.65
3		$(F) \sin \alpha$	+ 0.03	+ 0.03
4	Total	Left and right	+49.57	
5	$A_x$	$\Sigma y^2 \frac{\Delta s}{l}$	+ 641.1	+ 813.6
6		$\Sigma \frac{\Delta s}{l} \cos^2 \alpha$	+ 7.5	+ 7.6
7		$n \Sigma \frac{\Delta s}{l} \sin^2 \alpha$	+ 8.9	+ 10.2
8		$y_a^2(E)$	+ 75.9	+ 93.6
9		$2y_a(F) \sin \alpha$	+ 2.6	+ 3.2
10		$(G) \cos^2 \alpha$	+ 0.2	+ 0.2
11		$(H) \sin^2 \alpha$	+ 1.0	+ 1.1
12	Total	Left and right	+1668.7	
13	$A_y$	$\Sigma xy \frac{\Delta s}{l}$	-1464.6	+1752.0
14		$(n-1) \Sigma \frac{\Delta s}{l} \sin \alpha \cos \alpha$	- 6.8	+ 7.3
15		$x_a y_a(E)$	- 127.5	+ 147.1
16		$x_a(F) \sin \alpha$	- 2.2	+ 2.5
17		$(G) \sin \alpha \cos \alpha$	+ 0.4	- 0.4
18		$(H) \sin \alpha \cos \alpha$	- 0.5	+ 0.5
19		$y_a(F) \cos \alpha$	- 0.7	+ 0.7
20	Total	Left and right	+308.7	
21	$B_\alpha$	$\Sigma x \frac{\Delta s}{l}$	- 60.668	+ 66.182
22		$x_a(E)$	- 2.471	+ 2.587
23		$(F) \cos \alpha$	- 0.013	+ 0.012
24	Total	Left and right	+5.629	
25	$B_x$	$= A_y$	+308.7	
26	$B_y$	$\Sigma x^2 \frac{\Delta s}{l}$	+3651.6	+4134.1
27		$\Sigma \frac{\Delta s}{l} \sin^2 \alpha$	+ 3.2	+ 3.6
28		$n \Sigma \frac{\Delta s}{l} \cos^2 \alpha$	+ 20.9	+ 21.3
29		$x_a^2(E)$	+ 214.2	+ 231.2
30		$2x_a(F) \cos \alpha$	+ 2.2	+ 2.2
31		$(G) \sin^2 \alpha$	+ 0.7	+ 0.9
32		$(H) \cos^2 \alpha$	+ 0.3	+ 0.2
33	Total	Left and right	+8286.6	
34	$C_\alpha$	$\Sigma \frac{\Delta s}{l}$	+ 1.297	+ 1.360
35		$(E)$	+ 0.029	+ 0.029
36	Total	Left and right	+2.715	
37	$C_x$	$= A_\alpha$	+49.57	

TABLE 7—Continued

## ARCH EQUATION CONSTANTS, EXAMPLE 4

[Data:  $n = 2.80$ ,  $F = 20^\circ$ ,  $\Delta F = 8^\circ$ ,  $E = 3,000,000$  lb per sq in. = 432,000,000 lb per sq ft.]

Item	Terms	Functions	Left	Right
38	$C_y$	$= B_x$	+5.629	
39	$D_x$	$\sum \frac{\Delta s}{l} M_E$	-430.6	-494.7
40		$C_F \Delta F E \sum \frac{\Delta s}{l}$	-221.1	-232.9
41		$(E) M_E$	-22.8	-26.0
42		$(F) \sin \alpha \Sigma P_z$	+ 5.0	+ 4.9
43		$(F) \cos \alpha \Sigma P_y$	- 5.1	- 5.1
44	Total	Left and right	-1428.4	
45	$D_z$	$\Sigma y \frac{\Delta s}{l} M_E$	-12,327	-15,594
46		$(n-1) \sum \left( \frac{\Delta s}{l} \sin \alpha \cos \alpha \Sigma P_y \right)$	-1,798	-1,965
47		$\sum \left( \frac{\Delta s}{l} \cos^2 \alpha \Sigma P_z \right)$	+2,851	+2,875
48		$n \sum \left( \frac{\Delta s}{l} \sin^2 \alpha \Sigma P_z \right)$	+2,673	+2,911
49		$C_F \Delta F E \Sigma y \frac{\Delta s}{l}$	-3,830	-4,459
50		$C_F F E x_s$	+4,493	+4,633
51		$y_s(E) M_E$	+1,177	+1,479
52		$y_s(F) \sin \alpha \Sigma P_z$	+259	+280
53		$y_s(F) \cos \alpha \Sigma P_y$	-262	-288
54		$(G) \cos^2 \alpha \Sigma P_z$	+38	+29
55		$(G) \sin \alpha \cos \alpha \Sigma P_y$	+149	+156
56		$(H) \sin^2 \alpha \Sigma P_z$	+195	+189
57		$(H) \sin \alpha \cos \alpha \Sigma P_y$	-197	-194
58		$(F) \sin \alpha M_E$	-20	-25
59	Total	Left and right	-21,884	
60	$D_y$	$\Sigma x \frac{\Delta s}{l} M_E$	+28,794	-34,349
61		$\sum \left( \frac{\Delta s}{l} \sin^2 \alpha \Sigma P_y \right)$	+992	-1,173
62		$n \sum \left( \frac{\Delta s}{l} \cos^2 \alpha \Sigma P_y \right)$	+3,750	-3,887
63		$(n-1) \sum \left( \frac{\Delta s}{l} \sin \alpha \cos \alpha \Sigma P_z \right)$	-2,294	+2,373
64		$C_F \Delta F E \Sigma x \frac{\Delta s}{l}$	+10,550	-11,590
65		$C_F F E y_s$	+2,674	-2,947
66		$x_s(E) M_E$	+1,978	-2,326
67		$x_s(F) \sin \alpha \Sigma P_z$	-436	+441
68		$x_s(F) \cos \alpha \Sigma P_y$	+440	-452
69		$(G) \sin \alpha \cos \alpha \Sigma P_z$	+75	-67
70		$(G) \sin^2 \alpha \Sigma P_y$	+293	-355
71		$(H) \sin \alpha \cos \alpha \Sigma P_z$	-99	+83
72		$(H) \cos^2 \alpha \Sigma P_y$	+100	-85
73		$(F) \cos \alpha M_E$	+10	-11
74	Total	Left and right	-7518	

The first term of this appears as the seventh item of  $A_x$ , and the second is included in the fifth item.

All of these  $x$  movements are toward the abutments; hence all signs are plus.

The coefficient  $A_y$  for  $H_c$  in the  $y$  deflection equation is composed of the third term of Eq. 16 and the second terms of Eqs. 22 and 28, plus foundation movements. The turning due to a positive  $H_c$  displaces the crown point of the arch upward on both sides of the arch; hence the terms  $\Sigma(\Delta sxy)/I$  are negative for both sides but the right side becomes positive by transposition. The thrust component of a positive  $H_c$  causes a positive  $y$  displacement on both sides but the right side becomes negative by transposition. The shear component of a positive  $H_c$  produces negative  $y$  displacements on both sides, the right side becoming positive by transposition. The thrust and shear items are alike except for signs and the factor  $n$  and may be assembled as shown.

The derivation of abutment terms follows the reasoning used for  $A_x$ , changing  $x$  for  $y$  and  $\sin \alpha$  for  $\cos \alpha$  where required. The signs are determined by inspection.

The remaining coefficients and their signs are developed in the same manner, observing, however, that the reaction to a positive  $V_c$  on the left is a negative  $V_c$  on the right. The coefficient  $B_x$  is identical with  $A_y$ ; likewise,  $C_x = A_x$ , and  $C_y = B_x$ . Numerical values are taken from Tables 4 and 6. Values of  $\Sigma P_y$ ,  $\Sigma P_x$ , and  $M_E$  in the foundation items are, respectively, the end values of columns 23, 26, and 30, Table 4. The specified value of 3,000,000 lb per sq in. for  $E$  is converted to lb per sq ft to conform to other dimensions in the table.

The signs shown for the  $A$ ,  $B$ , and  $C$  coefficients are definite and do not change. Some of the signs for the  $D$  terms depend on the loading and must be specially evaluated for each analysis.

(g) *Computation of crown forces.* By substituting from Table 7, Eqs. 60, 61, and 62 are given numerical form and solved as follows:

$$49.57H_c + 5.629V_c + 2.715M_c = 1428.4$$

$$1666.7H_c + 308.7V_c + 49.57M_c = 21884$$

$$308.7H_c + 8286.6V_c + 5.629M_c = 7518$$

$$H_c + 0.11356V_c + 0.05477M_c = 28.8158$$

$$H_c + 0.18522V_c + 0.02974M_c = 13.1301$$

$$H_c + 26.84354V_c + 0.01824M_c = 24.3537$$

$$0.07166V_c - 0.02503M_c = -15.6857$$

$$25.65832V_c - 0.01150M_c = +11.2236$$

$$V_c - 0.34929M_c = -218.890$$

$$V_c - 0.00043M_c = +0.421$$

$$0.34886M_c = +219.311$$

$$M_c = 628.660 \text{ ft kips}$$

$$V_c = +0.693 \text{ kips}$$

$$H_c = -5.695 \text{ kips}$$

$$T_c = H_1 + H_c = 431.805 \text{ kips}$$

(h) *Computation of stresses.* Moments at points other than the crown are computed from Eq. 11 and thrusts and shears from Eqs. 20 and 26, respectively. Extreme fiber stresses are computed from the equations<sup>18</sup>

$$f_c = \left[ \frac{T}{t} + \frac{M}{I} (0.5t + e) \right] \frac{r}{r + 0.5t} \quad [72]$$

$$f_i = \left[ \frac{T}{t} - \frac{M}{I} (0.5t - e) \right] \frac{r}{r - 0.5t} \quad [73]$$

where  $r$  is the radius to the center line and  $e$  is the eccentricity of the neutral axis (see Art. 9b). If the thickness is constant,  $r + 0.5t = r_c$  and  $r - 0.5t = r_i$ . In Example 4, the eccentricity of the neutral axis is ignored, making  $e = 0$  and  $r_c = r_i = r$ . Computations of  $f_c$  and  $f_i$  at the crown and the abutments are shown in Table 8. No tension exists, and compressive stresses are moderate. Whether the arch is satisfactory depends on the allowable unit stresses which are not specified, as this example is concerned only with the method of analysis.

It will be noted that the moment at the abutment is less than at the crown. This unusual result is caused by the assumed radial temperature variation  $\Delta F$ . For the conditions of this example, thickening of the ends of the arches is not justified.

The cylinder stress computed by Eq. 2, using the dimensions of the central portion of the arch, is 325 lb per sq in., for comparison.

(i) *Line of pressures.* The arch thrust is actually a distributed force but is frequently represented by its equivalent concentrated resultant. The line of action of this resultant is called the "line of pressure." Its position at any point is given by the equation

$$e = \frac{M}{T} \quad [74]$$

where  $e$  is the eccentricity, or distance from the arch axis, and  $M$  and  $T$  are final moment and thrust. If there is no tension, the line of pressure is within the middle third (or kern).

(j) *Significance of foundation terms.* Inspection of Table 7 shows that many of the foundation items are small and could be omitted for the slender arch of Example 4. (See also Table 11, Art. 16c.)

**15. Example 5, Graphic Analysis.** (a) *Selection of example.* Most of the operations represented in Tables 4 and 7 can be performed graphically. The procedure will be illustrated by repeating the analysis of the arch of Fig. 17, Example 4.

(b) *Layout of arch and loading.* The arch is carefully drawn to a convenient scale and divided into voussoirs as in Fig. 18. Rules governing the number of divisions are the same as for arithmetical analysis. The value of  $e$ , Eq. 7, is again assumed zero. Voussoir lengths are measured as semi-chords.

<sup>18</sup> Adapted from Cain's Eq. (107), p. 533, *Trans. Am. Soc. Civil Engrs.*, Vol. 90, 1927 using also Cain's Eq. (94), p. 524.

TABLE 8

STRESS COMPUTATIONS, EXAMPLE 4

$[n = 2.8, \mu = \frac{1}{8} \text{ and } \frac{1}{8}, J = 0.75, F = 20^\circ, \Delta F = 8^\circ]$

Function	Left abut.	Crown	Right abut.
<b>MOMENTS: ft-kips</b>			
$M_c$ , Art. 14g	+628.7	+628.7	+628.7
$M_R$ , Table 4	-800.3		-898.9
$H_c y$	-293.8		-323.8
$V_c x$	- 60.0		+ 61.9
$M = \text{Total mom.}$	-525.4	+628.7	-532.1
<b>THRUSTS: kips</b>			
$H_c$ , Art. 14g	- 5.7	- 5.7	- 5.7
$\Sigma P_x$ , Table 4	+200.2	+437.5	+176.0
$T_x = x \text{ Comp. of thrust}$	+194.5	+431.8	+170.3
$T_x \cos \alpha$	+ 88.1	+431.8	+685.0
$V_c$ , Art. 14g, kips	+ 0.7		- 0.7
$\Sigma P_y$ , Table 4, kips	+398.3		+410.7
$T_y = y \text{ Comp. of thrust, kips}$	+399.0		+411.4
$T_y \sin \alpha$ , kips	+355.7		+376.6
$T = T_x \cos \alpha + T_y \sin \alpha$ , kips	+443.8	+431.8	+445.1
<b>STRESSES: lb per sq in.</b>			
$T \div 0.144t$	+274.4	+306.0	+273.3
$M \div 0.024t^2$	$\pm 173.6$	$\pm 272.8$	$\pm 173.3$
$r \div (r + 0.5t)$	0.941	0.953	0.942
$r \div (r - 0.5t)$	1.067	1.052	1.065
$f_c$ (Eq. 69, $\epsilon = 0$ )	+ 94.9	+551.6	+ 94.2
$f_t$ (Eq. 70, $\epsilon = 0$ )	+478.0	+ 34.9	+475.6

It is convenient to divide the loads at the voussoir centers rather than at the ends, as was done in Example 4. The load length for each division is found by scaling the chord between radii to the *outside curve*, drawn through adjacent voussoir centers. Each load is treated as if uniformly distributed and normal to its face chord. If the actual distribution is irregular, further subdivision or other special steps may be required for accuracy. The loads are recorded directly on the drawing in the positions and direction of their concentrated resultants. Table 5, for the abutment constants, will be required, as in Example 4.





Values of  $t$  are scaled and recorded in column 1 of Table 9 and values of  $\Delta s$  are recorded in column 2. Values of  $\Delta s_e$ , distances between voussoir centers, are recorded in column 3. Values of  $\Delta s/t$  and  $\Delta s/I$  are computed and set down in columns 4 and 5. The foundation factor ( $E$ ) enters all arch equation constants in exactly the same manner as  $\Delta s/I$  items; hence this factor may be treated as an abutment value of  $\Delta s/I$ . It is, accordingly, entered in column 5.

(c) *Algebraic functions.* The derivation of data equivalent to those of columns 10a, 10b, and 12 to 16, of Table 4, is accomplished on Fig. 18. Base lines  $a_x-C_x$  and  $a_y-C_y$  parallel respectively to the  $x$  axis and  $y$  axis are drawn and the voussoir centers are projected onto them. Values of  $\Delta s/I$  from column 5, Table 9, including the abutment factor ( $E$ ), are plotted consecutively from abutment to crown along the line  $C_x-13$ .

A pole distance is laid off from  $C_x$  to 29 and the line 29-9 is drawn, where  $C_x-9$  represents the plotted value of the abutment factor ( $E$ ). Then  $a_x-16$  is drawn parallel to 29-9. (See "Distorted Illustration.") Similar triangles  $C_x-29-9$  and  $C_x-a_x-16$  give the relation

$$(C_x-16)(C_x-29) = (C_x-9)(C_x-a_x) \quad .$$

or

$$p(C_x-16) = (E)x$$

where  $p$  is the pole distance. If ( $E$ ) is plotted to a scale of 1 in. =  $k$  units, then the length  $C_x-16$  represents ( $E$ ) $x$  to a scale of 1 in. =  $pk$  units.

Next, the line 29-10 is drawn to the top of the first value of  $\Delta s/I$  and 23-17 is drawn parallel to it. The length 16-17 represents  $x\Delta s/I$  for the end voussoir to a scale of 1 in. =  $pk$  units. This procedure is repeated in turn for each voussoir, ending with the line 28-20, which is parallel to a line from 29 to 13. Distances between points 16, 17, 18, etc., correspond to the individual values of column 12, Table 4. The distance 16-20 represents the total of this column and the distance  $C_x-20$  represents  $\Sigma x\Delta s/I$  plus ( $E$ ) $x$ , and may be scaled and entered as item 18 of Table 10, which corresponds to Items 21 and 22 of Table 7. The polygon  $a_x-23-24-25-28-20$  will be referred to as Curve A.

The pole length  $p$  and the scale of  $\Delta s/I$  are chosen to give a reasonable form of diagram and a convenient value for the scale factor  $pk$ . In the present example,  $p$  is made 50 ft and  $\Delta s/I$  is plotted to 1 in. = 0.2 units, giving a scale of 1 in. = 10 units for  $x\Delta s/I$ .

Coincidentally with the construction of Curve A, Curve D is constructed on the base  $a_y-C_y$ , each line being perpendicular to the corresponding line of Curve A. Distances  $C_y-31$ , 31-32, 32-33, etc., represent values of  $y_a(E)$  and  $y\Delta s/I$ , to the same scale as  $x\Delta s/I$ . The total length,  $C_y-34$ , is scaled and inserted as item 1 in Table 10, replacing items 1 and 2 of Table 7.

Next, Curve B is constructed on the base  $a_x-C_x$ , following the procedure of Curve A, except that values of  $x_a(E)$  and  $x\Delta s/I$ , points 16, 17, 18, etc., are substituted for values of  $\Delta s/I$ , points 9, 10, 11, etc. Extensions corresponding to the portion 26-19 of line 25-19, Curve A, are not required. The scaled length of  $C_x-15$  is entered as item 22 in Table 10, replacing  $x_a^2(E)$  and  $\Sigma x^2\Delta s/I$

TABLE 9  
TABULAR DATA FOR GRAPHIC ANALYSIS, EXAMPLE 5  
[Units are feet, pounds, and foot-pounds.]

Point	1	2	3	4	5	6	7	8	9	10	11	12	13
	$t$	$\Delta s$	$\Delta s_e$	$\frac{\Delta s}{t}$	$\frac{\Delta s}{l}$	Shear $= S$	AVRG. shear $= S'$	$S' \Delta s_e$ $= \Delta M$	$\Sigma(\Delta M)$ $= M_E$	$\frac{\Delta s}{l} M_E$	$\Sigma \left( \frac{\Delta s}{l} M_E \right)$ $= \partial \alpha$	AVRG. $\partial \alpha$ $= \partial' \alpha$	$\Delta s \partial' \alpha$
Crown	9.8	.....		.....	.....	0			.....	.....		.....	.....
Left Side	1	" 14.0	7.0	1.429	0.1785	1,500	750	5,200	.....	.....	454,300	.....	.....
	2	" "	14.0	"	"	4,500	3,000	42,000	5,200	900	453,400	453,800	6,350,000
	3	" "	"	"	"	7,500	6,000	84,000	47,200	8,400	445,000	449,200	6,290,000
	4	" "	"	"	"	10,500	9,000	126,000	131,200	23,500	421,500	433,200	6,060,000
	5	" "	"	"	"	13,500	12,000	168,000	257,200	45,900	375,600	398,600	5,580,000
	6	9.9	"	1.414	0.1731	12,000	12,750	178,500	425,200	75,900	299,700	337,600	4,730,000
	7	10.3	"	1.358	0.1536	6,800	9,400	131,600	603,700	104,500	195,200	247,400	3,460,000
	8	10.9	8.06	0.739	0.0747	2,800	4,800	52,900	735,300	112,900	82,300	138,800	1,940,000
Abut.	11.2	.....	4.03	.....	*0.0285	2,200	2,500	8,100	788,200	58,900	23,400	52,800	430,000
Total	.....	.....	.....	10.656	1.3224	.....	.....	.....	796,300	**23,400	.....	.....	.....

\* (E) From Table 5.      \*\* (E)  $M_E + S(F)$ .

TABLE 10  
ARCH EQUATION CONSTANTS, EXAMPLE 5

Item	Term	Function	Left	Right
1	$A_x$	$\Sigma y \frac{\Delta s}{I} + y_a(E)$ , Curve <i>D</i> , Fig. 18	+23.2	+26.6
2		( <i>F</i> ) sin $\alpha$ , computed	.....	.....
3	Total		+49.8	
4	$A_z$	$\Sigma y^2 \frac{\Delta s}{I} + y_a^2(E)$ , Curve <i>F</i> , Fig. 18	+722.0	+911.0
5		$\Sigma \frac{\Delta s}{t} \cos^2 \alpha$ , Curve <i>H</i> , Fig. 18	+7.5	+7.6
6		$n \Sigma \frac{\Delta s}{t} \sin^2 \alpha$ , Curve <i>H</i> , Fig. 18	+9.0	+10.2
7		$2y_a(F) \sin \alpha$ , Curve <i>K</i> , Fig. 18	+2.6	+3.2
8		( <i>G</i> ) $\cos^2 \alpha$ , Curve <i>J</i> , Fig. 18	+0.2	+0.2
9		( <i>H</i> ) $\sin^2 \alpha$ , Curve <i>I</i> , Fig. 18	+1.0	+1.1
10	Total		+1675.6	
11	$A_y$	$\Sigma xy \frac{\Delta s}{I} + x_a y_a(E)$ , Curve <i>E</i> , Fig. 18	-1595	+1900
12		$(n-1) \Sigma \frac{\Delta s}{t} \sin \alpha \cos \alpha$ , Curve <i>H</i> , Fig. 18	-7	+7
13		( <i>G</i> ) $\sin \alpha \cos \alpha$ , Curve <i>I</i> , Fig. 18	.....	.....
14		( <i>H</i> ) $\sin \alpha \cos \alpha$ , Curve <i>J</i> , Fig. 18	.....	.....
15		$x_a(F) \sin \alpha$ , compute	-2	+2
16		$y_a(F) \cos \alpha$ , compute	-1	+1
17	Total		+305	
18	$B_x$	$\Sigma x \frac{\Delta s}{I} + x_a(E)$ , Curve <i>A</i> , Fig. 18	-63.2	+68.9
19		( <i>F</i> ) $\cos \alpha$ , compute	.....	.....
20	Total		+5.7	
21	$B_z$	$-A_y$	+305	

TABLE 10—Continued  
ARCH EQUATION CONSTANTS, EXAMPLE 5

Item	Term	Function	Left	Right
22	$B_y$	$\Sigma x^2 \frac{\Delta s}{l} + x_a^2(E)$ , Curve $B$ , Fig. 18	+3,858	+4,374
23		$\Sigma \frac{\Delta s}{l} \sin^2 \alpha$ , Curve $H$ , Fig. 18	+3	+4
24		$n \Sigma \frac{\Delta s}{l} \cos^2 \alpha$ , Curve $H$ , Fig. 18	+21	+21
25		$2x_a(F) \cos \alpha$ , compute	+2	+2
26		$(G) \sin^2 \alpha$ , Curve $I$ , Fig. 18	+1	+1
27		$(H) \cos^2 \alpha$ , Curve $J$ , Fig. 18	.....	.....
28	Total		+8287	
29	$C_a$	$\Sigma \frac{\Delta s}{l} + (E)$ , Col. 5, Table 9	+1.322	+1.392
30	Total		+2.714	
31	$C_x$	$= A_a$	+49.8	
32	$C_y$	$= B_a$	+5.9	
33	$D_a$	$\Sigma \frac{\Delta s}{l} M_E + (E) M_E + S(F)$ , Col. 10, Table 9	-454.3	-515.8
34		$C_F \Delta F E \Sigma \frac{\Delta s}{l}$ , from Col. 5, Table 9	-221.0	-233.1
35	Total		-1424.2	
36	$D_x$	$\partial x$ (Moment), Curve $B$ , Fig. 19	-13,130	-17,390
37		$\partial x$ ( $S$ and $T$ ), Curve $A$ , Fig. 19	+3,900	+3,990
38		$C_F \Delta F E \Sigma y \frac{\Delta s}{l}$ , Curve $G$ , Fig. 18	-3,820	-4,460
39		$C_F F E x_a$ , compute	+4,490	+4,630
40	Total		-21,790	
41	$D_y$	$\partial y$ (Moment), Curve $B$ , Fig. 19	+30,000	-36,520
42		$\partial y$ ( $S$ and $T$ ), Curve $A$ , Fig. 19	+2,840	-3,090
43		$C_F \Delta F E \Sigma x \frac{\Delta s}{l}$ , Curve $C$ , Fig. 18	+10,610	-11,570
44		$C_F F E y_a$ , compute	+2,670	-2,950
45	Total		-7240	

items 29 and 26 in Table 7. The scale is again 1 in. =  $pk$  units, where  $k$  is the scale factor for Curve  $A$  and  $p$  the pole distance for Curve  $B$ . The same pole distance of 50 ft might have been used but a 40-ft pole is selected to separate the two curves for clearness. The scale is 1 in. =  $40 \times 10 = 400$  units.

Coincidentally with the construction of Curve  $B$ , Curve  $E$  is constructed on the  $a_v$ - $C_v$  axis, each segment being perpendicular to the corresponding segment of Curve  $B$ . The distance  $C_v$ -37 is scaled and entered as item 11 in Table 10, replacing  $x_a y_a(E)$  and  $\Sigma xy \Delta s/I$ , items 15 and 13 of Table 7.

Functions containing  $y^2$  (column 15, Table 4) require the construction of Curve  $F$  on the  $a_v$ - $C_v$  axis. This curve is based on pole point 30 and values of  $y_a(E)$  and  $y \Delta s/I$ , points 31, 32, 33, etc., following the procedure used for Curve  $B$ . A pole distance of 20 ft gives a scale of 1 in. =  $20 \times 10 = 200$  units. The length  $C_v$ -36 is scaled and entered as item 4 in Table 10, replacing  $y_a^2(E)$  and  $\Sigma y^2 \Delta s/I$ , items 8 and 5 in Table 7. To avoid confusion between Curves  $E$  and  $F$ , a portion of the latter is omitted from Fig. 18.

Functions involving variable temperature bending, columns 10a and 10b, Table 4, are derived from Curves  $C$  and  $G$ . The construction of these curves follows the procedure of Curves  $A$  and  $D$ , except that values of  $\Delta s/t$ , platted on the base 21-22, replace values of  $(E)$  and  $\Delta s/I$  on line  $C_x$ -13. The base 21-22 is offset from the axis for clearness. A pole distance of 30 ft and a scale of 1 in. = 2 units for  $\Delta s/t$  give a scale of 1 in. = 60 units for  $x \Delta s/t$  and  $y \Delta s/t$ . The lengths  $C_x$ -14 and  $C_v$ -35 are multiplied by  $C_F E \Delta F$  and entered in Table 10 as items 43 and 38, replacing items 64 and 49 in Table 7.

(d) *Trigonometric functions.* The trigonometric functions of columns 17, 18, and 19, Table 4, are derived from Curve  $H$ , Fig. 18. The construction of this diagram may be explained by means of the triangle 39-40-42 near the middle of the diagram. The line 39-42 represents to scale the value of  $\Delta s/t$  for voussoir 6 and 40-42 and 40-39 are, respectively, parallel and normal to the voussoir chord. The angle 39-42-40 is equal to the angle  $\alpha$  between the  $y$  axis and the radius to the center of the voussoir. If 40-43 is perpendicular to 39-42, then  $(39-43) = \sin^2 \alpha \Delta s/t$ ,  $(43-42) = \cos^2 \alpha \Delta s/t$ , and  $(40-43) = \sin \alpha \cos \alpha \Delta s/t$ .

Triangles are similarly constructed for the other voussoirs. For convenience they are assembled, beginning at the top, to form the continuous polygon 38-39-40-41. The  $x$  projection of this curve 44-41 represents  $\Sigma \sin^2 \alpha \Delta s/t$ , which is entered as item 23, Table 10, and used in item 6, replacing items 27 and 7 of Table 7. The  $y$  projection 38-34, Curve  $H$ , represents  $\Sigma \sin \alpha \cos \alpha \Delta s/t$  and is used in constructing item 12, Table 10, which replaces item 14, Table 7. The value of  $(n-1)$  is known. The value of  $\Sigma \cos^2 \alpha \Delta s/t$  is obtained by subtracting  $\Sigma \sin^2 \alpha \Delta s/t$  from  $\Sigma \Delta s/t$ , the sum of column 4, Table 9. It is entered as item 5 and used in item 24, Table 10, replacing items 6 and 28 of Table 7.

(e) *Thrust and shear functions.* Crown deflections from external loads are derived from a force polygon, Fig. 19. An arbitrary crown force  $H_1$ <sup>17</sup> is

<sup>17</sup> Taken from Table 4 for uniformity. See Art. 23g for other methods of computing  $H_1$ .

laid off in magnitude and direction from 0 to 0'. The external loads are plotted successively from crown to abutment in positions 0'-9, 9-11, 11-13, etc.,

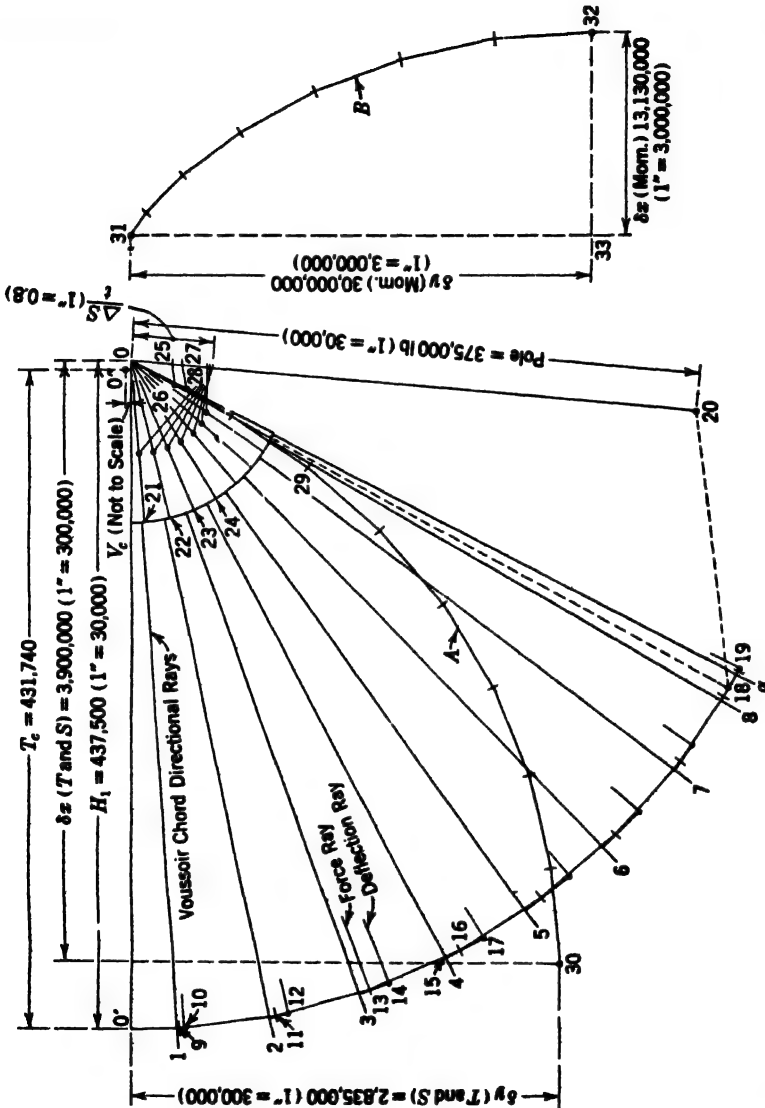


FIG. 19. Graphic analysis, thrust and shear functions, Example 5.

ending at point 19. Lines radiating from point 0 and parallel to the voussoir chords are drawn as 0-1 to 0-8, inclusive. Line 0-a is parallel to the tangent at the abutment. Portions of these rays near the center are omitted to avoid a confusion of lines in a subsequent step.

Line 0-4, for example, represents the direction of the chord in voussoir 4, and the thrust at the center of this voussoir is represented in magnitude and direction by a line from 0 to 16. This force, which is inclined to the center line of the voussoir, may be resolved into a thrust 0-15 and a shear 15-16. The thrust causes a shortening of the chord proportional to the length 0-15 times  $\Delta s/t$ . The shear causes a deformation normal to the chord and proportional to  $n(15-16) \Delta s/t$ . If 15-17 is made  $n$  times 15-16, it will bear the same relation to shear deflection that 0-15 bears to thrust deflection. Hence the line 0-17 multiplied by  $\Delta s/t$  becomes a measure of combined shear and thrust deflection in voussoir 4. Similar lines represent thrust-shear deflections in other voussoirs. When multiplied, each by its corresponding value of  $\Delta s/t$ , these lines may be added vectorially to give the total movement at the crown.

The shear line 15-16 may be scaled, multiplied by  $n$ , and replatted as 15-17, or it may be extended with proportional dividers.

Multiplication of the deflection rays is accomplished graphically, the scale being reduced simultaneously to facilitate vectorial addition.

A pole distance is laid off from 0 to 20, using any convenient combination of direction and length. Values of  $\Delta s/t$  for all the voussoirs are platted on this line to a convenient scale, each value being measured independently from point 0. Let line 0-18 represent the deflection ray and 0-25 the value of  $\Delta s/t$  for voussoir 8 and draw 25-26 parallel to 20-18. If  $\Delta s/t$  is platted to a scale of 1 in. =  $k$  units, (0-26) represents deflection to a scale of 1 in. =  $pk$  units,  $p$  being the pole length (0-20) to the scale of the force polygon. In Fig. 19,  $p$  and  $k$  are 375,000 and 0.8, respectively; hence the scale of 0-26 is 1 in. = 300,000 units. Other deflection rays are multiplied in the same way. The foundation movement is determined from an additional ray at the abutment, using the value of  $(G)$  from Table 5 in place of  $\Delta s/t$ . To get the direction of the abutment deflection ray, the abutment shear line  $a-19$  is multiplied by  $(H)/(G)$  (from Table 5) rather than by  $n$  as for other rays. For the present example this ratio is 1.33. The line 0-27 represents  $(G)$ , and 0-28 is the foundation movement due to the arbitrary crown force and external loads.

The nine deflection vectors thus obtained are added by platting one after another, beginning with 0-28 and proceeding through 29 along Curve A to point 30.

Usually, the radial deflection due to the  $(F)$  term of Eq. 56 may be ignored; otherwise its value may be computed, using the scaled value of the abutment shear, and the result inserted as a right-angle offset in line A at point 28.

The horizontal and vertical components of Curve A are scaled and entered as items 37 and 42 of Table 10, replacing items 46, 47, 48, 54, 55, 56, 57, 58, and 61, 62, 63, 69, 70, 71, 72, 73 of Table 7.

(f) *Moment functions.* Deformations caused by the moments from external loads are computed from the shears scaled from the force polygon of Fig. 19. The scaled values of 1-9, 2-11, 3-13, etc., are recorded in column 6, Table 9. If a shear curve using these values is platted on the developed arch axis line, the value of  $M_x$  at any point is the area under such curve from the crown to



the point. Area increments, which are also shear increments, are obtained by multiplying the average shears of column 7 by the length increments,  $\Delta s$ , from column 3. The results, column 8, are summated from crown to abutment to give the values of  $M_E$  shown in column 9. These values are multiplied by  $\Delta s/I$  to give the angular deflection increments of column 10. Foundation effect due to moment is allowed for by inserting the value of  $(E)$  from Table 5 as an abutment value of  $\Delta s/I$ , column 5, and carrying this value through as if it represented an additional voussoir. If the second term of Eq. 54 is not to be ignored, the product  $S(F)$  is added algebraically to the value of  $M(E)$  in column 10,  $S$  being the abutment value of the shear, column 6, and  $(F)$  the foundation factor from Table 5.

Values of column 10 summated from abutment to crown give accumulated angular deflections at the *ends* of voussoirs, column 11. The last term of this summation represents the angular deflection at the crown due to external forces and is entered as item 33 of Table 10, replacing items 39, 41, 42, and 43 of Table 7. Average values, column 12, are multiplied by  $\Delta s$ , column 2, to give the voussoir deflection increments of column 13. These deflections, each assumed normal to its voussoir chord, are platted successively from abutment to crown in the position 31 to 32, Curve *B*, Fig. 19. The length 33-32 represents

$$\Sigma x M_E \frac{\Delta s}{I} + x_a(E) M_E + x_a(F) \sin \alpha \Sigma P_x + x_a(F) \cos \alpha \Sigma P_y$$

items 60, 66, 67, and 68, Table 7, and is scaled and entered as item 41, Table 10. The length 31-33 similarly represents

$$\Sigma y M_E \frac{\Delta s}{I} + y_a(E) M_E + y_a(F) \sin \alpha \Sigma P_x + y_a(F) \cos \alpha \Sigma P_y$$

items 45, 51, 52, and 53, Table 7. The scaled value is entered as item 36, Table 10.

(g) *Remaining items of Table 10.* The influence of foundation deformation on  $D_u$ ,  $D_x$ , and  $D_y$  is fully included in Fig. 19. Items 8, 9, 13, 14, 26, and 27 of Table 10, containing the factors  $(G)$  and  $(H)$  from Table 5, are determined graphically from Curves *I* and *J*, Fig. 18, or they may be computed as in Table 6. Values of  $(F) \sin \alpha$  and  $(F) \cos \alpha$ , items 2 and 19, Table 10, are computed. The computed values are too small to record in this example but are used in computing items 7, 15, 16, and 25.

As was observed in Example 4, Art. 14j, many of the foundation terms are negligible for *this arch*. They are included to illustrate procedure.

Values of  $C_u$ , item 29, Table 10, is the total of  $\Delta s/I + (E)$ , column 5, Table 9, replacing items 34 and 35 of Table 7.

The value of  $\Sigma \Delta s/t$  used in computing item 34, Table 10, is the total of column 4, Table 9, which corresponds to item 40, Table 7. The temperature terms, items 39 and 44, Table 10, are identical with items 50 and 65, Table 7. This completes Table 10.

(h) *Crown forces and stresses.* Having completed the determination of constants for the left half of the arch, those for the right half are similarly determined and all are assembled in Table 10 to give the constants required for the solution of Eqs. 60, 61, and 62, following the procedure of Art. 14g. The computed crown forces are as follows:

$$M_c = 627.2 \text{ ft kips}$$

$$V_c = 0.654 \text{ kips}$$

$$H_c = -5.760 \text{ kips}$$

$$T_c = H_1 + H_c = 431.740 \text{ kips}$$

Moments at the abutments and at intermediate points are computed from Eq. 11. The abutment thrust is determined graphically from Fig. 19. The resultant of  $T_c$  and  $V_c$  is substituted for  $H_1$  by plating  $T_c$  from  $O'$  toward the right and then  $V_c$  vertically to get a new center  $O''$  for the force rays. True thrusts and shears are determined by redrawing the voussoir chord directional rays from this new center, following the procedure of Art. 15c.

The moments and measured thrusts are assembled and stresses computed in a manner similar to that illustrated in Table 8.

(i) *Comparative accuracy.* A comparison of Tables 7 and 10 shows close agreement for all individual items and reasonable agreement in final coefficients. Exact agreement is difficult to attain and is not essential. However, careful work is required, particularly in items carrying opposite signs for the right and left sides of the arch and in the determination of the shear values from which moments are computed. With good equipment, using a hard pencil (8H or 9H) on hard paper, a careful draftsman should have no trouble securing all necessary precision, except possibly for very slender arches. Graphic solution is most useful for arches of irregular form.

**16. Possible Simplifications.** (a) *Neglect of shear.* The effect of shear deformations on the computed stresses is small in slender arches, such as those encountered in bridges and near the tops of dams, but it may be important in thick arches. The shear effect may be removed from Example 4 by giving  $n$  a value of zero in Table 7. This eliminates eight items from Table 7 (four for each side of arch). Eight other factors containing  $(n - 1)$  are altered. The  $(\sin^2 \alpha/t) \Sigma P_x$  and  $(\cos^2 \alpha/t) \Sigma P_y$  items appear only in eliminated items; hence columns 36 and 39 may be omitted from Table 4. Only one of these occurs in a symmetrical arch. The reduction in effort is important only in the routine testing of many arches.

For graphical procedure with shear deformations ignored, the extension of the shear lines is not required. The thrust components of the force rays replace the rays 0-10, 0-12, etc., in the construction of Curve A, Fig. 19.

Fig. 20 shows the error resulting from neglect of shear in cylindrical arches under uniform normal loads for various thickness-radius ratios for all values

of the central angle. Although this diagram strictly applies only to cylindrical arches, it serves as a rough guide for other forms. The effect of shear deformation becomes very appreciable as the ratio of thickness to radius increases.

(b) *Partial neglect of shear.* The simplification due to making  $n = 1$ , i.e., by *partially* ignoring shear deformation, is greater than for  $n = 0$ , and the

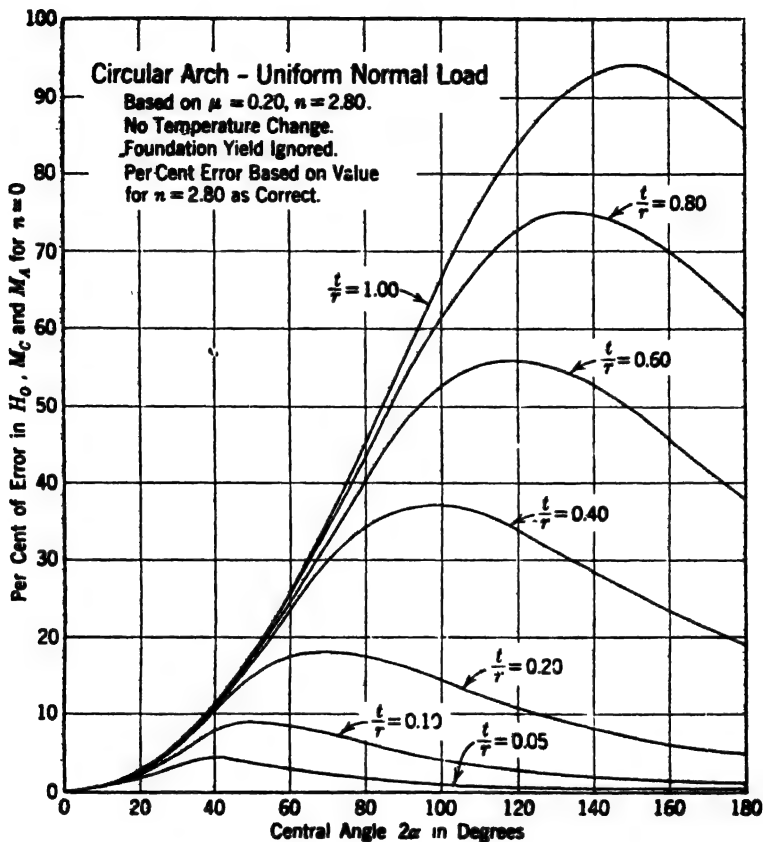


FIG. 20. Error caused by neglect of shear deformation.

error is less. The  $(n - 1)$  terms are eliminated from Table 7, and substituting unity for  $\sin^2 + \cos^2$  permits a combination and simplification of other terms. Twenty-four items are eliminated from Table 7 and six new simpler ones are added. All trigonometric columns except 2 and 3 are eliminated from Table 4. Two new columns are required for values of  $\Sigma \Delta s \Sigma P_x / t$  and  $\Sigma \Delta s \Sigma P_y / t$ .

In graphic work, the actual force rays replace the "deflection rays" in the construction of Curve A, Fig. 19. Making  $n = 1$  is equivalent to assuming that combined shear and thrust deflection from an inclined load on the end of a cantilever is in the direction of the load. A value of unity for  $n$  is permissible

for slender arches. There is never any need for making  $n$  zero, as  $n = 1.0$  involves less work and less error.

(c) *Neglect of foundation yielding.* If foundation yielding is ignored, Tables 5 and 6 and the foundation terms of Table 7, are eliminated, with an appreciable saving in work. Examination of Table 7 shows that the foundation items contribute appreciably to the arch equation constants. However, the influence on actual stresses is less marked and foundation deformations may be ignored for this relatively slender arch without serious error.

For thicker arches, the influence of foundation yielding may be important. Foundation yielding generally causes a relief in abutment stresses with an increase at the crown. Temperature stresses are relieved throughout. The many possible combinations of physical conditions, water load, and temperature change, make a general rule difficult. Table 11 gives some idea of the effect of foundation yielding on the load stresses for two typical series of cylindrical arches.

TABLE 11  
COMPARATIVE FOUNDATION EFFECTS

[Cylindrical arch, uniform normal load,  $h_2 = 100$  ft,  $E_M = E_F$ ,  $\psi = 40^\circ$ ,  $\mu$  (foundation) = 0.2,  $b \div a = 8.0$ ,  $n = 2.8$ ; no temperature stress.]

Radius-thickness ratio, $r/t$		1.0	2.0	4.0	8.0
$\alpha = 40^\circ$	$T_c$ Yielding foundation	3663r	3617r	4484r	5563r
	$T_c$ Rigid foundation	2857r	3022r	4103r	5180r
	$M_c$ Yielding foundation	863r <sup>2</sup>	493r <sup>2</sup>	252r <sup>2</sup>	96r <sup>2</sup>
	$M_c$ Rigid foundation	517r <sup>2</sup>	380r <sup>2</sup>	232r <sup>2</sup>	96r <sup>2</sup>
	$M_a$ Yielding foundation	- 474r <sup>2</sup>	489r <sup>2</sup>	344r <sup>2</sup>	156r <sup>2</sup>
	$M_a$ Rigid foundation	- 1008r <sup>2</sup>	741r <sup>2</sup>	453r <sup>2</sup>	187r <sup>2</sup>
$\alpha = 30^\circ$	$T_c$ Yielding foundation	6174r	5916r	6224r	6384r
	$T_c$ Rigid foundation	5432r	5350r	6047r	6350r
	$M_c$ Yielding foundation	758r <sup>2</sup>	388r <sup>2</sup>	153r <sup>2</sup>	46r <sup>2</sup>
	$M_c$ Rigid foundation	744r <sup>2</sup>	426r <sup>2</sup>	170r <sup>2</sup>	50r <sup>2</sup>
	$M_a$ Yielding foundation	- 843r <sup>2</sup>	560r <sup>2</sup>	251r <sup>2</sup>	82r <sup>2</sup>
	$M_a$ Rigid foundation	- 1407r <sup>2</sup>	805r <sup>2</sup>	322r <sup>2</sup>	94r <sup>2</sup>

(d) *Partial neglect of foundation yielding.* The items involving the foundation factor ( $F$ ) may be stricken from Table 7 without measurably changing the computed stresses. In fact, considering the approximate nature of the foundation treatment, it is doubtful if it is ever necessary to include these items.

(e) *Origin at elastic center.* The algebraic work is simplified if the center of gravity of the  $\Delta s/I$  quantities for the half arch, rather than the crown point, is used as the center of coordinates. If  $x$  and  $y$  are measured from this center,  $\Sigma x \Delta s/I$  and  $\Sigma y \Delta s/I$  become zero; hence, terms containing these summations disappear. If the arch is analyzed in two parts, as is usual, the elastic center must be determined separately for each side, and proper precautions must be taken in joining the results in the arch equations.

It is likewise possible to orient the coordinate system with origin at the elastic center to make

$$\Sigma xy \frac{\Delta s}{I} = 0 \quad [75]$$

If the foundation factor is included with  $\Delta s/I$  in finding the elastic center, then the  $x_a(E)$ ,  $y_a(E)$ , and  $x_a y_a(E)$  terms are likewise eliminated. Other foundation terms remain, except where they may be ignored.

The crown forces  $H_c$  and  $V_c$  are equal, respectively, to elastic center forces  $H_0$  and  $V_0$ . The moment at the crown or at any other point on the arch, is found by inserting proper values of  $y$  and  $x$  in the equation

$$M = M_0 + H_0 y + V_0 x \quad [76]$$

Where a single unaltered arch section is to be analyzed for many load combinations, the use of the elastic center appreciably reduces the work. If the arch itself is likely to be altered, the labor involved in finding the elastic center may exceed that saved by its use unless the arch is of some standard form for which the position of the elastic center is known.

(f) *Voussoir length constant.* If the arch is divided so that  $\Delta s$  is constant, this factor may be canceled from all items in which it appears. The temperature and foundation items which do not contain  $\Delta s$  must then be divided by  $\Delta s$ . The saving in labor is small and some complications are introduced if the arch is unsymmetrical or if deflections between arches of unequal arc lengths are to be compared.

(g) *Constant ratio of  $\Delta s$  to  $I$ .* The voussoir length may be chosen to make  $\Delta s/I$  constant. The result is a slight reduction of arithmetic work, but unless the same arch is to be analyzed for several load conditions, the work of dividing the ring more than offsets the savings.

**17. The Importance of Temperature Stresses.** An understanding of the contribution of temperature deformation to the total stress is helpful in the selection of arch shapes and also in considering justifiable expenditures for the control of temperature drop. (See Art. 14, Chapter 15.) Stresses due to temperature alone are found by making all external loads including the arbitrary crown thrust  $H_1$  equal to zero.

Fig. 21 shows graphically the temperature stresses at the four critical points in a cylindrical arch for thickness-radius ratios from 0.05 to 1.00 and for central angles up to 180°. Two sets of vertical scales are shown. The inner set is to be multiplied by  $C_r F E$  to get actual stresses. The outer set is in lb per sq in.

for  $F = 10^\circ \text{F}$  and  $C_F E = 20$ ,  $E$  being in lb per sq in. The diagram applies only to circular arches but may be used as a general guide for arches of other forms.

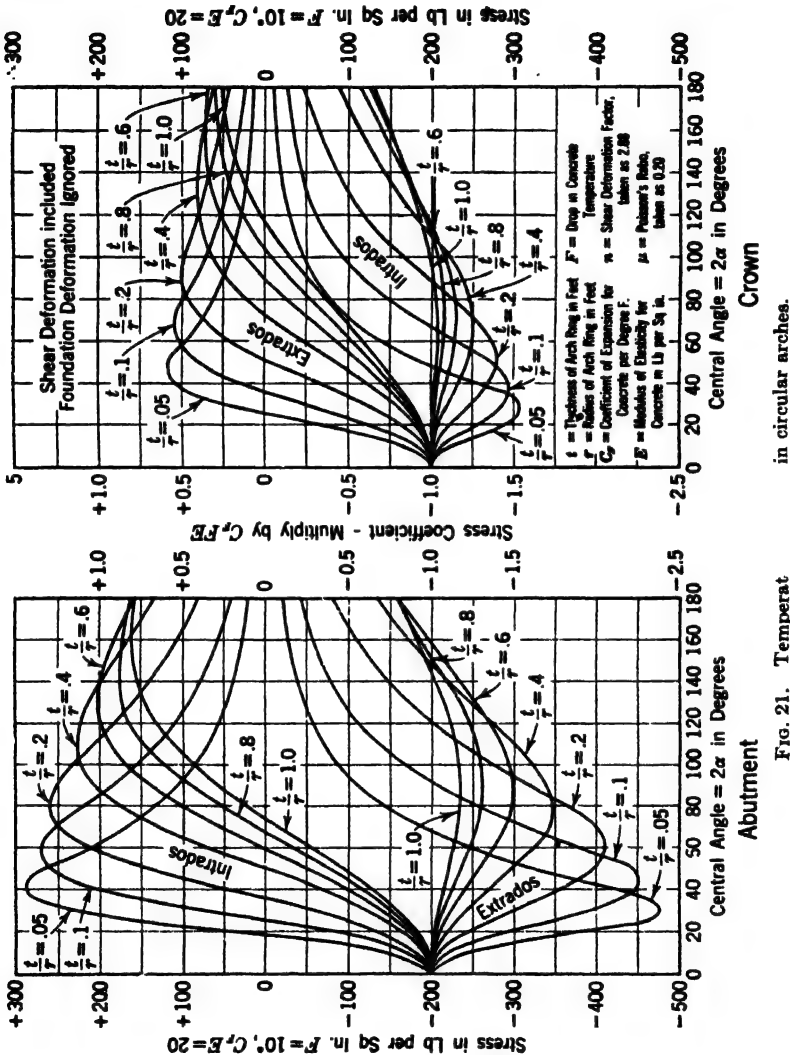


FIG. 21. Temperat

All the stress lines converge at a stress coefficient of  $-1$  for  $2\alpha = 0$  and have maximum positive or negative values for central angles which are related to the thickness-radius ratio. The highest peak stresses in arches of moderate thickness occur with central angles from  $20^\circ$  to  $60^\circ$ . Stresses in the thinner arches drop off rapidly with increasing central angles after the peak is passed

TABLE 12  
ARCH COMPUTATIONS, SYMMETRICAL ARCH, EXAMPLE 6

Point	1	2	3	4	5	6	7	8	9	10	10½	11	14	15	20	21	22
$\alpha$	$\alpha$	$\sin \alpha$	$\cos \alpha$	$r$	$\Delta r$	$y$	$\Delta y$	$\Delta s$	$t$	$\frac{\Delta s}{t}$	$\frac{s \Delta y}{t}$	$\frac{\Delta s}{I}$	$\frac{\Delta y}{I}$	$\frac{\Delta y^2}{I}$	$I'$	$\frac{I'}{\cos \alpha}$	$\frac{I'}{\sin \alpha}$
rown	..	...	....	...	...	...	...	..	9.80	..	....	...	...	...	...	....	437,500
1	4° 01'	0.07005	0.99751	7.00	...	0.25	0.25	11.00	"	1.42857	0.36	0.17850	0.04462	0.01	64,250	64,090	4,500
2	12° 02'	0.20848	0.97803	20.85	13.85	2.20	1.95	"	"	"	3.14	"	0.04462	0.86	"	62,840	13,490
3	20° 03'	0.34284	0.93949	34.28	13.43	6.06	3.86	"	"	"	8.66	"	0.39270	6.56	"	60,360	22,030
4	28° 04'	0.47050	0.88240	47.05	12.77	11.76	5.70	"	"	"	16.80	"	1.08171	24.69	"	56,690	30,290
5	36° 06'	0.59020	0.80799	58.02	11.87	19.20	7.44	"	"	"	27.43	"	3.42720	65.80	"	51,910	37,860
6	44° 34'	0.70174	0.71243	69.60	10.68	28.23	9.03	"	9.85	1.42132	40.12	0.17580	4.96283	110.10	64,270	45,700	45,100
7	53° 20'	0.80368	0.59506	78.77	9.17	38.80	10.57	"	10.20	1.46054	52.79	0.15120	5.98296	232.11	64,110	38,530	51,770
8	60° 30'	0.87036	0.49242	84.77	6.00	48.03	9.25	8.06	10.93	0.73742	35.42	0.07408	3.53806	170.80	37,290	18,320	32,380
Abut.	63° 04'	0.89153	0.43205	80.68	1.91	51.59	3.56	....	11.25	....	..	....	....	..	..	..	....
Total	....	..	....	....	..	..	....	....	..	10.06213	184.72	1.20638	21.54024	611.05	..	....	....

Left Side

Point	23	24	25	26	27	28	29	30	31	33	35	364
	$\Sigma P_y$	$\Delta r \Sigma P_y$	$\Sigma (\Delta r \Sigma P_y)$	$\Sigma P_z$	$\Delta r \Sigma P_z$	$\Sigma (\Delta r \Sigma P_z)$	$\left\{ \Delta r' \right.$	$\frac{M E}{\Sigma (\Delta r \Sigma P_y) - \Sigma (\Delta r \Sigma P_z) + \frac{1}{2} \Delta r'}$	$\frac{\Delta r M E}{I}$	$\frac{\Delta r M E}{I}$	Avrg. $\frac{\Sigma P_z}{\text{from Col. 26}}$	$\frac{\Delta r \Sigma P_z}{I}$
Crown			.....									
1	64,000	887,600	.....	437,300	100,400	100,400	112,400	3,000	536	100	435,250	621,800
2			887,600	433,000	844,400	553,900		46,200	8,247	18,100	436,300	606,000
3	126,930	1,704,700	2,592,300	419,610	1,619,700	2,573,300		131,200	23,119	141,000	408,600	582,700
4	187,200	2,301,700	4,084,000	397,380	2,206,200	4,839,700		236,700	43,821	558,300	382,400	546,300
5	243,080	2,808,000	7,880,000	367,450	2,733,100	7,572,800		419,600	74,860	1,438,100	448,420	497,800
6	295,890	3,160,100	11,040,100	329,400	2,975,300	10,348,100	112,200	604,500	106,271	3,000,000	396,940	436,200
7	341,680	3,133,200	14,173,300	284,300	3,006,000	13,554,100	112,700	731,900	112,879	4,378,900	258,500	351,700
8	380,010	2,280,100	16,453,400	232,620	2,146,900	15,701,000	37,200	786,900	58,516	2,810,500	216,400	216,400
Abut.	308,330	767,800	17,214,200	200,240	712,000	16,413,000	...	800,300	.....	.....	.....	.....
Total	.....	.....	.....	.....	.....	.....	.....	.....	430,568	12,326,500	.....	3,862,000

Left Side



Peaks for thicker arches occur at greater angles and are lower, and the stresses drop off less rapidly beyond the peak. The very great importance of temperature stresses is at once apparent.

### SPECIAL ARCH FORMS

**18. Symmetrical Arch.** (a) *Simplification of equations.* If the arch and its loading are symmetrical about the  $y$  axis, the labor of computation is greatly reduced. Computations for the right and left sides are identical and need be made only once. Also, from symmetry,  $V_c$  is zero and the angular and  $x$  deflections are each equal to zero for each half of the arch. In Eqs. 60, 61, and 62 the terms containing  $V_c$  drop out, also  $A_y$  and  $C_y$  are not required; hence there remains

$$A_a H_c + C_a M_c + D_a = 0 \quad [60a]$$

$$A_x H_c + C_x M_c + D_x = 0 \quad [61a]$$

(b) *Analytical analysis, Example 6.* As an example of a symmetrical analysis, take an arch of the same specifications as Example 4 except that both sides shall be identical with the left side of Fig. 17 and the shearing factor,  $n$ , is assumed unity. Based on previous experience (in Example 4), all foundation items are ignored except those containing ( $E$ ) and the ( $G$ ) items of  $D_x$ .

Computation proceeds exactly as for Example 4 except that many items may be omitted. Constants are computed and assembled in Tables 12 and 13 which correspond to Tables 4 and 7 of Example 4. The column numbers of Table 4 are retained for convenient reference.

Columns 10a, 12, 13, 14, 19, 32, 38, 39, and 40 are eliminated because not required for a symmetrical arch; 17, 18, 36, 37, and 41 because of shear modification; and 34 because of these two influences combined. The movement at the crown due to thrust and modified shear is completely given by a new column 36a.

Using the constants assembled in Table 13, the crown forces are computed thus:

$$23.02H_c + 1.326M_c = 674.5$$

$$727.6H_c + 23.02M_c = 8,790$$

$$H_c + 0.0576M_c = 29.30$$

$$H_c + 0.0316M_c = 12.08$$

$$0.0250M_c = 17.22$$

$$M_c = 688.8 \text{ ft kips}$$

$$H_c = -9.69 \text{ kips}$$

$$T_c = H_1 + H_c = 437.5 - 9.7 = 427.8 \text{ kips}$$

Stress computations follow the form of Table 8.

TABLE 13

## ARCH EQUATION CONSTANTS, EXAMPLE 6

[ $n = 1.0$ ,  $F = 20^\circ$ ,  $\Delta F = 8^\circ$ , forces in kips. ( $E$ ) and ( $G$ ) from Table 5, left side.]

Item	Term		Value	Item	Term		Value
1	$A_\alpha$	$\Sigma y \frac{\Delta s}{I}$	+21.55	12	$D_\alpha$	$\Sigma \frac{\Delta s}{I} M_E$	-430.6
2		$y_\alpha(E)$	+1.47	13		$C_F \Delta F E \Sigma \frac{\Delta s}{t}$	-221.1
3	Total		+23.02	14		$(E) M_\alpha$	-22.8
4	$A_z$	$\Sigma y^2 \frac{\Delta s}{I}$	+641.05	15	Total		-674.5
5		$\Sigma \frac{\Delta s}{t}$	+10.66	16	$D_z$	$\Sigma y \frac{\Delta s}{I} M_E$	-12,326
6		$y_z^2(E)$	+75.90	17		$\Sigma \left( \frac{\Delta s}{t} \Sigma P_x \right)$	+3,863
7	Total		+727.61	18		$C_F \Delta F E \Sigma y \frac{\Delta s}{t}$	-3,830
8	$C_\alpha$	$\Sigma \frac{\Delta s}{I}$	+1.297	19		$C_F F E x_\alpha$	+4,493
9		$(E)$	+0.029	20		$y_\alpha(E) M_\alpha$	-1,177
10	Total		+1.326	21		$(G) \cos^2 \alpha \Sigma P_x$	+38
11	$C_z$	$= A_\alpha$	+23.02	22		$(G) \sin \alpha \cos \alpha \Sigma P_y$	+149
				23	Total		-8,790

**19. Circular Arch of Uniform Thickness.** (a) *Variable loading.* If the arch is fully cylindrical and of uniform thickness, the totals for columns 10 to 19 of Table 4 may be computed from the integrals shown in Table 14; hence the individual items of these columns need be computed only if required in the construction of the remainder of the table. Integrals for columns 10a and 10b are identical with those for columns 12 and 14, except that the constant  $I$  must be replaced by  $t$ . If the arch is symmetrically divided and the loading is symmetrical, the simplification discussed in Art. 16 may be introduced.

Also, for symmetrical division, the  $\Sigma x \Delta s / I$  terms in the arch equation are not required and the benefits of using the elastic center (Art. 16e) are obtained if the origin is placed on the axis of symmetry a distance

$$y_0 = r \left( 1 - \frac{\sin \alpha}{\alpha} \right) \quad [77]$$

TABLE 14

INTEGRALS FOR GEOMETRIC FUNCTIONS, CIRCULAR ARCH, UNIFORM THICKNESS

Col. no.	Function	Integrals (origin at crown)	Integrals (origin at elastic center)
10	$\int \frac{1}{t} ds$	$\frac{s}{t}$	$\frac{s}{t}$
11	$\int \frac{1}{I} ds$	$\frac{s}{I}$	$\frac{s}{I}$
12	$\int \frac{x}{I} ds$	$\frac{r^2}{I} (1 - \cos \alpha)$	$\frac{*r^2}{I} (1 - \cos \alpha)$
13	$\int \frac{x^2}{I} ds$	$\frac{r^3}{I} (\frac{1}{2}\alpha - \frac{1}{4}\sin 2\alpha)$	$\frac{r^3}{I} (\frac{1}{2}\alpha - \frac{1}{4}\sin 2\alpha)$
14	$\int \frac{y}{I} ds$	$\frac{r^2}{I} (\alpha - \sin \alpha)$	Zero
15	$\int \frac{y^2}{I} ds$	$\frac{r^3}{I} (\frac{3}{2}\alpha - 2\sin \alpha + \frac{1}{4}\sin 2\alpha)$	$\frac{r^3}{I} (\frac{1}{2}\alpha + \frac{1}{4}\sin 2\alpha - \frac{\sin^2 \alpha}{\alpha})$
16	$\int \frac{xy}{I} ds$	$\frac{r^3}{I} (\frac{1}{2} - \cos \alpha + \frac{1}{4}\cos 2\alpha)$	$\frac{*r^3}{I} (\frac{\sin \alpha}{\alpha} - \frac{\sin \alpha \cos \alpha}{\alpha} - \frac{1}{4} + \frac{1}{4}\cos 2\alpha)$
17	$\int \frac{\sin^2 \alpha}{t} ds$	$\frac{r}{t} (\frac{1}{2}\alpha - \frac{1}{4}\sin 2\alpha)$	$\frac{r}{t} (\frac{1}{2}\alpha - \frac{1}{4}\sin 2\alpha)$
18	$\int \frac{\cos^2 \alpha}{t} ds$	$\frac{r}{t} (\frac{1}{2}\alpha + \frac{1}{4}\sin 2\alpha)$	$\frac{r}{t} (\frac{1}{2}\alpha + \frac{1}{4}\sin 2\alpha)$
19	$\int \frac{\sin \alpha \cos \alpha}{t} ds$	$\frac{r}{t} (1 - \frac{1}{2}\cos 2\alpha)$	$\frac{*r}{t} (1 - \frac{1}{2}\cos 2\alpha)$

\* These functions are zero when left and right sides are combined. Limits of integration,  $\alpha$  and 0.

from the crown toward the center, where  $\alpha$  is the angle between the center line and the abutment radius. This point is the elastic center of the arch as a whole. If the  $y$  axis coincides with the bisecting radius, the conditions of Eq. 75 are likewise satisfied. Integrals based on the origin at the elastic center, shown in the right-hand column of Table 14, involve the assumption of symmetrical division of the arch but not necessarily of the loads.

Such of the geometric columns of Table 4 as are required for the computation of load columns with variable loading are filled in. Totals are computed for the remainder from the integrals, the load columns are completed, and the results transferred to a table similar to Table 7. The remaining procedure is

is described for Example 4, taking full advantage of symmetry and other available simplifications.

(b) *Uniform normal loads.* If the loading consists solely of uniform water pressure normal to the cylindrical upstream face, arithmetical summation may be entirely eliminated by making the arbitrary crown force  $H_1$  equal to the full cylinder crown thrust as determined from Eq. 1. This force is applied at the true neutral axis or the center line whichever is being used. The resulting moments and shears from external loads on the free half-arch (including  $H_1$ ) are zero at all points on the arch axis; hence, all functions containing these factors disappear. This eliminates all of columns 20 to 41 of Table 4, except those giving crown movement due to thrust and these are replaced by the expressions

$$\delta x = \frac{H_1}{t} x_a = \frac{w_2 h r_c}{t} r \sin \alpha \quad [78]$$

The arch is treated as symmetrical and the origin may be taken at the elastic center. The equations take the form of 60a and 61a, Art. 18a. If  $\Delta F = 0$ , as is usually the case,  $D_a$  is zero. If foundation deformations are ignored,  $A_a$  is also zero (with origin at elastic center); hence  $M_0 = 0$ , and there remains the sole equation

$$H_0 = -\frac{D_x}{A_x} \quad [79]$$

The foundation constants, when included, are computed separately as in Table 5, using applicable simplifications.

(c) *Numerical example, Example 7.* An analysis will be made of a cylindrical arch under uniform normal load conforming to the following data:

*Arch:*

$$\alpha = 65^\circ, r_c = 120 \text{ ft}, t = 20 \text{ ft}, h = 100 \text{ ft}$$

$$E_M = 3,000,000 \text{ lb per sq in.}$$

$$\text{Temperature drop } F = 12^\circ, C_F = 0.000006$$

$$\text{Shear factor } n = 2.8$$

*Foundation:*

$$E_F = E_M, \mu = 0.2, b'a = 8, \psi = 50^\circ$$

Neglect foundation factor ( $F$ )

Proceeding as illustrated in Table 5, using  $k$  values from Figs. 10 to 14, values of the foundation functions are found as follows: ( $E$ ) = 0.011209, ( $G$ ) = 1.00117, ( $H$ ) = 1.669997. The constants are computed in Table 15 and represent deformations at the elastic center. For this simple symmetrical case they may be entered directly into the arch equations. (An unsymmetrical

arch requires alteration of the procedure illustrated in Table 15.) The arch equations are set up and solved as follows:

$$0.5050H_0 + 0.2149M_0 = 0$$

$$124.61H_0 + 0.5050M_0 = -8,128,600$$

$$H_0 + 0.4255M_0 = 0$$

$$H_0 + 0.0041M_0 = -65,232$$

$$0.4214M_0 = 65,232$$

$$M_0 = 154,800 \text{ ft lb}$$

$$H_0 = -65,900 \text{ lb}$$

Moments at the crown and abutment are computed from Eq. 76, and the corresponding thrusts are found by adding  $H_0$  and  $H_0 \cos \alpha$  (algebraically) to  $H_1$ . The fiber stresses are computed from Eqs. 72 and 73. The results are as follows:

	<i>Crown</i>	<i>Abutment</i>
$T$ , lb	746,600	784,600
$M$ , ft-lb	1,838,000	2,814,000
$f_c$ , lb per sq in.	+420	-27
$f_i$ , lb per sq in.	+80	+607

Stress conditions are least favorable at the abutment which follows from the fact that  $y_a$  is greater than  $y_0$ . This leads to the frequent practice of thickening the arch toward the ends.

(d) *Special formulas and diagrams.* Many papers have been published dealing with stresses in cylindrical arches under uniform normal loads. Notable among these are papers and discussions by Cain,<sup>18</sup> Jakobsen,<sup>19</sup> and Fowler.<sup>20</sup> Cain developed formulas equivalent to those of Art. 19b with the  $A$ ,  $C$ , and  $D$  terms written out in detail and solved to give direct expressions for fiber stresses at the crown and abutment. These equations allow for a uniform temperature drop but do not include shear deflections, abutment deformation, or radial temperature variation. Cain later revised his equations to allow for shear.<sup>19</sup>

<sup>18</sup> WILLIAM CAIN, "The Circular Arch Under Normal Load," *Trans. Am. Soc. Civil Engrs.*, Vol. 85, 1922, p. 233.

<sup>19</sup> B. F. JAKOBSEN, "Stresses in Thick Arches of Dams," *Trans. Am. Soc. Civil Engrs.*, Vol. 90, 1927, p. 475; also discussion of same by William Cain, p. 522.

<sup>20</sup> F. H. FOWLER, "A Graphic Method for Determining the Stresses in Circular Arches under Normal Loads by the Cain Formulas," *Trans. Am. Soc. Civil Engrs.*, Vol. 92, 1928, p. 1512.

TABLE 15  
ARCH EQUATION CONSTANTS, EXAMPLE 7

Item	Term	Integral	Value
1	$A_a$	$y_a(E)$	+0.5050
2	$A_z$	$\int \frac{y^2}{I} ds = \frac{r^3}{I} \left( \frac{1}{2}\alpha + \frac{1}{4}\sin 2\alpha - \frac{\sin^2 \alpha}{\alpha} \right)$	+89.47
3		$\int \frac{\cos^2 \alpha}{t} ds = \frac{r}{t} \left( \frac{1}{2}\alpha + \frac{1}{4}\sin 2\alpha \right)$	+4.54
4		$n \int \frac{\sin^2 \alpha}{t} ds = n \frac{r}{t} \left( \frac{1}{2}\alpha - \frac{1}{4}\sin 2\alpha \right)$	+6.30
5		$y_a^2(E)$	+22.75
6		$(G) \cos^2 \alpha$	+0.18
7		$(H) \sin^2 \alpha$	+1.37
8	Total		+124.61
9	$C_a$	$\int \frac{ds}{I} = \frac{s}{I} = \frac{12r\alpha}{t^3}$	+0.2037
10			+0.0112
11	Total		+0.2149
12	$C_z$	$= A_a$	+0.5050
13	$D_a$		0
14	$D_z$	$\frac{H_1}{t} x_a$	+4,407,800
15		$H_1(G) \cos \alpha$	+ 354,000
16		$C_F F E x_a$	+3,375,800
17	Total		+8,128,600

NOTE: Coordinates and deformations measured to elastic center of whole arch.

Jakobsen introduces shear deformation and shows that the neutral axis of a curved beam does not coincide with its center line. His equations, like Cain's, do not include abutment deformation or radial temperature variation.

Fowler presents a diagram for the solution of the Cain equations, both with and without modifications for shear and true neutral axis. He assumes Poisson's ratio ( $\mu$ ) to be zero, which gives  $n$ , Eq. 64, a value of 2.4. Because there is no fixed relation between temperature drop and water load, temperature effects are omitted and must be computed separately. No allowance is made for foundation deformations.

For the limited conditions to which they apply, the Fowler curves are a great convenience. They are particularly useful in preliminary work.

**20. Fillet Arches.** (a) *Special equations.* The analyses illustrated in Examples 4 and 5 are entirely general and applicable to arches and loads of any form. Actually, the arches of these examples are only partially irregular, and simplification of the analysis is possible.

The procedure is illustrated in Fig. 22. The extrados is circular and subjected to a uniform normal water pressure. The axis is represented by the compound curve 1-2-4, which should be the true neutral axis but may be taken as the center line if the arch is thin. The portion 2-4 need not be

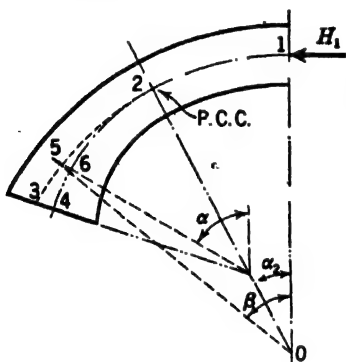


FIG. 22. Fillet arch.

circular. The arch thickness is constant from 1 to 2 and variable from 2 to 4. If the arbitrary crown force,  $H_1$ , is made equal to  $w_2hr$ , the moment,  $M_E$ , for the free arch, is zero at any point on the axis 1-2 or its extension 2-3. The tangential thrust,  $T$ , due to  $H_1$  and water loads, is equal to  $H_1$  at all points on 1-2-3, and the shear normal to 1-2-3 is zero. The value of  $M_E$  at any point, such as 6, on the axis 2-4 is given by the equation

$$M_E = 0.5H_1\Delta t \quad [80]$$

where  $\Delta t = (t - t_c)$ ,  $t$  being the thickness at the point and  $t_c$  the crown thickness. Corresponding thrusts and shears on the axis 2-4 are

$$T_E = H_1 \cos (\alpha - \beta) \quad [81]$$

$$S_E = H_1 \sin (\alpha - \beta) \quad [82]$$

where  $T_E$  and  $S_E$  are, respectively, the thrust and shear due to external loads, including  $H_1$ , and  $\alpha$  and  $\beta$  have the significance indicated in Fig. 22.

If  $(\alpha - \beta)$  is small,  $T_E$  differs only slightly from  $H_1$ , and  $V_E$  is negligible. If it is also permissible to assume the shear factor,  $n$ , equal to unity, combined rib

shortening and shear displacements follow the line 1-2-3 and corresponding crown deflections are

$$\partial x = \sum \frac{\Delta s}{t} H_1 \cos \beta \quad [83]$$

$$\partial y = \sum \frac{\Delta s}{t} H_1 \sin \beta \quad [84]$$

These expressions are subject to integration for the cylindrical portion of the arch, the result being

$$\partial x(1 \text{ to } 2) = \frac{H_1}{t} x_2 \quad [85]$$

$$\partial y(1 \text{ to } 2) = \frac{H_1}{t} y_2 \quad [86]$$

(b) *Example 8, fillet arch.* The symmetrical arch of Example 6 will be partially reanalyzed as a fillet arch. The constants are computed in Table 16. Many of the columns of Table 12 for the same arch by the general solution are omitted. Columns 5 and 7 and 20 to 29 are not required for the determination of  $M_E$  and are omitted. Column 35 is not required, and column 36a is replaced by 37a. If full shear effect is to be considered, the heading for column 37a becomes  $T_E \cos \alpha \Delta s/t$ , and an additional column is required to give the shear deformation  $S_E \sin \alpha \Delta s/t$ . (Note the change from  $\beta$  to  $\alpha$  as the deformations follow the line 2-3 only when  $n$  is assumed unity.) Values of  $T_E$  and  $S_E$  are computed from Eqs. 81 and 82, or determined graphically. Column 9a is added, also columns 1a and 3a when required. Except for these new columns, all entries for points 6, 7, 8 in columns up to and including 15 are identical with corresponding entries in Table 12. Other items are either omitted or obtained by integration, using the formulas of Table 14. Graphical determination of  $\beta$  is usually sufficient.

The horizontal crown thrust  $H_1$  computed from Eq. 1 is  $62.5 \times 70 \times 104.9 = 458,940$  lb or 458.94 kips. This force, multiplied by  $0.5\Delta t$ , gives the values of  $M_E$  shown in column 30. The construction of columns 31 and 33 is evident. Column 37a gives the horizontal component of the crown movement due to rib shortening,  $\beta$  being identical with  $\alpha$  for the cylindrical part of the arch. The total of the first five items is equal to  $r/tH_1 \cos 40^\circ 06'$ .

The remaining procedure is identical with that of Example 6 and will not be repeated. The totals of columns 10 and 11 are identical with the corresponding totals of Table 12, but for 10b, 14, and 15, the totals are somewhat increased. These differences result from the inexactness of arithmetical summation. Columns 30, 31, and 33 are different because of a different value for  $H_1$ . The foundation effects are added separately, as in Example 6.

If the arch is unsymmetrical, the simplification must be applied to Table 4 rather than to Table 12 and a duplicate of column 37a must be added to give  $y$  deflections due to  $H_1$ . If the shear factor,  $n$ , is taken at its actual value rather



TABLE 16  
ARCH COMPUTATIONS, FILLET ARCH, EXAMPLE 8

Point	1	1a	2	3	3a	4	6	8	9	9a
	$\alpha$	$\beta$	$\sin \alpha$	$\cos \alpha$	$\cos \beta$	$x$	$y$	$\Delta s$	$t$	$\Delta t$
1 to 5	.....	.....	.....	.....	.....	.....	.....	70.00	9.80	0
6	44° 34'	44° 07'	.....	0.71243	0.71792	.....	28.23	14.00	9.85	0.05
7	53° 29'	52° 08'	.....	0.59506	0.61383	.....	38.80	14.00	10.29	49
8	60° 30'	58° 29'	.....	0.49242	0.52275	.....	48.03	8.06	10.93	1.13
Abut.	63° 04'	60° 46'	0.89153	0.45295	.....	86.08	51.59	.....	11.23	1.43
<hr/>										
Point	10	10b	11	14	15	30	31	33	* 37a	* 37b
	$\frac{\Delta s}{t}$	$\frac{\Delta s}{t} y$	$\frac{\Delta s}{t}$	$\frac{\Delta s}{t} y$	$\frac{\Delta s}{t} y^2$	$\frac{M_E}{0.5 \Delta t H_1}$	$\frac{\Delta s}{t} M_E$	$\frac{\Delta s}{t} y M_E$	$\frac{\Delta s}{t} H_1 \cos \beta$	
1 to 5	7.1430	56.90	0.89250	7.109	101.1	.....	.....	.....	3,016	.....
6	1.4213	40.12	0.17580	4.963	140.1	15.5	2.022	49.4	468	.....
7	1.3605	52.79	0.15420	5.983	232.1	112.4	17.332	672.5	383	.....
8	0.7374	35.38	0.07408	3.581	173.1	259.3	20.167	928.6	177	.....
Abut.	.....	.....	.....	.....	.....	.....	.....	.....	.....	.....
Total	10.6622	185.19	1.29658	21.636	646.4	.....	39.521	1650.5	4,044	.....

\* For true value of  $n$ , col. 37a is  $\frac{\Delta s}{t} T \cos \alpha$  and 37b is  $\frac{\Delta s}{t} S \sin \alpha$ .

than unity, the shear functions must be retained. If the loading is irregular, the load columns must also be retained, which largely eliminates the advantage of the fillet analysis.

**21. Three-Centered Arches.** A three-centered arch, similar to that shown in Fig. 23, is sometimes superior to any feasible single-centered fillet arch.

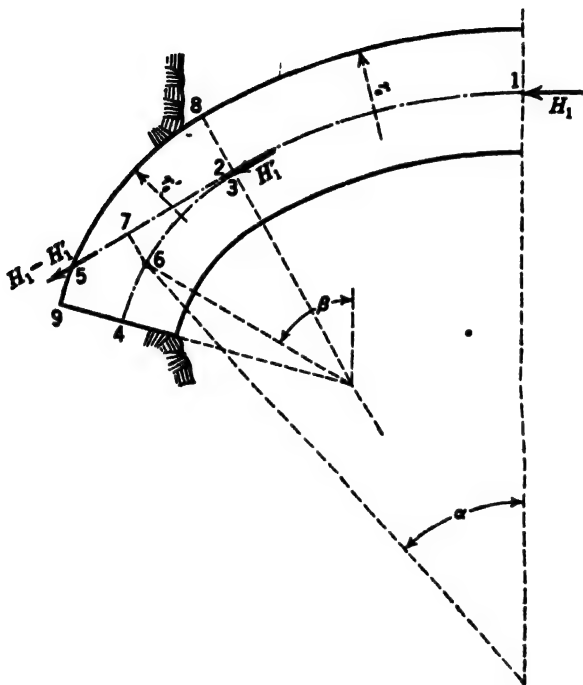


FIG. 23. Three-centered arch.

Such a design accentuates overhang and is thus subject to the limitations discussed in Art. 4c.

A three-centered arch may be analyzed by the general procedure, as illustrated in Examples 4, 5, and 6, or more simply by a modification of the fillet analysis, Example 8.

The axis of the arch follows the curve 1-2-3-4, the offset 2-3 resulting from a change in the value of  $\epsilon$ , Eq. 7, at the point of compound curve. If the arbitrary crown force,  $H_1$ , is made equal to  $w_2hr_s$ , there is no external moment or shear along the length 1-2. If the tangential axial force  $H'_1$ , at point 3, is made equal to  $w_2hr_s$ , there will be no external moments or shears along the length 3-4 due to water pressure on the face 8-9. However, the residual force  $H_1 - H'_1$  acting along the tangent 2-5 produces both moments and shears.

At point 6, for example, the net external moment is  $(H_1 - H'_1) \times (7-6)$  and shear is  $H_1 - H'_1 \sin (\beta - \alpha)$ . The thrust is  $H'_1 + (H_1 - H'_1) \cos (\beta - \alpha)$ . These alterations readily can be introduced into the procedure of Example 8.

## DETERMINING THE DIMENSIONS OF AN ELASTIC ARCH

**22. Best Shape for Elastic Arch.** The examples thus far given of elastic arches have related to the analysis of arches of predetermined form. Because of the many conflicting influences, the arch form must be selected largely by trial. In Art. 3*b*, it is shown that according to the cylinder theory an arch should be circular and that the best central angle is  $133^\circ 34'$ . These rules are not precisely applicable to the elastic analysis. The best shape for an elastic arch can be determined for a given set of conditions by analyzing a number of trial arches and plating concrete area against maximum stress. No specific general rule is available. Experience indicates that considering a whole dam, the central angles should be as large as practicable. Circular arches or circular arches with flared abutments, such as those of Examples 4, 5, 6, and 8, are favored even for variable loading but departure from these forms may be desirable at times.

**23. Selection of Arch Form.** (a) *Data.* The selection of an arch form will be illustrated for the following conditions:

### Example 9

#### Arch:

Clear span, at intrados, $l_i$	= 160 ft
Depth below surface, $h$	= 200 ft
Temperature drop, $F$	= $340/(t + 8)$

Radial temperature variation,  $\Delta F$  = 0

$E_M$ , lb per sq in. = 3,000,000

Shear factor,  $n$  = 2.80

Allowable tension = none

Allowable compression = 600 lb per sq in.

#### Foundation:

$E_F$ , lb per sq in. = 4,000,000

Abutment angle,  $\psi$  =  $60^\circ$

Poisson's ratio,  $\mu$  = 0.20

Foundation ratio,  $b/a$  = 5.0

(b) *Preliminary study.* The load being simple normal water pressure, a general idea of the relation of stress to dimensions may be gained quickly by analyzing a number of cylindrical arches. The stresses derived from a series of such analyses for central angles ( $2\alpha$ ) varying from  $60^\circ$  to  $120^\circ$  are shown in Fig. 24.

For a given thickness, maximum stresses decrease as  $2\alpha$  increases.

Appreciable tensile stresses are shown for the smaller angles and in the thicker arches for all angles. Compressive stresses are excessive at the abutment intrados; also at the crown except for the thickest arches. The possibility of thickened haunches suggests itself.

(c) *First trial.* Study of Fig. 24 suggests the dimensions shown in Fig. 25 for a first trial. It will be assumed that physical restrictions (not given) limit the curvature to about that shown. The crown thickness of 35 ft is derived

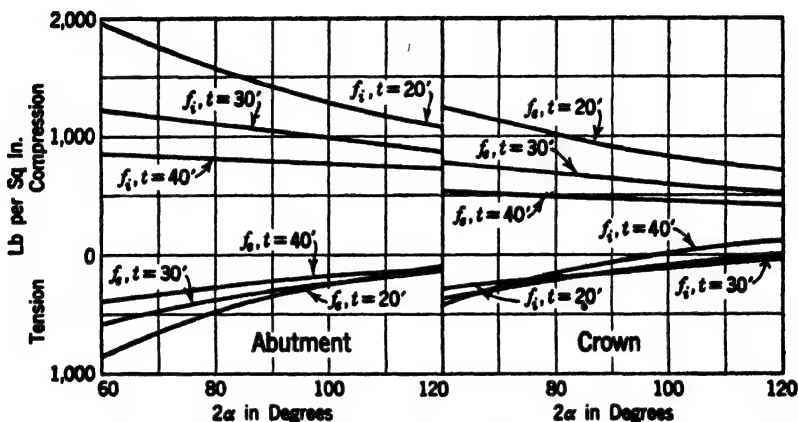


FIG. 24. Stresses in cylinder arches, conditions of Example 9.

from a study of Fig. 24. Flaring ends are relied upon to reduce abutment stresses.

The analysis is made by the procedure of Example 8. The resultant critical stresses in pounds per square inch are

$$\text{Crown, } f_e = +478, \quad f_i = -35$$

$$\text{Abutments, } f_e = -57, \quad f_i = +663$$

Although moderate tensile stresses are still found at both crown and abutment and the abutment compressive stress is somewhat above the specified value, the design is in better balance than any that could have been selected from Fig. 24, and in practice might be accepted.

(d) *Second trial.* The results of the first trial indicate a slightly thinner arch with increased abutment flare for a second trial, if avoidance of overhang and other limitations permit. If these expedients are not permissible, further thickening may be required. The possibility of using a three-centered arch should be considered. Successive trials should be made until the stresses come within the specified limits, or approach them as closely as is practicable.

(e) *Cracked arches.* Unless the temperature drop is small, and other conditions favorable, tension is difficult to eliminate in the thicker lower portions of an arch dam. Such dams are subject to cracking in the central portions and

near the abutments. This need not involve an element of danger if the uncracked portions of the structure are of adequate strength.

If the eccentricity of the reaction is appreciable, it may be desirable to investigate the extent of the cracking and its effect on actual stresses and deflections.

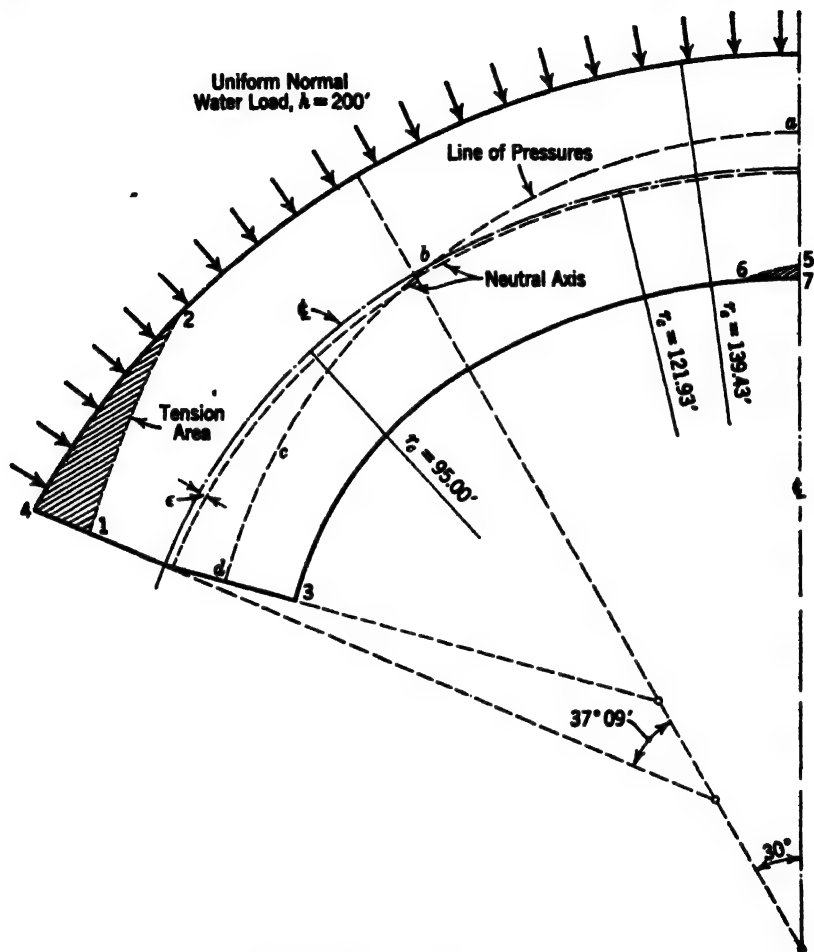


FIG. 25. Trial arch, Example 9.

An approximate investigation may be made by eliminating the tension areas and reanalyzing the arch.

The tension area may be found approximately by applying the middle third rule. The line of pressures (see Art. 14i) is platted as curve  $a-b-c-d$ , Fig. 25. If curve 1-2 is platted twice as far from  $b-c-d$  as  $b-c-d$  is from the intrados, the area 1-2-4 represents approximately the portion of the arch in tension near the abutment. The area 5-6-7 similarly represents the tension area at the crown.

If these areas are ignored, the computed flexibility of the arch is increased, which decreases the computed eccentricity of the line of pressures. This reduces the apparent tension area. Hence, as a first trial, the excluded area should be somewhat less than the estimated tension area. The percentage of reduction increases as the tension area increases.

(f) *Importance of cracking.* The influence of moderate cracking on compressive stresses usually is not important and it is generally permissible, so far as stresses are concerned, to ignore cracking. Cracking increases deformations and may be of importance in problems involving arch deflections. However, after careful investigation of many arch dam designs, Houk finds that the effect of cracking is of minor importance.<sup>21</sup> It is seldom, if ever, necessary to consider cracking in preliminary work. The cautious designer will wish to analyze at least a few cracked arches to ascertain the importance of cracking for his particular conditions.

(g) *Values of  $H_1$  for irregular arches or irregular loading.* Generally, in preceding articles of this chapter, values of  $H_1$  have been computed from Eq. 1. If the loading is irregular, or if the arch is irregular or cracked, some other method of estimating may be desirable. In discussing such methods it is necessary to remember that  $H_1$  is introduced to simplify the arithmetical work by keeping the computed moments due to "external" forces small. This avoids the necessity of carrying meaninglessly large numbers of digits. Whether  $H_1$  closely approximates the actual crown thrust is of secondary importance.

Consider the graphical arch analysis illustrated in Fig. 19. The value of  $H_1$  used in this figure was taken from Table 4 to maintain similarity between computed results for Examples 4 and 5. If computations for Example 4 had not been available, and particularly if either the arch or the loading in Example 5 had been irregular,  $H_1$  might have been determined thus:

Choose a position for  $O'$  (Fig. 19) at random and plot the load lines 0-9, 9-11, 11-13, etc. Extend a horizontal line from  $O'$  indefinitely to the right. Then, instead of drawing the "voussoir chord direction rays" 0-1, 0-2, etc., through a predetermined position of point 0, draw them from breaks in the load line, points 9, 11, 13, etc., using correct directions. There will result a multiplicity of intersections of these lines with the horizontal through  $O'$ . Choose a "round" value for  $H_1$  which when platted to the right of  $O'$  will cause 0 to fall about the middle of these intersections.

For arithmetical analysis, where the arch or loading is too irregular to permit the use of Eq. 1,  $H_1$  may be estimated as follows:

Upon reaching column 22, Table 4, or the corresponding point in any other type of analysis, make a preliminary run of columns 22 to 30 using zero or any other "guessed" value for  $H_1$ ; then find by graphics or otherwise a value of  $H_1$  which will reduce each item in column 30 to a reasonable value.

<sup>21</sup> IVAN E. HOUK, "Trial Load Analysis of Curved Concrete Dams," *The Engr.*, July 5 1935.

### THE TRIAL LOAD ANALYSIS OF ARCHED DAMS

**24. Outline of Trial Load Theory.** As pointed out previously, the cylinder theory may be used for the design of slender, simple arches, but it is a poor indication of stresses in thick arch dams, particularly where temperature variations and special loadings are involved. The elastic theory gives a better idea of actual stresses and permits allowance for temperature change, foundation yielding, earthquake forces, and irregular arch forms. This theory applies to separate arches, each acting independently of its neighbors. Actually, the flow of stress in an arch dam is complex, and adjacent arches restrain each other.

Just as there are simple cases for which the cylinder theory is adequate, there are others somewhat more complex for which it is adequate to design the arches as independent units. However, for structures of importance and for unusual profiles or conditions, a more complete knowledge of stress distribution is desirable.

An exact mathematical analysis is not practicable, but a method known as the "trial load method" gives a reasonably satisfactory approximation. The dam is assumed to be made up of two systems of elements—horizontal arches and vertical beams or cantilevers. Each system occupies the whole dam structure and the loading is assumed to be divided between them in such manner that the computed deflection for any point in the dam, considered as a point in the arch system, will be identical with its computed deflection, considered as a point in the cantilever system. The division of loading which will cause coincident deflections at all points is found by a succession of trials.

**25. Preparation of Preliminary Plan.** The trial load analysis is applied to a structure of predetermined dimensions; hence the first requisite is a preliminary plan. Such a plan may be based on judgment, comparison with a similar structure, the cylinder theory, or an elastic analysis. Errors in the trial design are revealed as the analysis proceeds.

**26. Horizontal Elements of Dam.** The dam structure is assumed divided by horizontal planes, a unit distance apart, into a continuous series of arches. Representative slices are selected for analysis.

**27. Vertical Elements.** The dam is likewise assumed to be divided into a continuous series of vertical elements, and representative units are chosen for analysis.

In a constant-radius dam, like that shown at *a*, Fig. 26, the upstream face may be considered as divided into unit chords as 1-2-3, etc., and vertical elements formed by passing vertical radial planes through these points. The units are simple with a constant trapezoidal cross-section at any given elevation. Unless the ratio of thickness to radius of curvature is small, the thinning of the cantilevers at the downstream face should be considered.

In a variable-radius dam, *vertical radial planes* are not possible, as the direction of the radius on a given vertical varies with elevation; hence some twisted cantilever form must be adopted which will permit the establishment of a set of

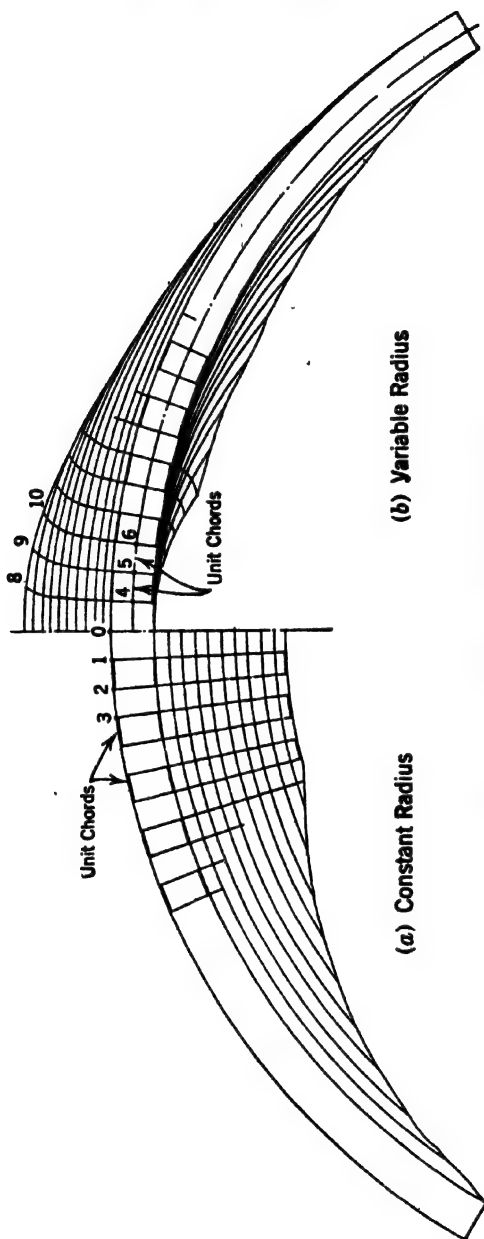


FIG. 26. Typical vertical elements, trial-load dams.



essentially similar or systematically changing units exactly filling the full volume of the dam. In one of many possible systems, the center line of the top arch, or any other selected axis, is divided into unit lengths, and warped radial planes are passed through vertical lines dropped from these divisions, as illustrated at *b*, Fig. 26. This system of division is more fully illustrated in Example 10.

**28. Interaction of Elements.** In Fig. 27, let 1-2-3-4 represent one of the arches to be investigated and let 5-6 represent one of the cantilevers, these two elements being assumed to intersect in a common prism *a-b*. Some portion of

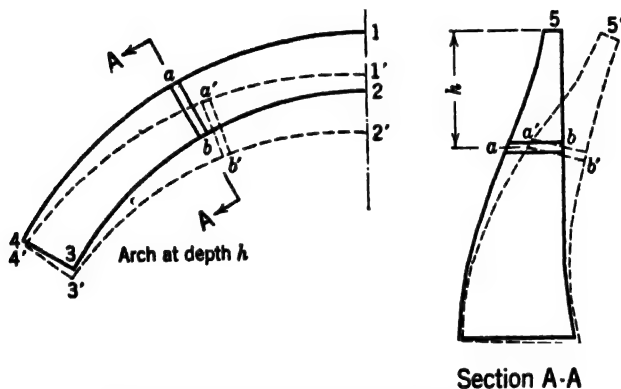


FIG. 27. Deflections of arches and cantilevers.

the load on the face of this prism will be borne by the arch, the remainder going to the cantilever. Similar load divisions occur at other points. The result is a reduced and variable load on the faces of both the arch and the cantilever.

The arch is deflected to some new position as 1'-2'-3'-4'. The intersecting prism is moved from *a-b* to *a'-b'*. This movement generally has radial, tangential, and angular components.

The new position of the prism of intersection in the deformed cantilever must coincide with its position in the deformed arch. Simple radial loads on the cantilever will not produce the required tangential and angular displacements. These movements are produced by forces internal to the dam as a whole but treated as external loads on individual arches and cantilevers. These forces are found by trial.

A system of lateral forces is applied to the cantilever to make lateral shear deflections at all elevations identical with corresponding tangential arch deflections. The tangential continuity of the structure prevents measurable lateral bending of cantilevers; hence only shear deflections need be considered. A system of tangential forces, equal and opposite to corresponding lateral forces on the cantilever, must be included in the loads used for computing arch deflections.

A system of twist loads (moments in horizontal planes) must be applied to the cantilevers to produce angular deflections identical with those for the arches. Equal and opposite moments must be included with the loads and forces used in computing the arch deflections.

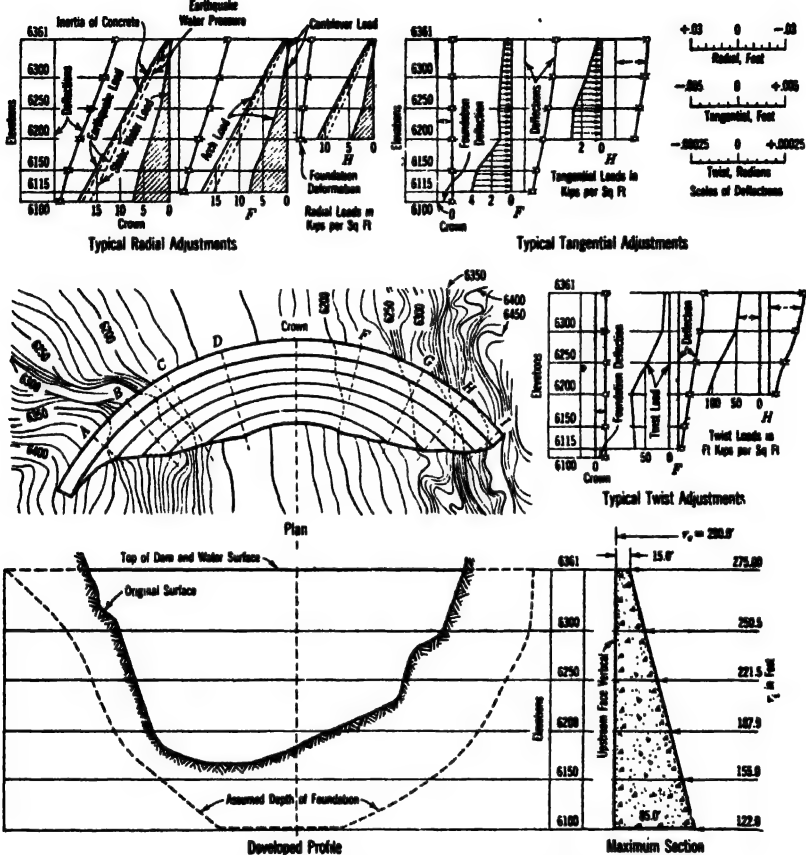


FIG. 28. Typical adjustments, Seminoe Dam.

The radial cantilever deflections have angular components in vertical planes. A system of twist loads (moments in vertical radial planes) must be applied to the arches to cause them to conform. Equal and opposite moments must be included with the loads used for computing the cantilever deflections.

It must not be concluded that these reactions give a complete picture of the internal forces in an arch dam. The actual situation is far more complex. However, experience indicates that a proper balancing of these elements gives results reasonably close to the truth. In simple structures, one or more of the enumerated influences may be negligible.

**29. Factors Influencing Division of Loads.** Not only the division of external loads between arch and cantilever but also all of the interactions discussed in Art. 28 must be determined by trial. The most important influences

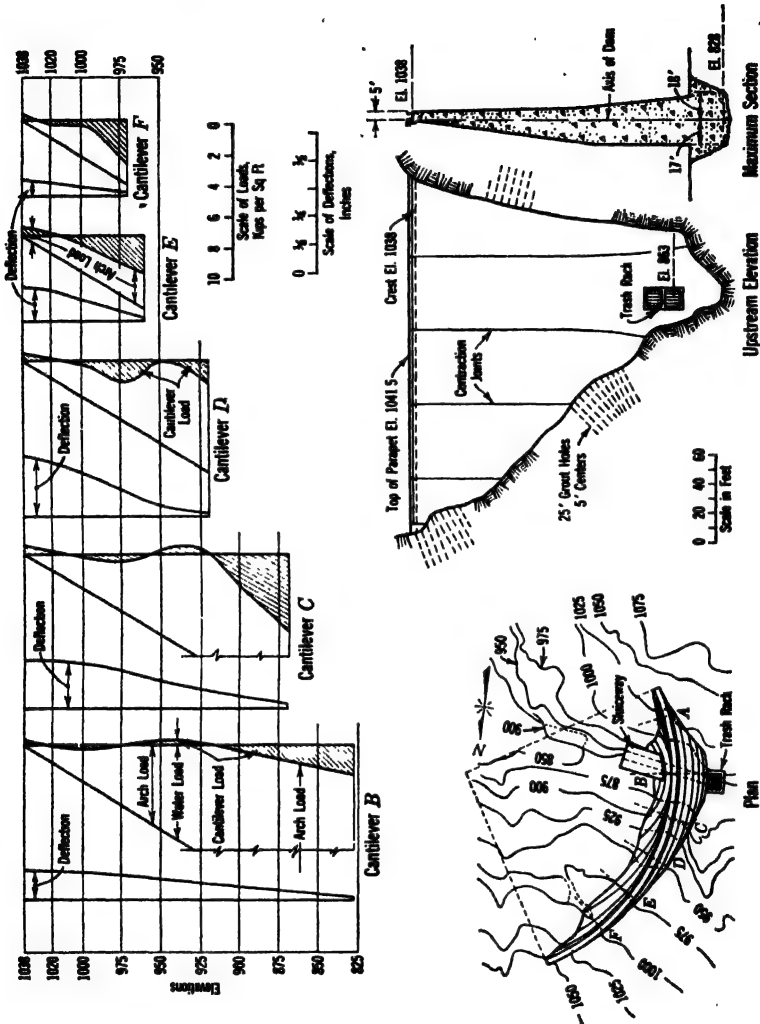


FIG. 29. Copper Basin Dam.

are radial loads and radial deflections. It is usual to bring these elements into at least approximate agreement before introducing tangential shear and twist.

The first trial division of external loads is made arbitrarily with only general experience on comparable dams as a guide. The division will vary from point to point. Frequently, one system carries a negative load, the other being subjected to more than the total local loading. This condition is usual at the

top of the dam where the freeboard arches are under stress from loads transferred to them by the vertical elements. Similar conditions may be found near irregularities in the foundation profile. The first trial division of loads is not likely to be accurate, but a skillful computer usually can arrive at a sufficiently close approximation with a moderate number of trials.

**30. Typical Load Division.** Typical load and deflection curves from the trial load analysis of a nearly symmetrical arch of simple cross-section are shown in Fig. 28. Radial, tangential, and twist data are shown for three out of nine analyzed cantilevers.<sup>22</sup> Earthquake forces resulting from the inertia of the concrete and increased water pressure are shown on the water pressure force diagram. In this chapter the whole earthquake load will be introduced separately.

Fig. 29 shows the division of radial load for a thin arch dam in an extremely unsymmetrical site.<sup>23</sup> The loads in the central portion of this dam and along the vertical left abutment go almost exclusively to the arches. The influence of irregularities in the right abutment on load distribution is evident. If stresses are critical, such irregularities may be removed during excavation.

The radial load pattern for the Ariel Dam,<sup>24</sup> which contains some interesting irregularities, is shown in Fig. 30.

#### NUMERICAL EXAMPLE OF TRIAL-LOAD ARCH DAM

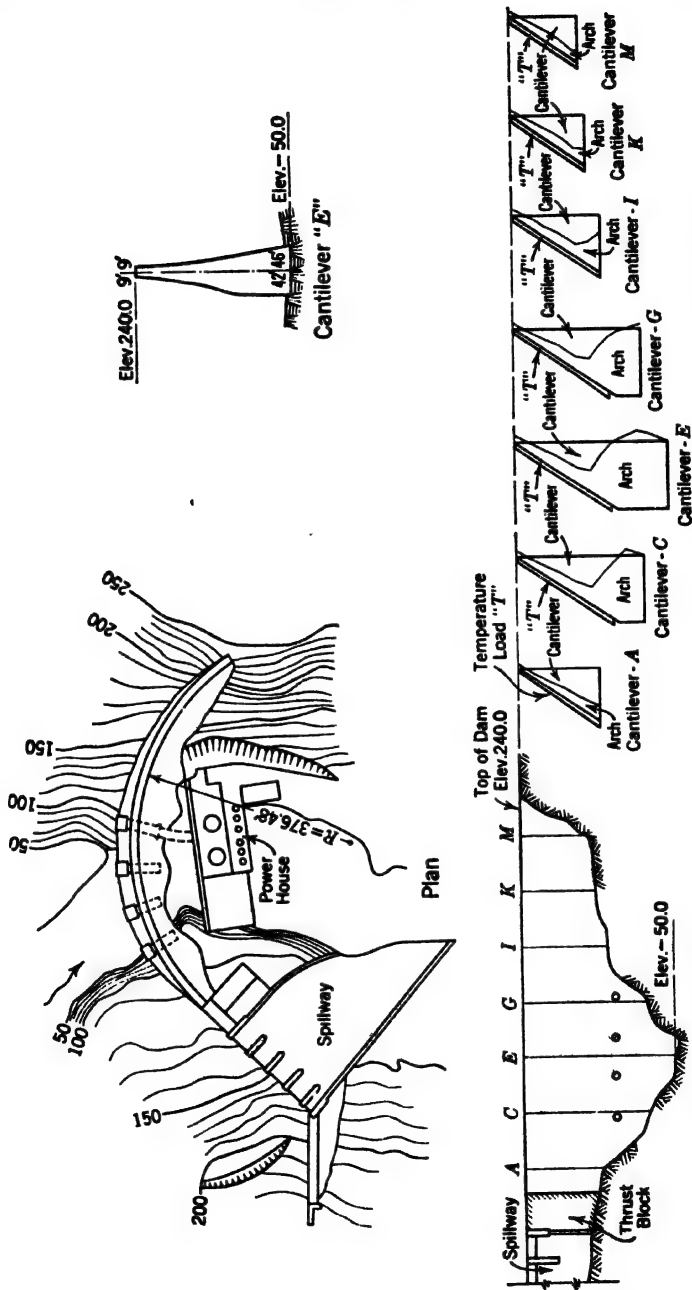
**31. Example 10, Data.** The presentation of a completely worked out example of a trial-load dam is impracticable. However, the procedure may be illustrated by beginning the design of a dam for the simple topographic conditions shown in Fig. 31. Design data are assumed as follows:

- Weight of concrete,  $w_1 = 150$  lb per cu ft,
- Joints in dam to be solidly grouted at mean annual temperature,
- Weight of water,  $w_2 = 62.5$  lb per cu ft,
- Earthquake acceleration  $= 0.1g$  (parallel to axis of symmetry),
- Temperature drop below mean,  $F = 340/(t + 8)$ ,
- Radial temperature drop,  $\Delta F = \text{ignore}$ ,
- Temperature coefficient,  $C_F = 0.000006$ ,
- Allowable tension  $= 0$ ,
- Allowable compression  $= 500$  lb per sq in.,
- Modulus of elasticity, dam  $= 3,000,000$  lb per sq in.,
- Modulus of elasticity, foundation  $= 4,000,000$  lb per sq in.,
- Shear modulus ratio,  $n = 2.80$  (may use  $n = 1.0$  for preliminary trials),
- Uplift, uncracked masonry,  $c = 1$ ,  $\zeta = 1$ ,
- Uplift, in cracks  $=$  full water pressure.

<sup>22</sup> IVAN E. HOUK, *Dams and Control Works*, U. S. Bur. Reclam., 1938, p. 235.

<sup>23</sup> *Copper Basin Dam*, The Metropolitan Water District of Southern California.

<sup>24</sup> From an unpublished report by Electric Bond and Share Co. Engineering Dept., Aug. 15, 1930. See also "Actual Deflections and Temperatures in a Trial-Load Arch Dam," *Trans. Am. Soc. Civil Engrs.*, Vol. 99, 1934, p. 897.



Load Distribution on Vertical Sections.

FIG. 30. Arch Dam.

The 500 lb per sq in. stress limit which is exceeded in many arch dams is chosen to yield relatively thick cantilevers which are desirable for illustrative purposes. The temperature stress is based on the assumption that the dam will be closed at the mean annual temperature. Many dams are now cooled

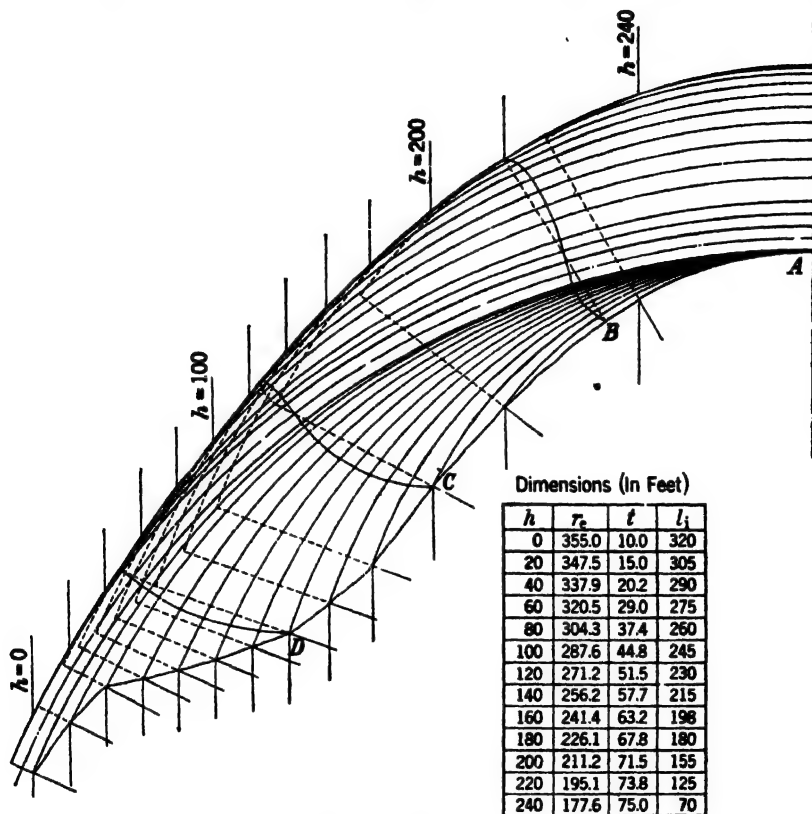


FIG. 31. Half plan of arch dam, Example 10.

below this mean before closing. Values of unity for  $c$  and  $\zeta$  are on the conservative side.

**32. Preliminary Dimensions.** Preliminary dimensions will be determined from the cylinder theory. Because actual stresses are appreciably greater than cylinder-theory stresses, the assumed trial cylinder stress must be less than the allowable compression. Assuming 300 lb per sq in., trial dimensions are as shown on Fig. 31. In thickness, this preliminary dam compares roughly with Ariel and Seminole Dams (see Art. 30). Many arch dams are thinner but most of them have local stresses above the 500 lb per sq in. limit here specified. The purpose of the analysis is to determine whether the trial dimensions are correct.

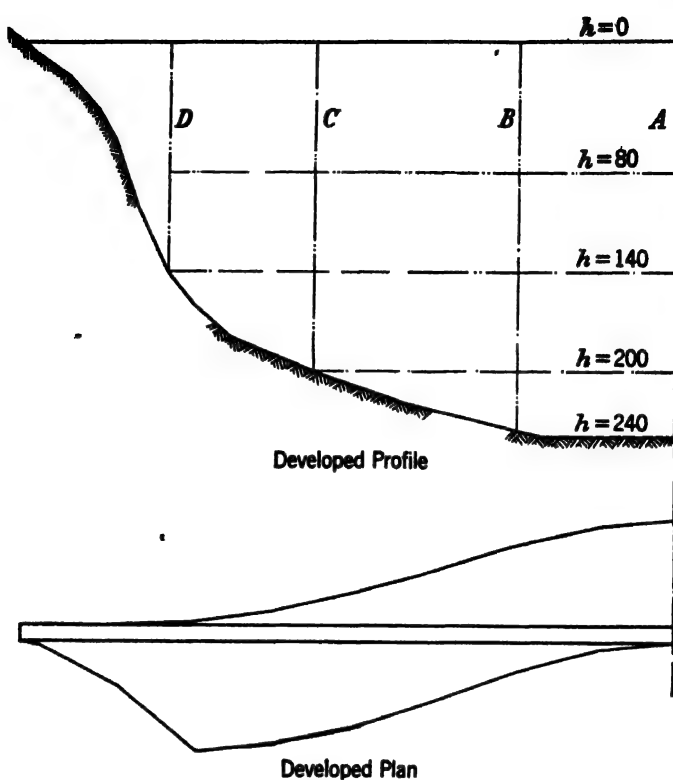


FIG. 32. Developed plan and elevation, Example 10.

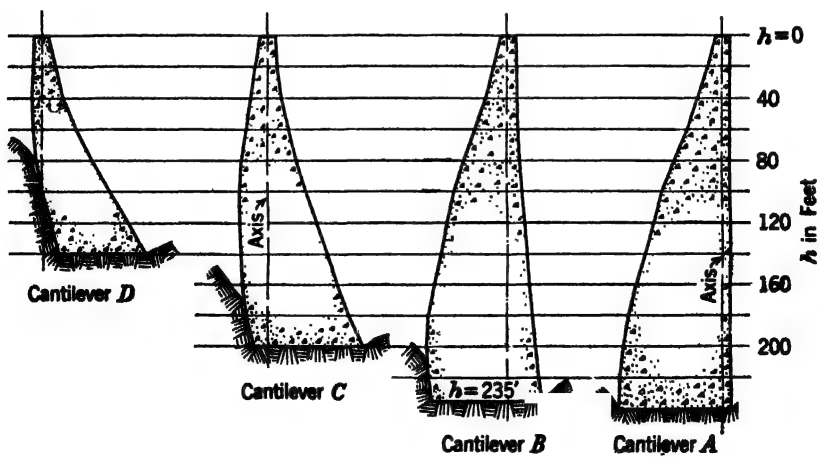


FIG. 33. Cantilevers, Example 10.

**33. Selection of Units for Analysis.** If the canyon cross-section is irregular (as Copper Basin and Ariel Dams, Art. 30), the cantilevers and arches to be analyzed are chosen to show the effect of the irregularities. In the present example, the choice may be made arbitrarily as shown on the developed half-elevation, Fig. 32. Arches are chosen at the top and at depths of 80, 140, and 200 ft below the top. Cantilevers are chosen at the axis of symmetry and at distances of 100, 226, and 325 ft along the center line of the top arch from the axis of symmetry. The cantilevers are designated as *A*, *B*, *C*, and *D*, respectively. The bases of *C* and *D* are purposely made coincident with the ends of the arches at  $h = 200$  and  $h = 140$ . These units represent the minimum permissible number. More are usually used, especially for irregular canyons. Cantilever forms are shown on Fig. 33. Arch dimensions may be taken from the table on Fig. 31.

**34. First Trial Division of Radial Loads.** Study of load divisions on previously designed dams is the best guide in the establishment of the first trial load. Inspection of the examples shown in Art. 30 (none of which, however, are closely similar to the present example) indicates that loads at the top of the cantilevers are likely to be negative.

The cantilevers are usually more sensitive to overload than the arches, hence are better criteria for preliminary study. Cracking usually occurs at the upstream side near the base and frequently at the downstream side near the top. Lacking a comparative design for a guide, the first trial load on the cantilevers in the central portion of the dam may be assumed to be of sufficient magnitude to cause slight cracking near the top and appreciable cracking near the bottom.

The central cantilever is frequently chosen for preliminary study, particularly in a constant-radius dam. However, any section in the central portion of the dam may be used. In the present case, cantilever *B* will be taken as a "pilot." The first trial load is shown in Fig. 34.

**35. Cantilever Analysis for Radial and Vertical Loads.** (a) *Dimensions.* The principles developed for the design of gravity dams are applicable to the radial load analysis of the cantilever but they require extension to provide for deflections and for the analysis of cracked sections. The analytical work is performed in Table 17.

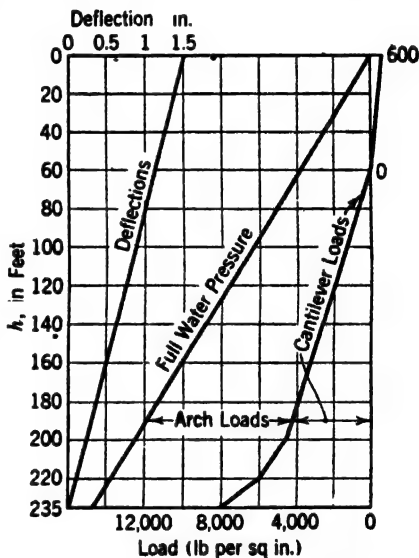


FIG. 34. First trial load, cantilever *B*, Example 10.







The cantilever is divided into blocks by joints at the depths shown in line 1 of the table. Water-pressure intensities  $w_2h$  are recorded in line 2. Values of  $t$ , line 3, and  $r_e$ , line 4, are taken from Fig. 31. Values of  $r_e$  and  $r_i$ , lines 5 and 6, are computed as shown. They are equal to the intrados and extrados radii only if the arch faces are concentric.

Values of  $a_c$ , line 7, and  $\Delta s$ , line 8, are determined graphically, as illustrated in Fig. 35. The axis 1-2 (not necessarily circular) is drawn to large scale. The top center of the cantilever whose dimensions are desired is marked as at  $B$ . A unit length laid off to exaggerated scale from 3 to 4, tangent to the axis at  $B$ , represents the thickness of the top cantilever section.

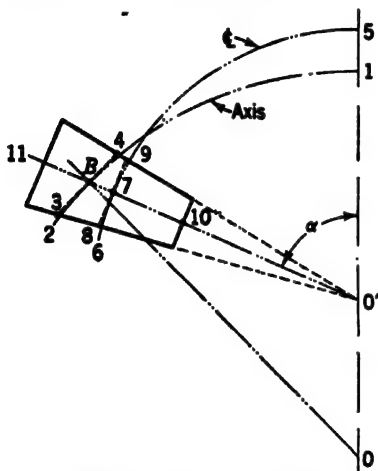


FIG. 35. Elemental voussoir.

Values of  $\Delta s$ , cantilever widths at the upstream face, are computed as indicated in line 9, or scaled from Fig. 35.

Values of  $t/r_e$ , required in subsequent computations, are recorded in line 10.

The distance from the center of the trapezoid to its center of gravity, line 11, is computed from the equation

$$e_1 = \frac{t^2}{12r_e} \quad [87]$$

It is convenient to plot values of  $e_1$  on profiles of the cantilever similar to those shown in Fig. 33 but to large scale. A distorted scale is usually convenient. Fig. 36 represents cantilever  $B$  of Example 10, with the horizontal scale doubled.

The line of centers is drawn by plating values in line 7, Table 17, from the axis.

Distances from axis to the center of gravity,  $a_g$ , line 12, are found by adding values from lines 7 and 11. Their successive differences recorded as  $\Delta a_g$  in line 13 represent horizontal projections of the center of gravity line (see Fig.

37). Values of  $a'_g$ , line 14, represent horizontal distances from the centers of gravity of blocks (located graphically) to the center of gravity of the base (see Fig. 37). Because they pertain to the blocks rather than to the joints, the values in lines 13 and 14 are set in an intermediate position.

Upstream and downstream kern distances are computed and recorded as  $k_e$  and  $k_i$ , respectively, lines 15 and 16.<sup>25</sup> These values may be plotted on Fig. 36

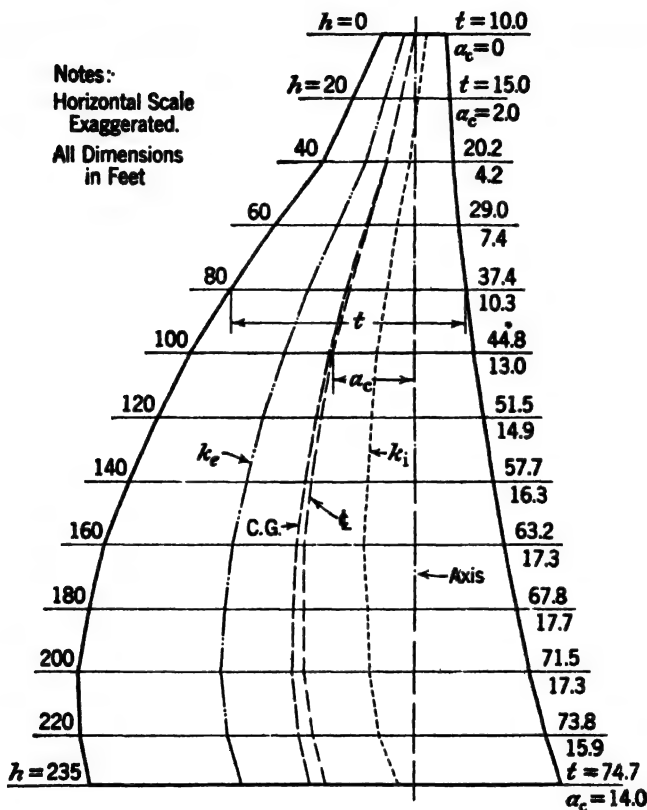


FIG. 36. Dimensions of cantilever B, Example 10.

to show the limits within which the resultant must fall for no tension or cracking. The kern distances are reexpressed as distances from the centers of gravity in lines 17 and 18.

(b) *Deflections, reservoir empty.* Final deflections are the result of combined dead and live loads. However, the cantilevers take their dead loads as soon as completed and if the vertical contraction joints are grouted solid after the dam has hardened and cooled to the mean annual temperature, and before

<sup>25</sup>  $k_e$  and  $k_i$  mark the boundaries of the kern within which the resultant must fall if there is to be no tension. Methods of computing are indicated in lines 15 and 16, Table 17.

water load is imposed, dead load deflection in the cantilevers and the no-stress condition in the arches occur simultaneously. Hence, in making trial load comparisons, only the net live load deflections for the cantilevers are considered. Because masonry is assumed to take no tension, it is not possible merely to ignore the dead loads. Deflections for both empty and full reservoir must be computed and differences taken.

Line 19 contains areas at successive joints and line 20 contains weights of blocks computed from average end areas. The prismoidal formulas may be used for extreme cases. Values of  $W_1$  in line 21, obtained by summation of the block weights in line 20, represent total weights on the respective joints.

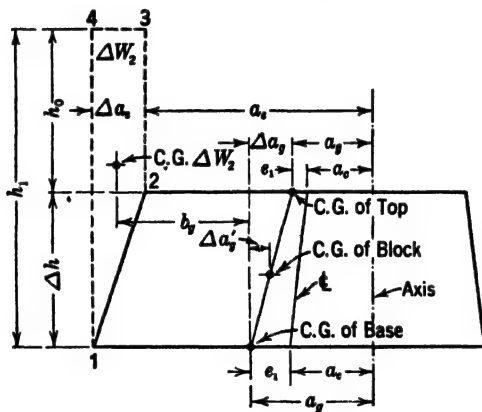


FIG. 37. Cantilever block dimensions.

Lines 22 and 23 contain partial moment increments which are summated simultaneously to give the moments  $M_1$  in line 24. These moments are about the centers of gravity of the sections. To avoid confusion between negative loads and negative moments, clockwise moments are considered positive. This convention is opposite to that used for arches (see Art. 14e).

Line 25 contains values of  $1/I$ ,  $I$  being the moment of inertia for the trapezoidal sections, computed from the equation shown. The parenthetical term of this equation is taken as unity in this example.

Products of lines 24 and 25, recorded in line 26 as  $\partial\phi_1$ , represent angular deflections per unit of vertical height, at the joints. These values are subsequently subtracted from similar values for the reservoir full to give the net effect of live load. It is not necessary to compute the actual deflections for reservoir empty.

(c) *Vertical water loads.* Each block of the cantilever is subjected to a vertical load  $\Delta W_2$  equal to the weight of the water in the prism 1-2-3-4, Fig. 37. This prism has a width  $\Delta a$ , (line 27) obtained by scaling, and a thickness  $\Delta s$ , (line 9) which is usually variable and may be averaged. Vertical loads per block  $\Delta W_2$  computed as indicated in line 28 are summated in line 29 to give

accumulated vertical water load. Note that  $\Delta a_2$  and  $\Delta W_2$  are negative at the bottom of cantilever *B* because of a slight overhang.

The center of gravity of 1-2-3-4, Fig. 37, is found graphically, and its horizontal distance from the center of gravity of the base of the block is scaled and recorded in line 30 as  $b_1$ . Partial moment increments are computed as indicated in lines 31 and 32 and simultaneously summated to give total values of  $M_2$  in line 33. These moments are about the centers of gravity of the bases of the blocks.

Vertical loads in lines 21 and 29 are added to give total vertical loads, exclusive of uplift  $W_0$ , line 34.

(d) *Normal uplift.* Where the resultant falls within the kern, uplift forces are computed by the rules established for gravity dams, Art. 5, Chapter 7. Under the stated assumptions and allowing for the trapezoidal shape of the cross-section, the equation for uplift in the unbroken cantilever is

$$W_u = \frac{1}{12} w_2 h \Delta st \left( 6 + \frac{t}{r_c} \right) \quad [88]$$

Values of  $W_u$  are recorded in line 35. The concentrated resultant of normal uplift acts at the upstream kern limit, i.e., at a distance  $k_u$  from the face, or  $e_u$  from the center of gravity of the base. Values in line 35 multiplied by  $e_u$ , line 17, give uplift moments about the center of gravity of the base, recorded as  $M_u$  in line 36. Net vertical loads for the unbroken cantilevers  $W_n$ , line 37, are found by subtracting  $W_u$  from  $W_0$ .

(e) *Horizontal loads.* Horizontal load intensities at each cantilever joint, determined from Fig. 34 and recorded in line 38, are multiplied by  $\Delta s_e$  (line 9) to give corresponding loads per unit of height  $p$  line 39. The total horizontal force against the face of a given block may be represented by the trapezoid 1-2-3-4, Fig. 38, which may be divided into the rectangle 1-2-3-5 and the triangle 1-5-4. The base of the triangle 4-5 is equal to  $\Delta p$ , line 40.

The rectangular and triangular load increments are computed and recorded in lines 41 and 42. The rectangular load is equal to  $\Delta h$  times  $p$  for the top or bottom of the block, whichever is smaller. Corresponding items of lines 41 and 42 are added in line 43 to give total shear increments. These values are summated vectorially<sup>26</sup> from crest to base to secure total shears at successive joints. The procedure is illustrated in Fig. 39. Beginning at point 0, the values in line 43 are platted successively, each in the direction of the radius at the mid-height of its block, to form the force line 0-20-40, etc., the numbers representing values of  $h$ . At  $h = 160$ , for example, the accumulated force is represented by a line 0-160, which may be resolved into components 0- $a$  and

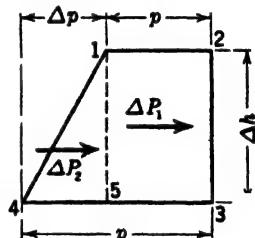


FIG. 38. Horizontal loads on cantilever block *B*, Example 10.

<sup>26</sup> For preliminary work, numerical summation is permissible, ignoring differences in direction.

$\alpha=160$ , respectively parallel and normal to the radius at  $h = 160$ . Accumulated forces at other depths are similarly resolved and radial components are scaled and recorded in line 44. The tangential components are used subsequently in the arch computations.

Moment increments for  $\Delta P_1$  and  $\Delta P_2$  are computed in lines 45 and 46, and those for "previous shear" in line 47. The lever arm of the triangular load is  $\frac{1}{3}\Delta h$  or  $\frac{2}{3}\Delta h$ , according to the position of its vertex. The values of  $P$  used in line 47 are those for the tops of the respective blocks. Corresponding values in lines 45, 46, and 47 are added in line 48 to give total moment increments

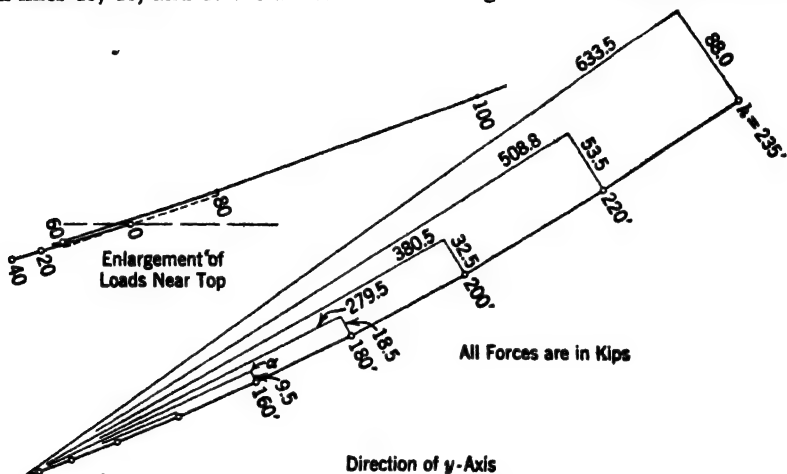


FIG. 39. Summation of horizontal loads, cantilever B, Example 10.

$\Delta M_3$ . These increments are added vectorially<sup>27</sup> and resolved into radial and tangential components, following the procedure of Fig. 39. The radial components are recorded as  $M_3$ , line 49. The tangential components are ignored, as lateral flexure is not considered. The twisting resistances of the arch slices to angular cantilever deflection  $M$  are recorded in line 50. This function is derived from cantilever computations not yet made; hence this line is blank in Table 17. Its computation for insertion in subsequent trials is discussed in Art. 40b.

(f) *Locating the resultant.* Moments without uplift and with normal uplift are assembled in lines 51 and 52. The distance  $e_r$  from the center of gravity to the resultant with normal uplift is  $M_n + W_n$ , line 53. At depths of 140 and below,  $e_r$  exceeds  $e_k$ , line 18; hence the resultant is outside the kern on the downstream side.

(g) *Broken cantilevers.* On the assumption that the masonry can take no tension, cracking will occur where the resultant is outside the kern. The cantilever is then assumed to stand on its unbroken portion. Cracking changes both uplift and uplift moment. Also, the center of gravity of the effective base is moved, which changes  $M_1$  and  $M_2$  (lines 24 and 33).

<sup>27</sup> Numerical summation ignoring direction is usually permissible.

The stated assumption that uplift in a crack equals full water pressure at the entrance to the crack results in the uplift patterns shown at *a* and *b*, Fig. 40, assuming no tailwater. To permit the determination of the unbroken thickness  $t'$  it is necessary to locate the resultant of the final vertical foundation reaction.

For a broken intrados, *a*, Fig. 40, the foundation reaction 2-3-4 and the uplift 1-2-4 have the same center of reaction, which is identical in position with

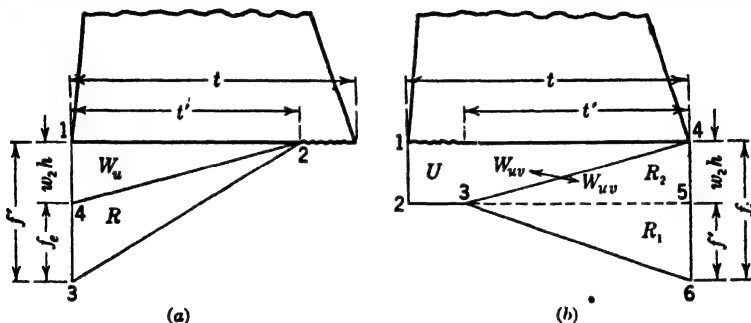


FIG. 40. Cracked cantilever reactions.

the reaction for zero uplift. Hence, the distance from the original center of gravity to the center of reaction for the cracked cantilever is

$$e'_r = \frac{M_0}{W_0} \text{ (broken intrados)} \quad [89]$$

The computed values, if any, are recorded in line 56 for values of  $h$  which show cracking on the downstream face, i.e., where  $e_r$ , line 53, is upstream and is greater than  $e_r$ , line 17. There are no such points in Table 17.

For a cracked extrados, the uplift 1-2-3-4 and the foundation reaction 3-4-6 are both of unknown position and magnitude. It is convenient to divide the reaction into two parts,  $R_1$  and  $R_2$ , and to add the part  $R_2$  to the uplift. The combination 1-2-5-4, called the virtual uplift, is of the magnitude

$$W_{uv} = w_2 h t \Delta s \quad [90]$$

where  $t$  and  $\Delta s$  are for the unbroken section. Values of  $W_{uv}$  are listed in line 54. The center of application is at the center of gravity of the original section; hence the moment remains  $M_0$ . The residual reaction, line 55, is

$$R_1 = W_0 - W_{uv} \quad [91]$$

The distance from the original center of gravity to the center of this reaction is

$$e'_r = \frac{M_0}{R_1} \text{ (broken extrados)}$$

The computed values are listed in the right-hand portion of line 56.

Distances from original centers of gravity to unbroken faces are recorded in line 57. Differences between corresponding items of lines 56 and 57 represent



distances from centers of reaction to unbroken faces,  $b_r$ , line 58. These values represent kern distances for the unbroken portions of the broken sections and may be used for determining the unknown values of  $t'$ , thus:

$$t' = b_r \left( \frac{3r_s - t'}{r_s - 0.5t'} \right) \text{ (broken intrados)} \quad [92]$$

and

$$t' = b_r \left( \frac{3r_i + t'}{r_i + 0.5t'} \right) \text{ (broken extrados)} \quad [93]$$

Tables 18 and 19 facilitate the solution of these equations. Entering these tables with  $b_r/r_s$ , or  $b_r/r_i$ , from line 59, values of  $t'/b_r$  are read and recorded in line 60. Values of  $t'$  are then computed as in line 61.

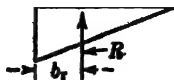
TABLE 18  
VALUES OF  $t'/b_r$  FOR GIVEN VALUES OF  $b_r/r_s$  FOR COMPUTING  $t'$  FOR  
CANTILEVERS BROKEN ON DOWNSTREAM FACE

$b_r/r_s$	0.000	0.001	0.002	0.003	0.004	0.005	0.006	0.007	0.008	0.009
0.00	3.0000	3.0015	3.0030	3.0045	3.0060	3.0076	3.0091	3.0106	3.0122	3.0137
.01	.0153	.0169	.0184	.0200	.0216	.0232	.0248	.0264	.0280	.0296
.02	.0312	.0328	.0344	.0361	.0377	.0394	.0411	.0428	.0444	.0461
.03	.0479	.0496	.0513	.0530	.0548	.0565	.0582	.0600	.0618	.0636
.04	.0653	.0671	.0689	.0708	.0726	.0744	.0762	.0781	.0799	.0818
.05	3.0836	3.0855	3.0874	3.0893	3.0912	3.0931	3.0950	3.0969	3.0988	3.1008
.06	.1027	.1047	.1067	.1086	.1106	.1126	.1146	.1166	.1186	.1207
.07	.1227	.1248	.1268	.1289	.1310	.1331	.1352	.1373	.1394	.1416
.08	.1438	.1459	.1481	.1503	.1526	.1548	.1570	.1593	.1616	.1639
.09	.1662	.1685	.1708	.1731	.1755	.1778	.1802	.1826	.1850	.1874
.10	3.1898	3.1923	3.1947	3.1972	3.1997	3.2022	3.2047	3.2072	3.2097	3.2122
.11	.2148	.2174	.2200	.2226	.2252	.2278	.2305	.2332	.2359	.2386
.12	.2414	.2442	.2469	.2497	.2526	.2554	.2583	.2611	.2640	.2670
.13	.2699	.2729	.2758	.2788	.2819	.2849	.2880	.2910	.2941	.2973
.14	.3004	.3036	.3068	.3100	.3132	.3165	.3198	.3232	.3265	.3299
.15	3.3333	3.3367	3.3402	3.3437	3.3472	3.3507	3.3543	3.3579	3.3616	3.3652
.16	.3689	.3726	.3764	.3802	.3840	.3879	.3918	.3957	.3997	.4037
.17	.4077	.4118	.4159	.4201	.4243	.4286	.4329	.4372	.4416	.4460
.18	.4504	.4549	.4594	.4640	.4686	.4733	.4781	.4829	.4877	.4926
.19	.4976	.5026	.5077	.5128	.5180	.5233	.5286	.5340	.5394	.5449
.20	3.5505	3.5561	3.5618	3.5676	3.5735	3.5795	3.5856	3.5917	3.5979	3.6042
.21	.6106	.6171	.6237	.6303	.6371	.6440	.6510	.6581	.6653	.6726
.22	.6801	.6877	.6954	.7032	.7112	.7194	.7277	.7362	.7448	.7536
.23	.7626	.7719	.7814	.7910	.8009	.8110	.8213	.8319	.8427	.8537
.24	.8649	.8764	.8881	.9001	.9124	.9251	.9382	.9520	.9666	.9824

$$\frac{t}{b_r} = \frac{r_s - t'}{r_s - 0.5t'}$$

$t$  = thickness,  $b_r$  = kern or reaction distance,  $r_s$  = upstream radius.

Left column computed; others interpolated.



$r_s$

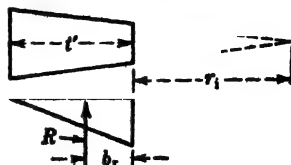
TABLE 19

VALUES OF  $t'/b_r$  FOR GIVEN VALUES OF  $b_r/r_1$  FOR COMPUTING  $t'$  FOR  
CANTILEVERS BROKEN ON UPSTREAM FACE

$b_r/r_1$	0.000	0.001	0.002	0.003	0.004	0.005	0.006	0.007	0.008	0.009
0.00	3.0000	2.9985	2.9970	2.9955	2.9940	2.9925	2.9911	2.9896	2.9881	2.9866
.01	2.9852	.9838	.9823	.9809	.9795	.9781	.9767	.9753	.9739	.9725
.02	.9711	.9697	.9684	.9670	.9656	.9643	.9629	.9615	.9602	.9588
.03	.9575	.9562	.9548	.9535	.9522	.9509	.9496	.9483	.9470	.9457
.04	.9444	.9431	.9418	.9406	.9393	.9380	.9368	.9355	.9342	.9330
.05	2.9317	2.9305	2.9292	2.9280	2.9268	2.9255	2.9243	2.9231	2.9219	2.9207
.06	.9195	.9183	.9171	.9159	.9147	.9135	.9123	.9111	.9099	.9088
.07	.9076	.9064	.9053	.9041	.9030	.9018	.9007	.8996	.8984	.8973
.08	.8962	.8951	.8940	.8928	.8917	.8906	.8895	.8884	.8873	.8862
.09	.8851	.8840	.8829	.8818	.8807	.8796	.8786	.8775	.8764	.8754
.10	2.8743	2.8732	2.8722	2.8711	2.8701	2.8690	2.8680	2.8670	2.8660	2.8649
.11	.8639	.8629	.8619	.8608	.8598	.8588	.8578	.8568	.8558	.8548
.12	.8538	.8528	.8518	.8508	.8498	.8488	.8479	.8469	.8459	.8450
.13	.8440	.8430	.8421	.8411	.8401	.8392	.8382	.8372	.8363	.8354
.14	.8344	.8335	.8325	.8316	.8306	.8297	.8288	.8279	.8269	.8260
.15	2.8251	2.8242	2.8233	2.8224	2.8215	2.8206	2.8197	2.8188	2.8179	2.8170
.16	.8161	.8152	.8143	.8134	.8125	.8117	.8108	.8099	.8090	.8082
.17	.8073	.8064	.8055	.8047	.8039	.8030	.8022	.8013	.8005	.7996
.18	.7988	.7980	.7971	.7963	.7954	.7946	.7938	.7930	.7921	.7913
.19	.7905	.7897	.7889	.7880	.7872	.7864	.7856	.7848	.7839	.7831
.20	2.7823	2.7815	2.7807	2.7799	2.7791	2.7783	2.7775	2.7767	2.7760	2.7752
.21	.7744	.7736	.7728	.7721	.7713	.7705	.7698	.7690	.7682	.7674
.22	.7667	.7659	.7652	.7644	.7637	.7629	.7621	.7614	.7606	.7599
.23	.7591	.7584	.7576	.7568	.7561	.7554	.7546	.7539	.7532	.7524
.24	.7517	.7510	.7502	.7495	.7488	.7481	.7474	.7466	.7459	.7452
.25	2.7445	2.7438	2.7431	2.7424	2.7417	2.7410	2.7403	2.7396	2.7389	2.7382
.26	.7375	.7368	.7361	.7354	.7347	.7340	.7334	.7327	.7320	.7313
.27	.7306	.7299	.7292	.7286	.7279	.7272	.7266	.7259	.7252	.7246
.28	.7239	.7232	.7226	.7219	.7213	.7206	.7199	.7193	.7186	.7180
.29	.7173	.7166	.7160	.7154	.7147	.7141	.7134	.7128	.7122	.7115
.30	2.7109	2.7103	2.7096	2.7090	2.7084	2.7078	2.7071	2.7065	2.7059	2.7053
.31	.7046	.7040	.7033	.7027	.7021	.7015	.7008	.7002	.6996	.6990
.32	.6984	.6978	.6972	.6966	.6960	.6954	.6948	.6942	.6936	.6930
.33	.6924	.6918	.6912	.6906	.6900	.6894	.6889	.6883	.6877	.6871
.34	.6865	.6859	.6853	.6848	.6842	.6836	.6830	.6824	.6819	.6813
.35	2.6807	2.6801	2.6796	2.6790	2.6784	2.6778	2.6773	2.6767	2.6761	2.6756
.36	.6750	.6744	.6739	.6733	.6728	.6722	.6716	.6711	.6705	.6700
.37	.6694	.6688	.6683	.6678	.6672	.6666	.6661	.6656	.6650	.6644
.38	.6639	.6634	.6628	.6623	.6618	.6612	.6607	.6602	.6597	.6591
.39	.6586	.6581	.6575	.6570	.6565	.6560	.6554	.6549	.6544	.6538
.40	2.6533	2.6528	2.6523	2.6518	2.6513	2.6508	2.6502	2.6497	2.6492	2.6487
.41	.6482	.6477	.6472	.6467	.6462	.6456	.6451	.6446	.6441	.6436
.42	.6431	.6426	.6421	.6416	.6411	.6406	.6401	.6396	.6391	.6386
.43	.6381	.6376	.6371	.6366	.6361	.6356	.6352	.6347	.6342	.6337
.44	.6332	.6327	.6322	.6318	.6313	.6308	.6303	.6298	.6294	.6289
.45	2.6284	2.6279	2.6275	2.6270	2.6265	2.6260	2.6256	2.6251	2.6246	2.6242
.46	.6237	.6232	.6228	.6223	.6218	.6214	.6209	.6204	.6199	.6195
.47	.6190	.6185	.6181	.6176	.6172	.6167	.6162	.6158	.6153	.6149
.48	.6144	.6140	.6135	.6130	.6126	.6122	.6117	.6112	.6108	.6104
.49	.6099	.6095	.6090	.6086	.6081	.6077	.6073	.6068	.6064	.6060
.50	.6055	.6051	.6046	.6042	.6038	.6034	.6029	.6025	.6021	.6016

$$\frac{t}{b_r} = \frac{2r_1 + t'}{r_1 + 0.5t'}$$

$t$  = thickness,  $b_r$  = kern or reaction distance,  $r_1$  = down-stream radius.



Values of  $r_o - 0.5t$  or  $r_i + 0.5t'$ , recorded in line 62, are for finding  $\Delta s'$ , line 63, the thickness of the cantilever at the middle of  $t'$ .

Values of  $f'$ , line 64, having the significance indicated in Fig. 40, are computed from the appropriate one of the following equations:

$$f' = \frac{6W_0 b_r}{\Delta s'(t')^2} \text{ (broken intrados)} \quad [94]$$

$$f' = \frac{6R_1 b_r}{\Delta s'(t')^2} \text{ (broken extrados)} \quad [95]$$

Values of  $f_o$  and  $f_i$ , line 65, representing net unit vertical reactions at the unbroken faces, are found by subtracting or adding  $w_2 h$ .

Unit angular deflections for the broken cantilevers, line 66, are found from the equations

$$\partial\phi_2 = \frac{f_o}{Et'} \text{ (broken intrados)} \quad [96]$$

or

$$\partial\phi_2 = \frac{f_i}{Et'} \text{ (broken extrados)} \quad [97]$$

The modulus of elasticity  $E$  is eliminated to conform to other parts of the computation (see Art. 12). For unbroken sections,  $\partial\phi_2$  is computed by multiplying the moment from line 52 by  $1/I$  for the original section, line 25.

(h) *Combined deflections.* The net unit angular deflections due to water load only are equal to  $\partial\phi_2 - \partial\phi_1$ , or the algebraic *differences* of corresponding items of lines 66 and 26. These differences, recorded in line 67, are averaged and multiplied by  $\Delta h$  to give  $\Delta\phi$ , the angular deflection increment per block, line 68. The right-hand term in this line and also the last terms in line 72 represent foundation deformation, computed in accordance with Art. 35i.

Values in line 68 are summated from abutment to crest to give accumulated angular deflections at the crown, line 69. Strictly, the summation should be made vectorially, following the procedure of Fig. 39 (but in reverse direction). However, because tangential components are not required, numerical summation usually is permissible.

Unit horizontal shears are computed in line 70. The values shown for the cracked portions of the cantilever are based on  $t'$ , the net unbroken thickness. The correctness of this procedure has not been demonstrated. The cracked portion of the section probably does not retain its full shear strength but no doubt contributes something. However, no reliable rule for a compromise shear thickness has been proposed. The designer may use either  $t$  or  $t'$ , which ever gives the least favorable result for the dam as a whole.<sup>22</sup>

Values of  $\phi$ , line 69, are averaged and multiplied by  $\Delta h$  to give the horizontal deflection increment caused by moment  $\Delta n_1$ , line 71. Unit shears are multi-

<sup>22</sup> Comments in this paragraph apply to tangential and twist deformations, to be discussed later.

plied by  $\Delta h$  times the shear factor  $n$  to give the shear deflection increments  $\Delta n_2$ , line 72. Values in lines 71 and 72 are added to give the total deflection increments  $\Delta n$ , line 73.

These values are summated vectorially in Fig. 41, each being platted in the direction of the arch radius at the mid-height of its block. Radial and tangential components of the deflection are scaled at intersections with the arches to be analyzed, or at other points where deflections are desired.

(i) *Foundation deformations.* As previously stated, the last values in lines 68 and 72 represent foundation deformations computed from Eqs. 51 and 53 or their simplifications, Eqs. 54 and 56. Because the vertical construction joints,

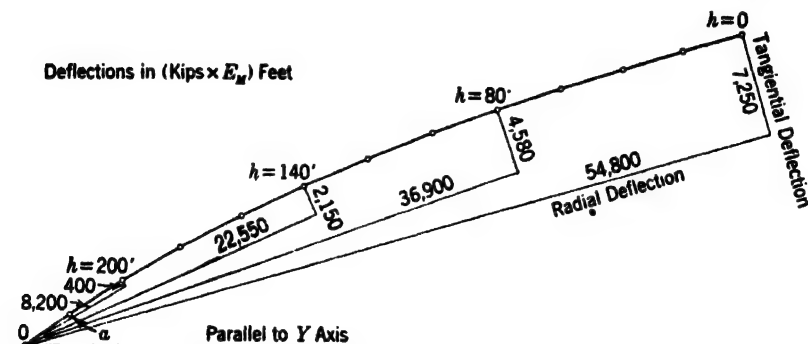


FIG. 41. Deflections, cantilever B, Example 10.

before grouting, are assumed to permit unrestrained vertical settlement, Eq. 55 is not used. For the cantilever,  $\psi$  is the angle between the plane of the cantilever and the abutment face, the complement of that used for an arch having the same abutment.

Computations for  $(E)$ ,  $(F)$ , and  $(H)$  follow the form of Table 5. Values of  $(E)$  and  $(F)$  must be computed for both  $t$  and  $t'$ .

The computed values are as follows:

Reservoir empty,  $t = 74.7$  ft,

$(E) = 0.000692$ ,  $(F) = 0.00538$ ,  $(H) = 1.62$ ;

Reservoir full,  $t' = 18.12$  ft,

$(E) = 0.0118$ ,  $(F) = 0.0222$ ,  $(H) = 1.62$ .

The foundation moment about the center of gravity of the cracked cantilever does not appear in Table 17 but may be computed from the equation

$$M_a = \frac{1}{12} f_i (t')^2 \left[ 1 - \frac{1}{12} \left( \frac{t'}{r_c} \right)^2 \right] \Delta s' \quad [98]$$

The bracketed term may be taken as unity except for large values of  $t'/r_c$ . In the present example the moment is approximately

$$M_a = \frac{1}{12} \times 137.44 \times (18.12)^2 \times 0.86 = 3230 \text{ ft-kips}$$

The shear is equal to the last value in line 44, Table 17, being 633.5 kips for Example 10.

Actual foundation deformations are computed as illustrated in Table 20. Items 1 and 2 are the angular deflection terms of Eq. 54 for reservoir full, item 3 being their total. In item 4 is the  $M(E)$  term in the same equation for reservoir empty. The  $S(F)$  term does not appear for the reservoir empty, as the shear is zero. The difference between items 3 and 4 gives the net angular foundation movement caused by cantilever loads.

TABLE 20  
FOUNDATION DEFORMATIONS, CANTILEVER B

1	$M(E)$ , reservoir full	= 3230(0.0118)	38.11
2	$S(F)$ , " "	= 633.5(0.0222)	14.06
3	Subtotal		52.17
4	$M(E)$ , reservoir empty	= 1623(0.000692)	1.12
5	Difference = $\partial_\alpha \alpha$ (Eq. 54)		51.05
6	From arch, $ \partial_\alpha \alpha$ , Arts. 38j and 38l		
7	Total, enter line 68, Table 17		51.05
8	$M(F)$ , reservoir full	= 3230(0.0222)	72
9	$S(H)$ , " "	= 633.5(1.62)	1026
10	Subtotal		1098
11	$M(F)$ , reservoir empty	= 1623(0.00538)	9
12	Difference = $\partial_\alpha n$ (Eq. 56)		1089
13	From arch, $ \partial_\alpha n$ , Arts. 38j and 38l		
14	Total, enter line 72, Table 17		1089

Angular cantilever deflection caused by the arch load, line 6, depends on arch computations not yet made, hence is temporarily omitted (see Art. 38l). The total, line 7, is entered as the right-hand value in line 68, Table 17.

The horizontal radial deflection based on Eqs. 56 and 56a is computed in a similar manner, items 8 to 14, Table 20, which cover movements due to both moment and shear, lines 71 and 72, Table 17. The single total is inserted in line 72.

After trial arch computations have been made, items 6 and 13 of Table 20 are taken directly from lines 3 and 6, respectively, of Table 23 (see Art. 38l), if any computed arch ends at the base of cantilever B. Actually no analyzed arch ends at this point; hence values must be obtained by interpolation or by

estimation from other arches. The arch ending at cantilever *B* in this example is very near the bottom of the dam and is of uncertain action; hence for the present its effect on cantilever foundation movement may be ignored. If it later appears that this effect is important, proper allowance may be made.

Values from lines 3 and 6, Table 23, for the arch at  $h = 80$  ft, apply to an 80-ft high cantilever with base at the end of the arch. As no such cantilever is used in the analyses (see Fig. 32), Table 23 is illustrative only. Values of similar tables for arches at  $h = 140$  ft and  $h = 200$  ft apply directly to cantilevers *D* and *C*.

(*g*) *Cantilever influence on arch foundation deformation.* The effects of cantilever foundation deformations on arch foundations, required subsequently for inclusion in the arch computations, should be computed at this point.

Transverse foundation constants  $\underline{E}$  and  $\underline{F}$ , Eq. 54*a*, are computed from Eqs. 44*a*, 45*a*, 46*a*, and 47*a*, using a table similar to Table 5. The results are as follows:

Reservoir empty,  $t = 74.7$  ft,  
 $\underline{E} = 0.000519$ ,  $\underline{F} = 0.00216$ ;  
 Reservoir full,  $t' = 18.1$  ft,  
 $\underline{E} = 0.00883$ ,  $\underline{F} = 0.00890$ .

On the assumption that vertical joints are to be left open until vertical strains are fully developed, the factor  $\underline{G}$ , Eq. 55*a*, is not required. Values of (*H*) and (*F*), Eq. 56*a*, are as given in Art. 35*i*.

Values of  $\underline{E}$  and  $\underline{F}$  are used in lines 1, 2, and 3, of Table 21, to compute arch components of angular deflections which are totaled in line 4. The radial movement, line 5, is brought forward from line 12 of Table 20 for convenience.

TABLE 21

CONTRIBUTION OF CANTILEVER *B* TO ARCH FOUNDATION DEFORMATIONS

1	$M/\underline{E}$ , reservoir full = 3230(0.00883)	+28.50
2	$S/\underline{F}$ , " " = 633.5(0.00890)	+5.64
3	$-M/\underline{E}$ , reservoir empty = -1623(0.000519)	-0.84
4	Total = $\partial_{\alpha}\alpha$ for arch comps.*	+33.32
5	$\partial_{\alpha}n = \partial_{\alpha}n$ from line 12, Table 20 *	1089

\* For use see Art. 38*k*.

Use *M*, line 1, from Art. 35*i*.

Use *M*, line 3, from line 24, Table 17.

Use *S*, line 2, from line 44 Table 17.

If the arches and cantilevers chosen for analysis have identical bases, the results from lines 4 and 5, Table 21, may be inserted directly into the appropriate arch computation; otherwise interpolation is required. The radial deflection, line 5, usually must be resolved into  $x$  and  $y$  components for use in the arch analysis. Inspection of Fig. 32 shows that in the present example no arch ends in the vicinity of the base of cantilever  $B$ ; hence the values in Table 21 are illustrative only. Similar values for cantilevers  $C$  and  $D$  are applicable to arches at  $h = 200$  ft and 140 ft, respectively.

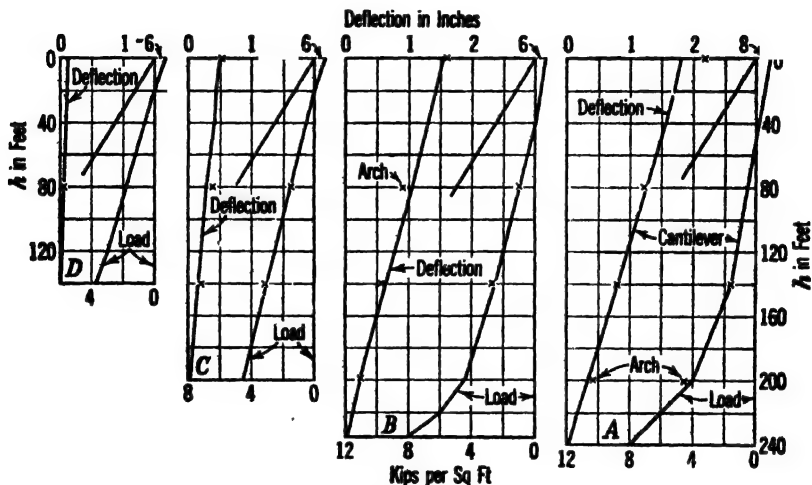


FIG. 42. Cantilever loads and deflections, Example 10.

(k) *Interpretation of results.* Radial deflections scaled from Fig. 41 are plotted on the left side of Fig. 34. If these deflections appear reasonable when compared with probable arch deflections (to be described later), the trial loading may be tentatively accepted; otherwise a new trial is made. Precision is not possible at this point. In the present case the results will be assumed satisfactory for preliminary purposes.

**36. First Complete Set of Trial Loads.** When a deflection curve of likely form has been obtained for the pilot cantilever, the preliminary work is repeated for each of the cantilevers leading to a set of trial loads, such as that shown in Fig. 42.

**37. Methods of Arch Analysis.** By placing the portion of the total water load not assumed to be carried by the cantilever, plus earthquake loads, on the arches, a trial set of radial arch loads is established. The arches are analyzed by the elastic theory. The loading is necessarily irregular. If the arches are of irregular form, graphical analysis is advantageous. Numerical analysis is somewhat more dependable for the thin arches near the top. If cracking of the thicker, lower arches is to be allowed for, graphical analysis is preferable.

**38. Sample Arch Analysis.** (a) *Arch data.* The arch at  $h = 80$  ft, Fig. 31, will be used for illustration. The arch being cylindrical (unless later found to be cracked), and the loading irregular, the analysis is in accordance with Art. 19a. The half-arch should be laid out to a scale of about 1 in. = 20 ft and divided into voussoirs as shown in Fig. 43. Because the thickness is constant, both  $\Delta s/I$  and  $\Delta s/t$  are constant if  $\Delta s$  is constant, permitting the simplifications mentioned in Arts. 16f and 16g. Ten voussoirs of equal length are assumed. A smaller number could be used.

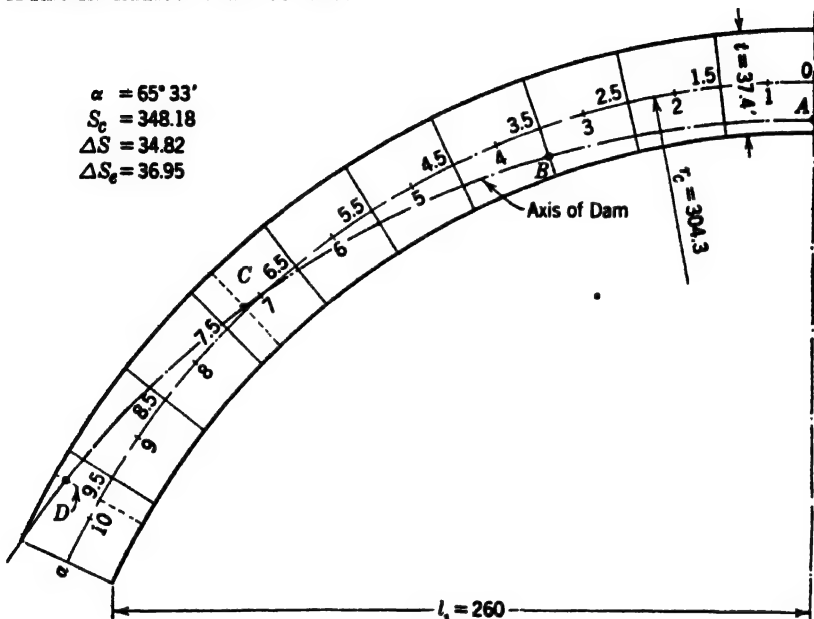


FIG. 43. Arch at  $h = 80$  ft, Example 10.

(b) *Form of computation.* In preliminary tests for this arch, the shear factor  $n$  may be assumed unity, even though the stated value of 2.80 is used for the cantilevers and the thicker arches. (See Art. 16b.) The analysis may take the general form of Table 12, Example 6, with permissible simplifications and necessary extensions. The computations are shown in Table 22. The analysis will be described by discussing the construction of this table.

(c) *Trigonometric data.* Columns 1 to 7, inclusive, are identical as to construction with the same numbered columns of Table 12 (see also Table 4), except that column 6 is totaled. With  $\Delta s/t$  and  $\Delta s/I$  constant, the totals of columns 10b and 14, Table 12, are derived from the total of column 6; hence 10b and 14 are omitted from Table 22.

Columns 8, 9, 10, and 11, Table 12, are omitted from Table 22 because the functions are constant. Column 15 is written merely as  $y^2$ , the constant factor  $\Delta s/I$  being introduced separately into the arch equations.



(d) *Water loads.* The determination of unit water loads is illustrated in diagram *a* of Fig. 44. The horizontal scale represents distance from the crown on the developed arch center line and vertical distances represent radial water loads. The cantilever positions are platted as at *A*, *B*, *C*, and *D*. Differences between cantilever loads, scaled from Fig. 42, and the full water load at  $h =$

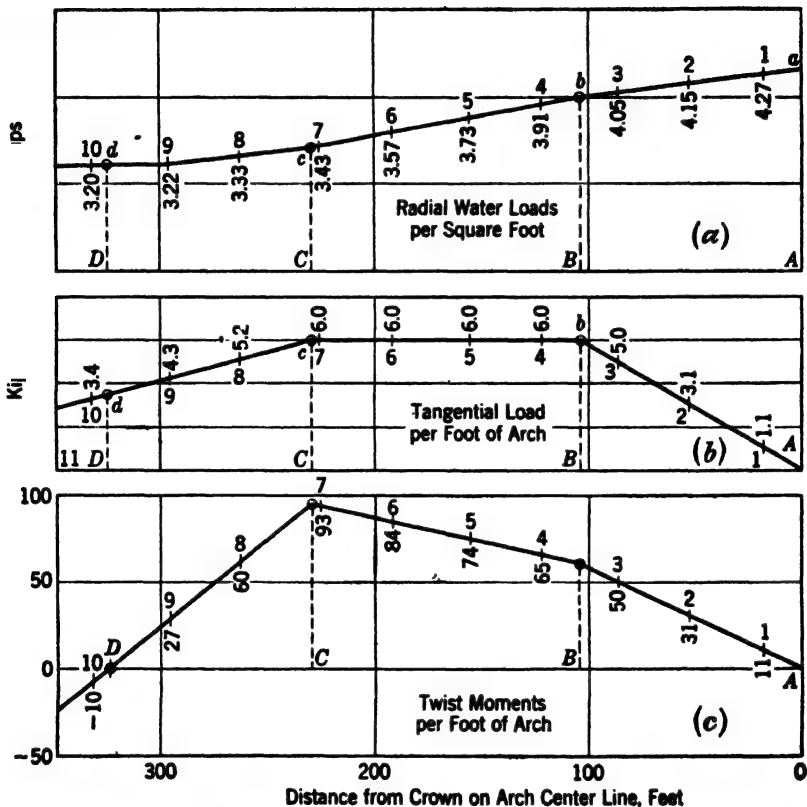


FIG. 44. Radial, tangential, and twist loads, arch at  $h = 80$  ft, Example 10.

80 ft are platted to give the arch load line  $a-b-c-d$ , arbitrarily extended to  $e$ . Voussoir center points 1, 2, 3, etc., are spotted, and the corresponding unit loads are scaled and recorded on the figure. These values, assumed to be averages for the voussoirs, are multiplied by  $\Delta s$ , and recorded in column 20*a*, Table 22.

(e) *Earthquake water loads.* The increased water pressure at the crown from earthquake movement is computed from Eq. 34*a*, Art. 13*e*, Chapter 7. The computed value for  $h = 80$  ft is 0.72 kips per sq ft. This pressure theoretically applies to a plane face normal to the line of earth movement. Pressures at other points are computed from Eq. 36*a*, Art. 13*e*, Chapter 7, or





simply by multiplying the crown value of 0.72 kips by  $\cos \alpha'$ , where  $\alpha'$  is measured from the line of earth movement. In the present example,  $\alpha' = \alpha$ .

If the earth movement is parallel to the  $x$  axis,  $\alpha'$  becomes  $90 - \alpha$ , and the tabular loads are  $P_n \sin \alpha$ . If the line of movement is oblique to both axes, new angular functions are required in Table 22, or unit pressures may be determined graphically as in Fig. 45. The line 0-11 is parallel to the line of earthquake action and its length is equal to  $p$  from Eq. 34a, Chapter 7. If lines 0-1, 0-2, 0-3, etc., are drawn parallel to the radii to corresponding voussoir

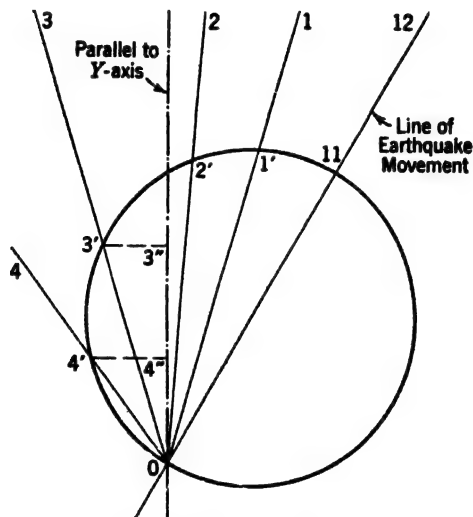


FIG. 45. Graphic resolution of earthquake water loads.

centers, chords 0-1', 0-2', 0-3', etc., represent normal unit pressures, which may be multiplied by  $\Delta s_n$  and recorded in column 20b of Table 22. If  $\Delta s_n$  is constant, multiplication may be accomplished by making 0-11 equal to  $P_n$ .

(f) *Total radial loads.* Corresponding values in columns 20a and 20b are added to give the total radial loads in column 20c.

(g) *Tangential loads.* Column 20d provides space for recording the arbitrary crown force  $H_1$  and the tangential force resulting from the interaction of adjacent arches. The interactions are never known for a first trial computation, hence are omitted in Table 22. Their computation for subsequent trials is discussed in Art. 39d.

(h) *Earthquake inertia loads.* Earthquake forces from the inertia of the masonry are computed from Eq. 32, Chapter 7, and act in the direction of earth movement, which is parallel to the  $y$  axis for this example. The voussoir volumes being constant (in this example), the force is constant at 19.5 kips. This value is entered for each voussoir in column 21c of Table 22.

When the arch is tested for movement parallel to the  $x$  axis, these values are transferred to column 22c, 21c being left blank.

If the line of action is oblique to both axes, proper components appear in both columns 21c and 22c. If the voussoir volume varies, the load will vary.

(i) *Axial components of forces.* The radial and tangential forces are resolved into  $y$  and  $x$  components in columns 21a, 21b, 22a, and 22b. Columns 21b and 22b are blank in the present trial (except for  $H_1$ ) because the tangential loads, column 20d, are ignored in this preliminary trial. Column 22c is blank because the assumed earth movement is parallel to the  $y$  axis. The totals in columns 21d and 22d correspond to  $P_y$  and  $P_x$ , columns 21 and 22, Table 12.

(j) *Total loads and moments.* Columns 23 to 30 are identical as to construction with columns of the same numbers in Table 12 or Table 4 except for the variation indicated by the heading in column 29 and provision for totals for columns 26 and 30. The twist moments, column 29a, represent cantilever twist resistances and are copied from column 4, Table 28, Art. 40d. The moments are not available for a first trial; hence column 29a is blank in Table 22. Because  $\Delta s/I$  is constant, the total of column 31, Table 12, can be produced from the total of column 30; hence 31 may be omitted. The total of column 26, *using half of the end values*, multiplied by the constant  $\Delta s/t$ , replaces the total of column 36a, Table 12; hence this latter column is not required.

(k) *Foundation constants.* Foundation constants for the direct effect of arch loads are computed in a table (not shown) similar to Table 5. The angle  $\psi$  scaled from the developed profile, Fig. 32, is  $80^\circ$ . Values of constants for Eqs. 54, 55, and 56 are

$$(E) = 0.00277$$

$$(G) = 1.383$$

$$(F) = 0.01100$$

$$(H) = 1.644$$

The cantilever contribution to foundation movement should be taken from a table similar to Table 21, computed for the cantilever at the end of the arch; but such a cantilever is not included in the computations. It will be adequate for present purposes to interpolate between zero and the values computed for cantilever  $D$ , thus:

As computed, cantilever  $D$  (computations not shown)

$$\left| \frac{\partial}{\partial \alpha} \right| = 10.85; \quad \left| \frac{\partial}{\partial n} \right| = 196.5$$

At  $h = 80$  ft by interpolation

$$\frac{80}{140} \left| \frac{\partial}{\partial \alpha} \right| = 6.21; \quad \frac{80}{140} \left| \frac{\partial}{\partial n} \right| = 112.2$$

These are downstream deformations; hence signs are changed to negative when used in the arch computations.

(l) *Arch influence on cantilever foundation deformations.* It is convenient at this point to illustrate the computation of the arch influence on cantilever

foundation movements. Values of  $|E|$  and  $|F|$  for Eq. 54a, computed in the same manner as other foundation constants, are as follows:

$$|E| = 0.000667 \quad |F| = 0.00137$$

In this example, vertical arching is ignored; hence  $|C|$ , Eq. 55a, is not required. Vertical deflections caused by loads applied after the closure of all open joints may at times merit consideration. Values of  $(H)$  and  $(F)$  are as computed in Art. 38k.

Moments and shears are taken from column 50, Table 22, and from Fig. 46, where  $\Sigma P_y$  and  $\Sigma P_x$  from Table 22 are platted, respectively, as 0-1 and 1-2. The resultant 0-2 is decomposed into a thrust 0-3 and a shear 3-2.

The computations are accomplished in Table 23, which is self-explanatory except as to signs. The radial arch deflection for a negative abutment moment is *downstream*, which is negative under the sign convention for the arches. (See Art. 14e.) For the cantilever, a downstream angular motion is positive (see Art. 35b); hence in totaling lines 1 and 2 in Table 23 the sign must be reversed. The same is true of the linear radial deflection, line 6.

Values from lines 3 and 6, Table 23, may be inserted directly into lines 6 and 13, respectively, Table 20, for a cantilever having the same base as the arch. Because the cantilever at the end of the arch at  $h = 80$  ft is not to be analyzed, actual values in Table 23 are illustrative only. Similar computations for arches at

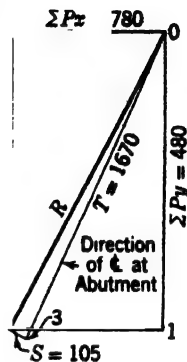


FIG. 46. Abutment reactions, arch at  $h = 80$  ft, Example 10.

TABLE 23

CONTRIBUTION OF ARCH,  $h = 80$  FT, TO CANTILEVER FOUNDATION DEFORMATION

1	$M E  = -1578 \times 0.000667$	-1.05
2	$S F  = -105 \times 0.00137$	-0.14
3	Total = $ \partial_a \alpha $ * (reverse sign)	+1.19
4	$S(H) = -105 \times 1.644$	-172.6
5	$M(F) = -1578 \times 0.0110$	-17.4
6	Total = $ \partial_a n $ * (reverse sign)	+190.0

\* For use, see Art. 35i. Use  $M$  from Table 22,  $S$  from Fig. 46.

$h = 140$  ft and  $h = 200$  ft give values for cantilevers  $D$  and  $C$ , respectively. Because no analyzed arch ends at the base of cantilever  $B$ , values must be estimated or interpolated. (See Art. 35i.)

(m) *Arch equation constants.* Ignoring minor foundation factors as negligible, at least in preliminary tests, the arch constants are assembled in Table 24, which follows the form of Table 13. (If full foundation effects are to be considered, follow the form of appropriate parts of Table 7.)

Items are provided under  $D_a$  and  $D_s$  for  $\frac{\partial \alpha}{\partial a}$  and  $\frac{\partial \alpha}{\partial n}$ , the foundation effects caused by the cantilevers. Numerical values are taken from Art. 38k.

(n) *Crown forces.* The constants from Table 24 are inserted in Eqs. 60a and 61a, Art. 18, and  $M_c$  and  $H_c$  are computed. The computed values are  $M_c = +7700$  ft-kips and  $H_c = -263.63$  kips. Adding  $H_c$  to  $H_1$  gives a net crown thrust of  $+1536$  kips.

(o) *True forces and deflections.* Net moments at voussoir centers are next computed from Eq. 11, as indicated in column 50 of Table 22. Also, values of  $\Sigma P_s$ , column 26, are corrected to true values by the algebraic addition of  $H_c$ , the results being recorded in column 51. There being no crown shear, values of  $\Sigma P_s$  require no correction.

Values of  $M\Delta s/I$ , column 52, represent angular deflection increments per voussoir. The bottom value represents turning in the foundation and is computed from Eqs. 54 and 54a, as follows:

$$\begin{array}{rcl} M(E) & = -1578 (0.00277) & = -4.37 \\ S(F) & = \text{neglected} & \\ \text{From cantilever (see Art. 38k)} & = & \underline{-6.12} \\ \text{Total} & & \underline{-10.49} \end{array}$$

Values of  $(E)$  and  $(F)$  are taken from Art. 38k and  $M$  from column 50, Table 22. The value of  $S$  is determined graphically from Fig. 46. The term  $S(F)$  is neglected in this example because similar terms are omitted in Table 24. The item for cantilever effect is taken from Art. 38k. The total is entered in column 52, Table 22.

Column 52 is summated from abutment to crown in column 53 to give accumulated angular deflections at voussoir ends. The arch and loading being symmetrical, the crown value should be zero.

Values in column 53 are averaged and multiplied by  $\Delta s$  to give the radial deflection increments per block, column 54. Because the shear factor  $n$  is assumed unity for this arch trial,  $\Sigma P_s$  produces only  $y$  deflections and  $\Sigma P_x$  only  $x$  deflections, as shown in columns 55 and 56.

If  $n$  is not assumed equal to zero, the thrust is determined graphically from a force diagram like that of Fig. 19 and thrust and shear deformations are computed for each voussoir using Eqs. 17 and 23. The headings of columns 55 and 56 then become  $T\Delta s/t$  and  $nS\Delta s/t$  and the deflections are respectively tangential and radial.

The last term in column 54 represents foundation deformation and is computed from Eqs. 56 and 56a thus:

$$\begin{array}{rcl} S(H) & = 105 \times 1.64 & = +172 \\ M(F) & = \text{neglected} & \\ \text{From cantilever (see Art. 38k)} & = & \underline{-112} \\ \text{Total} & & \underline{+ 60} \end{array}$$

TABLE 24  
ARCH EQUATION CONSTANTS,  $h = 80$  Ft, EXAMPLE 10

Item	Term	Function	Values
1	$A_\alpha$	$\frac{\Delta s}{I} \Sigma y = 0.00799 \times 620.3$	+4.956
2		$y_\alpha(E) = 178.35 \times 0.00277$	+0.494
3		Total	+5.450
4	$A_z$	$\frac{\Delta s}{I} \Sigma y^2 = 0.00799 \times 67,372$	+538.30
5		$\frac{s}{l}$	+9.31
6		$y_\alpha^2(E) = (178.35)^2 \times 0.00277$	+88.11
7		Total	+635.72
8	$C_\alpha$	$\sum \frac{\Delta s}{I} = 10 \times 0.00799$	+0.0799
9		(E)	+0.0028
10		Total	+0.0827
11	$C_z$	$= A_\alpha$	+5.450
12	$D_\alpha$	$\frac{\Delta s}{I} \Sigma M_E = 0.00799 \times 86,625$	+692
13		$M_E(E) = 36,932 \times 0.00277$	+102
14		* $\partial_\alpha \alpha$	-6
15		Total	+788
16	$D_z$	$\frac{\Delta s}{I} \Sigma y M_E = 0.00799 \times 10,721,000$	+85,661
17		$\frac{\Delta s}{l} \Sigma (\Sigma P_z) = 0.93101 \times 15,161$	+14,115
18		$C_F F E x_\alpha$	+5,385
19		$y_\alpha(E) M_\alpha$	+18,244
20		$(G) \sin \alpha \cos \alpha \Sigma P_y$	+770
21		$(G) \cos^2 \alpha \Sigma P_z$	+246
22		$y_\alpha \partial_\alpha \alpha = 178.35 \times * 6.21$	-1,108
23		$\partial_\alpha n \sin \alpha = * 112.2 \times 0.91032$	-102
24		Total	+123,211

\* From Art. 38k.



The tangential foundation deformation  $T(G)$ , Eq. 55, is

$$T(G) = 1670(1.38) = 2305$$

This value is written across the bottom of columns 55 and 56.

(*p*) *Platting deflections.* Because of the multiplicity of directions, the increments of columns 54, 55, and 56 are added vectorially as in Fig. 47. To illus-

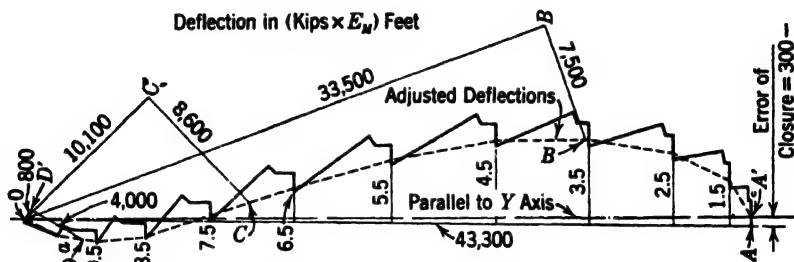


FIG. 47. Arch deflections, arch at  $h = 80$  ft, Example 10.

trate the procedure, a portion of Fig. 47 is enlarged in Fig. 48. Beginning at 0, the radial foundation movement (last value in column 54) is platted from 0 to 1, parallel to the abutment radius. Then the tangential abutment movement (from bottom of columns 55 and 56) is platted from 1 to  $a$ . The distance 0- $a$  represents the foundation displacement.

The radial deflection of voussoir number 10 (from column 54) is platted from  $a$  to 2, parallel to the radius at the voussoir center. Radial deflection due to temperature,  $C_F F E \Delta s$ , is platted from 2 to 3, the  $y$  deflection for block 10 (column 55) from 3 to 4, and the  $x$  deflection (column 56) from 4 to 9.5. The line  $a$ -9.5 represents the movement in voussoir 10 and 0-9.5 the total movement of point 9.5 (see Fig. 43).

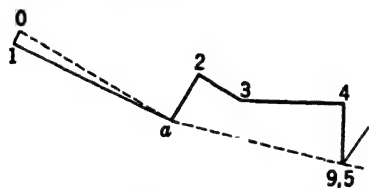


FIG. 48. Detail of part of Fig. 47.

This procedure is repeated for each of the voussoirs, finally arriving at the crown deflection 0-A, Fig. 47. For a symmetrical arch, the line 0-A should be parallel to the  $y$  axis. In Fig. 47 the error of closure is equal to  $A-A'$ , a relatively small amount. The deflections are adjusted for this error by moving points 1.5, 2.5, 3.5, etc., horizontal distances equal to the distance between lines 0-A and 0-A' at their respective levels.

The adjusted points are connected by dotted chords (or by a smooth curve if desired). Intersections with cantilevers B, C, and D are spotted by interpolation, and radial and tangential deflections at these points are drawn. As an example, lines 0-B' and B'-B are respectively parallel and normal to the

arch radius at the intersection of the center line with cantilever *B* and represent to scale the radial and tangential arch deflections at that point. The values are in feet times  $E$ . They are converted to inches by multiplying by  $12/E$ .

(*g*) *Comparison of arch and cantilever deflections.* The scaled radial deflections, converted to inches, are platted on their respective deflection diagrams at  $h = 80$  ft on Fig. 42.

Residual loads are applied in the same manner to arches at  $h = 140$  ft and  $h = 200$  ft; positive loads equivalent to the negative cantilever loads are applied to the arch at  $h = 0$ . The resulting arch deflections are marked on Fig. 42 by crosses. Agreement with cantilever deflections is excellent for a first trial except for cantilevers *A* and *D* at the top. These discrepancies can be adjusted in subsequent trials. It is useless to strive for an exact balance for radial loads alone, as such balance is disturbed when tangential and twist loads are introduced, which should be done as soon as reasonably good radial agreement has been achieved.

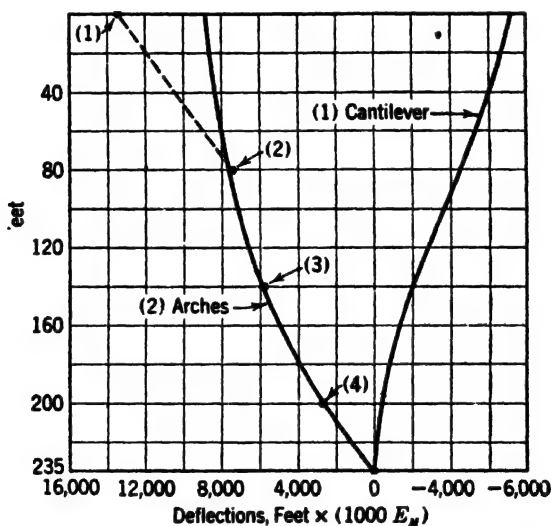


FIG. 49. Tangential deflections, cantilever *B*, Example 10.

**39. Tangential Loads.** (*a*) *Methods of estimating.* Consider cantilever *B*. Tangential cantilever deflection components, scaled from Fig. 41, are platted as curve 1, Fig. 49.

Tangential deflections for the various arches at their intersections with cantilever *B* are platted at 1, 2, 3, and 4. Point 2, for example, is obtained by scaling the tangential deflection component  $B'-B$  from the arch deflection curve of Fig. 47. Other points are similarly determined from the deflection curves for their respective arches. A smooth curve (curve 2) is drawn approxi-

mately through the points.<sup>29</sup> Point 1 for the top arch is out of line with the others. Because this arch is known to be in poor adjustment (see Art. 38*q*), the upper part of curve 2 is drawn arbitrarily, as shown. The horizontal distance between curves 1 and 2 represents lack of tangential conformity. Internal forces must be introduced to correct this condition.

The trial tangential forces may be based on judgment or estimated in any desirable way. A preliminary computation procedure is illustrated in Table 25. Values of arch and cantilever deflections, from Fig. 49, are shown in lines 2 and 3. Algebraic differences between these values, line 4, represent total radial disparity in computed cantilever and arch positions. Disparity values per block are shown in line 5. Values of  $t\Delta s$  in line 6 (or  $t'\Delta s'$  if broken)<sup>30</sup> are averaged and divided by  $n\Delta h$  to give the inverted shear deflection factors of line 7. These values multiplied by corresponding values from line 5 give the average shear values required to produce deflections equivalent to the disparities of line 3.

These average shear values, assumed to represent shears at the block centers, are plotted in Fig. 50 and fitted with a smooth curve, *A*.<sup>31</sup> Shears opposite assumed joints are scaled from this curve and recorded in line 9 of Table 25.

From these shears it is necessary to subtract the tangential components of the radial cantilever loads, which have not thus far been considered. These components are scaled from Fig. 39 and recorded in line 10. Algebraic subtraction gives the net shears of line 11. Differences in adjacent values in line 11 represent load accumulations per block, line 12. Dividing by  $\Delta h$  gives the average load per vertical foot of cantilever, line 13. These loads may be plotted opposite the block centers and a load curve *B*, Fig. 50, drawn approximately through them. Positive loads act toward the abutment.

Because the tangential forces deflect the arch as well as the cantilevers, the forces represented by curve *B* are likely to be appreciably in excess of the true tangential forces. Approximate arch computations (not shown) indicate a first trial load curve about in the position of curve *C*, Fig. 50.

(*b*) *Recomputation of tangential deflections.* The lateral deflections resulting from these loads are computed as illustrated in Table 26, which is a reversal of Table 25.

Values of  $h$  are recorded in line 1. Loads per vertical foot are scaled from curve *C*, Fig. 50, and recorded in line 2. Averages of these values are multiplied by  $\Delta h$ , to give the block loads of line 3. These loads are summated to give the shears of line 4. Strictly, this summation should be made graphically

<sup>29</sup> Mathematically, the tangential load at any point depends on the curvature of the deflection curve at that point. A sharp curve denotes a large force. Actually, sharp curves do not occur under ordinary circumstances. Hence, "smoothness" is more important than an accurate fit of computed points, particularly as points will change with recomputation. This comment applies to all deflection curves from which forces or moments are to be estimated.

<sup>30</sup> See footnote, Art. 35*h*, concerning broken cantilevers.

<sup>31</sup> See footnote 29, above.

TABLE 25  
TANGENTIAL LOADS, CANTILEVER B, FIRST TRIAL

1	$h = \text{depth to joint}$	0	20	40	60	80	100	120	140	160	180	200	220	235
2	Tangential arch deflection	+8.850	+8.680	+8.400	+8.050	+7.610	+7.100	+6.520	+5.850	+5.000	+4.000	+2.770	+1.300	0
3	Tangential cantilever deflection	-7.250	-6.830	-6.250	-5.300	-4.480	-3.630	-2.840	-2.100	-1.450	-860	-400	-160	0
4	Difference (algebraic) = $\delta_i$	16.100	15.510	14.650	13.350	12.090	10.730	9.360	7.950	6.450	4.860	3.170	1.460	0
5	Value per block = $\Delta\delta_i$	590	860	1,300	1,300	1,260	1,360	1,370	1,410	1,500	1,590	1,690	1,710	1,460
6	$\Delta\delta_i$ (use $\Delta\delta_i'$ if broken)	10.0	15.0	20.4	29.6	38.5	46.6	54.1	54.6	50.0	41.3	33.7	20.4	15.6
7	(Average $\Delta\delta_i$ ) $\div n\Delta h$	0.223	0.316	0.446	0.608	0.760	0.898	0.971	0.934	0.815	0.670	0.483	0.429	
8	$P_{10} = \text{average shear} = (7) \times (5)^*$	132	271	580	580	766	1,034	1,230	1,370	1,490	1,295	1,132	823	627
9	$P_i' = \text{shear at joint (curve A, Fig. 50)}$	0	190	410	650	900	1,150	1,310	1,390	1,370	1,210	960	710	550
10	$P_i'' = \text{tangential cantilever load (Fig. 36)}$	0	0	0	0	0	1	1	4	10	18	32	54	88
11	$P_i = \text{net shear} = (9) - (10)$	0	190	410	650	900	1,149	1,309	1,386	1,360	1,192	928	656	462
12	$\Delta P_i = \text{net block loads}$	190	220	240	240	250	249	160	77	-26	-188	-264	-272	-194
13	$P_{10} = \Delta P_i \div \Delta h = \text{avg. increment per ft}^{**}$	9.5	11.0	12.0	12.5	12.5	12.5	8.0	3.8	-1.3	-8.4	-13.2	-13.6	-12.9

\* Plat as curve A, Fig. 50. \*\* Plat as curve B, Fig. 50.

TABLE 26  
TANGENTIAL DEFLECTIONS, CANTILEVER  $P$ , FIRST TRIAL

1	$h$ = depth to joint	0	20	40	60	80	100	120	140	160	180	200	220	235
2	$p_1$ = tangential load per ft (curve $C$ , Fig. 50)	3.8	5.0	5.8	6.2	5.9	4.7	2.9	0.6	-2.0	-4.7	-6.5	-7.0	-6.5
3	(Avg. $p$ ) $\Delta h = \Delta P'$	88	108	120	121	121	106	76	35	-14	-67	-112	-135	-135
4	$Z\Delta P' = P'_i \rightarrow$	0	88	196	316	437	543	619	654	640	573	461	326	191
5	$P'_i$ = tangential cantilever load (Fig. 30)	0	0	0	0	0	1	1	4	10	18	32	54	88
6	$P_i = P'_i + P''_i$	0	88	196	316	437	544	620	658	650	591	493	380	279
7	$\Delta \delta_i$ (use $\Delta \delta'_i$ where broken)	10.0	15.0	20.4	29.6	38.5	46.6	54.1	54.6	50.0	41.3	33.7	20.4	15.6
8	$n + \Delta \delta_i$	0.280	0.187	0.137	0.095	0.073	0.060	0.052	0.051	0.056	0.068	0.083	0.137	0.180
9	$\delta_i(n) = P_i(n + \Delta \delta_i)$	0	16.5	26.9	30.0	31.9	32.6	32.2	33.6	36.4	40.2	40.9	52.1	50.2
10	$\delta_i$ (average $\delta_i$ ) $\Delta h$	165	434	569	619	645	648	648	658	700	766	811	980	767
11	$\delta_i$ = deflections = $Z\Delta \delta_i \leftarrow$	7712	7547	7113	6544	5925	5280	4632	3974	3274	2508	1697	767	0

so that radial components may be measured and added to the radial loads of Table 17. This need not be done for early trials and frequently not at all.

The tangential components of the radial shear, line 5, scaled from Fig. 39 (same as line 10, Table 25), are added to the shears in line 4 to give the totals of line 6. Values of  $t\Delta s$  (or  $t'\Delta s'$ ),<sup>32</sup> line 7, are divided into  $n$  to give the values of line 8. The shears are multiplied by values in line 8 to give shear distortions per unit height at the joints, line 9. These values, averaged and multiplied by  $\Delta h$ , give block deflections, line 10, which are summated to give the

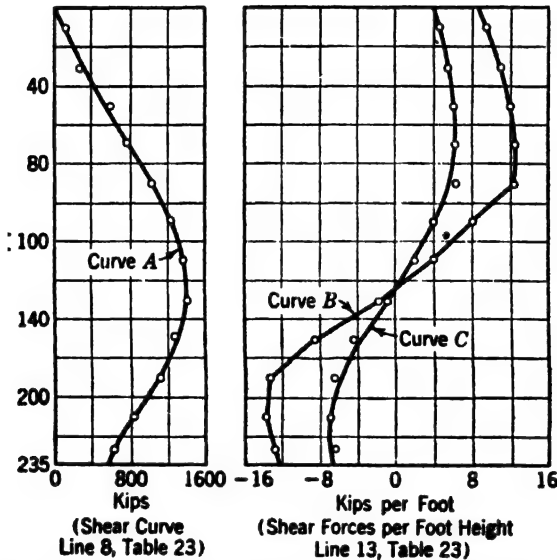


FIG. 50. Tangential shear loads, cantilever B, Example 10.

total deflections of line 11. This summation, again, strictly should be made graphically in order that radial components of the deflection may be measured and included with other radial deflections. This refinement may be ignored in early trials.

(c) *Other cantilevers.* Tangential loads are similarly computed for the other cantilevers, remembering that for a symmetrical dam, like Example 10, there is no tangential deflection at the crown. The only new element to be introduced is an allowance for tangential arch foundation deflection, where appreciable, as illustrated for cantilever D, Fig. 51.

Computed tangential arch deflections are represented by points 1, 2, and 3, 0-1 representing the foundation movement. This deformation may be considered as moving the unstrained position of the cantilever from curve 0-5 to the parallel curve 1-5'. Hence the strain producing disparities are represented by the distances between 1-5' and the polygon 1-2-3. Instead of moving the

<sup>32</sup> See footnote, Art. 35h.

curve 0-5, it is usual to move points 1, 2, and 3, as shown. A smooth trial curve 0-4 is drawn corresponding to curve 1, Fig. 49.

(d) *Application to arches.* The trial tangential forces from Table 26 must be introduced into the arch computation. Consider the arch at  $h = 80$  ft and let the horizontal scale, diagram *b*, Fig. 44, represent the developed length of its center line, intersections with cantilevers *A*, *B*, *C*, and *D* being located as shown.

The load of 6.2 kips per ft of height for cantilever *B* at  $h = 80$  ft, from curve *C*, Fig. 50, produces a reaction per foot of arch equal to 6.2 divided by the cantilever thickness, i.e.,  $6.2 \div 1.03 = 6.0$ . This value is plotted at *b*. Similar values for cantilevers *C* and *D* (computations not shown) are plotted

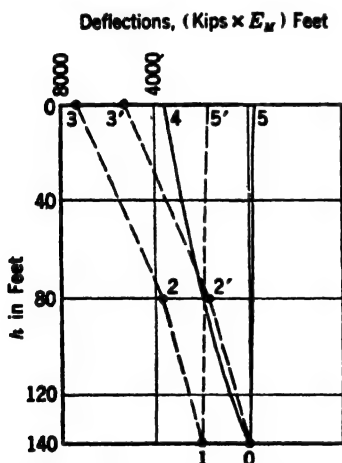


FIG. 51. Tangential deflections, cantilever *D*, Example 10.

at *c* and *d*, respectively. For a symmetrical arch, the tangential load at the crown is zero. The computed points are joined by a polygon (or a smooth curve) *A-b-c-d*, extrapolated to the abutment.

The voussoir center stations are spotted at 1-2-3, etc., and the corresponding loads are scaled and recorded on the diagram. The values shown are in kips per linear foot of arch center line. These values are multiplied by  $\Delta s$  and the products are inserted in column 20*d*, Table 22, for the next trial analysis. Notwithstanding the arbitrary reduction from curve *B* to curve *C*, Fig. 50, the tangential loads in diagram *b*, Fig. 44, are large compared to the radial loads of diagram *a*, and will no doubt be found to require further reduction as the trials proceed.

**40. Twisting of the Cantilevers.** (a) *Twist deflections.* In addition to being deflected radially and laterally, the cantilever must be twisted to conform to the angular deflection of the arches. The angular deflections for the first trial loading for the arch at  $h = 80$  ft are found in column 53, Table 22. The values shown are at the voussoir ends. Values at the cantilever intersections are found by interpolation. The value at cantilever *B* is plotted at 2 on diagram *a* of Fig. 52. Similar values for other arches are plotted at 1, 3, and 4, and a smooth curve is drawn to approximate them.<sup>23</sup> Point 1, for the top arch, is more or less ignored, for reasons previously given.

(b) *Estimating trial twist moments.* It is possible to apply a system of twisting moments to the cantilever which will cause it to conform to the angular movements represented by diagram *a*. Because the angular deflections of the arch are so far only approximately determined, and because in

<sup>23</sup> See footnote, Art. 39a.

any event they will be changed by the twist loads, such computation will not yield a final result but will serve as a guide in choosing a trial set of twist moments. The procedure is shown in Table 27.

Values of  $h$  at successive joints are shown in line 1. Required twists, scaled from diagram *a*, Fig. 52, are recorded in line 2. Differences in line 3 are divided by  $\Delta h$  to give average twists per foot, line 4. Values of the cantilever width  $t$  and its thickness  $\Delta s$ , transferred from Table 17, are recorded in lines 5 and 6 for convenience. Where the cantilever is cracked under the assumed radial loads,  $\Delta s'$  and  $t'$  are used.<sup>34</sup>

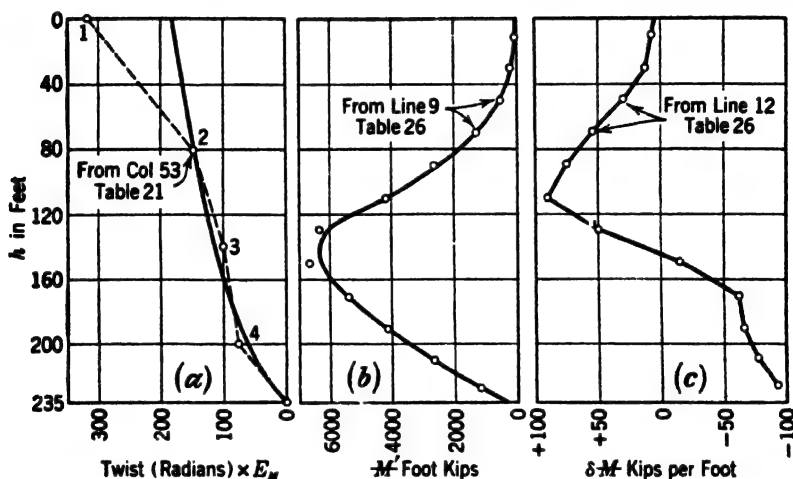


FIG. 52. Twist data for cantilever *B*, Example 10.

The twist deflection may be determined by the equation

$$\partial\theta = \frac{M}{2GI} \quad [99]$$

where  $\partial\theta$  is twist deflection per foot of height. In the present case,  $M$  is the unknown; hence

$$M = 2GI\partial\theta \quad [100]$$

or, substituting from Eq. 63,

$$M = \frac{EI}{(1 + \mu)} \partial\theta \quad [101]$$

If  $\mu$  is assumed to be  $\frac{1}{6}$ , Eq. 101 becomes

$$M = \frac{6}{7} EI\partial\theta = \Delta s \frac{t^3}{14} E\partial\theta \quad [102]$$

<sup>34</sup> See footnote, Art. 35h.



TABLE 27  
TWIST MOMENTS, CANTILEVER B, FIRST TRIAL

1	A = depth to joint																235
2	0	20	40	60	80	100	120	140	160	180	200	220	235				0
3	Angular deflection, diagram a, Fig. 52	180	172	164	155	146	136	126	114	100	84	63	33				33
4	Angular deflection per block	8	8	8	9	9	10	10	12	14	16	21	30				33
5	Angular deflection per ft = $\partial\theta$	0.40	0.40	0.40	0.45	0.45	0.50	0.50	0.60	0.70	0.80	1.05	1.50				2.20
6	$t$ (use $t'$ where broken)	10.0	15.0	20.2	29.0	37.4	44.8	51.5	52.6	48.4	41.3	34.6	22.5				18.1
7	$\Delta s$ (use $\Delta s'$ where broken)	1.00	1.00	1.01	1.02	1.03	1.04	1.05	1.04	1.03	1.00	0.96	0.90				0.86
8	$2GI = \Delta s^2 E + 14$ (omit $E$ )	72	241	594	1,780	3,850	6,630	10,170	10,720	8,300	5,020	2,840	732				364
9	Average $2GI$	156	418	1,187	2,815	5,240	8,400	10,445	9,510	6,660	3,930	1,786	548				548
10	$M' = (4) \times (8)$ , plat diagram b, Fig. 52	62	167	534	1,267	2,620	4,200	6,270	6,670	5,328	4,130	2,680	1,200				1,200
11	$M$ = twist moments at joints, from curve	0	110	350	940	2,000	3,450	5,250	6,250	5,950	4,700	3,350	1,800				400
12	$\Delta M$ per block	110	240	590	1,060	1,450	1,800	1,000	300	-1,250	-1,350	-1,550	-1,400				-1,400
13	$\partial M$ per ft, average, plat	5.5	12.0	29.5	53.3	72.5	90.0	50.0	15.0	-62.5	-67.5	-77.5	-93.4				-93.4
13C	$\partial M$ per ft at joints, from curve	+3	+9	+20	+40	+62	+80	+72	+20	-34	-56	-72	-85				-100
13D	$\partial M$ per ft at joints, from curve	+0	+13	+28	+53	+80	+133	+150	+127	+46	-25	-75					
13D	$\partial M$ per ft at joints, from curve	+6	+10	+11	+8	-1	-18	-44	-67								

Deflections in Table 27 already contain the factor  $E$ , brought over from the arch computations; hence  $E$  is ignored. Values of  $\Delta st^3/14$  are recorded in line 7, averaged in line 8, and used to compute average twist moments per foot of height,  $M'$  in line 9. These values are platted on diagram *b*, Fig. 52, and a smooth curve drawn from which the joint values of line 10 are scaled.<sup>35</sup> The differences in line 11 are divided by  $\Delta h$  to get the average moment increments per foot of height, line 12. These values are platted on diagram *c*, Fig. 52, from which the joint values in line 13 are read.

Twist moments for cantilevers *C* and *D* are similarly computed, the end results being shown in lines 13*C* and 13*D*, Table 27.

Whether these estimated twist moments should be used directly as trial values or reduced, as in the case of tangential shear, curve *C*, Fig. 50, depends on their magnitude compared to other arch moments.

(*c*) *Recomputation of cantilever twists.* If the trial twists are altered from the values estimated in Table 27, the corresponding cantilever twist deflections must be computed. This is accomplished by a reversal of the procedure of Table 27.

(*d*) *Application of cantilever twist moments to arches.* Consider the arch at  $h = 80$  ft. Twist moment increments for column  $h = 80$  ft from lines 13, 13*C*, and 13*D*, Table 27, are divided by their respective cantilever thicknesses to get twist moment increments per foot of arch, which are platted to produce diagram *c*, Fig. 44. The platted points are connected by a polygon (or smooth curve), and values at voussoir center stations are scaled and recorded on the diagram. The scaled values represent moment increments per foot of arch center line.

Because the moments thus introduced change the computed angular deflections of the arch, it is usually desirable to reduce the scale values for trial purposes. Computations for the full values are illustrated in Table 28. The scaled values are entered in column 1 and multiplied by  $\Delta s$  to get the increments of column 2. These values are averaged in column 3 and summated in column 4 to get area under the load curve of diagram *c*, Fig. 44, which represents accumulated values of  $M$ . Because the desired moments are at the voussoir centers, the first and last terms of column 3 are reduced one-half. The values of column 4 are transferred to column 29*a* of Table 22 and may be used to correct the previously completed arch computations, or held for the next trial.

The resulting moments in the present case are large compared to corresponding values of  $M_E$ , indicating that the values from diagram *c*, Fig. 44, should be appreciably reduced for a first trial. Final determination cannot be made until values for other points have been found and consideration has been given to possible effect of tangential loads, and possible changes in trial radial loads.

<sup>35</sup> See footnote, Art. 39*a*.

TABLE 28  
ACCUMULATED TWIST MOMENTS ARCH AT  $h = 80$  FT, FIRST TRIAL

	1	2	3	4
Point	$\frac{\partial M}{\partial s}$ From Fig. 44c	$\Delta M = \frac{\partial M}{\partial s} \Delta s$	Average $\Delta M$	$M =$ $\Sigma(\text{Avg. } \Delta M)$
Crown	0	0		
1	11	383	*96	96
2	31	1,079	731	827
3	50	1,741	1,410	2,237
4	65	2,263	2,002	4,239
5	74	2,577	2,420	6,659
6	84	2,925	2,751	9,410
7	93	3,238	3,082	12,492
8	60	2,089	2,664	15,156
9	27	940	1,515	17,671
10	-10	-348	296	17,967
Abut.			*-87	17,880

\* Use half values at ends (see Art. 40d).

**41. Twisting of the Arches.** (a) *Twist deflections.* The angular deflection of the cantilevers causes a twisting of the arches, producing moments which affect the deflection of the cantilevers. In Fig. 53, line 0-A represents the developed center line of the arch at  $h = 80$  ft, and points A, B, C, and D represent cantilever intersections. The angular deflection of cantilever B at  $h = 80$  ft from line 69, Table 17, is plotted from B to b. Corresponding values for other cantilevers (computations not shown) are plotted at a, c, and d. A smooth curve is drawn approximately through the plotted points.<sup>36</sup>

<sup>36</sup> See footnote, Art. 39a.

(b) *Estimating trial twist moments.* Values for the voussoir ends are read from the curve of Fig. 53 and recorded in line 2, Table 29. Differences between adjacent values recorded in line 3 represent twist increments per voussoir. Dividing by  $\Delta s$  gives twist increments per linear foot of arch center line,

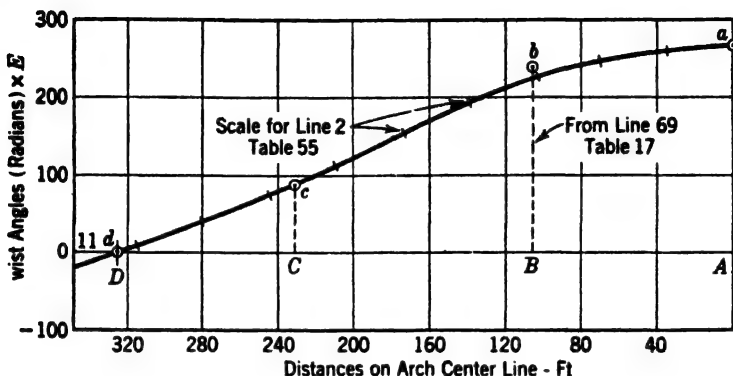


FIG. 53. Twist data, arch at  $h = 80$  ft, Example 10.

line 4. These values are voussoir averages. Applying Eq. 102 gives the voussoir average twist moments per linear foot. These averages are platted opposite the voussoir centers in Fig. 54 and a smooth curve is drawn approximately through them.<sup>37</sup> Values for voussoir ends read from this curve and recorded in line 6 represent twist moments, and their successive differences,

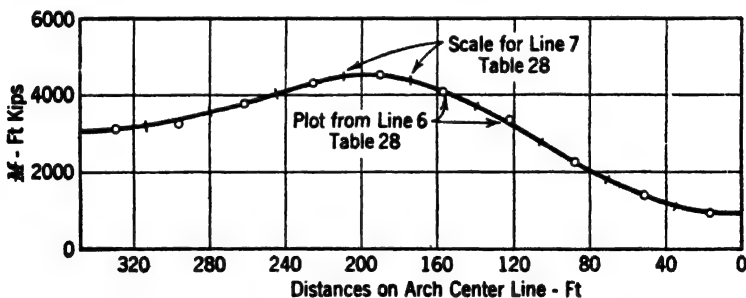


FIG. 54. Twist moments, arch at  $h = 80$  ft, Example 10.

line 7, represent twist moment increments per voussoir. These values are divided by  $\Delta s$  for the arch to give the average increments per foot, line 8.

These values may be platted opposite voussoir centers on a diagram not shown, similar to Fig. 53, to facilitate interpolation for values at the cantilever stations. Similar results for the other arches are appended to Table 29.

<sup>37</sup> See footnote, Art. 39a.

TABLE 29  
ARCH TWIST DATA AT  $h = 80$  FT, FIRST TRIAL

1	Voussoir end	0	1.5	2.5	3.5	4.5	5.5	6.5	7.5	8.5	9.5	Abut.
2	Angle of twist, scale from Fig. 53	269	260	247	226	195	157	115	75	40	10	-19
3	Angle of twist per voussoir	9	13	21	31	38	42	40	35	30	29	
4	Angle of twist per ft, average	0.259	0.373	0.603	0.890	1.092	1.206	1.148	1.005	0.862	0.833	
5	$M' = (4)t^3 + 14 = (4) \times 3,740$ (avg.), plat Fig. 54	960	1,390	2,250	3,330	4,080	4,510	4,300	3,750	3,220	3,120	
6	$M =$ twist moment at joints read from Fig. 54	950	1,150	1,800	2,780	3,720	4,350	4,450	4,000	3,550	3,200	3,060
7	$\Delta M$ (per voussoir)	200	650	980	940	630	100	-450	-450	-350	-150	
8	$\Delta M \div \Delta s =$ average increment per ft	5.74	18.68	28.20	27.00	18.10	2.87	-12.92	-12.92	-10.06	-4.31	
8	Last line $h = 0$ $\Delta M \div \Delta s =$ average increment per ft	0.44	0.51	0.49	0.37	0	0.32	-0.56	-0.42	-0.27	-0.24	
8	Last line $h = 140$ ft $\Delta M \div \Delta s =$ average increment per ft	63	88	129	207	116	-31	-14	-151	-192	-198	
8	Last line $h = 200$ ft $\Delta M \div \Delta s =$ average increment per ft	219	263	372	438	438	306	-158	-415	-350	-306	

Note:  $\Delta s = 34.82$  ft.

(c) *Application of twist moments to arch.* The twist moment increments shown in line 8, Table 29, are merely estimates of trial values. If these values are altered, the corresponding twist deflections are computed by a reversal of the procedure of Table 29. These reestimated twists are held for comparison with the next set of angular cantilever deflections. The reverse computation is not illustrated.

(d) *Application to cantilevers.* Cantilever *B* will be used as an example. Values in line 8, Table 29, for each arch, are interpolated to get twist moment increments per foot horizontally at each cantilever station, then multiplied by  $\Delta s$  for the cantilever (line 8 or 63, Table 17) to get twist moment increments per vertical foot of cantilever. The results for cantilever *B* are as follows:

Elevation	0	80	140	200
Increment per foot	0.49	28	150	380
$\Delta s$ or $\Delta s'$	1.00	1.03	1.04	0.96
Increment per foot, cantilever	0.49	29	156	365

These values are platted as curve 1, Fig. 55, from which the moment increments per foot of cantilever required to twist the arches into conformity with the first trial angular cantilever deflections may be scaled. The resulting moments reduce the computed cantilever deflection, which reduces the twisting of the arch and changes the position of curve 1. Consequently, trial values are arbitrarily reduced, somewhat as represented by curve 2.

Values scaled from this curve, entered in column 2, Table 30, represent trial twist moment increments per vertical foot. Averaged and multiplied by  $\Delta h$  they represent twist moments per block, column 3, and may be summated to get the accumulated twist moments of column 4. These values are entered in line 50, Table 17, and included with other cantilever moments in the next trial.

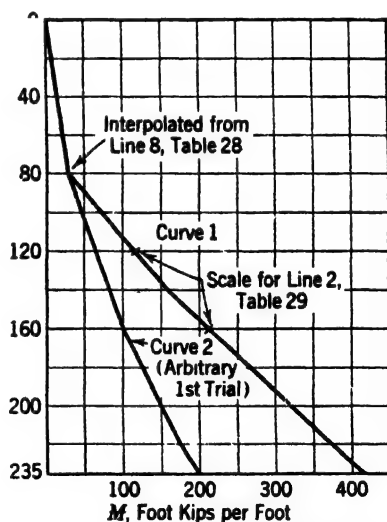


FIG. 55. Twist moments, cantilever *B*, Example 10.

**42. Adjustment for Poisson's Ratio.** Consider a half-arch slice at a given level in a dam, loaded with the vertical weight of the cantilevers above it. The pressure of this weight lengthens the arch and extends its radial width, according to Poisson's ratio. The circumferential lengthening influences the arch deflection. Usually, the cantilever pressure is not uniformly distributed.

**TABLE 30**  
**CANTILEVER TWIST MOMENTS FROM ARCH TWIST RESISTANCE**

1	2	3	4
$h$ (ft)	$\partial M$	$\Delta M$	$M$ (ft-kips)
0	0		0
20	7	70	70
40	15	220	290
60	22	370	660
80	30	520	1,180
100	48	780	1,960
120	65	1,130	3,090
140	83	1,480	4,570
160	100	1,830	6,400
180	125	2,250	8,650
200	150	2,750	11,400
220	175	3,250	14,650
235	200	3,810	17,460

Notes:  $h$  = Depth to joint, in ft.

$\partial M$  = Twist moment per foot of height.

$\Delta M$  =  $\Delta h$  times average  $\partial M$ .

= Twist moment per block.

$M$  =  $\Sigma \Delta M$  = Twist moments at block ends.

As a result, the circumferential extension of the arch fibers is not constant from face to face. This causes an angular deflection of the arch.

The pressure of the arches on a given cantilever similarly affects the cantilever deflection, only the angular effect being important in this case.

The radial thrusts produce similar effects in both arch and cantilever.

The deflections thus produced may be included in the computations if desired. However, their inclusion is involved and their influence on the final result is not usually important.<sup>38</sup>

**43. Principal Stresses.** (a) *In the interior.* The computation of inclined stresses and interior stresses in the combined arch-cantilever system of a gravity-arch dam involves the fundamental principles discussed in Chapter 12, but the problem is three-dimensional and consequently is more involved.

At any point within the dam there are three mutually perpendicular principal stresses. These principal stresses may be computed if the six unit forces acting on any three mutually perpendicular planes through the point are known. The six stresses are as follows:

(1) Vertical thrust (or tension). This is the vertical cantilever stress and may be computed by the rules of Chapter 12, using cantilever loads from the final trial.

(2) Radial shear in a horizontal plane. This is the cantilever shear which may be computed by the rules of Chapter 12, using cantilever loads from the final trial. For cracked cantilevers it is doubtful if the rules of Chapter 12 are accurate.

(3) Tangential thrust (or tension). This is the arch thrust and may be computed approximately, by rules of this chapter, assuming linear distribution for interior points.

(4) Radial shear in a vertical plane. This is the arch shear. The total shear across any radial section may be computed by the rules of this chapter. For a cylindrical arch, the intensity on a radial plane is zero at each face, and parabolic distribution similar to that for a prismatic beam may be assumed as a fair approximation.

(5) Radial thrust, which is made up of two parts. The portion derived from the cantilever analysis may be computed by the rules of Chapter 12. The portion derived from the arch load may be found from a similar computation applied to the arch section.

(6) Horizontal tangential shear derived from the trial loads data thus:

$$s_t = \frac{S_t}{t} \pm \frac{M}{I_c} c \quad [103]$$

where  $s_t$  is the unit tangential shear at any point,  $S_t$  is the total tangential shear per foot of arch at the point taken from the trial load analysis,  $t$  is the thickness of the arch,  $M$  is the cantilever twist moment from Table 17,  $I_c$  is

<sup>38</sup> "Trial Load Method of Analyzing Arch Dams," U. S. Bur. Reclam., Boulder Canyon Project Final Reports, Part V, Technical Investigations, Bull. 1, Sec. 178, p. 178.



the moment of inertia of the unit cantilever, and  $c$  is the distance from the arch axis to the point in question.

The determination of principal stresses at interior points is not usually required and will not be further discussed here.

(b) *At the faces.* As in gravity dams, maximum stresses occur at the faces where governing conditions are simpler than in the interior.

At the base of cantilever  $C$ , Fig. 32, Example 10, consider stresses in a unit thickness slab parallel to the face. There is no shear in the plane of the face and consequently no shears normal to the face. The shear acting parallel to the face in a horizontal plane may be computed from Eq. 103, using data from the trial load computations. Unless the inclination of the face exceeds that usually found in arched dams, this shear may be assumed to represent approximately the unit shear parallel to the face in a normal plane with a horizontal trace.

The inclined cantilever thrust parallel to the face is found as for a gravity dam, and the arch stress from the arch analysis. The principal stresses are then found from Mohr's circle, as explained in Chapter 12.

In the vicinity of the abutments the maximum stress is usually inclined to both the cantilever and the arch.

#### 44. Unit Load Patterns for Arches.

Just as influence lines are used for determining the effect of moving loads on bridges, standard load patterns may be utilized in the trial load analysis of an arched dam. In diagram *a*, Fig. 56, let 0-2-5-6-9 represent the water face of the left side of an arch, divided into voussoirs 0-2, 2-5, etc., and subjected to a variable radial loading represented by 1-3-4-7-8. The total load may be divided into the partial loads 1-0-2, 1-2-4, etc.

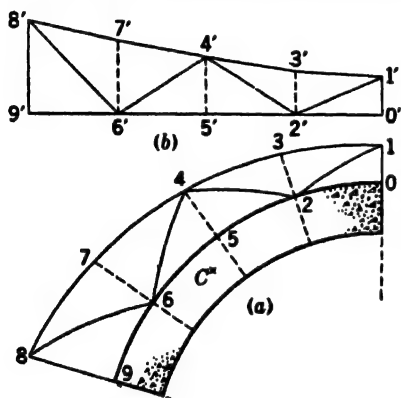


FIG. 56. Standard load patterns for arches.

The magnitude of the partial loads is represented more accurately in diagram *b*, Fig. 56. Intensities may be assumed to vary linearly within each voussoir, causing 1'-3', 3'-4', etc., Fig. 56*b*, to be straight lines. Accuracy is controlled by the number of voussoirs. The area of a figure like 1'-2'-4'-3' is the same as a triangle with base 0'-5' and altitude 3'-2'.

Prior to the completion of the trial load analysis, values of load intensities 1-0, 3-2, etc., are unknown. Following methods heretofore described, all of these intensities are simultaneously assumed and a trial analysis is made. If the result is unsatisfactory, one or more of the assumed intensities are changed and the analysis repeated.

As an alternative, the analysis may be based on a series of unit load computations. The intensity 1-0, diagram *a*, Fig. 56, is assumed to be unity and the

arch is analyzed for the partial load 1-0-2, acting alone or combined with the corresponding partial load immediately to the right of 0. The analysis is made complete, including stresses and deflections. Similar analyses are made separately for the partial loads 1-2-4, 2-4-5, 4-6-8, and 6-8-9, intensities 3-2, 4-5, 7-6, and 8-9 being assumed equal to unity.

If the arch is symmetrical and if it is known that the final trial loads will be symmetrical, the partial loads may be applied in symmetrical pairs; otherwise a separate analysis is required for each partial load on each side of the arch.

The deflections, stresses, and other required functions are determined for each of these unit radial loads for each point at which such functions are needed and the results are tabulated. Similar unit load computations are made for unit tangential loads and unit twist loads. Also, to allow for the effect of cantilever foundation movements on arch deflections, analyses must be made for concentrated unit thrust, unit shear, and unit moment at the abutment. An analysis for temperature drop is also required, but, the temperature change being known, this is a direct analysis. The results of all these analyses are tabulated. Radial, tangential, and twist deflections are listed separately.

Suppose that after the unit load analyses have been made it is desired to find the deflections at point *c*, diagram *a*, Fig. 56, caused by a given set of trial values for 1-0, 4-2, etc. From the table of results of unit load computations read the radial deflection caused by the load 1-0-2 with 1-0 = unity. Multiply this value by the trial value of 1-0. Do the same for 1-2-4, 2-4-6, etc., also for each of unit loads for tangential shear, twist, and concentrated abutment loads, and add the results to get the total radial deflection. The temperature deflections are also included. Find total tangential and angular deflections in the same way. Oblique loads, such as earthquake inertia, are resolved into components and included in the trial radial and tangential loads.

If the deflections thus computed do not agree with the cantilever deflections (computed separately), new trial values are assumed.

The application of the unit load system to isolated cases of special arch forms is of doubtful advantage. After the table of unit load deflections is computed, the effect of numerous sets of trial loads may be found with reasonable rapidity. However, the preparation of the table of deflections is laborious. With only four arch divisions, as illustrated in Fig. 56*a*, if the dam is unsymmetrical, a complete arch analysis is required for each of nine unit radial load patterns, also nine tangential loads, nine twist loads, three abutment concentrations, and one temperature, making a total of 31. The physical and trigonometric functions are constant for all of these analyses and load functions are much simplified. Nevertheless, the labor is appreciable. Consequently, unit pattern loads are generally useful only where a standard arch form can be adopted. In such case, tables can be computed once and for all and used repeatedly.

A set of such tables for cylindrical arches of uniform thickness has been prepared and published by the U. S. Bureau of Reclamation.<sup>30</sup> These tables are based on unit load patterns of the form shown in Fig 57 instead of those shown in Fig. 56. By multiplication and combination, a set of such loads may be made to conform to any trial load pattern, varying linearly in each arch division. Some of the loads may need to be negative. Values of  $\alpha$  vary by degrees and each half-arch is divided into four parts for load determination. Analysis is by integration.

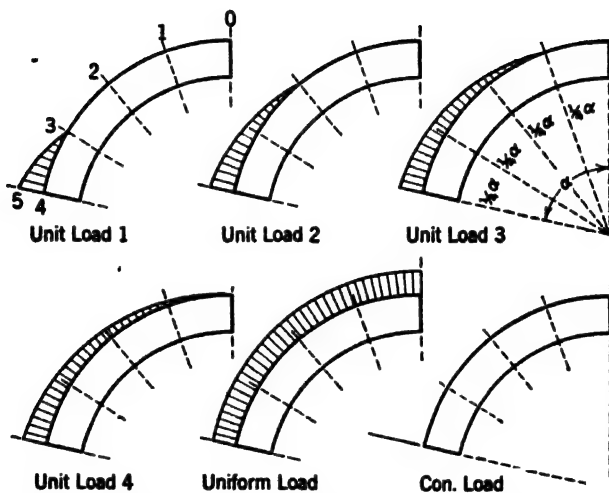


FIG. 57. U. S. Bureau of Reclamation standard load patterns.

It is claimed that the use of these tables, where applicable, saves much effort. Approximate means of applying them to fillet arches are discussed.

Unit load patterns cannot be used if cracking of the arches is to be recognized. They should not be used without a full understanding of the underlying principles.

**45. Unit Loads for Cantilevers.** A unit pattern, similar to diagram b, Fig. 56, may also be applied to the cantilever, unless the cantilevers are cracked. As many of the trial cantilevers usually are cracked, unit loads are seldom helpful.

**46. Recapitulation of Trial Load Method.** The trial load analysis thus presented is far from complete. It is necessary, upon completion of the first trial, to adopt a new set of trial loads, including tangential shears and twists, and to repeat the analysis. The necessary steps have been illustrated but space does not permit their completion.

The reader will recognize the complexity of the problem, which is inherent in the nature of combined arch-gravity action. The approximate nature of

<sup>30</sup> "Trial Load Method of Analysing Arched Dams," U. S. Bur. Reclam., Boulder Canyon Project Final Reports, Part V, Technical Investigations, Bull. 1.

many of the operations should be kept in mind. Computations must be made with extreme care and in some cases apparently absurd accuracy may be required to insure consistency, but any apparent precision of final results should be discounted. Nevertheless, comparisons of computations and experimental measurements show that a carefully made trial load analysis gives dependable results.

As previously stated, not all arched dams need be analyzed in this manner. Little would be gained by the trial load analysis of the simple thin dam of Fig. 6. In fact, with conservative unit stress the cylinder-theory design illustrated is acceptable. It would be preferable and not particularly laborious to apply the elastic theory, assuming independent arches. The analysis would be performed in accordance with an appropriate one of the examples of elastic analysis. In such an analysis the ends might be flared, earthquake loads considered, and other special conditions recognized, as required. Vertical elements in such a dam are no doubt stressed beyond their strength, but this is not necessarily dangerous as long as the arches are able to carry the full load alone.

In the thicker dam of Example 10, vertical beam action is more important, although with a perfectly regular profile it might be ignored without great danger. This might be classed as a borderline example but usually would be analyzed by the trial load method.

In irregular canyons, such as Copper Basin and Ariel, Figs. 29 and 30, stress concentrations may exist which can be revealed only by a trial load analysis or a model test. A complete analysis is essential in such cases.

Also, the trial load analysis (or model test) is the only means of economic design for a massive curved dam such as Boulder.

An experienced designer not familiar with the trial load procedure is likely to be bewildered by the work involved. Indeed, such analysis is a major undertaking but not at all impossible or impracticable and the cost need not be out of proportion to the importance of the structure. An ingenious squad leader soon develops short-cuts and processes which lead with reasonable rapidity to satisfactory results. It is essential that the work be done under the leadership of someone with a complete but practical comprehension of the process. Such a comprehension is readily acquired.

The procedure illustrated is general. Simplifications are sometimes permissible. For example, minor foundation factors will frequently be found to have small effect and the twist factors may at times be negligible, particularly in preliminary trials. Possible simplifications suggest themselves as the work progresses.

#### MODEL TESTS AND EXAMPLES OF ARCH DAMS

**47. Model Analysis of Arch Dams.** (a) *General statement.* As an alternative to computations made as hereinbefore described, or as a supplemental check, arch dams may be analyzed by measuring the stresses in a loaded scale model. The tests may be applied to a monolithic model of the whole structure

or to "one dimensional" slices. Both mechanical and photoelastic methods have been used.

(b) *Stevenson Creek Dam.* One of the earliest arched dams to be subjected to model test was the Stevenson Creek Dam, constructed in 1926 for experimental purposes near Big Creek, Calif., under the auspices of the Engineering Foundation. This dam was a thin, single-arch structure, 60 ft high. Provision was made for rapidly filling and emptying the very small basin above the dam and equipment was provided for measuring strains and deflections. Also, small scale models of concrete were tested at Boulder, Colo., by U. S. Bureau of Reclamation engineers, and a celluloid model by Prof. George E. Beggs at Princeton University. The results were recorded in a series of bulletins issued by the American Society of Civil Engineers.<sup>40</sup>

Although the difficulties inherent in the measurement of stresses in an actual structure or a model of it, particularly if of concrete, were found to be greater than had been anticipated, the results obtained by mathematical analysis and by measurement on the full-sized structure and models were reasonably concordant. These comparative studies went far toward establishing confidence in the trial load method of analysis.

(c) *Boulder Dam.* Because of its outstanding importance, Boulder Dam was analyzed with the greatest care. It was subjected to a very extensive mathematical analysis and to exhaustive model tests. Descriptions of these analyses and tests, and of many other technical matters concerning the design and construction of Boulder Dam, are to be covered in a series of bulletins issued by the U. S. Bureau of Reclamation, Denver, Colo. A number of the bulletins already have been printed (1943), and others are to appear as available time for their preparation permits. Anyone interested should write to the Chief Engineer, U. S. Bureau of Reclamation, Denver, Colo., for an up-to-date list.

The work done at Boulder has contributed in an outstanding manner to the theory of arch dam design, particularly in substantiating some of the more obscure facts of the trial load theory.

(d) *Photoelastic analysis.* The analysis of loaded transparent models of celluloid or other suitable material by polarized light has become well established in the last decade or so. In this process, polarized light passed through flat models under stress show color bands, the number and nature of which indicate the magnitude and distribution of stresses. Such tests are very effective in showing stress patterns and concentrations at corners, around holes, and in all kinds of structures of special shape. For example, photoelastic analysis is very helpful in the study of stresses at the base of a gravity dam and around openings, some of the rules in Chapter 12 having been checked or deduced in this manner.

It is possible to analyze individual arch or cantilever slices from an arch dam photoelastically. However, such an analysis involves more time, equip-

<sup>40</sup> Engineering Foundation, Committee on Arch Dam Investigations, Vol. 1, 1928; Vol. 2, 1931; Vol. 3, 1933.

ment, and skill than a mathematical analysis, and because of the difficulty of accurately reproducing physical conditions and loading, the results are not more dependable. Consequently, a photoelastic study is valuable chiefly as a check under unusual conditions and as an aid in visualizing conditions at corners and at other irregularities.

(e) *Practicability of model tests as a method of design.* Any competent mathematician, mechanically inclined, well-informed theoretically, and naturally inclined to painstaking research, should be able to approximate the stresses in an arch dam by model tests. However, model testing has not yet been developed to such a point as to justify its substitution for mathematical analysis of dams.

Strains and deflections in models are minute, and their precise measurement involves difficulties. Physical similarity is difficult to obtain. A concrete scale model of a dam loaded with water is stressed and deflected very little. Consequently, other more yielding elastic materials, such as rubber compounds, special plasters, and plastics, usually are required, and they must be loaded with mercury or by some system of loading greatly in excess of normal water pressure. Special materials are of variable characteristics and all of their properties must be determined for each test. Their action is not in all cases similar to the action of the concrete in the dam.

In gravity dam studies the element of weight must be considered. Stresses and strains produced by the weight of a 6-foot-high model of any ordinary material are negligible. This has led to the use of gelatins.

The overcoming of these difficulties and many others not mentioned requires vigilance and resourcefulness. Unless the work is done with extreme care, too much dependence cannot be placed on the accuracy of the results. However, model testing is a valuable check on the correctness of the mathematical analysis of important dams although not yet a practical tool for use alone. Such tests should be undertaken only by competent personnel with adequate equipment.

It must be remembered in making comparisons that mathematical analyses likewise involve uncertainties, as pointed out elsewhere in this chapter. It is not the intention to discourage the use and development of model work but rather to sound a warning that, for the present, model testing must be considered as supplemental to mathematical analysis rather than as a substitute for it.

**48. Examples of Arch Dams.** The Boulder Dam, the most notable dam in the world, towering 726 ft above its foundation, is of the gravity-arch type. Much of its tremendous water load is transferred to the abutments by arch action. The general arrangement of this structure is shown in Fig. 58. A photographic view is shown in the frontispiece.

Quite naturally, plans for this dam were subjected to an analytical study far surpassing anything done before. It was here that the trial load method received its greatest advancement. Extensive model studies also were undertaken for the determination of stresses and hydraulic performance. It was

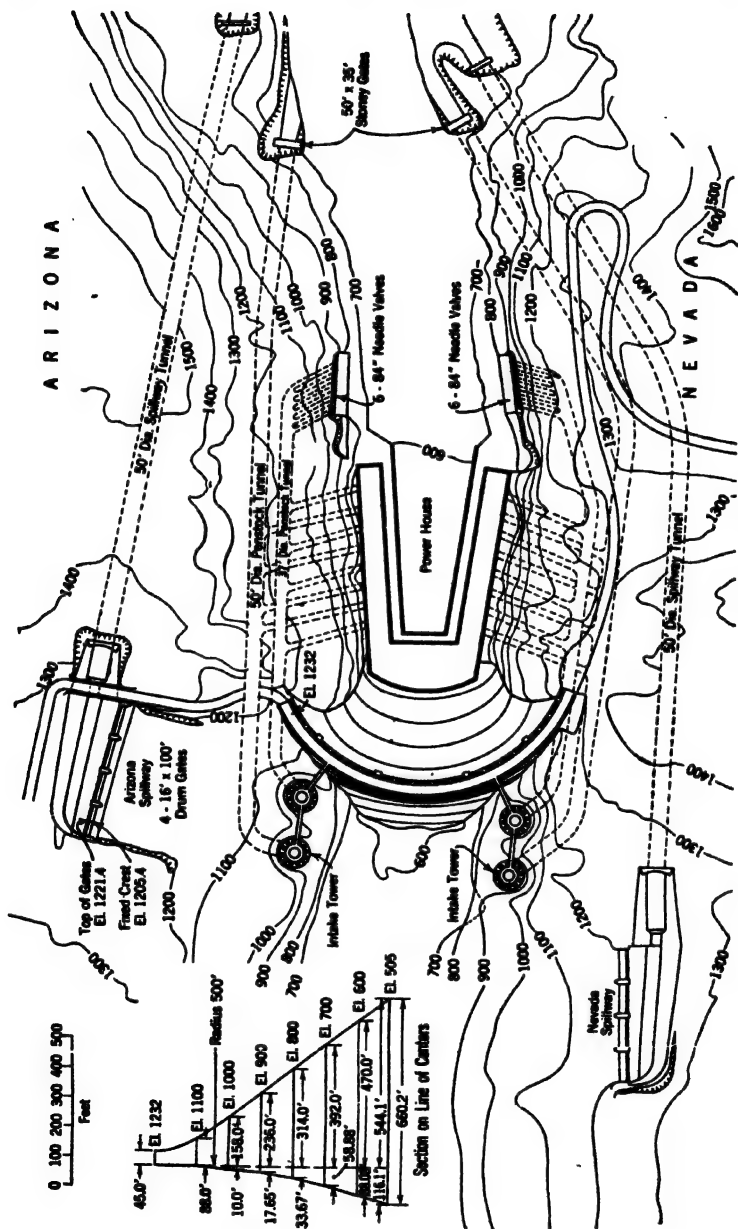


Fig. 58. Boulder Dam and appurtenant work.

among the first dams to be constructed with low-heat cement and the first in which artificial cooling was extensively used. To control cracking due to shrinkage and to insure adequate arch action, it was divided both axially and transversely by contraction joints. The result was a columnar effect. After cooling, these joints were grouted to produce a virtual monolith.

Space does not permit a complete description of the dam, its design or its construction, but many published articles concerning it are available.<sup>41</sup>

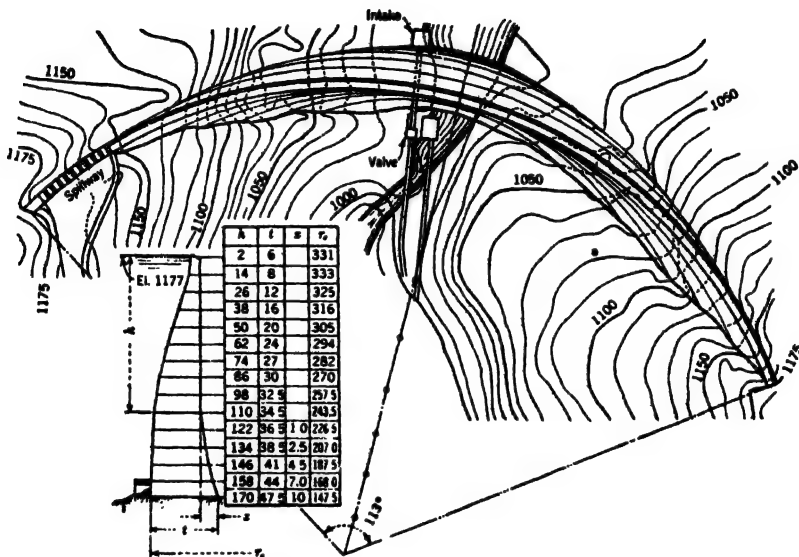


FIG. 59. Salmon Creek Dam, Alaska (*Trans. Am. Soc. Civil Engrs.*, Vol. 78).

A variable-radius dam of more usual dimensions is shown in Fig 59. This dam was constructed by the Alaska Gastineau Mining Company on Salmon Creek, Alaska, in 1914. It was not based on the trial load theory.

Fig. 60 represents a relatively small arch dam at Cheyenne, Wyo. The maximum cylinder stress is only 23,000 lb per sq ft, and slenderness ratio at the top is 35. A spillway is provided around the end of the dam.

Fig. 61 shows one of a number of notably slender small arch dams in Australia.

Fig. 62 shows the arrangement of the Calles Dam, Aguascalientes, Mexico, completed by the Mexican Government in 1928, and one of the early trial load structures.

Figs. 29 and 30 show other examples of trial load designs for arch dams.

<sup>41</sup> Dams and Control Works, 1938. Final Report, Boulder Dam, Part IV, Design and Construction Bulletin, and other bulletins of the same series, all by the U. S. Bur. Reclam.



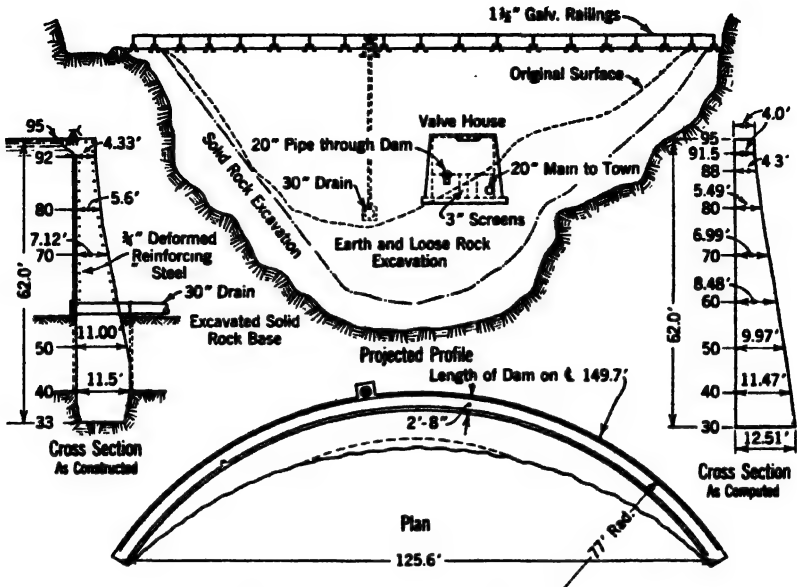


FIG. 60. North Crow Dam. (*Eng. Record*, Vol. 67, p. 149.)

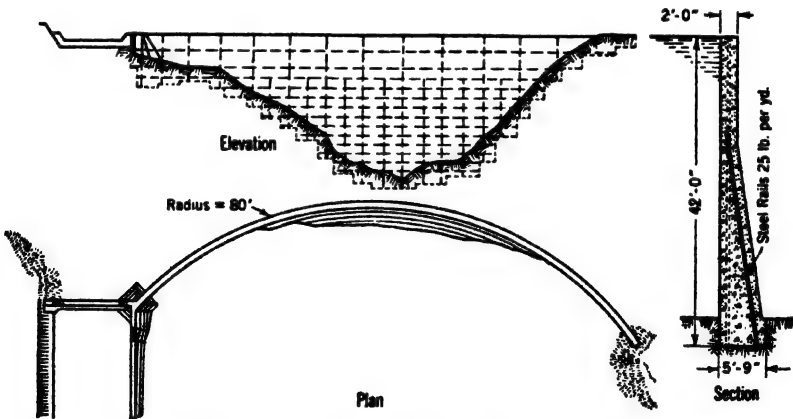


FIG. 61. Barren Jack Creek Dam Australia. (*Eng. Record*, Vol. 61, p. 664.)





Table 31 contains a compilation of data for a number of arch dams. This table, which was compiled by R. A. Sutherland, is an extension of a similar table contained in *Masonry Dams*.<sup>42</sup>

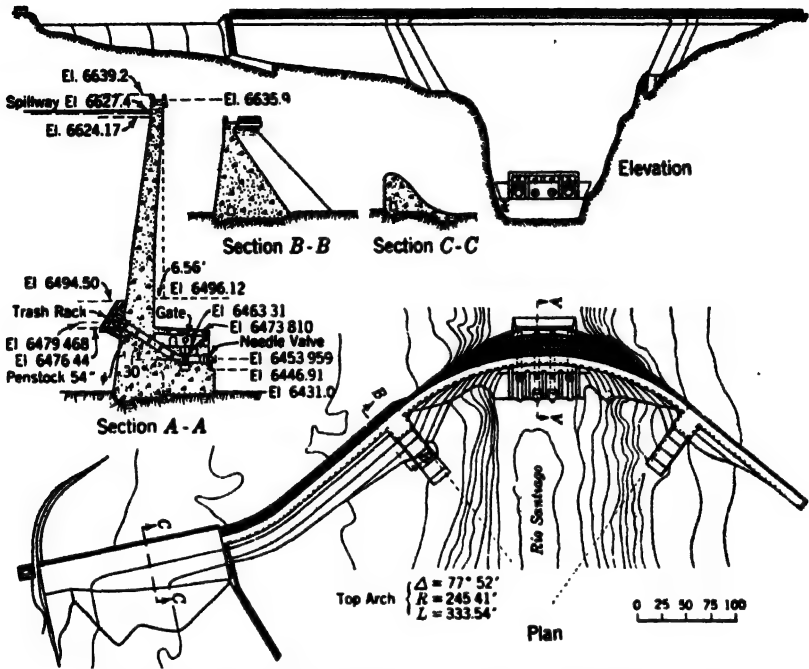


FIG. 62. The Calles Dam, Mexico. (*Civil Eng.*, Aug. 1931, p. 1010.)

For data on additional dams see Table XXIV of *Masonry Dams* and also Proceedings, American Society of Civil Engineers, May 1928, "Report on Arch Dam Investigation," Vol. 1, p. 24.

<sup>42</sup> WILLIAM P. CREAGER, 2nd Ed., John Wiley & Sons, 1929.

## CHAPTER 14

### BUTTRESSED CONCRETE DAMS

**1. Advantages of Buttressed Dams.** As has been explained in other chapters, solid gravity dams resist the forces acting against them primarily by weight alone. Strength of masonry is critical only when the height is great, and then only over limited areas. In massive arch dams, described in Chapter 13, the strength of the masonry is more fully developed. However, not all dam sites are suitable for massive arches.

Frequently, a reduction in cost with no sacrifice in safety can be effected by a dam of structural form. Because of the more efficient development of latent strength, masonry quantities are reduced. More intricate form work and the need for reinforcement increase unit costs, but under favorable conditions an appreciable net saving in total cost may be achieved. This is particularly true in locations where the cost of procuring or transporting the cement required for a more massive structure is prohibitive, or where other construction materials are scarce.

The more efficient use of masonry strength does not necessarily mean higher maximum pressures than are permitted in gravity structures. However, with carefully placed reinforced concrete, increased stresses may be allowed. If these occur at the base, better and more carefully prepared foundations may be needed. This can be offset by the use of spread footings. (See Art. 12.)

Buttressed dams are more subject to damage or destruction by sabotage or military attack than massive dams. Because of the thinness of their members they are sensitive to even moderate deterioration of the concrete; hence they must be carefully built and careful consideration must be given to any unusual exposure conditions.

**2. Types of Buttressed Dams.** The use of buttresses to reinforce and strengthen masonry structures is of ancient origin. Many early solid gravity dams of otherwise relatively thin sections were made stable by such means. One of many such old dams found in the Republic of Mexico is shown in Fig. 1.

The present chapter deals with more recent types where a relatively thin facing is supported by buttresses in such manner as to secure true structural action. Buttressed dams are adaptable to overflow as well as nonoverflow conditions. In overflow dams a downstream deck is provided to guide the falling stream. Typical buttressed sections are shown in Figs. 2 and 3, which are taken from an unpublished preliminary study for a U. S. Bureau of Reclamation dam in Idaho (1924).

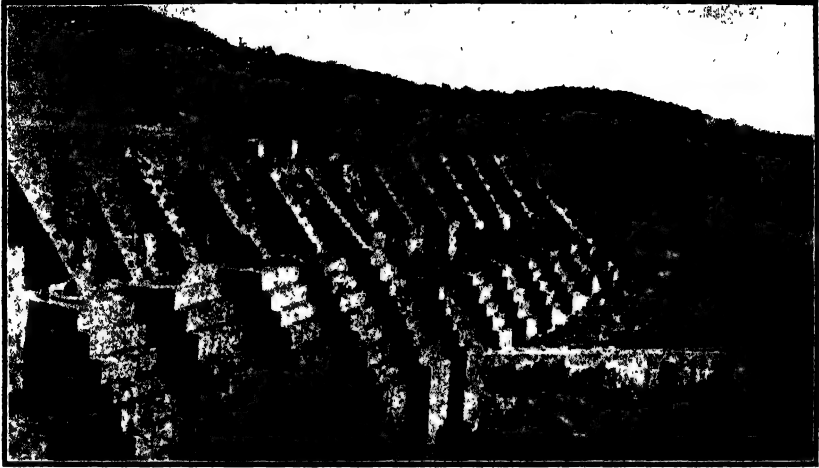


FIG. 1. Los Arcos Dam, Aguascalientes, Mexico.

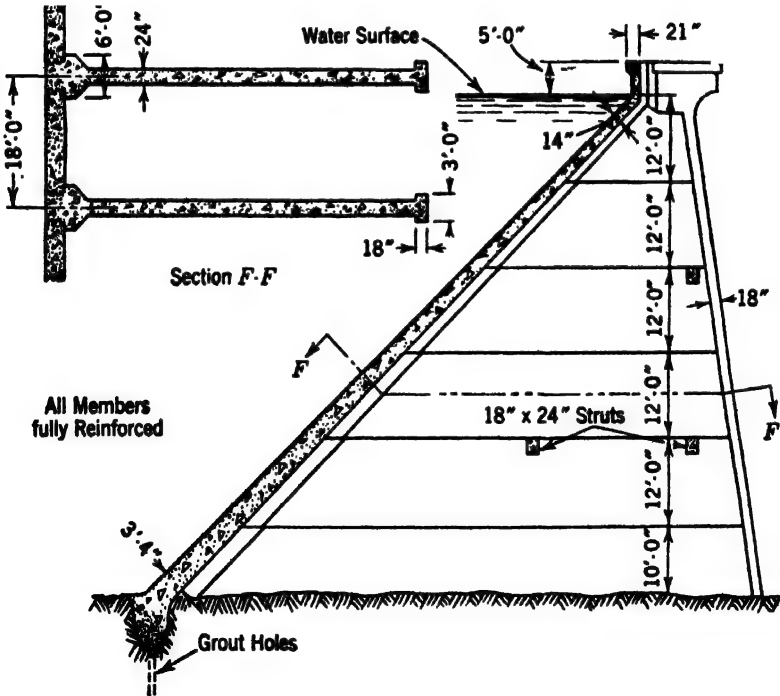


FIG. 2. Slab and buttress dam.

Because of the small volume of masonry, the upstream face is inclined so that a portion of the water pressure may be utilized to provide a safe sliding factor. Five typical forms of facing are illustrated in Fig. 4.

Of the three flat slab decks shown, the simple beam type shown at *a* is most commonly used. Action of the continuous deck type shown at *b* is uncertain if there is any unequal settlement of foundations. Also, occasional joints are required to minimize shrinkage and temperature effects. The authors know of no actual use of the cantilever deck type, shown at *c*.

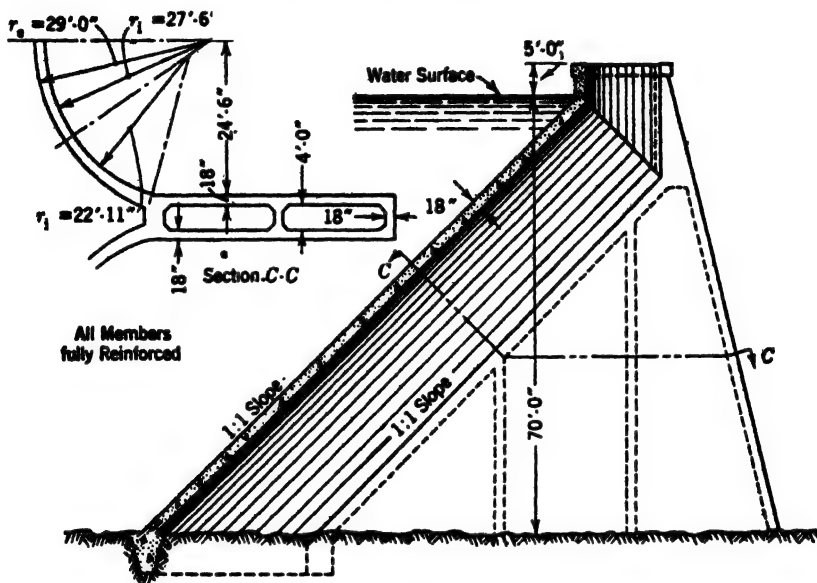


FIG. 3. Multiple-arch dam.

The round-head buttress type, shown at *d*, was proposed by the late F. A. Noetzi about 1925.<sup>1</sup> The buttress heads are enlarged to full span width and the faces are curved in such manner that the water pressure is transmitted to the buttress in compression. Buttress heads are not reinforced.

In the multiple-arch type shown at *e*, the water load is taken by a series of inclined arches which span the spaces between the buttresses. The arches are analyzed according to the principles established in Chapter 13. If tensile stresses are encountered, reinforcement may be used.

A number of types of buttress dams are illustrated in the examples and figures which follow. Also, Table 1, compiled by Robert A. Sutherland in 1940, lists the principal dimensions of 39 of the world's most notable buttress dams.

<sup>1</sup> See EDWARD WEGMANN, *Design and Construction of Dams*, John Wiley & Sons, Inc., N. Y., 1927, p. 523.

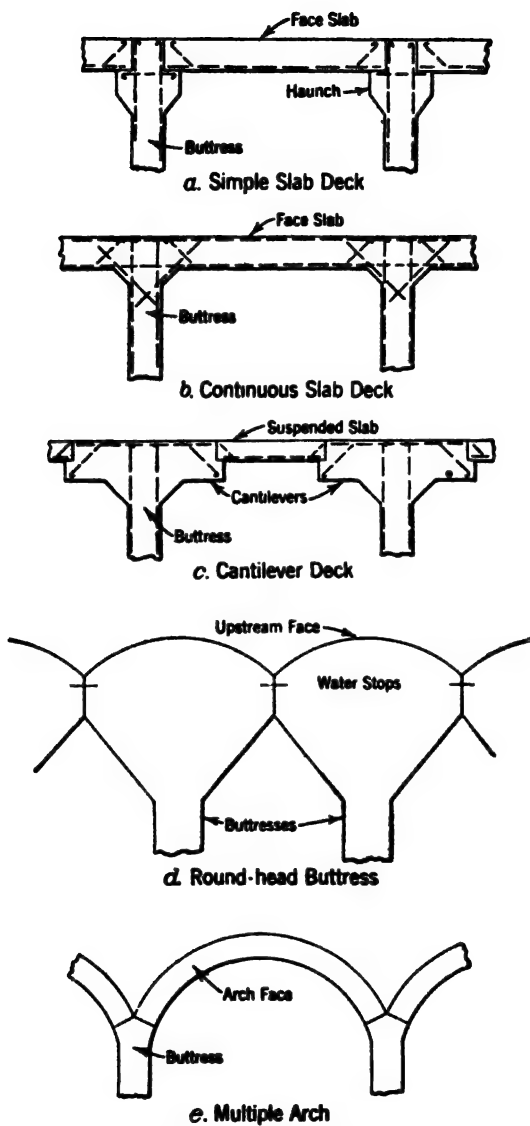


FIG. 4. Types of buttress dams.



**TABLE**  
**DIMENSIONS OF NOTABLE**  
[Compiled by

Item	Name	Location	Type	Max. Height (ft)	Up- stream Slope (deg)	But- tress Spacing (ft) (in)	Buttress Thickness	
							Top (ft) (in)	Bottom (ft) (in)
1	Aasensire	Norway	Multiple arch	190	Varies	43	2	8 3
2	Anyox	Canada	Multiple arch	156	Varies	24	18	10 1
3	Beni Bahdel	Algeria	Multiple arch	164				
4	Big Dalton	Calif., U. S. A.	Multiple arch	180	48	60	2	4 3 <sup>1</sup>
5	Bristol	N. H., U. S. A.	Slab	100				
6	Bartlett	Aris., U. S. A.	Multiple arch	286	48	60	2	7 <sup>1</sup>
7	Castrola	Italy	Multiple arch	226				
8	Cave Creek	Calif., U. S. A.	Multiple arch	107	Varies	44	12	8 10
9	Combamala	Italy	Slab	138	55	18	14	6 1
10	Coolidge	Aris., U. S. A.	Multiple dome	249	Varies	180	20	80
11	Don Martin	Mexico	Round-head buttress	105	57	29 6	6 7	6 7
12	Florence Lake	Calif., U. S. A.	Multiple arch	149	48	50	2 3	7 10
13	Gem Lake	Calif., U. S. A.	Multiple arch	112	50	40	18	4 3
14	Gleno	Italy	Multiple arch	164	53	26 3	6 6	11 3
15	Guajabal	Puerto Rico	Slab	120	44	18	14	3 6
16	Hamilton	Texas, U. S. A.	Multiple arch	154	48	35 70	3	9
17	Jordan River	Canada	Slab	126	77	18	12	3 6
18	Lago d'Avio	Italy	Multiple arch	105	60	40		
19	Lago Nero	Italy	Multiple arch	112	62	20		
20	Lake Hodges	Calif., U. S. A.	Multiple arch	136	45	24	18	4 2
21	Lake Lure	N. C., U. S. A.	Multiple arch	122	45	41	24	7 6
22	Lake Pleasant	Aris., U. S. A.	Multiple arch	256	47	60	18	5 6 <sup>4</sup>
23	Mountain Dell	Utah, U. S. A.	Multiple arch	150	50	35	18	8
24	Murray	Calif., U. S. A.	Multiple arch	112	45	30	12	4 4
25	Ogden	Utah, U. S. A.	Multiple arch	100	65	49		16 6
26	Palmdale	Calif., U. S. A.	Multiple arch	175	45	24	15	5
27	Pavana	Italy	Multiple arch	177	60	54	6 6	20
28	Pensacola	Okla., U. S. A.	Multiple arch	155	48	84	24	4 6 <sup>1</sup>
29	Pit River No. 4	Calif., U. S. A.	Slab	120				
30	Possum Kingdom	Texas, U. S. A.	Slab	180	50		8	9
31	La Prele	Wyo., U. S. A.	Slab	148	40	18	14	4 2
32	Rodriguez	Mexico	Slab	240	45	22	19	5 6
33	Stony Gorge	Calif., U. S. A.	Slab	125	45	18	18	
34	Sutherland	Calif., U. S. A.	Multiple arch	180	45	60	3 4	10
35	Tidone	Italy	Multiple arch	171	45	32 10	2 4	7 2
36	Tiger Creek	Calif., U. S. A.	Slab	100				
37	Tinco	Italy	Multiple arch	239	57	49 3	8 2	23 10
38	Venina	Italy	Multiple arch	170	Vertical	50 6		
39	Webber	Calif., U. S. A.	Multiple arch	120	76	140 93 87	4	

<sup>1</sup> Each wall hollow.<sup>2</sup> Increased in height in 1933.<sup>3</sup> Subsequently failed.<sup>4</sup> At 180 ft from top.<sup>5</sup> At 200 ft from top.<sup>6</sup> Increased in height in 1924.<sup>7</sup> Foundation arch over fault.<sup>8</sup> Provided with foundation slab.

1

## BUTTRESS DAMS

Robert A. Sutherland, 1940]

Arch Sub-tended Angle (deg)	Slab or Arch Thickness		Foundation	Width of Footing (ft)	Sliding Ratio	Concrete (cu yd)	Length (ft)	Year Built	Reference
	Top (ft) (in)	Bottom (ft) (in)							
180	16	6 3					690	1922	17
100	12	3 6		172	0.72		684	1924	16
	2	5 6		204		45,000	1,050	1937	<sup>a</sup> 4-36
							480	1928	16
							525	1924 <sup>†</sup>	<sup>P</sup> 8-17-33
180	2 4	7	Granite	360		180,000	740	1938	<sup>Y</sup> 11-39
130	12	4	Cemented gravel	89	1.07	18,700	680	1923	
	16	4 6				15,000	310	1916	17
Varies	4	20 1	Quartzite	258	0.73	204,000	600	1929	16
			Limestone		0.87		800	1930	<sup>†</sup> 1932
156	18	4 6	Granite	164		57,000	3,160	1926	16
120	12	3 7	Rock			8,500	640	1916	<sup>†</sup> 1917
180	16	2 7	Porphyry				730	1922 <sup>‡</sup>	16
	12	4 7				44,000	920	1913	17
	2 4	3 4	Granite				8,377	1937	<sup>†</sup> 9-37
	12	3 2				21,000	780	1912	17
121	21	2						1924	17
								1924	17
120	12	2 7	Rock			18,200	558	1917	16
130	12	3 8				40,000	585	1927	16
96	18	5 6 <sup>a</sup>		253		103,000	1,975	1927	16
133	15	4 10	Seamy rock				560	1917 <sup>a</sup>	16
	12	2 6	Porphyry			8,200	900	1917	
	6	8					340	1896	17
100	15	4 3		200		25,000	648	1924	16
180	24	5 7				47,000	470	1925	16
150	2 4	4 4	Limestone	200		230,000	4,284	1940	<sup>P</sup> 2-1-40
						42,700		1928	
	5	9	Shale	256	0.46	325,000	1,640	1940	<sup>P</sup> 6-8-39
	12	4 6				22,500	365	1910	17
	2 1	5 6	Rhyolite and Granite <sup>†</sup>	256		190,000	2,200	1935	<sup>P</sup> 10-16-30
	15	4 2	Shale		0.60	37,000	808	1928	2
130	18	6 4	Granite				1,100	1928	16
180	14	3 0	Shale <sup>a</sup>				900	1925	16
						13,500	470	1932	
	20	5 6	Trachyte			214,000	930	1923	16
	20	4 1						1926	16
130	24	12 10					320	1923	16
114									
62									

<sup>a</sup> Travaux, Paris, France.<sup>P</sup> Engineering News-Record, New York.<sup>Y</sup> New Reclamation Era (now Reclamation Era), Washington, D. C.<sup>†</sup> Transactions, Am. Soc. Civil Engineers.<sup>‡</sup> Construction Methods, New York.

**3. Forces on Buttressed Dams.** Buttressed dams on rock foundations are subject to the same forces as other dams except that the downward component of the water pressure is greater and uplift is less. In fact, because of the easy lateral escape of pressure under the buttresses, uplift from headwater in the case of rock foundations is usually neglected. However, where the rock is liable to uplift pressures on horizontal seams, the foundation should be drilled for drainage. Full uplift from tailwater should always be included. Buttressed dams on pervious foundations may require footing slabs designed to resist uplift loading. Such dams are briefly discussed in Art. 12. Wind pressure, which is neglected in other dams, may merit consideration if a diagonal wind of high velocity can reach the downstream side. On high thin buttresses, such pressures may increase the danger of buckling. Because the wind cannot strike the buttress face normally, a pressure of 10 lb per sq ft over a width not exceeding the clear distance between buttresses should be safe. Authoritative data are lacking. For well-braced or double-walled buttresses, such pressures are of little importance.

**4. Earthquake Loading for Buttressed Dams.** Earthquake forces are computed by rules established in Chapter 7. Slab and round-head buttress dams are particularly efficient in resisting such forces, because of small mass relative to rigidity for individual units, coupled with ability of the dam as a whole to yield to slight permanent displacements.

For general stability, the most unfavorable direction of motion for such dams is upstream horizontally. For the deck slabs, the maximum masonry inertia load is for motion normal to the face. Definite rules for the computation of the increased water pressure on the inclined face are lacking. The approximate rules established in Arts. 13e and 13f of Chapter 7 may be followed.

Cross-stream acceleration is unimportant for straight-faced dams. Unreinforced buttresses may need checking for slab strength under lateral loading, but the buttresses cannot overturn sidewise.

For multiple-arch dams, the most important earthquake effect may come from transverse motion.

The force resulting from the inertia of the masonry in the arch barrels is readily computed. Unless the buttresses are stable in themselves or are securely braced against lateral displacement, they must be held against overturning sidewise by the arches. This introduces an accumulating transverse load, applied at the spring lines and transmitted to the abutments by the arches. The resulting stress may be of appreciable magnitude. The load is difficult to compute but may be approximated by dividing the buttress into blocks and computing the force required to prevent overturning, proceeding step by step from the top downward.

The small volume of water in the troughs over the piers adds to the uncertainty of increased water pressure from cross-stream acceleration. This effect has generally been ignored, although not on the side of safety.

**5. Spacing of Buttresses.** The spacing of the buttresses is governed by economy. If the spans are short, face slabs or arches may be thin with a small volume of masonry. On a simple unit stress basis, the buttress thickness would be proportional to the span, and total thickness for the dam would be constant. Practical considerations preclude the use of very thin walls; hence beyond certain limits the volume of individual buttresses remains constant regardless of spacing. The result is a more or less definite economic limit to the spacing.

Many factors enter into the determination of this limit. Two buttresses each 2 ft thick cost more to construct than one buttress 4 ft thick. The cost of excavation and foundation treatment is also greater for two thin buttresses than for one thick one. For very long spans the cost of falsework for the facing may be high, and secondary stresses in the haunches may be troublesome.

Economic buttress spacing increases with the height of the dam. Usually the height is variable, giving a variable economic spacing. Variable spacing is usually avoided by the adoption of a standard for the entire dam. Separate standards for the abutments and the central portion of the dam may be used if desired, but this is not the usual practice.

**6. Design of the Buttresses.** Buttresses for all of the dam types shown in Fig. 4 are analyzed for stability in a manner similar to that used for gravity dams, Chapters 10 and 11. The design element, instead of being a slice of unit thickness, is taken as a full panel.

In addition to meeting the stability requirements for gravity dams, the buttress must conform to the design rules for structural concrete members.

The buttresses may be considered as vertical cantilever beams of variable cross-section. Both the width and the thickness may vary. The width must be sufficient to avoid tension at the upstream face when fully loaded and also to avoid excessive compression at the downstream face. As in all beams, simple bending stresses are smallest for a given cross-sectional area if the buttress is made wide and thin. However, if too thin, failure may occur by buckling.

In order to fix the required thickness of buttresses to prevent buckling, they are considered to be bearing walls instead of beams, the minimum allowed thickness being the same as for columns. According to the "Joint Committee" report on "Recommended Practice and Standard Specifications for Concrete and Reinforced Concrete,"<sup>2</sup> a reduction in stress must be made where the unsupported length exceeds ten times the thickness.

It is usual to reduce the unsupported length by means of struts or to increase the width of the compression face by adding a flanged section. Both of these devices are illustrated in Fig. 2 and both may be used.

In high dams, additional flanges or pilasters may be added along the width of the buttress, either in place of or in addition to the struts. The Florence

<sup>2</sup> Sec. 804b, p. 45, *Proc. Am. Soc. Civil Engrs.*, June 1940

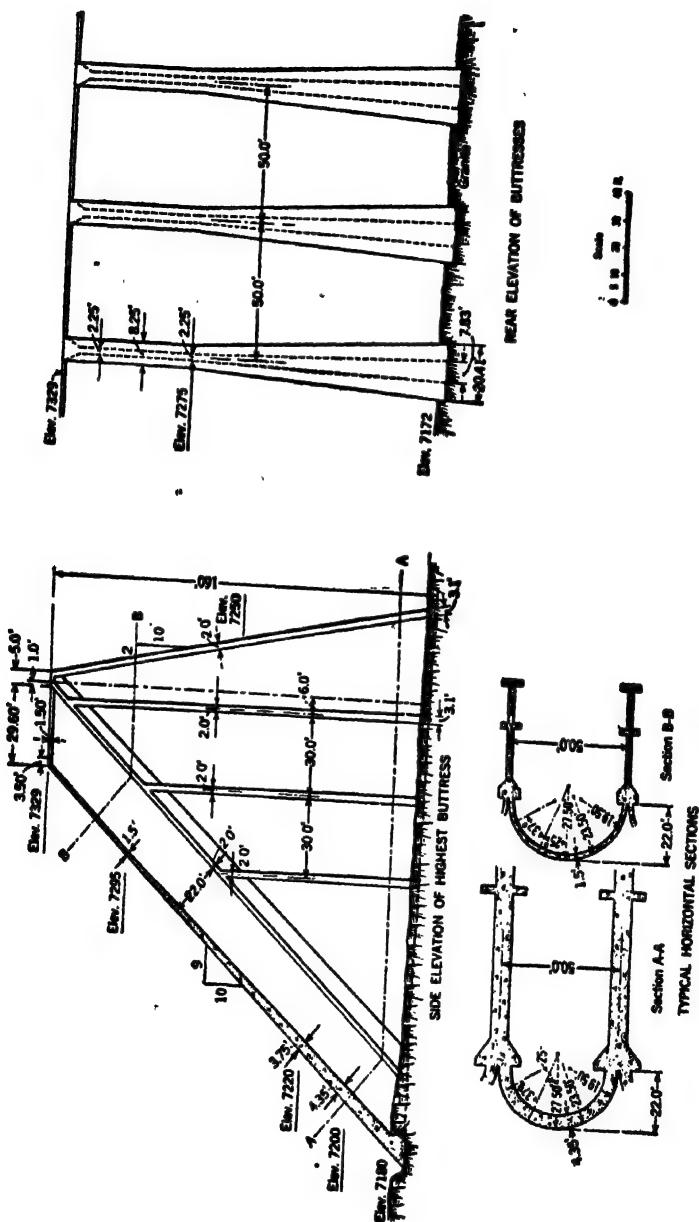


FIG. 5. Florence Lake Dam.

Lake Dam, California, shown in Fig. 5,<sup>3</sup> illustrates the use of pilasters. There are no established rules for the dimensions or spacing of pilasters and struts. However, the unsupported length in the highly stressed portions of the buttress should not exceed ten times the effective thickness. At other places the unsupported length may be increased to 15, provided the stresses are not in excess of 50 per cent of allowed stresses.

The reinforcement in the struts is usually continuous through at least three bays, but in some cases it has been carried continuously throughout the structure, with no deleterious effects from contraction. The struts should abut solidly against the abutments. The horizontal building joints in the buttresses should be at the elevation of the struts if practicable.

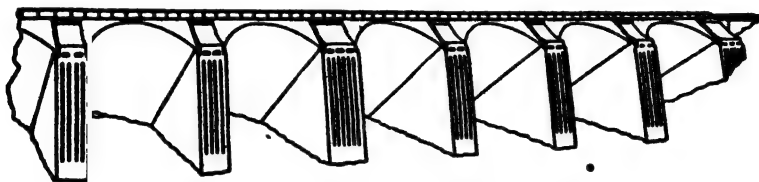


FIG. 6. Architectural use of double buttresses.

In multiple-arch dams, where the economic span is usually greater than for other buttressed types, the need for struts and pilasters may be eliminated by using double-wall or hollow buttresses, each stable within itself. This type, proposed by Noetzli in 1924,<sup>4</sup> has been used in a number of dams. Mr. Noetzli's example is described under Example 3, Arts. 27 to 32 of this chapter. Essential details are shown in Fig. 15.

A system of tie walls and struts between the webs assures unity of action. A buttress of this type can be made secure against buckling without resort to long struts between buttresses.

Double-walled buttresses have a distinct advantage as to appearance, particularly in high dams. An architectural treatment of the buttresses and the top of the arches, suggested by V. H. Cochran<sup>5</sup> is reproduced in Fig. 6.

**7. Beam Stresses in Buttresses.** Horizontal and vertical forces and moments on the buttresses are computed as for gravity dams. The joint between the facing and the buttress is sufficiently rough that the facing will follow the buttress in case of overturning; hence the full weight of the facing and of all other parts of the dam above any section being analyzed is included with the downward forces.

Examples of alternative buttress-slab connections are shown in Fig. 4. For monolithic deck and buttress, as illustrated in Fig. 4b, and for multiple arches actually tied to the buttresses, Fig. 4e, the buttress and a half-span

<sup>3</sup> WEGMANN, *The Design and Construction of Dams*, 1927, Pl. JJJ.

<sup>4</sup> F. A. NOETZLI, "Improved Type of Multiple Arch Dam," *Trans. Am. Soc. Civil Engrs.*, Vol. 87, 1924, p. 346.

<sup>5</sup> *Idem*, discussion, p. 371.

of deck on each side act as a T-beam. In the simple slab type, Fig. 4a, T-beam action is rendered somewhat uncertain by reduced shearing strength along the joint between the slab and the buttress. However, friction is assumed to hold the slab against movement on this joint, and it is not unreasonable to assume monolithic action. Also, because of increased eccentricity of the vertical loads, the maximum compressive stress in the buttress, which occurs at the downstream face, is greater for the buttress-slab T-beam combination than for the buttress alone. The reverse is true at the upstream face, but buttress compression there is not critical, hence it is on the side of safety to assume unit action. (See Art. 18 for numerical illustration.) If there is any possibility of a critical upstream cantilever stress in the buttress, the condition of buttress alone should be investigated. As in structural T-beams, only the web (buttress) is assumed to resist shear.

With the cantilever deck, Fig. 4c, the suspended deck is excluded in computing buttress stresses.

For round-head buttresses, the buttress and buttress head are treated as a unit.

Vertical unit pressures are assumed to be linearly distributed, as for gravity dams. They are computed from Eq. 41 or 41a, Chapter 7. Values at the faces are found from Eqs. 42 and 43, or 42a and 43a, Chapter 7. These equations are of the general form applicable to nonrectangular bases. If uplift is considered, it is treated in accordance with the rules of Chapter 7.

Rules for computing the moment of inertia for irregular sections will be found in works on mechanics.

Inclined stresses at the faces are computed by Eqs. 5a and 6a, Chapter 8. The normal pressure  $p_n$  at the upstream face is the water pressure, as for a solid dam.

Shearing stresses and principal stresses at interior points may be computed according to principles discussed in Chapter 12. Because of complexity of form and action, the applicability of the ordinary assumptions of stress distribution to buttresses is more uncertain than in the case of gravity sections. However, they give a general idea of buttress action. Any uncertainty is absorbed in the factor of safety used for stresses. In especially important cases, resort may be had to model studies.

There is an intensified normal force along the junction between the buttress and the buttress head or facing. As an approximation, the principal stress along this junction plane may be assumed to be equal to the "normal" pressure due to the panel water load and the normal component of the weight of the facing and buttress head. This approximate stress usually will be less than the true principal stress by a small percentage, which may be assumed to be absorbed in the factor of safety. If the stress computed in this manner approaches the danger point, an internal stress analysis may be made.

The resultant must be so located that  $p''$  (Eq. 6a, Chapter 8) will be positive even though  $p_n$  and  $\tan^2 \phi''$  have appreciable values. This is accom-

plished by adjustment of the buttress width. In fact, the resultant usually can be made to fall near the center of gravity of the buttress, thus approximating a uniform distribution of vertical pressures.

**8. Inclination of Buttress Faces.** The upstream face of a buttressed dam is inclined to provide the vertical water load required to insure stability. The downstream face is inclined only as required to provide an adequate buttress width. In most existing dams, the upstream slope,  $\tan \phi''$ , ranges from 1.00 to about 0.70. The steepest slope that will satisfy stability requirements is economical.

Near the top of the dam the face can usually be steeper than at lower elevations, because the width of the top is greater than needed for stability, and the amount of masonry may be reduced by using a variable slope for the water face. This principle has been utilized in a few dams,<sup>6</sup> but the general practice is to use a straight upstream face except for a short vertical lift at the top.

**9. Shrinkage Cracks and Buttress Reinforcement.** Concrete in buttresses as in all other structures is subject to shrinkage. The base of the buttress is prevented from shrinkage on account of contact with the foundation, particularly when on rock. As a result, vertical or inclined shrinkage cracks tend to form in the buttresses. Such cracks, observed in many dams, usually run more or less in the direction of the planes of minimum principal stress (see Chapter 12), although apparently not specifically related to stresses caused by loading. Should such a crack assume a disadvantageous direction, it would weaken the buttress. Cracking can be avoided or controlled by reinforcement, by contraction joints, or by a combination of these means.

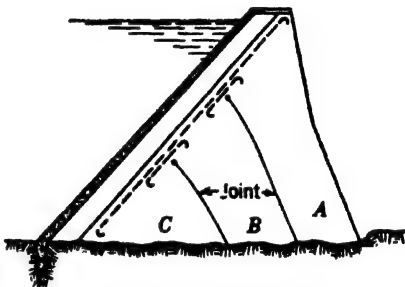


FIG. 7. Big Dalton Dam.

The use of contraction joints is illustrated in Fig. 7, which shows a buttress of the Big Dalton Dam, California.<sup>7</sup> This buttress is reinforced, and part of the steel passes through the joints which no doubt influences their effectiveness. No appreciable cracking has been observed. Similar joints were used in the Possum Kingdom Dam, illustrated in Fig. 2 of Chapter 23.

Buttresses built in vertical columns, separated by gaps filled in after the main portions of the buttress has shrunk, are discussed in Art. 36 of this chapter.

<sup>6</sup> WEGMANN, *Design and Construction of Dams*, Cave Creek Dam, Arizona, and Anyox Dam, Canada, 1927, pp. 482 and 500.

<sup>7</sup> F. A. NOETTL, "Stresses in Buttressed and Gravity Dams," Discussion, *Trans. Am. Soc. Civil Engrs.*, Vol. 98, 1933, p. 1006.



A special type of joint used in the Pensacola Dam is illustrated in Fig. 1 of Chapter 23.

**10. Buttresses of Uniform Strength.** Schorer has suggested that buttresses should be so shaped that the first principal stress will be equal to the allowable limit in compression, and the second principal stress zero at all points.<sup>8</sup> How this is to be accomplished is illustrated in Fig. 8.

Any small portion of the face, 1-2, is assumed to be supported by a curved column, 1-2-3-4-5-6, which constitutes part of the buttress. The curvature of the center line of the column is found by combining weight elements with the force,  $P$ . It is possible to compute the form of the curve and the area of the column for the face segment, 1-2, and for other similar segments.

The widths and thicknesses of the "columns" may be adjusted to produce a continuous buttress, which may be poured monolithically or with joints following theoretical "column" boundaries. The thickness, of course, is variable. Schorer presents equations and curves for use in computations.

This example is presented because of its value in illustrating buttress action. So far as the authors know, no dam utilizing this principle has been constructed. As illustrated in Fig. 8, the separate columns would be in exact equilibrium with maximum load and

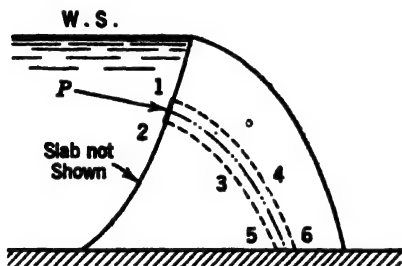


FIG. 8. Buttress of uniform strength.

consequently would have a factor of safety against overturning of only one. This would need to be remedied in an actual design by making the weight of each column exceed its theoretical value by a factor of safety.

**11. Connection of Facing with the Foundation.** Particular care must be taken with the connection of the facing of a buttressed dam with the foundation rock. A connection tight against leakage under high pressure must be secured in a relatively short distance. Usually a cutoff trench is excavated into sound rock. Fissures are closed by grout or other means. Important fissures may need to be cleaned out and refilled with concrete. At the Rodriguez Dam in Lower California, Mexico, a shaft was excavated to a depth of 300 ft in a (presumably) dead fault, and refilled with concrete.<sup>9</sup> Similar but much less extensive treatment is frequently required.

The facing may be made monolithic with the cutoff or may be joined to it in any satisfactory manner. The joint must be tight under all conditions of deformation. For multiple-arch dams, the effect of foundation restraint on normal arch action must be considered.

<sup>8</sup> HERMAN SCHORER, "The Buttressed Dam of Uniform Strength," *Trans. Am. Soc. Civil Engrs.*, Vol. 96, 1932, p. 666.

<sup>9</sup> C. P. WILLIAMS, "Foundation Treatment at Rodriguez Dam," *Trans. Am. Soc. Civil Engrs.*, Vol. 99, 1934, p. 295.

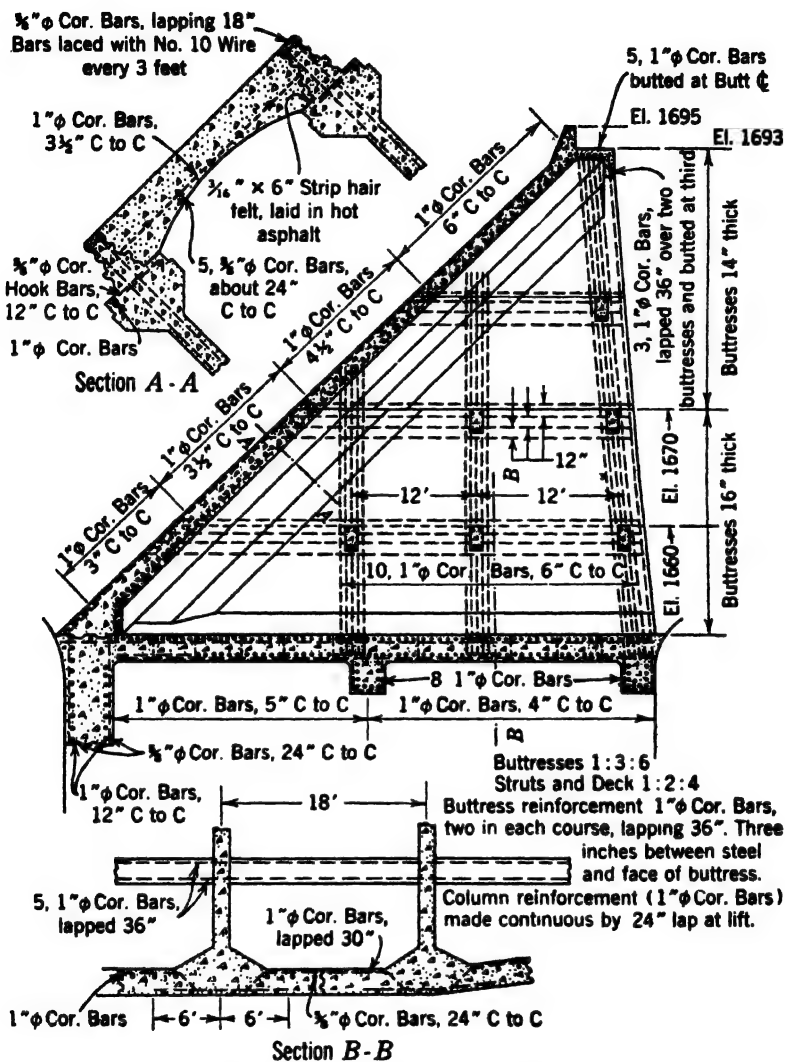


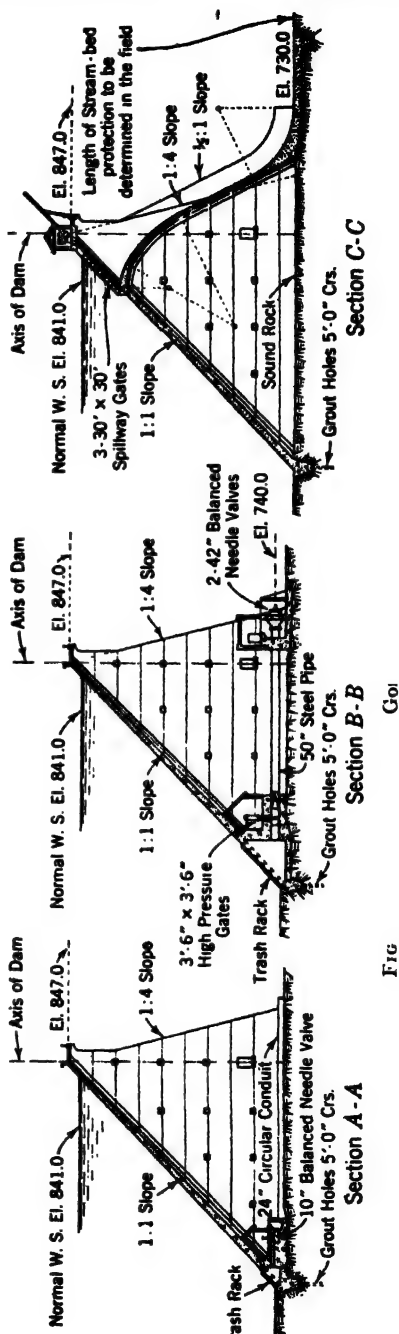
FIG. 9. Details of Mathis Dike Dam.

**12. Buttressed Dams on Soft Foundations.** Any of the buttressed dams described in this chapter may be adapted to soft foundations by the use of spread footings, or if necessary, complete foundation slabs or inverted arches may be provided as in Fig. 9 to reduce the foundation pressure to allowable limits. If the foundation is porous, the upstream cutoff must be carried to an impervious stratum, or, if this is not possible, the foundation slab must be designed for uplift and made of sufficient length to provide the required percolation distance. (See Chapter 3 for treatment of porous foundations.) If uplift is not allowed for, the foundation slab should be provided with large weep holes which should be protected from freezing, and the foundation must be safe against piping through the weep holes.

### EXAMPLES OF SLAB AND BUTTRESS DAMS

#### 13. Example 1, Simple Slab Dam.

No attempt will be made to present all of the computations for a buttressed dam, but the method of checking the stability and stresses at a given level in a previously designed structure will be shown. The Stony Gorge Dam, constructed by the U. S. Bureau of Reclamation in 1928<sup>10</sup> is chosen for this purpose. General dimensions and arrangements are shown in Fig. 10.<sup>11</sup> Because of the spillway near its central portion, this structure illustrates both the over-



FIG

<sup>10</sup> S. E. ROCKWELL, *Dams and Control Works*, U. S. Bur. Reclam., 2nd Ed., 1938, p. 70.

<sup>11</sup> "Stony Gorge Dam," Drawing No. 3, U. S. Bur. Reclam. Spec. 449,

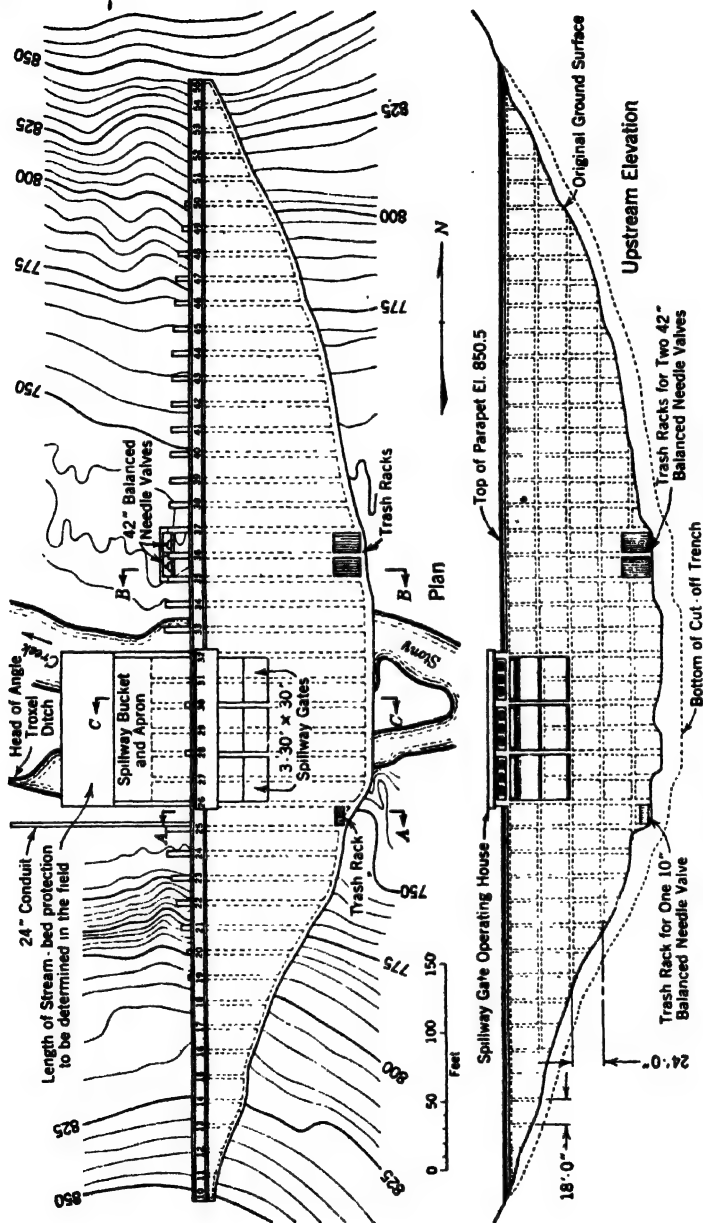


FIG. 10 (continued). Example 1, Stony Gorge Dam, general plan.

flow and nonoverflow types. Example No. 1 will relate to the analysis of the nonoverflow section, using the following data:

Flood level at elevation 847, top of roadway slab, and 6.0 ft above "normal" water level,

$h_1$  = depth of water on joint to be analyzed = 109 ft,

Buttress spacing = 18 ft, center to center,

$w_1$  = weight of reinforced concrete = 150 lb per cu ft,

$w_2$  = weight of water = 62.5 lb per cu ft,

$h_2$  = depth of tailwater at joint to be analyzed = 0,

$p'_i$  and  $p''_i$  = maximum allowed inclined compressive stress in buttress = 50,000 lb per sq ft,

$J$  = working value of the coefficient of friction of the joints and base = 0.65,

$s_a$  = allowable value of average unit shear on a horizontal plane = 100 lb per sq in.,

$f_c$  = ultimate compressive strength of concrete at 28 days = 3000 lb per sq in.,

$f_s$  = allowable stress in reinforcing steel = 18,000 lb per sq in.,

$n$  = modulus of elasticity for steel divided by same for concrete = 12.

Use "Joint Committee" specifications for reinforced concrete design.<sup>12</sup>

The specification of both a sliding factor and a unit shear for the buttress is a duplication. The buttress being in compression throughout should withstand greater average shear than that allowed for beams in flexure. The limitations here specified are not necessarily those used in the original design.

**14. Form and Spacing of Buttresses.** The designer of this dam followed the usual practice of using a straight upstream buttress slope. The best slope to use is found by trial; for economy it should be as steep as will yield satisfactory sliding factors and stresses. It is usual to assume a trial slope and to correct it as the design proceeds. The slope of the *under side* of the slab in the example is 45°.

The buttress spacing of 18 ft was chosen by comparative estimates. Because the economic spacing varies with the height, such estimates must embrace the whole structure. According to Rockwell<sup>13</sup>

Studies and estimates were made of comparative costs for the finished structure, with buttress spacings of 16, 18, 20, 22, and 24 feet, and with face slabs of corresponding thicknesses; also for heights of dam varying by 12-foot lifts up to 120 feet. The results of the estimates indicated that the usual buttress spacing of 18 feet was the most economical for this structure.

A maximum section of the nonoverflow portion of the dam is shown in Fig. 11.<sup>14</sup> The analysis is to be made on the horizontal section *B-C*, using dimensions for the lift above the joint.

<sup>12</sup> See *Proc. Am. Soc. Civil Engrs.*, June 1940, or current revision of this specification

<sup>13</sup> S. E. ROCKWELL, *op. cit.*, p. 78.

<sup>14</sup> Drawing No. 6, "Stony Gorge Dam," *U. S. Bur. Reclam. Spec.* 449.

**15. Slab Analysis, Example 1.** With the moments and shears known, the slab thickness at any depth is computed as for other reinforced concrete structures. According to Fig. 11, the slab begins with an arbitrary minimum thickness of 15 in. at the top and increases to 46.5 in. at the section chosen for analysis. As tabulated on the figure, the slab is reinforced at section B-C with 1-in. round bars on 4-in. centers.

The normal water load is  $109 \times 62.5 = 6812$  lb per sq ft. The slab itself weighs 581 lb per sq ft, the component normal to the buttress face being  $581 \sin \phi'' = 411$  lb per sq ft. Therefore, the total load to be borne by the slab in flexure is  $6812 + 411 = 7223$  lb per sq ft.

Assuming, for the time being, that the buttress head and corbel dimensions tabulated on Fig. 11 will be found correct, the distance, center to center, of end bearings is  $12 \text{ ft } 3\frac{1}{2} \text{ in.}$  The resulting bending moment on the slab is

$$M = 0.125 \times 7223 \times 12.3^2 = 137,000 \text{ ft-lb per ft width, or in.-lb per in. width of slab}$$

The clear span is 10 ft 7 in. and the maximum shear is

$$0.5 \times 7223 \times 10.58 = 38,600 \text{ lb}^*$$

With 1-in. round bars on 4-in. centers, 3 in. from the face of the slab, the percentage of reinforcement is 0.45 and

$$\frac{M}{d^2} = \frac{138,600}{(43.5)^2} = 73$$

For  $n = 12$ , the resulting concrete and steel stresses are approximately <sup>15</sup>

$$f_c = 580 \text{ lb per sq in.}$$

and

$$f_s = 18,000 \text{ lb per sq in.}^{16}$$

The average unit shear at the face of the corbel is 81.7 lb per sq in. These stresses are within the limits allowed by the standard specifications, provided the bars are turned up and shear steel is used.

**16. Corbel Details, Example 1.** A typical detail of the junction of buttress and slab is shown at *a*, Fig. 11. A buttress extension separates and anchors the face slabs. Corbels are used to support the edges of the face slabs. The width, *S*, of the bearing face of the corbel must be such that the allowable bearing pressure will not be exceeded. The exact form of the reaction diagram between the slab and the corbel is not known. In computing the slab strength (see Art. 15), the center of bearing is taken at the center of the corbel face. It is probable that the stress concentration increases toward the end of the corbel. To be on the safe side in computing the strength of the corbel, the

<sup>15</sup> TURNHAURE and MAURER, *Principles of Reinforced Concrete Construction*, John Wiley & Sons, 1935, diagram 4, p. 415.

<sup>16</sup> Tabulated stresses in Fig. 11 are based on design assumptions probably different from those used here.

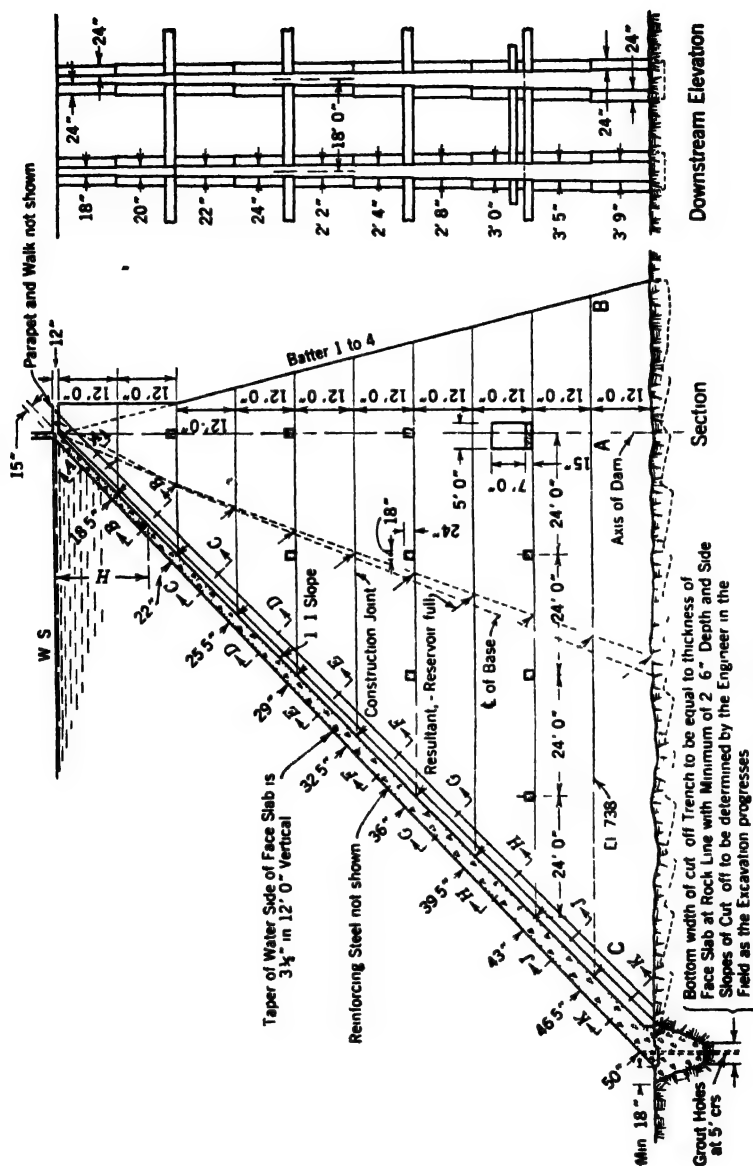


FIG. 11. Example 1. Stony Gorge Dam, nonoverflow section.



(a) Typical Section thru Face Slab

(b) Section thru Buttress Footing

H	Section	Dimensions				Face Slab				Buttress Corbel				Buttress					
		M	N	S	T	Reinforcing Steel		Concrete		Reinforcing Steel		Concrete		Maximum Compression		Sliding Factor	H Ft		
						Spacing of 1'-φ	f <sub>s</sub> # / □ "	u # / □ "	f <sub>c</sub> # / □ "	v @ O # / □ "	f <sub>s</sub> # / □ "	f <sub>c</sub> # / □ "	v @ R # / □ "	# / □ "	Tons / □ "				
6	A-A	16 3/4"	9"	9"	18"	12"	12,500	133	380	20	14"	5,200	81	19	25	50	3.5	.45	.12
18	B-B	20 3/4"	11"	10"	20"	7"	15,600	139	573	42	14"	12,900	181	42	45	81	5.9	.56	.24
30	C-C	23 3/4"	13"	11"	22"	5 1/4"	16,400	145	623	55	10 1/2"	15,000	227	59	61	106	7.6	.60	.36
42	D-D	2'-3 3/4"	15"	12"	24"	4 1/4"	16,000	142	624	66	8"	15,400	252	73	75	130	9.3	.62	.48
54	E-E	2'-6 3/4"	17"	13"	2'-2"	4"	15,400	137	594	72	6 3/4"	15,200	261	82	87	145	10.4	.63	.60
66	F-F	2'-10 3/4"	19"	14"	2'-4"	4"	16,800	145	587	76	5 1/4"	16,700	298	90	97	170	12.3	.63	.72
78	G-G	3'-1 3/4"	21"	16"	2'-8"	4"	16,800	148	566	77	4 1/4"	15,200	286	97	98	176	12.7	.63	.84
90	H-H	3'-5 3/4"	23"	18"	3'-0"	4"	17,000	150	542	78	4"	16,000	307	102	100	183	13.2	.62	.96
102	I-I	3'-8 3/4"	2'-1"	20 3/4"	3'-5"	4"	17,000	149	513	78	3 3/4"	15,500	293	99	99	185	13.4	.61	1.08
114	K-K	4'-0 3/4"	2'-3"	22 3/4"	3'-9"	4"	16,900	148	502	77	3 3/4"	16,500	292	97	100	195	14.0	.60	1.20

FIG. 11 (continued). Example 1, Stony Gorge Dam, stability and stress data.



reaction diagram may be assumed to be triangular, with the maximum at the outer end.

All of the details should be proportioned in accordance with current rules for the design of reinforced concrete structures.<sup>17</sup>

The thickness of the buttress extension need not be the same as that of the buttress. The buttress reinforcement should be anchored into the extension. The corbels should be tied together with sufficient steel to assure adequate flexural and shearing strength.

As a general guide, the following relations for corbel dimensions are suggested:

$$\begin{aligned} R &= >0.8M, \text{ but not greater than } t, \text{ unless required for standardization of} \\ &\quad \text{slab spans,} \\ N &= 0.75 \text{ depth of face slab to steel,} \\ S &= 0.50T, \\ C &= S + 0.5(R - T), \\ D &= 1.25C, \end{aligned}$$

where notations are as shown at *a*, Fig. 11.

The corbel dimensions of Example 1, as tabulated on Fig. 11, are somewhat smaller than suggested above and at section *B-C* are as follows:

$$\begin{aligned} M &= 46.5 \text{ in., net } 43.5 \text{ in.,} \\ R &= 4 \text{ ft } 0 \text{ in. (constant),} \\ N &= 2 \text{ ft } 2 \text{ in.,} \\ T &= 3 \text{ ft } 5 \text{ in.,} \\ S &= 0.5T = 20.5 \text{ in.,} \\ C &= 24 \text{ in. (constant),} \\ D &= 24 \text{ in. (constant).} \end{aligned}$$

Falsework and forms are simplified if the clear distance, face to face of corbels, on adjacent buttresses is made constant, i.e., if the buttress heads are of constant width. In low dams this can be accomplished without difficulty. In high dams buttress heads adequate for lower elevations are unwieldy near the top. In such case the clear distance may be changed in stages, i.e., two or more standard buttress heads may be used.

In Example 1, the width of the buttress head is variable, changing in each 12-ft lift. The buttress extension is of a uniform thickness of 4 ft 0 in., giving a constant total slab span of 14 ft. This simplifies main slab reinforcement and adds to upstream appearance. Constant values for *C* and *D* simplify corbel form work.

The stresses in the adopted corbel must, of course, be checked, and dimensions changed if necessary. The bearing area of the flange is  $20.5 \times 12 = 246$  sq in. The total load for a half-slab slice is  $7223 \times 7.00 = 50,560$  lb, which is 206 lb per sq in., average, or 412 lb per sq in. at the edge of the

<sup>17</sup> See Joint Committee Report, *Proc. Am. Soc. of Civil Engrs.*, June 1940.

assumed triangular reaction. This is within the limits allowed by the specifications.

The bending moment at the foot of the short cantilever is  $13.67 \times 50,560 = 691,200$  in.-lb per ft width. Standard rules for concrete beams apply only approximately to this short cantilever of variable depth. The beam depth is  $N + D - 3$  in. = 47 in. The steel consists of  $\frac{5}{8}$ -in. round bars at  $3\frac{1}{2}$ -in. centers, which is 1.06 sq in. per ft, or 0.19 per cent in a 47-in. beam, and  $M/bd^2 = 28$ . The steel stress is about 16,000 lb per sq in., and the concrete stress is low. These ties should be securely anchored by bending or hooking over longitudinal bars.

The unit shear, at the foot of the corbel, allowing 3 in. to the center of the ties, is  $50,560 \div (12 \times 47) = 90$  lb per sq in., which is within allowable limits.

**17. Stability of Buttresses, Example 1.** Forces, moments, and location of resultants for the buttress are shown in Table 2. Moments are taken about a reference point *A* on the joint *B-C*, Fig. 11. Units of kips and foot-kips are used.

TABLE 2

STONY GORGE DAM, EXAMPLE 1 •

[Analysis at 108 ft below top of face slope; water depth 109 ft]

Line	Item	Forces (kips)		Arm (ft)	Moment (ft-kips)
		Horis.	Vert.		
1	$W_1$ Concrete (comps. not shown)		4.415	39.02	172,250
2	$W_2$ Water, $0.5 \times 62.5 \times 18 \times 109 \times 113.7$		6.971	74.60	521,430
3	$P_1$ Water, $0.5 \times 62.5 \times 18 \times 109^2$	6,683		36.33	-242,790
4	Totals, reservoir full	6,683	11,386	(39.6)	450,890

The total weight of the masonry above the joint is recorded in line 1 of the table, also the corresponding lever arm and moment. Detailed computations for this line are not shown. A full panel length of slab, a complete buttress, and appurtenances for a panel, are included.

The vertical component of the water pressure for a full panel width is computed in line 2, horizontal water pressure for a full panel width in line 3, and totals for reservoir full in line 4.

The lever arm in line 1 represents the distance from point *A* to the resultant, reservoir empty, and that in line 4 the same for reservoir full. The position of the resultant never is a problem in a dam of this type, and the condition of reservoir empty is not likely to require investigation.

Dividing the total horizontal force by the total vertical force, both from line 4, the inclination of the resultant is found to be

$$\tan \theta = \frac{6,683}{11,386} = 0.59$$

This value is smaller than that shown on Fig. 11, probably due to variation in assumptions, and is well within the specified limits. Should a similar condition be found at all heights, the upstream face could be steepened. It is usually economical to have as steep an upstream face as the allowed maximum value of  $\tan \theta$  will permit.

**18. Vertical Pressures, Buttresses of Example 1.** The section of the buttress (including the corbels and slab) is not rectangular and  $p'_u$  and  $p''_u$  are assumed zero; hence the vertical compressive stresses are found by Eqs. 42a and 43a of Chapter 7.

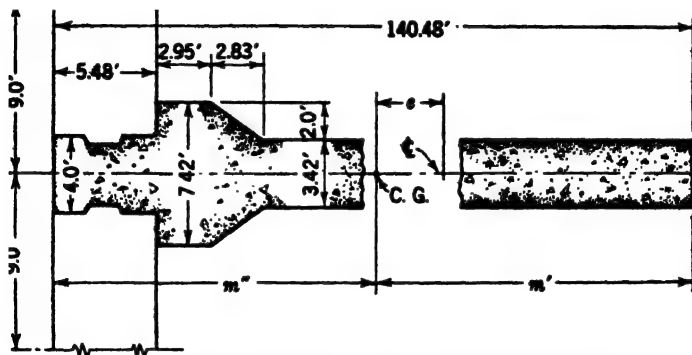


FIG. 12. Horizontal section at elevation 738, Example 1.

To illustrate numerically the influence of the slab and corbels on the computed cantilever stresses, as discussed in Art. 7, consideration will be given to four cases as follows:

- (a) Full T-section, including corbels and slab,
- (b) T-section with slab but without corbels,
- (c) buttress and corbels without the slab, and
- (d) buttress alone, ignoring slab and corbels.

All computations are for a horizontal section, as shown in Fig. 12. Areas, moments of inertia, and dimensions for the four cases are shown in Table 3. Values of  $e'$ , in the last column, represent distances from the point at which the resultant cuts the base to the center of gravity of the base. These values are found by subtracting the lever arm from Table 2 (39.6 ft) and the distance  $A-B$ , Fig. 11 (27 ft), from  $m'$ . The vertical pressure computations are completed as follows:

In case *a*

$$p'_s = \frac{\Sigma(W)}{A} + \frac{e'm'\Sigma(W)}{I}$$

$$\frac{11,386,000}{576.92} + \frac{14.78 \times 81.38 \times 11,386,000}{1,065,000}$$

$$32,600 \text{ lb per sq ft}$$

**TABLE 3**  
**DATA FOR SECTIONS SHOWN IN FIG. 12**

Item	$A$ (sq ft)	$I$ (ft) <sup>4</sup>	$e$ (ft)	$m''$ (ft)	$m'$ (ft)	$e'$ (ft)*
Case <i>a</i> , buttress, slab, and corbel	576.92	1,065,000	11.14	59.10	81.38	14.78
Case <i>b</i> , buttress and slab	559.46	1,018,000	9.55	60.69	79.79	13.19
Case <i>c</i> , buttress and corbels	497.90	775,000	2.19	68.05	72.43	5.83
Case <i>d</i> , buttress alone	480.44	709,000	0.00	70.24	70.24	3.64

\*  $e'$  = distance from center of gravity of base to resultant.

The value of  $\Sigma(W)$  is from Table 2, and other values are from Table 3. Changing the plus sign to minus and substituting  $m''$  (59.10 ft) for  $m'$  gives the corresponding value of  $p''$  at the upstream face. The vertical pressures for the other cases are found in the same way, the results, in pounds per square foot, being as follows:

In case *a*,  $p'_c = 32,600$ ;  $p'' = 10,400$

In case *b*,  $p'_c = 32,100$ ;  $p'' = 11,400$

In case *c*,  $p'_c = 29,100$ ;  $p'' = 17,000$

In case *d*,  $p'_c = 27,800$ ;  $p'' = 19,600$

This tabulation illustrates (1) that in computing the vertical pressures at the downstream face it is on the side of safety to use the combined buttress, slab, and corbel sections (case *a*); (2) that at the upstream face it is safer to omit the slab or even the slab and corbels, although as a rule this is unimportant because upstream vertical pressures are not critical; and (3) in view of the inaccuracy of computed cantilever stresses in a wedge-shaped beam, such as the buttress of Example 1, it is permissible to simplify computations by omitting the corbels where the buttress width is great.

**19. Inclined Pressures, Buttresses of Example 1.** Maximum inclined pressures at the ends of the joint, for full reservoir, are computed from Eqs. 5a and 6a, Chapter 8. There being no tailwater,  $p'_n$ , Eq. 5a, is zero. Also, at the downstream face

$$\tan \phi' = 0.25; \sec^2 \phi' = 1.0625$$

Using these values and the computed values of  $p'_c$ , the inclined pressure at the downstream faces for the combined buttress, slab, and corbel, is found thus:

$$p'_i = 32,600 \times 1.0625 = 34,600 \text{ lb per sq ft}$$

At the upstream face  $\tan \phi'' = 1.00$ ,<sup>18</sup>  $\sec^2 \phi'' = 2.00$ , and  $p_n$  is simple water pressure, which is  $109 \times 62.5 = 6810$  lb per sq ft.

The corresponding inclined stress at the upstream face, for case *a*, using vertical pressures from Art. 18, is

$$p_i'' = 10,400 \times 2 - 6810 = 13,990 \text{ lb per sq ft}$$

For case *c*, combined buttress and corbel, the corresponding stress is

$$p_i'' = 2 \times 17,000 - 6810 = 27,190 \text{ lb per sq ft.}$$

The maximum stress in the upstream portion of the buttress is not necessarily at the face but may occur at the junction of the corbel with the buttress. As explained in Art. 7, an approximate value of this stress may be obtained by assuming the first principal stress to be normal to the plane of the junction between corbel and buttress and equal to the total normal panel load divided by the thickness of the buttress. For this purpose, the panel load should include the normal component of the weight of the buttress head. For Example 1, the total panel load to the bottom of the corbel at elevation 738 is

$$\begin{aligned} \text{Water load} &= 109 \times 62.5 \times 18 &= 122,600 \text{ lb} \\ \text{Slab} &= 3.88 \times 18 \times 150 \sin \phi'' &= 7,400 \text{ lb} \\ \text{Buttress head} &= 22.85 \times 150 \sin \phi'' &= 2,400 \text{ lb} \\ \text{Total for panel strip 1 ft wide} &&= 132,400 \text{ lb} \end{aligned}$$

Dividing by the buttress thickness, the corresponding approximate value of the first principal stress is

$$p_i'' = \frac{132,400}{3.42} = 38,700 \text{ lb per sq ft}$$

which is the highest stress found in the section but is still within the specified limit.

**20. Horizontal Shear, Buttresses of Example 1.** Although the sliding factor, separately determined, is low, the average horizontal shearing stress is one of the limiting factors specified in Art. 13 and will be computed. In computing this average shear, only the true buttress web area is used, ignoring slab, corbel, and any flanges or pilasters. For Example 1, using the horizontal force from line 4, Table 2, the average shear is

$$s_a = \frac{6,683,000}{140.48 \times 3.42 \times 144} = 97 \text{ lb per sq in.}$$

which is slightly below the specified value of 100 lb per sq in.

<sup>18</sup> Neglecting slight difference in slope of two sides of face slab.

**21. Recapitulation of Stresses, Buttresses of Example 1.** All of the inclined stresses and the approximately determined principal stress at base of the corbel, Art. 19, are well within the specified limit of 50,000 lb per sq ft. The average shear, computed in Art. 20, is slightly less than the 100 lb per sq in. limit, and the slab and corbel stresses, Arts. 15 and 16, and the sliding factor, Art. 17, are safe. Stresses must of course be checked at other levels.

**22. Reinforcement of Buttresses, Example 1.** The buttresses of Stony Gorge Dam, Example 1, were built in 12-ft lifts and were provided with a triple network of reinforcing bars near each face. In describing this dam, S. E. Rockwell<sup>19</sup> states that:

The buttresses were first designed with  $\frac{5}{8}$ -inch round bars, 18 inches on centers, placed diagonally and parallel to the face slabs in both sides of the buttresses; and with  $\frac{5}{8}$ -inch round bars 3 feet on centers, placed vertically in both sides of the buttresses. After several of the largest buttresses were started, vertical shrinkage cracks began to appear, and it was decided to add horizontal reinforcement in all buttresses below the bottom of the third lift. The horizontal bars were distributed along both faces of the buttresses, and the area of the steel used amounted to approximately 0.3 of 1 per cent of the vertical cross-sectional area of the concrete. This percentage of longitudinal steel appears to have stopped all vertical cracking.

Many buttressed dams have been constructed without buttress reinforcement. Generally, the buttresses have cracked, some so seriously as to require extensive betterments. Other buttresses, reinforced less elaborately than Stony Gorge, are giving satisfactory service. In fact, a moderate amount of cracking is not necessarily disastrous. However, any appreciable cracking is disturbing, and the modern tendency is toward adequate reinforcement.

**23. Example 2, Overflow Slab Dam.** A typical section of the overflow portion of Stony Gorge Dam is shown at C-C, Fig. 10. The crest and upper portion of the downstream slab are of (approximate) standard shape for an overflow crest with a 1 : 1 upstream slope, as established in Art. 2, Chapter 11. Except for low dams, the lower portion of the downstream slab may be made straight, as for the solid overflow dam. The radius of the bucket can be determined from Fig. 12, Chapter 11.

The downstream slab theoretically carries no water load at maximum overflow but carries some weight at lower discharges. Failure of the back slab during a flood might cause much damage, for which reason it is usual to provide ample strength. The extreme requirement would be that the slab have strength to support the full normal component of the weight of the over-falling sheet. This conservative rule usually does not give excessive slab thicknesses.

The downstream slab may be attached to the buttresses in any convenient manner, connections similar to (a) and (b), Fig. 4, being permissible. If continuous construction is used, an occasional contraction joint is advisable. In any event, the anchorage of the slab to the buttress must be substantial. The connection used at Stony Gorge is shown in Fig. 13.

<sup>19</sup> *Dams and Control Works*, U. S. Bur. Reclam., 2nd Ed., 1938, p. 78.

Drainage holes should be provided near the base of the dam, to relieve pressure on the back side of the slab, and the interior space should be vented to avoid any tendency to vacuum.

Slide gates are shown on the spillway in Fig. 10. Radial gates, drum gates, flash boards, etc., also may be used; or there may be no control whatever.

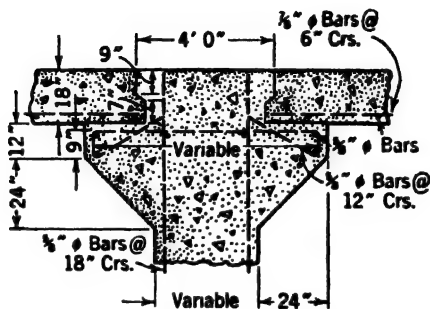


FIG. 13. Downstream slab connection, Example 2

### MULTIPLE-ARCH DAMS

**24. Principles of Design.** Most of the principles involved in the design of a multiple-arch dam have been developed in other examples. The arches may be analyzed either graphically or algebraically, as in the case of massive arch dams of Chapter 13. The principles are the same. Principles covering buttress design are the same as for slab dams, as set forth in the first part of this chapter, only details requiring adjustment.

Because arches are relatively stronger than flat slabs, the facing is thinner than for the slab type, which permits a wider economic spacing of buttresses. This requires thicker and more substantial buttresses. As mentioned in Art. 6, double-walled or hollow buttresses are frequently used.

**25. Form of Arches.** The arches are usually relatively slender and of regularly varying form from top to bottom. Consequently, the transverse beam effect (see Chapter 13) is negligible, possibly excepting a short distance near the connection with the foundation. Trial load analysis is not required. The arch faces may be and frequently are simple cylindrical surfaces. A closer fit between line of pressure and center line of arch can be secured with a noncircular or multicentered arch. Also, the moment at the spring line is usually greater than at the crown (see Art. 19c, Chapter 13), for which reason a thickening toward the haunches is desirable. This is accomplished by using a single-centered extrados and a three-centered intrados, as illustrated in Fig. 22, Chapter 13, or by any other convenient means.

Central angles as small as  $100^\circ$  have been used. The tendency at present is toward central angles approaching  $180^\circ$ . The larger angles reduce lateral reaction on the buttresses, in case of unbalanced loading, and involve smaller rib shortening and temperature stresses.

**26. Loading and Arch Analysis.** The usual unit of arch analysis is a unit width slice, normal to slope of the upstream face. Because the arch barrel is inclined, the water load on such a unit is variable from spring to crown. Also, a component of the masonry weight contributes to the arch load. Consequently, the simplified equations of Chapter 13 for uniform normal loads are not applicable.

If the arch form is simple, the variable loads may be expressed mathematically and equations and curves for stress computations are possible. George Goodall and Ivan M. Nelidov have developed equations and curves for such use for cylindrical inclined arches.<sup>20</sup> Space does not permit the inclusion of these computation aids.

Yielding of the arch abutments (the buttresses) is usually ignored for balanced loading.

Elastic yielding of the foundations under the buttresses is assumed to have no effect on arch stresses. Unequal settlement is objectionable and should be guarded against. Lateral deflections of the buttresses may require consideration where there are lateral earthquake forces (Arts. 3 and 4) or other lateral forces.

The thin arches respond rather rapidly to climatic changes and because of the inclination of the arches, it is not feasible to leave closing gaps or joints to be grouted at low temperature. Consequently, temperature ranges may be expected to be relatively high. This is compensated for, at least in part, by the flexibility of the slender arches and by using large central angles and reinforcing steel.

Frost may penetrate the thin slab or arch and cause an accumulation of ice on the water face. Such a condition, at Gem Lake Dam, was described by Fred O. Dolson and Walter L. Huber in 1926.<sup>20c</sup>

### EXAMPLE OF A MULTIPLE-ARCH DAM

**27. Example 3, Nonoverflow Multiple-Arch Dam.** The complete design of a multiple-arch dam would involve duplication of arch analysis work illustrated in Chapter 13 and of the buttress design in Example 1 of this chapter and will not be attempted. An example of an actual design will be described.

The example chosen is the design for the Horseshoe site on the Rio Verde in Arizona, as presented in Noetzli's paper on the "Improved Multiple Arch Dam."<sup>21</sup>

Fig. 14, taken from Noetzli's paper, shows the plan and downstream elevation of the dam, which has a maximum height of about 210 ft. The double-walled buttresses are spaced 60 ft center to center. Fig. 15, from the same source, shows details of the maximum section.

<sup>20</sup> "Stresses in Inclined Arches of Multiple Arched Dams," *Trans. Am. Soc. Civil Engrs.* Vol. 98, 1933, p. 1200.

<sup>20c</sup> FRED O. DOLSON and WALTER L. HUBER, "Multiple-Arch Dam at Gem Lake on Rush Creek, Calif.," *Trans. Am. Soc. Civil Engrs.*, Vol. 89, 1926, p. 713.

<sup>21</sup> *Trans. Am. Soc. Civil Engrs.*, Vol. 87, 1924, p. 342.



**28. Description of Arches, Example 3.** In describing this dam, Noetzli states that

A uniform distance of 8.0 ft. was chosen between buttress walls, so that the ratio of thickness to height of the H-column is about  $\frac{1}{14}$  for a section at the middle of the column, and about  $\frac{1}{10}$  for a section at the base, which resulted in a span of about 52 ft. for the extrados of the arches. In order to minimize the side thrust of the arches as much as practicable, and at the same time to diminish the secondary arch stresses resulting from rib-shortening and temperature, an arch with a rise of about 20 ft. was selected.

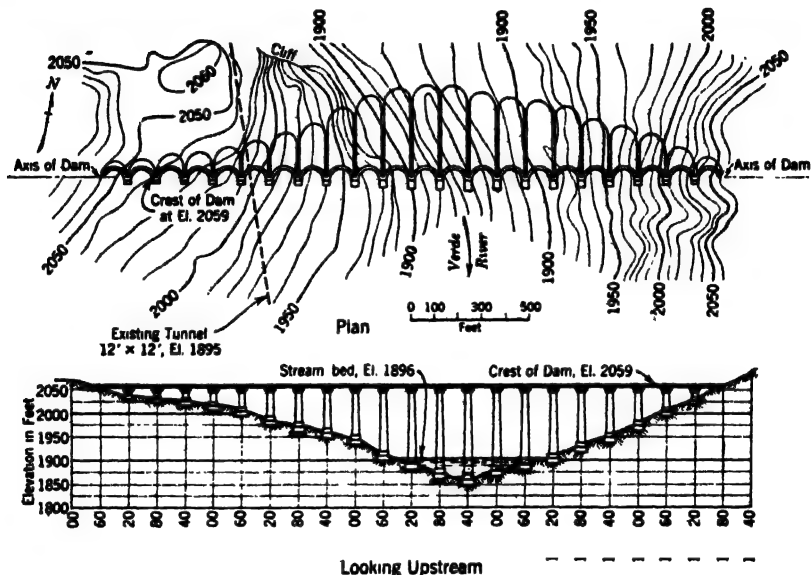


FIG. 14. Noetzli's improved type multiple-arch dam.

A maximum unit stress of 400 lbs. per sq. in. was chosen for axial arch compression. For practical reasons, the minimum thickness of the arches was made 18 in., and, in order to provide additional strength for the arch barrel near the crest, where uneven loading occurs, due to the inclination of the elementary arches, the crest arch was widened and an auxiliary arch was added about 10 ft. below the crest, as shown in Plate I [Fig. 15].

There is always a complication at the top of the arch barrel because of the large relative variation in arch load from crown to spring, and because of the support required for the partial corner arches, the crowns of which are cut away. This condition can be met effectively by a wide horizontal arch rib at the top and a normal rib a short distance below the top, as shown in Fig. 15; or it may be met by an increased minimum thickness for the upper portion of the barrel.

**29. Arch Stresses, Example 3.** Computations for arch stresses in Example 3 were made by the elastic theory, but they involved some simplification of

the rules given in Chapter 13. Apparently the slight thickening of the corbels was ignored, as was also the influence of the reinforcing steel on the moment of inertia. The effect of these approximations is probably not great and can be checked by a few comparative analyses.

The following assumptions were made:

(1) Temperature drop below mean, reservoir full to top of dam, 25° F at top, decreasing uniformly to 10° F at stream bed (163 ft below top), constant at 10° F below stream bed.

(2) Temperature drop below mean, reservoir full to spillway level (14 ft below top), 50° F at top decreasing uniformly to 20° F at stream bed; constant below.

(3) Temperature change from mean, reservoir empty,  $\pm 50^\circ$  F at top and  $\pm 20^\circ$  F at stream bed and below.

(4)  $E = 2,000,000$  lb per sq in. for concrete.

$C_F = 0.0000055$  per °F for concrete.

The arch stresses as computed by Noetzli at crown depth of 70 ft below the top, reservoir full, are all compression, as follows:

At the crown:

$$f'_c \text{ (intrados) } = 302 \text{ lb per sq in.}$$

$$f''_c \text{ (extrados) } = 487 \text{ lb per sq in.}$$

At the abutments:

$$f'_c \text{ (intrados) } = 579 \text{ lb per sq in.}$$

$$f''_c \text{ (extrados) } = 210 \text{ lb per sq in.}$$

According to Noetzli:

The ratio between the rise and span of the arches of the Horseshoe Dam is such that no tension exists at any point of the arches when the dam is under pressure, duly considering the effect of rib-shortening and temperature. However, small tension stresses caused by temperature changes will occur when the reservoir is empty. The arches are reinforced at the upper elevations by  $\frac{1}{2}$ -in. round bars, 18 in. apart, at the extrados and intrados, and, at the lower elevations, by 1-in. round bars, 9 in. apart, at the extrados and intrados.

The size and general arrangement of the reinforcement are shown in detail on Plate I [Fig. 15]. Although the calculations show that practically no steel would be required for the arches of this dam, largely because of the efficient ratio between rise and span, it was considered good practice to use what is believed to be a minimum of reinforcement for concrete arches of this size. The fact that probably no tension cracks in the concrete will occur also assures a perfect protection of the steel from rusting, although this is a rather superfluous precaution in view of the numerous examples of successfully built reinforced concrete structures for holding water, such as tanks, Ambursen dams, etc.

**30. Stability Computations, Example 3.** The stability of an arch-buttress unit is computed in the manner illustrated for the buttress-slab unit of Example 1, using a tabulation similar to Table 2. The volume of water above the

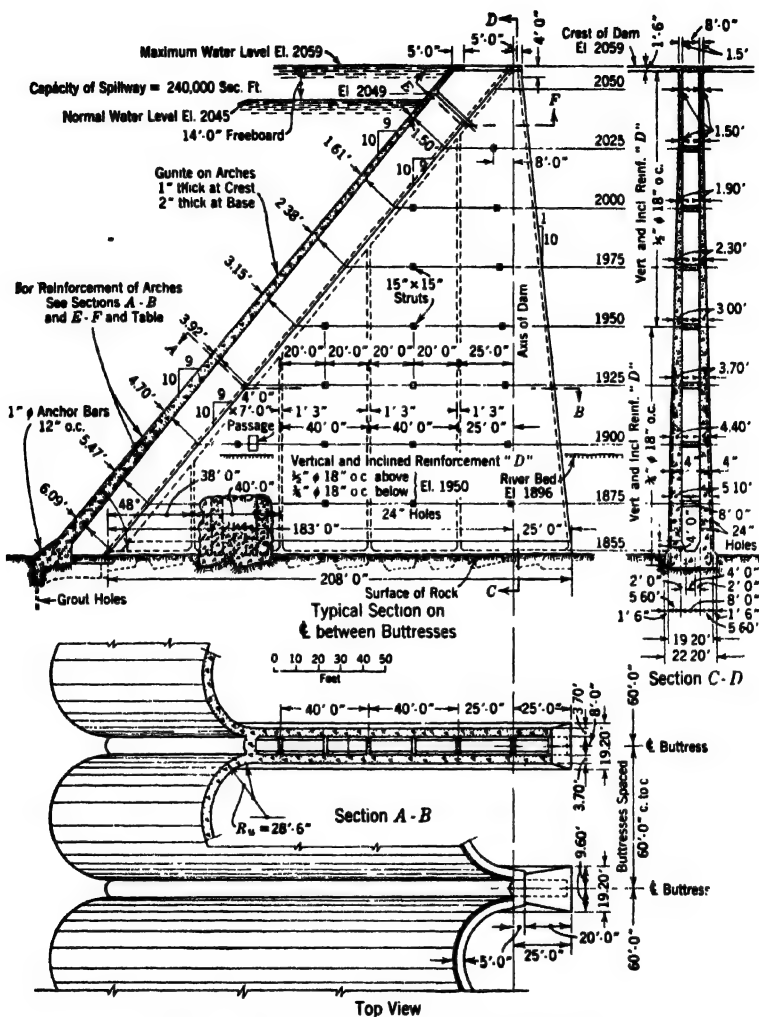


FIG. 15. Noetzel's improved type multiple-arch dam.



arch barrel for any depth,  $h$ , is represented in plan by 11-12-13-14, Fig. 16. Triangle 1-2-3 represents the water prism area at the crown. In Example 3 the extradosal surface of the barrel is a true cylinder; hence the curves 11-13 and 12-14 are ellipses and all vertical sections parallel to 11-12 are of the same shape and size as 1-2-3. A vertical section along 13-14 is represented by 4-5-6.

The center of gravity of 1-2-3 is at point 7 in elevation and at point 8 in plan. Centers of gravity for other sections lie on the ellipse 8-9. The center

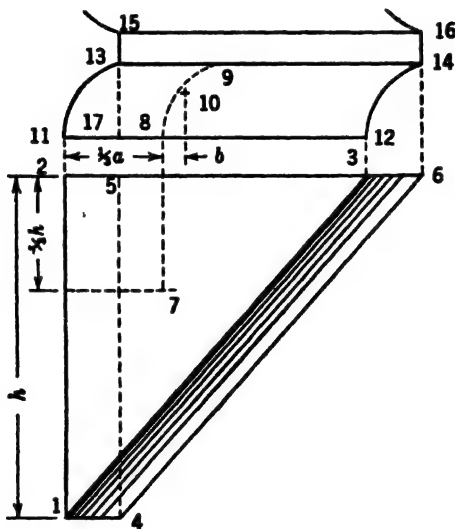


FIG. 16. Water load on arch barrel.

of gravity of the volume is at point 10, which is the center of gravity of the elliptical arc 8-9. This point can be found mathematically or by appropriate approximate methods.

Ignoring the arching of the upstream face of the buttress, the vertical water load between arches is represented in elevation by 4-5-6 and in plan by 13-14-15-16.

The volume of the water over the arch barrel is equal to the area of 1-2-3 times twice the distance 13-17.<sup>22</sup> The volume over the pier is equal to the same area times the distance 13-15.

Geometrical determination of the volume and center of gravity of the arch barrel usually is possible, or the barrel may be divided into a number of sections. The volume of the sections may be found by average end areas and the centers of gravity approximated. Precise methods may be applied if desired, but this usually is not necessary.

<sup>22</sup> If the extradosal surface is not cylindrical, appropriate alteration of geometrical computation of water load must be made.

The buttresses may be divided for computation in any convenient manner. The finding of volumes, weights, and centers of gravity is merely a problem in geometry.

Horizontal forces are the same as if the face were vertical. Moments, forces, and lever arms are computed as for the flat-slab dam of Example 1, using a tabulation similar to Table 2. The computations are not shown.

**31. Stresses in Buttresses of Example 3.** Following the reasoning developed in Art. 7 and because the arches and buttresses are actually tied together with reinforcing steel, monolithic action should be assumed. The unit for analysis may be a buttress and two half-arches or an arch and two half-buttresses.

Vertical pressures, reservoir full, computed in the manner indicated in Art. 18 for the monolithic section, at a depth of 204 ft below the crest, are as follows:

At upstream face:

$$p_v'' = 60 \text{ lb per sq in.}$$

At downstream face:

$$p_v' = 468 \text{ lb per sq in.}$$

The batter of the downstream face is 1 : 10,  $\tan \phi' = 0.1$ ,  $\sec^2 \phi' = 1.01$ ; hence the inclined pressure is

$$p_i' = 468 \times 1.01 = 473 \text{ lb per sq in.}$$

The batter of the upstream face is 9 : 10; hence  $\sec^2 \phi''$  is 1.81. The normal water pressure is  $204 \times 62.5 \div 144 = 89 \text{ lb per sq in.}$  From Eq. 6a, Chapter 8,

$$p_i'' = 60 \times 1.81 - 89 \times 0.81 = 38 \text{ lb per sq in.}$$

The pressure under the haunches at this same depth of 204 ft below the crest is found thus:

Average head on a normal arch with spring at  $h = 204 \text{ ft}$  is about 197 ft.

Outside span of arch barrel, 54 ft.

Thickness of arch barrel, 6.09 ft.

Radius of extrados, 28.5 ft.

Span of extrados, 54 ft.

Central angle of extrados,  $140^\circ 40'$ .

Area of arch, 396 sq ft.

Also

Total width of buttress head, 19.20 ft.

Average thickness of buttress head, about 6 ft.

Width of water on buttress head, 6.00 ft.

$$\sin \phi'' = \frac{0.9}{\sqrt{1.81}} = 0.6689$$

Thickness, two buttress barrels, 11.20 ft.

Therefore the forces are as follows:

Weight of arch ring = $396 \times 150 =$	59,400 lb
Weight of buttress head = $19.2 \times 6 \times 150 =$	17,300 lb
Total weight of concrete =	76,700 lb
Normal component = $76,700 \sin \phi'' = 76,000 \times 0.6689$	50,800 lb
Water pressure on arch = $197 \times 5 \times 54 =$	664,900 lb
Water pressure on pier center = $204 \times 62.5 \times 6 =$	76,500 lb
Total normal panel load =	792,200 lb
Unit pressure $\frac{792,200}{11.20 \times 144}$	491 lb per sq in.

This is the highest stress shown in the analysis. As explained in Art. 7, it may be assumed to approximate the principal stress at the buttress head.

Noetzli investigated these buttresses for a wind pressure of 15 lb per sq ft, inclined at  $45^\circ$  to the face of the piers,<sup>23</sup> and found a flexural stress of about 7 lb per sq in., which is negligible.

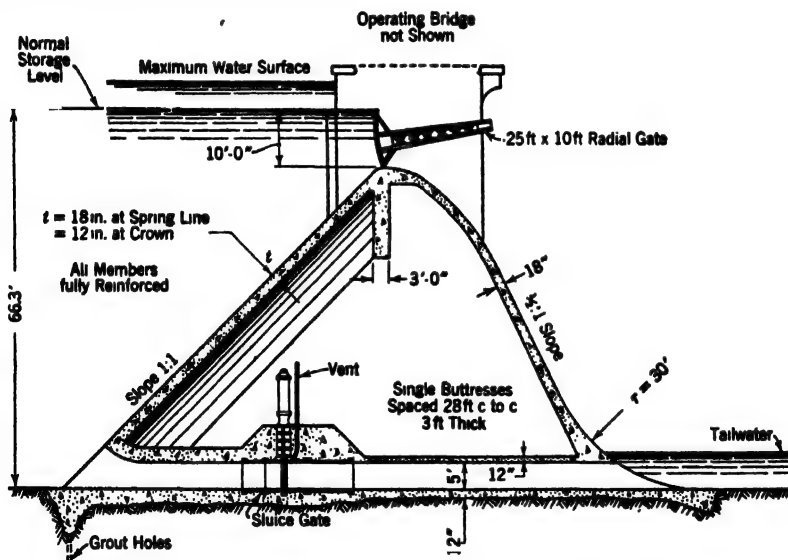


FIG. 17. Overflow multiple-arch dam with radial gate control.

In regard to reinforcement of buttresses, Noetzli states that

In these calculations the reinforcement of the buttresses was not considered, and, theoretically, none would be required. However, it was considered good practice to reinforce the lower part of each buttress wall with  $\frac{3}{4}$ -in. round bars, cross-wise, 18 in. apart, and by  $\frac{1}{2}$ -in. round bars in the upper elevations. In addition,  $1\frac{1}{2}$ -in. round bars were placed opposite each other in the webs of the H and C.

<sup>23</sup> The assumption of such a wind pressure is not recommended by the authors.

**32. Recapitulation, Example 3.** The computations of the preceding paragraph must be repeated at a number of levels. If all the stresses thus found are within allowable limits and sliding factors are satisfactory, the design may be considered safe. The uniform outside radius simplifies load computations and the uniform inside width facilitates the construction of the buttresses. However, a constant intrados curve has many advantages in construction. The inside forms and centering carry heavy loads and where of constant form they may be substantially constructed and moved upward as the work progresses. This requires constant outside thickness of buttresses and a variable extrados curve.

**33. Overflow Multiple-Arch Dam.** Fig. 17 illustrates how a multiple-arch dam may be adapted to the same spillway conditions shown for a slab dam in section C-C, Fig. 10. Fig. 17 is based on a preliminary study by the U. S. Bureau of Reclamation for a dam in Idaho (1924). The use of the crest control gate is of course optional. The installation of a sluice gate is also illustrated. The buttresses must be extended downstream to support the back slab. The beam immediately below the radial gate serves as a curtain wall against which the inclined arch barrels may end. Other arrangements are of course possible.

**34. Lake Hodges Multiple-Arch Dam.** The Lake Hodges Dam, illustrated in Fig. 18, is typical of the single-buttress, multiple-arch dam with struts. It was constructed in 1917. Fig. 18 is adapted from Plate AAA, *The Design and Construction of Dams*, Wegmann, 1927. On page 475 of this book, Noetzli describes the Lake Hodges Dam as follows:

The buttresses are spaced 24 feet on centers. The thickness is 1 foot 6 inches at the top and 4 feet 1 inch at a distance of 130 feet below the crest of the dam. The buttresses are stiffened by a Tee at the down-stream side and braced by horizontal struts, spaced from 30 feet to 35 feet apart. They are not reinforced. There is a passageway leading through openings in the buttresses from one side hill to the other.

The arch barrels are inclined at an angle of  $45^\circ$  except near the crest, where they are vertical. The thickness is 12 inches for the upper 50 feet and from there increases to 2 feet 7 inches at an elevation of 130 feet below the crest. The central angle of the arches is  $120^\circ$ . The radius of the extrados is 13.85 feet and is constant, from top to bottom. The reinforcement of the arches consists of  $\frac{1}{2}$ -inch rib bars spaced 12 inches apart, both at extrados and intrados. There are vertical bars  $\frac{1}{2}$  inch round, 24 inches on centers.

The concrete of the arches is of 1 : 2 : 4 mixture. For the buttresses the proportions are about 1 :  $2\frac{1}{2}$  : 5. The up-stream face of the arches is covered by a layer of gunite.

Inasmuch as the length of the buttresses is quite considerable, the contraction of the concrete due to shrinkage and changes in temperature has produced cracks in the unreinforced concrete. These cracks start approximately at the junction of the arches with the buttresses and extend in an inclined direction to a short distance above the bedrock. They pass through the openings in the buttresses which were left for the passage-way.



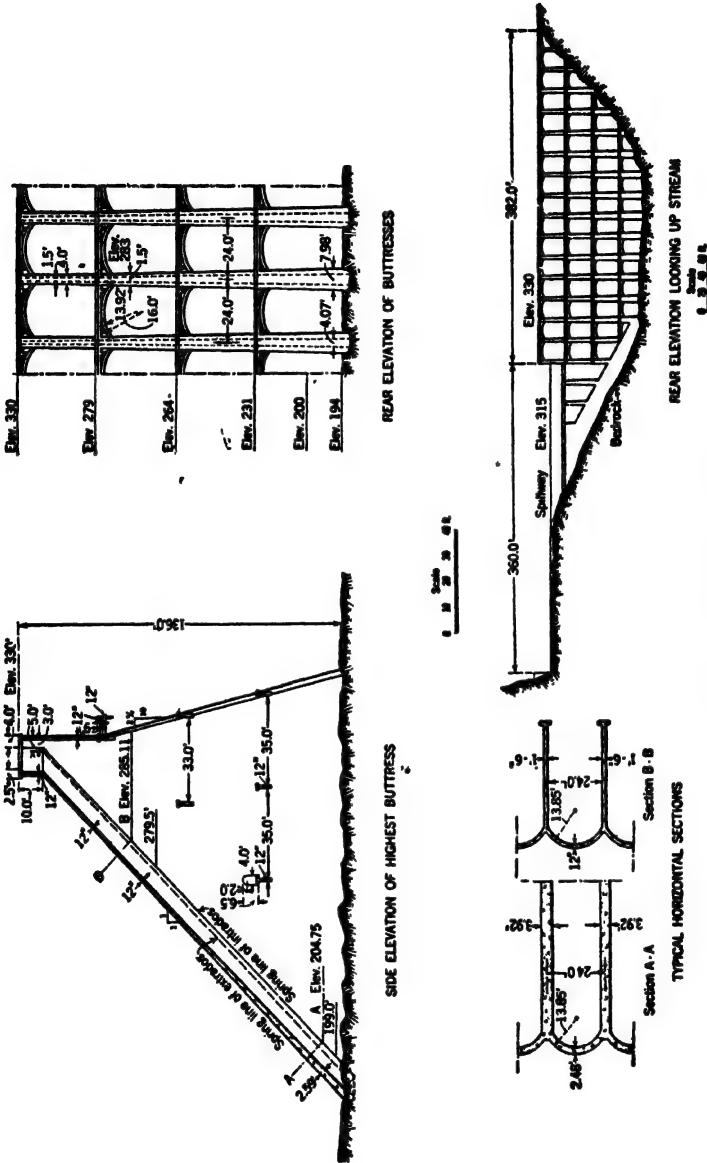


Fig. 18. Lake Hodges Dam.

The cracks have been under observation for a number of years. The width is measured periodically with a strain gage. It has been found that there exists no definite relation between width of crack and height of water in the reservoir. The width of the cracks generally increases with a decrease in temperature. The cracks almost close up when the temperature rises to the seasonal maximum in summer. This seems to indicate that these cracks merely facilitate "breathing" of the concrete with changes of temperature.

Subsequent to the writing of Noetzi's description, the main buttresses of Lake Hodges Dam were reinforced with clusters of reinforcing bars laid diagonally across the cracks, on the buttress faces, anchored into the uncracked portions, prestressed, and encased in concrete pilasters or beams. The structure thus repaired has a very substantial appearance. The face is exceptionally watertight.

**35. Florence Lake Multiple-Arch Dam.** The Florence Lake Dam, Fig. 5, is a typical example of a single-buttress, multiple-arch dam without struts between buttresses. Strength against buckling is supplied by flanges and pilasters. Fig. 5 is adapted from Plate JJJ, *The Design and Construction of Dams*, Wegmann, 1927. Noetzi, on pages 492 and 493 of this book, describes this dam as follows:

The Florence Lake Dam (Plates III and JJJ) was built in 1925-26 by the Southern California Edison Company as a part of its hydro-electric development in the Sierra Nevada. The dam stores the water of the South Fork of the San Joaquin River and diverts it through the 13-mile Florence Lake tunnel into Huntington Lake. The dam is located at an elevation of 7200 feet above sea level. The maximum height is 150 feet and the total length about 3300 feet. On account of the topographic conditions of the dam site, the axis of the dam forms several angles. The bends are formed by specially heavy buttresses. The slope of the arch barrels is 9 horizontal to 10 vertical. The arches are nearly semi-circular, in order to minimize the rib-shortening and temperature stresses. The thickness of the arches is 18 inches at the crest and 4 feet 6 inches at a depth of 150 feet.

The buttresses are spaced 50 feet on centers. They are strongly reinforced and provided with counterforts and a large Tee at the down-stream side for stiffening purposes. There are no horizontal struts between the buttresses. The thickness of the buttress walls is 2.25 feet at the crest, and 7.8 feet at a depth of 150 feet. The concrete was mixed and placed with great care. Special attention was given to a good grading of the aggregate and to a proper water-cement ratio. The mixture was about 1 : 2 : 4 for the arches, and 1 : 2½ : 5 for the buttresses. The up-stream face of the dam was waterproofed with Inertol.

As will be noted from Fig. 5, Florence Lake Dam is 7200 feet above sea level. As a consequence, it is subject to severe cold. In this particular location, it is also subject to much winter sunshine. The plan of operation is such that the reservoir is normally empty during the winter months. Many of the arches have a southerly exposure for the water face and are covered with a black waterproofing compound which accentuates the absorption of solar heat. The result is a large number of freezing and thawing cycles for the face concrete each winter; also, at times, a heavy temperature gradient from face to face. Result-

ing maintenance problems are discussed by W. L. Chadwick in a paper read before the 1943 summer convention of the American Society of Civil Engineers.<sup>23a</sup>

**36. Bartlett Multiple-Arch Dam.** A recently constructed multiple arch is the Bartlett Dam, built by the U. S. Bureau of Reclamation, in Arizona.

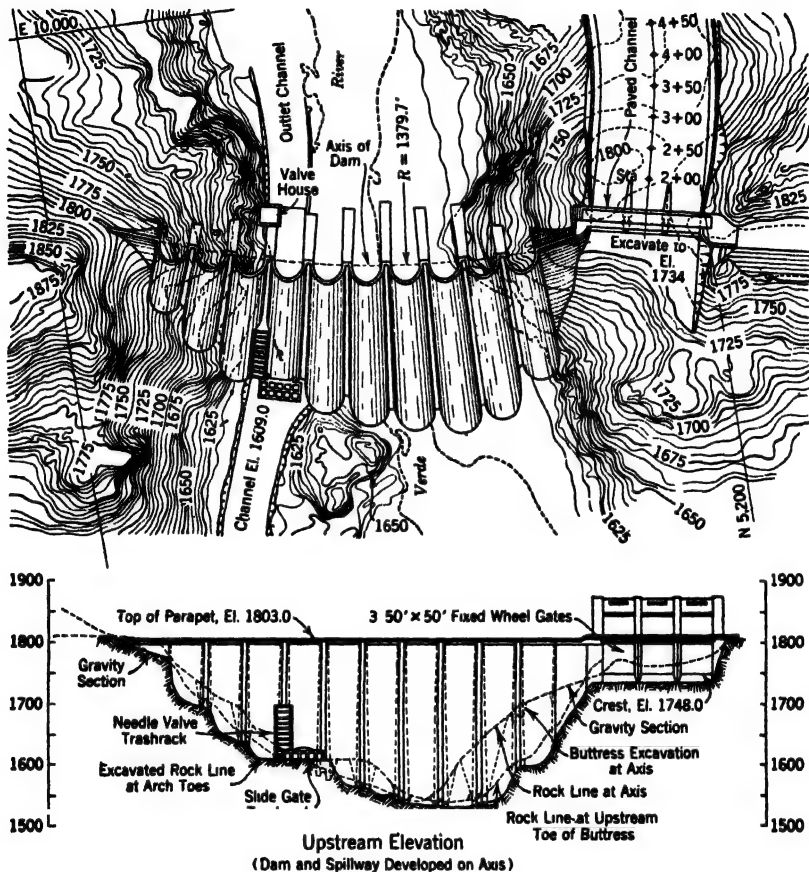


FIG. 19. Bartlett Dam, general plan.

Plan and elevation of this dam are shown in Fig. 19, elevation of the maximum buttress in Fig. 20, and important details in Fig. 21. All of these figures are adapted from drawings in Specifications No. 674 of the U. S. Bureau of Reclamation.

This dam has several features not illustrated in any other examples. The arches are cylindrical, full half-circles. The intrados has a constant radius of 24.0 ft and the interior space in the buttress has a uniform width of 8.00 ft.

<sup>23a</sup> W. L. CHADWICK, "Experience with Maintenance of Concrete Dams in High Altitudes." (Publication pending.)

Simultaneously constant values for these dimensions were made possible by giving the axis of the dam a slight curvature. Lines of equal buttress thickness are inclined.

A notable feature is the use of stepped contraction joints, 18 in. in minimum width, dividing the buttress walls into vertical columns 40 ft wide. Positions of these openings are indicated in the sectional plan of Fig. 21, and the detailed form is shown on that figure. These openings were filled in after the main portion of the buttress had taken its shrinkage. Notches are provided to

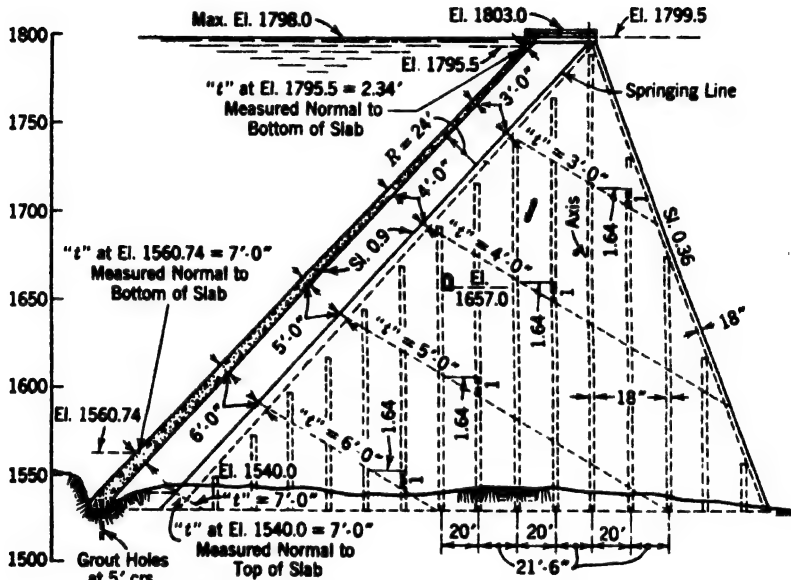


FIG. 20. Bartlett Dam, maximum section.

assist in carrying stresses across the openings, and the reinforcement is lapped within the notch for the same purpose.

### ROUND-HEAD BUTTRESS DAMS

**37. Characteristics of Round-Head Type.** Rules for the design of buttresses of round-head buttress dams are identical with those for other buttress dams. The object of the "round-head" is the elimination of reinforcement; hence it is logical that the buttresses should be made massive and unreinforced. In fact, the type is usually looked upon as a modified gravity dam free from appreciable uplift, and more stable against overturning than the conventional gravity structure.

By use of wide buttresses (upstream and downstream) and spread footings, such dams can be adapted to relatively weak foundations; and by controlling

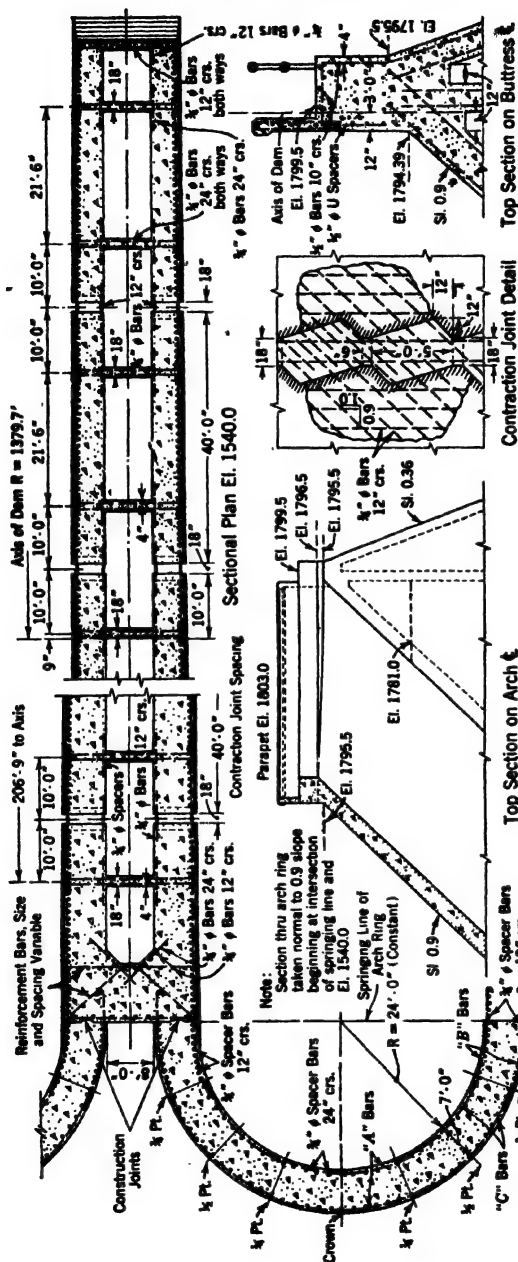


FIG. 21. Bartlett Dam, arch and buttress details.

the upstream face slope, a low sliding factor can be obtained. It offers rigidity in individual units and flexibility as a whole, which adapt it to earthquake regions.

Stability can be achieved with less concrete than in a gravity dam but more formwork is required, and if the foundation overburden is great excavation quantities may be large. The spacing of buttresses is determined by economy.

Although this type has been rather favorably discussed, little actual use has been made of it to date.

**38. Rio Salado Round-Head Buttress Dam.** The spillway section of the Rio Salado Dam, on the Don Martin Project in northern Mexico, is an example of a round-head buttress overflow dam.<sup>24</sup> Plan and typical section are shown in Fig. 22. Principal data are as follows:

Radius of head,	20.9 ft
Width of buttress head,	29.5 ft
Width of contact plane,	6.6 ft
Thickness of buttress walls,	6.6 ft
Thickness of spillway slab,	2.5 ft
Maximum height,	105.0 ft
Height of radial gate,	14.5 ft
Width of radial gate,	25.0 ft
Number of radial gates,	26

The dimensions shown are translated from metric dimensions and are approximate. The buttress wall thickness (2.0 meters) was chosen as about the minimum favored by the designers for this type of structure. The corresponding dimensions for the buttress head were based largely on judgment. It was thought that the width of the buttress head should not be more than four or five times the buttress wall thickness. The spacing also was influenced by the span of the downstream slab.

The downstream face conforms only approximately to theoretical curve of Fig. 3, Chapter 11. The crest is surmounted by 26 float-controlled radial gates, each 25 ft wide and 14.5 ft high. Joints between the buttress heads are provided with water stops but are not designed to transmit shear. The downstream extension of the buttresses was determined by the contour of the overflow face. With this limitation, a vertical upstream face provided ample stability for about 35 ft below the fixed crest. Below that depth the upstream face was battered 0.65 to 1, to control sliding factor and location of resultant. The deep heavy cutoff was provided to seal a weak foundation stratum. Pier trenches also were carried below this stratum. The foundation is limestone.

<sup>24</sup> ANDREW WEISS, "The Don Martin Project," *Trans. Am. Soc. Civil Engrs.*, Vol. 96, 1932, p. 833.

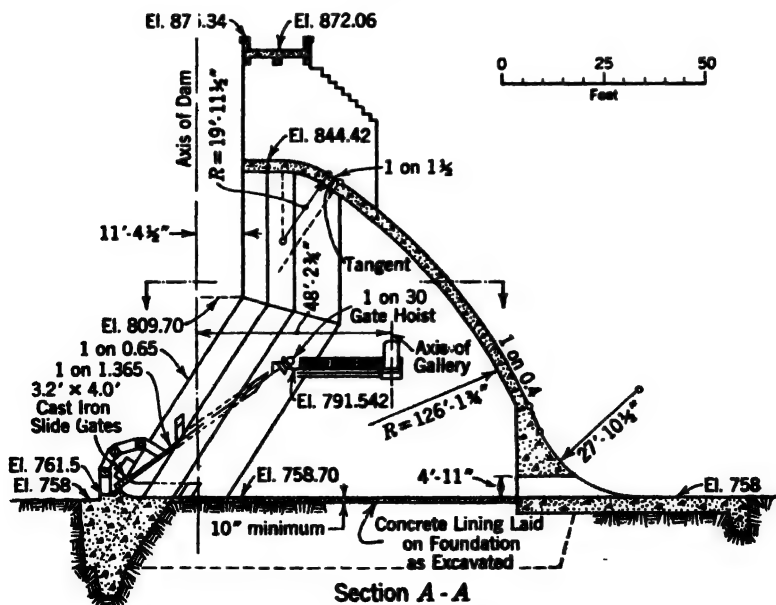
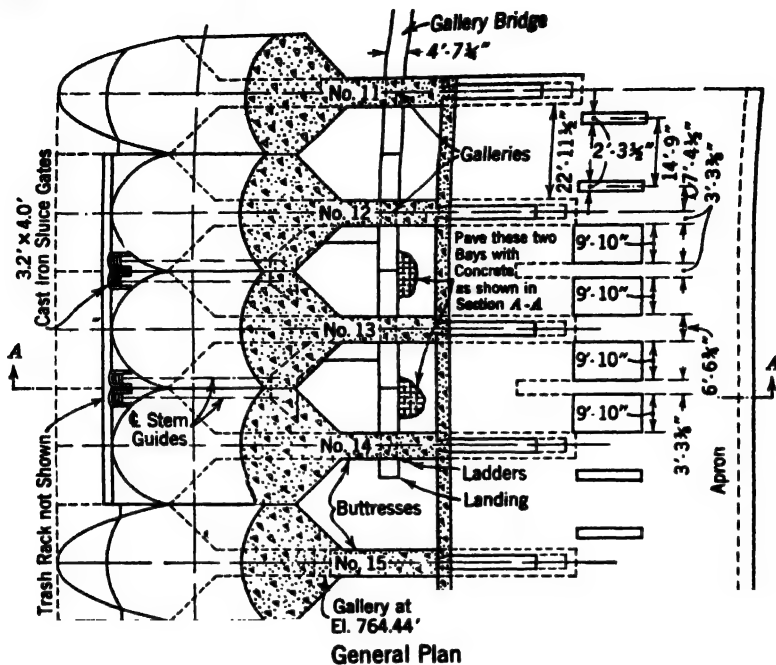
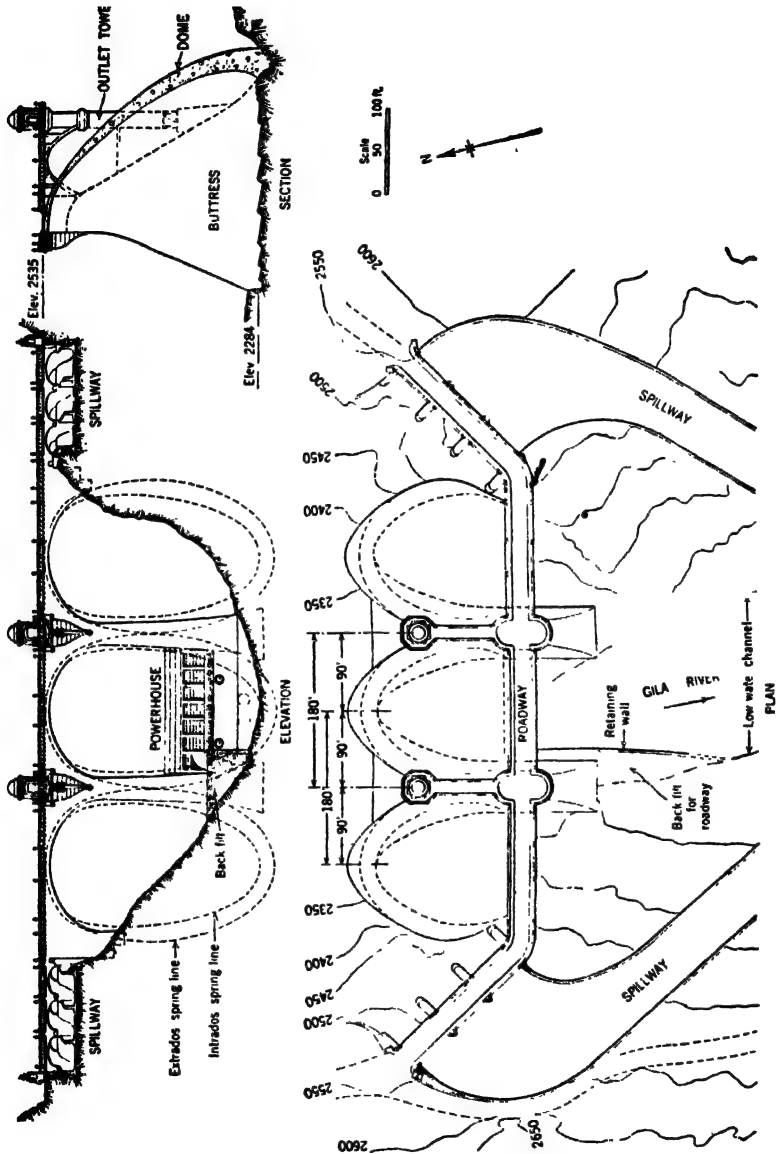


FIG. 22. Rio Salado Dam, Don Martin Project, Mexico.



G. 23. Coolidge Dam

## OTHER TYPES OF STRUCTURAL CONCRETE DAMS

**39. Multiple-Dome Dams.** That there is no definite limit to the variety of forms that reinforced concrete dams may take is illustrated by the unusual design of the Coolidge Dam on the Gila River, near San Carlos, Ariz., which



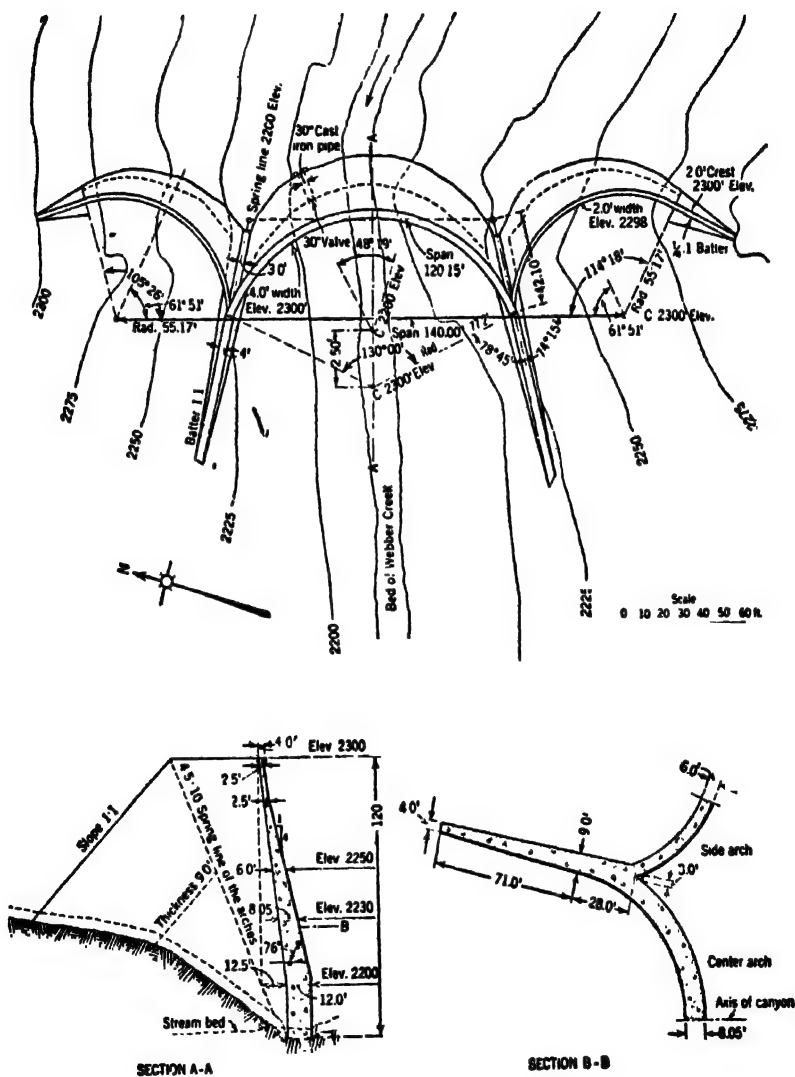


FIG. 24. Webber Creek Dam.

See note 27, page 603.

consists of three domes supported on two intermediate piers and the canyon walls.<sup>25</sup> The piers are 180 ft center to center. The dam is about 210 ft high and resembles a long span multiple arch. However, the arrangement is such that the arch radius shortens as the depth increases.

An elevation and a section of this dam are shown in Fig. 23, which is adapted from Plate UUU, Wegmann.<sup>26</sup>

This dam was estimated to be slightly cheaper for this site than a multiple-arch dam. It involves continually changing formwork, which no doubt offsets some of its apparent economy.

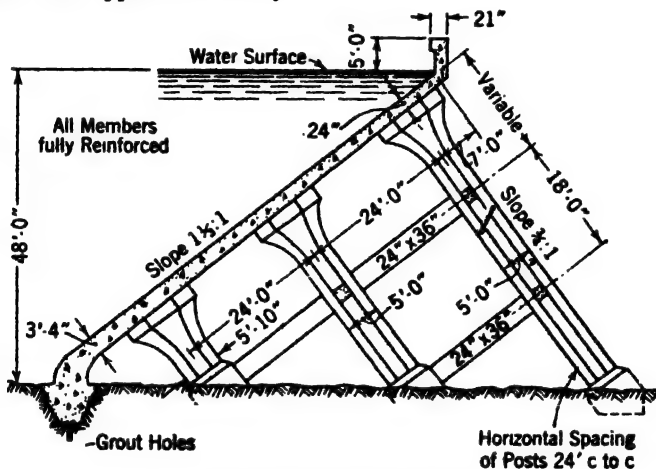


FIG. 25. Slab and column dam.

**40. Triple-Arch Dams.** Sometimes it is possible to span a stream with a system of three vertical or nearly vertical arches, of the form shown in Fig. 24, which represents the Webber Creek Dam in California.<sup>27</sup> The arches are supported on the canyon walls and two intermediate piers, which are in turn anchored into the canyon wall. The piers in this dam act primarily as struts, vertical weights playing a minor role.

**41. Slab and Column Dams.** The dam shown in Fig. 25 is taken from an unpublished preliminary study by the U. S. Bureau of Reclamation for a dam in Idaho (1924). It consists of a continuous flat slab designed and reinforced in accordance with concrete floor practice and supported on inclined columns. The columns are stiffened by a two-directional system of struts. It is claimed that this type eliminates the uncertainties of buttress action. The authors have no information concerning actual installations of this type.

<sup>25</sup> This description is based on a more complete statement in WEOMANN'S *The Design and Construction of Dams*, 1927, p. 520.

<sup>26</sup> Idem.

<sup>27</sup> Idem, adapted from Pl. GGG. This dam was not built to dimensions shown but was constructed to a lesser height and later was submerged within a higher hydraulic-fill dam.

## CHAPTER 15

### CONCRETE FOR CONCRETE DAMS

*By Byram W. Steele*<sup>1</sup>

**1. General.** Concrete is a graded mixture of either natural or manufactured rock particles embedded in a slowly hardening paste composed of cement and water, in which the water content plays a dual part. A limited amount only of the water content is vital to the hardening of the cement, but the total water content is a necessary vehicle in the differential movement of the rock particles during placement.

Because of the heat-generating qualities of cement during the setting process, and the resulting change in volume of the mass as this excess heat is dissipated, it is not an ideal structural material. Its coefficient of volume change varies through a wide range of values, depending on the minerals of which the rocks are formed and upon the raw materials from which the cement is manufactured. Compared to brick and building tile, which have a much lower coefficient of expansion, this is one of the most objectionable features in concrete as a structural material, and one which necessitates the use of joints at every critical section if future troubles relative to expansion and contraction are to be avoided.

In the early days of concrete construction, bank-run mixtures of sand and gravel were used, but gradually as the art and science of good uniform concrete were developed the rock particles were separated into fine and coarse aggregate and then gradually the coarse aggregate was split into two or more sizes, depending on what maximum size of rock particle could be used in the mix. For many years in dam construction plum stones or derrick stones were embedded in the concrete as it was placed so as to effect greater economy in the use of cement, but this practice has now been almost abandoned in favor of the more economical and workable method of putting all ingredients through the mixer and thus simplifying placing costs and procedure.

The structural quality of concrete is so closely related to the structural quality of the aggregate of which it is composed that it is hazardous to conclude that if the cement and aggregate tested alone prove durable, the concrete will be equally durable. There are too many examples to the contrary, and hence a thorough and comprehensive series of tests of all ingredients alone, and also in the proposed mixes, is mandatory for important structures if later failures are to be avoided. The testing of concrete ingredients is a

<sup>1</sup>Head Engineer, Office of Chief of Engineers, War Department, Washington, D. C.

good deal like the examination of a dam site—rarely is it sufficiently exhaustive to leave no regrets.

The specifications for the concrete in a structure should be comprehensive but at the same time should be couched in generalizations rather than in too much detail. Results rather than methods should be specified, if practicable. And then, an experienced and well-qualified inspection force should be provided and clothed with the authority necessary to secure the desired results.

**2. Cement.** Since cement is the least stable ingredient in concrete, it has an important influence on the life of a concrete structure, especially a hydraulic structure in a climate where a large number of alternate freezings and thawings annually result in progressive surface disintegration.

Natural cement was first used in this country for hydraulic structures. After the discovery of the Portland cement process, Portland cement gradually displaced natural cement for nearly all types of hydraulic structures. During this transition period combinations of Portland and natural cement were used quite extensively for massive sea-water work.

To overcome the inherent weaknesses of Portland cement various kinds and types of cement have been investigated and tried out in service. American Society for Testing Materials Specifications are available for five types of Portland cement—I, general purpose; II, moderate heat; III, high early strength; IV, low heat; and V, sulphate resistant. Federal Specifications also are available on four of these cements and the Federal Specifications Committee is now working on a specification for type IV.

The tricalcium aluminate content of all five types is limited as follows: I, 15%; II, 8%; III, 15%; IV, 7%; and V, 5%.

Type II, commonly known as modified cement, is becoming quite popular for hydraulic structures exposed to moderate sulphate action, or where moderate heat of hydration is an essential feature, and where it is desired to specify certain chemical and physical test requirements.

Type IV, low-heat cement, is used for massive concrete work in which it is desired to limit the maximum temperature in the concrete to the smallest value practicable and to produce as crack-resistant a concrete as possible.

Type V cement is used where specially resistant qualities are necessary on account of severe alkali conditions.

Although natural and Portland-pozzolana cement are sometimes used in the construction of dams, the vast majority of dams are built with Portland cement. Bonneville Dam on the Columbia River was built with a factory-produced blend of Portland-pozzolana cement in the proportions of 75 to 25, and Friant Dam, now under construction, is using 80 per cent Portland and 20 per cent Punicite. The Punicite is quarried near the site and batched in a separate batcher at the mixer without processing.

In the early days of Portland cement manufacture, the product of the average mill was decidedly coarse ground as compared to modern practice which varies from an average specific surface of 1700 sq cm per gm for type I cement to at least 2200 for type III. The rate of heat generation and strength

gain in concrete is influenced to a marked degree by the fineness of grinding, hence the extremely fine grinding for the high-early strength cements.

**3. Fine Aggregate.** Specifications, as a rule, stipulate that the fine aggregate shall be a natural sand because of the superior qualities of workability and placeability that well-rounded particles impart to the concrete. However, manufactured sand is becoming more common as the machinery for its production is improved and perfected so that the particle shape (cubical rather than thin and elongated) and the gradation can be controlled within desirable limits; but, because of its angularity and sharp edges and corners manufactured sand will never be as satisfactory as a good natural sand of equal durability. Sand showing a darker color than the Standard in the colorimetric test for organic impurities should be tested further to determine whether there is sufficient organic matter present to affect the durability and strength of the concrete.

The gradation, or particle size distribution, of the sand has an important bearing on the workability, durability, and cement content of concrete. The allowable grading limits depend to some extent on the shape and surface characteristics of the particles. For example, a sand having smooth, well-rounded particles will give satisfactory results with a much coarser grading than a manufactured sand with angular particles. The fineness modulus of sand, which is the sum of the percentages retained on the number 4, 8, 16, 30, 50, and 100 Standard sieves divided by 100, should, for general concrete work, be maintained between 2.50 and 3.00, and the variation from the average on any job should be held to plus or minus 0.1 if uniformity and close control of placement are desirable. Gradually the maximum and minimum limits of material passing the different screens are being drawn closer together as aggregate processing plants become better equipped to meet desirable limits. The present Federal and A.S.T.M. aggregate specifications give rather wide percentage limits for the number 4, 16, 50, and 100 sieves only, whereas some large mass concrete jobs now in progress limit the percentages on each one of the 4, 8, 16, 30, 50, and 100 sieves to a rather narrow range in the interests of better control. This limitation is well illustrated in Fig. 14 on page 68 of the January 1941 edition of the Bureau of Reclamation's "Manual for the Control of Concrete Construction," which is reproduced as Fig. 1 in this chapter. It is now generally recognized that the percentages passing the number 50 and 100 sieves should never be less than 10 per cent and 2 per cent respectively, and preferably somewhat greater. Manufactured sand generally requires a greater percentage of fines than natural sand to produce satisfactory workability. Experience has demonstrated that very fine or coarse sand or a deficiency or excess of any size fraction produces undesirable results in the concrete. In other words, a smooth grading curve between recognized limits produces the most desirable concrete.

**4. Coarse Aggregate.** The number 4 screen, which has a square opening of  $\frac{3}{16}$  in., is generally used as the dividing point between fine and coarse aggregate. For mass concrete in dams the maximum size of stones incorporated in

Screen Size	% Retained		Comb. % Ret.	
	Individual	Cumulative	Individual	Cumulative
6 inch	0	0	0	0
3 inch	28	28	21	21
1½ inch	26	54	20	41
¾ inch	22	76	16	57
½ inch	16	92	12	69
No. 4	8	100	6	75
F M		8.50		
No. 4	0	0	0	
No. 8	12	12	3	78
No. 16	20	32	5	83
No. 30	24	56	6	89
No. 50	24	80	6	95
No. 100	16	96	4	99
Pan	4	100	1	100
F M		2.79		7.07
Percent sand (clean separation) 25				
(Screen sizes are based on square openings)				

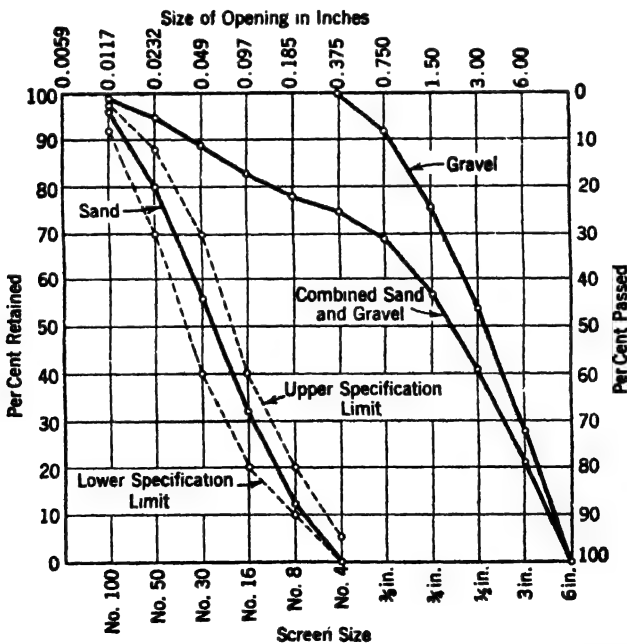


FIG. 1. Typical size distribution of suitably graded natural aggregate.

the concrete has gradually decreased until now 6 in. has been generally adopted as the largest cobble practicable to put through the mixer and hence the largest particle of rock that can be economically incorporated in the concrete. To avoid undesirable segregation, coarse aggregate should be divided into 2, 3, or 4 sizes, depending on the maximum size of the cobble permitted. The selection of screens to produce these sizes depends on the natural gradation of the coarse aggregate. A common size division is  $\frac{3}{16}$  to  $\frac{3}{4}$  in.,  $\frac{3}{4}$  to  $1\frac{1}{2}$  in.,  $1\frac{1}{2}$  to 3 in., and 3 to 6 in. The dividing point between sizes is more or less arbitrary but in some cases it is necessary to modify the usual size limitations to prevent too much difference in size of batching units.

**5. Water.** The water used in concrete, mortar and grout must be reasonably clean and free from objectionable quantities of silt, organic matter, alkali, salts, and other impurities.

**6. Admixtures.** If deficiency of the fines in the sand produces concrete that is difficult to place, an admixture may improve the workability; but if concrete is decidedly harsh, the most satisfactory way to improve its placing qualities is to correct the grading deficiency in the sand. Lean mixes are benefited by an admixture much more than rich ones.

**7. Concrete Mixes.** The designing of the concrete mixes for a dam involves the combination of available materials so as to produce concrete of the desired durability, impermeability and strength at minimum costs. Theoretical mix-design methods found in the literature may well be used in designing concrete mixes, but these methods are often too complicated for general use; so it is advisable to select trial mixes which will approximate the desired characteristics and then adjust these trial mixes to suit local aggregates and conditions. For details of this procedure reference is made to the report of Committee 613 in the November 1943 Journal of the American Concrete Institute, which report is proposed as an A.C.I. Standard on Concrete Mix Design. The Trial Mix design procedure given in the committee report is an excellent approach to this subject and one of the most direct and simple yet devised.

In a massive structure, economy dictates the use of the maximum size of aggregate that is available and can be handled advantageously through the mixers. Strength, impermeability, and resistance to weathering can generally be secured in mass concrete containing cobbles with about 1 bbl of cement per cu yd for the exterior and less for the interior, depending on the gradation of the aggregate and whether it is natural or manufactured. It should be remembered that the cement paste is the most soluble and least durable portion of the concrete and that any more water in the mix than is absolutely necessary as a vehicle for proper placement is a detriment.

If the structure, however, is of the multiple-arch or slab and buttress type the thickness of the members and the reinforcement details generally dictate the maximum size of aggregate that can be used to advantage, and durability and impermeability rather than strength will be the factors that will influence the selection of the cement content. The water-cement ratio is the most important factor in the control of permeability, small changes in water-ratio

producing large differences in the degree of imperviousness. The maximum water-cement ratio permissible under the requirements of durability and impermeability will generally produce concrete of a much higher average strength than the specifications for the structure require.

When the essential qualities of durability are present, the resulting strength of any mix is generally ample to meet ordinary design requirements for strength. The cement content of any mix should never exceed the minimum necessary to meet the requirements of durability, impermeability and strength, because excess cement results in more heat generation, a higher maximum temperature in the concrete, and consequently greater volume change with all the attendant possibilities of undesirable cracking.

In the following tabulation appears typical mix data taken from mixes used on construction jobs.

Nat. or mfg. agg.	Max. size agg. (in.)	Mix	Sum of aggregate	Gravel-sand ratio	Fine-ness Modulus sand	Average slump (in.)	Water-cement ratio by wt	Cement content (bbl/cu yd)
Nat.	8	1-2.45-7.05	9.50	2.88	2.70	3.6*	0.53	1.02
Nat.	6	1-2.7-7.0	9.70	2.59	2.67	2.25	0.53	1.00
Mfg.	6	1-3.68-7.55	11.23	2.02	2.88	2.0	0.67	0.90
Nat.	6	1-2.51-7.04	9.56	2.80		1.75	0.58	0.80
Nat.	4	1-2.44-7.05	9.49	2.88		1.0	0.53	1.00
Mfg.	3	1-2.58-4.40	6.98	1.70	2.88		0.55	1.33
Nat.	2½	1-2.32-5.68	8.00	2.45	2.71	5.3*	0.56	1.16
Nat.	2½	1-2.10-4.70	6.80	2.24	2.75	4.4	0.50	1.32
Nat.	1½	1-2.46-4.44	6.90	1.80	2.70	5.5*	0.57	1.29
Mfg.	1½	1-2.50-3.40	5.90	1.35	2.88		0.55	1.50
	1½	1-2.1-4.2	6.3	2.00	2.72	5.0	0.51	1.40
Nat.	¾	1-2.20-3.50	5.70	1.60	2.69	6.1*	0.56	1.47

\* Average slump at plant, in inches.

The narrow spread in water-cement ratios for these mixes should be noted. In the absence of any other test data the water-cement ratio may be accepted as the best indication of the actual quality of concrete. A lower water-cement ratio than is ordinarily adopted and a lower cement content than is usually permitted in hydraulic structures will still produce a satisfactory mix, providing a well-rounded, well-graded aggregate is available. Vibration has contributed more than any other factor in making low water-cement ratios and low cement contents possible. These refinements, however, contemplate that the coarse aggregate is graded up to the maximum size practicable to use and that the highest practicable gravel-sand ratio is also employed, both of which contribute the minimum surface area to be coated with cement and the minimum void ratio.

The slump test is the most practicable method yet devised for controlling workability and maintaining uniformity in the field. Taking everything into



consideration, it is believed that the ideal slump to attempt to maintain in mass concrete at the forms—not at the mixing plant where the test specimens are usually made and the slump is taken—lies between  $1\frac{1}{2}$  in. and  $2\frac{1}{2}$  in. When the air is cool and the humidity is high a slump of  $1\frac{1}{2}$  in. is high enough, but when the air is hot and dry a  $2\frac{1}{2}$  in. slump permits proper consolidation with less chance of rock pockets and honeycomb streaks and other undesirable results. The best stipulation that can be made as to the proper slump for any mix is that it shall be no greater than is absolutely necessary to permit proper (near-maximum) consolidation of the concrete in the structure or part of the structure in question.

To compute the weights of the various ingredients in 1 cu yd of concrete of a certain mix, proceed to determine the absolute (solid) volume of the materials as indicated in the chart below. If more than two sizes of aggregate are used add columns accordingly. In the absence of actual specific gravity determinations, average values of 3.15 for cement and 2.65 for sand and gravel will

Feature	Cement	Water	Sand	Gravel
Mix parts by weight	1	0.53	2	4
Specific gravity	3.15	1.00	2.65	2.65
Weight of material for a 1 sack batch (lb)	94	$\frac{94}{\times 0.53}$ 49.8	$\frac{94}{\times 2}$ 188	$\frac{94}{\times 4}$ 376
Weight of 1 cu ft of solid material (lb)	$\frac{62.4}{\times 3.15}$ 196.5	62.4	$\frac{62.4}{\times 2.65}$ 165.4	$\frac{62.4}{\times 2.65}$ 165.4
Absolute (solid) volume per sack of cement	$\frac{94}{196.5} = 0.48$	$\frac{49.8}{62.4} = 0.80$	$\frac{188}{165.4} = 1.13$	$\frac{376}{165.4} = 2.27$

Sum of absolute volumes =  $0.48 + 0.80 + 1.13 + 2.27 = 4.68$  cu ft per sack of cement

Material for 1 cu yd of concrete (4074 lb)	$\frac{27}{4.68} = 5.76$ $\frac{\times 94}{541}$	$\frac{541}{\times 0.53}$ 287	$\frac{541}{\times 2}$ 1082	$\frac{541}{\times 4}$ 2164
--	---	----------------------------------	--------------------------------	--------------------------------

give fairly satisfactory results. For actual determinations of specific gravity and other test methods desired see A.S.T.M. or Bureau of Reclamation Concrete Manual Designations for the test in question.

**8. Batching and Mixing.** Constant pressure for more speed and better concrete in recent years has resulted in radical improvements in batching and mixing equipment. The concrete plants for large jobs are now well-equipped factories with highly trained personnel, automatic batching, weighing, and recording equipment; and the resulting product embodies a degree of uniformity comparable to other factory products. The measurement of all materials by weight instead of by volume is one of the principal factors contributing to the present high degree of uniformity.

In the batching and mixing plants now in general use for dam construction, the aggregate is delivered to the top of the storage bins by belt conveyor and the cement is pumped through pipes. The storage bins are above the batchers and the mixers below them. All materials descend through the plant and into the buckets by gravity. Batching equipment is usually air-operated and electrically controlled from a single board. In the latest plants the tilting mixers are charged from a common central collecting cone, and discharged through a central common hopper into the bottom dump buckets.

The tilting mixer is the only type that will satisfactorily handle mixes containing cobbles. The shape of the mixer drum and the shape and location of the blades within the drum, as well as the method and sequence of charging, have a marked effect upon the uniformity of the batch. All mixers should be so located and arranged as to permit the operator to view the mixing operation during its progress rather than to judge the qualities of the mix after it is dumped. The proper mixing time for any batch depends on the speed of rotation of the mixer and the other factors mentioned above; it varies from 1 min for small mixers to  $2\frac{1}{2}$  to 3 min for 4-yd mixers.

**9. Transportation and Placing.** The demand for an increase in uniformity and the elimination of segregation forced the long-used chuting system out of the concrete field and in its place came the cableway, the trestle, the concrete pump, and the belt conveyor.

The belt conveyor, however, is not permitted on many jobs because of the tendency for segregation and erratic loss of moisture in transit and the consequent effect on the placing qualities of the concrete.

The trestle and the cableway are the most common systems of distributing concrete over the structure. If a cableway is used, bottom dump buckets are transported from the mixer to the cableway on cars; and the cableway, in order to serve any point on the dam, is equipped with a movable tower at one or both ends, depending on the plan layout of the dam. If a trestle is used, the cars transport the buckets from the mixer along the trestle to the point of deposit, where a crane picks the bucket off the car and spots it in the forms.

Concrete should be transported from the mixer as a unit mixture, deposited as near as practicable in its final position, and consolidated by vibration with

as little segregation as possible. The vibrator, by permitting the satisfactory placement of concrete too dry to place by hand, has done more than any other agency to promote the benefits of the water-cement ratio law; but even so, vibration has its objectionable features, one of which is the tendency among too many operators to cause objectionable lateral flow within the mass and its attendant segregation, rather than consolidation only. There is a definite trend in recent years toward higher speeds in vibrators, but as yet the relative merits of speed versus amplitude have not been well established.

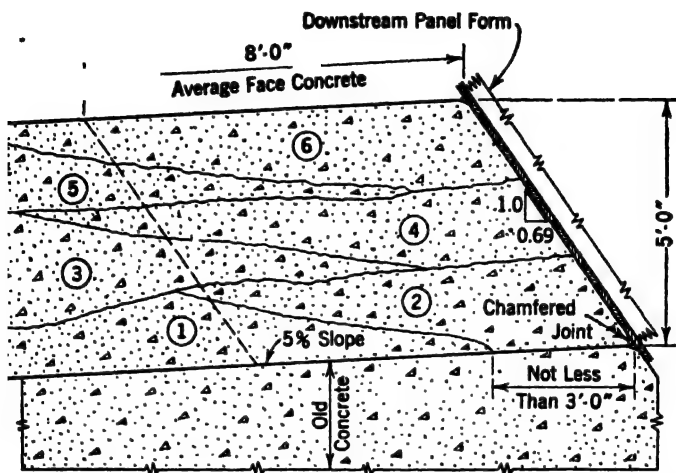


FIG. 2. Sequence of pours (circled numerals) for concrete on downstream face of dam. (O. Laurgaard in *Proc. Am. Soc. C. E.* March 1941.)

In massive concrete dams, the exterior shell generally contains more cement than the interior and a common stipulation relative to the control and placing of this face mix is as follows: "The concrete to a depth of 5 ft normal to the face shall contain more cement per cubic yard than the concrete in the interior of the dam; it shall be placed as nearly simultaneously with the adjacent interior mix as plant operations will permit, so that the two mixtures will unite in their plastic state to form an integral mass." The last clause contemplates an overlapping and dovetailing of the batches as they are dumped and consolidated by vibration. For a schematic picture of this concrete face-mix placing operation see Fig. 2.

**10. Forms and Formed Surfaces.** Steel forms are admirably adapted to tunnel-lining jobs and other similar work, but after many attempts to use structural and sheet metal in the construction of mass concrete dams, timber is still the only material that will economically permit the flexibility necessary in the forming of mass concrete, regardless of whether this is paneled or built in place formwork. Because of wrinkling and buckling, sheet steel is not adapted to the surfacing of forms for concrete exposed to view. Tongue

and grooved narrow lagging for ordinary surfaces outranks any other form material since it permits the escape of more air and water bubbles than sheet metal and such materials as masonite, thus eliminating much objectionable sand streaking and pitting. Wherever a dense, durable, pock-free, matt surface is desired, some form of absorptive form lining, such as Celotex, Firtex, or U. S. Rubber Co. lining should be used. For parapets, penthouses, retaining walls, and the exterior and interior of structures to house the control works an absorptive form lining produces an ideal surface, if due care is used in the building of the forms and the placing and consolidation of the concrete. In effect, it case-hardens the concrete at the surface by straining out the air and water, holding back the cement and thus producing more intimate particle contact and increased impermeability.

In the construction of spillway buckets, ogee crests, and other structures, there is the disposition on the part of many constructors to screed the concrete to the required grade on steep slopes, rather than to form such slopes. Such practice nearly always results in early indications of disintegration because it is impossible to compact the concrete on such steep slopes to a durable density; and consequently heat, moisture, and frost soon leave the indications that are the forerunners of early disintegration. For such conditions as here indicated slopes steeper than 1 on  $1\frac{3}{4}$  should be formed. Concrete properly placed against a formed surface is more resistant to the elements and to erosion than a surface that has been disturbed by screeding, floating, and troweling. If a surface, after being floated and troweled, could be compressed sufficiently to squeeze out the water that permitted the finishing operations the durability factor would be materially increased. Recent experience in the use of absorptive form lining indicates attractive possibilities for increased resistance to weathering by virtue of the "case-hardening" effect produced at the surface.

**11. Height of Lifts.** In order to control the maximum temperature in mass concrete, it is generally specified that it shall be poured in 5-ft lifts, but multiple-arch dams, slab and buttress dams, and retaining walls are ordinarily carried up in 10-ft, 12-ft or even higher lifts since the dissipation of excess heat from such structures and the prevention of cracks are more readily accomplished. Lifts higher than 5 ft have been used in mass concrete, but the form work difficulties increase rapidly with height for mass concrete types of forms. From a purely construction standpoint, lifts higher than 5 ft may be desirable for mass concrete work but, after all factors entering into this question have been given due consideration, the 5-ft lift seems preferable on most mass concrete jobs. One of the objections to high lifts, especially in the arches and face slabs of dams, is the tendency toward the accumulation of water and cement at the top of the lift, thus producing a thin band of high water-cement ratio, porous, nondurable concrete. This condition in high lifts can be avoided and satisfactory concrete secured, but to do so requires eternal vigilance on the part of the inspection force.

**12. Curing and Protection.** Concrete to be adequately cured must be protected against rapid radical changes in temperature and also against extremes

in temperature during the curing period; and it must have available at its surface at all times—not just periodically—a blanket of moisture applied in some convenient form. It is hard for many persons to appreciate the detrimental effect on the formation of the cement gel of temporary surface drying and to realize that the curing process to be most effective must be continuous.

Vertical surfaces can be cured very satisfactorily by arranging a system of pipes with spray nozzles at such intervals that the entire surface is covered with a fine spray. For horizontal surfaces the most positive means of securing continuous moist curing is a blanket of saturated sand applied immediately after placement is completed. This method of curing results in a surface that is as near ideal for starting the next lift as it is possible to produce and is equally good for finished surfaces.

Curing compounds, both colored and colorless, are permitted on many jobs, and when properly applied the degree of perfection of the curing is probably as good as the average water-cured job but it is universally recognized that no curing compound will give the equivalent of *continuous* moist-cure. Colored compounds, to be most effective in reducing surface cracking, should be covered with a coat of whitewash so that the heat of the sun will be reflected instead of absorbed. Moisture, in addition to that present as mixing water, will be taken up by the cement if this excess moisture is readily available at the right time.

Winter concreting involves protection against freezing until the concrete has attained sufficient strength to permit normal construction operations without damaging the concrete. This length of time varies according to the temperature of the mix when placed and the kind of cement used. One of the chief objections to low-heat cement for dams in northern climates is the increase in time between lifts necessary to accommodate its slower-setting characteristics.

**13. Joints—Horizontal and Vertical.** Joints in dams are a necessary evil. They are necessary to permit systematic and economical construction and to prevent the formation, owing to volume change that cannot be prevented, of haphazard and ragged cracks. (For further discussion of the spacing of joints see Art. 1 of Chapter 23.)

The proper treatment of horizontal lift joints is one of the moot questions in mass concrete construction. If the concrete immediately below the joint surface is of normal consistency and there is no accumulation of water (water-gain) and fluffy inert cement as the lift is completed there does not appear to be a logical reason for any treatment of the surface prior to starting another lift except to wash it off. If, however, there is an accumulation of water and cement immediately below the surface of the lift this should be removed to such depth as is necessary to expose concrete of the desired qualities. Surface clean-up is best accomplished by the use of a high velocity jet of water and air applied at the proper time during the setting period. Once the concrete is hardened, clean-up is best accomplished by the use of the wet-sand blasting process, which will remove any undesirable material rather effectively and

economically. Regardless of what kind of treatment the joint receives before another lift is started,  $\frac{1}{2}$  in. of mortar should be applied immediately before concrete placing begins, to permit the proper bedding of the aggregate in the fresh concrete and the proper bond of old and new concrete.

**14. Temperature Control, Cracking and Checking.** For every stress crack produced by the actual live load for which a structure is designed, there are millions of volume-change cracks due to temperature; and hence temperature is fast becoming the most important problem to deal with in the construction of a dam. Deep cracking is all too prevalent, but even so, it does not deserve as much attention as surface cracking and checking because these are the entering wedges of wholesale disintegration.

Deep cracking is caused by high interior temperatures, which create steep temperature gradients between the interior and the surface for long periods of time, while surface cracking and checking is due to high daily differentials in temperature between the surface and near-surface areas. Surface cracks, once started, may progress into the interior or clear through the structure, depending on conditions.

The following are some of the various operations that may be incorporated into the construction program for a dam as a practical solution of the elimination of cracks: (1) starting off all rock foundations or concrete surfaces that have set for several weeks with two or three  $2\frac{1}{2}$ -ft lifts and 5 days between lifts; (2) limiting the height of all other lifts to 5 ft and 5 days between lifts; (3) sprinkling the coarse aggregate and blowing compressed air through it in summer to standardize the moisture content and reduce the temperature (this operation at Hiwassee Dam reduced the temperature about 3 degrees); (4) refrigeration of the mixing water, including use of ice if it can be properly batched and discharged into the mixer; (5) use of low-heat cement; (6) use of low cement content—0.8 bbl per cu yd for interior and 1.0 bbl for exterior or surface shell. If the gradation and particle shape of the aggregate permit, 3 sacks of cement per cu yd can be successfully used for interior concrete in a massive dam; (7) circulating cold water or ice water through pipes embedded in the concrete of each lift as soon as the pipes are covered and until the temperature of the mass has been reduced to mean annual temperature for that locality; (8) control of form removal so that high differentials in temperature between the surface and near-surface areas do not take place. The size of the dam, the amount of concrete, and the form in which the concrete is placed will be important factors in determining how many of these operations are applicable.

The construction refinements and cooling operations used in the attempt to eliminate or reduce cracks in the concrete made Hiwassee Dam, recently completed by the Tennessee Valley Authority, an outstanding structure among those built in recent years. When examined in the late fall of 1940, it was as near crack-free as any dam it has ever been the good fortune of the writer to examine.

Impermeability is the all-important characteristic of concrete if *permanent durability* is desired. To produce *durable* concrete *too much* emphasis cannot be

placed on *minimum water content and minimum permeability*, and this does not necessarily mean *maximum density*. If concrete is rendered impervious by virtue of structurally sound aggregate, properly selected cement, proper mixture design, proper mixing and placing, and adequate curing, the resulting concrete will resist hundreds of cycles of freezing and thawing without appreciable deterioration. Cement containing Vinsol resin or other approved air-entraining agent is now generally acknowledged as superior to plain cement in preventing the deterioration due to frost action. The best indication of deterioration in the structural qualities of a concrete specimen is a continued reduction in its sonic modulus. Low temperatures cannot impair the structural qualities of concrete, unless moisture is present within the mass to produce expansion at critical temperatures and a consequent disruption of that close association between the matrix and the aggregate particles commonly referred to as bond. The plane of contact between the matrix and the aggregate particles must remain an impervious plane of contact and not gradually degenerate into a series of interconnected voids, which provide the entering wedges of deterioration through frost action. This degree of perfection is possible, but it is not often attained with careless and indifferent workmanship. Hence, eternal vigilance from the quarry to the cured product is the only way to produce good, uniform, durable concrete. In buttressed dams, and other hydraulic structures in cold climates, impermeability in thin walls subject to water pressure is very important. Such walls, if exposed on one side, may freeze entirely through several times during a single winter. Unless the moisture-absorbing capacity of these walls is held to the absolute minimum, trouble may be expected.

There is ample evidence of durable and nondurable concrete. It is not a question of whether durable concrete can be produced, it is a question of whether we are willing to submit to the monotonous grind of eternal vigilance in each and every detailed operation connected with production. It will never be easy to produce good, uniform, durable concrete, but it can be produced if there are no missing links in the process. The production of such concrete is an intricate manufacturing process in which the necessity for proper control of all the ingredients and careful supervision of all the steps in the process are not yet sufficiently appreciated by the average constructor to enable him to produce the desired results. He is too often high-pressured into sacrificing the very detail that is mandatory if the desired results are to be attained.

Variation in the coefficients affecting volume change of the various ingredients of concrete is a potential source of cracking and checking that has not yet been given careful consideration. Materials combined into a synthetic conglomerate cannot expand and contract at different rates under rapid temperature changes (thermal shock) without tending to disrupt the paste, or the aggregate, or both.

**15. Waterproofing.** Concrete is inherently a more or less porous material, and its degree of impermeability is dependent upon so many factors that the question of when to waterproof and what method to use cannot be answered except in very general terms. If well-graded aggregates are available and

the mixture is properly designed, mixed and placed, and then adequately cured, concrete can be made tight for all practical purposes, even under high pressures. However, cold joints between pours, settlement or shrinkage cracks, careless placement, segregation, laitance bands at the tops of lifts, and other defects are the common sources of leakage which make waterproofing necessary in relatively thin concrete structures having one side exposed to direct water pressure when the other side must be absolutely dry.

The art of placing mass concrete has now progressed to the point where the 5 ft horizontal lift joints are no longer a common source of trouble from the penetration of water under pressure. Thinner wall sections could also eliminate much of this trouble if lower lifts and the same care were used in joint treatment as in massive work. This, however, is not always possible, nor is it always practicable; and hence it may be necessary to waterproof the outside of a structure because of these inherent weaknesses.

There are available a number of tar and asphaltic coatings with which to treat concrete surfaces. Some of these should be applied hot and others cold, since the asphaltic coatings depend for their hardening on the evaporation of the solvent. As noted in the first paragraph, the extent to which these materials will render a concrete surface watertight depends so much upon the construction materials and the conditions of placement, and of exposure that each and every case must be studied carefully, the basic condition analyzed and the proper material and procedure for each individual case determined.

Bituminous coatings, oil paints, oil resin combinations, Portland cement paint, powdered iron preparations, and other proprietary surface treatments have been used with varying degrees of success. Bituminous membrane waterproofing has been used extensively in Europe in connection with hydroelectric projects.

Integral waterproofing should also be mentioned; but the use of powdered admixtures to improve watertightness is limited to the leaner mixes, where the additional fines increase the workability and thus make possible a more dense and impervious mass.

**16. Tests of Concrete and Concrete Materials.** Owing to the unsatisfactory service record of many structures, the tendency today is toward closer inspection and an increase in the types of tests conducted on concrete and the ingredients of concrete. The American Society for Testing Materials has available standard methods for all such tests, and the 1940 report of the Joint Committee on Standard Specifications covers in detail Recommended Practice and Standard Specifications for Concrete and Reinforced Concrete.

Cement should be sampled and thoroughly tested as provided for under both Federal and A.S.T.M. standard specifications. Chemical interaction between the cement and the aggregate several months after the structure is completed is now causing much concern relative to ultimate durability of the structures affected.

The sand should be tested for the possible and occasional but not probable presence of injurious organic compounds. Both fine and coarse aggregate



should be tested for specific gravity and absorption. Light-weight aggregates (2.40 sp. gr. or less) or those having a high rate of absorption rarely ever produce durable concrete for hydraulic structures.

The sand should be tested for the approximate quantity of clay, silt, and shale. A frequent screen analysis of the coarse aggregate, and a constant check on the analysis of the sand, especially, is imperative if uniformity in the concrete produced is to be maintained. The structural soundness of the aggregate should be determined by the sodium or magnesium sulphate tests, and resistance to abrasion of the coarse aggregate by the Los Angeles testing machine.

Before any concrete is placed, a series of tests should be made of the mixes proposed for use in the dam, these mixes being composed of the aggregates and cement selected for construction. After the dam is started a sufficient number of specimens—6-in. by 12-in. or 8-in. by 16-in. cylinders or 6-in. by 6-in. by 36-in. beams—should be taken to secure a complete and representative record of the construction procedure. Concrete beams, while generally used for road and pavement tests, offer a type of test specimen that has many desirable features for use in dam construction. Cores drilled from the finished structures at various points offer the advantage of an independent check on the concrete as poured and cured under field rather than laboratory control.

Last, but not least, is the question whether freezing and thawing tests of concrete made from the cement and aggregate selected should be a part of the testing program for any important structure. At least some poor concrete and occasionally a regrettable later development might be avoided under such procedure; and hence it is urgently recommended for all important work. The effect of freezing and thawing on the structural soundness of concrete can be measured quite satisfactorily by determining the sonic modulus of elasticity of the specimens at regular intervals.

# INDEX

- Aaensire Dam, 562
- Aare Dam, 355
- Abrasion tests, coarse aggregate, 618
- Absorptive linings, concrete forms, 613
- Abutments, effect on flow, 365
- Acceleration, earthquake, 247, 279, 330
- Admixtures, concrete, 608
- Aeration, weirs, 256, 257
- Aerial photographs, 8
- Aeroplane mapping, 5, 7, 8
- Aero-projection method, 6
- A-frame, timber dam, 843
- Aggregate, abrasion tests, 618
  - batching, 611
  - coarse, 606
  - cobbles, 608, 611
  - derrick stone, 604
  - fine, specifications for, 606
  - fineness modulus, 606
  - gradation of, 607, 609
  - light-weight, 618
  - maximum sizes, 604, 608
  - plum stones, 604
  - specific gravity, 610, 617
  - tests for, 617, 628
  - weight per cubic yard of concrete, 610
- Air bubbler, 912
- Air vents for gates, 916
- Alamogorda Dam, 778
- Alcova Dam, 778
  - grouting of, 90
- Alexander Dam, 660, 778, 790, 792
- Alin, A. L., chute spillways, 208
- Alouette Dam, 792
- Alpine Dam, 350
- Amawalk Dam, seepage line in, 677, 678
- Ambursen dams, *see* Buttressed dams
- American Falls Dam, uplift, 265
- Anaglyph maps, 9
- Anchorage, dam to foundation, 278, 296
  - for chute spillways, 215
- Angle of internal friction, 274, 619, 620, 632, 639, 716, 733
- Anxox Dam, 562
- Apishapa Dam, 660, 778
- Apron, 58, 63
  - downstream, 71, 72
  - sloping, 79
  - uplift under, 87
  - upstream, 69, 70, 302, 696
- Arch dams, application of, 42
  - classification of, 425
  - cylinder theory, 425
    - angle, best central, 427
    - constant angle, 429
    - constant radius, 427
    - design examples, 427, 429, 431
    - overhang, 431
    - stresses, 425
    - variable radius, 431
  - design of, 425
  - elastic theory, 434
    - angle, best central, 496
    - arch dimension, 496
    - arch form, 496
    - arch forms, special, 486
    - circular arch, 487
    - cracked arch, 497
    - crown deflections, 436, 448, 449
    - crown forces, 435, 436, 460, 467, 476, 486, 490, 499, 530
    - deformations, 434
    - design examples, analytical analysis, 454
      - best shape, 496
      - cylindrical arch, 489
      - fillet arch, 493
      - graphic analysis, 468
      - symmetrical arch, 486
    - earthquake effects, 284, 452
    - elastic center, 482, 487, 489
    - fillet arches, 492
    - flexure, 436
    - foundation deformation, 440
    - graphic analysis, 468
    - gravity axis, 436
    - integrals for, 488
    - line of pressure, 468
    - moment deformation, 436

- Arch dams, elastic theory, moment theorem, 460**  
 neutral axis, 436  
 Poisson's ratio, 442, 443, 444, 452, 453, 454  
 reactions, statically indeterminate, 434  
 shape, best, 496  
 shear, neglect of, 479, 480  
 shear deformation, 439  
 shrinkage, effect of, 434  
 special formulas and diagrams, 490  
 stresses, computation of, 468, 489, 490  
     cylindrical arches, 497  
     symmetrical arch, 486  
 temperature stresses, 434, 439, 450, 482, 483  
 three-centered arches, 495  
 thrust deformation, 488  
 water loads, 453  
 weight of masonry, 454  
 erosion below spillways, 82  
 investigation, A.S.C.E., 279  
 list of, 556  
 loads, *see* Loads on dams  
 multiple arches, 584  
 overhang, 431  
 steel, 841  
 trial load theory, 500  
     arch analysis, 524  
     arch twisting, 541, 542  
     cantilever, tangential loads, 533  
     cantilever analysis, 509 to 524  
     cantilever deflection, 502, 503, 504, 513, 520, 521, 524, 530 to 541, 545  
     cantilever twisting, 538, 545  
     cantilevers, broken, 516  
     design examples, 505  
     earthquake inertia loads, 527  
     earthquake water loads, 526  
     foundation deformation, 521, 523, 528  
     horizontal elements, 500  
     interaction of elements, 502  
     kern distance, 513  
     load, division of, 504  
     loads and deflections, Ariel Dam, 506  
         Copper Basin Dam, 504  
         Seminole Dam, 503  
     model tests, 551  
     photoelastic analysis, 552  
     Poisson's ratio, 545  
     recapitulation, 550
- Arch dams, trial load theory, resultant, 516**  
 stresses, broken cantilevers, 520  
     principal, 547  
 tangential deflection, 502, 503, 504, 505, 532, 533, 534, 536  
 trial loads, 500, 503, 504, 505, 506, 509, 524, 526, 527, 528, 533, 537, 538, 543  
 twist deflection, 538, 542  
 twist moment, 538  
 unit load for arches, 548  
 unit load for cantilever, 550  
 uplift, 505, 515, 517  
 vertical elements, 500  
 triple arch, 602, 603
- Arch equations, cylinder theory, 425, 426, 427**  
 elastic theory, fillet arches, 492  
 foundation deformation, 440  
 integrals for circular arches, 488  
 summary, 449  
 symmetrical arches, 486
- Arches, fillet, 492**  
 Architectural treatment, 857  
 Ariel Dam, 265, 506, 556  
 Arkabutla Dam, 684, 778  
 Arnold and Gregory, snow melt, 206  
 Arnold Dam, 350  
 Arrowrock Dam, 305, 348, 350  
 Artesian pressure under dams, 71  
 Ash Fork Dam, 834, 836, 837, 838, 841  
 Ashley, Carl, rock fill dams, 806  
 Ashokan Dam, 350  
 Ashokan Dikes, 683, 699, 778  
 Ashti Dam, 661  
 Asphalt coating for waterproofing, 617  
 Asphalt grouting, 52  
 Atterburg plastic limit, 620, 761  
 Auger, clean out, 19, 28  
     earth, 15  
 Automatic gates, 898, 901  
 Automatic spillway, 882  
 Aziscolhos Dam, log chute, 868  
 Azucar, El, Dam, 778
- Baby dredge, 795**  
 Backwater curves, 374  
 Baffles for energy dissipation, 78, 79, 84  
 Bagnell Dam, 353  
 Bailey, S. M., floods, 206  
 Bainbridge, F. H., steel dams, 836  
 Baker, Ira O., allowable stresses in masonry, 300

- Baker River Dam, 556
- Bakhadda Dam, 808, 831, 832
- Bakhmeteff, B. A., hydraulic jump, 91, 98
- Balsam Dam, 660
- Barker Dam, 350
- Barnes, B. E., floods, 206
- Barnes, George E., tests, hydraulic models, 91, 98
- Barossa Dam, 556
- Barren Jack Creek Dam, 556
- Barrett Dam, 350
- Bartlett Dam, 562, 596, 597, 598
- Bartlett's Ferry Dam, 350
- Basins, stilling, 80, 83, 86
- Bassell, Burr, drainage of earth dams, 683
- Batching, concrete and aggregate, 611
- Bazin, M., weirs, 372
- Beach pipe, 784, 789
- Beach slope, 785
- Beam, pick up, 898
- Beams, flexure in curved, 436
  - T-sections, 568
- Bear River Dam, 808
- Bear trap dams, 871, 882
- Bear Valley Dam, 556
- Beaufield, R. McC., grouting, 90
- Beaver Park Dam, 807, 808, 822
- Bee Tree Dam, 792
- Beggs, George E., model arch dam tests, 552
- Belle Fourche Dam, 660, 764, 778
- Belt conveyors, concrete placement, 611
- Beni Bahdel Dam, 562
- Bentonite grouting, 51
- Berms on earth dams, 766
- Bernard, Merrill, rainfall, 206
- Bernard, snow-melt, 206
- Bernoulli's theorem, 376
- Bertram, G. C., filters, 688
- Bertram ratio, 689
- Bibliography, earth dams, details, 805
  - general principles of design, 714
  - stability, 748
  - flood flows, 205
  - foundations, preparation and protection, 90
  - headwater control, 929
  - hydraulic model tests, 98
  - infiltration, 205
  - rainfall, 205
  - rock-fill dams, 832
  - siphons, 929
  - snow-melt, 205
- Bibliography, soil tests, 654
  - steel dams, 841
- Big Creek Dam No. 1, 350
- Big Dalton Dam, 562, 569
- Big Santa Anita Dam, 556
- Big Tujunga Dam, 556
- Birch Hill Dam, 778
- Bit, chopping, 15
- Bits, improved efficiency of diamond, 32
- Bituminous coating for waterproofing, 617
- Black Canyon Dam, 350
- Blackbrook Dam, 350
- Blanket, 58, 63, 69, 696
- Blasting, care in, 45
- Bligh's line of creep, 58, 65
- Blow sand, 624, 636, 757, 803
- Blue Ridge Dam, 778, 792
- Bluestone Dam, jet deflectors, 86
- Boca Dam, 778
- Bog Brook Dam, seepage line in, 677
- Bogert, C. L., 305, 356
- Boils, 708
- Bond to foundation, 45
- Bonding earth dams to foundations, 713
  - 751, 770
- Bonito Dam, 808
- Bonneville Dam, cement for, 605
  - fish lock, 866
  - fishways, 864
- Boonton Dam, 350
- Borings, accurate data important, 34
  - churn, 14
  - core, 15, 31, 34
  - core barrel, 31, 33
  - core recovery, 34
  - diamond bits for, 32
  - diamond drill, 10, 31
  - feeler, inspection with, 36
  - of large size, 34
  - periscope inspection of, 36
  - pressure testing device, 35
  - pressure testing of, 36
  - program for, 10
  - records of, 35
  - rotary drilling of overburden, 15
  - size of, 33
  - wash, 14
- Borrow pit, hydraulic fill analysis, 790
  - prewetting, 769, 771
- Bortz diamond bit, 31, 32
- Boston Soc. C. E., floods, 207
- Bou Hanifa Dam, 808, 830

- Boulder Dam, 224, 348, 350, 552, 553, 554, 862  
 Bouquet Canyon Dam, 778  
 Bowman Dam, 808  
 Bowman, J. S., air bubbler, 913  
 Boyd's Corners Dam, seepage line in, 677  
 Boz-su Dam, seepage line in, 678  
 Brahtz, J. H. A., photoelasticity, 414, 415  
     seepage, 90  
 Bridgewater Dam, 792  
 Bristol Dam, 562  
 Broome gate, 920, 921  
 Brown, Ernest, ice thrust, 270, 271  
 Browning, G. M., infiltration, 205  
 Brule River Dam, uplift, 265  
 Bubbler system, 876, 913  
 Bucket, 76, 374  
     surface finish of, 613  
     upturned, 78, 81, 82  
 Buckingham, E., model tests, hydraulic, 98  
 Bucks Dam, concrete facing, 808, 818  
 Bull Run Dam, 265, 305, 348, 350  
 Bullards Bar Dam, 556  
 Bulldozers, 751  
 Burrowing animals, 712  
 Burton Dam, 354  
 Butte City Dam, 350  
 Butterfly valves, 916, 922, 923, 924  
 Buttressed dams, 558  
     application of, 41  
     buckling of buttresses, 564  
     buttress, inclined pressures, 581  
     buttress cracks, 569, 593  
         Lake Hodges Dam, 593  
     buttress design, 565  
     buttress form and spacing, 574  
     buttress joints, Bartlett Dam, 597, 598  
         Possum Kingdom Dam, 569, 850  
     buttress pressures, vertical, 580  
     buttress reinforcement, 569, 571, 583, 589, 592, 593, 595, 598  
         Lake Hodges Dam, 593, 595  
     buttress shear, 582  
     buttress spacing, 565, 574  
     buttress stability, 579, 587  
     buttress stresses, 567, 580, 591  
     buttresses, beam stresses, 567  
         of uniform strength, 570  
     concrete mixes for, 608  
     corbels, 575, 577, 578  
     cutoffs, 570, 572, 599  
     double buttresses, 560, 567, 585, 586, 588, 589, 598  
     Buttressed dams, drains, 572  
         earthquake loading, 285, 564  
         forces on, 564  
         foundation, connection, 570  
         soft, 572  
         list of, 562  
         multiple-arch type, 560, 561  
         on earth, 54  
         overflow, 572, 583, 592, 593  
         round-head buttresses, 560, 561, 597  
         slab analysis, 575  
         slab and buttress type, 559  
         types, 558  
     Buttresses, cutoff, earth dams, 713  
 Cableways, concrete placement, 611  
 Caddoa Dam, 779  
 Cain, William, extreme fiber stress arch dams, 468  
     geometric analysis of shear, 405  
     stresses in cylindrical arches, 490, 492  
 Cajalco Dam, 778  
 Calaveras Dam, 660, 778, 792  
 Calderwood Dam, 82, 556  
 Calles Dam, 557  
 Calyx, 19, 27, 28  
 Camarasa Dam, 355  
 Camp and Howe, circular weirs, 228  
 Campbell (Lane-Price), flow net, 90  
 Cantilever type, steel dams, 835  
 Cantilevers, 509 to 524  
 Capillary fringe, 664  
 Carmel Dam, seepage line in, 677  
 Carothers, D., elastic theory, 728  
 Carpenter Dam, 350  
 Casagrande, A., notes on soil testing, 619  
     seepage through dams, 665  
     seepage through earth foundation, 60  
     shear tests, 633  
 Castillon Dam, 556  
 Castlewood Dam, 808  
 Castrola Dam, 562  
 Caterpillar gates, 888, 920, 921  
 Cave Creek Dam, 562  
 Cavitation, of baffle piers, 84  
     on spillway aprons, 73  
 Cedar River Dam, 350  
 Cement, concrete ratio, 277  
     specific gravity, 610  
     specifications, 605  
     tests for, 617  
     types, 605  
     water-cement ratio, 608, 609, 610  
 Center of gravity, trapezoidal section, 512  
 Volume I, pages 1-246; Volume II, pages 247-618; Volume III, pages 619-929

- Chadwick, W. L., dams at high altitudes, 596
- Chambon Dam, 355
- Chatsworth Park, 808
- Cheat Haven Dam, 350
- Checking of concrete surfaces, 615
- Cheesman Dam, 305, 348, 350
- Chemical grouting, Lewin on, 90
- Cheoah Dam, 350
- Cherokee Bluffs Dam, 352
- Chopping bit, 15
- Christians, G. W., grouting, 90
- Churn drilling, 14
- Chute spillway, 208  
     anchorage, 215  
     cutoffs, 214  
     drainage, 215  
     hydraulics of, 216  
     joints, 213  
     paving, 212  
     San Gabriel No. 1, 211  
     Tionesta Dam, 208, 209
- Chutes, concrete placement, 611
- Clark, George C., ice thrust, 270
- Classification of soils, 621, 624
- Clay, 623  
     consolidation of, 636  
     drive sampling of, 16  
     foundation bearing power, 302  
     grouting with, 51  
     samplers for, 17  
     tests of, 627  
     varved, 19
- Claytor Dam, 351
- Cle Elum Dam, 778
- Clean-out auger, 19
- Clearing for earth dams, 750
- Clendening Dam, 660, 772
- Clyde, G. D., snow-melt, 206
- Coarse sands, consolidation, 635
- Cobble Mountain Dam, 778, 784, 792
- Cobbles, concrete aggregate, 608, 611
- Cochiti Dam, foundation, 69
- Cochran, A. L., floods, 140
- Cochran, V. H., double-walled buttresses, 567
- Coefficient of discharge, broad-crested weirs, 372, 373  
     between piers, 365, 372  
     curved standard crests, 370  
     end contractions, 365  
     Francis formula, 364  
     gates, partly open, 374  
     influence of special details, 370
- Coefficient of discharge, overflow dams, 364  
     special spillway types, 370  
     standard crests, 367  
     submerged spillways, 373
- Coefficient of expansion, concrete, 604  
     thermal, 451, 453
- Coefficient of friction, 295  
     various substances, 904
- Coefficient of permeability, 647
- Coefficient of sliding, 295
- Cogoti Dam, 808
- Cohesion, definition of, 619
- Cohesionless materials, sampling of, 27
- Cohesive material, suitability of, 37
- Colloidal material, 38, 622, 793
- Colorado Springs Dam, 661
- Columns, slab and column dams, 603
- Combamala Dam, 562
- Compaction, degree of, definition of, 620  
     excessive, 755  
     pervious material, 757
- Composite earth dam, seepage line, 672
- Compressed air tampers, 758
- Conchas Dam, 10, 38, 305, 348, 351, 859
- Conchas Dikes, 769, 778  
     core analysis, 771
- Conconully Dam, 790
- Concrete, admixtures, 608  
     batching and mixing, 611  
     composition, 604  
         Florence Lake Dam, 595  
         for various uses, 608  
         Lake Hodges Dam, 593  
     contraction, 604  
     cracking of, 615  
     curing, and protection, 613  
         effect on durability, 616  
     cutoff, 47, 70  
     density, 616  
     durability, 604, 606, 608, 609, 613, 615, 616  
     expansion, 604  
     facing, rock fill dams, 818  
     fineness modulus of aggregate, 606  
     forms, 612  
     freezing and thawing, 605, 614, 616, 618  
         Florence Lake Dam, 595  
     heat generation, 604  
     lift, height of, 613  
     joints in, 614  
     mixers, 611  
     mixes, 608, 609  
     modulus of elasticity, 452

- Concrete, permeability, 608, 613, 615
  - placing, 611
  - plastic flow, 452
  - Poisson's ratio, 452
  - porous, for slope protection, 764
  - protection of, 613
  - reinforcement, *see* Reinforcement
  - shrinkage, 451
  - slump, 609
  - specific gravity of ingredients, 610, 618
  - specifications, 605
  - strength of, 300
  - stresses allowable, 300
  - structural quality, 604
  - surface cracking, 615
  - surface finish, 613
  - temperature changes, 615
    - control, 615
    - variation, 450
  - testing, 604, 617
  - thermal coefficient of expansion, 451
  - transportation, 611
  - vibration, 611
  - water-cement ratio, 608, 609, 610
  - waterproofing, 616
  - weight of, 277, 328, 454
  - weight of ingredients, 610
- Concrete aggregate, coarse, 606
  - fine, 606
  - gradation, 607, 609
  - requirements, 604, 606, 608
- Concrete dams, application of, 41
  - architectural treatment, 857
  - foundation drainage, 53
  - gravity, application of, 41
  - height on earth, 54
  - horizontal joints, 848
  - joints, spacing of, 851
  - keyway, 852
  - longitudinal joints, 855
  - temperature control, 848
  - water stops, 853
- Concrete lining for upstream slope, 763
  - of square concrete blocks, 764
- Concrete material, tests of, 628
- Conduits through earth dams, 710
- Conklingville Dam, 778, 792
- Conowingo Dam, 351
- Consolidation, 633
  - clay, 636
  - curves, 638
  - device, 637
  - effect on shear strength, 639
  - fine sands, 634
- Consolidation, grouting, 63
  - shear strength curve, 639
  - significance of, 633
  - silt, 636
  - time of, 640
  - void ratio curve, 641
- Constant-angle arch dam, 429
- Constant-radius arch dam, 427
- Construction joints, 298
- Construction methods, 304
  - for earth dams, 749
- Construction materials for earth dams, 656
- Contents, of concrete gravity dams, 349, 400
  - of earth dams, 775
- Contour interval, 5, 9
- Contours, 7
- Contraction of concrete, 604
- Control, spillway, 870, 871
- Control of temperature, in concrete dams, 848
- Controlled crests, overflow dams, ice on, 399
- Controlling devices, outlets, 914
- Conveyors, belt, for concrete placing, 611
- Coolidge Dam, 562, 601, 603
- Cooling of dams, 615
- Coordinate system, 9
- Copeo Dam No. 1, 351
- Copper Basin Dam, 504, 556
- Coquilla Dam, seepage line in, 678
- Corbels, buttresses, 575, 577, 578, 584
- Core, care of samples of, 34
  - Conchas Dam analysis, 771
  - desirability of narrow, 793
  - drilling for grouting, 50
  - Fort Peck Dam, 798
  - lenses in shell, 796
  - location in rock fill, 829
  - mechanical analysis of, 792, 793
  - minimum width, 794
  - pool depth, 786
  - pool operation, 786
  - recovery of, 34
  - removal of sand lenses, 795
  - sand lenses in, 794
  - size of, 33
  - tightness of, 794
- Core barrel, 31, 33
- Core boxes, 35
- Corewall, 698
  - expansion joints, 701
  - rockfill dams, 823

- Counterweighted gates, 898, 902
- Cove Creek Dam, 353
- Cracks, arches, 497
  - buttresses, 569, 593
  - concrete dams, 848, 856
  - concrete structures, 615
  - Lake Hodges Dam, 593
- Crane, Albert S., mechanical analysis, 793
- Crane, gantry, 899
- Creager, W. P., extension of Bazin's data, 358
  - flood flows, 100, 125, 132
  - floods, 207
  - horizontal velocity components of overflow, 257
  - influence of silt deposits, 263
  - shape of crest, 357, 364
  - shearing strength of dams, 269, 297
  - top width of non-overflow dams, 307
- Creep, line of, 58, 65, 696, 703, 709
  - bibliography, 90
- Crest control, 871
- Crest gate, heating of, 871, 884, 912, 913
  - operation, 895
  - weight, 906
- Crests, ogee, surface finish, 613
- Crib, rock-fill dam, 816
- Critical density, 636, 757
- Critical depth, spillway intakes, 371
- Crocodile River Dam, 556
- Crosby, I. B., geology, 90
- Cross Cut Dam, drainage, 71
- Cross River Dam, 351
- Croton Falls Dam, 351
- Crown deflections, elastic arches, 436, 448, 449
- Crown forces, elastic arches, 435, 460, 467, 479, 486, 490, 499, 530
- Crystal Springs Dam, 353
- Cucharas Dam, 808
- Cummum Dam, 778
- Curing of concrete, 613
  - effect on durability, 616
- Curtain grouting, 48
- Cushman Dams, 556
- Cutoff, 47, 262, 693 to 701
  - anchorage, 296
  - buttress dams, 570, 572, 599
  - buttresses, earth dams, 713
  - chemical grouting, 70
  - chute spillways, 214
  - concrete, 47, 70
  - control of uplift or underflow, 267, 268, 570, 572
- Cutoff, dams on earth, 70
  - downstream, 72
  - grouted, 47
  - partial, 695
  - prevent sliding, 55, 296
  - rock-fill dams, 806
  - Rodriguez Dam (300 feet), 570
  - seepage, 695
  - steel sheet piling, 70, 302, 694
  - upstream at John Martin Dam, 768
  - walls, 701
  - wood piling, 70
- Cutting edge, diameter of, 21, 23
- Cylinder theory for arch dams, 425
- Dams, arch, *see* Arch dams
  - buttressed, *see* Buttressed dams
  - concrete, *see* Concrete dams
  - earth, *see* Earth dams
  - hollow, *see* Buttressed dams
  - list of existing, arch, 556
    - buttressed, 562
    - composite rock-fill and earth, 810
    - earth, 778
    - gravity, 305, 350
    - rock-fill, 808
  - list of failures, earth, 660
  - safety of, first consideration, 40
  - short life, 40
  - steel, *see* Steel dams
  - timber, *see* Timber dams
- Dangerous circle analysis, abbreviated method, 738
  - by slices, 735
  - failure below toe, 734
  - failure through toe, 732
- Darcy, H., 647
- Darcy formula, 647
- Davis, Albion, spillway discharge, 366
- Davis, A. P., irrigation engineering, 356
- Davis, C. V., applied hydraulics, 98
- Davis Bridge Dam, 779, 790, 792
  - flat-crested shaft spillway, 236, 237
  - permanent flashboard, 877
- Davis Reservoir, 661
- Dean, J. P., hydraulic model tests, 98
- Debris Barrier No. 1 Dam, Yuba River, 661
- Debris dams, earth and silt pressure, 272
- Deck girders, steel dams, 838
- Deer Creek Dam, 778
- Definitions, soil mechanics, 619
- Deformation, cantilever, 502, 512, 523, 528, 529, 534



- Deformation, elastic, in arches, 434, 435  
   foundation, 440  
   moment, arch dams, 436  
   shear, arch dams, 439, 479, 480  
   thrust, arch dams, 438  
   twist, arch dams, 538, 542  
 Denison Dam, 778  
 Density, concrete, 616  
   critical, 636, 757  
   definition, 621  
   effect on permeability, 650  
   method of determining, 760  
   required for rolled fill, 760  
   various moisture contents, 643, 644  
 Dentated end sills, 84  
 Depletion curves, ground water, 157  
 Depth duration, 181  
 Depth of core pool, 786  
 Derrick stones, concrete aggregate, 604  
 Design of earth dams, bibliography of, 714  
   gravity dams, general, 306, 313, 357  
   head, discharge for, 367  
   standard crest, 357  
   storm, 180  
 Devil's Gate Dam, 351  
 Dewell, H. D., earthquake acceleration, 279  
 Diablo Dam, 556  
 Diamond bits, improved efficiency of, 32  
 Diamond drilling, 10, 31  
 Dillman, O., coefficient of discharge, 369  
 Direct shear machine, 629  
 Discharge capacity, overflow dams, 364  
 Discharge formula, 364, 368  
 Distortion of undisturbed samples, 17, 18  
 Diversion dams, silt above, 272  
 Dix River Dam, 808, 811, 815, 820  
 Dodder Dam, 778  
 Dodge, Russell A., fluid mechanics, 259  
 Dolson, Fred O., frost action, Gem Lake Dam, 585  
 Don Martin Dam, 562, 599, 600  
 Don Pedro Dam, 351  
 Dore, Stanley M., 651  
 Dover Dam, 351  
 Dow valve, 923  
 Downstream rock protection, Clendenning Dam, 773  
   Conchas Dikes, 770  
 Downstream slope protection, earth dams, 766  
 Drainage, Arkabutla Dam, 684  
   chute spillways, 215  
   earth dams, 682  
   effect on seepage line, 685  
   foundations, 53  
   Tabeaud Dam, 682  
 Drainage wells, Arkabutla Dam, 684  
 Drains, blind, 713  
   buttressed dams, 572  
   control of uplift, 263, 296  
   dams on earth, 71  
   pile foundations, 302  
   pipe, 686  
     Kingsley Dam, 687  
     Sardis Dam, 688  
   position of, 693  
   rock, 689  
     foundations, 53  
 Drawdown, analysis for, 740  
 Dredge, baby, 795  
 Dredges, suction, 784  
 Drew's Dam, 808  
   timber facing, 816  
 Drilling, *see* Borings  
 Drive sampling of clays and silts, 16  
 Druids Lake Dam, 779  
 Drum gates, 871, 878, 880  
   overflow dams, 398  
 Dry density, definition, 621  
 Dry weight, 760  
 du Pont, R. B., on circular weirs, 228  
 Dumped riprap, 761  
 Durability, of concrete, 604, 606, 608, 609, 613, 615, 616  
   of steel dams, 841  
 Dwinnell Dam, 792  
 Dynamic effect, tailwater, 259  
 Dynamic forces on dams, 255  
 Earth, angle of internal friction, 274, 619, 620, 632, 639, 716, 733  
   augers, 15  
   dry weight, 273  
   foundation, 268, 296, 300, 302  
   pressure on dams, 272  
   submerged weight of, 273, 719, 721  
 Earth dam, abbreviated method for dangerous circle, 738  
   analysis for drawdown, 740  
   application of, 42  
   bibliography on details, 805  
   principles of design, 714  
   stability, 748  
   bonding to foundations, 713, 751, 770  
   buttresses, 713

**Earth dam, clearing, 750**  
 composite, seepage line, 672  
 conduits through, 710  
 construction, importance of careful, 750  
   methods, 749  
 contents, 775  
 criteria for design, 662  
 cutoff walls, 70, 701  
 dangerous circle analysis, 732, 734  
   by slices, 735  
 design for available material, 657  
 details, 749  
 drainage in, 682  
 elastic theory, foundation, 728  
 equipment improvements, 749  
 equivalent liquid pressure, 722  
 factor of safety, hydraulic fill, 747  
 failure, 662  
   table, 660  
 filters for, 688  
 flotation gradient, 706  
 flow net, 670  
 foundation of, 53, 656  
   shear, 725  
 hydraulic fill, formula, Gilboy, 744  
   safety during construction, 783  
 list of, 775  
 piezometer pipes, 705  
 pipes through, 710  
 piping, 708  
 plastic foundation, 731  
 pressure cells, 704  
 quick sand foundation, 706  
 rolled fill, 753  
 rolled layers, depositing, 754  
 safety, against foundation shear, 727  
   against overtopping, 663  
   against shear, 719, 720  
   against sudden drawdown, 723  
 safety requirements, 662  
 seepage, 663  
 seepage line, 664, 672, 675, 677  
   determination of, 665  
   in composite structure, 672  
   in existing, 677  
 shear, in downstream portion, 717  
   in hydraulic fill, 744  
   in plastic foundation, 731  
   in upstream portion, 718  
 settlement, 758  
 stability, 715  
   against headwater pressure, 716  
   hydraulic fill, 742  
   numbers, Taylor, 737

**Earth dam, stability, rough methods of**  
   determining, 715  
     Swedish geophysical method, by, 731  
 stripping, 750  
   trimming of slopes, 759  
 upstream blankets, 696  
**Earth foundations, piping, 61, 708**  
   recommended design, 68  
   uplift, 63  
**Earthquake acceleration, 247, 279, 330**  
**Earthquake forces, 527**  
   arch dams, 452, 526, 527  
   buttressed dams, 285, 564  
   direction of, 284  
   discussion, 279  
   fault movements, 285  
   ice and silt, 285  
   masonry inertia, 281  
   resonance, 281  
   Rossi-Foré scale, 280, 281  
   uplift, 284  
   vibration periods, 282  
   water load, 282, 284, 330, 526, 564  
**East Canyon Dam, 808**  
**East Park Dam, 351**  
**Echo Dam, 779**  
**Eddy, H. P., Jr., floods, 207**  
**Eel River, 351**  
 Effective size, sand, definition, 620  
**El Capitan Dam, 779**  
**El Fuerte Dam, 355**  
 Elastic arches, 434  
 Elastic center, 482, 487  
 Elastic theory, 434  
   for foundation shear, 728  
**Electrical analogy, model test, 57, 671**  
**Electrical resistivity prospecting, 12**  
**Electrolytic determination of permeabil-**  
   ity coefficient, 653  
**Elephant Butte Dam, 305, 351, 858, 859**  
   profile, 330, 348  
**Embankments, application of, 42**  
   in layers, building, 753  
   weaving, 754  
   wetting, 754  
**Emergency spillways, 243**  
**End contractions, overflow dams, 365**  
**End sills, 84**  
   dentated, 84  
**Energy dissipation, arch dams, 82**  
   baffles, 77, 78  
   below spillways, 74  
   jet deflectors, 86  
   low dams, 83

- Energy dissipation, sloping aprons, 79  
 Engineering Foundation, 16  
 Englewood Dam, 791, 792  
 English Dam, 808  
 Equipment improvements, effect of, 749  
 Equivalent liquid pressure, 722  
 Equivalent liquid weight of core, 743  
 Erosion, a cause of failure, 293  
     timber dams, 846  
     below spillways, 73, 82, 86  
         baffle piers, 78  
         causes of, 73  
         cavitation, 84  
         end sills, 83, 84  
         general requirements of control, 76  
         jet deflectors, 86  
         low dams, 83  
         sloping aprons, 79  
         upturned bucket, 81  
 Erosion control, 76  
     end sill, 78  
     stilling pool, 77  
 Escape gradient, 707, 708  
 Escondido Dam, 808  
 Estimating diagram, gravity dams, 349, 400  
 Euclid, 753  
 Exchequer Dam, 351  
 Expansion, thermal, coefficient, for concrete, 451  
     for stone, 453  
     steel dams, 838  
 Expansion of concrete, 604  
 Expansion joints, concrete facing of rock-fill dams, 818  
     in corewalls, 701  
 Experiments, hydraulic, 98  
 Exploration, subsurface, 9, 10  
     churn drilling, 14  
     earth augers, 15  
     electrical, 12  
     methods of, 12  
     rotary drilling of overburden, 15  
     seismic, 12, 39  
     test pits, 13  
     wash borings, 14  
 Explosion wave method, 39  
  
 Facing, concrete, rock-fill dams, 816, 817, 818  
 Factor of safety, against foundation shear, 727  
     hydraulic fill, 744, 747  
 Fadum, R. E., 633  
 Fahlquist, Frank E., 62  
 Fahlquist sampler, 27, 28  
 Failure, Belle Fourche Dam, concrete facing, 764  
     below toe, dangerous circle analysis, 734  
     chute spillways, of, 210  
     Clendenen Dam, 772  
     dams, causes of, 293  
     earth dams, 662  
         table, 660  
     Tappan Dam, 756  
     through toe, dangerous circle analysis, 732  
 Fargo Engineering Co., 913  
 Faults, earthquake movement on, 285  
 Faure, Henry, Boulder Dam, spillway tests, 98  
 Feagin, L. B., 55  
 Feeler inspection of borings, 36  
 Fetch, 274, 276  
 Field laboratory, 626  
 Field tests, 37, 760  
 Fifteen Mile Falls Dam, 351  
 Fillet arches, 492  
 Fillets in corners, 414  
 Filter, for earth dams, 688  
     gradation, 688  
     position of, 693  
     required thickness, 692  
 Filter drains, 71, 72  
     under aprons, 88  
 Fine sands, tests of, 627  
 Fineness modulus, concrete aggregate, 606  
 Fines, wasting, 793  
 Fish, ladders, 863  
     lifting, 865, 866  
     lock, 865  
     protection, 862  
 Fishways, 862  
 Fixed roller gate, 871, 889  
 Flashboard pins, failure stress, 872, 873, 875  
 Flashboards, 871  
     ice against, 876  
     on overflow dams, 397  
     permanent, 876, 877, 878  
 Flexural stresses, dam foundation, 288  
 Flexure, curved beams, 436  
 Flinn, A. D., arch dam investigation, 279  
     "Water Works Handbook," 305  
 Flood, characteristics, 128, 130  
     control economics, 131  
     flows, 99

- Flood, formula, 139
- frequency studies, 131
  - defects in, 135
- hydrographs, 140, 157
  - natural, 155
  - subdivision of, 157
- probability curves, 136
- symposium, Am. Soc. C. E., 207
- Floods, accuracy of estimates, 203
  - Am. Meteorological Soc., 207
  - basic stage method, 132
  - bibliography, 205
  - coefficient of variation, 134, 136
  - depletion curves, 157
  - effect of forests, 129
  - effect of physical characteristics, 128
  - effect of snow, 130
  - effect of vegetation, 129
  - emergency spillways, 243
  - freeboard, 201, 203
  - ground-water depletion, 157
  - hypothetical hydrographs, 192
  - infiltration, 143
    - index, 145
  - initial loss, 145
  - lag, 100
  - margin of safety, 201, 204
  - peak, 99, 139
  - physical characteristics, 128
  - physical indication of, 137
  - publications of record, 123
  - rainfall depth-duration, 181
  - recession curves, 156
  - record of history, 99
  - reservoir inflow, 177
  - routing, 195, 196, 198, 200
  - runoff, 155
  - S-curves, 167
  - snow, 186
  - spillway design flood, 204
  - storage effect on, 128
  - surcharge storage, 202
  - synthetic unit hydrograph, 162, 169
  - table of, 101
  - Thiessen polygons, 154
  - transposed storms, 185
  - unit hydrograph, 158, 160, 162, 170, 173, 175
  - unit rainfall duration, 158
  - unit storms, 159
  - unusual, 101
  - valley storage, 129
  - variation, coefficient of, 100
  - yearly flood method, 132
- Florence Lake Dam, 562, 566, 595
- Floris, A., uplift pressures, 266
- Flotation gradient, 706
- Flow, plastic, 452
  - types of, 93
- Flow net, 55, 64, 262, 668
  - bibliography, 90
  - in earth dams, 670
  - in foundation, 669
  - porous foundation, 261
- Folse and Hayford, flood factors, 139
- Forces on dams, 247, 252; *see also* Loads on dams
- Fordyce Dam, 808
- Forests, effect on floods, 129
- Forms, concrete, 612
- Fort Peck Dam, 27, 70, 660, 779, 791, 793, 795, 797
- Foster, H. A., flood flows, 134
- Foum-El-Guëias Dam, 808
- Foundation, 55
  - bearing strength, 300, 302
  - bibliography, 90
  - bond, 45
  - bonding earth dams to, 713, 751
    - Conchas Dike, 770
  - buttressed dams, connection with facing, 570
    - on soft, 572
  - cutoff, 693, 694, 695
    - effect on seepage, 693
    - for rock-fill dams, 806
  - dam anchorage to, 278
  - defects, treatment of, 46
  - definition of, 44
  - deformation, 463
    - arch dams, cantilevers, 521, 523, 528
    - constants, 462
    - effect on elastic arch, 434
    - equations and constants, 440
    - neglect of, 481
    - significance of, 468
  - drainage, 53
  - earth, 53, 268, 296, 300, 302
    - bearing strength of, 54, 302
    - limiting height of dam, 54
    - pipings, 61, 708
    - recommended design, 68
    - roofing, 54
    - seepage through, 59
    - sliding on, 54
    - strength of, 54
    - uplift, 63
  - earth dams, 656

- Foundation, engineering, 16  
 flow net, 669  
 grouting, 48, 262, 296  
 inclined stresses, 301  
 material, tests of, 628  
 modulus of elasticity, 442, 629  
 permeability of, 57  
 piles, 54, 55, 302  
 preparation of, 44  
 pressure, 288  
 protection of, 44  
 reaction, elastic effects, 286  
   equations for vertical pressures, 288  
   horizontal, 292  
   irregular bases, 290  
   law of middle third, 291  
   rectangular bases, 290  
   stability requirements, 291  
   static requirements, 286  
   trapezoidal form, 287  
   with uplift, 290  
 rock, care in blasting, 45  
   leakage through, 47  
   suitability of, 37  
 seams, effect on underflow and uplift, 263  
 shear strength, 269, 292, 297  
 shearing stresses in, 725  
 sliding coefficient, 295  
 steel dams, 840  
 stratified, 296  
 strength of, 300  
 stress, concentrations, 415  
   Grand Coulee Dam, 415, 416  
   Morris Dam, 415  
 test of bond to Conchas Dam, 770  
 test of strength, 301  
 timber dams, 846  
 toe protection, 53  
 treatment, 44, 46  
   Grand Coulee, 45  
 uplift, 63, 264  
 weight, 278  
 Fowler, F. H., circular arches graphic methods, 490, 492  
 Francis, J. B., weir discharge, 364, 365, 366, 368  
 Francis's formula, 364, 365  
 Franklin Falls Dam, 779  
 Free, G. R., infiltration, 205  
 Freeboard, 201, 203, 274, 276, 313, 663, 822  
   rock-fill dams, 822  
 Freeman, John R., earthquake, 281  
 Freeman, John R., "Hydraulic Laboratory Practice," 92, 98  
 Freezing and thawing concrete, 614, 616, 618  
 Freezing method of sampling, 27  
 Freezing of crest gates, 912  
 French Lake Dam, 808  
 Frequency studies, floods, 131  
 Friant Dam, 351  
   cement for, 605  
 Friction, coefficient of, 295, 904  
   combined with shear, 297  
   gates, 903, 904, 905  
   internal, 619  
     angle of, 274, 619, 620, 632, 639, 716, 719 to 728, 733 to 748  
     resistance to sliding, 294  
 Friction loss in sluicing pipes, 787  
 Frost damage, buttressed dams, 585, 595  
 Froude number, 92, 93, 94  
 Frozen plug, use of, in sampling, 28, 31  
 Fuller, W. E., flood flows, 100, 125, 207  
 Galleries, 422  
 Galloway, J. D., rock-fill dams, 811  
 Gantry crane, 899  
 Gârza Dam, 791  
 Gate, air vents, 916  
   automatic, 898, 901  
   spillway, 882  
   broome, 920, 921  
   butterfly, 916, 922, 923, 924  
   caterpillar, 888, 920, 921  
   counterweighted, 898, 902  
   crest, 871, 884  
   discharge coefficient, 374  
   Dow valve, 923  
   drum, 398, 871, 878, 880  
   fixed roller, 871, 889  
   forces to operate, 905, 906  
   friction, 903, 904, 905  
   guard, 915  
   hoist, 896, 897  
   ice troubles at, 911  
   location for sluice, 916  
   Reclamation Service, drum gate, 880  
   slide gate, 921  
   ring follower, 919, 921  
   roller bearing, 871  
   rolling, 871, 894  
   seals, 898, 902, 903, 921  
   sector, 881  
   Sidney, 894  
   slide, 871, 916, 917, 918, 921

- Gate, sluice, 927, 929
  - Stauwerke, 884
  - Stickney drum, 878
  - stone, 885
  - taintor, 871, 891, 892, 893
  - tilting, 871, 884
  - tractor, 920, 921
  - truck mounted, 871, 891
  - ventilation of, 916
  - wheeled, 920
- Gatun Dam, 10, 11, 81, 779
- Gem Lake Dam, 562, 585
- Genissiat Dam, 355
- Geologic investigations, 9
- Geologic sections, 10
  - Conchas Dam, 10
  - Gatun Dam, 10, 11
- Geologist, 10
- Geology for dams, 38
- Geophysical foundation study, 39
- Germantown Dam, 791, 792
- Ghrib Dam, 808, 830
- Giant for sluicing, 783
- Gibbs, E. F., tests, hydraulic model, 98
- Gibson, A. H., tests, hydraulic, model studies, 98
- Gibson Dam, 556
  - uplift, 265
- Gilboa Dam, 351
- Gilboy, Glennon, hydraulic fill formula, 744
  - rock-fill dams, 829
- Gilchrest, B. R., floods, 206
- Glacial deposits, for hydraulic fill, 791
- Gleno Dam, 562
- Glenville Dam, 810, 825
- Glines Canyon Dam, 556
- Glover, R. E., heat flow in dams, 450
- Goodall, George, on inclined arch stresses, 585
- Goose Creek Dam, 779
- Grand Coulee Dam, 45, 81, 305, 348, 351, 415
- Granite Reef Dam, 59, 68
- Graphic analysis, elastic arch, 468
- Grass for slope protection, 766
- Grassey Lake Dam, 779
- Gravel, 624
  - concrete aggregate, 609, 610
  - foundation, bearing power, 302
  - suitability of, 37
  - tests of, 627
- Gravelly Valley Dam, 351
- Graves, Q. B., "Flood Routing," 206
- Gravity acceleration  $g$ , 248, 256, 279
- Gravity axis, arch dams, 436
- Gravity dams, block depths, 329
  - compressive stresses, 299
  - design, general, 306, 307, 308, 309, 310, 311, 312
    - multiple-step, 345
  - earthquake forces, 330
  - existing, uplift, 265
  - freeboard, 309, 313, 338
  - nonoverflow, comparison of sections, 330, 346, 347, 348
    - design of, 306, 313
    - estimating curves, 349
    - examples, 313, 330, 337
    - ice pressure, 315
    - list of existing, 350
    - practical profile, 329
    - stability requirements, 293
    - top details, 306, 314, 331
    - zones, 309, 314, 331, 337
  - overflow, comparison of, 399
    - controlled crests, 397
    - crest gates, discharge, 374
    - design, 306, 357
      - examples, 377, 385, 391
      - head, 258, 357
    - discharge, 364
      - coefficient, 364, 372, 373
      - formula, 364, 368
    - drum gates, 398
    - dynamic forces, 259
    - end contractions, 365
    - estimating diagram, 400
    - flashboards, 397
    - flow over crest, 258, 357, 392
    - ice loads, 385
    - ice on controlled crests, 399
    - jet, adherence of, 361
    - jet velocities, 364
    - list of existing, 305, 350
    - practical profile, 384
    - pressure on crest, 258
    - reinforcement for ice pressure, 386
    - shape of crest, 357, 377, 393
    - special crest details, 361, 370, 397
    - stability, with crest gates, 364, 397
    - stability requirements, 293
    - standard crest, 357
    - stresses, crest, 384, 386
    - submerged, 372
    - surface finish, crests and buckets, 613
    - tailwater reaction, 259

- Gravity dams, overflow, top details, 380,**  
     388, 395, 397  
     zones, 311, 378  
     practical profiles, 329, 384  
     safety factor, 303  
     shear, 405, 411  
     stability requirements, 293  
     stresses, base, 413, 415  
         compressive, 299  
         existing dams, 304  
         faces, 404  
         foundation, 288  
         interior, 401  
         margin of safety, 303  
         numerical values, 385, 391  
         oblique planes, 402  
         openings, at, 418  
         principal, 402  
         secondary, 401  
         tension, 302  
     theoretical cross-sections, 306  
     top details, 306, 314, 331, 380, 388, 395,  
         397  
     triangular section, 306  
     zones, 309, 311, 314, 331, 337, 378  
**Green, W. E., reservoir temperatures, 451**  
**Green Mountain Dam, 779**  
**Greenlich Dam, 661**  
**Gregory (with Arnold), runoff, 206**  
**Grimsel Dam, 355**  
**Groat, Benjamin F., hydraulic model**  
     tests, 98  
**Ground control for multiplex mapping, 7**  
**Ground-water depletion, 157**  
**Grout holes, 50**  
**Grouted cutoff, 47**  
**Grouting, 262, 296**  
     asphalt, 52  
     bibliography, 90  
     chemical, 70, 90  
     consolidation, 53  
     curtain, 48  
     foundation, Labontan Dam, 49  
     longitudinal joints, 856  
     in stages, 49  
     mixtures, 50  
     of seams, 48, 49, 50, 51, 52  
     pressures, 51  
     rock foundation, 48  
     uplift caused by, 51  
     with bentonite, 51  
     with clay, 51  
**Growdon, J. P., earth core rock fill, 825**  
**Guajabal Dam, 562**  
**Guard Gates in sluices, 516**  
**Guernsey Dam, 779**  
**Gulf Island Dam, 351**  
**Gumensky, D. B., 374, 425**  
  
**Hamilton Dam, 562**  
**Hanna, Frank W., dams, 356**  
**Hansen Dam, 779**  
**Harriman Dam, 779**  
**Harrison, C. L., ice pressures, 271**  
**Harris, L. F., Dix River Dam, 811**  
     uplift and seepage, 90, 261, 671  
**Hathaway, G. A., floods, 140, 206**  
**Hatchtown Dam, 661**  
**Hauser Lake Dam, 351, 834, 839**  
**Hawley, George W., "900 Dams In-**  
     spected," 356  
**Hayford and Folse, flood factors, 139**  
**Hays, J. B., grouting, 90**  
**Hasen, Allen, core material, 793**  
     floods, 125, 132, 135, 206  
**Head loss in sluicing pipe, 787**  
**Headwater control, bibliography, 929**  
**Hebron Dam, 661**  
**Heel trench, 45**  
**Heilbron, Carl H., Jr., arch dams, 425**  
**Hemet Dam, 351**  
**Henny, D. C., stability of dams, 266, 297**  
**Henshaw Dam, 790, 792**  
**Hetch Hetchy Dam, 353**  
**Hill, H. M., flow net, 90**  
**Hinds, Julian, canal headgate discharge,**  
     374  
     side channel spillways, 217, 218, 224  
**Hiwassee Dam, 305, 330, 348, 352, 615,**  
     856, 861  
**Hodges, flood flows, 125**  
**Hoffman Dam, 792**  
**Hogan, M. H., tests, hydraulic models, 98**  
**Hoist, gate, 897**  
     oil pressure, 915  
**Hollow Dam, see Buttressed dams**  
**Holmes, Harlan B., fishways, 862**  
**Holter Dam, 352**  
**Hoopess Dam, 352**  
**Horizontal piping, 709**  
**Horse Creek Dam, 661**  
**Horse Mesa Dam, 556**  
**Horseshoe Dam, 585**  
**Horton, R. E., floods, 137**  
     infiltration, 205  
     snow-melt, 206  
     values of Kutter's  $n$ , 138  
     weir experiments, 364, 370, 372, 374

- Houk, Ivan E., arch dams, 499, 505  
 design assumptions, masonry dams, 298  
 rainfall, 207  
 uplift pressure in masonry dams, 264
- Howe (with Camp), circular weirs, 228
- Howell-Bunger valve, 928
- Hoyt, W. G., runoff, 206
- Huber, Walter L., frost action, Gem Lake Dam, 585
- Hume Dam, 779
- Huntington Dam, 352
- Hvorslev, Dr. M. Juul, sampling, 16
- Hydraulic electric analogy, 671
- Hydraulic fill dam, 782, 783  
 analysis, 746  
 borrow-pit analysis, 790  
 formula, Gilboy, 744  
 lenses, recommended requirements, 797  
 materials suitable, 791  
 stability, 742  
 uniformity coefficients of shells, 791
- Hydraulic jump, 75, 77  
 on sloping aprons, 79  
 overflow dams, 396
- Hydraulic models, 91
- Hydraulic similitude, 92  
 examples of, 95
- Hydraulicking, suitability of material for, 38, 791
- Hydraulics, chute spillways, 216  
 morning glory spillway, 229, 236  
 shaft spillways, 229, 236, 241  
 side channel spillways, 218, 225
- "Hydro-Electric Handbook," Creager and Justin, 356
- Hydrograph, computations, 193  
 hypothetical, 192  
 natural, 155  
 reservoir inflow, 177  
 S-curves, 167  
 spillway design, flood, 204  
 subdivision of, 157  
 unit, 160, 173  
 adjustments, 170  
 isolated storms, 160  
 major flood records, 162  
 peak discharge, 164  
 selection of, 175  
 synthetic, 162
- Hydrostatic pressure, relief of, 53
- Hyetographs, rainfall, 143  
 snow-melt plus rainfall, 192
- Ice, against flashboard, 876  
 air jets for preventing, 913  
 melting by air bubblers, 876, 913
- Ice pressure, 270, 271  
 earthquake effect, 272, 285  
 on controlled crests, 399  
 gravity dams, 315  
 reinforcement for, 386
- Ice troubles, 911
- Imperial Dam, 55  
 drainage, 71, 72  
 end sill, 83  
 foundation, 68
- Impervious material, suitability of, 37  
 upstream facing for rock-fill dams, 816
- Inertia, earthquake loads, 527
- Infiltration, initial loss, 145  
 rainfall, 143
- Infiltration index, 145  
 computation of, 146
- Inflow flood, 177
- Inflow storage-discharge curves, 196, 197
- Inland Dam, 810, 825, 826
- Internal friction, angle of, 274, 619, 620, 632, 639, 716, 733
- Internal stresses, horizontal, 404, 406, 410, 416, 547  
 inclined, 402, 416, 547  
 principal, 402, 403, 413, 416, 547  
 secondary, 401  
 shears, 407, 410, 411, 416  
 vertical, 404, 411, 413, 416
- Intrusions in core, 794
- Investigation of dam site, 1, 3
- Irrigation engineering, A. P. Davis, 356
- Isohyetal map, 141
- Iwan earth auger, 15
- Jaenichen, P. H., on shaft spillways, 235
- Jakobsen, B. F., stresses in thick arches, 437, 490
- Jarvis, C. S., floods, 100, 123, 127, 206
- Jet, adherence, overflow dams, 361  
 deflectors, 86  
 shape, with piers, 366  
 velocities, overflow dams, 364
- Jobes, J. G., tests, hydraulic model, 98
- John Martin Dam, 767, 779
- Johnson, J. B., elastic properties of rocks, 452
- Johnstown Dam, 661
- Joints, buttress, 569, 597  
 chute spillways, 213



- Joints, concrete structures, 614  
   construction, effect on sliding, 298  
   diagonal, 850  
   horizontal, concrete dams, 848  
   longitudinal, grouting of, 856  
   spacing of, in dams over 200 feet high, 851  
   transverse, concrete dams, 848  
 Jones and Minear, grouting, 90  
 Jordan Dam, 352  
 Jordan River Dam, 562  
 Jorgensen, Lars, 556  
 Jumbo Dam, seepage line in, 678  
 Jump, hydraulic, 75, 77, 396  
 Jürgeonson, Leo, elastic theory, 728  
   formula, 731  
 Justin, Joel D., flood flows, 100  
  
 Kebir Dam, 808  
 Kellog, F. H., grouting, 00  
 Kendorco classification, 624  
 Kenerson, W. I., 624  
 Kennedy, Robert C., dams, 356  
 Kensico Dam, 305, 347, 352, 856, 857  
 Keokuk Dam, spillway discharge, 366  
 Kern, 513, 518, 519  
 Keyways, concrete dams, 852, 855  
 Khosla (Bose and Taylor), foundations, 90  
 King, Horace, "Handbook of Hydraulics," 372  
 Kingsley Dam, 70, 231, 234, 687, 779, 791, 793, 795, 803  
 Knightville Dam, 779, 791, 793, 795  
 Kochess spillway, 210  
 Koehlin, "Mecanisme de l'Eau," 356  
 Koon Dam, 352  
 Kurtz, Ford, on shaft spillways, 236, 240  
  
 La Grange Dam, 352  
 La Jagne Dam, 556  
 La Prele Dam, 562  
 La Regadera Dam, 660  
 Laboratory, field, 626  
 Lackawak Dam, 779  
 Lago d'Avio Dam, 562  
 Lago Nero Dam, 562  
 Laguna weir, 822  
 Lahontan Dam, 49, 779  
 Lake Avalon Dam, 661, 810  
 Lake Cheesman Dam, 305, 348, 350  
 Lake Francis Dam, 661  
 Lake George Dam, 661  
 Lake Hodges Dam, 562, 593, 594  
  
 Lake Lure Dam, 562 \*  
 Lake McClure Dam, 351  
 Lake Pleasant Dam, 562  
 Lake Spaulding Dam, 556  
 Laminar flow, 93  
 Lancha Plana Dam, 353  
 Lane, Campbell, and Price, flow net, 90  
 Lane, E. W., "Flow Net and Electric Analogy," 261  
   foundations, 90  
 Lane's line of creep, 58, 65  
 Langbein, W. B., floods, 156  
   infiltration, 206  
 Larner Johnson valve, 925  
 Laurgard, O., on pours of concrete, 612  
 Layers, thickness of, 754  
   Conchas Dike, 757, 771  
 Le Tourneau scraper, 752  
 Lenses, criteria for, 797  
   recommended requirements, 797  
 Levy, Maurice, 266  
 Lewin, J. D., chemical grouting, 90  
 Life of dams, 40  
 Light, Philip, on snow-melt, 189, 206  
 Limnology, Welch, Paul S., 276  
   line of creep, 58, 65, 696, 703, 709  
   line of pressure, elastic arch, 468  
   liner of sampler, 23  
   lining of sluice, 916  
   Linville Dam, 790  
 Liquid limit, definition, 621  
 Lithgow No. 2 Dam, 556  
 Little Bear Creek Dam, 779  
 Loads on dams, Ariel Dam, 506  
   buttressed dams, 285, 564  
   Copper Basin Dam, 504  
   division, trial load theory, 504, 509, 524  
   dynamic, 255, 259  
   earth pressure, 272  
   earthquake forces, 279, 330, 452, 526, 564  
   foundation reaction, 286  
   horizontal, cantilever, trial load theory, 515  
   ice pressure, 270, 314, 385, 399  
   radial, cantilevers, trial load theory, 509  
   Seminole Dam, 503  
   silt pressure, 272, 377, 381  
   subatmospheric, 255  
   tailwater, 255, 259, 383, 396  
   tangential, 502, 527, 533  
   trial loads, 500  
   twist moments, cantilevers, 538

- Loads on dams, uplift, *see* Uplift**
  - variable, on arches, 434
  - vertical, cantilever, 509, 514
  - water pressure, 252, 258, 260, 377, 425, 453, 489, 514, 590
    - earthquake, 282, 330, 526, 564
  - wave pressure, 274, 314
  - weight of dam, 277
  - wind pressure, 274
- Location, choice of, 4**
- Loch Raven Dam, 352**
- Lockington Dam, 792**
- Loess, 624, 647, 648, 650**
- Log chute, 866, 867, 868**
- Long Valley Dam, 779**
- Longitudinal joints, concrete dams, 855**
  - grouting of, 856
  - Shasta Dam, 855
- Los Arcos Dam, 559**
- Lower Otay Dam, 660, 808, 823, 824**
- Loyalhanna Dam, stilling basin, 80**
- Lugeon, Maurice, "Barrages et Géologie," 356, 556**
- Lyman Dam, 661**
- Macyscope, 9**
- Madden Dam, sloping apron, 79**
- Magic Dam, 790**
- Mahoning Dam, 305, 348, 352**
- Maney, G. A., indeterminate stresses, 439**
- Manganese in sluicing pipe, 791**
- Manning's formula, 76, 94**
- Mapping, aeroplane, 5, 7, 8**
  - multiplex, accuracy of, 7
  - plane table, 8, 9
- Maps, anaglyph, 9**
  - site, 9
  - topographic, 5
  - aeroplane, 8
- Mareges Dam, 556**
- Marichal, Arthur, 358**
- Marsh, L. E., floods, 206**
- Marshall Creek Dam, 660, 662**
- Marshall Ford Dam, 352**
- Martin Dam, 352**
- Masonry, 300**
  - allowable stresses, 300
  - construction, Baker, Ira O., 300
  - inertia of, 281
  - modulus of elasticity, 452
  - sliding coefficients, 295
  - weight of, 277, 454
- Mass rainfall curves, 143**
- Material, cohesive, suitability of, 37**
- Material, colloidal, 38**
  - impervious, suitability of, 37
  - rough tests for, 37
  - selection of, 37, 759
  - uncompacted, passage of water through, 713
- Materials of construction for earth dams, 656, 657**
- Mathis Dike Dam, 571**
  - sliding, 55
- Matrimony vine for slope protection, 766**
- Matzke, A. E., on hydraulic jump, 98**
- Maurer, E. R., on slab analysis, 575**
- Mayer, L. C., infiltration, 205**
- McCarthy, E. F., forests and floods, 207**
- McCarthy, G. T., flood flows, 131**
- McConaughy, Boulder Dam spillway tests, 98**
- McMillan Dam, 810, 824, 825**
- Mead, W. J., geology, 90**
- Meadow Lake Dam, 808**
- Mechanical analysis, 621**
  - blow sand, 623
  - borrow pit, hydraulic fill, 790
  - clayey silt, 623
  - Conchas core, 771
  - core, 792, 793
  - core and shell, Fort Peck Dam, 800
  - fat clay, 623
  - loess, 623
  - pervious section, Conchas Dam, 772
  - sandy silts, 623
  - sandy gravel, 624
  - sandy loess, 648
  - sandy silty clay, 637
  - shell, 795
  - silty clay, 623
  - silty sand, 623
- Medina Dam, 352**
  - uplift, 265
- Medleri Embankment, seepage line in, 679**
- Merriman Dam, 779**
- Miami Dams, 785**
- Miami Conservancy District, floods, 137**
  - rainfall, 206
- Microscope, field, 38**
- Middle Branch Dam, seepage line in, 677**
- Middle third, law of, 291**
- Middlebrooks, T. A., 708**
- Milner Dams, 810**
- Minatare Dam, seepage line in, 679**
- Miner and Jones, grouting, 90**
- Minidoka Dam, 810**

- Mississippi River, emergency spillways, 244
- Mitchell Dam, 352
- Mixers, concrete, 611
- Mixing, concrete, 611
- Model, spatial, 5, 7
- Model tests, arch dams, 551  
     electrical analogy, 57  
     photoelastic, 552  
     spillways, 74
- Models, flow nets, 57  
     hydraulic, 91
- Modified Kendorco classification, 624, 625
- Modulus of elasticity, arch equations, 449  
     concrete, 452  
     foundation, 442, 629  
     masonry, 452  
     stone, 452, 453
- Mohawk Dam, 91, 685, 779
- Mohicanville Dam, 779
- Mohr, H. A., 21
- Mohr's circle, 403, 413
- Moisture content, Clendening Dam, 774  
     definition, 621  
     determining, 760  
     optimum, 642
- Molitor, D. A., wave pressures, 274
- Moment deformation, elastic arch, 436
- Moment tailwater effects, 259
- Moment theorem, elastic arch, 460
- Moment, twist, 526, 538
- Monolithic concrete lining, 763
- Monongahela Dam, baffle piers, 78, 79
- Montejaque Dam, 556
- Morena rock-fill dam, 808, 811, 814
- Mormon Flat Dam, 556
- Morning glory spillway, 227  
     Davis Bridge, 236  
     flat-crested, 236  
     hydraulics of, 229, 236, 238  
     standard crest, 228
- Morris Dam, 305, 348, 353, 779  
     stresses at base, 415
- Mountain Dell Dam, 562
- Mud Mountain Dam, 779
- Mudduk Dam, 779
- Mulholland Dam, 353
- Multiple-arch dam, 560, 562, 566, 592, 596  
     arch analysis, 585  
     arch forms, 584  
     arch stresses, 586  
     buttress stresses, 591
- Multiple-arch dam, cracks, Lake Hodges Dam, 593  
     design, 584  
     "improved type," 585, 588, 589  
     loading, 585  
     overflow type, 592, 593  
     reinforcement, Lake Hodges Dam, 593, 595  
     stability, 587  
     typical section, 560, 561
- Multiple-dome dams, 601
- Multiple-step design, gravity dams, 345
- Multiplex, equipment for aeroplane mapping, 5, 6  
     mapping, 7  
     plotting, 7
- Murray Dam, 562
- Muscle Shoals Dam, 355
- Musgrave, G. W., infiltration, 205
- Musk rats, 712
- Myer, A. F., flood flows, 125, 127
- Nagler and Davis, spillway discharge, 366
- Namias, Jerome, rainfall, 206
- Nantahala Dam, 808, 821, 825, 827
- Nappe, aeration of, 256, 257  
     coordinates for, 359, 360, 362  
     overflow dam, 258  
     shape of, 359
- Narrow cores, desirability of, 793
- Narrows Dam, 305, 353
- Natural cement, 605
- Natural hydrographs, 155
- Necaxa Dam, 661, 779
- Needle valve, 924, 927
- Needles, 871, 908
- Nelidov, Ivan M., inclined arch stresses, 585
- Neutral axis, 436
- New Croton Dam, 305, 347, 353, 779
- Neye Dam, uplift, 265
- Niederwartha Dam, 780
- Noetzi, F. A., Florence Lake Dam, 595  
     Lake Hodges Dam, 593  
     multiple-arch dam, 567, 585  
     round-head buttress dam, 560  
     stresses in buttress and gravity dams, 569  
     wind stresses in buttresses, 592
- Nomenclature for masonry dams, 247
- Norris Dam, 305, 353  
     holes grouted under, 38  
     profile, 348

- Norris Dam, sloping aprons, 79  
 Norristown rock-fill crib dam, 816  
 North African rock-fill dam, 830  
 North Bowman Dam, 808  
 North Crow Dam, 556
- Ocmulgee River Dam, 353  
 Oester Dam, uplift, 264, 265  
 Ogden Dam, 562  
 Olive Bridge Dam, 347, 350  
 Openings in dams, multiple, 423  
     numerical example, 421  
     reinforcing, 420, 422  
     stress concentrations, 418, 422  
 Operation of core pool, 786  
 Operation of crest gates, 895  
 Optimum moisture content, 621, 642, 760  
 Optimum water content, definition, 621  
 Organic impurities, 606, 617  
 Osage Dam, 353  
 O'Shaughnessy Dam, 353  
 Otay Dam (Lower), 353  
 Outlet control devices, 314  
 Overhang, arch dams, 431  
 Overrolling, danger of, 755  
 Overtopping, safety against, for earth dams, 663  
 Overturning, cause of failure, 293  
 Owyhee Dam, 353
- Pacoima Dam, 556  
 Paddy Creek Dam, 790  
 Paint, for waterproofing concrete, 617  
     on steel dams, 841  
 Palmdale Dam, 562  
 Parcel, J. I., indeterminate stresses, 439  
 Pardee Dam, 305, 348, 353  
 Parker Dam, 269, 556  
 Pathfinder Dam, 556  
 Patterson, K. E., Swedish geophysical method, 731  
 Paulsen, C. G., floods, 207  
 Pavana Dam, 562  
 Peak flows, 99  
 Penrose-Rosemont Dam, 808  
     steel facing, 817  
 Pensacola Dam, 562, 848, 862  
 Per cent voids, definition, 620  
 Percolation, control of piling foundations, 302  
     path of 58, 696, 703, 709  
 Percussion drill holes for grouting, 50  
 Periscopic inspection of drill holes, 36  
 Permeability, 645  
     Permeability, coefficient of, 646 647  
         concrete, 608, 613, 615  
         definition, 621  
         electrolytic determination, 653  
         table of, 649  
         determined by Thiern method, 650  
         foundation, 57, 650, 653  
         horizontal, 668  
         vertical, 668  
     Pervious material, compaction of, 757  
     Peter, E. Meyer, Boulder Dam spillway tests, 98  
     Philippe, R. R., piping experiments, 708  
     Photoelastic analysis, arch dams, 552  
     Photographs, aerial, 8  
     Pick-up beam, 898, 900  
     Piedmont Dam, 780  
     Piers, 365  
         restriction of flow by, 365, 371  
     Piezometers, 73, 705  
     Pigeon River Dam, 556  
     Pile foundations, 54, 55, 302  
     Piling cutoff, 70, 767, 798, 803  
     Pine Canyon Dam, *see* Morris Dam  
     Pins, flashboard, 872, 873, 875  
     Pipe, rubber lining for sluicing, 791  
         sluicing, 789  
         composition of, 790  
         wear of, 790  
         trap, 789  
     Pipe drains, 686  
         Kingsley Dam, 687  
         Sardis Dam, 688  
     Pipes, beach, 784, 789  
         sluicing, friction loss, 787  
         velocity, 787  
         through earth dams, 710  
         window, 789  
     Piping, 61, 708  
         blow-out gradient, 706, 708  
         buttressed dams, 572  
         escape gradient, 709  
         factor for safety, 63, 709  
         flotation gradient, 706, 708  
         horizontal, 709  
         pile foundations, 302  
         vertical, 708  
     Piston-type sampler, 23, 25  
     Pit River Dam No. 3, 265, 353  
     Pit River Dam No. 4, 562  
     Plane table mapping, 8, 9  
     Plastic flow, concrete arches, 452  
     Plastic foundation, shear in, 731  
     Plastic limit, 620, 761

- Pleasant Hill Dam, cutoff walls, 702  
 Pleasant Valley Dam, 660  
 Plotting, multiplex, 7, 8  
 Plum stones, concrete aggregate, 604  
 Poisson's ratio, adjustments for, 545  
     foundation equations, 442, 443, 444  
     values, for concrete, 452  
     for stone, 453  
 Polson Dam, 556  
 Ponte Alto Dam, 556  
 Porosity, definition, 620  
 Porous concrete for slope protection, 764  
 Portland cement, 605  
 Possum Kingdom Dam, 562, 569, 850, 855  
 Pozzolana cement, 605  
 Prado Dam, 780  
 Precipitation stations, 141  
 Preconsolidation loading, 634  
 Preliminary investigation, 3  
 Pressure, allowable compressive, 299  
     dynamic, 255, 259, 394  
     earth, 272  
     foundation, 288  
     hydrostatic, relief of, 53  
     ice, 270, 272, 285, 315, 385, 399  
     inclined, 301, 340, 581  
     internal, uplift, 260  
     overflow crest, 258  
     silt, 272, 377, 381  
     sluicing, 783, 787  
     stability against headwater, earth dams, 716  
     subatmospheric, 255  
     tailwater, 255, 259, 383  
     under dams, 71  
     vertical, 301, 405, 580  
     void ratio curve, 638  
     water, earthquake, 282, 330, 526, 564  
         external, 252, 258, 377, 425, 453, 489, 514, 590  
         wave, 274, 314  
     wind, 274  
     within dam, 264  
     within foundation, 264  
 Pressure cells, 704  
     readings, in hydraulic fill, 743  
 Pressure testing device, 35  
 Prettyboy Dam, 353  
 Prewetting, 769, 771  
 Price (Lane-Campbell) flow net, 90  
 Priest Dam, 780  
 Probability curves for floods, 131  
 Proctor, R. R., dry density, 274  
     Proctor analysis, 643, 644  
     Proctor needle, 645, 760  
     Protection of top and downstream slope, 768  
     Puddingstone No. 1 Dam, 660, 780  
     Puddle clay, 767  
     Puddling, 711, 752  
     Puls, L. G., Wilson Dam, 366  
     Pumicite in cement, 605  
     Quabbin Diike, 780, 791, 793, 795  
     Quaker Bridge Dam (New Croton Dam), 353  
     Quarry, suitability of, 37  
     Quick sand, 706  
     Quick shear strength curves, 639  
     Racks for sluices, 915  
     Rainfall, analysis, 141  
         bibliography, 205  
         excess, 181, 184, 185  
         hyetographs, 143  
         mass curves, 141  
         snow melted by, 190  
         Thiessen polygons, 154  
         transposed storms, 185  
         unit rainfall duration for floods, 158  
         unit storms, 159  
     Ralston Creek Dam, 780  
     Ramser, C. E., values of Kutter's  $n$ , 138  
     Randolph, R. R., on hydraulic jump, 79  
     Randolph model tests, 98  
     Rankine formula, 272, 273, 718, 722  
     Rawhouser, Clarence, temperature control, 440  
     Recession curves, floods, 156  
     Reconnaissance, equipment for, 1  
     Record storm, transposition of, 184  
     Red Bank Creek Dam, baffle piers, 85  
         jet deflectors, 86, 88  
     Redridge Dam, 834, 836, 838, 840, 841  
     Reid, Lincoln, spillway crests, 259, 358, 361, 369  
     Reinforcement, buttressed dams, 569, 571, 575, 583, 589, 592, 593, 595, 598  
         ice pressure, 386  
         openings in dams, 420, 422  
     Relief Dam, 808  
     Reservoirs, flood routing, 195, 196, 198, 240  
         inflow hydrograph, 177  
         life of, 39  
         siltling of, 39

- Resin, Vinsol, 616\*
- Resistance to sliding, 45, 294, 321
- Resonance, earthquake forces, 281
- Resultant, cantilever, 516
  - forces on dam, 286
  - required location of, 294
- Retrogression, 89
- Reynolds' number, 92, 94
- Ricobaya Dam, 355
- Ring follower gate, 919, 921
- Rio Puerco Dam, 353
- Rio Salado Dam (Don Martin), 562, 599, 600
- Ripley, Theron M., taintor gate discharge, 374
- Riprap, 761
  - bedding, 763
  - concrete, 763
  - dumped, 761
  - hand-placed, 762
  - monolithic concrete, 763
  - stone, 763
- Rock, foundation for dams, 300, 301
  - on downstream slope, Clendenning Dam, 773
  - Conchas Dike, 770
- Rock drain, 689
- Rock fill, main, 811
- Rock-fill dams, 806
  - bibliography, 832
  - composite type, 823
  - concrete facing, 818
  - core, 829
  - corewall type, 823
  - earth-core type, 825
  - freeboard, 822
  - impervious facing, 816
  - North African, 830
  - rock size, 813
  - rubble backing of face, 813
  - settlement, 820
  - sluicing, 820
  - spillways, 822
  - steel facing, 817
  - timber facing, 816
- Rock foundation, care in blasting, 45, 46
  - treatment, 46
- Rock Island Dam, 353
- Rock toe, 690, 693
- Rockwell, S. E., on Stony Gorge Dam, 572, 574, 583
- Rocky River Dam, 679, 790, 792
- Rodriguez Dam, 562, 570
- Rolled fill, 753
  - Rolled-fill dam, engineering control, 759
  - Rolled layers, depositing, 754
    - thickness of, 754
  - Roller, passes of, 755
    - pressure of, 754
    - sheep's-foot, 754, 755
  - Roller bearing gates, 871
  - Rolling, danger of overrolling, 755
    - embankment, 754
    - gates, 871, 894
  - Roofing in earth foundations, 54, 66, 302
  - Roosevelt Dam, 353
  - Rossi-Forel scale, earthquake forces, 280, 281
  - Rotary drilling of overburden, 15
  - Roughness, coefficient of, model tests, 94
  - Round-head buttressed dams, 560, 561, 597, 599
    - Rio Salado (Don Martin), 562, 599, 600
  - Round Hill Dam, 353
  - Rouse, Hunter, experimental hydraulics, 98, 361, 369
    - spillway crests, 259, 358
  - Routing floods, 195
  - Rubber lining for sluicing, 791
  - Rubber seal, 853
  - Rubble backing, rock-fill dams, 813
  - Ruby Dam, 556
  - Rugen, O. N., snow-melt, 206
  - Runoff, bibliography, 205
    - concentration near peak, 165
    - floods, 155
    - ground-water depletion, 157
    - infiltration, 143
    - initial loss, 145
  - Rutter, E. J., floods, 206
  - S-curve hydrograph, 167
  - Sabrina Dam, 808
    - timber facing, 816
  - Safe Harbor Dam, 353
  - Safety, against foundation shear, 727
    - against sliding of rock fill, 807
  - Safety factor, concrete, 300
    - earth dam, against shear, 719, 720
    - gravity dams, 303
    - hydraulic fill dam, 744, 747
    - piping, 62, 709
    - psychological considerations, 304
    - shear friction, 297
    - sliding, 295
      - on earth, 296

- Safety of shells, hydraulic fill, against shear, 744
- Safety requirements, earth dams, 662
- Saint Francis Dam, 354, 629
- Salmon Creek Dam, 555, 556
- Salmon River Dam, 556
- Salt Springs Dam, 808, 812, 819, 820, 822, 823
- Saluda Dam, 680, 790, 792
- Sampler, application of, 25  
     diameter of cutting edge, 21, 23  
     Fahlquist, 27  
     importance of fast, uninterrupted motion, 25  
     large size, 23  
     liner of, 23  
     piston type, 23  
     small diameter, 21
- Samples, care of, 34  
     failure, prevention of, 13  
     silt and clay, 17  
     undisturbed, 16, 39  
         distortion of, 17, 18
- Sampling, cohesionless materials, 27  
     drive, 16  
     freezing method, by, 27  
     frozen plug, use of, 28  
     minimum disturbance, 25  
     undisturbed, 16
- San Dimas Dam, 353
- San Gabriel No. 1 Dam, 211, 810, 821
- San Gabriel No. 2 Dam, 808, 821
- San Leandro Dam, 780
- San Mateo Dam, 353
- Sand, blow, 624, 636, 757, 803  
     concrete aggregate, 606, 608, 609, 610, 617  
     consolidation, 634  
     foundation bearing power, 302  
     lenses in core, 794  
     suitability of, 37  
     tests of, 627  
     trinity, 15, 634
- Sandy gravel, 624
- Sandy silt, 623
- Santee Cooper Dam, porous concrete  
     slope protection, 764
- Santeetlah Dam, 556
- Santiago Creek Dam, 780
- Sardis Dam, 780, 785, 791, 795
- Sarrans Dam, 355
- Saturation, degree of, definition, 621
- Savage Dam, 354
- Saylor, William H., arch dams, 425
- Schley, General Juliafi L., Fort Peck slide, 801
- Schneider, G. R., floods, 206
- Schoklitsch, Armin, hydraulic structures, 356
- Schorer, Herman, buttresses of uniform strength, 570
- Schraeh Dam, 355
- Schrontz, C. C., setup, 277
- Schuyler, J. D., arch dams, 556
- Scimemi, Ettore, "Dighe," 356, 358
- Scott Dam, 351
- Scottsdale Dam, 661
- Scraper, 752
- Screens, 627
- Seals, for gates, 898, 902, 903, 921  
     transverse joints, 853
- Seams, cleaning out, 52  
     grouting of, 48, 52
- Secondary stresses, discussion, 401  
     Grand Coulee Dam, 415, 416
- Sections, geologic, 10
- Sector gate, 881
- Seepage, bibliography, 90  
     earth dams, 663  
     earth foundations, 59  
     effect of foundation cutoff, 693  
     parabola, 666  
     partial cutoff, 695  
     quantity of, 680  
     tests on, 59  
     total through and under earth dams, 682  
     without cutoff, 59, 693
- Seepage line, composite earth dam, 672  
     computed position, 673  
     determination of, 665  
     earth dams, 664  
     effect of drainage on, 685  
     existing earth dams, 677  
     observation devices, 704  
     pervious foundation, 676  
     prediction of, 664, 672, 675  
     under cutoff, 695
- Seiches, 276
- Seismic prospecting, 12, 39
- Semihydraulic fill dams, 782
- Seminole Dam, 556  
     loads and deflections, 503
- Senecaville Dam, 780
- Sepulveda Canyon Dam, 661
- Settlement, 640  
     embankments, 758  
     rock-fill dams, 820

- Setup, 276, 277\*
- Shaft spillway, 227
  - flat-crested, 236
  - hydraulics of, 229, 236, 241
- Shasta Dam, 79, 305, 348, 354, 854
- Shaver Lake Dam, 354
- Shear, analysis of, in dams, 405, 411
  - buttresses, 582
  - combined with friction, 297
  - deformation equations, 439
  - direct machine, 629
  - elastic theory, 728
  - foundation, 269, 292
    - approximate stresses, 725
    - elastic theory, 728
    - Fort Peck Dam, 801
  - safety against, 727
  - friction factor, 297
- Grand Coulee Dam, 416
- horizontal, downstream portion of earth dam, 717
  - upstream portion of earth dam, 718
- hydraulic fill dam, 744
- neglect of, arch dams, 479, 480
- plastic foundation, 731
- Shear machine, triaxial, 631
- Shear sliding factor, gravity dams, 321
- Shear strength, definition, 620
  - effect of consolidation, 639
  - relation to height of dam, 269
- Shear tests of soils, 629
- Sheep's-foot roller, 754, 755
- Sheet piling cutoff, 70, 763, 798, 803
- Shell, criteria for lenses, 797
  - Fort Peck Dam, 800
  - hydraulic fill, 791
  - lenses of core in, 796
  - mechanical analysis of, 795
  - uniformity coefficient, hydraulic fill, 791
- Sherman, L. K., floods, 205
- Sherman Dam, 792
- Shing Mun Dam, 355
- Shoshone Dam, 556
- Shovel, diesel, 750
- Shrinkage, arch dams, 434, 439, 450
  - cracks in buttresses, 569, 593
  - setting of concrete, 451
- Side channel spillways, 216
  - hydraulics of, 218
- Sidney gate, 894
- Sill, dentated, 81
- Silt, 623
  - above diversion dams, 272
- Silt, angle of internal friction, 274, 632
  - backwater effect, 376
  - carried by streams, 3
  - consolidation of, 636
  - drive sampling, 16
  - dry weight, 273
  - earthquake effect on, 285
  - effect on uplift, 263
  - pressure, direction of action, 273
    - on dams, 272, 377, 381
  - samplers for, 17
  - sluicing of, 272, 805
  - specific gravity, 273
  - submerged weight, 273
- Silting of reservoirs, 39
- Silts, tests of, 627
- Silty clay, 623
- Silty sand, 624
- Silvan Dam, 780
- Silverman, I. K., stress around holes, 419
- Similarity, hydraulic model tests, 92
- Similitude/hydraulic, 92, 95
- Siphons, bibliography, 929
  - spillways, 871, 909
- Site maps, 9
- Skaguay Dam, 808
  - steel facing, 817
- Slab analysis, 575
- Slab and buttress dam, 558
- Slab and column dams, 603
- Slichter, C. S., permeability, soils, 650, 653
- Slickensides, 756
- Slide, 662, 755, 756, 772, 801
- Slide gate, 871, 916, 917, 918, 921
- Sliding, cause of failure, 293
  - coefficient of, 295
  - construction joints, 298
  - cutoff to prevent, 55
  - earth foundation, 296
  - prevention of, 296
  - resistance to, 45, 294
  - safety against rock fill, 807
  - shear and friction, 297
  - shear sliding factor, 321
  - stability requirements, 292, 715
- Slope, of beach, 785
  - of layers, 757
  - protection upstream, 761
    - porous concrete, 764
- Slope design, rough methods of, 724
- Slopes, trimming of, 759
- Sluice, 870, 914
  - lining, 916



- Sluice, racks for, 915
  - silt removal, 272
- Sluice gate, 917, 929
- Sluice lines, mixture carried, 787
- Sluice pipe, 789
  - composition of, 791
  - friction loss, 787
  - head loss, 787
  - rubber lining, 791
  - velocity required, 787
  - wear of, 790
- Sluicing and rock-fill dams, 820
- Sluicing box, 788
  - Winsor Dam, 788
- Sluicing pressure, 784
- Slump, concrete, 609
- Smith, Chester W., dams, 356
- Snake Ravine Dam, 661
- Snow, effect on floods, 130, 186
  - free water in, 187
  - heat transfer, 188, 190
  - melt, bibliography, 205
  - degree-day method, 191
  - melting, 188
    - by rainfall, 190
  - water equivalent of, 187
- Snyder, F. F., floods, 163, 205, 206
- Soft Maple Dam, 680, 792
- Soil, classification of, 621
  - flow of water through, 646
  - kinds of, 621, 623
  - sample, prevention of failure of, 18
  - shear tests of, 629
  - tests, 619
    - bibliography on, 654
    - clays, silts and fine sands, 627
    - of coarse sands and gravels, 627
    - standardization of, 619
- Soil mechanics, definitions, 619
  - utilization of, 655
- Solids, percentage, in sluicing, 787
- Somerset Dam, 790, 792
- South Lake Dam, 808, 816
- Spacing of buttresses, 565, 574
- Spatial model, 5, 7
- Specific gravity, 277
  - aggregate, 610, 617
  - cement, 610
  - definition, 621
  - silt, 273
- Specifications, cement, 605
  - concrete, 605
- Spiers Falls Dam, 354
- Spillway, 208, 870
  - arch dams, 82
    - automatic, 882
    - Boulder Dam side channel, 224
    - chute, 208, 210
    - control, 870, 871
    - crests, model research, 259
    - critical depth, 371
    - Davis Bridge morning glory, 236
    - design hydrograph, 204
    - design storm, 178, 180
    - discharge, restricted openings, 366, 372
    - emergency, 243
    - flat-crested shaft, 236
    - model tests, 74
    - morning glory, 227
      - hydraulics of, 229, 236, 238
    - standard crest, 228
    - required capacity, 192
    - rock-fill dams, 822
    - rock-fill timber crib, 816, 822
    - shaft, 227
      - hydraulics of, 229, 236
      - standard crest, 228
    - side channel, 216
      - hydraulics, 218
    - Tieton Dam side, 217
  - siphon, 909
  - special type, discharge formula, 370
  - submerged, flow over, 372
- Spitallamm Dam, 355
- Stability, buttressed dams, 579, 587
  - concrete dams, by D. C. Henny, 266, 297
  - crest gates, 364, 397
  - earth dams, 715
    - bibliography, 748
  - gravity dams, 266, 293, 297
  - hydraulic fill, 742
  - masonry dams, 291
  - multiple-arch dams, 587
  - numbers, Taylor, 737
  - requirements, sliding, 292
  - Swedish geophysical method, 731
  - timber dams, 845
- Stadia, 9
- Stage grouting, 49
- Standard crests, classification, 358
  - coordinates for, 359, 360, 362
  - design head, 357
  - discharge coefficient, 367
  - shape and dimensions, 357 to 364
- Standley Lake Dam, 780
- Stanislaus Dam, 807
- Stanley, C. M., stilling basin design, 98

- Stauwerke gate, 834
- Steel arch dams, 841
- Steel dams, 834
  - application of, 43
  - bents, 838
  - bibliography, 841
  - cantilever type, 835
  - contraction, 838
  - costs, 841
  - deck girders, 838
  - durability, 841
  - expansion, 838
  - face plates, 836
  - foundation, 840
  - painting, 841
  - quantities, 841
  - slope of face, 836
- Steel facing, rock-fill dams, 817
- Steel sheet piling cutoff, 70, 694, 695, 768, 798, 803
- Steele, Byram W., concrete, 604
  - concrete cooling, 451
  - construction joints, 849
- Steele, I. C., rock-fill dams, 813
- Salt Springs Dam, 818
- Sterns, Frederic P., earth dams, 683, 688
- Stevens, J. C., model tests, 98
- Stevens Dam, 779, 828
- Stevenson, Thomas, wave height, 274
- Stevenson Creek Dam, model tests, 552
- Stevenson Dam, 354
- Stewart Mountain Dam, 556
- Stickney drum gate, 878
- Stilling basin, 77, 80, 82, 83, 86
  - Mohawk Dam, 91
- Stone for riprap, 763
  - downstream slope protection, 766
  - properties of, 452, 453
- Stoney gate, 885, 886, 887, 888
- Stoney River Dam, 46
  - cutoff, 55
- Stony Gorge Dam, 562, 572, 573, 574, 576, 577, 579, 583
- Stop logs, 871, 907
- Stops, water, 701, 820, 853
- Storage, effect on floods, 128
  - valley, 129
- Storms, transposed, 184, 185
- Stratton, J. H., Conchas Dam, 305
- Strawberry Dam, 808
- Stress concentrations, fillets, 414
  - Grand Coulee Dam, 415
  - holes in plates, 417
  - Morris Dam base, 415
- Stress concentrations, openings in dams, 418
  - reinforcement for, 420
- Stress-strain curves, 632
- Stresses, allowable, in concrete, 300
  - in masonry, 300
  - base of dams, 415
  - beam, in buttresses, 567
  - compressive, rules for, 299
  - concentrations in foundations, 415
  - dam faces, 404
  - foundation, 288, 290, 415, 416
  - Grand Coulee Dam, 415, 416
  - heel and toe, 413
  - horizontal, 404, 406, 410, 416, 547, 582
  - inclined, 299, 302, 402, 581
  - Morris Dam, 415
  - oblique planes, 402
  - principal, 402, 403, 413, 415, 416, 547
  - secondary, 401, 415, 416
  - temperature, 434, 439, 450, 482
  - vertical, 238, 302, 404, 411, 416, 547, 568, 580
- Stripping for earth dams, 750
- Structures, precaution around, 758
- Sturgeon Pool Dam, 354
- Subatmospheric pressure, 255
- Submerged dams, discharge coefficient, 373
- Subsurface exploration, 9, 10
  - churn drilling, 14
  - earth augers, 15
  - electrical, 12
  - methods of, 12
  - rotary drilling, overburden, 15
  - seismic, 12
  - test pits, 13
  - wash borings, 14
- Suction dredges, 784
- Sudden drawdown, earth dam, 723, 740, 747
- Surcharge storage, 202
- Surface finish, concrete, 612, 613
- Surry Mountain Dam, 780
- Sutherland, Robert A., dams, 350, 556, 562, 778
- Sutherland Dam, 562
- Svirstroy Dam, foundation, 70
- Swansea Dam, 661
- Swedish geophysical method, 731
- Swedish piston-type sampler, 23, 25
- Sweetwater Dam, 354
- Swift Dam, 808
- Swinging Bridge Dam, 790, 792

- Symbols for masonry dams, 247  
 Synthetic unit hydrographs, 162, 169
- T-beams, buttressed dams, 568  
 Tabeaud Dam, 682, 780  
 Table Rock Cove Dam, 660  
 Tailwater, dynamic effect, 255, 259  
   hydraulic jump, 75, 396  
   reaction, 259, 383, 396  
 Taintor gate, 871, 891, 892, 904  
 Talla Dam, 766  
 Tallulah Dam, 354  
 Tampers, compressed air, 758  
 Tangential loads, 502, 527, 533  
 Tappan Dam, 660, 756  
 Tar coating for water proofing, 617  
 Taylor Park Dam, 780  
 Taylor's stability numbers, 737  
 Taylorsville Dam, 792  
 Temescal Dam, 780  
 Temperature, control, concrete, 615, 848  
   cracks, concrete structures, 615  
   stresses, 434, 439, 450, 482  
   variation, arch dams, 434, 439, 450  
     Florence Lake Dam, frost damage, 595  
     ice pressure, 270  
     multiple arches, 585, 587  
     radial, 440, 451  
 Tepuxtepec Dam, 808  
 Terrace Dam, 780, 792  
 Terzaghi, Karl, elastic theory, 728  
   piping experiments, 708  
   retaining-wall design, 273  
   stability of gravity dams, 266  
 Test pits, 13  
 Testing, borings by pressure, 36  
   concrete, 604, 617  
   device for borings, 35  
 Tests, clays, 627  
   coarse sands and gravels, 627  
   concrete and concrete materials, 617, 628  
   field, during construction, 626, 760  
   fine sands, 627  
   foundation materials, 628  
   hydraulic model, bibliography, 98  
     similarity, 92, 95  
   model, spillways, 74  
   rough field, 37  
   shear of soils, 629  
   silt, 627  
   soil, 619, 627, 654  
   soils, bibliography, 654
- Volume I, pages 1-246; Volume II, pages 247-618; Volume III, pages 619-929
- Tests, triaxial shear, 601  
 Thermal expansion, coefficient of, 451  
   concrete, 604  
 Thiem, G., permeability determination, 650  
 Thiessen polygons, 154  
 Thomas, D., 369  
 Thomas, Harold A., erosion control, 73  
 Thompson, Milton J., fluid mechanics, 259  
 Three-centered arch, 495  
 Tides, 276  
 Tidone Dam, 562  
 Tieton Dam, 217, 780, 790, 792  
 Tiger Creek Dam, 562  
 Tilting gates, 871, 884  
 Timber crib dam, 844  
 Timber dams, 843  
   A-frame type, 843  
   advantages of, 843  
   application of, 42  
   beaver type, 845  
   choice of type, 846  
   erosion, 846  
   foundation, 846  
   limitations of, 847  
   stability, 845  
 Timber facing for rock-fill dams, 816  
 Time of consolidation, 640  
 Time per cent consolidation curve, 638  
 Timoshenko, S., elastic theory, 417, 728  
   location of neutral axis, 436  
   shear modulus, 449  
 Tionesta Dam chute spillway, 208  
 Tirso Dam, 562  
 Titicus Dam, 354, 780  
   seepage line in, 677  
 Toe, rock, 690  
 Toe hold, 45  
 Top protection, earth dams, 766  
 Top width, nonoverflow dam, 307  
 Topographic maps, 5  
   aeroplane, 8  
   drafting, 8  
 Topography, 5  
   aeroplane mapping, 5  
 Trac-truck, 753  
 Tractor gate, 920, 921  
 Tranco de Beas Dam, 355  
 Transmission constant, definition, 621, 647  
 Transposed storms, 185  
 Transposition of record storm, 184  
 Transverse joints, concrete dams, 848

- Trap pipe, 789 •
- Trapezoidal section, 287
- Trautwine, J. C., 358
- Trestles, concrete placement, 611
- Trial load theory for arch dams, 500
- Trial mix of concrete, 608
- Trimming of slopes, 759
- Trinity sand, 15, 634
- Triple-arch dam, 602, 603
- Truck-mounted gate, 871, 891
- Truyere Dam, 355
- Tubing, thin-walled, 21, 23
- Turbulent flow, 93
- Turlock Dam, 352
- Turneure, F. E., on slab analysis, 575
- Twin Falls Dam, 354
- Twist deflection, arches, 541, 542
  - cantilevers, 538, 545
- Twist moment, cantilevers, 538
  - estimating for arches, 526, 543
- Tygart Dam, 305, 348, 355, 859
- Tytam Bay Dam, 683
  
- Uncompacted material, passage of water through, 713
- Undermining, cause of failure, 293
- Undisturbed samples, distortion of, 17, 18
  - report on, 39
- Undisturbed sampling, 16
- Uniformity coefficient, definition, 620
  - hydraulic fill shells, 791
- Unit hydrograph, 158, 162, 170, 173
  - adjustment, 170
  - major flood records, 162
  - peak discharge, 164
  - selection of, 175
  - synthetic, 162, 169
- Unit loads, for arches, 548
  - for cantilevers, 550
- U. S. Bureau of Reclamation, dams and control works, 90
- U. S. Engineers, Los Angeles, flow net, 90
- Uplift, 260
  - areas subject to, 260, 264
  - bibliography, 90
  - buttressed dams, 264, 564, 572
  - caused by grouting, 51
  - constants recommended, 269
  - control of, 262, 296
  - earth foundations, 268
  - earthquake effect, 284
  - effect of silt, 263
  - effect on resultant, 294
  - equation for, 267
  - Uplift, examples of assumptions, 268
    - existing gravity dams, 265
    - explanation of, 260
    - flow-net, 55, 64, 261
    - Levy, Maurice, 266
    - measured by piezometers, 73
    - normal, 515
    - observed intensities, 265
    - pervious foundation, 55, 261
    - practical diagram, 267
    - under aprons, 87
    - value of constants for design, 268
    - with foundation reaction, 290
  - Uplift and seepage under dams on sand, 261
  - Uplift pressure on dams, 63, 260
  - Upstream blanket, 68, 685, 696, 785, 805
  - Upstream slope, concrete lining, 763
  - Upstream slope protection, 761
  - Upturned bucket, 81
    - Grand Coulee Dam, 82
  - Utica Dam, 61
  
  - Vacuum, overflow dam crest, 357
  - Vallecito Dam, 780
  - Valley storage, 129
  - Valve, 917, 929
    - Howellunger, 928
    - Larner Johnson, 925
    - location in sluices, 916
    - needle, 924 to 927
      - Reclamation Service, 925
    - sleeve, 928
    - slide, 871, 916, 917, 918, 921
  - Valves and sluices, 915
  - Van den Broek, J. A., elastic energy theory, 439
  - Variable-radius arch dam, 431
  - Variation, coefficient of, 134, 136
  - Vegetable matter, removal of, 751
  - Velocity, critical, 93, 371
    - in sluicing pipes, 787
    - of approach, effect on discharge, 366
      - 369, 371, 392
    - effect on shape of crest, 358, 392
  - Velocity head, backwater curves, 376
    - effect on pressure, 256
  - Venina Dam, 562
  - Ventilation of sluice gates, 916
  - Vertical elements of arch dams, 500
  - Vibration, concrete, 611
    - periods, 282
  - Vinsol resin, 616
  - Viscosity of water, 92

- Vogel, H. D., tests, hydraulic models, 98  
 Vogt, Frederik, deformation equations, 441  
 Void ratio, critical, 636  
   definition, 620, 635  
   Trinity sands, 15, 634  
 Wachusett Dam, 355  
 Wachusett Dike, 678, 780  
 Waggital Dam, 355  
 Walnut Grove Dam, 808  
 Warnock, J. E., crests for overfall dams, 359 -  
 Wash borings, 14  
 Water, for concrete, quantity, 608, 609, 610  
   flow through soils, 646  
   free passage of, through dams, 710  
   passage through uncompacted material, 713  
   viscosity of, 92  
   weight of, 252  
 Water cement ratio, 608, 609, 610  
 Water content, definition, 621  
 Water pressure, arch dams, 453  
   center of application, 253  
   dynamic effect, 255  
   earthquake, 282, 330, 526, 564  
   external, 252  
   internal uplift, 260  
   multiple-arch dams, 590  
   tailwater, 255  
   vertical, 514  
 Water stops, 701, 820, 853  
 Waterproofing concrete, 616  
 Wave pressure and heights, 274, 314  
 Wear of sluice pipe, 790  
 Weaver, Warren, uplift, 64, 261  
 Weaving of embankment, excessive, 754, 756  
 Webber Creek Dam, 602  
 Webber Dam, 562  
 Weber's number, 93  
 Weep holes, foundation slabs, 572  
 Wegmann, Edward, dams, 309, 356, 556, 560, 567, 569, 593, 595, 603  
 Weight, *see also* Density  
   of concrete, 277  
   of crest gates, 906  
   of earth, 273  
   of foundation,\*278  
     of masonry, 277, 454  
     of silt, 273  
     of sluicing mixture, 787  
 Weir, aeration of, 256, 257  
   broad-crested, 370, 372, 373  
   discharge capacity, 364  
   forces on, 255  
   negative pressure on, 258  
   shape of nappe, 357  
   sharp-crested (not aerated), 257  
 Weiss, Andrew, Don Martin Dam, 599  
 Weisse Dam, 660  
 Welch, Paul S., limnology, 276  
 Well drilling, 15  
 Well point drains, 71, 684  
 Wenzel, Leland K., 651  
 West Julesburg Dam, 661  
 Westergaard, H. M., earthquake pressures, 282, 283  
 Weston, R. S., 305, 356  
 Wetting embankment, 754  
 White Salmon Dam, 355  
 Wichita Falls Dam, 791, 792  
 Williams, C. P., Rodriguez Dam foundation, 570  
 Willocks, Sir William, floods, 138  
 Wilson, H. M., irrigation engineering, 356  
 Wilson, W. T., on snow-melt, 189, 206  
 Wilson Dam, 355, 366  
 Wilwood Dam, uplift, 265  
 Wind pressure, 274  
 Wind velocity, 274  
 Window pipe, 789  
 Winsor Dam, 781, 788, 791, 795  
 Wire cutting, 23  
 Wissota Dam, 683  
   seepage line in, 680  
 Wolf Creek Dam, 355  
 Yadkin Narrows Dam, 305, 353  
 Yarnell, D. L., rainfall, 206  
 Yarrow Dam, 781  
   typical cross-section, 699  
 Youghiogheny Dam, jet deflectors, 86  
 Ziegler, P., "Der Talsperrenbau," 356  
 Zola Dam, 556  
 Zuider Zee formula for setup, 277  
 Zuni Dam, 661, 810



















